






# Morpho-phylogenetic evidence reveals four novel species of *Coniella* (Diaporthales, Schizoparmaceae) from southern China

Duhua Li<sup>1,2</sup>, Zixu Dong<sup>2</sup>, Qiyun Liu<sup>2</sup>, Yaling Wang<sup>2</sup>, Zhaoxue Zhang<sup>2</sup>, Xiuguo Zhang<sup>2</sup>, Jiwen Xia<sup>1</sup>

<sup>1</sup> College of Agriculture and Forestry, Linyi University, Linyi, Shandong, 276000, China

<sup>2</sup> College of Plant Protection, Shandong Agricultural University, Taian, Shandong, 271018, China

Corresponding author: Jiwen Xia (xiajiwen@lyu.edu.cn)



This article is part of:

**Exploring the Hidden Fungal Diversity:  
Biodiversity, Taxonomy, and Phylogeny of  
Saprobic Fungi**

Edited by Samantha C. Karunarathna,  
Danushka Sandaruwan Tennakoon, Ajay  
Kumar Gautam

Academic editor:

Danushka Sandaruwan Tennakoon

Received: 3 January 2025

Accepted: 26 February 2025

Published: 4 April 2025

**Citation:** Li D, Dong Z, Liu Q, Wang Y, Zhang Z, Zhang X, Xia J (2025) Morpho-phylogenetic evidence reveals four novel species of *Coniella* (Diaporthales, Schizoparmaceae) from southern China. MycoKeys 116: 1–23. <https://doi.org/10.3897/mycokeys.116.145857>

Copyright: © Duhua Li et al.

This is an open access article distributed under terms of the Creative Commons Attribution License (Attribution 4.0 International – CC BY 4.0).

## Abstract

*Coniella* species are distributed worldwide and have been reported as plant pathogens, endophytes, or saprobes. In our ongoing survey of terrestrial plant fungi in southern China, we obtained *Coniella* isolates from diseased plant leaf tissues in Fujian, Hainan, and Yunnan provinces. Maximum likelihood and Bayesian inference based on four loci (ITS, LSU, *rpb2*, and *tef1-α*) were used to clarify the taxonomic placement of the species. We confirmed that they represent four new species, namely *Coniella diaoluoshanensis*, *C. dongshanlingensis*, *C. grossedentatae*, and *C. veri* based on both morphology and phylogeny support. The new species are compared with other *Coniella* species, comprehensive descriptions and micrographs are provided.

**Key words:** Morphology, multigene phylogeny, new taxa, taxonomy

## Introduction

*Coniella* was formally introduced by Von Höhnel (1918) with *C. pulchella* (= *C. fragariae* (Oudem.) B. Sutton) as the type species (Von Höhnel 1918; Sutton 1977; Crous et al. 2014a). Samuels et al. (1993) initially recognized the uniqueness of *Schizoparme* and its relationship to *Coniella* and *Pilidiella*, these were initially placed in the Melanconidaceae. Both Castlebury et al. (2002) and Van Niekerk et al. (2004) revealed that these species within the Diaporthales, which they collectively designated as the *Schizoparme* complex. Rossman et al. (2007) introduced a new family, Schizoparmaceae, which comprises the distinctive teleomorph genus *Schizoparme*, its asexual state *Pilidiella*, and the closely related anamorph genus *Coniella*. These genera are cosmopolitan fungal pathogens associated with foliar, fruit, stem, and root diseases on a wide variety of hosts, including some economically important hosts (Van Niekerk et al. 2004; Alvarez et al. 2016). They occur as parasites on unrelated dicotyledonous hosts (Samuels et al. 1993) or sometimes as secondary invaders of injured plant tissues (Ferreira et al. 1997).

*Coniella* has undergone comprehensive morpho-molecular studies and experienced several taxonomic adjustments over the years. Petrak and Sydow (1927) classified *Coniella* into two subgenera: *Euconiella* (dark conidia),

typified by *C. pulchella*, and *Pseudoconiella* (hyaline to pale conidia), typified by *C. granati*. Von Arx (1973, 1981) classified *Coniella* and *Pilidiella* as distinct genera, with *Coniella* characterized by dark brown conidia and *Pilidiella* by hyaline conidia that darken to a pale brown when mature. Nonetheless, Sutton (1980) and Nag Raj (1993) disregarded conidial pigmentation as a defining trait and still opted to employ the earlier name *Coniella*. Samuels et al. (1993) stated *Schizoparme* as the sexual morph and positioned it in Melanconidaceae. Castlebury et al. (2002) classified *Pilidiella* and *Coniella* as members of the *Schizoparme* complex. Van Niekerk et al. (2004) demonstrated that these taxa form a distinct evolutionary lineage within the Diaporthales based on ITS, LSU, and *tef1-α* sequences. Subsequently, Rossman et al. (2007) established a new family, Schizoparmaceae, including the above three genera, viz. *Coniella*, *Pilidiella*, and *Schizoparme*. Alvarez et al. (2016) demonstrated that *Coniella*, *Pilidiella*, and *Schizoparme* formed a monophyletic clade in Schizoparmaceae and suggested adopting *Coniella* (the older asexual typified name) instead of *Pilidiella* and *Schizoparme*, in accordance with Article 59.1 of the International Code of Nomenclature for Algae, Fungi, and Plants (ICN, Melbourne Code; McNeill et al. 2012). Additionally, due to the many numbers of species and the similarity in morphological characteristics, they suggested that the identification of new species within *Coniella* must be based on a combination of DNA sequence data and morphological characteristics. Chethana et al. (2017) used a combination of morphological analysis and multigene phylogeny with the genealogical concordance phylogenetic species recognition (GCPSR) method to delineate species boundaries. Hyde et al. (2020) and Tennakoon et al. (2021) conducted the recent phylogenetic analyses for *Coniella* species within the Schizoparmaceae. Currently, there are 66 accepted *Coniella* species (Index Fungorum: <https://indexfungorum.org>; MycoBank: <http://www.mycobank.org>; Mu et al. 2024).

In this study, we conducted extensive sample collection in southern China, primarily collecting plant leaves with obvious fungal necrosis or typical blight spot symptoms. Several *Coniella* fungi were collected from the diseased leaves of *Ampelopsis grossedentata*, *Cinnamomum verum*, *Kadsura longipedunculata*, and *Lygodium circinnatum*. Based on morphological and multi-locus analysis employing internal transcribed spacer (ITS), 28S large subunit ribosomal RNA gene (LSU), partial RNA polymerase II second largest subunit (*rpb2*), and translation elongation factor 1-α gene (*tef1-α*), four new *Coniella* species, namely *C. diaoluoshanensis*, *C. dongshanlingensis*, *C. grossedentatae*, and *C. veri*, were proposed.

## Materials and methods

### Sample collection and isolation

During 2022 to 2024, a large number of plant leaves that exhibited obvious signs of fungal necrosis or typical blight spot symptoms were collected from Fujian, Hainan, and Yunnan provinces in China. This study used tissue isolation methods to isolate fungi (Li et al. 2024). These diseased leaves were cut into small pieces of about 25 mm<sup>2</sup> and surface sterilized by immersion in a 75% ethanol solution for 60 s, washed one time in sterile deionized water

for 20 s, transferred to 5% sodium hypochlorite (NaOCl) for 90 s, and then washed three times in sterile deionized water for 60 s, subsequently dried on sterilized filter paper. The tissue pieces were transferred to the potato dextrose agar (PDA, 200 g potato, 20 g dextrose, 20 g agar, add deionized water and fill to 1000 mL, natural pH) plates and placed in a biological incubator at 25 °C for 3–4 days. The hyphal tips of individual colonies were transferred to new PDA plates to obtain pure cultures, which were then cut into 25 mm<sup>2</sup> pieces using a sterile scalpel and stored in 2 mL frozen tubes containing 20% sterilized glycerin, with 8–10 pieces placed in each tube, for fungal strain preservation at -20 °C for further study.

### Morphological and cultural characterization

The culture characteristics of the colonies were observed and photographed using a Sony Alpha 6400L digital camera (Sony Group Corporation, Tokyo, Japan) on 7 and 14 days, respectively. The micromorphological characteristics of the colonies were observed with the Olympus SZX10 stereomicroscope and Olympus BX53 microscope (Olympus Corporation, Tokyo, Japan), along with the BioHD-A20c color digital camera (FluoCa Scientific, China, Shanghai). Structural measurements were carried out using Digimizer software (v5.6.0) with a minimum of 30 measurements taken for each structure, such as conidiophores, conidiogenous cells, and conidia. The voucher specimens have been deposited in the Herbarium of the Department of Plant Pathology, Shandong Agricultural University, Taian, China (HSAUP). Additionally, the ex-type living cultures were deposited in the Shandong Agricultural University Culture Collection (SAUCC) and the China General Microbiological Culture Collection Center (CGMCC). The taxonomic information of the new taxa were submitted to MycoBank (<http://www.mycobank.org>, accessed on 2 Jan. 2025).

### DNA extraction, PCR amplification, and sequencing

The DNA of the fungal genome was extracted using the modified cetyltrimethylammonium bromide (CTAB) method (Guo et al. 2000; Wang et al. 2023) or the magnetic bead kit method (OGPLF-400, GeneOnBio Corporation, Changchun, China) (Zhang et al. 2023). PCR amplifications of four genes (ITS, LSU, *rpb2*, and *tef1-a*) were done, and the corresponding primer pairs and PCR conditions were listed in Table 1. The PCR reaction was conducted in a 12 µL reaction volume, with a composition of 6 µL of 2 × Hieff Canace® Plus PCR Master Mix (with dye) (Cat. No. 10154ES03, Yeasen Biotechnology, Shanghai, China), 0.5 µL each of forward and reverse primer (10 µM TsingKe, Qingdao, China), and 0.5 µL of template genomic DNA (about 10 ng/µL), with the volume adjusted to 12 µL using distilled deionized water. PCR products were separated using 1% agarose gel and GelRed (TsingKe, Qingdao, China). Gel extraction was purified using a Gel Extraction Kit (Cat. No. AE0101-C, Shandong Sparkjade Biotechnology Co., Ltd., Jinan, China). The purified PCR products were subjected to bidirectional sequencing by Sangon Biotech Company Limited (Shanghai, China). The raw data were analyzed using MEGA v. 7.0 to obtain consistent sequences (Kumar et al. 2016). The sequence data have been deposited in GenBank, and their accession numbers were listed in Table 2.

**Table 1.** The primer sequences and PCR programs in this study.

Locus	Primers	Sequence (5' – 3')	PCR cycles	References
ITS	ITS5	GGA AGT AAA AGT CGT AAC AAG G	(94 °C: 30 s, 55 °C: 30 s, 72 °C: 45 s) × 29 cycles	White et al. 1990
	ITS4	TCC TCC GCT TAT TGA TAT GC		
LSU	LR0R	GTA CCC GCT GAA CTT AAG C	(94 °C: 30 s, 48 °C: 50 s, 72 °C: 1 min 30 s) × 35 cycles	Vilgalys and Hester 1990; Rehner and Samuels 1994
	LR5	TCC TGA GGG AAA CTT CG		
<i>rpb2</i>	RPB2-5F2	GGG GWG AYC AGA AGA AGG C	(94 °C: 45 s, 60 °C: 45 s, 72 °C: 2 min) × 5 cycles, (94 °C: 45 s, 54 °C: 45 s, 72 °C: 2 min) × 30 cycles	Liu et al. 1999; Sung et al. 2007
	RPB2-7CR	CCC ATR GCT TGY TTR CCC AT		
<i>tef1-a</i>	EF1-728F	CAT CGA GAA GTT CGA GAA GG	(95 °C: 30 s, 51 °C: 30 s, 72 °C: 1 min) × 35 cycles	O'Donnell et al. 1998; Carbone and Kohn 1999
	EF2	GGA RGT ACC AGT SAT CAT GTT		

**Table 2.** Species names, strain numbers, hosts or substrates, regions, and corresponding GenBank accession numbers of DNA sequences used in this study.

Species	Strain numbers	Host/Substrate	Region	GenBank accession numbers				References
				ITS	LSU	<i>rpb2</i>	<i>tef1-a</i>	
<i>Coniella africana</i>	CBS 114133* = CPC405	<i>Eucalyptus nitens</i>	South Africa	AY339344	AY339293	KX833421	KX833600	Van Nierkerk et al. 2004; Alvarez et al. 2016
<i>Coniella castanea</i>	SAUCC200313*	<i>Castanea mollissima</i>	China	OL757537	OL757563	OL770463	OL780610	Wang et al. 2022
	SAUCC200314	<i>Castanea mollissima</i>	China	OL757538	OL757564	OL770464	OL780611	Wang et al. 2022
<i>Coniella cili</i>	GUCC 194020.1	<i>Rosa roxburghii</i>	China	ON791171	ON791212	ON815908	ON815944	Zhang et al. 2024b
	GUCC 196007.1*	<i>Rosa roxburghii</i>	China	ON791172	ON791213	ON815909	ON815945	Zhang et al. 2024b
<i>Coniella crousii</i>	NFCCI 2213	<i>Terminalia chebula</i>	India	HQ264189	NA	NA	NA	Rajeshkumar et al. 2011
<i>Coniella diaoluoshanensis</i>	CGMCC3.27786* = SAUCC 7481-1	<i>Kadsura longipedunculata</i>	China	PQ357094	PQ357134	PQ361030	PQ404804	This study
	SAUCC 7481-4	<i>Kadsura longipedunculata</i>	China	PQ357095	PQ357135	PQ361031	PQ404805	This study
<i>Coniella diospyri</i>	CBS 145071* = CPC 34674	<i>Diospyros mespiliformis</i>	South Africa	MK047439	MK047489	MK047543	MK047562	Crous et al. 2018
<i>Coniella diplodiella</i>	CBS 111858* = CPC3708	<i>Vitis vinifera</i>	France	AY339323	KX833335	KX833423	KX833603	Van Nierkerk et al. 2004; Alvarez et al. 2016
	CBS 112729 = CPC3927	<i>Vitis vinifera</i>	South Africa	KX833520	KX833345	KX833433	KX833613	Alvarez et al. 2016
<i>Coniella diplodiopsis</i>	CBS 109.23 = CPC 3933	<i>Vitis vinifera</i>	Switzerland	NA	AY339287	KX833440	KX833624	Van Nierkerk et al. 2004; Alvarez et al. 2016
	CBS 590.84* = CPC 3940	<i>Vitis vinifera</i>	Italy	AY339334	AY339288	NA	NA	Van Nierkerk et al. 2004
	CBS 116310 = CPC 3793	<i>Vitis vinifera</i>	Italy	KX833532	KX833357	KX833443	KX833627	Alvarez et al. 2016
<i>Coniella dongshanlingensis</i>	CGMCC3.27785* = SAUCC 7265-5	<i>Lygodium circinnatum</i>	China	PQ357090	PQ357130	PQ361026	PQ404800	This study
	SAUCC 7265-6	<i>Lygodium circinnatum</i>	China	PQ357091	PQ357131	PQ361027	PQ404801	This study
<i>Coniella duckerae</i>	CBS 142045* = VPRI 13689	<i>Lepidospermum concavum</i>	Australia	KY924929	NA	NA	NA	Marin-Felix et al. 2017
<i>Coniella erumpens</i>	CBS 523.78*	Rotten wood	Chile	KX833535	KX833361	KX833446	KX833630	Alvarez et al. 2016
<i>Coniella eucalyptigena</i>	CBS 139893* = CPC 24793	<i>Eucalyptus brassiana</i>	Malaysia	KR476725	KR476760	NA	NA	Crous et al. 2015a
<i>Coniella eucalyptorum</i>	CBS 112640* = CPC 3904 = DFR 100185	<i>Eucalyptus grandis</i> × <i>E. tereticornis</i>	Australia	AY339338	AY339290	KX833452	KX833637	Van Nierkerk et al. 2004; Alvarez et al. 2016
	CBS 114852	<i>Eucalyptus</i> sp.	Australia	KX833556	KX833380	KX833464	KX833652	Alvarez et al. 2016



Species	Strain numbers	Host/Substrate	Region	GenBank accession numbers				References
				ITS	LSU	<i>rpb2</i>	<i>tef1-a</i>	
<i>Coniella fici</i>	MFLU 18-2578*	<i>Ficus septica</i>	China	MW114356	MW114417	NA	NA	Tennakoon et al. 2021
<i>Coniella fragariae</i>	CBS 172.49* = CPC 3930	<i>Fragaria</i> sp.	Belgium	AY339317	AY339282	KX833472	KX833663	Van Niekerc et al. 2004; Alvarez et al. 2016
	CBS 454.68	<i>Malus sylvestris</i>	Denmark	KX833571	KX833393	KX833477	KX833670	Alvarez et al. 2016
<i>Coniella fujianensis</i>	CGMCC3.25353	<i>Canarium album</i>	China	OR623057	OR623054	OR637413	OR637415	Mu et al. 2024
	CGMCC3.25354*	<i>Canarium album</i>	China	OR623058	OR623055	OR637414	OR637416	Mu et al. 2024
<i>Coniella fusiformis</i>	CBS 141596* = CPC 19722	<i>Eucalyptus</i> sp.	Indonesia	KX833576	KX833397	KX833481	KX833674	Alvarez et al. 2016
	CBS 114850	<i>Eucalyptus pellita</i>	Australia	KX833574	KX833395	KX833479	KX833672	Alvarez et al. 2016
<i>Coniella granati</i>	CBS 132860	<i>Punica granatum</i>	Turkey	KX833577	KX833400	KX833484	KX833677	Alvarez et al. 2016
	CBS 252.38 = ATCC 12685 = CPC 3714	<i>Vitis vinifera</i>	Italy	KX833581	AY339291	KX833488	KX833681	Van Niekerc et al. 2004; Alvarez et al. 2016
<i>Coniella grossedentatae</i>	SAUCC 1354-1	<i>Ampelopsis grossedentata</i>	China	PQ357062	PQ357102	PQ361000	PQ404774	This study
	CGMCC3.27783* = SAUCC 1354-3	<i>Ampelopsis grossedentata</i>	China	PQ357063	PQ357103	PQ361001	PQ404775	This study
<i>Coniella heterospora</i>	CBS 143031* = FMR 15231	Herbivorous dung	Spain	LT800501	LT800500	LT800502	LT800503	Crous et al. 2017
<i>Coniella hibisci</i>	CBS 109757* = AR 3534	<i>Hibiscus</i> sp.	Africa	KX833589	AF408337	NA	KX833689	Castlebury et al. 2002; Marin-Felix et al. 2017
<i>Coniella javanica</i>	CBS 455.68*	<i>Hibiscus sabdariffai</i>	Indonesia	KX833583	KX833403	KX833489	KX833683	Alvarez et al. 2016
<i>Coniella koreana</i>	CBS 143.97*	NA	South Korea	KX833584	AF408378	KX833490	KX833684	Alvarez et al. 2016
<i>Coniella lanneae</i>	CBS 141597* = CPC 22200	<i>Lannea</i> sp.	Zambia	KX833585	KX833404	KX833491	KX833685	Alvarez et al. 2016
<i>Coniella limoniformis</i>	CBS 111021* = PPRI 3870 = CPC 3828	<i>Fragaria</i> sp.	South Africa	KX833586	KX833405	KX833492	KX833686	Alvarez et al. 2016
<i>Coniella lustricola</i>	DAOMC 251731*	NA	America	MF631778	MF631799	MF651900	MF651899	Raudabaugh et al. 2018
	DAOMC 251732	NA	America	MF631779	MF631800	NA	NA	Raudabaugh et al. 2018
	DAOMC 251733	NA	America	MF631780	MF631801	NA	NA	Raudabaugh et al. 2018
	DAOMC 251734	NA	America	MF631781	MF631802	NA	NA	Raudabaugh et al. 2018
<i>Coniella macrospora</i>	CBS 524.73* = CPC 3935	<i>Terminalia ivoriensis</i> stem	Ivory Coast	KX833587	AY339292	KX833493	KX833687	Alvarez et al. 2016
<i>Coniella malaysiana</i>	CBS 141598* = CPC 16659	<i>Corymbia torelliana</i>	Malaysia	KX833588	KX833406	KX833494	KX833688	Alvarez et al. 2016
<i>Coniella nicotianae</i>	CBS 875.72* = PD 72/793	<i>Nicotiana tabacum</i>	Jamaica	KX833590	KX833407	KX833495	KX833690	Alvarez et al. 2016
<i>Coniella nigra</i>	CBS 165.60* = IMI 181519 = IMI 181599 = CPC 4198	Soil	India	AY339319	KX833408	KX833496	KX833691	Van Niekerc et al. 2004; Alvarez et al. 2016
<i>Coniella obovata</i>	CBS 111025 = CPC 4196 = IMI 261318	Leaves	South Africa	AY339313	KX833409	KX833497	KX833692	Van Niekerc et al. 2004; Alvarez et al. 2016
<i>Coniella paracastaneicola</i>	CBS 141292* = CPC 20146	<i>Eucalyptus</i> sp.	Australia	KX833591	KX833410	KX833498	KX833693	Alvarez et al. 2016
<i>Coniella peruensis</i>	CBS 110394* = RMF 74.01	Soil of rain forest	Peru	KJ710463	KJ710441	KX833499	KX833695	Crous et al. 2015b; Alvarez et al. 2016
<i>Coniella pseudodiospyri</i>	CBS 145540* = CPC 35725	<i>Eucalyptus microcorys</i>	Australia	MK876381	MK876422	MK876479	MK876493	Crous et al. 2019
<i>Coniella pseudogranati</i>	CBS 137980* = CPC 22545	<i>Terminalia stuhlmannii</i>	Zambia	KJ869132	KJ869189	NA	NA	Crous et al. 2014b

Species	Strain numbers	Host/Substrate	Region	GenBank accession numbers				References
				ITS	LSU	<i>rpb2</i>	<i>tef1-a</i>	
<i>Coniella pseudokoreana</i>	MFLU 13-0282* = MFLUCC 12-0427	Leaves	Thailand	MF190145	NA	NA	NA	Senanayake et al. 2017
<i>Coniella pseudostraminea</i>	CBS 112624* = IMI 233050	<i>Fragaria</i> sp.	South Africa	KX833593	KX833412	KX833500	KX833696	Alvarez et al. 2016
<i>Coniella quercicola</i>	CBS 283.76	Excrements of <i>Glomerus</i> , which had eaten forest soil	The Netherlands	KX833594	KX833413	KX833501	KX833697	Alvarez et al. 2016
	CBS 904.69*	<i>Quercus robur</i>	The Netherlands	KX833595	KX833414	KX833502	KX833698	Alvarez et al. 2016
<i>Coniella solicola</i>	CBS 766.71*	Soil	South Africa	KX833597	KX833416	KX833505	KX833701	Alvarez et al. 2016
<i>Coniella straminea</i>	CBS 149.22 = CPC 3932	<i>Fragaria</i> sp.	USA	AY339348	AY339296	KX833506	KX833704	Van Niekerk et al. 2004; Alvarez et al. 2016
<i>Coniella tibouchinae</i>	CBS 131594* = CPC 18511	<i>Tibouchina granulosa</i>	Brazil	JQ281774	KX833418	KX833507	JQ281778	Miranda et al. 2012; Alvarez et al. 2016
<b><i>Coniella veri</i></b>	<b>CGMCC3.27787* = SAUCC 8877-4</b>	<b><i>Cinnamomum verum</i></b>	<b>China</b>	<b>PQ357098</b>	<b>PQ357138</b>	<b>PQ361034</b>	<b>PQ404810</b>	<b>This study</b>
	<b>SAUCC 8877-7</b>	<b><i>Cinnamomum verum</i></b>	<b>China</b>	<b>PQ357099</b>	<b>PQ357139</b>	<b>PQ361035</b>	<b>PQ404811</b>	<b>This study</b>
<i>Coniella vitis</i>	MFLUCC 16-1399* = JZB3700001	<i>Vitis vinifera</i>	China	KX890008	KX890083	NA	KX890058	Chethana et al. 2017
<i>Coniella wangiensis</i>	CBS 132530* = CPC 19397	<i>Eucalyptus</i> sp.	Australia	JX069873	JX069857	KX833509	KX833705	Crous et al. 2012; Alvarez et al. 2016
<i>Dwiroopa lythri</i>	CBS 109755* = AR 3383	<i>Lythrum salicaria</i>	USA	MN172410	MN172389	MN271801	MN271859	Jiang et al. 2020

**Notes:** New species established in this study are shown in bold. Those marked “\*” in the table are represented as ex-type or ex-epitype strains. NA: Not available.

## Sequence alignment and phylogenetic analyses

The nucleotide sequences of four new species were submitted to the NCBI's GenBank nucleotide database (<https://www.ncbi.nlm.nih.gov/>, accessed on 2 Jan. 2025), and all related species were retrieved for phylogenetic analysis. Multiple sequences were aligned using MAFFT version 7 (<http://mafft.cbrc.jp/alignment/server/index.html>, accessed on 2 Jan. 2025) with default settings, and manual correction was applied if necessary (Kato et al. 2019). For phylogenetic analyses, single and concatenated sequences were subjected to analysis by Maximum Likelihood (ML) and Bayesian Inference (BI) algorithms, respectively. Both ML and BI were executed on the CIPRES Science Gateway portal (<https://www.phylo.org/>, accessed on 2 Jan. 2025) or offline software (ML was executed in RaxML-HPC2 on XSEDE v8.2.12 and BI analysis was executed in MrBayes v3.2.7a with 64 threads on Linux) (Miller et al. 2012; Ronquist et al. 2012; Stamatakis 2014). For the ML analysis, the default parameters were used, and 1,000 rapid bootstrap replicates were run with the GTR+G+I model of nucleotide evolution; for BI, it was performed using a rapid bootstrapping algorithm with an automatic stop option and utilized MrModeltest v.2.3 to determine the best evolutionary model for each partition (Nylander 2004; Zhang et al. 2024a). Bayesian Inference posterior probabilities (BIPP) were evaluated by Markov Chain Monte Carlo (MCMC) (Rannala and Yang 1996; Zhaxybayeva and Gogarten 2002). The BI analyses encompassed two parallel runs spanning 5,000,000 generations, with a stop rule incorporated and a sampling frequency of 50 generations. The burn-in fraction was set at 0.25, and posterior probabilities were calculated

from the remaining trees. The resulting trees were generated using FigTree v. 1.4.4 (<http://tree.bio.ed.ac.uk/software/figtree>, accessed on 2 Jan. 2025) or ITOL: Interactive Tree of Life (<https://itol.embl.de/>, accessed on 2 Jan. 2025) (Letunic and Bork 2021), and the final layout of the trees was refined in Adobe Illustrator CC 2019. The names of the isolates in this study are marked in red in the phylogenetic tree.

## Results

### Molecular phylogeny

Initially, based on the ITS sequence data, we preliminarily determined that the eight strains belong to *Coniella*. Subsequently, based on ML and BI methods, we conducted a combined analysis of ITS, LSU, *rpb2*, and *tef1-a* gene data to construct phylogenetic trees for further determination of the phylogenetic position of these strains. The phylogenetic analysis of *Coniella* strains included 63 sequences, with *Dwiroopa lythri* (CBS 109755) serving as the outgroup. The final alignment comprised 2800 concatenated characters, viz. 1–600 (ITS), 601–1380 (LSU), 1381–2140 (*rpb2*), and 2141–2800 (*tef1-a*). The ML optimization likelihood was calculated to be -23461.791405. The matrix exhibited 1116 distinct alignment patterns, with 18.42% of characters or gaps remaining undetermined. The optimal models, evaluated by MrModeltest and selected in the BI, are as follows: the SYM+I+G model for ITS and the GTR+I+G model for LSU, *rpb2*, and *tef1-a*. The alignment exhibited a total of 1121 unique site patterns (ITS: 211, LSU: 78, *rpb2*: 322, *tef1-a*: 510). The topology of the ML tree concurred with that derived from BI; thus, only the ML tree is presented (Fig. 1). Combining morphological characteristics and molecular phylogenetic analyses, the eight strains in this study were introduced as four new species, namely *Coniella diaoluoshanensis*, *C. dongshanlingensis*, *C. grossedentatae*, and *C. veri*.

### Taxonomy

***Coniella diaoluoshanensis* D.H. Li, J.W. Xia & X.G. Zhang, sp. nov.**

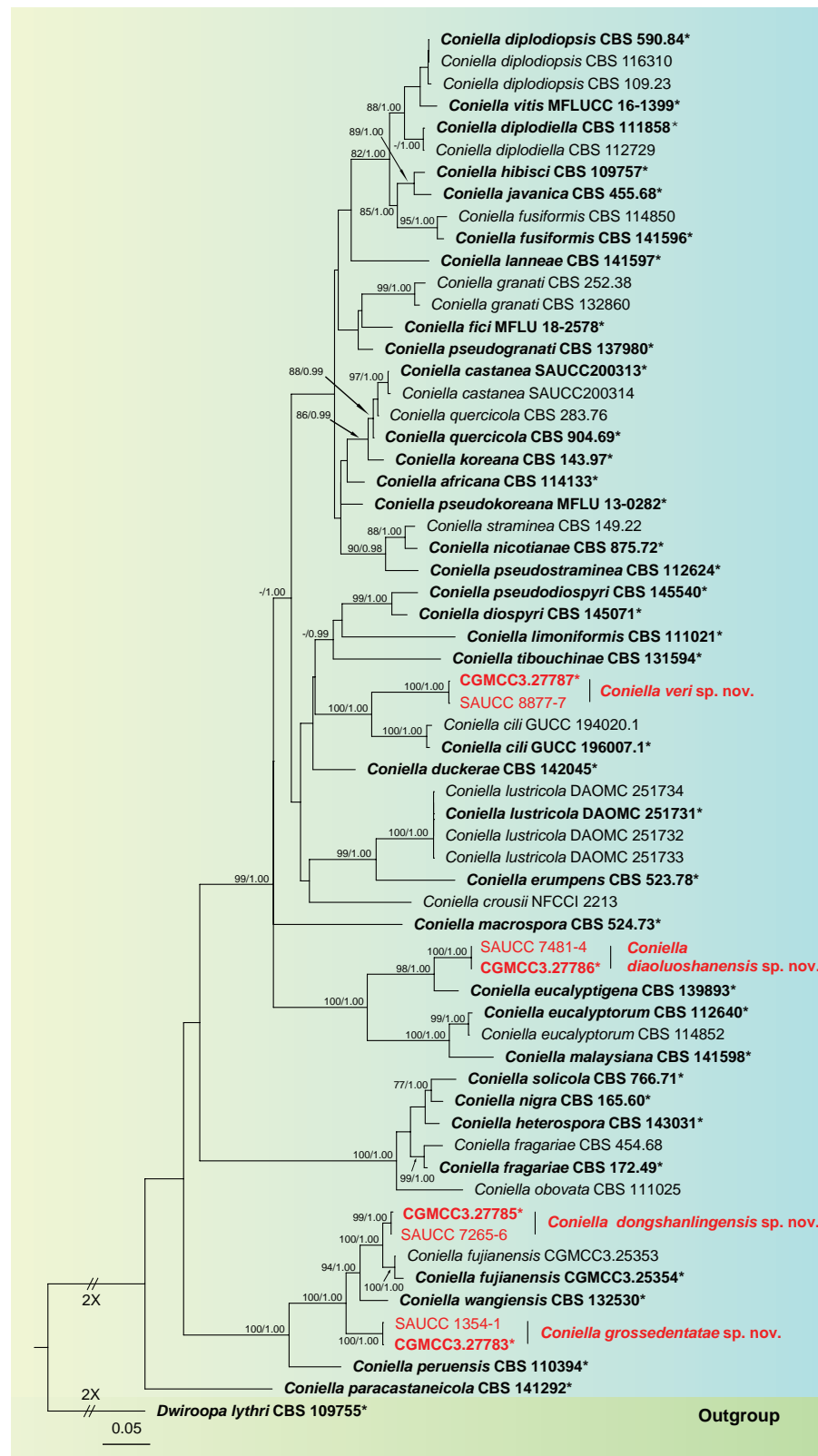
MycoBank No: 856520

Fig. 2

**Holotype.** CHINA • Hainan Province: Diaoluoshan National Forest Park, on diseased leaves of *Kadsura longipedunculata* (Schisandraceae), 18.660546°N, 109.936445°E, 94.1 m asl., 27 Mar. 2024, D.H. Li, holotype HSAUP 7481-1, ex-type living culture SAUCC 7481-1 = CGMCC3.27786.

**Etymology.** Named after the collection site of the type specimen, Diaoluoshan National Forest Park.

**Description.** *Hypha* immersed, 1.9–6.5 µm wide, branched, multi-septate, enlarged towards septum and terminal, hyaline. Asexual morph: ***Conidiomata*** nearly spherical, separate, scarce, immersed or superficial, surface uneven, sizes inconsistent, black. ***Conidiophores*** cylindrical, aseptate, straight or slightly curved, densely aggregated, simple, smooth, usually reduced to conidiogenous cells. ***Conidiogenous cells*** phialidic, simple, aggregative, hyaline, smooth, 8.1–11 × 1.4–2.6 µm (mean ± SD = 9.6 ± 0.8 × 2.1 ± 0.4 µm, n = 30), with apical periclinal



**Figure 1.** Phylogenetic relationship of *Coniella* based on concatenated sequences of ITS, LSU, *rpb2*, and *tef1-a* sequence data with *Dwiroopa lythri* (CBS 109755) as the outgroup. The Maximum Likelihood Bootstrap Value (left, MLBV  $\geq 75\%$ ) and the Bayesian Inference Posterior Probability (right, BIPP  $\geq 0.90$ ) are shown as MLBV/BIPP above the nodes. The ex-type strains are marked with “\*” and indicated in boldface. Strains from this study are shown in red. The scale bar at the bottom left represents 0.05 substitutions per site. Some branches are shortened according to the indicated multipliers to fit the page size, and these are indicated by the symbol (//).

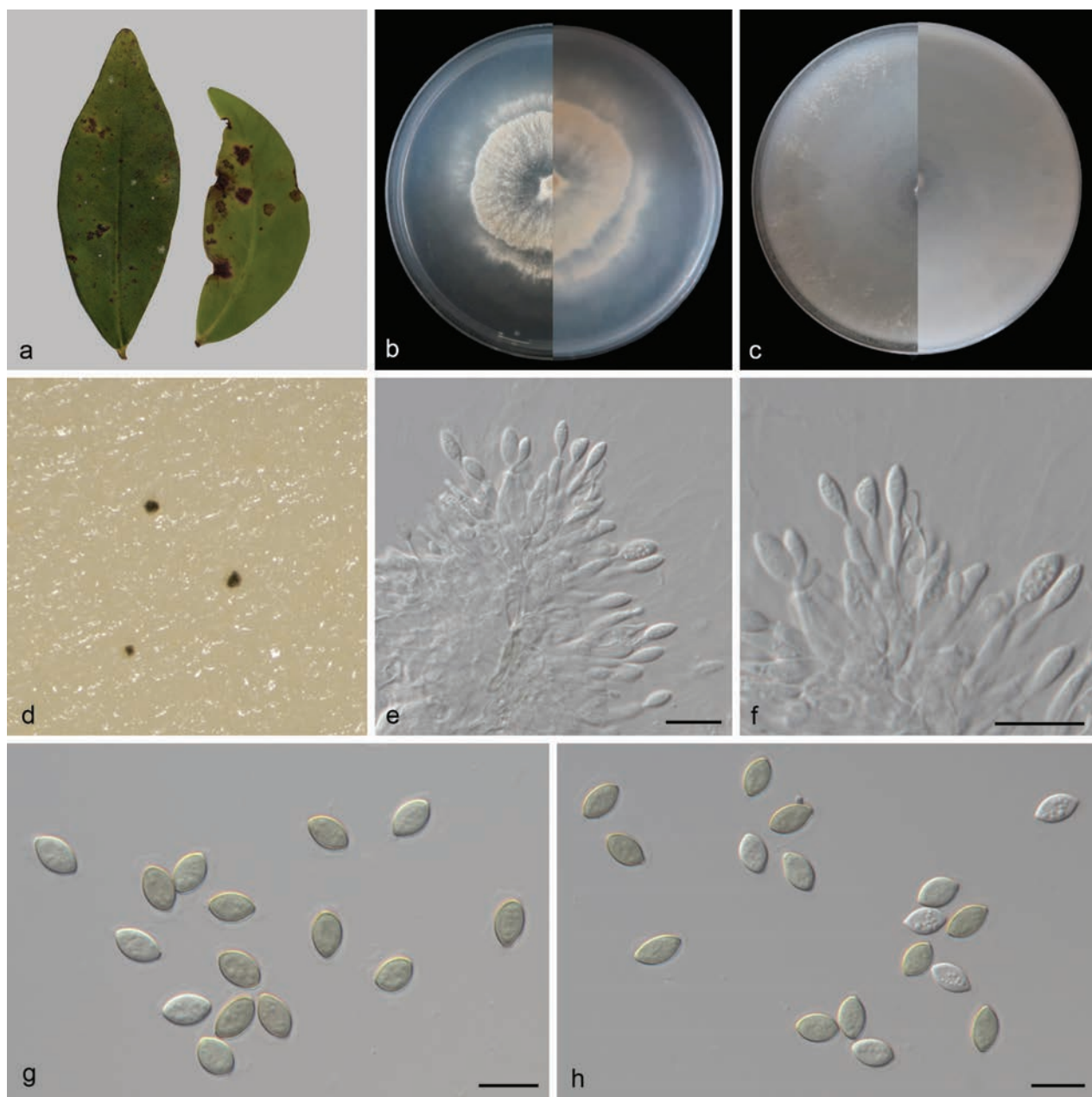


**Figure 2.** *Coniella diaoluoshanensis* (CGMCC3.27786) **a** leaves of *Kadsura longipedunculata* **b, c** surface and reverse sides of colony after 14 days on PDA **(b)** and OA **(c)** **d** conidiomata forming on OA **e, f** conidiophores and conidiogenous cells with developing conidia **g, h** conidia. Scale bars: 10  $\mu$ m **(e–h)**.

thickening, blastospore at the apex. **Conidia** elliptical or fusiform, apices tapering, subobtuse, apically rounded, widest at the middle, bases tapering to a truncate hilum, multi-guttulate, immature conidia hyaline, mature conidia pale olivaceous, wall darker than pale olivaceous body of conidium, smooth,  $7.5\text{--}9.3 \times 4.7\text{--}5.5 \mu\text{m}$  (mean  $\pm$  SD =  $8.4 \pm 0.5 \times 5.1 \pm 0.3 \mu\text{m}$ ,  $n = 30$ ). Sexual morph unknown.

**Culture characteristics.** Colonies on PDA after 14 days of cultivation in the dark at 25 °C, reaching 75–77 mm in diam., with a growth rate of 5.4–5.5 mm/day; from above: white to cream-colored with age, sparse aerial mycelium at the center, irregularly circular, slightly low; peripheral mycelium dense, concentric rings, flat; colony edge irregular, sparse aerial mycelium, dispersed, striped; reverse: similar in color. Colonies on OA covering entire plate after 14 days of cultivation in



the dark at 25 °C; from above: white, devoid of aerial mycelium at the center, with dispersed and sparse aerial mycelium at the edges; reverse: even white texture.

**Additional material studied.** CHINA • Hainan Province: Diaoluoshan National Forest Park, on diseased leaves of *Kadsura longipedunculata* (Schisandraceae), 18.660546°N, 109.936445°E, 94.1 m asl., 27 Mar. 2024, D.H. Li, HSAUP 7481-4, living culture SAUCC 7481-4.

**Notes.** Phylogenetic analyses showed that *Coniella diaoluoshanensis* formed an independent clade (Fig. 1) and was closely related to *C. eucalyptigena* (CBS 139893), *C. eucalyptorum* (CBS 112640 and CBS 114852), and *C. malaysiana* (CBS 141598). *Coniella diaoluoshanensis* was distinguished from *C. eucalyptigena* by 4/573 and 7/791 base-pair differences in ITS and LSU sequences, from *C. eucalyptorum* (CBS 112640) by 19/565, 7/793, 68/765, and 164/539 base-pair differences in ITS, LSU, *rpb2*, and *tef1-α* sequences, and from *C. malaysiana* by 16/553, 7/783, 67/767, and 154/488 base-pair differences in ITS, LSU, *rpb2*, and *tef1-α* sequences, respectively. Morphologically, *C. eucalyptigena* lacks asexual sporulation description, making it impossible to compare microscopic structures with *C. diaoluoshanensis*. However, their macroscopic colony colors differ greatly: on PDA, *C. diaoluoshanensis* is cream-colored while *C. eucalyptigena* is salmon; on OA, *C. diaoluoshanensis* is white on the surface, whereas *C. eucalyptigena* is rosy buff. Morphologically, since *C. eucalyptigena* only had a description of sexual morphology, it could not be directly compared with the asexual morphology in this study. Then, *C. eucalyptorum* and *C. malaysiana*, which were closely related on the evolutionary tree, were selected for comparison. The conidiogenous cells of *C. diaoluoshanensis* (8.1–11 × 1.4–2.6 μm) shorter than those of *C. eucalyptorum* (10–17 × 3–3.5 μm) and *C. malaysiana* (8.5–18 × 1.5–3.5 μm); the conidia of *C. diaoluoshanensis* (7.5–9.3 × 4.7–5.5 μm) shorter than those of *C. eucalyptorum* (9–14 × 6–8 μm) and *C. malaysiana* (8–11.5 × 3–5 μm); and the mature conidial color of *C. diaoluoshanensis* (pale olivaceous) was lighter than that of *C. eucalyptorum* (medium to dark red-brown) and *C. malaysiana* (pale brown) (Van Niekerk et al. 2004; Crous et al. 2015a; Alvarez et al. 2016; Zhang et al. 2024b). Therefore, we describe our collection as a novel species.

***Coniella dongshanlingensis* D.H. Li, J.W. Xia & X.G. Zhang, sp. nov.**

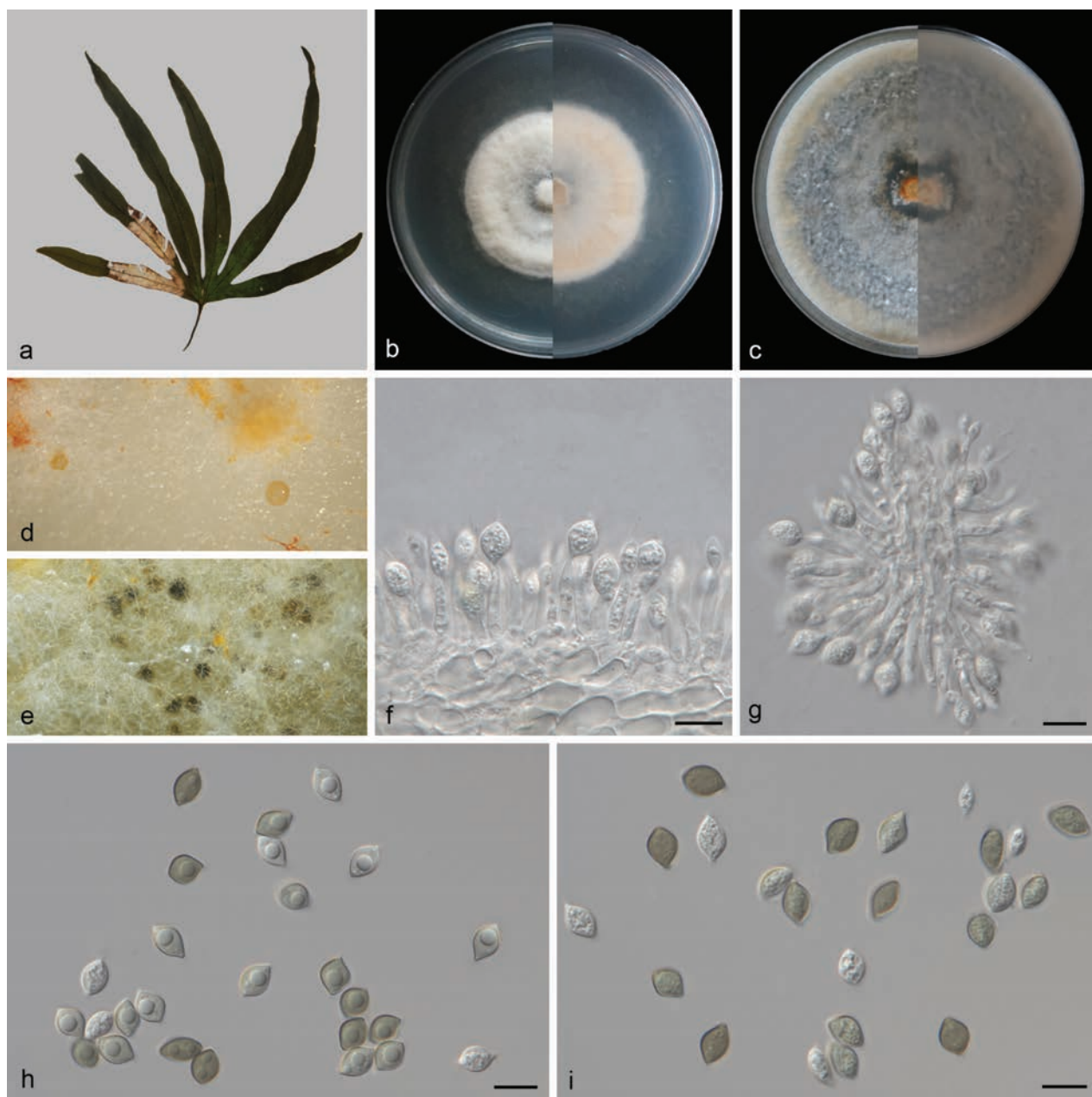
MycoBank No: 856519

Fig. 3

**Holotype.** CHINA • Hainan Province: Dongshanling Scenic Area, on diseased leaves of *Lygodium circinnatum* (Lygodiaceae), 18.802153°N, 110.421473°E, 18.8 m asl., 26 Mar. 2024, D.H. Li, holotype HSAUP 7265-5, ex-type living culture SAUCC 7265-5 = CGMCC3.27785.

**Etymology.** Named after the collection site of the type specimen, Dongshanling Scenic Area.

**Description.** *Hypha* superficial, 1.1–3.2 μm wide, less branched, multi-septate, hyaline to pale yellow. Asexual morph: **Conidiomata** pycnidial to nearly spherical, separate, superficial, surface enveloped in a gelatinous sheath, sizes inconsistent, initially appearing hyaline, becoming black with mature. **Conidiophores** cylindrical, aseptate, straight or slightly curved, densely aggregated, simple, smooth, usually reduced to conidiogenous cells. **Conidiogenous cells** phialidic,



**Figure 3.** *Coniella dongshanlingensis* (CGMCC3.27785) **a** a leaf of *Lygodium circinnatum* **b, c** surface and reverse sides of colony after 14 days on PDA (**b**) and OA (**c**) **d, e** conidiomata forming on PDA **f, g** conidiophores and conidiogenous cells with developing conidia **h, i** conidia. Scale bars: 10 µm (**f–i**).

simple, aggregative, hyaline, smooth,  $7.3\text{--}19.2 \times 1.5\text{--}3.3$  µm (mean  $\pm$  SD =  $12.6 \pm 2.6 \times 2.4 \pm 0.5$  µm,  $n = 30$ ), with apical periclinal thickening, blastospore at the apex. **Conidia** elliptical to fusiform, apices tapering, subobtuse, apically rounded, bases tapering to a truncate hilum, immature conidia hyaline, multi-guttulate, mature conidia olivaceous, 1–2 guttulate, wall darker than olivaceous body of conidium, smooth,  $7.8\text{--}10 \times 5.1\text{--}7$  µm (mean  $\pm$  SD =  $8.7 \pm 0.6 \times 6.2 \pm 0.4$  µm,  $n = 30$ ). Sexual morph unknown.

**Culture characteristics.** Colonies on PDA after 14 days of cultivation in the dark at 25 °C, reaching 47–50 mm in diam., with a growth rate of 3.4–3.6 mm/day; from above: white to pale orange with age, medium aerial mycelium, circular, slightly low at the center, slightly higher at the edges; reverse: similar in color.

Colonies on OA covering entire plate after 14 days of cultivation in the dark at 25 °C; from above: pale orange, interspersed with extensive black pycnidia, medium aerial mycelium, flat; reverse: similar in color.

**Additional material studied.** CHINA • Hainan Province: Dongshanling Scenic Area, on diseased leaves of *Lygodium circinnatum* (Lygodiaceae), 18.802153°N, 110.421473°E, 18.8 m asl., 26 Mar. 2024, D.H. Li, HSAUP 7265-6, living culture SAUCC 7265-6.

**Notes.** Phylogenetic analyses showed that *Coniella dongshanlingensis* formed an independent clade (Fig. 1) and was closely related to *C. fujianensis* (CGMCC3.25353 and CGMCC3.25354). *Coniella dongshanlingensis* was distinguished from *C. fujianensis* (CGMCC3.25354) by 5/589, 9/657, and 19/306 base-pair differences in ITS, *rpb2*, and *tef1-α* sequences, respectively. Morphologically, the conidiogenous cells of *C. dongshanlingensis* (7.3–19.2 × 1.5–3.3 μm) are longer than those of *C. fujianensis* (3.5–8 × 2.5–3.5 μm); the conidia of *C. dongshanlingensis* (7.8–10 × 5.1–7 μm) slightly shorter than those of *C. fujianensis* (8–10.5 × 5.5–7.5 μm), and the mature conidial color of *C. dongshanlingensis* (olivaceous) is lighter than that of *C. fujianensis* (brown) (Mu et al. 2024). Therefore, we describe our collection as a novel species.

***Coniella grossedentatae* D.H. Li, J.W. Xia & X.G. Zhang, sp. nov.**

MycoBank No: 856518

Fig. 4

**Holotype.** CHINA • Fujian Province: Wuyishan City, Xingcun Town, on diseased leaves of *Ampelopsis grossedentata* (Vitaceae), 27.749556°N, 117.679038°E, 751.68 m asl., 15 Oct. 2022, D.H. Li, holotype HSAUP 1354-3, ex-type living culture SAUCC 1354-3 = CGMCC3.27783.

**Etymology.** Named after the species epithet of the host plant, *Ampelopsis grossedentata*.

**Description.** *Hypa* superficial, 1.3–3.5 μm wide, branched, multi-septate, hyaline to pale orange. Asexual morph: **Conidiomata** spherical or narrowly ellipsoid, separate, immersed or superficial, some surfaces enveloped in a gelatinous sheath, some surface uneven, sizes inconsistent, black. **Conidiophores** cylindrical, aseptate, straight or slightly curved, densely aggregated, simple, usually reduced to conidiogenous cells. **Conidiogenous cells** phialidic, simple, aggregative, hyaline, smooth, 10.6–23.1 × 1.7–3.8 μm (mean ± SD = 16.8 ± 3 × 2.5 ± 0.6 μm, n = 30), with apical periclinal thickening, blastospore at the apex. **Conidia** nearly spherical, apices acute, widest at the middle, bases tapering to a truncate hilum, multi-guttulate, immature conidia hyaline, mature conidia medium brown, wall darker than medium brown body of conidium, smooth, 8–10.5 × 7.5–9.5 μm (mean ± SD = 9.4 ± 0.6 × 8.4 ± 0.5 μm, n = 30). Sexual morph unknown.

**Culture characteristics.** Colonies on PDA after 14 days of cultivation in the dark at 25 °C, reaching 86–90 mm in diam., with a growth rate of 6.1–6.4 mm/day; from above: orange in the middle and edges, with white in between, medium aerial mycelium, granular, circular, flat; reverse: similar in color. Colonies on OA covering entire plate after 14 days of cultivation in the dark at 25 °C; from above: white in the middle and edges, with orange in between, sparse aerial mycelium, flat; reverse: similar in color.



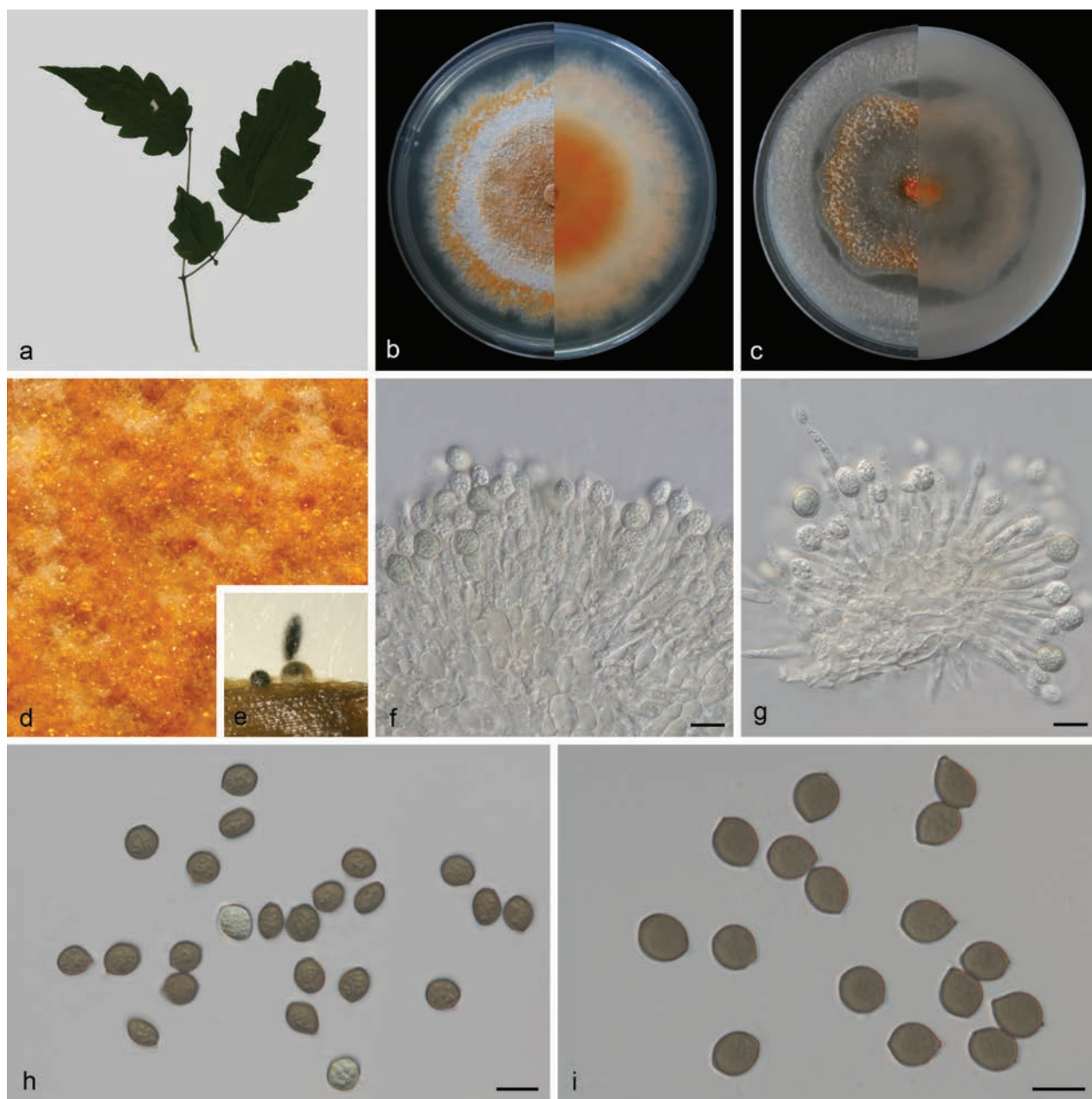


**Figure 4.** *Coniella grossedentatae* (CGMCC3.27783) **a** leaves of *Ampelopsis grossedentata* **b, c** surface and reverse sides of colony after 14 days on PDA **(b)** and OA **(c)** **d** colony on PDA **e** conidiomata forming on pine needle **f, g** conidiophores and conidiogenous cells with developing conidia **h, i** conidia. Scale bars: 10 µm **(f–i)**.

**Additional material studied.** CHINA • Fujian Province: Wuyishan City, Xingcun Town, on diseased leaves of *Ampelopsis grossedentata* (Vitaceae), 27.749556°N, 117.679038°E, 751.68 m asl., 15 Oct. 2022, D.H. Li, HSAUP 1354-1, living culture SAUCC 1354-1.

**Notes.** Phylogenetic analyses showed that *Coniella grossedentatae* formed an independent clade (Fig. 1) basal to *C. dongshanlingensis* (CGMCC3.27785, SAUCC 7265-6), *C. fujianensis* (CGMCC 3.25353, CGMCC 3.25354), and *C. wangiensis* (CBS 132530). *Coniella grossedentatae* can be distinguished from *C. dongshanlingensis* by 4/604, 1/793, 52/902, and 80/532 base-pair differences in ITS, LSU, *rpb2*, and *tef1-α* sequences, and from *C. fujianensis* by 8/588, 1/798, 34/657, and 64/313 base-pair differences in ITS, LSU, *rpb2*, and *tef1-α*.

sequences, and from *C. wangiensis* by 2/603, 5/798, 35/767, and 79/329 base-pair differences in ITS, LSU, *rpb2*, and *tef1-α* sequences, respectively. Morphologically, the conidiogenous cells of *C. grossedentatae* ( $10.6\text{--}23.1 \times 1.7\text{--}3.8\ \mu\text{m}$ ) are longer than those of *C. dongshanlingensis* ( $7.3\text{--}19.2 \times 1.5\text{--}3.3\ \mu\text{m}$ ), *C. fujianensis* ( $3.5\text{--}8 \times 2.5\text{--}3.5\ \mu\text{m}$ ), and *C. wangiensis* ( $15\text{--}20 \times 3\text{--}4\ \mu\text{m}$ ); the conidia of *C. grossedentatae* ( $8\text{--}10.5 \times 7.5\text{--}9.5\ \mu\text{m}$ ) are wider than those of *C. dongshanlingensis* ( $7.8\text{--}10 \times 5.1\text{--}7\ \mu\text{m}$ ) and *C. fujianensis* ( $8\text{--}10.5 \times 5.5\text{--}7.5\ \mu\text{m}$ ), and shorter than those of *C. wangiensis* ( $9\text{--}13 \times 7\text{--}10\ \mu\text{m}$ ) (Crous et al. 2012; Alvarez et al. 2016). Therefore, we describe our collection as a novel species.

***Coniella veri* D.H. Li, J.W. Xia & X.G. Zhang, sp. nov.**

MycoBank No: 856521

Fig. 5

**Holotype.** CHINA • Yunnan Province: Pu'er City, Yixiang Town, Pu'er Sun River Forest Park, on diseased leaves of *Cinnamomum verum* (Lauraceae), 22.593953°N, 101.086217°E, 1596.44 m asl., 15 May 2024, D.H. Li, holotype HSAUP 8877-4, ex-type living culture SAUCC 8877-4 = CGMCC3.27787.

**Etymology.** Named after the species epithet of the host plant, *Cinnamomum verum*.

**Description.** **Hypha** superficial,  $1.3\text{--}3.3\ \mu\text{m}$  wide, branched, multi-septate, hyaline. Asexual morph: **Conidiomata** spherical, aggregated or solitary, immersed or superficial, some surfaces enveloped in a gelatinous sheath, some surface uneven, sizes inconsistent, initially appearing hyaline, becoming black with mature. **Conidiophores** cylindrical, septate, branched, straight or slightly curved, densely aggregated, simple, usually reduced to conidiogenous cells. **Conidiogenous cells** phialidic, simple, aggregative, or solitary, hyaline, smooth,  $9.5\text{--}17.5 \times 1.2\text{--}2.5\ \mu\text{m}$  (mean  $\pm$  SD =  $12.5 \pm 1.5 \times 1.8 \pm 0.4\ \mu\text{m}$ ,  $n = 30$ ), with apical periclinal thickening, blastospore at the apex. **Conidia** elliptical to fusiform, apices acute, widest at the middle, bases tapering to a truncate hilum, multi-guttulate gather at both ends, hyaline, thick-walled, smooth,  $6.2\text{--}8.8 \times 3.6\text{--}4.7\ \mu\text{m}$  (mean  $\pm$  SD =  $7.7 \pm 0.6 \times 4 \pm 0.3\ \mu\text{m}$ ,  $n = 30$ ). Sexual morph unknown.

**Culture characteristics.** Colonies on PDA after 14 days of cultivation in the dark at 25 °C, reaching 81–85 mm in diam., with a growth rate of 5.8–6.1 mm/day; from above: white, medium aerial mycelium, slightly higher at the center, circular, radial, flat; reverse: pale orange in the middle, orange in the edges. Colonies on OA after 14 days of cultivation in the dark at 25 °C, reaching 72–77 mm in diam., had a growth rate of 5.1–5.5 mm/day; from above: white, sparse aerial mycelium, black pycnidia formed in the center, flat; reverse: similar in color.

**Additional material studied.** CHINA • Yunnan Province: Pu'er City, Yixiang Town, Pu'er Sun River Forest Park, on diseased leaves of *Cinnamomum verum* (Lauraceae), 22.593953°N, 101.086217°E, 1596.44 m asl., 15 May 2024, D.H. Li, HSAUP 8877-7, living culture SAUCC 8877-7.

**Notes.** Phylogenetic analyses showed that *Coniella veri* formed an independent clade (Fig. 1) and was closely related to *C. cili* (GUCC 194020.1 and GUCC 196007.1). *Coniella veri* can be distinguished from *C. cili* (GUCC 196007.1) by 31/597, 8/791, 52/869, and 125/516 base-pair differences in ITS, LSU, *rpb2*, and *tef1-α* sequences, respectively. Morphologically, the conidiogenous cells



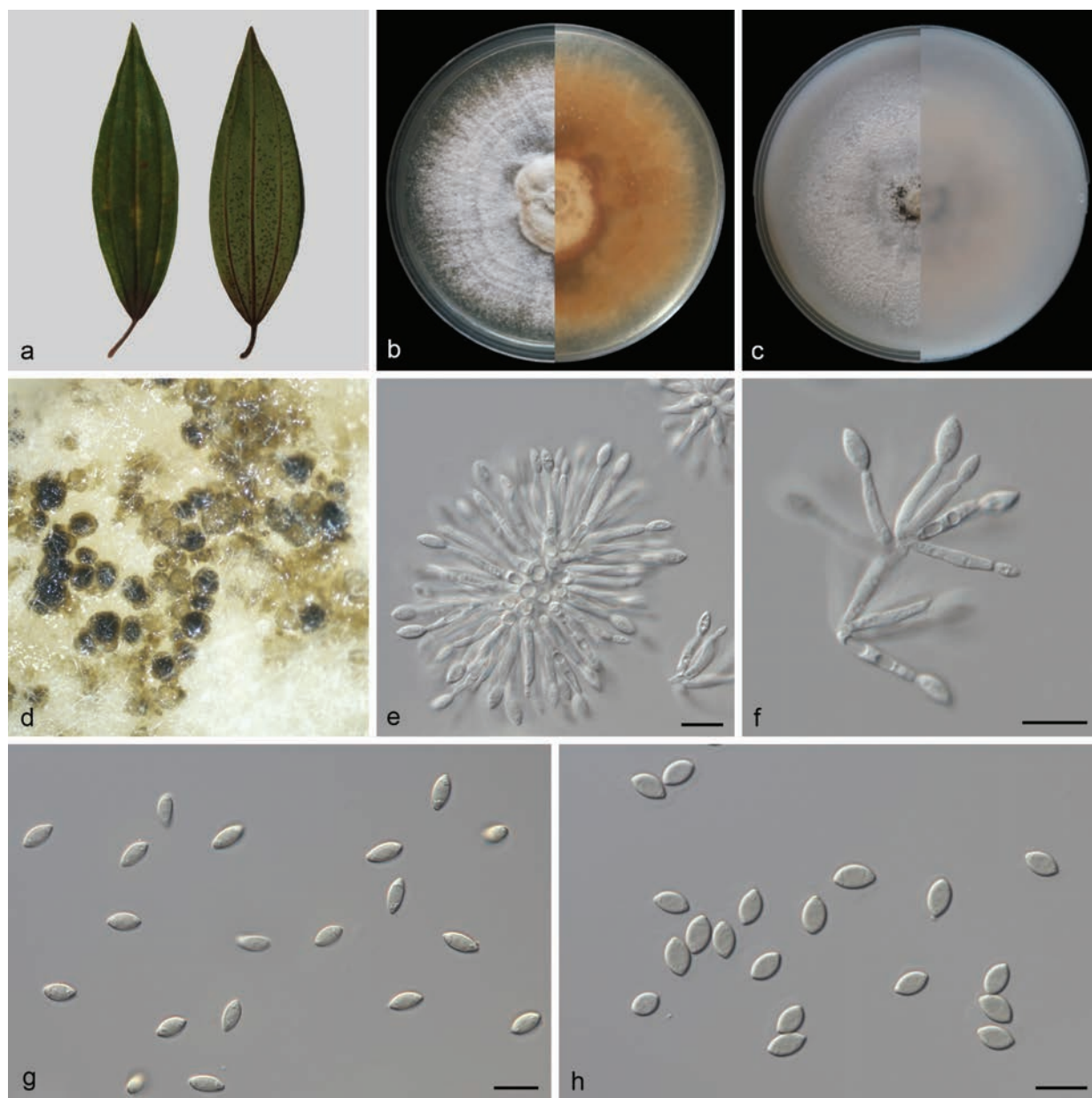


**Figure 5.** *Coniella veri* (CGMCC3.27787) **a** leaves of *Cinnamomum verum* **b, c** surface and reverse sides of colony after 14 days on PDA (**b**) and OA (**c**) **d** conidiomata forming on OA **e, f** conidiophores and conidiogenous cells with developing conidia **g, h** conidia. Scale bars: 10 µm (**e–h**).

of *C. veri* ( $9.5\text{--}17.5 \times 1.2\text{--}2.5 \mu\text{m}$ ) are shorter than those of *C. cili* ( $13\text{--}23.5 \times 1\text{--}2 \mu\text{m}$ ); the conidia of *C. veri* ( $6.2\text{--}8.8 \times 3.6\text{--}4.7 \mu\text{m}$ ) are shorter than those of *C. cili* ( $5.5\text{--}17.5 \times 2.5\text{--}5 \mu\text{m}$ ); the conidial shape of *C. veri* is elliptical to fusiform, whereas the conidial size and shape of *C. cili* exhibit considerable variation, including limoniform, fusoid, clavate, cylindrical, and elongated elliptical forms (Zhang et al. 2024b). Therefore, we describe our collection as a novel species.

## Discussion

*Coniella* species have a worldwide distribution, reported in countries across all continents (Van Niekerk et al. 2004; Alvarez et al. 2016). They have been found in Asia (e.g., China, India, Indonesia, Malaysia, South Korea, and Thailand), Europe (e.g.,

Belgium, Denmark, France, Italy, the Netherlands, Switzerland, and Spain), Africa (e.g., Ivory Coast, South Africa, and Zambia), the Americas (e.g., the United States, Brazil, Peru, Jamaica, and Chile), and Oceania (e.g., Australia). These countries, ranging from landlocked nations such as Zambia and Switzerland to coastal countries like China, Brazil, and Australia, as well as island nations including Jamaica and Indonesia, are geographically diverse. They are distributed on both sides of the equator and span multiple climatic zones, from tropical to frigid, coastal to inland, and plain to mountain, encompassing diverse climate types such as tropical, temperate, and alpine. Many countries, including most of Africa, northern Brazil, Indonesia, and Malaysia, have tropical climates with high temperatures and abundant precipitation year-round. China, with its vast territory, large latitudinal span, wide longitudinal extent, and complex and diverse topography, nearly covers all major climate types, providing favorable conditions for the formation of *Coniella* species diversity (Castlebury et al. 2002; Van Niekerk et al. 2004; Alvarez et al. 2016; Raudabaugh et al. 2018; Wang et al. 2022; Mu et al. 2024; Zhang et al. 2024b).

Currently, *Coniella* has accepted 66 species, many of which were introduced solely based on morphological studies (Index Fungorum: <https://indexfungorum.org>; MycoBank: <http://www.mycobank.org>; Alvarez et al. 2016; Mu et al. 2024). Morphological characteristics of some conidia are highly similar and can be classified into two categories: one comprises olivaceous brown to brown conidia that are ellipsoid or globose, while the other category consists of hyaline conidia that are fusiform or clavate, often with very similar shapes and sizes. Rendering precise identification of *Coniella* species difficult solely on morphological characteristics (Crous et al. 2014a). Consequently, there is a strong current trend towards integrating morphological and molecular methods to assess or clarify the taxonomic placement and phylogenetic relationships of *Coniella* species (Alvarez et al. 2016). Based on phylogenetic analyses of ITS, LSU, and *tef1-α* sequence data, Van Niekerk et al. (2004) demonstrated that *Coniella* represents a distinct evolutionary lineage within the Diaporthales (Van Niekerk et al. 2004). Based on phylogenetic analyses of ITS, LSU, *rpb2*, and *tef1-α* sequence data, Alvarez et al. (2016) conducted a taxonomic revision of the genus. Since then, phylogenetic analyses of *Coniella* have largely continued to use these four genetic loci (Alvarez et al. 2016).

According to previous studies, *Coniella* species have been recorded as plant pathogens, endophytes, and saprobes (Samuels et al. 1993; Ferreira et al. 1997; Alvarez et al. 2016; Chethana et al. 2017). Their hosts encompass multiple categories, including plants (such as trees, shrubs, herbs, and ferns), animal excreta, and soils (Crous et al. 2015b; Alvarez et al. 2016). In recent years, several *Coniella* species have been reported and described in China. For example, Fröhlich and Hyde (2000) discovered *C. calamicola* on both living and dead leaves of *Daemonorops margaritae* in Hong Kong. Chen et al. (2014) first reported that *C. granati* can cause fruit rot and twig blight in pomegranate (*Punica granatum*) in Anhui Province. Chethana et al. (2017) reported that *C. vitis* is the pathogenic fungus causing white rot in grapes (*Vitis vinifera*) in Beijing Municipality, Guangxi, Hebei, Henan, and Jilin Provinces. Tennakoon et al. (2021) isolated a new species, *C. fici*, from dead leaves of *Ficus septica* (Moraceae) on the island of Taiwan. Wang et al. (2022) isolated a new species, *C. castanea*, from symptomatic leaves of *Castanea mollissima* (Fagaceae) in an orchard in Shandong Province. Mu et al. (2024) isolated a new species, *C. fujianensis*, from dis-

eased leaves of *Canarium album* (Burseraceae) in Fujian Province. Zhang et al. (2024b) isolated the endophytic species *C. cili* from healthy fruits and seeds of *Rosa roxburghii* (Rosaceae) in Guizhou Province.

During a continuous survey of terrestrial plant fungi in certain regions of southern China, four new species of *Coniella* were discovered from diseased leaf tissues of infected plants in Fujian, Hainan, and Yunnan provinces. These new species are named *Coniella diaoluoshanensis*, *C. dongshanlingensis*, *C. grossedentatae*, and *C. veri*. Among them, *C. grossedentatae* utilizes *Ampelopsis grossedentata* (Vitaceae) as its host. Van Niekerk et al. (2004) have previously reported species of *C. diplodiopsis* isolated from *Vitis vinifera* (Vitaceae) collected in Italy. In contrast, *C. diaoluoshanensis*, *C. dongshanlingensis*, and *C. veri* are the first reports that are associated with the hosts *Kadsura longipedunculata*, *Lygodium circinnatum*, and *Cinnamomum verum*, respectively. This will further broaden the host range of *Coniella* species and contribute to the fields of plant pathology and fungal taxonomy. With the increasing number of *Coniella* species, we believe that comprehensive research on this genus will uncover more hidden *Coniella* species from terrestrial plants.

## Additional information

### Conflict of interest

The authors have declared that no competing interests exist.

### Ethical statement

No ethical statement was reported.

### Funding

This research was funded by the National Natural Science Foundation of China (nos. 32370001, 32270024, 31900014, U2002203), the Key Technological Innovation Program of Shandong Province, China (no. 2022CXGC020710), the Jinan City's 'New University 20 Policies' Initiative for Innovative Research Teams Project (no. 202228028) and the Innovative Agricultural Application Technology Project of Jinan City (no. CX202210).

### Author contributions

Sampling, molecular biology analysis: Duhua Li and Zixu Dong; fungal isolation: Qiyun Liu and Yaling Wang; description and phylogenetic analysis: Duhua Li and Zhaoxue Zhang; microscopy: Duhua Li and Jiwen Xia; writing-original draft preparation: Duhua Li; writing-review and editing: Xiuguo Zhang and Jiwen Xia. All authors read and approved the final manuscript.

### Author ORCIDs

Duhua Li  <https://orcid.org/0009-0006-5200-2034>

Qiyun Liu  <https://orcid.org/0009-0009-9545-7962>

Zhaoxue Zhang  <https://orcid.org/0000-0002-4824-9716>

Xiuguo Zhang  <https://orcid.org/0000-0001-9733-8494>

Jiwen Xia  <https://orcid.org/0000-0002-7436-7249>

### Data availability

All of the data that support the findings of this study are available in the main text.

## References

- Alvarez LV, Groenewald JZ, Crous PW (2016) Revising the Schizoparmaceae: *Coniella* and its synonyms *Pilidiella* and *Schizoparme*. *Studies in Mycology* 85(1): 1–34. <https://doi.org/10.1016/j.simyco.2016.09.001>
- Carbone I, Kohn LM (1999) A method for designing primer sets for speciation studies in filamentous ascomycetes. *Mycologia* 91(3): 553–556. <https://doi.org/10.1080/00275514.1999.12061051>
- Castlebury LA, Rossman AY, Jaklitsch WJ, Vasilyeva LN (2002) A preliminary overview of the Diaporthales based on large subunit nuclear ribosomal DNA sequences. *Mycologia* 94(6): 1017–1031. <https://doi.org/10.1080/15572536.2003.11833157>
- Chen Y, Shao DD, Zhang AF, Yang X, Zhou MG, Xu YL (2014) First report of a fruit rot and twig blight on Pomegranate (*Punica granatum*) caused by *Pilidiella granati* in Anhui Province of China. *Plant Disease* 98(5): 695. <https://doi.org/10.1094/PDIS-09-13-1012-PDN>
- Chethana KWT, Zhou Y, Zhang W, Liu M, Xing QK, Li XH, Yan JY, Chethana KWT, Hyde KD (2017) *Coniella vitis* sp. nov. is the common pathogen of white rot in Chinese vineyards. *Plant Disease* 101(12): 2123–2136. <https://doi.org/10.1094/PDIS-12-16-1741-RE>
- Crous PW, Summerell BA, Shivas RG, Burgess TI, Decock CA, Dreyer LL, Granke LL, Guest DI, Hardy GE, Hausbeck MK, Hüberli D, Jung T, Koukol O, Lennox CL, Liew EC, Lombard L, McTaggart AR, Pryke JS, Roets F, Saude C, Shuttleworth LA, Stukely MJ, Vánky K, Webster BJ, Windstam ST, Groenewald JZ (2012) Fungal Planet description sheets: 107–127. *Persoonia* 28(1): 138–182. <https://doi.org/10.3767/003158512X652633>
- Crous PW, Giraldo A, Hawksworth DL, Robert V, Kirk PM, Guarro J, Robbertse B, Schoch CL, Damm U, Trakunyingcharoen T, Groenewald JZ (2014a) The Genera of Fungi: Fixing the application of type species of generic names. *IMA Fungus* 5(1): 141–160. <https://doi.org/10.5598/ima fungus.2014.05.01.14>
- Crous PW, Shivas RG, Quaedvlieg W, van der Bank M, Zhang Y, Summerell BA, Guarro J, Wingfield MJ, Wood AR, Alfenas AC, Braun U, Cano-Lira JF, García D, Marin-Felix Y, Alvarado P, Andrade JP, Armengol J, Assefa A, den Breejën A, Camele I, Cheewangkoon R, De Souza JT, Duong TA, Esteve-Raventós F, Fournier J, Frisullo S, García-Jiménez J, Gardiennet A, Gené J, Hernández-Restrepo M, Hirooka Y, Hospenhal DR, King A, Lechat C, Lombard L, Mang SM, Marbach PAS, Marincowitz S, Marin-Felix Y, Montañó-Mata NJ, Moreno G, Perez CA, Pérez Sierra AM, Robertson JL, Roux J, Rubio E, Schumacher RK, Stchigel AM, Sutton DA, Tan YP, Thompson EH, Vanderlinde E, Walker AK, Walker DM, Wickes BL, Wong PTW, Groenewald JZ (2014b) Fungal Planet description sheets: 214–280. *Persoonia* 32(1): 184–306. <https://doi.org/10.3767/003158514X682395>
- Crous PW, Wingfield MJ, Guarro J, Hernández-Restrepo M, Sutton DA, Acharya K, Barber PA, Boekhout T, Dimitrov RA, Dueñas M, Dutta AK, Gené J, Gouliamova DE, Groenewald M, Lombard L, Morozova OV, Sarkar J, Smith MT, Stchigel AM, Wiederhold NP, Alexandrova AV, Antelmi I, Armengol J, Barnes I, Cano-Lira JF, Ruiz RFC, Contu M, Courtécuisse PR, da Silveira AL, Decock CA, de Goes A, Edathodu J, Ercole E, Firmino AC, Fourie A, Fournier J, Furtado EL, Geering ADW, Gershenzon J, Giraldo A, Gramaje D, Hammerbacher A, He XL, Haryadi D, Khemmuk W, Kovalenko AE, Krawczynski R, Laich F, Lechat C, Lopes UP, Madrid H, Malysheva EF, Marín-Felix Y, Martín MP, Mostert L, Nigro F, Pereira OL, Picillo B, Pinho DB, Popov ES, Peláez CAR, Rooney-Latham S, Sandoval-Denis M, Shivas RG, Silva V, Stoilova-Disheva MM, Telleria MT, Ullah C, Unsicker SB, van der Merwe NA, Vizzini A, Wagner HG, Wong PTW, Wood AR, Groenewald JZ (2015a) Fungal Planet description sheets: 320–370. *Persoonia* 34(1): 167–266. <https://doi.org/10.3767/003158515X688433>

- Crous PW, Schumacher RK, Wingfield MJ, Lombard L, Giraldo A, Christensen M, Gardienet A, Nakashima C, Pereira OL, Smith AJ, Groenewald JZ (2015b) Fungal systematics and evolution: FUSE 1. *Sydowia* 67: 81–118. <https://doi.org/10.12905/0380-sydowia67-2015-0081>
- Crous PW, Wingfield MJ, Burgess TI, Carnegie AJ, Hardy GESJ, Smith D, Summerell BA, Cano-Lira JF, Guarro J, Houbraken J, Lombard L, Martín MP, Sandoval-Denis M, Alexandrova AV, Barnes CW, Baseia IG, Bezerra JDP, Guarnaccia V, May TW, Hernández-Restrepo M, Stchigel AM, Miller AN, Ordoñez ME, Abreu VP, Accioly T, Agnello C, Agustin Colmán A, Albuquerque CC, Alfredo DS, Alvarado P, Araújo-Magalhães GR, Arauzo S, Atkinson T, Barili A, Barreto RW, Bezerra JL, Cabral TS, Camello Rodríguez F, Cruz RHSF, Daniëls PP, da Silva BDB, de Almeida DAC, de Carvalho Júnior AA, Decock CA, Delgat L, Denman S, Dimitrov RA, Edwards J, Fedosova AG, Ferreira RJ, Firmino AL, Flores JA, García D, Gené J, Giraldo A, Góis JS, Gomes AAM, Gonçalves CM, Gouliamova DE, Groenewald M, Guéorguiev BV, Guevara-Suarez M, Gusmão LFP, Hosaka K, Hubka V, Huhndorf SM, Jadan M, Jurjević Ž, Kraak B, Kučera V, Kumar TKA, Kušan I, Lacerda SR, Lamlerthton S, Lisboa WS, Loizides M, Luangsa-Ard JJ, Lysková P, Mac Cormack WP, Macedo DM, Machado AR, Malysheva EF, Marinho P, Matočec N, Meijer M, Mešić A, Mongkolsamrit S, Moreira KA, Morozova OV, Nair KU, Nakamura N, Noisripoom W, Olariaga I, Oliveira RJV, Paiva LM, Pawar P, Pereira OL, Peterson SW, Prieto M, Rodríguez-Andrade E, Rojo De Blas C, Roy M, Santos ES, Sharma R, Silva GA, Souza-Motta CM, Takeuchi-Kaneko Y, Tanaka C, Thakur A, Smith MT, Tkálčec Z, Valenzuela-Lopez N, van der Kleij P, Verbeken A, Viana MG, Wang XW, Groenewald JZ (2017) Fungal Planet description sheets: 625–715. *Persoonia* 39: 270–467. <https://doi.org/10.3767/persoonia.2017.39.11>
- Crous PW, Luangsa-Ard JJ, Wingfield MJ, Carnegie AJ, Hernández-Restrepo M, Lombard L, Roux J, Barreto RW, Baseia IG, Cano-Lira JF, Martín MP, Morozova OV, Stchigel AM, Summerell BA, Brandrud TE, Dima B, García D, Giraldo A, Guarro J, Gusmão LFP, Khamsuntorn P, Noordeloos ME, Nuankaew S, Pinruan U, Rodríguez-Andrade E, Souza-Motta CM, Thangavel R, van Iperen AL, Abreu VP, Accioly T, Alves JL, Andrade JP, Bahram M, Baral HO, Barbier E, Barnes CW, Bendiksen E, Bernard E, Bezerra JDP, Bezerra JL, Bizio E, Blair JE, Bulyonkova TM, Cabral TS, Caiafa MV, Cantillo T, Colmán AA, Conceição LB, Cruz S, Cunha AOB, Darveaux BA, da Silva AL, da Silva GA, da Silva GM, da Silva RMF, de Oliveira RJV, Oliveira RL, De Souza JT, Dueñas M, Evans HC, Epifani F, Felipe MTC, Fernández-López J, Ferreira BW, Figueiredo CN, Filippova NV, Flores JA, Gené J, Ghorbani G, Gibertoni TB, Glushakova AM, Healy R, Huhndorf SM, Iturrieta-González I, Javan-Nikkhah M, Juciano RF, Jurjević Ž, Kachalkin AV, Keochanpheng K, Krisai-Greilhuber I, Li YC, Lima AA, Machado AR, Madrid H, Magalhães OMC, Marbach PAS, Melanda GCS, Miller AN, Mongkolsamrit S, Nascimento RP, Oliveira TGL, Ordoñez ME, Orzes R, Palma MA, Pearce CJ, Pereira OL, Perrone G, Peterson SW, Pham THG, Piontelli E, Pordel A, Quijada L, Raja HA, Rosas de Paz E, Ryvarden L, Saitta A, Salcedo SS, Sandoval-Denis M, Santos TAB, Seifert KA, Silva BDB, Smith ME, Soares AM, Sommai S, Sousa JO, Suetrong S, Susca A, Tedersoo L, Telleria MT, Thanakitpipattana D, Valenzuela-Lopez N, Visagie CM, Zapata M, Groenewald JZ (2018) Fungal Planet description sheets: 785–867. *Persoonia* 41(1): 238–417. <https://doi.org/10.3767/persoonia.2018.41.12>
- Crous PW, Carnegie AJ, Wingfield MJ, Sharma R, Mughini G, Noordeloos ME, Santini A, Shouche YS, Bezerra JDP, Dima B, Guarnaccia V, Imrefi I, Jurjević Ž, Knapp DG, Kovács GM, Magistà D, Perrone G, Rămă T, Rebriv YA, Shivas RG, Singh SM, Souza-Motta CM, Thangavel R, Adhasure NN, Alexandrova AV, Alfenas AC, Alfenas RF,



- Alvarado P, Alves AL, Andrade DA, Andrade JP, Barbosa RN, Barili A, Barnes CW, Baseia IG, Bellanger JM, Berlanas C, Bessette AE, Bessette AR, Biketova AY, Bomfim FS, Brandrud TE, Bransgrove K, Brito ACQ, Cano-Lira JF, Cantillo T, Cavalcanti AD, Cheewangkoon R, Chikowski RS, Conforto C, Cordeiro TRL, Craine JD, Cruz R, Damm U, de Oliveira RJV, de Souza JT, de Souza HG, Dearnaley JDW, Dimitrov RA, Dovana F, Erhard A, Esteve-Raventós F, Félix CR, Ferisin G, Fernandes RA, Ferreira RJ, Ferro LO, Figueiredo CN, Frank JL, Freire KTLS, García D, Gené J, Gęsiorska A, Gibertoni TB, Gondra RAG, Gouliamova DE, Gramaje D, Guard F, Gusmão LFP, Haitook S, Hirooka Y, Houbraeken J, Hubka V, Inamdara A, Iturriaga T, Iturrieta-González I, Jadan M, Jiang N, Justo A, Kachalkin AV, Kapitonov VI, Karadelev M, Karakehian J, Kasuya T, Kautmanová I, Kruse J, Kušan I, Kuznetsova TA, Landell MF, Larsson K-H, Lee HB, Lima DX, Lira CRS, Machado AR, Madrid H, Magalhães OMC, Majerova H, Malysheva EF, Mapperson RR, Marbach PAS, Martín MP, Martín-Sanz A, Matočec N, McTaggart AR, Mello JF, Melo RFR, Mešić A, Michereff SJ, Miller AN, Minoshima A, Molinero-Ruiz L, Morozova OV, Mosoh D, Nabe M, Naik R, Nara K, Nascimento SS, Neves RP, Olariaga I, Oliveira RL, Oliveira TGL, Ono T, Ordoñez ME de M, Ottoni A, Paiva LM, Pancorbo F, Pant B, Pawłowska J, Peterson SW, Raudabaugh DB, Rodríguez-Andrade E, Rubio E, Rusevska K, Santiago ALCMA, Santos ACS, Santos C, Sazanava NA, Shah S, Sharma J, Silva BDB, Siquier JL, Sonawane MS, Stchigel AM, Svetasheva T, Tamakeaw N, Telleria MT, Tiago PV, Tian CM, Tkalčec Z, Tomashevskaya MA, Truong HH, Vecherskii MV, Visagie CM, Vizzini A, Yilmaz N, Zmitrovich IV, Zvyagina EA, Boekhout T, Kehlet T, Læssøe T, Groenewald JZ (2019) Fungal Planet description sheets: 868–950. *Persoonia* 42: 291–473. <https://doi.org/10.3767/persoonia.2019.42.11>
- Ferreira FA, Alfenas AC, Coelho L (1997) Portas-de-entrada para *Coniella fragariae* em folhas de eucalipto. *Revista Árvore* 21: 307–311.
- Fröhlich J, Hyde KD (2000) Palm microfungi. *Fungal Diversity Research Series* 3: 1–375.
- Guo LD, Hyde KD, Liew ECY (2000) Identification of endophytic fungi from *Livistona chinensis* based on morphology and rDNA sequences. *The New Phytologist* 147(3): 617–630. <https://doi.org/10.1046/j.1469-8137.2000.00716.x>
- Hyde KD, Norphanphoun C, Maharachchikumbura SSN, Bao DF, Bhat DJ, Boonmee S, Bundhun D, Calabon MS, Chaiwan N, Chen YJ, Chethana KWT, Dai DQ, Dayarathne MC, Devadatha B, Dissanayake AJ, Dissanayake LS, Doilom M, Dong W, Fan XL, Goonasekara ID, Hongsanan S, Huang SK, Jayawardena RS, Jeewon R, Jones EBG, Karunarathna A, Konta S, Kumar V, Lin CG, Liu JK, Liu N, Lu YZ, Luangsa-ard J, Lumyong S, Luo ZL, Marasinghe DS, McKenzie EHC, Niego AGT, Niranjana M, Perera RH, Phukhamsakda C, Rathnayaka AR, Samarakoon MC, Samarakoon SMBC, Sarma VV, Senanayake IC, Shang QJ, Stadler M, Tibpromma S, Wanasinghe DN, Wei DP, Wijayawardene NN, Xiao YP, Xiang MM, Yang J, Zeng XY, Zhang SN (2020) Refined families of Sordariomycetes. *Mycosphere* 11(1): 305–1059. <https://doi.org/10.5943/mycosphere/11/1/7>
- Jiang N, Fan XL, Tian CM, Crous PW (2020) Reevaluating Cryphonectriaceae and allied families in Diaporthales. *Mycologia* 112(2): 267–292. <https://doi.org/10.1080/00275514.2019.1698925>
- Katoh K, Rozewicki J, Yamada KD (2019) MAFFT online service: Multiple sequence alignment, interactive sequence choice and visualization. *Briefings in Bioinformatics* 20(4): 1160–1166. <https://doi.org/10.1093/bib/bbx108>
- Kumar S, Stecher G, Tamura K (2016) MEGA7: Molecular evolutionary genetics analysis version 7.0 for bigger datasets. *Molecular Biology and Evolution* 33(7): 1870–1874. <https://doi.org/10.1093/molbev/msw054>

- Letunic I, Bork P (2021) Interactive Tree of Life (iTOL) v5: An online tool for phylogenetic tree display and annotation. *Nucleic Acids Research* 49(1): 293–296. <https://doi.org/10.1093/nar/gkab301>
- Li D, Zhang M, Zhang J, Ma L, Zhang Z, Zhang J, Zhang X, Xia J (2024) Three new microfungi (Ascomycota) species from southern China. *MycKeys* 111: 87–110. <https://doi.org/10.3897/mycokeys.111.136483>
- Liu YJ, Whelen S, Hall BD (1999) Phylogenetic Relationships among Ascomycetes: Evidence from an RNA polymerase II subunit. *Molecular Biology and Evolution* 16(12): 1799–1808. <https://doi.org/10.1093/oxfordjournals.molbev.a026092>
- Marin-Felix Y, Groenewald JZ, Cai L, Chen Q, Marincowitz S, Barnes I, Bensch K, Braun U, Camporesi E, Damm U, de Beer ZW, Dissanayake A, Edwards J, Giraldo A, Hernández-Restrepo M, Hyde KD, Jayawardena RS, Lombard L, Luangsa-ard J, McTaggart AR, Rossman AY, Sandoval-Denis M, Shen M, Shivas RG, Tan YP, van der Linde EJ, Wingfield MJ, Wood AR, Zhang JQ, Zhang Y, Crous PW (2017) Genera of phytopathogenic fungi: GOPHY 1. *Studies in Mycology* 86(1): 99–216. <https://doi.org/10.1016/j.simyco.2017.04.002>
- McNeill J, Barrie FR, Buck WR, Demoulin V, Greuter W, Hawksworth DL, Herendeen PS, Knapp S, Marhold K, Prado J, Prud'homme van Reine WF, Smith GF, Wiersema JH, Turland NJ (2012) International Code of Nomenclature for algae, fungi, and plants (Melbourne Code). *Regnum Vegetabile* 154. ARG Gantner Verlag KG, 240 pp. <http://www.iapt-taxon.org/nomen/main.php>
- Miller MA, Pfeiffer W, Schwartz T (2012) The CIPRES science gateway: Enabling high-impact science for phylogenetics researchers with limited resources. In *Proceedings of the 1<sup>st</sup> Conference of the Extreme Science and Engineering Discovery Environment. Bridging from the Extreme to the Campus and Beyond*, Chicago, IL, USA, Association for Computing Machinery, San Diego, CA, USA 39: 1–8. <https://doi.org/10.1145/2335755.2335836>
- Miranda BEC, Barreto RW, Crous PW, Groenewald JZ (2012) *Pilidiella tibouchinae* sp. nov. associated with foliage blight of *Tibouchina granulosa* (quaresmeira) in Brazil. *IMA Fungus* 3(1): 1–7. <https://doi.org/10.5598/imafungus.2012.03.01.01>
- Mu TC, Lin YS, Pu HL, Keyhani NO, Dang YX, Lv HJ, Zhao ZY, Heng ZA, Wu ZY, Xiong CJ, Lin LB, Chen YX, Su HL, Guan XY, Qiu JZ (2024) Molecular phylogenetic and estimation of evolutionary divergence and biogeography of the family Schizoparmaceae and allied families (Diaporthales, Ascomycota). *Molecular Phylogenetics and Evolution* 201: 108211. <https://doi.org/10.1016/j.ympev.2024.108211>
- Nag Raj TR (1993) *Coelomycetous Anamorphs with Appendage-bearing Conidia*. Mycologue Publications, Waterloo, Canada, 1101 pp. [https://doi.org/10.1016/S0953-7562\(09\)80334-1](https://doi.org/10.1016/S0953-7562(09)80334-1)
- Nylander JAA (2004) MrModeltest v2. Program distributed by the author. Evolutionary Biology Centre, Uppsala University.
- O'Donnell K, Kistler HC, Cigelnik E, Ploetz RC (1998) Multiple evolutionary origins of the fungus causing Panama disease of banana: Concordant evidence from nuclear and mitochondrial gene genealogies. *Proceedings of the National Academy of Sciences of the United States of America* 95(5): 2044–2049. <https://doi.org/10.1073/pnas.95.5.2044>
- Petrak F, Sydow H (1927) Die Gattungen der Pyrenomyzeten, Sphaeropsiden und Melanconieen. I. Der phaeosporen Sphaeropsiden und die Gattung *Macrophoma*. *Feddes Repertorium Speciarum Novarum Regni Vegetabilum Beihefte* 42: 1–551.
- Rajeshkumar KC, Hapat RP, Gaikwad SB, Singh SK (2011) *Pilidiella crousii* sp. nov. from the northern Western Ghats, India. *Mycotaxon* 115(1): 155–162. <https://doi.org/10.5248/115.155>

- Rannala B, Yang Z (1996) Probability distribution of molecular evolutionary trees: A new method of phylogenetic inference. *Journal of Molecular Evolution* 43(3): 304–311. <https://doi.org/10.1007/BF02338839>
- Raudabaugh DB, Iturriaga T, Carver A, Mondo S, Pangilinan J, Lipzen A, He G, Amirebrahimi M, Grigoriev IV, Miller AN (2018) *Coniella lustricola*, a new species from submerged detritus. *Mycological Progress* 17(1–2): 191–203. <https://doi.org/10.1007/s11557-017-1337-6>
- Rehner SA, Samuels GJ (1994) Taxonomy and phylogeny of *Gliocladium* analysed from nuclear large subunit ribosomal DNA sequences. *Mycological Research* 98(6): 625–634. [https://doi.org/10.1016/S0953-7562\(09\)80409-7](https://doi.org/10.1016/S0953-7562(09)80409-7)
- Ronquist F, Teslenko M, van der Mark P, Ayres DL, Darling A, Höhna S, Larget B, Liu L, Suchard MA, Huelsenbeck JP (2012) MrBayes 3.2: Efficient Bayesian Phylogenetic Inference and Model Choice Across a Large Model Space. *Systematic Biology* 61(3): 539–542. <https://doi.org/10.1093/sysbio/sys029>
- Rossman AY, Farr DF, Castlebury LA (2007) A review of the phylogeny and biology of the Diaporthales. *Mycoscience* 48(3): 135–144. <https://doi.org/10.1007/S10267-007-0347-7>
- Samuels GJ, Barr ME, Lowen R (1993) Revision of *Schizoparme* (Diaporthales, Melanconidaceae). *Mycotaxon* 46: 459–483.
- Senanayake IC, Crous PW, Groenewald JZ, Maharachchikumbura SSN, Jeewon R, Phillips AJL, Bhat JD, Perera RH, Li QR, Li WJ, Tangthirasun N, Norphanphoun C, Karunarathna SC, Camporesi E, Manawasighe IS, Al-Sadi AM, Hyde KD (2017) Families of Diaporthales based on morphological and phylogenetic evidence. *Studies in Mycology* 86(1): 217–296. <https://doi.org/10.1016/j.simyco.2017.07.003>
- Stamatakis A (2014) RAxML version 8: A tool for phylogenetic analysis and post-analysis of large phylogenies. *Bioinformatics* 30(9): 1312–1313. <https://doi.org/10.1093/bioinformatics/btu033>
- Sung GH, Sung JM, Hywel-Jones NL, Spatafora JW (2007) A multi-gene phylogeny of Clavicipitaceae (Ascomycota, Fungi): Identification of localized incongruence using a combinational bootstrap approach. *Molecular Phylogenetics and Evolution* 44(3): 1204–1223. <https://doi.org/10.1016/j.ympev.2007.03.011>
- Sutton BC (1977) Coelomycetes VI. Nomenclature of generic names proposed for Coelomycetes. *Mycological Papers* 141: 1–253.
- Sutton BC (1980) The Coelomycetes. Fungi imperfecti with pycnidia, acervuli and stromata. Commonwealth Mycological Institute, Kew, UK. <https://doi.org/10.1007/BF03213663>
- Tennakoon DS, Kuo CH, Maharachchikumbura SSN, Thambugala KM, Gentekaki E, Phillips AJL, Bhat DJ, Wanasinghe DN, de Silva NI, Promputtha I, Hyde KD (2021) Taxonomic and phylogenetic contributions to *Celtis formosana*, *Ficus ampelas*, *F. septica*, *Macaranga tanarius* and *Morus australis* leaf litter inhabiting microfungi. *Fungal Diversity* 108(8): 1–215. <https://doi.org/10.1007/s13225-021-00474-w>
- Van Niekerk JM, Groenewald JZE, Verkley GJM, Fourie PH, Wingfield MJ, Crous PW (2004) Systematic reappraisal of *Coniella* and *Pilidiella*, with specific reference to species occurring on *Eucalyptus* and *Vitis* in South Africa. *Mycological Research* 108(3): 283–303. <https://doi.org/10.1017/S0953756204009268>
- Vilgalys R, Hester M (1990) Rapid genetic identification and mapping of enzymatically amplified ribosomal DNA from several *Cryptococcus* species. *Journal of Bacteriology* 172(8): 4238–4246. <https://doi.org/10.1128/jb.172.8.4238-4246.1990>
- Von Arx JA (1973) Centraalbureau voor Schimmelcultures Baarn and Delft. Progress Report 1972. Verhandelingen der Koninklijke Nederlandsche Akademie van Wetenschappen. Afdeling Natuurkunde 61: 59–81.

- Von Arx JA (1981) The genera of fungi sporulating in pure culture, 3<sup>rd</sup> edn. J Cramer, Vaduz.
- Von Höhnelt F (1918) Dritte vorläufige Mitteilung mycologischer Ergebnisse (Nr. 201–304). Berichte der Deutschen Botanischen Gesellschaft 36(6): 309–317. <https://doi.org/10.1111/j.1438-8677.1918.tb07278.x>
- Wang S, Mu TC, Liu RY, Liu SB, Zhang ZX, Xia JW, Li Z, Zhang XG (2022) *Coniella castanea* sp. nov. on *Castanea mollissima* from Shandong Province, China. Phytotaxa 559(1): 025–034. <https://doi.org/10.11646/phytotaxa.559.1.3>
- Wang S, Liu XM, Xiong CL, Gao SS, Xu WM, Zhao LL, Song CY, Liu XY, James TY, Li Z, Zhang XG (2023) ASF1 regulates asexual and sexual reproduction in *Stemphylium eturmiunum* by DJ-1 stimulation of the PI3K/AKT signaling pathway. Fungal Diversity 123(1): 159–176. <https://doi.org/10.1007/s13225-023-00528-1>
- White TJ, Bruns T, Lee S, Taylor J (1990) Amplification and direct sequencing of fungal ribosomal RNA genes for phylogenetics. In: Innis MA, Gelfand DH, Sninsky JJ (Eds) PCR Protocols: A Guide to Methods and Applications. Academic Press, New York, 315–322. <https://doi.org/10.1016/B978-0-12-372180-8.50042-1>
- Zhang ZX, Liu XY, Tao MF, Liu XY, Xia JW, Zhang XG, Meng Z (2023) Taxonomy, phylogeny, divergence time estimation, and biogeography of the family Pseudoplagiostomataceae (Ascomycota, Diaporthales). Journal of Fungi 9(1): 82. <https://doi.org/10.3390/jof9010082>
- Zhang ZX, Shang YX, Zhang MY, Zhang JJ, Geng Y, Xia JW, Zhang XG (2024a) Phylogenomics, taxonomy and morphological characters of the Microdochiaceae (Xylariales, Sordariomycetes). MycoKeys 106: 303–325. <https://doi.org/10.3897/mycokeys.106.127355>
- Zhang H, Mao YT, Ma MX, Tao GC, Wei TP, Jiang YL (2024b) Culturable endophytic Sordariomycetes from *Rosa roxburghii*: New species and lifestyles. Journal of Systematics and Evolution 62(4): 637–676. <https://doi.org/10.1111/jse.13035>
- Zhaxybayeva O, Gogarten JP (2002) Bootstrap, Bayesian probability and maximum likelihood mapping: Exploring new tools for comparative genome analyses. BMC Genomics 3(1): 1–15. <https://doi.org/10.1186/1471-2164-3-4>





# New fungal genus, three novel species and one new record from mangroves, with reclassification of *Melanconiella* (Melanconiellaceae) species

Carlo Chris S. Apurillo<sup>1,2,3,4</sup>, Chayanard Phukhamsakda<sup>3</sup>, Kevin D. Hyde<sup>1,3</sup>, Vinodhini Thiagaraja<sup>1</sup>, E. B. Gareth Jones<sup>5,6</sup>

<sup>1</sup> Key Laboratory of Phytochemistry and Natural Medicines, Kunming Institute of Botany, Chinese Academy of Sciences, Kunming, Yunnan 650201, China

<sup>2</sup> School of Science, Mae Fah Luang University, Chiang Rai 57100, Thailand

<sup>3</sup> Center of Excellence in Fungal Research, Mae Fah Luang University, Chiang Rai 57100, Thailand

<sup>4</sup> Department of Science and Technology-Center for Research in Science and Technology (CRST), Philippine Science High School-Eastern Visayas Campus, Palo, Leyte 6501 Philippines

<sup>5</sup> Department of Botany and Microbiology, College of Science, King Saud University, P.O. Box 2455, Riyadh, 11451, Saudi Arabia

<sup>6</sup> Nantgaredig, 33B St Edwards Road, Southsea, Hants., UK PO5 3DH, UK

Corresponding authors: E. B. Gareth Jones (torperadgj@gmail.com); Kevin D. Hyde (kdhyde3@gmail.com)

## Abstract

Mangrove ecosystems, located in the land-sea interface, host a diverse array of fungi. In this paper, we introduce a novel genus, three novel species and one new record of fungi collected from mangrove environments in Pranburi, Prachuap Khiri Khan, Thailand. We establish *Pseudomelanconiella* as a new genus in Melanconiellaceae, to accommodate *Pseudomelanconiella mangrovei*, a saprobe from submerged decomposing wood of *Avicennia marina*. Phylogenetic analysis indicates its close relation with *Septomelanconiella*, but they differ in the morphology of the conidia. Additionally, our analysis of Melanconiellaceae led to the reclassification of *Melanconiella loropetalii* to *Sinodiscula loropetalii* and synonymizing *Sinodiscula camellicola* and *Melanconiella camelliae*. This paper also introduces two other novel species: *Peroneutypa hibisci*, a saprobe found on *Hibiscus tiliaceus* and *Pseudochaetosphaeronema bruguiera* from *Bruguiera cylindrica*, the first species in this genus reported as a mangrove fungus. A new record of *Rimora mangrovei* from *Ceriops tagal* is also reported. These discoveries emphasize the rich fungal diversity in mangrove ecosystems supporting further exploration of this unique environment.

**Key words:** Fungi, mangrove, novel species, Pranburi, *Pseudomelanconiella*, saprobic fungi, taxonomy



Academic editor: Rajesh Jeewon

Received: 18 September 2024

Accepted: 19 December 2024

Published: 7 April 2025

**Citation:** Apurillo CCS, Phukhamsakda C, Hyde KD, Thiagaraja V, Jones EBG (2025) New fungal genus, three novel species and one new record from mangroves, with reclassification of *Melanconiella* (Melanconiellaceae) species. MycoKeys 116: 25–52. <https://doi.org/10.3897/mycokeys.116.137351>

**Copyright:** © Carlo Chris S. Apurillo et al. This is an open access article distributed under terms of the Creative Commons Attribution License (Attribution 4.0 International – CC BY 4.0).

## Introduction

Mangroves, found in unique intertidal habitats, are vital ecosystems hosting diverse flora and fauna. Though they cover only 1% of tropical forests, they support various plants and animals including mammals, birds, fish, and insects (Jia et al. 2020). Mangroves are also diverse hosts to a high number of fungal species (Norphanphoun et al. 2018; Devadatha et al. 2021).

The fungal kingdom, with an estimated 2.2–13 million species has a rich evolutionary history deeply intertwined with that of terrestrial, aquatic, and marine ecosystems (Hyde and Jones 1988; Wu et al. 2019; Hyde et al. 2020, 2024; Phukhamsakda et al. 2022). However, only about 10 percent of these have been described and reported (Hyde et al. 2024). This is the lowest percentage of described species among the eukaryotes compared to plants (83–96%) and animals (19%) (Wang et al. 2020; Bhunjun et al. 2022; Phukhamsakda et al. 2022). This highlights the need to continuously survey for fungal species, especially in unique ecological niches such as the mangrove environment.

Fungal study in mangroves began in the 1920s with the report of Stevens (1920) from mangroves in Puerto Rico, followed by the work of Cribb and Cribb (1955) in Australia. Kohlmeyer (1968) listed 75 species of mangrove fungi, noting their taxonomic diversity and host preferences. Later, Hyde and Jones (1988) documented 90 species of intertidal mangrove fungi across 26 tree species. Many species are widespread across different ocean basins, indicating their adaptability to diverse environmental conditions (Hyde and Jones 1988). Jones and Alias (1997) identified 268 mangrove fungi species, observing limited host-specificity but some host preferences, indicating a nuanced relationship between fungal communities and host plant diversity within the mangrove ecosystem. They suggested higher fungal diversity in Asian tropics due to greater host diversity, although this assertion is somewhat complicated since more studies were being conducted in Asia (Hyde and Lee 1995; Jones and Alias 1997).

Schmit and Shearer (2003) published the first checklist of mangrove fungi recognizing 625 species, including some freshwater and terrestrial taxa. Devadatha et al. (2021) updated this to 850 species, marking an increase of more than 200 taxa within the 18-year between the checklists. However, Devadatha et al. (2021) focused exclusively on marine fungi from mangrove substrates, excluding those from freshwater and terrestrial environments. Over the years, the number of fungi associated with mangroves has steadily increased due to a wider interest in their study, especially in bioprospecting for bioactive compounds useful in medicine, agriculture, and biotechnology (Tan et al. 2015; Dela Cruz et al. 2020; Cadamuro et al. 2021; Sopalun et al. 2021; Chen et al. 2022).

In this study, we introduce one new genus, three novel species and one new record of fungi from mangroves in Prachuap Khiri Khan province in Thailand.

## Methods

### Collection, observation, and isolation

Mangrove samples were collected from Pranburi Forest Park (No. 0907.4/23579) and the Pranburi River area in Prachuap Khiri Khan, Thailand. The samples included dead branches attached to mangroves and decomposing branches submerged in brackish water. They were sealed in plastic bags and transported to the laboratory at the Center of Excellence in Fungal Research, Mae Fah Luang University in Chiang Rai, Thailand.

Fungi on the samples were examined using a stereomicroscope, and their morphological features were documented with a Nikon Eclipse Ni compound microscope equipped with a Nikon DS-Ri2 camera (Nikon, Japan). Measurements were taken using Tarosoft® Image Framework software calibrated for the microscope. Photo plates were created using Adobe Photoshop 24.0 (Adobe Systems, USA).

To cultivate the fungi, single-spore isolation technique was employed (Chomnunti et al. 2014; Senanayake et al. 2020). Cultures were incubated at room temperature for 2–4 weeks and then used for DNA extraction. These cultures were deposited in the Mae Fah Luang University Culture Collection (MFLUCC). Additionally, herbarium samples were deposited at the Mae Fah Luang University Herbarium (MFLU). Novel fungal species were registered in Index Fungorum (2024) and Faces of Fungi (Jayasiri et al. 2015).

## DNA extraction and PCR

DNA extraction from mycelia of pure fungal cultures was carried out using the E.Z.N.A® Tissue DNA kit (Omega Biotek, USA) according to the manufacturer's instructions. Initial tissue lysis was performed using the Qiagen Tissuelyzer (Qiagen, Netherlands), with the samples mixed with lysis solution. Subsequent steps followed the protocol outlined in the extraction kit.

Multi-locus amplification was conducted on all isolates. PCR reactions were prepared in 25 µl volumes, comprising 21 µl of Vazyme® Rapid Taq Master Mix, 1 µl each of forward and reverse primer, and 2 µl of template DNA. The internal transcribed spacer region (ITS) and different loci were amplified for the isolates using distinct primers (Table 1). For *Pseudomelanconiella mangrovei*, nuclear large subunit ribosomal DNA (LSU), RNA polymerase II second largest subunit (*rpb2*), and translation elongation factor 1-alpha (*tef1-a*) were amplified with *tef1-a* using EF1-728F/TEF1-LLeReV primers. For *Peroneutypa hibisci*, beta-tubulin (*tub2*) was also amplified. For *Pseudochaetosphaeronema bruguierae* and *Rimora mangrovei*, LSU, 18S small subunit ribosomal gene (SSU), and *tef1-a* were amplified, using EF1-983F and EF1-2218R primers for *tef1-a*. For *R. mangrovei*, only LSU, SSU and TEF were used for the phylogenetic analysis, as detailed in the results section. The list of primers and PCR conditions for each primer pair is provided in Table 1.

Following PCR, the resulting products were electrophoresed on a 1% agarose gel to verify the sizes of the amplicons. If single bands matching the expected sizes were observed in the gel, the PCR products were forwarded for Sanger sequencing at Sangon Biotech (China).

## Phylogenetic analysis

The sequences were assembled using Seqman II v. 5.0 to produce a contig. Subsequently, the contigs were searched in the Basic Local Alignment Search Tool (Madden 2003) to check for closely related sequences. Based on the results, related sequences to the isolates were retrieved based on previous studies. The National Center of Biotechnology Information (NCBI) Nucleotide database was checked to ensure the inclusion of all related species with molecular data in the analysis. The accession numbers of the sequences used in this study are shown in Suppl. material.

**Table 1.** Primers and PCR conditions used in the study.

Locus	Primers	Sequence (5'-3')	Reference	PCR Conditions
ITS	ITS5	GGAAGTAAAAGTCGTAACAAGG	White et al. (1989)	95 °C, 5 min; 35 cycles of 95 °C 45 s, 53 °C 45 s, 72 °C 2 min; 72 °C 5 min
	ITS4	TCCTCCGCTTATTGATATGC		
LSU	LR0R	ACCCGCTGAACCTTAAGC	Vilgalys and Hester (1990)	94 °C 3 min;; 35 cycles of 94 °C 1 min, 52 °C 50 s, 72 °C 1 min; 72 °C 10 min
	LR5	ATCCTGAGGGAAACTTC		
<i>rpb2</i>	fRPB2-5F	GAYGAYMGWGATCAYTTYGG	Liu et al. (1999)	94 °C 3 min;; 35 cycles of 94 °C 1 min, 52 °C 50 s, 72 °C 1 min; 72 °C 10 min
	fRPB2-7CR	CCCATRGCTTGYTTRCCCAT		
SSU	NS1	GTAGTCATATGCTTGCTCTC	White et al. (1989)	95 °C 2 min; 35 cycles of 95 °C 30 s, 55 °C 50 s, 72 °C 1 min; 72 °C 10 min
	NS4	CTTCCGTCAATTCCTTTAAG		
<i>tef1-a</i>	EF1-728F	CATCGAGAAGTTCGAGAAGG	Carbone and Kohn (1999)	95 °C 2 min; 35 cycles of 95 °C 30 s, 56 °C 45 s, 72 °C 1 min; 72 °C 8 min
	TEF1-LLeReV	AACTGTCAGGCAATGTGG	Jaklitsch et al. (2005)	
	EF1-983f	GCYCCYGGHCAYCGTGAYTTYAT	Rehner and Buckley (2005)	95 °C 2 min; 35 cycles of 95 °C 30s, 55 °C 50s, 72 °C 1 min; 72 °C 10 min
	EF1-2218R	CCRAACRGCRCRGTYTGCTCAT		
<i>tub2</i>	Bt2a	GGTAACCAAATCGGTGCTGCTTTC	Glass and Donaldson (1995)	95 °C 5 min; 35 cycles of 94 °C 30 s, 54 °C 30 s, 72 °C 1 min; 72 °C 8 min
	Bt2b	ACCCTCAGTGTAGTGACCCTTGCC		

The sequences of the isolates and related species were aligned using Multiple Alignment using Fast Fourier Transform (MAFFT) version 7.4 with strategy set to auto, a gap extend penalty of 0.123, a gap opening penalty of 1.53, with adjust direction selected (Kato and Standley 2013). The alignment was cleaned up by Block Mapping and Gathering with Entropy (BMGE; Criscuolo and Gribaldo 2010), with the following settings: DNAPAM matrix, a sliding window size of 3, gap rate cut-off of 0.5, maximum entropy threshold of 0.5, and minimum block size of 5. MAFFT and BMGE were performed on the NGPhylogeny site (Lemoine et al. 2019).

The aligned sequences were then subjected to maximum likelihood (ML), maximum parsimony (MP), and Bayesian inference (BI) analyses. For ML, RAxML-HPC2 on ACCESS v. 8.2.12 (Stamatakis 2014) was utilized, using the default GTRGAMMA model and 1,000 bootstrap iterations. For MP, PAUP on XSEDE v.4.168 (Swofford 2002) set to 1,000 bootstrap iterations was employed.

Model testing was conducted prior to Bayesian analysis using MEGA v. 11 (Tamura et al. 2021), and specific models were applied during the analysis. For the multi-locus analysis, specific models for each partition of the concatenated sequences were specified in the command block. Bayesian posterior probability analysis was conducted using Markov chain Monte Carlo (MCMC) sampling in MrBayes v.3.2 on XSEDE (Ronquist et al. 2012), with four simultaneous Markov chains run for 10,000,000 generations, sampling every 1,000<sup>th</sup> generation. The run discarded 25% of the trees as the burn-in phase, using the remaining trees to compute the posterior probability (PP) in the consensus tree. Trace files of individual and combined runs were assessed using Tracer v.1.7.2 (Rambaut et al. 2018).

Phylogenetic analyses were initially performed on individual loci before multi-locus analyses were conducted. Trees generated from individual locus and multi-locus analyses for each taxon were compared, and only reported if they exhibited similar topologies. Trees were visualized using FigTree v.14.4 (Rambaut 2018), and then edited using Adobe Illustrator v.27.0 (Adobe

Systems, USA), combining the bootstrap values from ML and MP with the posterior probabilities (PP) from Bayesian analysis. The decisions as to whether to introduce new genera or species follow Jeewon and Hyde (2016) and Maharachchikumbura et al. (2021).

## Results

**Sordariomycetes O.E. Erikss. & Winka**

**Diaporthales Nannf.**

**Melanconiellaceae Senan., Maharachch. & K.D. Hyde**

Phylogenetic analysis for *Pseudomelanconiella* isolates was performed using ITS, LSU, *rpb2* and *tef1-α* loci. The ML, MP and Bayesian multi-locus analysis consisted of a total of 3,957 characters, including gaps in the concatenated sequence. The lengths of each region were as follows: ITS (1-592), LSU (593-1,469), *rpb2* (1,470-2,631), *tef1-α* (2,632-3,957).

For ML analysis, the alignment had 1,527 distinct alignment patterns with 23.52% gaps and undetermined characters. The best-scoring tree (shown in Fig. 1) had a final optimization likelihood of -25,438.87, tree length of 1.744101 and alpha of 0.239245. The base frequencies are: A = 0.227229, C = 0.273128, G = 0.273187 and T = 0.226456, with the following substitution rates: AC = 1.270018, AG = 3.717788, AT = 1.313118, CT = 5.037061, and GT = 1.00000.

The MP analysis of the multi-locus data included 3,957 characters, with 2,470 constant characters, 1,318 parsimony-informative and 169 parsimony-uninformative characters. The most parsimonious tree had a similar topology to the maximum likelihood tree (Fig. 1), with the *Pseudomelanconiella* clade in the same position on the tree.

For the Bayesian analysis, different evolutionary models were used for each locus based on the results from MEGA: Kimura 2-parameter with gamma distribution and proportion of invariable sites (K2P+G+I) for ITS, General Time Reversible model with gamma distribution (GTR+G) for LSU and General Time Reversible model with gamma distribution and proportion of invariable sites (GTR+G+I) for *rpb2* and *tef1-α*. The final average standard deviation of split frequencies after the total MCMC generations is 0.002019. Effective sample size (ESS) values for all factors of the combined trace files ranged from 7,577 to 15,002 with the trace plots showing two independent runs have converged. The topology of the tree from the Bayesian analysis is similar to the one obtained from the maximum likelihood analysis.

Based on the ML, MP, and BI analyses, which included sequences from species belonging to Melanconiellaceae, *Pseudomelanconiella* isolates (MFLU 24-0189, MFLU 24-0190) formed a distinct clade closely related to *Septomelanconiella* (Fig. 1). Although the node that separates *Pseudomelanconiella* and *Septomelanconiella* has low support in ML and MP, it has a good support for BI and is consistently recovered in all trees generated in the three analyses. Furthermore, the base differences of ITS, LSU and *rpb2* between *Septomelanconiella* and *Pseudomelanconiella* are higher than the least base difference between genera in Melanconiellaceae. Morphologically, *Pseudomelanconiella* differs from *Septomelanconiella*, as detailed in the taxonomy notes. *Pseudomelanconiella* is also phylogenetically distant from *Sinodiscula*, the most recent genus to be added to Melanconiellaceae.



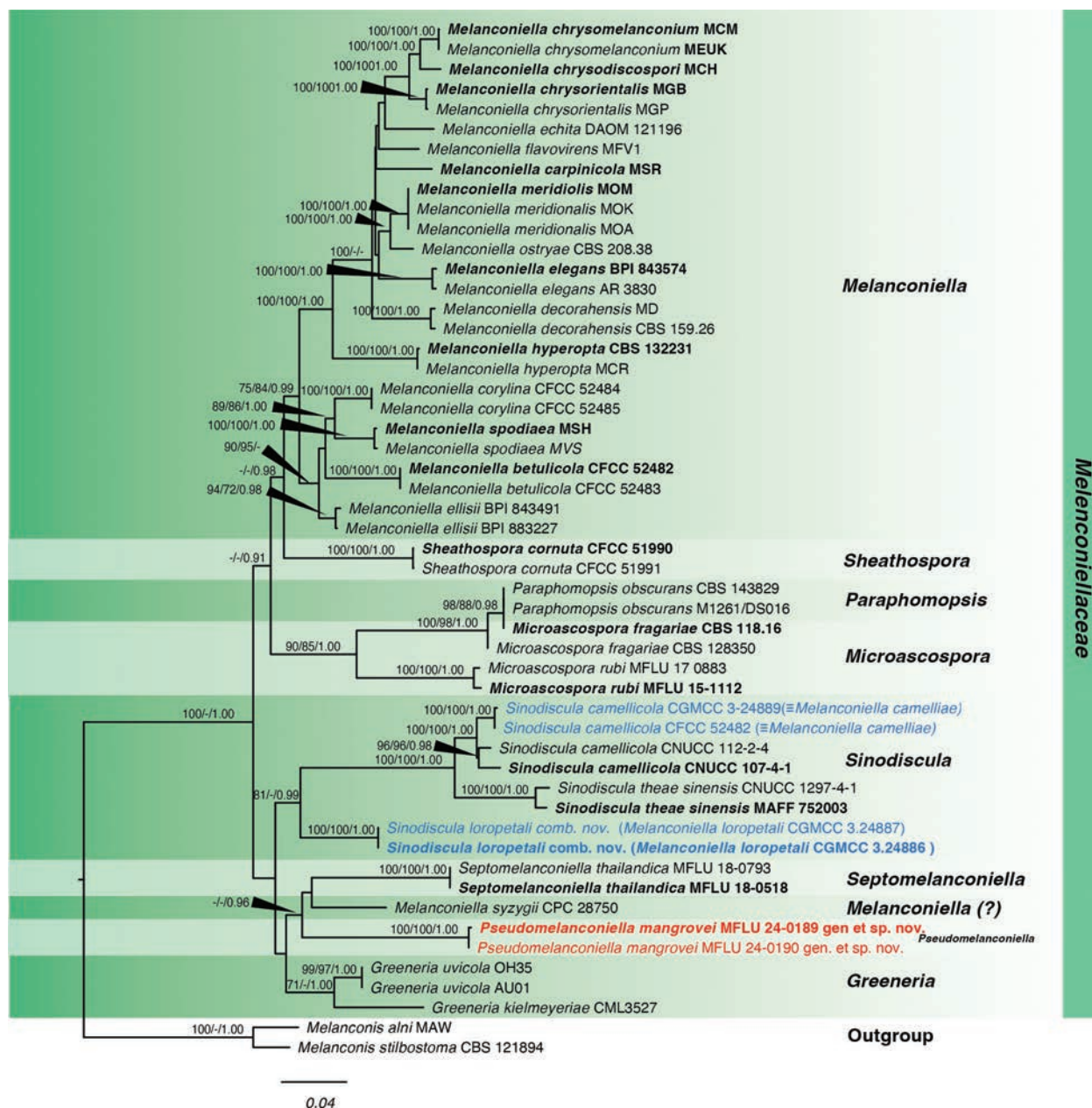


**Figure 1.** Phylogram of Melanconiellaceae based on a combined analysis of ITS, LSU, *rpb2*, and *tef1-α*. Values above the branches indicate bootstrap support from maximum likelihood (ML) and maximum parsimony (MP) equal to or above 70 and Bayesian posterior probabilities (PP) equal to or above 0.90. Novel species are in red, and species for synonymization and reclassification are in blue. Sequences from type species are indicated in bold. The tree is rooted with *Melanconis alni* MAW and *Melanconis stilbostoma* CBS 121894.

Our analysis shows that three *Melanconiella* species do not group within the *Melanconiella* clade. Thus, *Melanconiella camelliae* is synonymized with *Sinodiscula camellicola* while *Melanconiella loropetali* is reclassified as *Sinodiscula loropetali*. The third species, *Melanconiella syzygii*, forms a lineage with *Septomelanconiella*. However, the phylogenetic position of this isolate is not yet well-supported in the present analysis. Additional data are required to provide a more stable phylogenetic position, possibly leading to its reclassification under *Septomelanconiella*. The morphology of *M. syzygii* is similar to *Septomelanconiella* as they both possess septate conidia.

***Pseudomelanconiella* Apurillo, Phukhams., E.B.G. Jones & K.D. Hyde, gen. nov.**

Index Fungorum: IF902576

Facesoffungi Number: FoF16488

**Etymology.** From the Greek “pseudo” meaning false, due to the close morphologic similarity of isolates with *Melanconiella* species.

**Type species.** *Pseudomelanconiella mangrovei*.

**Description.** **Sexual morph:** Undetermined. **Asexual morph:** **Conidiomata** globose to subglobose, immersed to erumpent, develop under a clypeus with variable stromata, confluent, mostly with a long, conical, central ostiole, black. **Ostiole** present. **Peridium** light brown to brown, composed of textura angularis cells. **Conidiophores** hyaline, septate. **Conidiogenous cells** hyaline, phialidic. **Conidia** oblong to ellipsoid, light-brown, unicellular, aseptate, verrucose, without gelatinous sheath.

**Notes.** Combined phylogenetic analysis of ITS, LSU, *rpb2* and *tef1-a* sequences reveal that *Pseudomelanconiella* forms a distinct, well-supported clade separate from other genera in Melanconiellaceae. The sister taxon is *Septomelanconiella*, however, this monotypic genus is distinguished by its septate, laminate conidia, which is not observed in *Pseudomelanconiella* (Phookamsak et al. 2019). Both *Pseudomelanconiella* and *Septomelanconiella* are coelomycetous and have no reported sexual morphs (Phookamsak et al. 2019). Pairwise differences between the *Septomelanconiella* and *Pseudomelanconiella* in ITS (13.2%), LSU (1.6%), *rpb2* (16.1%) are all higher than the lowest base difference observed between genera in Melanconiellaceae. *Septomelanconiella* was isolated as a saprobe from *Syzygium samarangense* in a terrestrial environment while *Pseudomelanconiella* was isolated from mangroves in a brackish water environment (Phookamsak et al. 2019). These support the establishment of a new genus with *Pseudomelanconiella mangrovei* as the type species.

***Pseudomelanconiella mangrovei* Apurillo, Phukhams., E.B.G. Jones & K.D. Hyde, sp. nov.**

Index Fungorum: IF902577

Facesoffungi Number: FoF16489

Fig. 2

**Etymology.** Based on its mangrove host.

**Holotype.** MFLU 24-0189.

**Description.** **Saprobic** on decomposing branch of *Avicennia marina* submerged in brackish water. **Sexual morph:** Undetermined. **Asexual morph:** **Conidiomata** 100–590 µm × 200–815 µm ( $\bar{x}$  = 386.3 × 566.2 µm, n = 10), globose to subglobose, immersed to erumpent, black, confluent, mostly with a central stromatic column. **Peridium** light-brown to brown, made of cells of textura angularis. **Conidiophores** 8–20 × 1–2 µm ( $\bar{x}$  = 14.6 × 1.8 µm, n = 30), mostly straight, hyaline, septate, smooth unbranched. **Conidiogenous cells** 2–7 × 1–2 µm ( $\bar{x}$  = 4.2 × 1.8 µm, n = 30), monopialidic, determinate, discrete, cylindrical to subcylindrical, smooth-walled, hyaline, arising from inner layers of conidioma. **Conidia** 11–14 × 3–4 µm ( $\bar{x}$  = 11.4 × 3.3 µm,



**Figure 2.** *Pseudomelanconiella mangrovei* (MFLU 24-0189, holotype). **a** host **b, c** conidiomata on host **d** section of peridium **e** squash mount showing conidiophores and conidia **f** conidiophores, conidiogenous cells with attached conidia **g–j** conidia **k** germinated conidium **l** culture on MEA. Scale bars: 500  $\mu\text{m}$  (**b**); 100  $\mu\text{m}$  (**c**); 50  $\mu\text{m}$  (**e, f**); 20  $\mu\text{m}$  (**d, g**); 10  $\mu\text{m}$  (**h–k**).

$n = 50$ ), oblong to ellipsoid, hyaline to light-brown, unicellular, aseptate, verrucose, without gelatinous sheath.

**Known distribution.** Thailand.

**Culture characteristics.** Conidia germinate in malt extract agar (MEA) within 24 hours, with germ tubes arising from one end of the conidia. Colonies on MEA grow up to 14 cm after 7 days of incubation at room temperature, circular, mostly flat or effuse with a raised ring near the center, undulate, white, translucent; reverse does not exhibit pigments.

**Material examined.** THAILAND • Prachuap Khiri Khan Province, Pranburi District, 12°23'9"N, 99°56'51"E, on decomposing branch of *Avicennia marina* L.



(Acanthaceae) submerged in brackish water, 4 February 2023, Carlo Chris S. Apurillo, P30201 (MFLU 24-0189, **holotype**); • *ibid.*, P30301 (MFLU 24-0190); ex-type living culture MFLUCC 24-0512 = MFLUCC 24-0513 .

**GenBank numbers.** MFLU 24-0189 = ITS: PP989291, LSU: PP989287, *rpb2*: PP993004, *tef1-α*: PP993001; MFLU 24-0190 = ITS: PP989292, LSU: PP989288, *tef1-α*: PP993002.

**Notes.** Based on combined analysis of ITS, LSU, *rpb2*, and *tef1-α* sequences, *Pseudomelanconiella mangrovei* formed a distinct clade within Melanconiellaceae, with *Septomelanconiella thailandica* as the closest taxon. *Pseudomelanconiella mangrovei* differs from *Septomelanconiella thailandica* based on the appearance of the conidia. The distinguishing characteristic of *S. thailandica* is its septate conidia (Phookamsak et al. 2019). In contrast, *Pseudomelanconiella mangrovei* conidia are aseptate. While the morphology of *Pseudomelanconiella mangrovei* is similar to *Melanconiella* species, particularly the appearance of conidiomata, conidiogenous cells and the shape of the conidia, its phylogenetic position is distinct from other *Melanconiella* species (Voglmayr et al. 2012). Thus, this isolate is classified under a novel genus, *Pseudomelanconiella*.

#### **Sinodiscula M.J. Guo & C.L. Hou**

***Sinodiscula loropetali* (T.C. Mu & Jun Z. Qiu) Apurillo, Phukhams., K.D. Hyde & E.B.G. Jones, comb. nov.**

MycoBank No: 855635

Facesoffungi Number: FoF16612

*Melanconiella loropetali* T.C. Mu & Jun Z. Qiu, Front. Microbiol. 14(1229705):3 (2023). Basionym. MycoBank No: 848666.

**Description.** **Sexual morph:** Undetermined. **Asexual morph:** Descriptions and illustrations refer to Mu et al. (2023).

**Notes.** *Melanconiella loropetali* was introduced in *Melanconiella* by Mu et al. (2023), isolated from diseased *Loropetalum sinense* in China. *Melanconiella loropetali*, *Melanconiella camelliae* and *Melanconiella syzygii*, formed a basal clade distinct from other *Melanconiella* species in Mu et al. (2023). However, only *Melanconiella* species were used in the analysis, leading to their classification as *Melanconiella*. We included other genera in Melanconiellaceae in our analysis and *M. camelliae*, *M. loropetali* and *M. syzygii* are phylogenetically distant from *Melanconiella*. The phylogenetic tree of the combined ITS, LSU, *rpb2* and *tef1-α* sequences showed that *Melanconiella loropetali* formed a sister clade to *Sinodiscula* species. Thus, we reclassified *M. loropetali* as *Sinodiscula loropetali*. *Melanconiella loropetali* is similar to *Sinodiscula* species. It fits the generic description of *Sinodiscula*, and like other *Sinodiscula* species, *Melanconiella loropetali* was isolated as a plant pathogen (Mu et al. 2023; Guo et al. 2024). Given the similarities in morphology and ecology of *M. loropetali* and *Sinodiscula* species, and the well-supported phylogenetic position of *Melanconiella loropetali*, we reclassify it as *Sinodiscula loropetali*.

***Sinodiscula camellicola* S.Y. Zhao, M.J. Guo & C.L. Hou, Journal of Fungi 10 (2, no. 141): 9 (2024)**

Index Fungorum: IF851775

MycoBank No: 851775

≡ *Melanconiella camelliae* T.C. Mu & Jun Z. Qiu, Front. Microbiol. 14(1229705):6 (2023). MycoBank No: 848667.

**Description.** Descriptions and illustrations refer to Mu et al. (2023) and Guo et al. (2024).

**Notes.** In the present analysis, *Melanconiella camelliae* formed a well-supported clade with *Sinodiscula camellicola*. Detailed morphological comparison reveals that these two species are similar with no notable differences. Both species were isolated as pathogens from *Camellia sinensis*, from Fujian Province (China) for *Melanconiella camelliae* and from Anhui Province (China) for *Sinodiscula camellicola* (Guo et al. 2024). Moreover, the ITS sequences of *Melanconiella camelliae* and *Sinodiscula camellicola* differ by only 1%. Due to these similarities in morphology, ecology and molecular data of the two species, we propose to synonymize *M. camelliae* and *S. camellicola* under *Sinodiscula* (Melanconiellaceae).

#### **Xylariales Nannf.**

#### **Diatrypaceae Nitschke**

#### **Peroneutypa Berl.**

Phylogenetic analysis of *Peroneutypa* was based on the combined ITS and *tub2* sequence data. The combined multi-locus analysis consisted of 927 characters, including gaps with the following lengths: ITS (1-531) and *tub2* (532-927). ML, MP, and BI analyses were done using single and concatenated sequences.

For ML, there were 540 distinct alignment patterns with 31.95% gaps and undetermined characters in the concatenated sequences. The maximum likelihood tree (Fig. 3) has a final ML optimization likelihood of -8,464.76, tree length of 3.225995 and alpha of 0.362736. The base frequencies are: A = 0.222507, C = 0.268440, G = 0.239063 and T = 0.269990. The rates of substitution are as follows: AC = 0.825859, AG = 2.247793, AT = 1.238868, CG = 0.697931, CT = 3.237131 and GT = 1.00000.

The MP analysis consisted of 927 total characters, 452 of which were constant, 396 parsimony-informative and 79 parsimony-uninformative. The most parsimonious tree had a similar topology as the best-scoring ML tree (Fig. 3).

For the Bayesian analysis, the model used for ITS was K2P+G and Hasegawa-Kishino-Yano with gamma distribution (HKY+G) for *tub2*. After the total MCMC generations, the average standard deviation of split frequencies is 0.002628. Analysis in Tracer showed that the two independent runs have converged based on the trace plots with the ESS values of all factors for the combined runs ranging from 4,877 to 14,599. The topology of the Bayesian tree is similar to the best-scoring tree in ML shown in Fig. 3, especially with respect to the position of *Peroneutypa hibisci*.



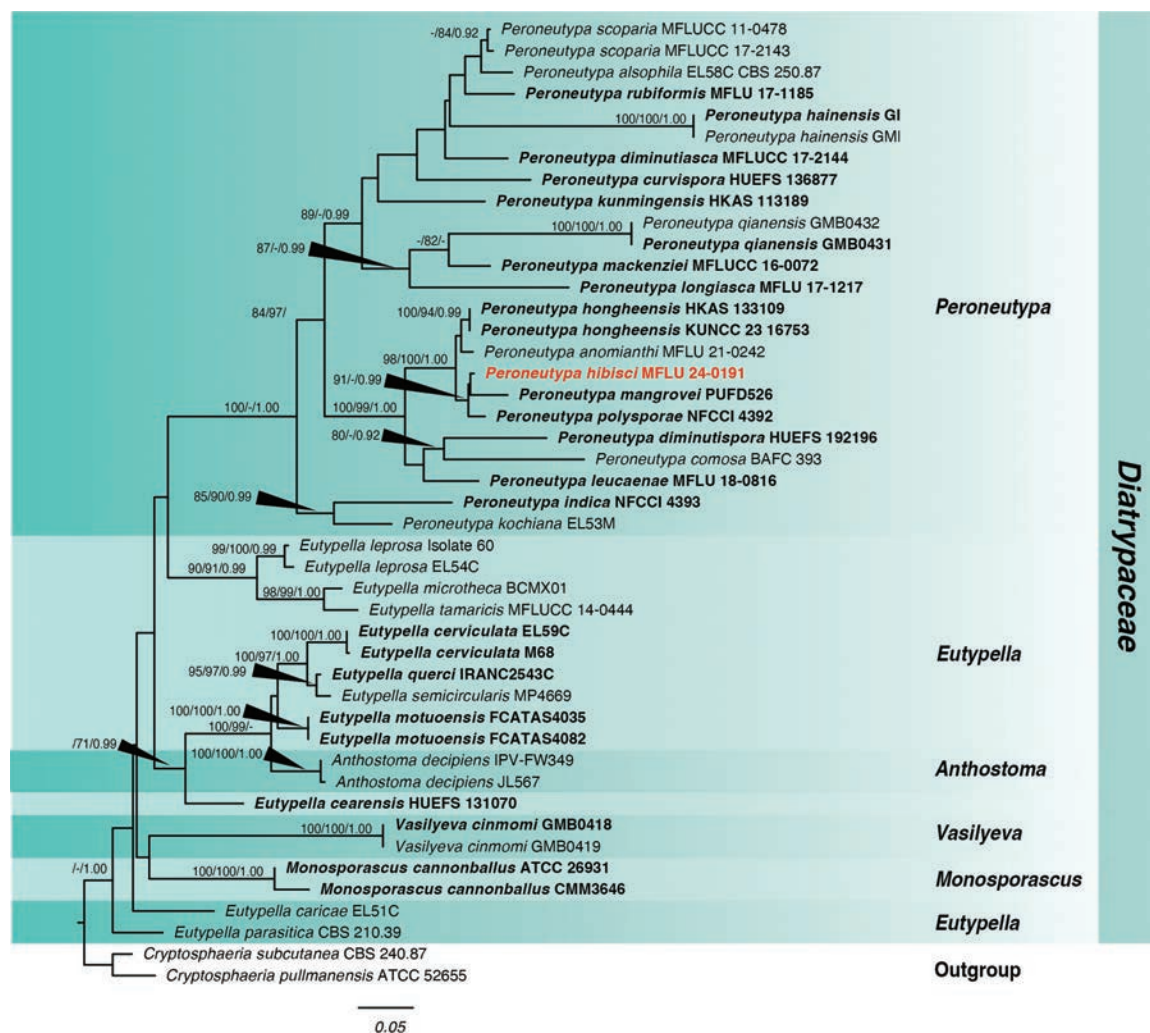


**Figure 3.** Phylogram of the combined ITS and *tub2* analysis of *Peroneutypa* and related genera in Diatrypeaceae. Values above the branches indicate bootstrap support values from maximum likelihood (ML) and maximum parsimony (MP) equal to or above 0.70 and Bayesian posterior probability (PP) equal to or above 0.90. The novel species is indicated in red bold. Sequences from type species are indicated in bold. The tree is rooted with *Cryptosphaeria subcutanea* CBS 240.87 and *Cryptosphaeria pullmanensis* ATCC 52655.

The ML, MP, BI analyses showed that *Peroneutypa hibisci* formed a distinct lineage with *Peroneutypa mangrovei*, the latter showing a longer branch length (Fig. 3). Although the two species were isolated from mangroves, they differ in morphology as discussed in the taxonomy notes. Furthermore, the base pair difference in ITS and *tub2* are greater than 1.5%.

***Peroneutypa hibisci* Apurillo, Phukhams., E.B.G. Jones & K.D. Hyde, sp. nov.**

Index Fungorum: IF902578

Facesoffungi Number: FoF16490

Fig. 4

**Etymology.** Based on the host, *Hibiscus tiliaceus*.

**Holotype.** MFLU 24-0191.

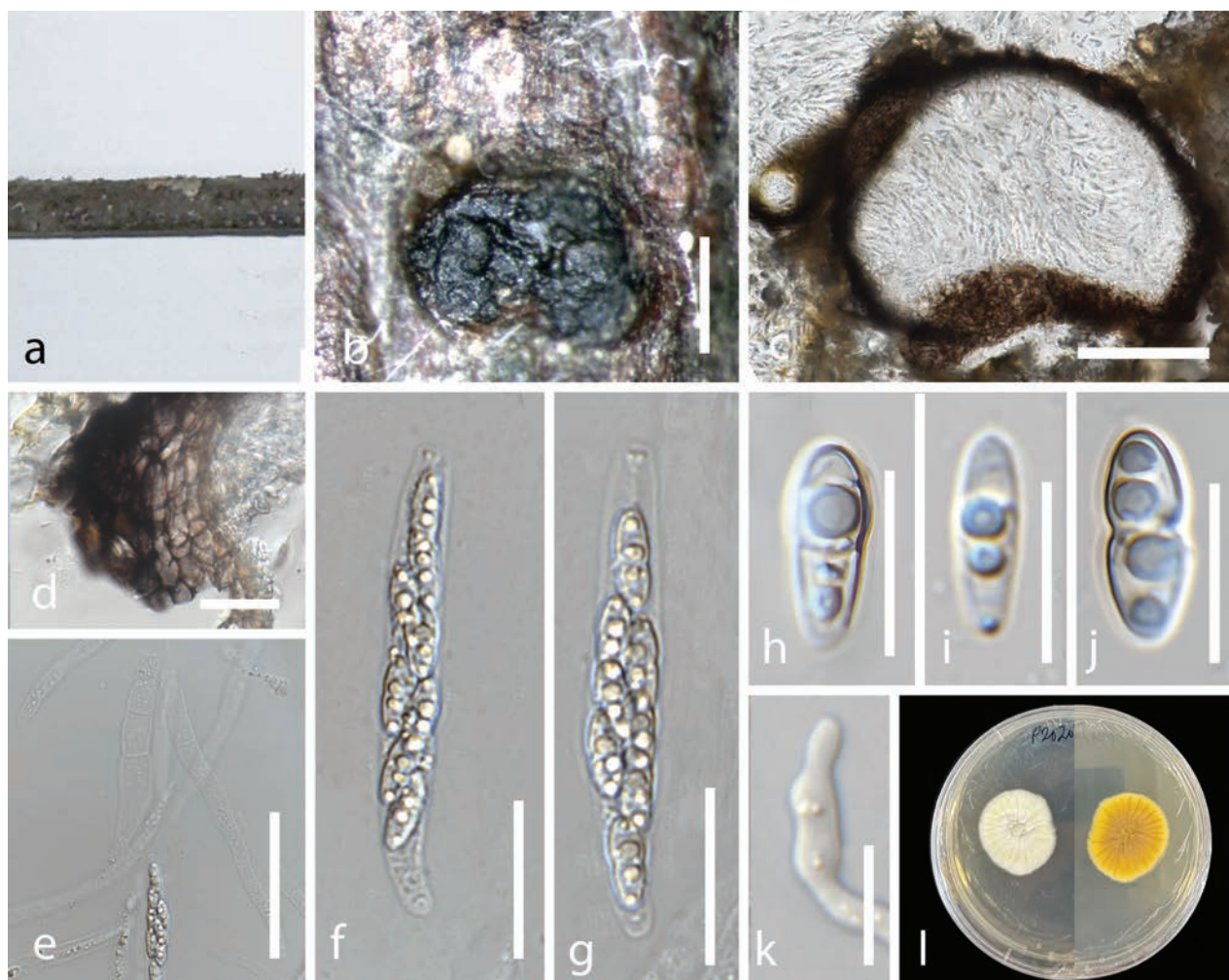


**Figure 4.** *Peroneutypa hibisci* (MFLU 24-0191, holotype). **a** host **b** ascoma on host **c** section of ascoma **d** peridium **e** ascus with hamathecium **f, g** asci **h–j** ascospores **k** germinated ascospore **l** culture on MEA. Scale bars: 200  $\mu$ m (**b**); 100  $\mu$ m (**c**); 50  $\mu$ m (**d**); 20  $\mu$ m (**e, f**); 10  $\mu$ m (**g–j**).

**Description.** Saprobic on decomposing branches of *Hibiscus tiliaceus* submerged in brackish water. **Sexual morph: Stromata** 1.0–1.5 mm ( $\bar{x}$  = 1.2,  $n$  = 5), poorly developed, non-sulcate, solitary to gregarious, immersed to erumpent, dark brown to black. **Perithecia** 200–300  $\mu$ m ( $\bar{x}$  = 238,  $n$  = 5) in diameter, immersed to erumpent, globose, brown to black, ostiolate. **Peridium** 20–45  $\mu$ m ( $\bar{x}$  = 32,  $n$  = 5) wide, composed of two layers, outer layer dark brown to black comprising of textura angularis cells, inner layer of textura angularis cells, brown to dark-brown. **Hamathecium** 90–125  $\mu$ m  $\times$  3–4  $\mu$ m ( $\bar{x}$  = 104  $\times$  3.4  $\mu$ m,  $n$  = 5) wide, hyaline, aseptate, unbranched. **Asci** 57–68  $\mu$ m  $\times$  6–8  $\mu$ m ( $\bar{x}$  = 59.4  $\times$  7.6  $\mu$ m,  $n$  = 5), 8-spored, clavate, unitunicate, short stipitate, with inamyloid apical rings. **Ascospores** 8–12  $\mu$ m  $\times$  3–4  $\mu$ m ( $\bar{x}$  = 10.7  $\times$  3.6  $\mu$ m,  $n$  = 45), hyaline, ellipsoid, with constricted median septum when mature, 2–4 guttules. **Asexual morph:** Undetermined.

**Known distribution.** Thailand.

**Culture characteristics.** Ascospores germinated in MEA within 24 hours, the germ tubes arising from both ends of the ascospore. Colonies on MEA grow up to 10 cm after 7 days of incubation at room temperature, white, filamentous, with aerial mycelium, reverse with gray pigment toward the center.

**Material examined.** THAILAND • Prachuap Khiri Khan: Pranburi District, 12°23'8.74"N, 99°56'51.47"E, on decomposing branches of *Hibiscus tiliaceus* submerged in brackish water. 4 February 2023, Carlo Chris S. Apurillo, P20201 (MFLU 24-0191, **holotype**), ex-type living culture, MFLUCC 24-0514.

**GenBank Numbers.** ITS: PP989294, *tub2* = PP993003.

**Notes.** *Peroneutypa hibisci* formed a lineage with *Peroneutypa mangrovei*, the latter showing a longer branch length than *Peroneutypa hibisci*. Although this clade has low support, this was consistently observed in ML, MP and BI trees. Comparison of base pair differences between these two closely related species revealed a difference of 23 out of 459 bases (5.0%) in ITS and 7 out of 349 bases (2.0%) in *tub2* sequences. Morphologically, they differ significantly: *P. hibisci* has larger, ellipsoid, guttulate ascospores ( $8\text{--}12 \times 3\text{--}4\ \mu\text{m}$ ), while *P. mangrovei* has smaller, cylindrical to clavate ascospores ( $3\text{--}5 \times 1\text{--}1.5\ \mu\text{m}$ ) without guttules. The asci of *P. hibisci* ( $57\text{--}68 \times 6\text{--}8\ \mu\text{m}$ ) are also much larger than those of *P. mangrovei* ( $14\text{--}20 \times 3\text{--}4\ \mu\text{m}$ ) (Phookamsak et al. 2019). Compared to another related species, *P. polysporae*, *P. hibisci* differs by producing median-septate, ellipsoid ascospores, whereas *P. polysporae* has smaller, unicellular, allantoid spores. Additionally, *P. polysporae* has larger asci ( $110\text{--}155 \times 5\text{--}7.5\ \mu\text{m}$ ) than *P. hibisci* (Dayarathne et al. 2020). Morphological and sequence data support the introduction of *Peroneutypa hibisci* as a novel species based on the guidelines of Jeewon and Hyde (2016) and Maharachchikumbura et al. (2021).

**Dothideomycetes O.E. Erikss. & Winka**

**Pleosporales Luttr. Ex M.E. Barr**

**Macrodiplodiopsidaceae Voglmayr, Jaklitsch & Crous,**

**Pseudochaetosphaeronema Punith.**

The ML, MP, and BI phylogenetic analyses of *Pseudochaetosphaeronema* utilized a combined multi-locus phylogeny including ITS, LSU, SSU, and *tef1-a* sequences. The alignment had a total of 3,313 characters, including gaps, with the lengths of the regions as follows: ITS (1-523), LSU (524-1,384), SSU (1,385-2,414), and *tef1-a* (2,415-3,313). For ML, the alignment has 607 distinct patterns with 20.91% gaps and completely undetermined characters. The best-scoring tree (Fig. 5) had a final optimization likelihood of -10,102.09 with tree length of 0.507278 and  $\alpha = 0.103258$ . The base frequencies are as follows: A = 0.237153, C = 0.250803, G = 0.270592, T = 0.241452 and the following substitution rates: AC = 1.724291, AG = 4.038401, AT = 2.171255, CG = 1.954009, CT = 11.161818, GT = 1.00000.

For MP, out of the 3,313 characters in the dataset, 2,715 were constant, 368 were parsimony-informative while 230 were parsimony-uninformative. The topology of the ML tree from the combined analysis was similar to that of the best-scoring tree.

In the Bayesian analysis, the models used for the different loci were as follows: K2P+G for ITS and SSU, K2P+G+I for LSU and GTR+G+I for *tef1-a*. The average standard deviation of split frequencies after the total MCMC runs is 0.001383. Evaluation of the trace files in Tracer showed ESS values for all factors ranging 4,963 to 13,845. The plots showed that the two independent runs have converged. The topology of the BI tree was similar to the best-scoring ML tree, especially the position of *Pseudochaetosphaeronema bruguierae*.



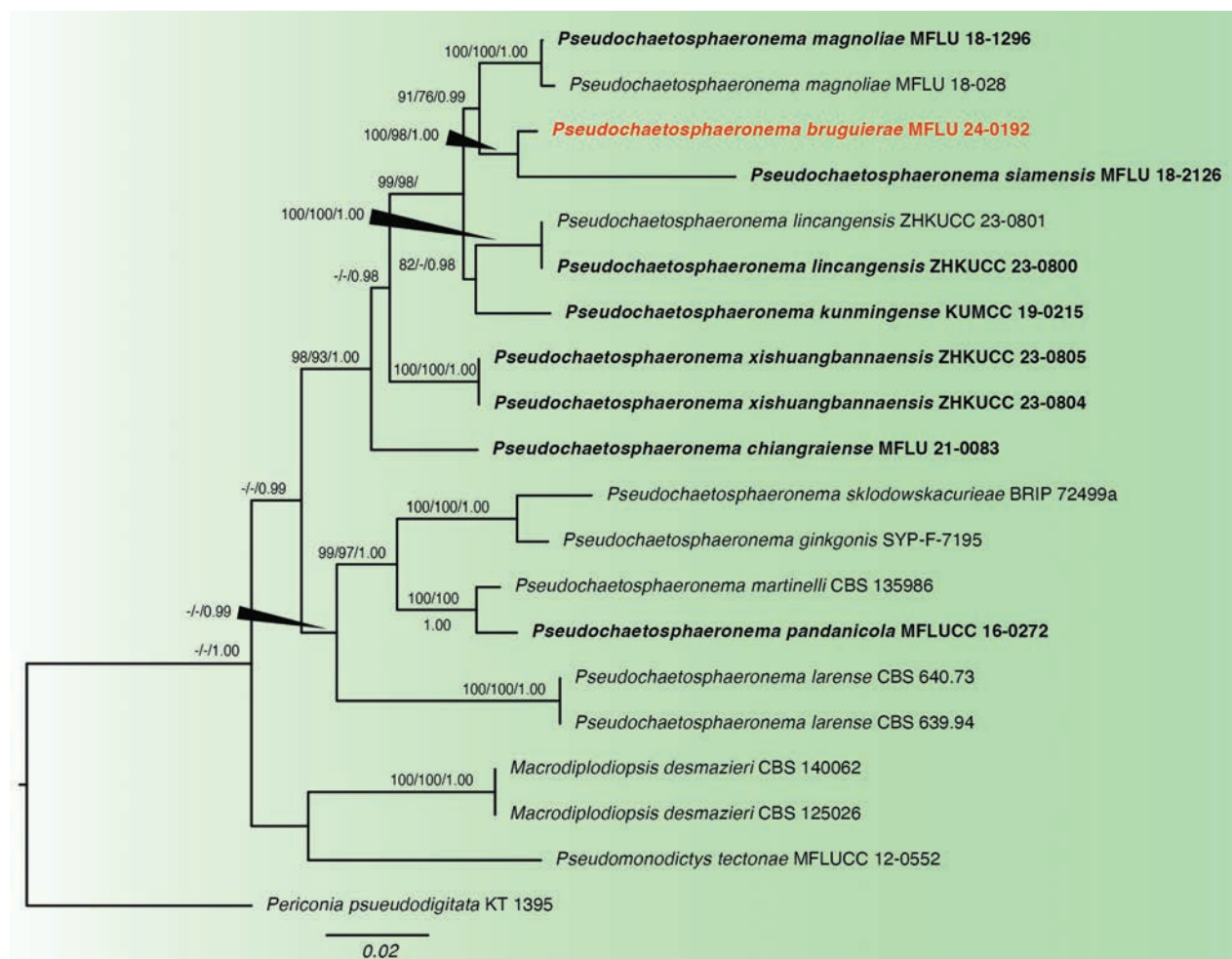


**Figure 5.** Phylogram of the combined ITS, LSU, SSU and *tef1-α* analysis of *Pseudochaetosphaeronema* and related genera. Values above the branches indicate bootstrap support values from maximum likelihood (ML) and maximum parsimony (MP) equal to or above 0.70 and Bayesian posterior probability (PP) equal to or above 0.90. The novel species is indicated in bold red. Sequences from type species are indicated in bold. The tree is rooted with *Periconia pseudodigitata*.

Based on the ML, MP, and BI analyses, *Pseudochaetosphaeronema bruguierae* is found in a distinct, well-supported clade with *Pseudochaetosphaeronema siamensis* as the sister taxon (Fig. 5). Notably, *P. siamensis* has a significantly longer branch length compared to *P. bruguierae*. Base differences in their sequences are also higher than 1.5%. In addition, *P. bruguierae* and *P. siamensis* differ in morphology of their conidiogenous cells and conidia, as discussed in the taxonomy notes.

***Pseudochaetosphaeronema bruguierae* Apurillo, Phukhams., E.B.G Jones & K.D. Hyde, sp. nov.**

Index Fungorum: IF902579

Facesoffungi Number: FoF16491

Fig. 6

**Etymology.** Based on the host *Bruguiera cylindrica*.

**Holotype.** MFLU 24-0192.

**Description.** *Saprobic* on aerial dead branch of *Bruguiera cylindrica*. **Sexual morph:** Undetermined. **Asexual morph:** Coelomycetous. **Conidiomata** 230–400 × 300–370 µm diameter ( $\bar{x}$  = 344.5 × 339.0 µm, n = 10), dark brown to black, immersed to erumpent, solitary to gregarious, globose to subglobose, without ostiole. **Conidiomata wall** 22–66 µm, composed of dark brown, thick-walled cells. **Conidiophores** reduced to conidiogenous cells. **Conidiogenous cells** 7–10 µm × 1–2.7 µm ( $\bar{x}$  = 10.2 × 1.7 µm, n = 20), hyaline, cylindrical or ampulliform, monophialidic, smooth. **Conidia** 5–10 × 2–3 µm ( $\bar{x}$  = 6.5 × 2.2 µm, n = 30), hyaline to pale brown, fusiform, 2–3 septate, with constriction in the septa, with 26 guttules.

**Known distribution.** Thailand.

**Culture characteristics.** Conidia germinate in MEA within 24 hours, with germ tubes arising from one end of the conidia. Colonies on MEA grow up to 30 cm after 3 weeks of incubation at room temperature, circular, white, with light green pigment, flat or effuse, entire edge, reverse exhibits a dark green to pale brown pigmentation.

**Material examined.** THAILAND • Prachuap Khiri Khan Province: Pranburi District, 12°24'48"N, 99°56'51"E, on aerial dead branch of *Bruguiera cylindrica* (Rhizophoraceae), 25 October 2022, Carlo Chris S. Apurillo, P11601 (MFLU 24-0192, **holotype**), ex-type living culture MFLUCC 24-0515.

**Genbank Numbers.** ITS: PP989295, LSU: PP989290, SSU: PP989296, *tef1-α*: PQ273803.

**Notes.** Based on a combined phylogenetic analysis of ITS, LSU, SSU, and *tef1-α* sequence data, *Pseudochaetosphaeronema bruguierae* formed a clade with *Pseudochaetosphaeronema siamensis*, with the latter showing longer branch length. Base pair comparison of ITS and *tef1-α* sequences revealed a 1.8% and 15% difference, respectively. The most significant difference between the two closely related species is their conidial morphology. *Pseudochaetosphaeronema bruguierae* has larger conidia (6.5 × 2.2 µm) which are fusiform, septate, with multiple guttules. In contrast, *Pseudochaetosphaeronema siamensis* has smaller conidia (3 × 2 µm) which are subglobose to oval without septation (Jayasiri et al. 2019). Furthermore, the conidiogenous cells of *Pseudochaetosphaeronema siamensis* are cylindrical with collarettes at the tips, while some appear flask-shaped with no collarettes for *Pseudochaetosphaeronema bruguierae* (Jayasiri et al. 2019). The conidiomata of *Pseudochaetosphaeronema bruguierae* is also larger than that of *Pseudochaetosphaeronema siamensis*. *Pseudochaetosphaeronema bruguierae* is similar to *Pseudochaetosphaeronema magnoliae* but they are phylogenetically distinct, with *P. magnoliae* forming a sister clade to *P. bruguierae* and *P. siamensis* (De Silva et al. 2022). Furthermore, *P. bruguierae* and *P. magnoliae* have a higher pairwise difference in the ITS sequences (9.3%). Although the shape of conidiogenous cells and the conidia of *P. bruguierae* and *P. magnoliae* are similar, they differ in terms of size, with *P. bruguierae* having larger conidiogenous cells and smaller conidia. Additionally, the conidia of *P. bruguierae* are septate with pronounced multiple guttules, which are not observed in the conidia of *P. magnoliae*. These support the introduction of *Pseudochaetosphaeronema bruguierae* as a novel species in *Pseudochaetosphaeronema* following the guidelines of Jeewon and Hyde (2016) and Maharachchikumbura et al. (2021).



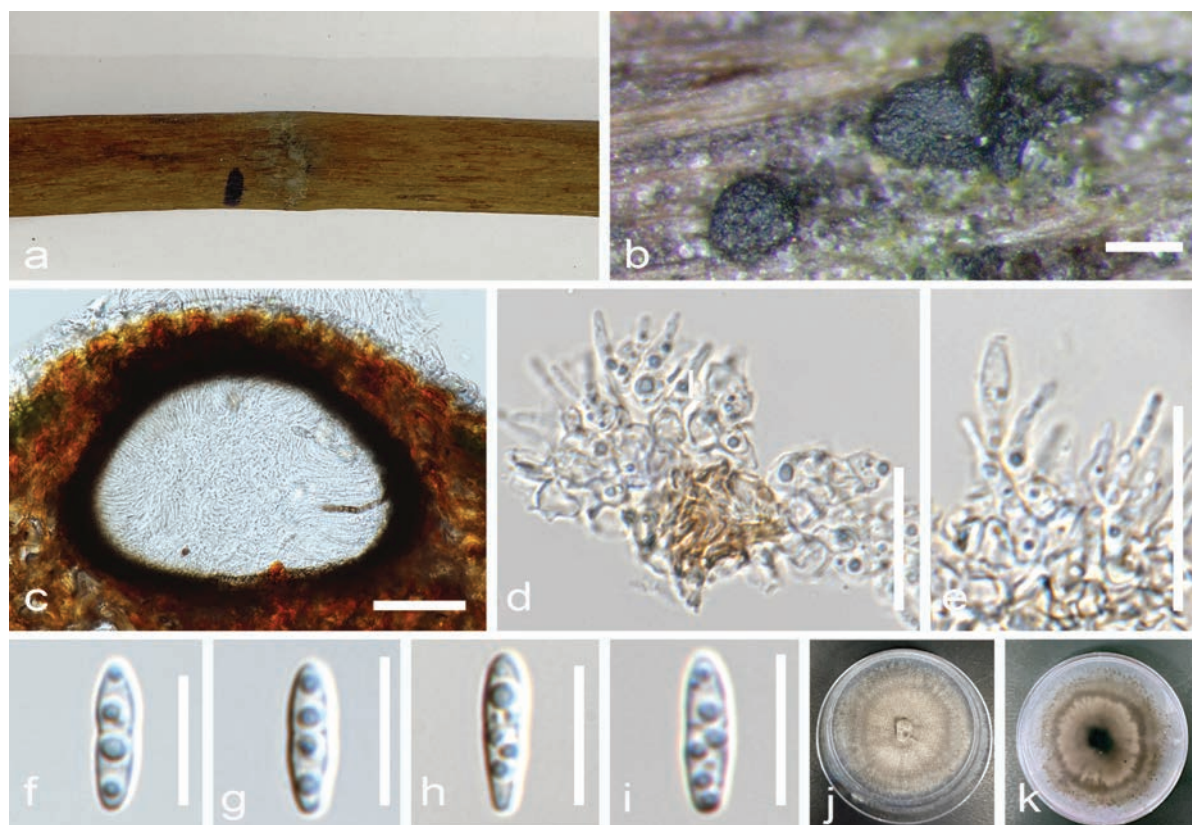


**Figure 6.** *Pseudochaetosphaeronema bruguierae* (MFLU 24-0192, holotype). **a** host **b** conidiomata on host **c** section of conidioma **d, e** conidiogenous cells **f–i** conidia **j** culture on MEA (obverse) **k** culture on MEA (reverse). Scale bars: 500 µm (**b**); 100 µm (**c**); 50 µm (**d, e**); 20 µm (**f**); 10 µm (**g–i**).

#### **Pleosporales Luttr. ex M.E. Barr**

**Aigialaceae Suetrong, Sakay, E.B.G. Jones, Kohlm., Volkm.-Kohlm. & C.L. Schoch**  
**Rimora Kohlm., Volkm.-Kohlm., Suetrong, Sakay & E.B.G. Jones**

Multi-locus analysis of *Rimora* was done using LSU, SSU and *tef1-α*. The alignment of concatenated sequences had a total length of 2,797 characters, including gaps. The specific lengths of each locus are as follows: LSU (1-853), SSU (854-1,876), *tef1-α* (1,877-2,797). In ML, the alignment has 720 distinct alignment patterns with 13.99% gaps and completely undetermined characters. After the analysis, the best-scoring ML tree (Fig. 5) had a final optimization value of -10,511.38, alpha = 0.162554 and tree length of 0.579899. The base frequencies are: A = 0.246335, C = 0.243918, G = 0.280712, and T = 0.229035 with the following substitution rates: AC = 1.97470, AG = 3.553768, AT = 1.000390, CG = 1.272768, CT = 13.114709 and GT = 1.00000.

For the BI analysis, different models were applied for each locus as follows: GTR+G for LSU and *tef1-α* and K2P+G+I for SSU. After the total MCMC generations, the average standard deviation of split frequencies is 0.003756. Analysis of trace files in Tracer showed ESS values ranging from 8,004 to 15,002 for the combined runs with the two independent runs showing convergence based on the plots. The topology of the BI tree was similar to the best-scoring ML tree (Fig. 5).

Based on the ML and BI multi-locus analyses, *Rimora mangrovei* MFLU 24-0193 is in a distinct clade with good support together with the holotype and other strains of *Rimora mangrovei* (Fig. 7). This strain, isolated from *Ceriops tagal*, represents a new host record for *Rimora mangrovei*.

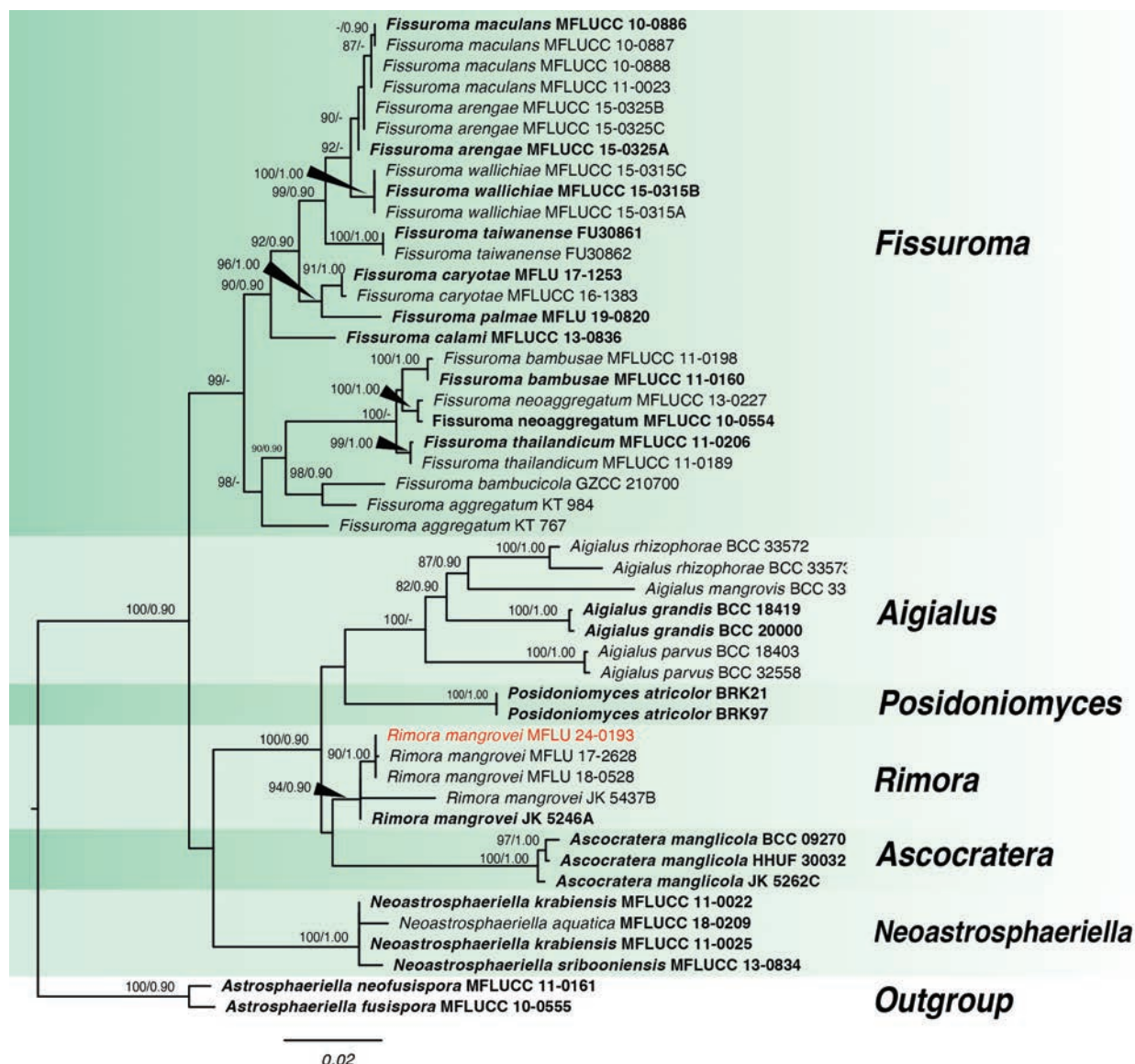


**Figure 7.** Phylogram of *Rimora* and closely-related genera based on a combined dataset of LSU, SSU and *tef1-α*. Values above the branches indicate bootstrap support from Maximum Likelihood (ML) and Bayesian posterior probability (PP). New record is indicated in red. Sequences from type species are indicated in bold. The tree is rooted with *Astroasphaeriella* species.

***Rimora mangrovei* (Kohlm. & Vittal) Kohlm., Volkm.-Kohlm., Suetrong, Sakay. & E.B.G. Jones**

Index Fungorum: IF515959

MycoBank No: 515959

Facesoffungi Number: FoF08152

Fig. 8

**Description.** *Saprobic* on decomposing wood of *Ceriops tagal* submerged in brackish water. **Sexual morph:** *Ascomata* 336–634 µm × 200–483 ( $\bar{x}$  = 494 µm × 329 µm, n = 10) wide, globose to subglobose, black, carbonaceous, solitary to gregarious, immersed at first then later erumpent, with cleft-like ostiole, epapillate. **Peridium** 73–162 µm ( $\bar{x}$  = 112 µm, n = 10) thick, cells forming textura angularis. **Pseudoparaphyses** up to 2 µm, trabeculate (*sensu* Liew et al. 2000), branched, numerous. **Asci** 175–181 × 9–15 µm ( $\bar{x}$  = 178.8 × 12.4 µm,



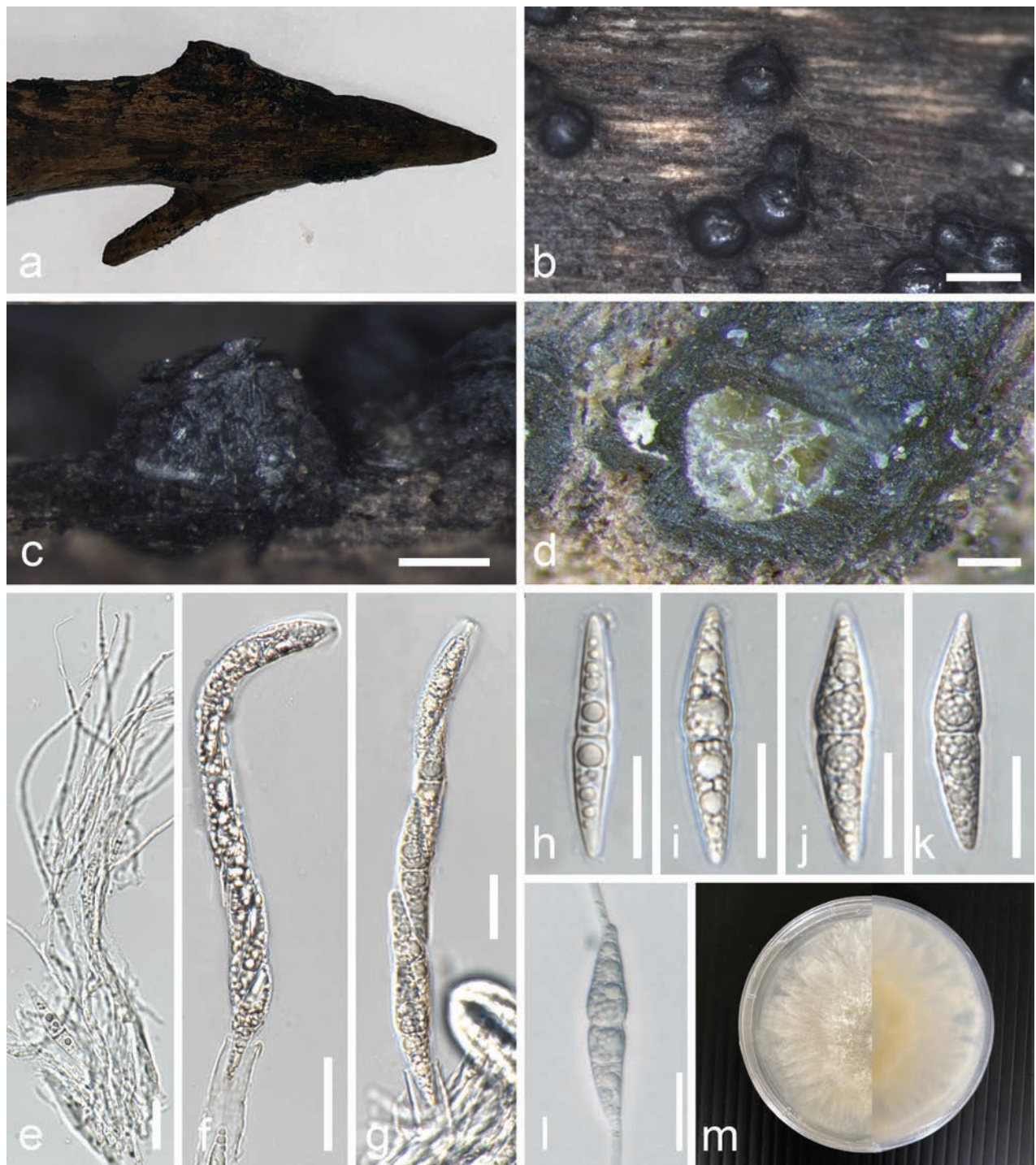


**Figure 8.** *Rimora mangrovei* (MFLU 24-0193). **a** host **b, c** ascomata on host **d** section of ascoma on host **e** paraphyses **f** immature ascus **g** mature ascus **h–k** ascospores **l** Germinated ascospore. **m** Colony on PDA. Scale bars: 500  $\mu\text{m}$  (**b**); 200  $\mu\text{m}$  (**c**); 250  $\mu\text{m}$  (**d**); 20  $\mu\text{m}$  (**e–l**).

$n = 10$ ), 8-spored, bitunicate, cylindrical, short pedicellate, with an apical apparatus. **Ascospores** 40–47  $\mu\text{m} \times 7$ –11  $\mu\text{m}$  ( $\bar{x} = 46.7 \times 8.9 \mu\text{m}$ ,  $n = 20$ ), fusiform, hyaline, biseriate, 1-septate, constricted at the septum, with multiple prominent guttules. **Asexual morph:** Undetermined.

**Known distribution.** Thailand.

**Culture characteristics.** Ascospores germinate in MEA within 24 hours, with germ tubes arising from one end of the ascospore. Colonies on MEA grow up to 6 cm after 14 days of incubation at room temperature, white, raised, fimbriated edge, reverse with light yellow pigment at the center which does not spread to the periphery.

**Material examined.** THAILAND • Prachuap Khiri Khan Province: Pranburi District, 12°24'48.672"N, 99°56'51.47"E, on decomposing wood of *Ceriops tagal* (Rhizophoraceae) submerged in brackish water, 25 October 2022, by Carlo Chris S. Apurillo, P10705 (MFLU 24-0193), ex-type living culture MFLUCC 24-0516.

**GenBank Numbers.** ITS: PP989293, LSU: PP989289, SSU: PP989297.

**Notes.** Based on a combined analysis of LSU, SSU and *tef1-α* sequences, *Rimora mangrovei* MFLU 24-0193 formed a well-supported clade with the holotype and other strains of *Rimora mangrovei* in Aigialaceae. This study identifies new characteristics not previously described for this species, including the presence of an apical apparatus in the asci and 1-septate ascospores with multiple prominent guttules. *Rimora mangrovei* has been reported from various mangrove hosts such as *Avicennia* species, *Bruguiera gymnorhiza*, *Ceriops decandra*, *Nypa fruticans*, *Rhizophora* species, and *Sonneratia* species across countries in the Atlantic, Indian and Pacific regions (Devadatha et al. 2021). This is the first record of isolation of *Rimora mangrovei* from *Ceriops tagal* in Prachuap Khiri Khan, Thailand.

## Discussion

In this study, we introduce one novel genus, three novel species and one new record of fungi isolated from mangroves in Thailand. Two of these, *Pseudomelanconiella mangrovei* and *Pseudochaetosphaeronema bruguierae*, belong to genera not previously reported from mangroves. Based on morphological and molecular data, we establish *Pseudomelanconiella* as a novel genus in Melanconiellaceae (Diaporthales). This family is typified by *Melanconiella*, and also includes *Dicarpella*, *Greeneria*, *Melanconiella*, and *Microascospora* (Senanayake et al. 2017). Later additions included *Sheathospora* (Fan et al. 2018), *Septomelanconiella* (Phookamsak et al. 2019), *Paraphomopsis* (Udayanga et al. 2021), and most recently, *Sinodiscula* (Guo et al. 2024). Except for *Septomelanconiella*, all genera in this family contain species that cause plant diseases such as canker, dieback, leaf blight, and anthracnose (Du et al. 2017; Fan et al. 2018; Udayanga et al. 2021; Guo et al. 2024). However, *Pseudomelanconiella* is unique in being a saprobe in mangrove environments rather than a pathogen. While it groups with *Septomelanconiella*, it is distinct both morphologically and ecologically. Notably, it thrives in intertidal zones—an environment not previously reported for the family Melanconiellaceae.

*Melanconiella loropetali* is reclassified as *Sinodiscula loropetali* and *Melanconiella camelliae* was synonymized with *Sinodiscula camellicola*. *Melanconiella* species, typically found in Europe and North America on Betulaceae, have a narrow host and geographical range (Voglmayr et al. 2012). However, *M. syzygii* was reported from *Syzygium* sp. in Malaysia, the first time this genus was isolated outside Europe and North America from a different host (Crous et al. 2016). *Melanconiella loropetali* and *M. camelliae* were also introduced to expand the host

range of the genus (Mu et al. 2023). Our analysis confirms that *M. loropetali*, *M. camelliae* and *M. syzygii* do not belong to *Melanconiella*, thereby restricting the genus again to Betulaceae hosts (Voglmayr et al. 2012; Fan et al. 2018).

*Peroneutypa hibisci*, a novel species, is also introduced in a genus with 43 known species (Index Fungorum 2024). Only two *Peroneutypa* species are from mangroves: *P. mangrovei* and *P. scoparia* while another two were reported from *Suaeda* plants in saline habitats: *P. indica* and *P. polysporae* (Jones et al. 2019; Devadatha et al. 2021). Our analysis groups *P. hibisci*, *P. mangrovei*, and *P. polysporae* together, suggesting that *Peroneutypa* species adapted to brackish or marine environments may have diverged separately from fungi in other ecological niches. For instance, these species may exhibit specialized traits such as salt tolerance or unique metabolic pathways for nutrient acquisition in saline conditions, distinguishing them from terrestrial *Peroneutypa* species that thrive in freshwater or soil habitats.

*Pseudochaetosphaeronema bruguierae* is also a novel species, the first in the genus to be reported from mangroves. *Pseudochaetosphaeronema* was established in 1979 to accommodate *P. larense* ( $\equiv$  *Chaetosphaeronema larense*), a pathogenic fungus isolated from human foot (Punithalingham 1979). This remained a monotypic genus until 2015 when Ahmed et al. (2015) introduced *Pseudochaetosphaeronema martinelli*, isolated as a pathogen in immunosuppressed humans. Currently, there are 12 species recorded for this genus, many of which have been isolated as saprobes of terrestrial plants and soil (Phookamsak et al. 2019; Boonmee et al. 2021; Tan and Shivas 2022; Xu et al. 2024). Although *Pseudochaetosphaeronema* is known as a human pathogen due to the first two species introduced, the other members of this genus are saprobes. Notably, none have been isolated from mangroves. In this study, *Pseudochaetosphaeronema bruguierae* was isolated from the dead branch of a mangrove that was not submerged in brackish water, thus, it is not considered a marine fungus. Currently, there is no evidence that the isolate can survive in a saline environment. Initially classified as *incertae sedis* in Pleosporales (Dothideomycetes), *Pseudochaetosphaeronema* was later accepted under Macrodiploidiopsidaceae (Pleosporales) by Wijayawardene et al. (2022).

*Rimora mangrovei* is introduced with *Ceriops tagal* as a new host record. *Rimora* is a monotypic genus typified by *Rimora mangrovei* (Suetrong et al. 2009). *Rimora* is one of three genera in Aigialaceae alongside *Aigialus* and *Ascocratera*, whose type species were first isolated from mangroves (Kohlmeyer and Schatz 1985; Kohlmeyer 1986). Another species in Aigialaceae, *Posidoniomyces atricolor*, the only species in the genus, was isolated as an endophyte of seagrass (Vohník et al. 2019). These examples highlight that many members of Aigialaceae can survive in marine environment, establishing it as a well-known marine family. The addition of a new record from mangroves in this family further confirms the ecological niche of Aigialaceae.

In conclusion, this study underscores the vital importance of ongoing exploration in mangrove ecosystems to uncover the diverse fungal species and their significance (Hyde and Lee 1995; Rampadarath et al. 2018). Despite considerable research, numerous fungal species in mangroves remain undiscovered. The discovery of novel genus and species, such as *Pseudomelanconiella*, *Peroneutypa*, *Pseudochaetosphaeronema*, highlights the species richness of these environments. Further exploration is crucial not only for taxonomic understanding



but also for discovering potential bioactive compounds with pharmaceutical and biotechnological applications. Indeed, many fungi from mangroves, including endophytes, have been reported to possess bioactive compounds with antibacterial, antimutagenic, and antioxidant properties among others (Dela Cruz et al. 2020; Cadamuro et al. 2021; Sopalun et al. 2021). This study emphasizes the necessity of sustained efforts in studying mangrove fungi, both as a means of understanding ecological interactions and for potential beneficial discoveries.

## Acknowledgments

CCS Apurillo would like to thank the following: Mae Fah Luang University for the partial PhD scholarship (GR-ST-PS-65-21); the Philippines Department of Science and Technology-Philippine Science High School-Eastern Visayas Campus for the study leave grant; and Thailand Department of National Parks, Wildlife and Plant Conservation for the permission granted to study in National and Forest Parks (No. 0907.4/23579). Gareth Jones is supported under the Distinguished Scientist Fellowship Program (DSFP), King Saud University, Kingdom of Saudi Arabia. We also thank Dr. Shaun Pennycook for the Latin name check.

## Additional information

### Conflict of interest

The authors have declared that no competing interests exist.

### Ethical statement

No ethical statement was reported.

### Funding

This study was funded by the Mushroom Research Foundation and Chinese Research Fund (CRF) grant number E1644111K1-Flexible introduction of high-level expert program-Kevin David Hyde to Kunming Institute of Botany, Chinese Academy of Sciences.

### Author contributions


Conceptualization: KDH, CCSA, EBGJ. Data curation: CCSA. Formal analysis: CCSA. Funding acquisition: CP, VT, KDH, EBGJ. Investigation: EBGJ, CCSA, CP. Methodology: CCSA. Project administration: KDH, VT. Supervision: EBGJ, KDH, CP, VT. Validation: EBGJ, VT, CP, KDH, CCSA. Visualization: CCSA. Writing - original draft: CCSA. Writing - review and editing: KDH, CP, CCSA, VT, EBGJ.


### Author ORCIDs

Carlo Chris S. Apurillo  <https://orcid.org/0000-0003-4348-0887>

Chayanard Phukhamsakda  <https://orcid.org/0000-0002-1033-937X>

Kevin D. Hyde  <https://orcid.org/0000-0002-2191-0762>

Vinodhini Thiyagaraja  <https://orcid.org/0000-0002-8091-4579>

E. B. Gareth Jones  <https://orcid.org/0000-0002-7286-5471>

### Data availability

All of the data that support the findings of this study are available in the main text or Supplementary Information.

## References

- Ahmed SA, Desbois N, Quist D, Miossec C, Atoche C, Bonifaz A, De Hoog GS (2015) Phaeohyphomycosis caused by a novel species, *Pseudochaetosphaeronema martinelli*. *Journal of Clinical Microbiology* 53(9): 2927–2934. <https://doi.org/10.1128/JCM.01456-15>
- Bhunjun CS, Niskanen T, Suwannarach N, Wannathes N, Chen YJ, McKenzie EHC, Maharachchikumbura SSN, Buyck B, Zhao CL, Fan YG, Zhang JY, Dissanayake AJ, Marasinghe DS, Jayawardena RS, Kumla J, Padamsee M, Chen YY, Liimatainen K, Ammirati JF, Phukhamsakda C, Liu JK, Phonrob W, Randrianjohany É, Hongsan S, Cheewangkoon R, Bundhun D, Khuna S, Yu WJ, Deng LS, Lu YZ, Hyde KD, Lumyong S (2022) The numbers of fungi: Are the most speciose genera truly diverse? *Fungal Diversity* 114(1): 387–462. <https://doi.org/10.1007/s13225-022-00501-4>
- Boonmee S, Wanasinghe DN, Calabon MS, Huanraluek N, Chandrasiri SKU, Jones GEB, Rossi W, Leonardi M, Singh SK, Rana S, Singh PN, Maurya DK, Lagashetti AC, Choudhary D, Yu CD, Zhao CL, Mu YH, Yuan HS, He SH, Phookamsak R, Jiang HB, Martín MP, Dueñas M, Telleria MT, Kałucka IL, Jagodziński AM, Liimatainen K, Pereira DS, Phillips AJL, Suwannarach N, Kumla J, Khuna S, Lumyong S, Potter TB, Shivas RG, Sparks AH, Vaghefi N, Abdel-Wahab MA, Abdel-Aziz FA, Li GJ, Lin WF, Singh U, Bhatt RP, Lee HB, Nguyen TTT, Kirk PM, Dutta AK, Acharya K, Sarma VV, Niranjana M, Rajeshkumar KC, Ashtekar N, Lad S, Wijayawardene NN, Bhat DJ, Xu R, Wijesinghe SN, Shen HW, Luo ZL, Zhang JY, Sysouphanthong P, Thongklang N, Bao DF, Aluthmuhandiram JVS, Abdollahzadeh J, Javadi A, Dovana F, Usman M, Khalid AN, Dissanayake AJ, Telagathoti A, Probst M, Peintner U, Garrido-Benavent I, Bóna L, Merényi Z, Boros L, Zoltán B, Stielow JB, Jiang N, Tian CM, Shams E, Dehghanizadeh F, Pordel A, Javan-Nikkhah M, Denchev TT, Denchev CM, Kemler M, Begerow D, Deng CY, Harrower E, Bozovov T, Kholmuradova T, Gafforov Y, Abdurazakov A, Xu JC, Mortimer PE, Ren GC, Jeewon R, Maharachchikumbura SSN, Phukhamsakda C, Mapook A, Hyde KD (2021) Fungal diversity notes 1387–1511: Taxonomic and phylogenetic contributions on genera and species of fungal taxa. *Fungal Diversity* 111(1): 1–335. <https://doi.org/10.1007/s13225-021-00489-3>
- Cadamuro RD, Da Silveira Bastos IMA, Silva IT, Da Cruz ACC, Robl D, Sandjo LP, Alves Jr S, Lorenzo JM, Rodríguez-Lázaro D, Treichel H, Steindel M, Fongaro G (2021) Bioactive compounds from mangrove endophytic fungus and their uses for microorganism control. *Journal of Fungi (Basel, Switzerland)* 7(6): 455. <https://doi.org/10.3390/jof7060455>
- Carbone I, Kohn LM (1999) A method for designing primer sets for speciation studies in filamentous ascomycetes. *Mycologia* 91(3): 553–556. <https://doi.org/10.1080/00275514.1999.12061051>
- Chen S, Cai R, Liu Z, Cui H, She Z (2022) Secondary metabolites from mangrove-associated fungi: Source, chemistry and bioactivities. *Natural Product Reports* 39(3): 560–595. <https://doi.org/10.1039/D1NP00041A>
- Chomnunti P, Hongsan S, Aguirre-Hudson B, Tian Q, Peršoh D, Dhami MK, Alias AS, Xu J, Liu X, Stadler M, Hyde KD (2014) The sooty moulds. *Fungal Diversity* 66(1): 1–36. <https://doi.org/10.1007/s13225-014-0278-5>
- Cribb A, Cribb J (1955) Marine fungi from Queensland-1. University of Queensland Papers. Department of Botany 3: 77–81.
- Criscuolo A, Gribaldo S (2010) BMGE (Block Mapping and Gathering with Entropy): A new software for selection of phylogenetic informative regions from multiple sequence alignments. *BMC Evolutionary Biology* 10(1): 210. <https://doi.org/10.1186/1471-2148-10-210>

- Crous PW, Wingfield MJ, Burgess TI, Hardy GESTJ, Crane C, Barrett S, Cano-Lira JF, Leroux JJ, Thangavel R, Guarro J, Stchigel AM, Martín MP, Alfredo DS, Barber PA, Barreto RW, Baseia IG, Cano-Canals J, Cheewangkoon R, Ferreira RJ, Gené J, Lechat C, Moreno G, Roets F, Shivas RG, Sousa JO, Tan YP, Wiederhold NP, Abell SE, Accioly T, Albizu JL, Alves JL, Antoniolli ZI, Aplin N, Araújo J, Arzanlou M, Bezerra JDP, Bouchara J-P, Carlavilla JR, Castillo A, Castroagudín VL, Ceresini PC, Claridge GF, Coelho G, Coimbra VRM, Costa LA, Da Cunha KC, Da Silva SS, Daniel R, De Beer ZW, Dueñas M, Edwards J, Enwistle P, Fiuza PO, Fournier J, García D, Gibertoni TB, Giraud S, Guevara-Suarez M, Gusmão LFP, Haituk S, Heykoop M, Hirooka Y, Hofmann TA, Houbroken J, Hughes DP, Kautmanová I, Koppel O, Koukol O, Larsson E, Latha KPD, Lee DH, Lisboa DO, Lisboa WS, López-Villalba Á, Maciel JLN, Manimohan P, Manjón JL, Marincowitz S, Marney TS, Meijer M, Miller AN, Olariaga I, Paiva LM, Piepenbring M, Poveda-Molero JC, Raj KNA, Raja HA, Rougeron A, Salcedo I, Samadi R, Santos TAB, Scarlett K, Seifert KA, Shuttleworth LA, Silva GA, Silva M, Siqueira JPZ, Souza-Motta CM, Stephenson SL (2016) Fungal Planet description sheets: 469–557. *Persoonia - Molecular Phylogeny and Evolution of Fungi* 37: 218–403. <https://doi.org/10.3767/003158516X694499>
- Dayarathne M, Jones EBG, Maharachchikumbura SSN, Devadatha B, Sarma VV, Khongphinitbunjong K, Chomnunti P, Hyde KD (2020) Morpho-molecular characterization of microfungi associated with marine based habitats. *Mycosphere* 11(1): 1–188. <https://doi.org/10.5943/mycosphere/11/1/1>
- De Silva N, Hyde K, Lumyong S, Phillips A, Bhat D, Maharachchikumbura S, Thambugala K, Tennakoon D, Suwannarach N, Karunarathna S (2022) Morphology, phylogeny, host association and geography of fungi associated with plants of Annonaceae, Apocynaceae and Magnoliaceae. *Mycosphere* 13(1): 955–1076. <https://doi.org/10.5943/mycosphere/13/1/12>
- Dela Cruz TEE, Notarte KIR, Apurillo CCS, Tarman K, Bungihan ME (2020) Biomineral fungal endophytes from tropical plants and seaweeds for drug discovery. *Biodiversity and Biomedicine*. Elsevier, 51–62. <https://doi.org/10.1016/B978-0-12-819541-3.00004-9>
- Devadatha B, Jones EBG, Pang KL, Abdel-Wahab MA, Hyde KD, Sakayaroj J, Bahkali AH, Calabon MS, Sarma VV, Suetrong S, Zhang SN (2021) Occurrence and geographical distribution of mangrove fungi. *Fungal Diversity* 106(1): 137–227. <https://doi.org/10.1007/s13225-020-00468-0>
- Du Z, Fan XL, Yang Q, Tian CM (2017) Host and geographic range extensions of *Melanconiella*, with a new species *M. cornuta* in China. *Phytotaxa* 327(3): 252. <https://doi.org/10.11646/phytotaxa.327.3.4>
- Fan X, Du Z, Bezerra JDP, Tian C (2018) Taxonomic circumscription of melanconis-like fungi causing canker disease in China. *MycKeys* 42: 89–124. <https://doi.org/10.3897/mycokeys.42.29634>
- Glass NL, Donaldson GC (1995) Development of primer sets designed for use with the PCR to amplify conserved genes from filamentous ascomycetes. *Applied and Environmental Microbiology* 61(4): 1323–1330. <https://doi.org/10.1128/aem.61.4.1323-1330.1995>
- Guo M, Zhao S, Gao Y, Shen X, Hou C (2024) A phylogenetic and taxonomic revision of *Discula theae-sinensis*, the causal agents of anthracnose on *Camellia sinensis*. *Journal of Fungi* (Basel, Switzerland) 10(2): 141. <https://doi.org/10.3390/jof10020141>
- Hyde KD, Jones EBG (1988) Marine mangrove fungi. *Marine Ecology* (Berlin) 9(1): 15–33. <https://doi.org/10.1111/j.1439-0485.1988.tb00196.x>
- Hyde KD, Lee SY (1995) Ecology of mangrove fungi and their role in nutrient cycling: What gaps occur in our knowledge? *Hydrobiologia* 295(1–3): 107–118. <https://doi.org/10.1007/BF00029117>

- Hyde KD, Jeewon R, Chen YJ, Bhunjun CS, Calabon MS, Jiang HB, Lin CG, Norphanphoun C, Sysouphanthong P, Pem D, Tibpromma S, Zhang Q, Doilom M, Jayawardena RS, Liu JK, Maharachchikumbura SSN, Phukhamsakda C, Phookamsak R, Al-Sadi AM, Thongklang N, Wang Y, Gafforov Y, Jones EBG, Lumyong S (2020) The numbers of fungi: Is the descriptive curve flattening? *Fungal Diversity* 103(1): 219–271. <https://doi.org/10.1007/s13225-020-00458-2>
- Hyde KD, Baldrian P, Chen Y, Thilini Chethana KW, De Hoog S, Doilom M, De Farias ARG, Gonçalves MFM, Gonkhom D, Gui H, Hilário S, Hu Y, Jayawardena RS, Khyaju S, Kirk PM, Kohout P, Luangharn T, Maharachchikumbura SSN, Manawasinghe IS, Mortimer PE, Niego AGT, Phonemany M, Sandargo B, Senanayake IC, Stadler M, Surup F, Thongklang N, Wanasinghe DN, Bahkali AH, Walker A (2024) Current trends, limitations and future research in the fungi? *Fungal Diversity* 125(1): 1–71. <https://doi.org/10.1007/s13225-023-00532-5>
- Index Fungorum (2024) Index Fungorum. <https://www.indexfungorum.org/> [April 22, 2024]
- Jaklitsch WM, Komon M, Kubicek CP, Druzhinina IS (2005) *Hypocrea voglmayrii* sp. nov. from the Austrian Alps represents a new phylogenetic clade in *Hypocrea/Trichoderma*. *Mycologia* 97(6): 1365–1376. <https://doi.org/10.1080/15572536.2006.11832743>
- Jayasiri SC, Hyde KD, Ariyawansa HA, Bhat J, Buyck B, Cai L, Dai Y-C, Abd-Elsalam KA, Ertz D, Hidayat I, Jeewon R, Jones EBG, Bahkali AH, Karunarathna SC, Liu J-K, Luangsa-ard JJ, Lumbsch HT, Maharachchikumbura SSN, McKenzie EHC, Moncalvo J-M, Ghobad-Nejhad M, Nilsson H, Pang K-L, Pereira OL, Phillips AJL, Raspé O, Rollins AW, Romero AI, Etayo J, Selçuk F, Stephenson SL, Suetrong S, Taylor JE, Tsui CKM, Vizzini A, Abdel-Wahab MA, Wen T-C, Boonmee S, Dai DQ, Daranagama DA, Dissanayake AJ, Ekanayaka AH, Fryar SC, Hongsanan S, Jayawardena RS, Li W-J, Perera RH, Phookamsak R, De Silva NI, Thambugala KM, Tian Q, Wijayawardene NN, Zhao R-L, Zhao Q, Kang J-C, Promputtha I (2015) The Faces of Fungi database: Fungal names linked with morphology, phylogeny and human impacts. *Fungal Diversity* 74(1): 3–18. <https://doi.org/10.1007/s13225-015-0351-8>
- Jayasiri S, Hyde K, Jones EBG, McKenzie E, Jeewon R, Phillips A, Bhat D, Wanasinghe D, Liu J, Lu Y, Kang J, Xu J, Karunarathna S (2019) Diversity, morphology and molecular phylogeny of Dothideomycetes on decaying wild seed pods and fruits. *Mycosphere : Journal of Fungal Biology* 10(1): 1–186. <https://doi.org/10.5943/mycosphere/10/1/1>
- Jeewon R, Hyde KD (2016) Establishing species boundaries and new taxa among fungi: Recommendations to resolve taxonomic ambiguities. *Mycosphere* 7(11): 1669–1677. <https://doi.org/10.5943/mycosphere/7/11/4>
- Jia S-L, Chi Z, Liu G-L, Hu Z, Chi Z-M (2020) Fungi in mangrove ecosystems and their potential applications. *Critical Reviews in Biotechnology* 40(6): 852–864. <https://doi.org/10.1080/07388551.2020.1789063>
- Jones EBG, Alias SA (1997) Biodiversity of mangrove fungi. In: Hyde KD (Ed.) *Biodiversity of Tropical Microfungi*. Hongkong University Press, Hongkong, 71–92.
- Jones EBG, Pang KL, Abdel-Wahab MA, Scholz B, Hyde KD, Boekhout T, Ebel R, Rateb ME, Henderson L, Sakayaroj J, Suetrong S, Dayarathne MC, Kumar V, Raghukumar S, Sridhar KR, Bahkali AHA, Gleason FH, Norphanphoun C (2019) An online resource for marine fungi. *Fungal Diversity* 96(1): 347–433. <https://doi.org/10.1007/s13225-019-00426-5>
- Katoh K, Standley D (2013) MAFFT Multiple Sequence Alignment Software Version 7: Improvements in performance and usability. *Molecular Biology and Evolution* 30(4): 772–780. <https://doi.org/10.1093/molbev/mst010>
- Kohlmeyer J (1968) Marine fungi from the tropics. *Mycologia* 60(2): 252–270. <https://doi.org/10.1080/00275514.1968.12018567>

- Kohlmeyer J (1986) *Ascocratera manglicola* gen. et sp. nov. and key to the marine Loculoascomycetes on mangroves. Canadian Journal of Botany 64(12): 3036–3042. <https://doi.org/10.1139/b86-401>
- Kohlmeyer J, Schatz S (1985) *Aigialus* gen.nov. (Ascomycetes) with two new marine species from mangroves. Transactions of the British Mycological Society 85(4): 699–707. [https://doi.org/10.1016/S0007-1536\(85\)80266-7](https://doi.org/10.1016/S0007-1536(85)80266-7)
- Lemoine F, Correia D, Lefort V, Doppelt-Azeroual O, Mareuil F, Cohen-Boulakia S, Gascuel O (2019) NGPhylogeny.fr: New generation phylogenetic services for non-specialists. Nucleic Acids Research 47(W1): W260–W265. <https://doi.org/10.1093/nar/gkz303>
- Liew ECY, Aptroot A, Hyde KD (2000) Phylogenetic significance of the pseudoparaphyses in Loculoascomycete Taxonomy. Molecular Phylogenetics and Evolution 16(3): 392–402. <https://doi.org/10.1006/mpev.2000.0801>
- Liu YJ, Whelen S, Hall BD (1999) Phylogenetic relationships among ascomycetes: Evidence from an RNA polymerase II subunit. Molecular Biology and Evolution 16(12): 1799–1808. <https://doi.org/10.1093/oxfordjournals.molbev.a026092>
- Madden T (2003) The BLAST Sequence Analysis Tool. The NCBI Handbook. National Center for Biotechnology Information, USA.
- Maharachchikumbura SSN, Chen Y, Ariyawansa HA, Hyde KD, Haelewaters D, Perera RH, Samarakoon MC, Wanasinghe DN, Bustamante DE, Liu JK, Lawrence DP, Cheewangkoon R, Stadler M (2021) Integrative approaches for species delimitation in Ascomycota. Fungal Diversity 109(1): 155–179. <https://doi.org/10.1007/s13225-021-00486-6>
- Mu T, Chen J, Zhao Z, Zhang W, Stephenson SL, Yang C, Zhu M, Su H, Liu P, Guan X, Qiu J (2023) Morphological and phylogenetic analyzes reveal two new species of *Melanconiella* from Fujian Province, China. Frontiers in Microbiology 14: 1229705. <https://doi.org/10.3389/fmicb.2023.1229705>
- Norphanphoun C, Raspé O, Jeewon R, Wen T-C, Hyde KD (2018) Morphological and phylogenetic characterisation of novel Cytospora species associated with mangroves. MycoKeys 38: 93–120. <https://doi.org/10.3897/mycokeys.38.28011>
- Phookamsak R, Hyde KD, Jeewon R, Bhat DJ, Jones EBG, Maharachchikumbura SSN, Raspé O, Karunarathna SC, Wanasinghe DN, Hongsan S, Doilom M, Tennakoon DS, Machado AR, Firmino AL, Ghosh A, Karunarathna A, Mešić A, Dutta AK, Thongbai B, Devadatha B, Norphanphoun C, Senwanna C, Wei D, Pem D, Ackah FK, Wang GN, Jiang HB, Madrid H, Lee HB, Goonasekara ID, Manawasinghe IS, Kušan I, Cano J, Gené J, Li J, Das K, Acharya K, Raj KNA, Latha KPD, Chethana KWT, He MQ, Dueñas M, Jadan M, Martín MP, Samarakoon MC, Dayarathne MC, Raza M, Park MS, Telleria MT, Chaiwan N, Matočec N, De Silva NI, Pereira OL, Singh PN, Manimohan P, Uniyal P, Shang QJ, Bhatt RP, Perera RH, Alvarenga RLM, Nogal-Prata S, Singh SK, Vadthanarat S, Oh SY, Huang SK, Rana S, Konta S, Paloi S, Jayasiri SC, Jeon SJ, Mehmood T, Gibertoni TB, Nguyen TTT, Singh U, Thiyagaraja V, Sarma VV, Dong W, Yu XD, Lu YZ, Lim YW, Chen Y, Tkalčec Z, Zhang ZF, Luo ZL, Daranagama DA, Thambugala KM, Tibpromma S, Camporesi E, Bulgakov TS, Dissanayake AJ, Senanayake IC, Dai DQ, Tang LZ, Khan S, Zhang H, Promputtha I, Cai L, Chomnunti P, Zhao RL, Lumyong S, Boonmee S, Wen TC, Mortimer PE, Xu J (2019) Fungal diversity notes 929–1035: Taxonomic and phylogenetic contributions on genera and species of fungi. Fungal Diversity 95(1): 1–273. <https://doi.org/10.1007/s13225-019-00421-w>
- Phukhamsakda C, Nilsson RH, Bhunjun CS, De Farias ARG, Sun YR, Wijesinghe SN, Raza M, Bao DF, Lu L, Tibpromma S, Dong W, Tennakoon DS, Tian XG, Xiong YR, Karunarathna SC, Cai L, Luo ZL, Wang Y, Manawasinghe IS, Camporesi E, Kirk PM, Promputtha I, Kuo CH, Su HY, Doilom M, Li Y, Fu YP, Hyde KD (2022) The numbers of fungi:



- Contributions from traditional taxonomic studies and challenges of metabarcoding. *Fungal Diversity* 114(1): 327–386. <https://doi.org/10.1007/s13225-022-00502-3>
- Punithalingham E (1979) Sphaeropsidales in culture from humans. *Nova Hedwigia* 31: 119–158.
- Rambaut A (2018) FigTree v1.4.4. Institute of Evolutionary Biology, University of Edinburgh, Edinburgh. <http://tree.bio.ed.ac.uk/software/figtree/>
- Rambaut A, Drummond AJ, Xie D, Baele G, Suchard MA (2018) Posterior summarization in Bayesian Phylogenetics using Tracer 1.7. *Systematic Biology* 67(5): 901–904. <https://doi.org/10.1093/sysbio/syy032>
- Rampadarath S, Bandhoa K, Puchooa D, Jeewon R, Bal S (2018) Metatranscriptomics analysis of mangroves habitats around Mauritius. *World Journal of Microbiology & Biotechnology* 34(4): 59. <https://doi.org/10.1007/s11274-018-2442-7>
- Rehner SA, Buckley E (2005) A *Beauveria* phylogeny inferred from nuclear ITS and EF1- $\alpha$  sequences: Evidence for cryptic diversification and links to *Cordyceps* teleomorphs. *Mycologia* 97(1): 84–98. <https://doi.org/10.3852/mycologia.97.1.84>
- Ronquist F, Teslenko M, van der Mark P, Ayres DL, Darling A, Höhna S, Larget B, Liu L, Suchard MA, Huelsenbeck JP (2012) MrBayes 3.2: Efficient Bayesian phylogenetic inference and model choice across a large model space. *Systematic Biology* 61(3): 539–542. <https://doi.org/10.1093/sysbio/sys029>
- Schmit J, Shearer CA (2003) A checklist of mangrove-associated fungi, their geographical distribution and known host plants. *Mycotaxon* 80: 423–477.
- Senanayake IC, Crous PW, Groenewald JZ, Maharachchikumbura SSN, Jeewon R, Phillips AJL, Bhat JD, Perera RH, Li QR, Li WJ, Tangthirasun N, Norphanphoun C, Karunarathna SC, Camporesi E, Manawasighe IS, Al-Sadi AM, Hyde KD (2017) Families of Diaporthales based on morphological and phylogenetic evidence. *Studies in Mycology* 86(1): 217–296. <https://doi.org/10.1016/j.simyco.2017.07.003>
- Senanayake I, Rathnayaka A, Marasinghe D, Calabon M, Gentekaki E, Lee H, Hurdeal V, Pem D, Dissanayake L, Wijesinghe S, Bundhun D, Nguyen T, Goonasekara I, Abeywickrama P, Bhunjun C, Jayawardena R, Wanasinghe D, Jeewon R, Bhat D, Xiang M (2020) Morphological approaches in studying fungi: Collection, examination, isolation, sporulation and preservation. *Mycosphere* 11(1): 2678–2754. <https://doi.org/10.5943/mycosphere/11/1/20>
- Sopalun K, Laosripaiboon W, Wachirachaikarn A, Iamtham S (2021) Biological potential and chemical composition of bioactive compounds from endophytic fungi associated with thai mangrove plants. *South African Journal of Botany* 141: 66–76. <https://doi.org/10.1016/j.sajb.2021.04.031>
- Stamatakis A (2014) RAxML version 8: A tool for phylogenetic analysis and post-analysis of large phylogenies. *Bioinformatics (Oxford, England)* 30(9): 1312–1313. <https://doi.org/10.1093/bioinformatics/btu033>
- Stevens F (1920) New or noteworthy Porto Rican fungi. *Botanical Gazette (Chicago, Ill.)* 70(5): 399–402. <https://doi.org/10.1086/332764>
- Suetrong S, Schoch CL, Spatafora JW, Kohlmeyer J, Volkmann-Kohlmeyer B, Sakayaroj J, Phongpaichit S, Tanaka K, Hirayama K, Jones EBG (2009) Molecular systematics of the marine Dothideomycetes. *Studies in Mycology* 64: 155–173. <https://doi.org/10.3114/sim.2009.64.09>
- Swofford D (2002) PAUP\*. Phylogenetic Analysis Using Parsimony (\*and Other Methods). Version 4.0b10. Sinauer Associates, Sunderland. <https://doi.org/10.1111/j.0014-3820.2002.tb00191.x>

- Tamura K, Stecher G, Kumar S (2021) Molecular Evolutionary Genetics Analysis version 11. Molecular Biology and Evolution 38(7): 3022–3027. <https://doi.org/10.1093/molbev/msab120>
- Tan YPT, Shivas RG (2022) Index of Australian Fungi no. 3. <https://doi.org/10.5281/ZENODO.7430436>
- Tan MA, Dela Cruz TE, Apurillo CC, Proksch P (2015) Chemical constituents from a Philippine mangrove endophytic fungi *Phyllosticta* sp. Der Pharma Chemica 7: 43–45.
- Udayanga D, Miriyagalla SD, Manamgoda DS, Lewers KS, Gardiennet A, Castlebury LA (2021) Molecular reassessment of diaporthean fungi associated with strawberry, including the leaf blight fungus, *Paraphomopsis obscurans* gen. et comb. nov. (Melanconiellaceae). IMA Fungus 12(1): 15. <https://doi.org/10.1186/s43008-021-00069-9>
- Vilgalys R, Hester M (1990) Rapid genetic identification and mapping of enzymatically amplified ribosomal DNA from several *Cryptococcus* species. Journal of Bacteriology 172(8): 4238–4246. <https://doi.org/10.1128/jb.172.8.4238-4246.1990>
- Voglmayr H, Rossman AY, Castlebury LA, Jaklitsch WM (2012) Multigene phylogeny and taxonomy of the genus *Melanconiella* (Diaporthales). Fungal Diversity 57(1): 1–44. <https://doi.org/10.1007/s13225-012-0175-8>
- Vohník M, Borovec O, Kolaříková Z, Sudová R, Réblová M (2019) Extensive sampling and high-throughput sequencing reveal *Posidoniomycetes atricolor* gen. et sp. nov. (Aigialaceae, Pleosporales) as the dominant root mycobiont of the dominant Mediterranean seagrass *Posidonia oceanica*. MycoKeys 55: 59–86. <https://doi.org/10.3897/mycokeys.55.35682>
- Wang K, Kirk PM, Yao Y (2020) Development trends in taxonomy, with special reference to fungi. Journal of Systematics and Evolution 58(4): 406–412. <https://doi.org/10.1111/jse.12538>
- White TJ, Bruns T, Lee S, Taylor J (1989) Amplification and direct sequencing of fungal ribosomal RNA genes for phylogenetics. Academic Press, San Diego, 315–322. <https://doi.org/10.1016/B978-0-12-372180-8.50042-1>
- Wijayawardene N, Hyde K, Dai D, Sánchez-García M, Goto B, Saxena R, Erdoğdu M, Selçuk F, Rajeshkumar K, Aptroot A, Błaszczowski J, Boonyuen N, Da Silva G, De Souza F, Dong W, Ertz D, Haelewaters D, Jones EBG, Karunarathna S, Kirk P, Kukwa M, Kumla J, Leontyev D, Lumbsch H, Maharachchikumbura S, Marguno F, Martínez-Rodríguez P, Mešić A, Monteiro J, Oehl F, Pawłowska J, Pem D, Pfliegler W, Phillips A, Pošta A, He M, Li J, Raza M, Sruthi O, Suetrong S, Suwannarach N, Tedersoo L, Thiyagaraja V, Tibpromma S, Tkálčec Z, Tokarev Y, Wanasinghe D, Wijesundara D, Wimalaseana S, Madrid H, Zhang G, Gao Y, Sánchez-Castro I, Tang L, Stadler M, Yurkov A, Thines M (2022) Outline of Fungi and fungus-like taxa – 2021. Mycosphere 13(1): 53–453. <https://doi.org/10.5943/mycosphere/13/1/2>
- Wu B, Hussain M, Zhang W, Stadler M, Liu X, Xiang M (2019) Current insights into fungal species diversity and perspective on naming the environmental DNA sequences of fungi. Mycology 10(3): 127–140. <https://doi.org/10.1080/21501203.2019.1614106>
- Xu RF, Karunarathna SC, Phukhamsakda C, Dai DQ, Elgorban AM, Suwannarach N, Kumla J, Wang XY, Tibpromma S (2024) Four new species of Dothideomycetes (Ascomycota) from Pará Rubber (*Hevea brasiliensis*) in Yunnan Province, China. MycoKeys 103: 71–95. <https://doi.org/10.3897/mycokeys.103.117580>

## Supplementary material 1

### Additional information

Authors: Carlo Chris S. Apurillo, Chayanard Phukhamsakda, Kevin D. Hyde, Vinodhini Thiyagaraja, E. B. Gareth Jones






Data type: xlsx

Explanation note: **table S1.** Genbank accession codes for the sequences of Melanconiellaceae species and outgroup used in this study. **table S2.** Genbank accession numbers of *Peroneutypa* and related genera used in this study. **table S3.** Genbank accession numbers of *Pseudochaetosphaeronema* and related genera used in this study. **table S4.** Genbank accession numbers of Aigialaceae strains used in this study.

Copyright notice: This dataset is made available under the Open Database License (<http://opendatacommons.org/licenses/odbl/1.0/>). The Open Database License (ODbL) is a license agreement intended to allow users to freely share, modify, and use this Dataset while maintaining this same freedom for others, provided that the original source and author(s) are credited.

Link: <https://doi.org/10.3897/mycokeys.116.137351.suppl1>

# Morphological and phylogenetic analyses reveal new species and records of *Fusarium* (Nectriaceae, Hypocreales) from China

Congcong Ai<sup>1</sup>, Qiyun Liu<sup>1</sup>, Yaling Wang<sup>1</sup>, Zhaoxue Zhang<sup>1</sup>, Duhua Li<sup>1</sup>, Yun Geng<sup>2</sup>, Xiuguo Zhang<sup>1</sup>, Jiwen Xia<sup>1,3</sup>

<sup>1</sup> Shandong Provincial Key Laboratory for Biology of Vegetable Diseases and Insect Pests, College of Plant Protection, Shandong Agricultural University, Taian, 271018, China

<sup>2</sup> Institute of Crop Germplasm Resources, Shandong Academy of Agricultural Sciences, Jinan, 250100, China

<sup>3</sup> College of Agriculture and Forestry, Linyi University, Linyi, Shandong, 276000, China

Corresponding authors: Qiyun Liu (liuqiyun0416@163.com); Jiwen Xia (xiajiwen1@126.com)

## Abstract

Species of *Fusarium* are important phytopathogens, saprobes, and endophytes around the world. Some species can affect plant health and cause yield loss of economic plants. *Fusarium* species are widely distributed in China, and many species were found from different plant hosts. The *Fusarium incarnatum-equiseti* species complex (FIESC) is one of the most significant species complexes within the genus. Based on morphological and three-gene (*cal*, *rpb2*, and *tef1*) phylogenetic analyses, two new species are in the *Incarnatum* clade, and two new host records are identified and described, viz. *Fusarium fici* **sp. nov.**, *Fusarium xylosmatis* **sp. nov.**, *Fusarium fecundum*, and *Fusarium weifangense*.

**Key words:** *Fusarium incarnatum-equiseti* species complex, multigene phylogeny, new taxa



Academic editor: Xin-Cun Wang

Received: 15 February 2025

Accepted: 28 February 2025

Published: 7 April 2025

**Citation:** Ai C, Liu Q, Wang Y, Zhang Z, Li D, Geng Y, Zhang X, Xia J (2025) Morphological and phylogenetic analyses reveal new species and records of *Fusarium* (Nectriaceae, Hypocreales) from China. MycoKeys 116: 53–71. <https://doi.org/10.3897/mycokeys.116.150363>

Copyright: © Congcong Ai et al.

This is an open access article distributed under terms of the Creative Commons Attribution License (Attribution 4.0 International – CC BY 4.0).

## Introduction

Johann Heinrich Friedrich Link first proposed the genus *Fusarium* (Nectriaceae, Hypocreales) in 1809 and typified it with *Fusarium roseum* (= *F. sambucinum*), with falcate or banana-shaped macroconidia and oval, subglobose, or kidney-shaped microconidia (Link 1809; Gams et al. 1997; Leslie and Summerell 2006; Liu et al. 2023; Zhang et al. 2023a). *Fusarium* is one of the most renowned and extensively spread genera in the Kingdom Fungi because of its morphological and phylogenetic diversity (Leslie and Summerell 2006; Sandoval-Denis et al. 2018; Crous et al. 2021). *Fusarium* species are known as plant pathogens, endophytes, and saprophytes (Leslie et al. 1990; Bacon and Yates 2006; Maryani et al. 2019; He et al. 2024). More than 1800 epithets of *Fusarium* have been listed in Index Fungorum (<https://www.indexfungorum.org>), but many species of *Fusarium* were identified solely based on morphological studies. Excessive overlap of conidial characteristics makes it difficult to morphologically distinguish *Fusarium* species. Currently, *Fusarium* taxonomy is dominated by morphological and molecular phylogenetic studies (Crous et al. 2021; He et al. 2024).

At present, *Fusarium* contains 23 monophyletic species complexes and several single-species lineages (Xia et al. 2019; O'Donnell et al. 2020; Geiser et al.



2021; He et al. 2024). The FIESC includes over 30 recognized phylogenetic species (O'Donnell et al. 2009; Villani et al. 2016; Maryani et al. 2019; Santos et al. 2019; Wang et al. 2019; Xia et al. 2019). Based on the haplotype nomenclature system, O'Donnell et al. (2009) implemented an informal classification system for FIESC and introduced the Equiseti and Incarnatum clades. The *Fusarium camptoceras* species complex (FCAMSC) was proposed for three lineages that are sister clades to the FIESC by phylogenetic studies by Xia et al. (2019). However, Han et al. (2023) included the FCAMSC in FIESC as the Camptoceras clade because the FCAMSC and FIESC clearly represent a distinct evolutionary lineage that is strongly supported by the phylogenomic tree. Thus, FIESC comprises three clades, viz. Camptoceras, Equiseti, and Incarnatum clades.

In this study, samples were collected from Hainan, Sichuan, and Yunnan Provinces of China. Two new species and two new host records were identified and classified by multi-locus analysis of calmodulin (*cal*), RNA polymerase II second largest subunit (*rpb2*), and translations elongation factor 1-alpha (*tef1*) datasets. They were described and discussed based on their morphological characteristics along with their molecular sequence data.

## Materials and methods

### Strain isolation and preservation

Plant specimens with necrotic spots were collected from three provinces (Hainan, Sichuan, and Yunnan) of China in 2023. Pure colonies were obtained by tissue isolation techniques (Zhang et al. 2024). Fragments (25 mm<sup>2</sup>) were cut from the edges of diseased tissues, immersed in a 75% ethanol solution for 1 min, then rinsed in sterile water for 30 s and 10% sodium hypochlorite solution for 1 min. Fragments were rinsed three times with sterile water for 30 s, then using sterilized filter paper to absorb dry, placed on PDA for incubation at 25 °C for 3 days. The strains were preserved in 10% sterilized glycerol and stored them at 4 °C for future detailed studies. Specimens were deposited in the Herbarium of the Department of Plant Pathology, Shandong Agricultural University, Taian, China (HSAUP), and the Herbarium Mycologicum Academiae Sinicae, Institute of Microbiology, Chinese Academy of Sciences, Beijing, China (HMAS). The living ex-type cultures were deposited in the Shandong Agricultural University Culture Collection (SAUCC) and the China General Microbiological Culture Collection Center (CGMCC).

### DNA extraction, amplification, and sequencing

Total genomic DNA was extracted from fresh fungal mycelia grown on potato dextrose agar (PDA) after 7 days using the genomic DNA purification kit (OG-PLF-400, GeneOnBio Corporation, Changchun, China) according to the product manual. The calmodulin (*cal*), RNA polymerase second largest subunit (*rpb2*), and translation elongation factor 1-alpha (*tef1*) gene loci were amplified using the primer pairs listed in Table 1 (Xia et al. 2019; Han et al. 2023). The reaction was performed in a 25 µL reaction volume, consisting of 12.5 µL of 2 × Hieff Canace® Plus PCR Master Mix (Cat. No. 10154ES03, Yeasen Biotechnology, Shanghai, China), 1 µL each of forward and reverse primer (TsingKe, Qingdao, China), and 1 µL of template genomic DNA, and at last replenished the total

**Table 1.** Molecular markers and their PCR primers and programs used in this study.

Loci	PCR Primers	Sequence (5'→3')	PCR Cycles	References
<i>cal</i>	CL1	GARTWCAAGGAGGCCTTCTC	(94 °C: 30 s, 55 °C: 30 s, 72 °C: 15 s) × 35 cycles	O'Donnell et al. (2020)
	CL2A	TTTTTGCATCATGAGTTGGAC		
<i>rpb2</i>	5f2	GGGGWGAYCAGAAGAAGGC	(94 °C: 45 s, 57 °C: 45 s, 72 °C: 15 s) × 35 cycles	Liu et al. (1999)
	7cr	CCCATRGCTTGYTTRCCCAT		
<i>tef1</i>	EF-1	ATGGGTAAGGARGACAAGAC	(94 °C: 45 s, 55 °C: 45 s, 72 °C: 15 s) × 35 cycles	O'Donnell et al. (1998)
	EF-2	GGARGTACCAGTSATCATG		

volume to 25 µL with double distilled water. PCR products were separated and purified using 1% agarose gel and Safe Red (RM02852 and RM19009 ABclonal, Wuhan, China) and UV light to visualize the fragments. Gel was extracted using a gel extraction kit (Cat. No. AE0101-C, Shandong Sparkjade Biotechnology Co., Ltd., Jinan, China) (Wang et al. 2023). The purified PCR products were sequenced by Youkang Company Limited (Zhejiang, China). All sequences generated in this study were deposited in GenBank under the accession numbers provided in Suppl. material 1.

### Phylogenetic analyses

The reference sequences were downloaded from NCBI's GenBank. All sequences were initially aligned with the MAFFT v. 7 (<http://mafft.cbrc.jp/alignment/server/>) online service and MEGA 7.0. The concatenated aligned *cal*, *rpb2*, and *tef1* sequences were used for maximum likelihood (ML) and Bayesian inference (BI), which were run on RaxML-HPC2 with XSEDE v. 8.2.12 and MrBayes v. 3.2.7a with 64 threads on Linux (Zhang et al. 2024). For ML analyses, 100 rapid bootstrap replicates and the GTR+FO+I+G4m model as default parameters were used. For BI analyses, a fast bootstrap algorithm with an automatic stop option was performed (Zhang et al. 2023b). The SYM+G model for *cal*, the SYM+I+G model for *rpb2*, and the GTR+I+G model for *tef1* were selected and incorporated into the analyses. The Markov chain Monte Carlo (MCMC) analysis of the sequence data was performed over 5,000,000 generations, yielding 34,652 trees. Following the discard of 8,663 trees during the burn-in phase, the remaining trees were used to calculate posterior probabilities in the consensus trees.

### Morphological characterization

All isolates were inoculated on potato dextrose agar (PDA) medium and oatmeal agar (OA) medium. Colony morphology, pigmentation, and growth rates were recorded. The above and reverse of the PDA and OA flat plates were captured with the Alpha 6400L digital camera (Canon Powershot G7X, Canon, Tokyo, Japan) on the 7<sup>th</sup> day. Used Carnation leaf agar (CLA; Fisher et al. 1982) medium to describe morphological features, such as shape, size, and septum number of the conidia (Wang et al. 2019). Used a stereomicroscope (Olympus SZ61, Olympus Corporation, Tokyo, Japan) and a microscope (Olympus BX53, Olympus Corporation, Tokyo, Japan) with Differential Interference Contrast (DIC) to observe the microscopic morphology. Stereomicroscope and microscope were equipped with BioHD-A20c color digital cameras (FluoCa Scientific, Shanghai, China) to capture the microscopic fungal structures. Microstructures were

randomly measured using Digimizer software v5.6.0 (<https://www.digimizer.com>, accessed on 18 November 2024) and calculated the mean size (av.). The “n” represents the number of measurements.

## Results

### Phylogenetic analyses

The combined dataset comprised 133 ingroup strains with *Fusarium concolor* (NRRL 13459) as the outgroup. The final alignment comprised 1,654 concatenated characters, spanning from positions 1 to 535 (*cal*), 536 to 1,192 (*rpb2*), and 1,193 to 1,654 (*tef1*). The ML was carried out to be -9,907.383240. MrModelTest recommended using Dirichlet base frequencies for the *cal*, *rpb2*, and *tef1* data partitions. The alignment showed a total of 563 unique site patterns (*cal*: 156, *rpb2*: 168, *tef1*: 239). Based on the three-gene (*cal*, *rpb2*, and *tef1*) phylogeny, the 134 strains were classified into 57 species. The topology of the ML tree confirmed the topology obtained from BI, with only the ML tree presented (Fig. 1). Furthermore, single gene trees were evaluated, respectively, for FIESC (Suppl. material 2).

### Taxonomy

***Fusarium fecundum* S.L. Han, M.M. Wang & L. Cai, Studies in Mycology 104: 87–148. 2023.**

Fig. 2

**Description.** On CLA, conidiophores arising from aerial mycelia, 13–71 µm long, unbranched or irregularly branched, bearing terminal or lateral phialides, often reduced to single phialides; Periclinal thickening inconspicuous; Aerial conidia hyaline, smooth, rarely ovoid to falcate, on the apical half, the dorsal side is more curved than the ventral side, and the apical cell is either blunt or hooked, basal cell barely to distinctly notched. 1-septate conidia: (16–)22–21(–27) × 4–6 µm (av. 20 × 5 µm, n = 9); 2-septate conidia: (18–)21–28(–33) × 5–7 µm (av. 26 × 6 µm, n = 9); 3-septate conidia: (32–)33–36(–41) × 5–8 µm (av. 35 × 7 µm, n = 16); 4-septate conidia: (32–)37–43(–43) × 6–9 µm (av. 39 × 7 µm, n = 18); 5-septate conidia: (41–)43–48(–53) × 7–9 µm (av. 46 × 8 µm, n = 12).

**Culture characteristics.** Colonies on PDA incubated at 25 °C in the dark, reaching 84–90 mm diameter in 7 d; aerial mycelia dense, white, radiate, colony margin erose; reverse surface greyish yellow in the center, odor absent. On OA in the dark, occupying an entire 90 mm diameter in 7 d; surface white and aerial mycelia scant, crateriform, reverse white, odor absent.

**Materials examined.** CHINA • Yunan Province, Nanuo Mountain, on leaves of *Setaria palmifolia*, 3 March 2023, Q.Y. Liu (HSAUP41424, HSAUP51424), living cultures CGMCC 3.27792 = SAUCC 2414-4, CGMCC 3.27793 = SAUCC 2414-5.

**Notes.** Phylogenetic analysis showed that isolates (SAUCC 2414-4 and SAUCC 2414-5) were closely related to *Fusarium fecundum* (LC15875, ex-type strain) (Fig. 1). There are no nucleotide position differences between *Fusarium fecundum* (SAUCC 2414-4) and *Fusarium fecundum* (LC15875, ex-type strain). Morphologically, *Fusarium fecundum* (SAUCC 2414-4) and *Fusarium fecundum* (LC15875, ex-type strain) are the lack of sporodochia. The aerial conidia of *Fusarium fecundum*

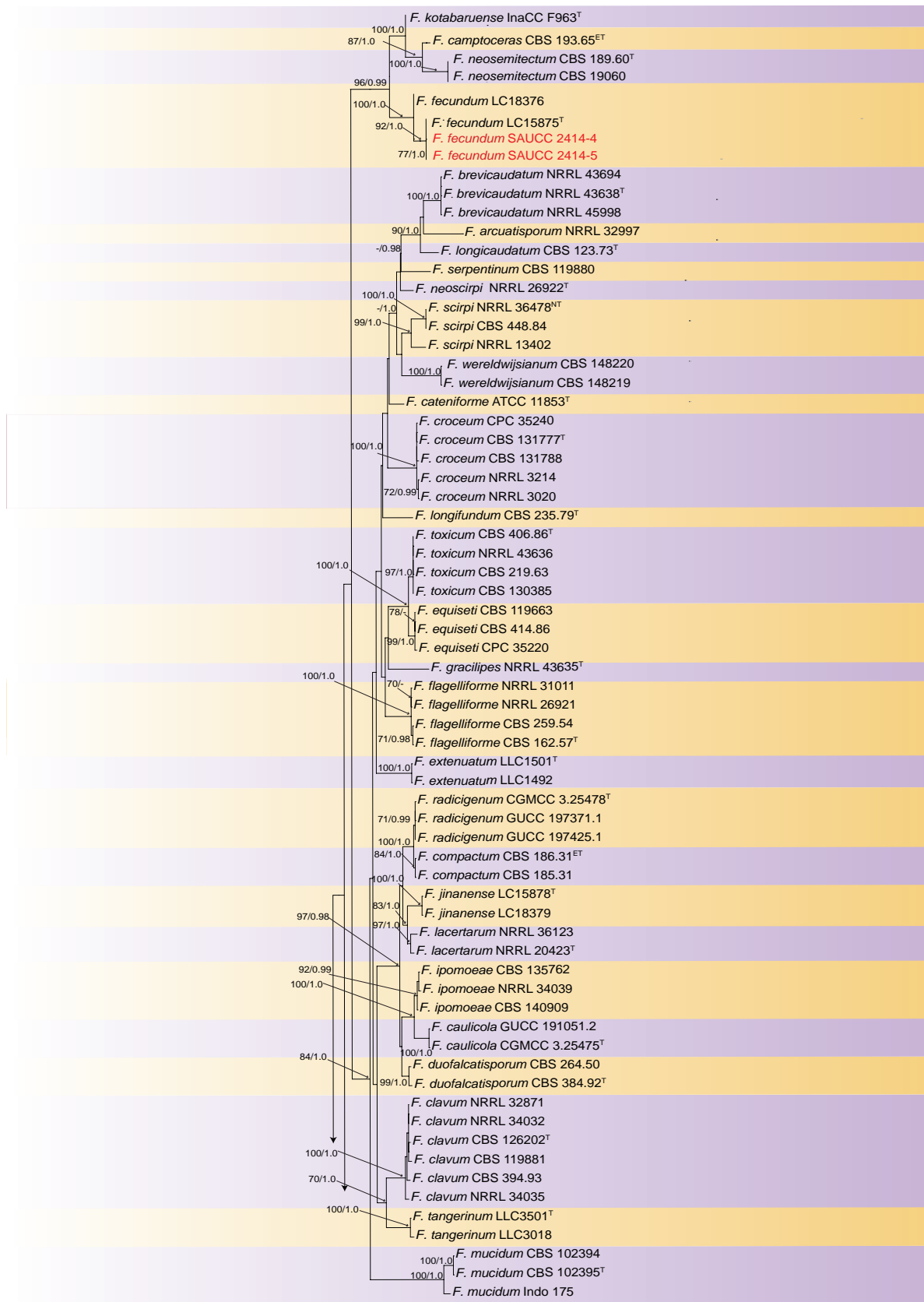


**Figure 1.** Phylogeny inferred based on the combined *cal-rpb2-tef1* sequence dataset of the *Fusarium incarnatum-equiseti* species complex (FIESC), with *Fusarium concolor* (NRRL 13459) as the outgroup. The RAxML Bootstrap support values (MLBS ≥ 70%) and Bayesian inference posterior probabilities (BIPP ≥ 0.90) were shown at the nodes. Ex-type, ex-epitype, and ex-neotype strains were indicated by T, ET, and NT, respectively. Strains isolated in this study were indicated in red.



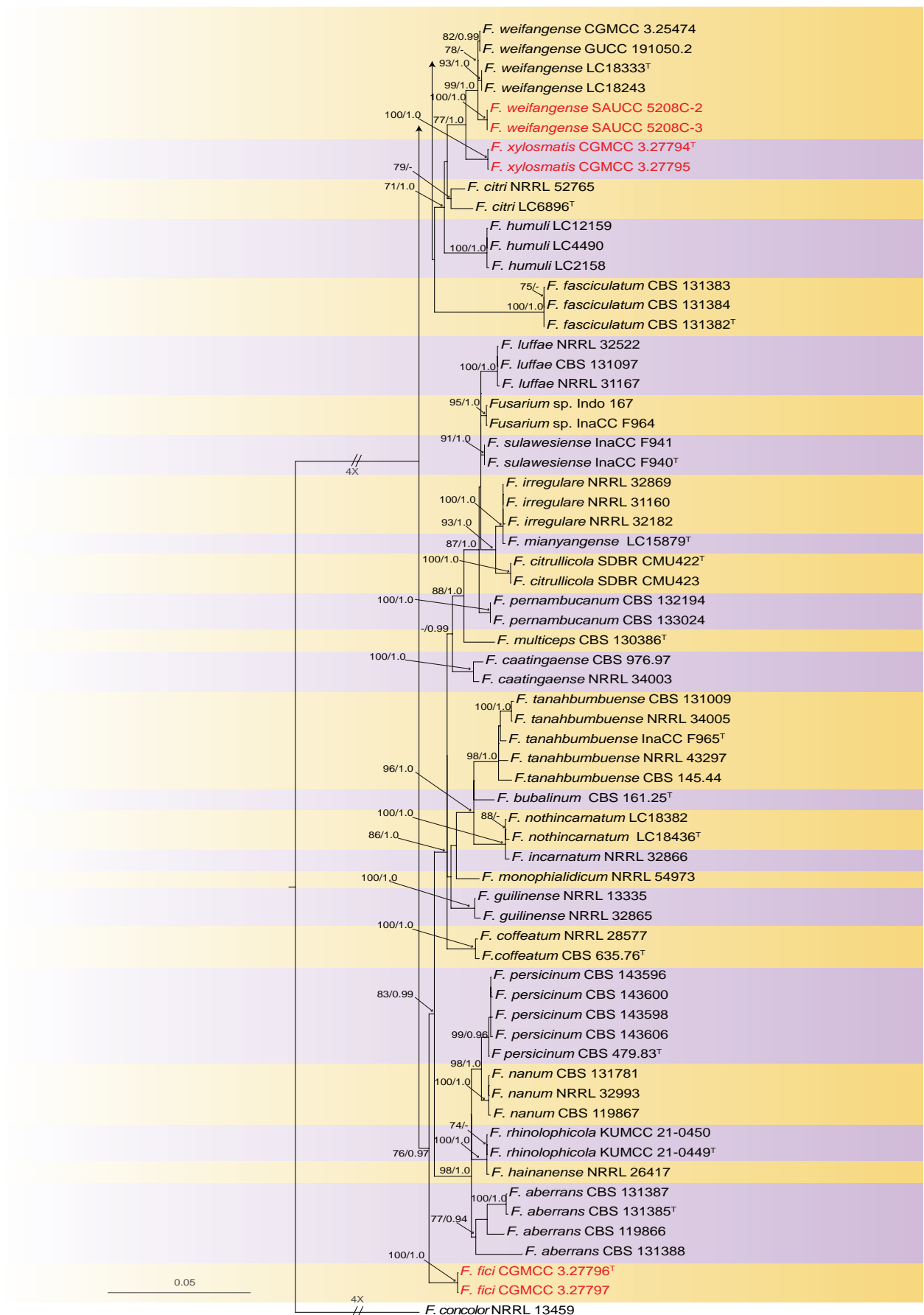
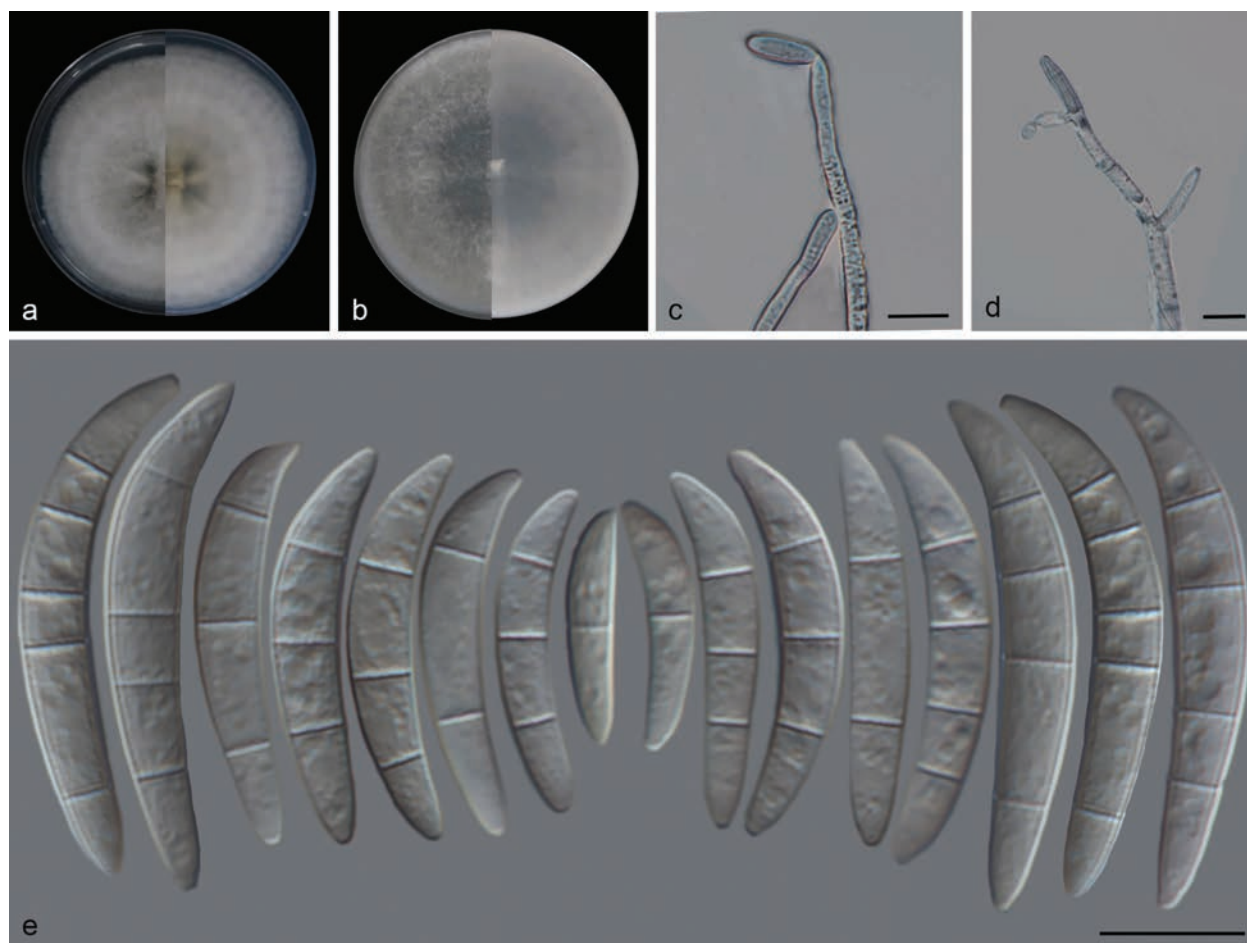


Figure 1. Continued.



**Figure 2.** *Fusarium fecundum* (SAUCC 2414-4) **a** colony on PDA after 7 days at 25 °C (left: above, right: reverse) **b** colony on OA after 7 days at 25 °C (left: above, right: reverse) **c**, **d** conidiophore on aerial mycelium with monophialides **e** aerial conidia. Scale bars: 10 µm (**c–e**).

(SAUCC 2414-4) are smaller than those of *Fusarium fecundum* (LC15875, ex-type strain). *Fusarium fecundum* was previously isolated from wheat and rice, and it has now been reported for the first time on *Setaria palmifolia* (Han et al. 2023).

***Fusarium fici* Q.Y. Liu, X.G. Zhang & J.W. Xia, sp. nov.**

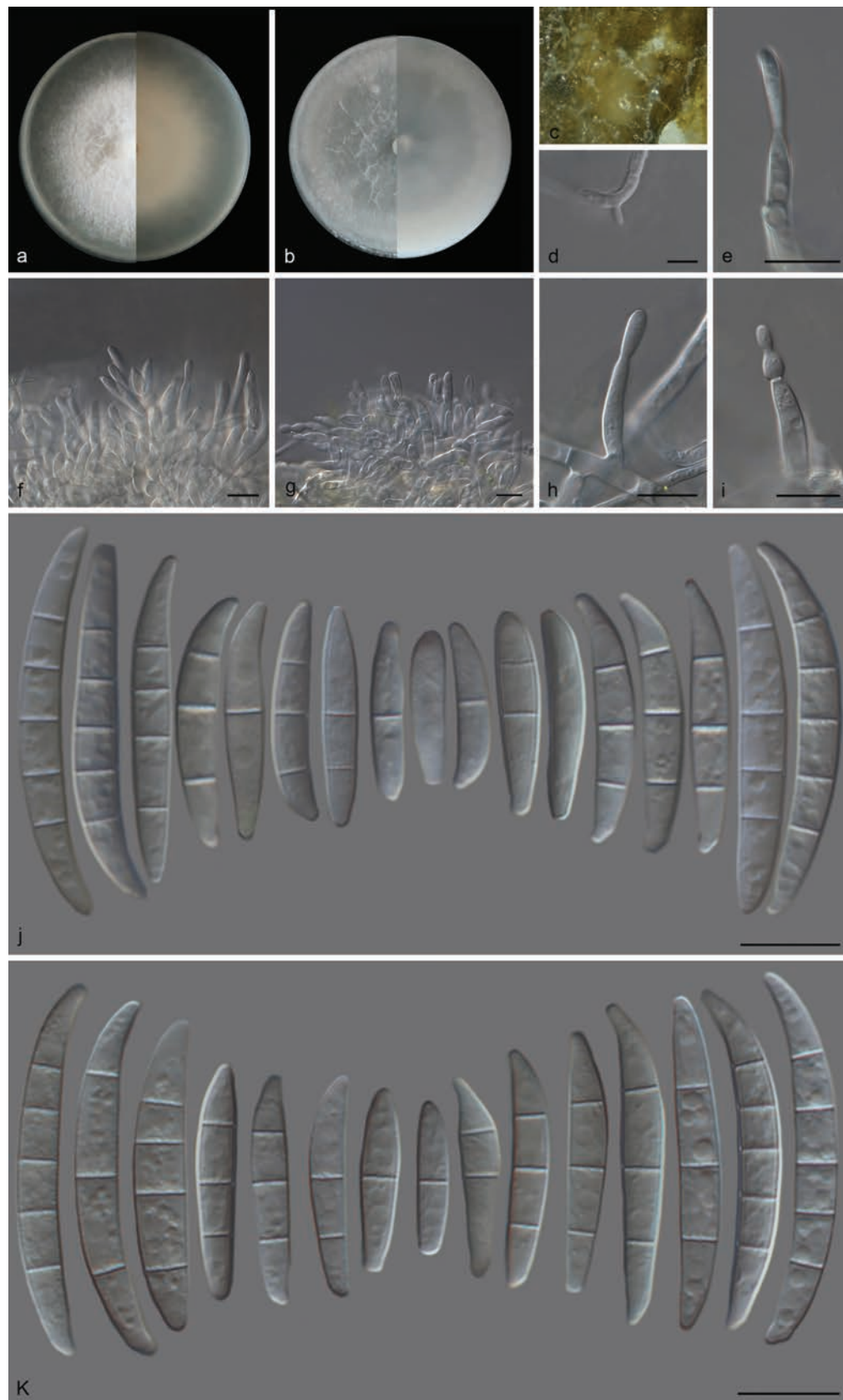
MycoBank No: 856644

Fig. 3

**Etymology.** Referring to the genus name of the host plant *Ficus fistulosa*.

**Typus.** CHINA • Hainan Province, Baoting Li and Miao Autonomous County, on leaves of *Ficus fistulosa*, 10 April 2023, Q.Y. Liu (HMAS 353395, holotype), ex-holotype culture CGMCC 3.27796 = SAUCC 3249C-3.

**Description.** Conidiophores arising from aerial mycelium, 17–21 µm long, unbranched, reduced to single phialidic pegs, subulate to subcylindrical; aerial conidia hyaline, smooth, and thin-walled, rarely ellipsoidal to falcate, straight to curved dorsiventrally, a blunt apical cell and barely notched basal cell, 1–3(–5)-septate; 1-septate conidia: (12–)12–16(–28) × 3–5 µm (av. 17 × 3 µm, n = 18); 2-septate conidia: (16–)17–21 (–26) × 3–5 µm (av. 19 × 4 µm, n = 17); 3-septate conidia: (20–)22–28 (–36) × 3–6 µm (av. 26 × 4 µm, n = 31); 4-septate conidia:



**Figure 3.** *Fusarium fici* (CGMCC 3.27796) **a** colony on PDA after 7 days at 25 °C (left: above, right: reverse) **b** colony on OA after 7 days at 25 °C (left: above, right: reverse) **c** sporodochia on carnation leaves **d** lateral phialidic peg on aerial mycelium **e** monophialide **f, g** sporodochial conidiophores **h, i** monophialides on aerial mycelium **j** sporodochial conidia **k** aerial conidia. Scale bars: 10 µm (**d–k**).

(28–)31–34 (–39) × 4–5 µm (av. 33 × 5 µm, n = 14); 5-septate conidia: (23–)32–33 (–36) × 4–5 µm (av. 31 × 4 µm, n = 5). Sporodochia salmon to saffron, formed abundantly on surface of carnation leaves. Sporodochial conidiophores densely and bearing apical whorls of 1 phialide; sporodochial phialides subulate to subcylindrical, 9–11 × 3–4 µm, smooth, thin-walled, with inconspicuous periclinal thickening; sporodochial conidia falcate, straight to curved dorsiventrally, tapering towards both ends, with slightly papillate, a conical to slightly papillate apical cell, a notched to foot-like basal cell, (0–)1–3(–5)-septate, hyaline, smooth, and thin-walled; 0-septate conidia: (10–)15–20(–21) × 2–4 µm (av. 16 × 3 µm, n = 9); 1-septate conidia: (13–)15–22(–25) × 2–5 µm (av. 18 × 4 µm, n = 23); 2-septate conidia: (13–)16–18(–23) × 2–5 µm (av. 18 × 3 µm, n = 23); 3-septate conidia: (19–)20–25(–29) × 3–5 µm (av. 24 × 4 µm, n = 37); 4-septate conidia: (28–)31–34(–36) × 4–5 µm (av. 33 × 4 µm, n = 12); 5-septate conidia: (34–)34–36(–38) × 3–5 µm (av. 35 × 4 µm, n = 5). Chlamydospores not observed.

**Culture characteristics.** Colonies on PDA incubated at 25 °C in the dark, reaching 76–80 mm diameter in 7 d, flat, convex, with abundant aerial mycelium, colony margin lightly erose; surface white, odor absent; reverse yellowish white, odor absent. On OA in the dark, reaching 85–90 mm diameter in 7 d; aerial mycelium scant in the center forming a vacant circle, reverse white, odor absent.

**Additional material studied.** CHINA • Hainan Province, Baoting Li and Miao Autonomous County, on leaves of *Ficus fistulosa*, 10 April 2023, Q.Y. Liu (HSAUP44932), living culture CGMCC 3.27797 = SAUCC 3249C-4.

**Notes.** Phylogenetic analyses of three combined sequences (*cal*, *rpb2*, and *tef1*) showed that *F. fici* constitutes a distinct clade, closely related to *F. aberrans*. Between *F. fici* (CGMCC 3.27796) and *F. aberrans* (CBS 131385), there were 11/535 differences in *cal*, 13/657 in *rpb2*, and 34/462 in *tef1*. The mycelium on OA of *F. fici* (CGMCC 3.27796) is sparser than that of *F. aberrans* (CBS 131385). Morphologically, *F. fici* (CGMCC 3.27796) and *F. aberrans* (CBS 131385) have different sporodochial conidial septa (0–5-septate in *F. fici* vs. 1–3-septate in *F. aberrans*) and sporodochial phialides (1 phialide in *F. fici* vs. 2–3 phialides in *F. aberrans*). The aerial conidiophores of *F. aberrans* (16–110 µm) are longer than *F. fici* (17–21 µm) (Xia et al. 2019).

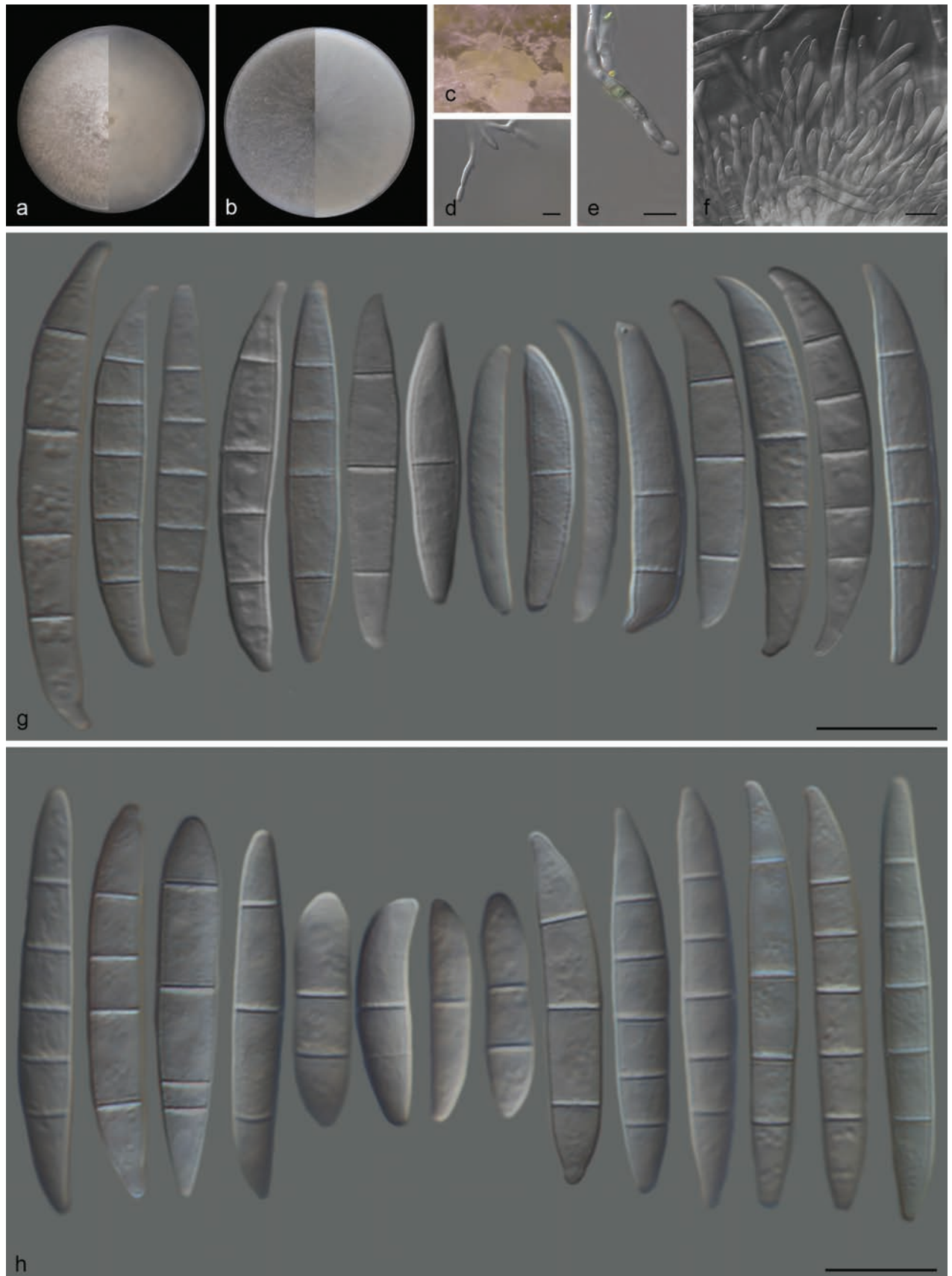
***Fusarium weifangense* S.L. Han, M.M. Wang & L. Cai, Studies in Mycology 104: 87–148. 2023.**

Fig. 4

**Synonym.** *Fusarium caulendophyticum* H. Zhang & Y.L. Jiang, Mycosphere 14(1): 2092–2207. 2023.

**Description.** Conidiophores arising from aerial mycelium, 14–18 µm long, unbranched or irregularly branched, often reduced to single phialides; aerial phialides monophialidic, subulate to subcylindrical, smooth- and thin-walled, with inconspicuous or absent periclinal thickening, 9.2–12.2 × 4.0–4.4 µm; aerial conidia hyaline, rarely ellipsoidal to falcate, slightly curved with almost parallel sides, tapering towards both ends, with a blunt to conical and slightly curved apical cell, blunt to barely notched basal cell, smooth and thin-walled, (1–)3–5-septate; 1-septate conidia: (14–)15–19(–20) × 3–4 µm (av. 17 × 3 µm, n = 8); 2-septate conidia: (19–)19–21(–24) × 3–5 µm (av. 21 × 4 µm, n = 14); 3-septate conidia: (22–)26–31(–34) × 3–6 µm





**Figure 4.** *Fusarium weifangense* (SAUCC 5208C-2) **a** colony on PDA after 7 days at 25 °C (left: above, right: reverse) **b** colony on OA after 7 days at 25 °C (left: above, right: reverse) **c** sporodochia on carnation leaves **d** polyphialide **e** monophialide **f** sporodochial conidiophores **g** sporodochial conidia **h** aerial conidia. Scale bars: 10 µm (**d-h**).

(av.  $28 \times 4 \mu\text{m}$ ,  $n = 22$ ); 4-septate conidia:  $(30-35-36(-45) \times 3-6 \mu\text{m}$  (av.  $36 \times 5 \mu\text{m}$ ,  $n = 17$ ); 5-septate conidia:  $(31-34-37(-46) \times 4-6 \mu\text{m}$  (av.  $38 \times 5 \mu\text{m}$ ,  $n = 15$ ). Sporodochia salmon to orange, formed abundantly on surface of carnation leaves. Sporodochial conidiophores densely, bearing apical whorls of one phialide; sporodochial phialides monophialidic, subulate to subcylindrical,  $16-24 \times 2-3 \mu\text{m}$ , smooth. Sporodochial conidia falcate, slightly curved, tapering towards both ends, with a slightly elongated conical or whip-like curved apical cell, a foot-like to notched basal cell, (0-)4-5-septate, hyaline, thin, and smooth-walled; 0-septate conidia:  $26-28 \times 3-4 \mu\text{m}$ ; 1-septate conidia:  $(17-26-36(-37) \times 3-6 \mu\text{m}$  (av.  $28 \times 4 \mu\text{m}$ ,  $n = 10$ ); 2-septate conidia:  $(20-21-37 \times 3-5 \mu\text{m}$  (av.  $25 \times 4 \mu\text{m}$ ,  $n = 7$ ); 3-septate conidia:  $21-33(-38) \times 3-5 \mu\text{m}$  (av.  $32 \times 5 \mu\text{m}$ ,  $n = 12$ ); 4-septate conidia:  $(31-32-35(-44) \times 3-6 \mu\text{m}$  (av.  $36 \times 4 \mu\text{m}$ ,  $n = 22$ ); 5-septate conidia:  $(34-40-45(-48) \times 3-6 \mu\text{m}$  (av.  $42 \times 4 \mu\text{m}$ ,  $n = 16$ ). Chlamydospores not observed.

**Culture characteristics.** Colonies on PDA incubated at  $25^\circ\text{C}$  in the dark, reaching 86–90 mm diameter in 7 d; surface white, flat, felty to velvety, aerial mycelia dense, colony margin entire; reverse white, odor absent. Colonies on OA incubated at  $25^\circ\text{C}$  in the dark, reaching 85–89 mm diameter in 7 d; surface white and aerial mycelia scant, radiate, reverse white, radiate, odor absent.

**Materials examined.** CHINA • Sichuan Province, Baoting Li and Miao Autonomous County, on leaves of *Prunus salicina*, 2 July 2023, Q.Y. Liu (HSAUP20852, HSAUP30852), living cultures SAUCC 5208C-2 = CGMCC 3.27939, SAUCC 5208C-3.

**Notes.** *Fusarium weifangense* (LC18333, ex-type strain) was proposed by Han et al. (2023). *Fusarium caulendophyticum* (CGMCC 3.25474, ex-type strain) was proposed by Zhang et al. (2023a). *Fusarium weifangense* (LC18333, ex-type strain) was the first to be discovered. *Fusarium weifangense* (LC18333 and LC18243) are clustered with *Fusarium caulendophyticum* (CGMCC 3.25474 and GUCC 191050.2) clade in the combined phylogenetic tree (Fig. 1, Suppl. material 4). *Fusarium weifangense* (LC18333, ex-type strain) and *Fusarium caulendophyticum* (CGMCC 3.25474, ex-type strain) were similar in *cal* (0/535), *rpb2* (1/657), and *tef1* (2/462) sequences. We therefore considered the *Fusarium caulendophyticum* synonym of *Fusarium weifangense*. In this study, our strains (SAUCC 5208C-2 and SAUCC 5208C-3) are clustered with the *Fusarium weifangense* (LC18333 and LC18243) clade in the combined phylogenetic tree (Fig. 1). SAUCC 5208C-2 and SAUCC 5208C-3 were similar to the latter in *cal* (with 100% sequence identity), *rpb2* (99.85%), and *tef1* (98.70%) sequences. *Fusarium weifangense* was previously isolated from wheat, *Capsicum* sp., *Triticum* sp., *Medicago sativa*, *Lactuca sativa*, *Chenopodium quinoa*, and *Rosaceae roxburghii*, and it has now been reported for the first time on *Prunus salicina* (Wang et al. 2019; Xia et al. 2019; Yin et al. 2021; Han et al. 2023; Zhang et al. 2023a) (Suppl. material 3).

***Fusarium xylosmatis* Q.Y. Liu, X.G. Zhang & J.W. Xia, sp. nov.**

MycoBank No: 856642

Fig. 5

**Etymology.** Referring to the genus name of the host plant *Xylosma congesta*.

**Typus.** CHINA • Yunan Province, Nanuo Mountain, on leaves of *Xylosma congesta*, 3 March 2023, Q.Y. Liu (HMAS 353394, holotype), ex-holotype culture CGMCC 3.27794 = SAUCC 2416-1.

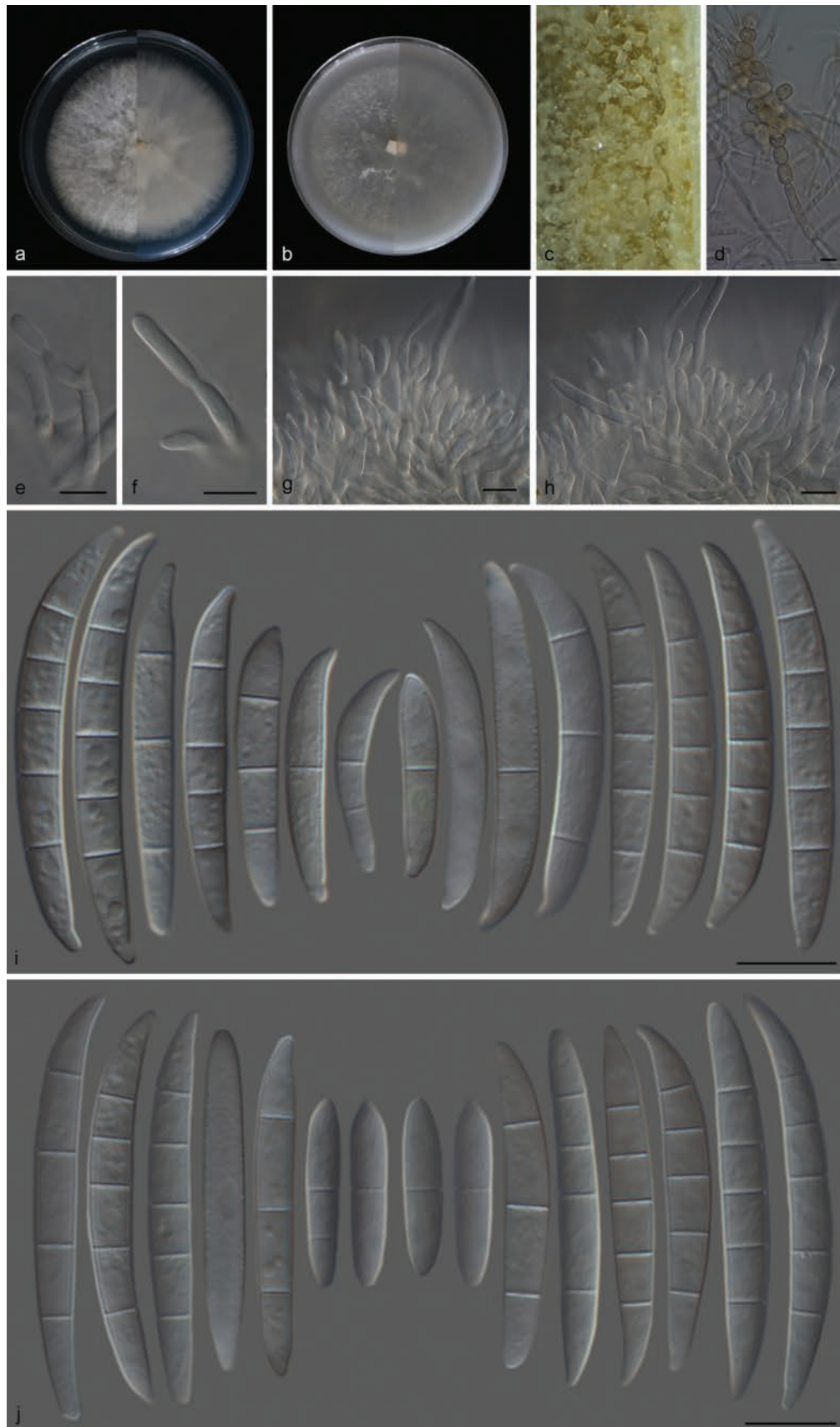


**Figure 5.** *Fusarium xylosmatis* (CGMCC 3.27794) **a** colony on PDA after 7 days at 25 °C (left: above, right: reverse) **b** colony on OA after 7 days at 25 °C (left: above, right: reverse) **c** sporodochia on carnation leaves **d** chlamydospores **e** polyphialide **f** monophialide **g, h** sporodochial conidiophores **i** sporodochial conidia **j** aerial conidia. Scale bars: 10 µm (**d-j**).

**Description.** Conidiophores arising from aerial mycelium, 25–35 µm long, unbranched or irregularly branched, often reduced to single phialides, subulate to subcylindrical, smooth, 12–15 × 4–5 µm, periclinal thickening inconspicuous; aerial conidia ellipsoidal to falcate, slightly curved, tapering towards both ends, with a blunt to conical and slightly curved apical cell and papillate basal cell, (0–)3–5-septate; 0-septate conidia: 16–20 × 3–4 µm (av. 21 × 4 µm, n = 5); 1-septate conidia: (12–)15–19(–29) × 3–4 µm (av. 18 × 4 µm, n = 33); 2-septate conidia: (16–)16–23(–29) × 3–5 µm (av. 21 × 4 µm, n = 18); 3-septate conidia: (20–)30–36(–41) × 4–5 µm (av. 31 × 5 µm, n = 45); 4-septate conidia: (31–)30–36(–34) × 4–6 µm (av. 34 × 5 µm, n = 26); 5-septate conidia: (30–)37–41(–43) × 4–6 µm (av. 38 × 5 µm, n = 26). Sporodochia pale orange, formed abundantly on surface of carnation leaves. Sporodochial conidiophores densely and irregularly branched, 15–19 × 2–3 µm, bearing apical whorls of 1–2 phialides; sporodochial phialides monophialidic, subulate to subcylindrical, 10–12 × 2–3 µm, smooth, and thin-walled; sporodochial conidia falcate, curved dorsiventrally, straight to slightly curved, tapering towards both ends, with slightly papillate, curved apical cell and a notched to foot-like basal cell, (0–)3–4(–5)-septate, hyaline, smooth, and thin-walled; 0-septate conidia: 28–30 × 3–4 µm (av. 29 × 4 µm, n = 5); 1-septate conidia: (16–)21–32(–36) × 3–5 µm (av. 27 × 4 µm, n = 11); 2-septate conidia: 22–23 × 3–4 µm (av. 23 × 4 µm, n = 4); 3-septate conidia: (22–)25–33(–41) × 3–6 µm (av. 32 × 4 µm, n = 38); 4-septate conidia: (33–)35–38(–43) × 4–6 µm (av. 37 × 5 µm, n = 26); 5-septate conidia: (36–)38–40(–44) × 4–6 µm (av. 40 × 5 µm, n = 16). Chlamydospores abundant, globose, subglobose to ellipsoid, terminal or intercalary, solitary, in pairs, or forming long chains, 8–12 µm diameter.

**Culture characteristics.** Colonies on PDA incubated at 25 °C in the dark, reaching 71–79 mm diameter in 7 d; aerial mycelia dense, flat, white, colony margin entire; reverse yellowish white, radiate, aerial mycelia dense, odor absent. Colonies on OA grown in the dark, reaching 69–77 mm diameter after 7 d at 25 °C, flat, aerial mycelia scant, colony margin entire, white; reverse white, odor absent.

**Additional material studied.** CHINA • Yunan Province, Nanuo Mountain, on leaves of *Xylosma congesta*, 3 March 2023, Q.Y. Liu (HSAUP21624), living culture CGMCC 3.27795 = SAUCC 2416-2.

**Notes.** Phylogenetically, *F. xylosmatis* (CGMCC 3.27794) is closely related to the species *F. weifangense* (LC18333); there were 7/535 differences in *cal*, 9/657 in *rpb2*, and 8/462 in *tef1*. Morphologically, *F. xylosmatis* (CGMCC 3.27794) is distinguished from *F. weifangense* (LC18333) by the number of sporodochial conidial septa (0–5-septate in *F. xylosmatis* (CGMCC 3.27794) vs. 3–7-septate in *F. weifangense* (LC18333)) (Han et al. 2023; Zhang et al. 2023a).

## Discussion

The genus and species concepts in *Fusarium* have endured significant changes (Leslie and Summerell 2006; Crous et al. 2021; He et al. 2024). Traditionally, the identification of *Fusarium* is mainly based on morphological characteristics (Wollenweber and Reinking 1935; Snyder and Hansen 1940; Toussoun and Nelson 1968; Gerlach and Nirenberg 1982; Leslie and Summerell 2006). However, identification is difficult due to the high morphological variation that complicates morphological identification among the closely related species (Leslie and Summerell 2006; Crous et al. 2021). Therefore, it is important to identify *Fusarium*



species through molecular analysis (Wang et al. 2019; Xia et al. 2019; Crous et al. 2021; Wang et al. 2022; He et al. 2024). The internal transcribed spacer (ITS), the large subunit (LSU), ATP citrate lyase (*ac1*), calmodulin (*cal*), RNA polymerase II largest subunit (*rpb1*), RNA polymerase second largest subunit (*rpb2*), translation elongation factor 1-alpha (*tef1*), and beta-tubulin (*tub2*) are used in current studies (Lombard et al. 2015; Sandoval-Denis et al. 2018; Xia et al. 2019; Crous et al. 2021; Suwannarach et al. 2023; He et al. 2024). However, the identification of *Fusarium* at the species level could not be resolved using the ribosomal DNA gene (ITS and LSU) alone (Balajee et al. 2009; O'Donnell et al. 2015; Suwannarach et al. 2023). Thus, the protein-coding genes (*ac1*, *cal*, *rpb1*, *rpb2*, *tef1*, and *tub2*) are added (Xia et al. 2019; Crous et al. 2021; Suwannarach et al. 2023; He et al. 2024). Different complexes of *Fusarium* require different gene combinations to identify.

In this study, we collected parasitic or saprotrophic fungi from terrestrial habitats in Hainan, Sichuan, and Yunnan Provinces of China on four plant specimens: *Setaria palmifolia*, *Ficus fistulosa*, *Prunus salicina*, and *Xylosma congesta*. Morphologically, these species exhibit a range of variations in spore size, shape, and ornamentation, as well as colony characteristics such as growth rate, pigmentation, and texture. We also conducted phylogenetic analyses using *cal*, *rpb2*, and *tef1* sequences and can be recognized as two new phylogenetic species (*Fusarium. fici* sp. nov. and *Fusarium xylosmatis* sp. nov.), along with two known species (*Fusarium fecundum* and *Fusarium weifangense*). The discovery of two new species underscores the rich fungal diversity in Hainan, Sichuan, and Yunnan Provinces and emphasizes the need for further exploration of understudied habitats. *Fusarium fecundum* was first reported from *Setaria palmifolia*; *Fusarium weifangense* was first reported from *Prunus salicina*. It can contribute to our knowledge of host specificity and ecological adaptation in fungal pathogens. These findings have significant implications for fungal taxonomy, ecology, and potential applications in plant pathology and biocontrol.

## Additional information

### Conflict of interest

The authors have declared that no competing interests exist.

### Ethical statement

No ethical statement was reported.

### Funding

This research was funded by the National Natural Science Foundation of China (nos. 32370001, 32270024, 31900014, U2002203), the Key Technological Innovation Program of Shandong Province, China (no. 2022CXGC020710), the Jinan City's 'New University 20 Policies' Initiative for Innovative Research Teams Project (no. 202228028), and the Innovative Agricultural Application Technology Project of Jinan City (no. CX202210).

### Author contributions

Sampling, molecular biology analysis: Qiyun Liu and Congcong Ai; fungal isolation: Yaling Wang; description and phylogenetic analysis: Zhaoxue Zhang; microscopy: Duhua Li and Yun Geng; writing—original draft preparation: Qiyun Liu; writing—review and editing: Jiwen Xia and Xiuguo Zhang. All authors read and approved the final manuscript.

## Author ORCIDs

Qiyun Liu  <https://orcid.org/0009-0009-9545-7962>

Zhaoxue Zhang  <https://orcid.org/0000-0002-4824-9716>

Duhua Li  <https://orcid.org/0009-0006-5200-2034>

Xiuguo Zhang  <https://orcid.org/0000-0001-9733-8494>

Jiwen Xia  <https://orcid.org/0000-0002-7436-7249>

## Data availability

The sequences were deposited in the GenBank database.

## References

- Bacon CW, Yates IE (2006) Endophytic root colonization by *Fusarium* species: histology, plant interactions, and toxicity. *Microbial Root Endophytes*, 133–152. [https://doi.org/10.1007/3-540-33526-9\\_8](https://doi.org/10.1007/3-540-33526-9_8)
- Balajee SA, Borman AM, Brandt ME, Cano J, Cuenca-Estrella M, Dannaoui E, Guarro J, Haase G, Kibbler CC, Meyer W, O'Donnell K, Petti CA, Rodriguez-Tudela JL, Sutton D, Velegraki A, Wickes BL (2009) Sequence-based identification of *Aspergillus*, *Fusarium*, and Mucorales species in the clinical mycology laboratory: Where are we and where should we go from here? *Journal of Clinical Microbiology* 47: 877–884. <https://doi.org/10.1128/JCM.01685-08>
- Crous PW, Lombard L, Sandoval-Denis M, Seifert KA, Schroers HJ, Chaverri P, Gené J, Guarro J, Hirooka Y, Bensch K, Kema GHJ, Lamprecht SC, Cai L, Rossman AY, Stadler M, Summerbell RC, Taylor JW, Ploch S, Visagie CM, Yilmaz N, Frisvad JC, Abdel-Azeem AM, Abdollahzadeh J, Abdolrasouli A, Akulov A, Alberts JF, Araújo JPM, Ariyawansa HA, Bakhshi M, Bendiksby M, Ben Hadj Amor A, Bezerra JDP, Boekhout T, Câmara MPS, Carbia M, Cardinali G, Castañeda-Ruiz RF, Celis A, Chaturvedi V, Collemare J, Croll D, Damm U, Decock CA, de Vries RP, Ezekiel CN, Fan XL, Fernández NB, Gaya E, González CD, Gramaje D, Groenewald JZ, Grube M, Guevara-Suarez M, Gupta VK, Guarnaccia V, Haddaji A, Hagen F, Haelewaters D, Hansen K, Hashimoto A, Hernández-Restrepo M, Houben J, Hubka V, Hyde KD, Iturriga T, Jeewon R, Johnston PR, Jurjević Ž, Karalti I, Korsten L, Kuramae EE, Kušan I, Labuda R, Lawrence DP, Lee HB, Lechat C, Li HY, Litovka YA, Maharachchikumbura SSN, Marin-Felix Y, Matio Kemkuignou B, Matočec N, McTaggart AR, Mičoch P, Mugnai L, Nakashima C, Nilsson RH, Nourmou SR, Pavlov IN, Peralta MP, Phillips AJL, Pitt JI, Polizzi G, Quaedvlieg W, Rajeshkumar KC, Restrepo S, Rhaïem A, Robert J, Robert V, Rodrigues AM, Salgado-Salazar C, Samson RA, Santos ACS, Shivas RG, Souza-Motta CM, Sun GY, Swart WJ, Szoke S, Tan YP, Taylor JE, Taylor PWJ, Tiago PV, Váczky KZ, van de Wiele N, van der Merwe NA, Verkley GJM, Vieira WAS, Vizzini A, Weir BS, Wijayawardene NN, Xia JW, Yáñez-Morales MJ, Yurkov A, Zamora JC, Zare R, Zhang CL, Thines M (2021) *Fusarium*: More than a node or a foot-shaped basal cell. *Studies in Mycology* 98(4): e100116. <https://doi.org/10.1016/j.simyco.2021.100116>
- Fisher NL, Burgess LW, Toussoun TA, Nelson PE (1982) Carnation leaves as a substrate and for preserving cultures of *Fusarium* species. *Phytopathology* 72: 151–153. <https://doi.org/10.1094/Phyto-72-151>
- Gams W, Nirenberg HI, Seifert KA, Brayford D, Thrane U (1997) Proposal to conserve the name *Fusarium sambucinum* (Hyphomycetes). *Taxon* 46(1): 111–113. <https://doi.org/10.2307/1224298>
- Geiser DM, Al-Hatmi AMS, Aoki T, Arie T, Balmas V, Barnes I, Bergstrom GC, Bhattacharya MK, Blomquist CL, Bowden RL, Brankovics B, Brown DW, Burgess LW, Bushley K,

- Busman M, Cano-Lira JF, Carrillo JD, Chang HX, Chen CY, Chen W, Chilvers M, Chulze S, Coleman JJ, Cuomo CA, de Beer ZW, de Hoog GS, Del Castillo-Munera J, Del Ponte EM, Dieguez-Uribeondo J, Di Pietro A, Edel-Hermann V, Elmer WH, Epstein L, Eskalen A, Esposto MC, Everts KL, Fernandez-Pavia SP, da Silva GF, Foroud NA, Fourie G, Frandsen RJN, Freeman S, Freitag M, Frenkel O, Fuller KK, Gagkaeva T, Gardiner DM, Glenn AE, Gold SE, Gordon TR, Gregory NF, Gryzenhout M, Guarro J, Gugino BK, Gutierrez S, Hammond-Kosack KE, Harris LJ, Homa M, Hong CF, Hornok L, Huang JW, Ilkit M, Jacobs A, Jacobs K, Jiang C, Jimenez-Gasco MDM, Kang S, Kasson MT, Kazan K, Kennell JC, Kim HS, Kistler HC, Kuldau GA, Kulik T, Kurzai O, Laraba I, Laurence MH, Lee T, Lee YW, Lee YH, Leslie JF, Liew ECY, Lofton LW, Logrieco AF, Lopez-Berges MS, Luque AG, Lysoe E, Ma LJ, Marra RE, Martin FN, May SR, McCormick SP, McGee C, Meis JF, Migheli Q, Mohamed Nor NMI, Monod M, Moretti A, Mostert D, Mule G, Munaut F, Munkvold GP, Nicholson P, Nucci M, O'Donnell K, Pasquali M, Pfenning LH, Prigitano A, Proctor RH, Ranque S, Rehner SA, Rep M, Rodriguez-Alvarado G, Rose LJ, Roth MG, Ruiz-Roldan C, Saleh AA, Salleh B, Sang H, Scandiani MM, Scauflaire J, Schmale DG 3<sup>rd</sup>, Short DPG, Sisic A, Smith JA, Smyth CW, Son H, Spahr E, Stajich JE, Steenkamp E, Steinberg C, Subramaniam R, Suga H, Summerell BA, Susca A, Swett CL, Toomajian C, Torres-Cruz TJ, Tortorano AM, Urban M, Vaillancourt LJ, Vallad GE, van der Lee TAJ, Vanderpool D, van Diepeningen AD, Vaughan MM, Venter E, Vermeulen M, Verweij PE, Viljoen A, Waalwijk C, Wallace EC, Walther G, Wang J, Ward TJ, Wickes BL, Wiederhold NP, Wingfield MJ, Wood AKM, Xu JR, Yang XB, Yli-Mattila T, Yun SH, Zakaria L, Zhang H, Zhang N, Zhang SX, Zhang X (2021) Phylogenomic analysis of a 55.1kb 19-gene dataset resolves a monophyletic *Fusarium* that includes the *Fusarium solani* species complex. *Phytopathology* 111: 1064–1079. <https://doi.org/10.1094/PHYTO-08-20-0330-LE>
- Gerlach W, Nirenberg HI (1982) The genus *Fusarium* – a pictorial atlas. *Mitteilungen der Biologischen Bundesanstalt für Land-und Forstwirtschaft Berlin-Dahlem* 209: 1–406.
- Han SL, Wang MM, Ma ZY, Raza M, Zhao P, Liang JM, Gao M, Li YJ, Wang JW, Hu DM, Cai L (2023) *Fusarium* diversity associated with diseased cereals in China, with an updated phylogenomic assessment of the genus. *Studies in Mycology* 104: 87–148. <https://doi.org/10.3114/sim.2022.104.02>
- He J, Li DW, Cui WL, Zhu LH, Huang L (2024) Morphological and phylogenetic analyses reveal three new species of *Fusarium* (Hypocreales, Nectriaceae) associated with leaf blight on *Cunninghamia lanceolata* in China. *MycKeys* 101: 45–80. <https://doi.org/10.3897/mycokeys.101.113128>
- Leslie JF, Summerell BA (2006) *The Fusarium Laboratory Manual*. Blackwell Publishing Professional, USA. <https://doi.org/10.1002/9780470278376>
- Leslie JF, Pearson CAS, Nelson PE, Toussoun TA (1990) *Fusarium* spp. from corn, sorghum, and soybean fields in the central and eastern United States. *Phytopathology* 80(4): 343–350. <https://doi.org/10.1094/Phyto-80-343>
- Link JHF (1809) *Observationes in ordines plantarum naturales*. *Dissertatio Ima. Gesellschaft Naturforschender Freunde zu Berlin. Magazin* 3(1): 3–42.
- Liu YJ, Whelen S, Hall BD (1999) Phylogenetic relationships among ascomycetes: Evidence from an RNA polymerase II subunit. *Molecular Biology and Evolution* 16(12): 1799–1808. <https://doi.org/10.1093/oxfordjournals.molbev.a026092>
- Liu XF, Tibpromma S, Hughes AC, Chethana KWT, Wijayawardene NN, Dai DQ, Du TY, Elgorban AM, Stephenson SL, Suwannarach N, Xu JC, Lu L, Xu RF, Maharachchikumbura SSN, Zhao CL, Bhat DJ, Sun YM, Karunarathna SC, Mortimer PE (2023) Culturable mycota on bats in central and southern Yunnan Province, China. *Mycosphere* 14: 497–662. <https://doi.org/10.5943/mycosphere/14/1/7>

- Lombard L, van der Merwe NA, Groenewald JZ, Crous PW (2015) Generic concepts in Nectriaceae. *Studies in Mycology* 80: 189–245. <https://doi.org/10.1016/j.simyco.2014.12.002>
- Maryani N, Sandoval-Denis M, Lombard L, Crous PW, Kema GHJ (2019) New endemic *Fusarium* species hitch-hiking with pathogenic *Fusarium* strains causing Panama disease in small-holder banana plots in Indonesia. *Persoonia* 43: 48–69. <https://doi.org/10.3767/persoonia.2019.43.02>
- O'Donnell K, Kistler HC, Cigelnik E, Ploetz RC (1998) Multiple evolutionary origins of the fungus causing Panama disease of banana: Concordant evidence from nuclear and mitochondrial gene genealogies. *Proceedings of the National Academy of Sciences of the United States of America* 95: 2044–2049. <https://doi.org/10.1073/pnas.95.5.2044>
- O'Donnell K, Sutton DA, Rinaldi MG, Gueidan C, Crous PW, Geiser DM (2009) Novel multilocus sequence typing scheme reveals high genetic diversity of human pathogenic members of the *Fusarium incarnatum*-*F. equiseti* and *F. chlamydosporum* species complexes within the United States. *Journal of Clinical Microbiology* 47: 3851–3861. <https://doi.org/10.1128/JCM.01616-09>
- O'Donnell K, Ward TJ, Robert VARG, Crous PW, Geiser DM, Kang S (2015) DNA sequence-based identification of *Fusarium*: Current status and future directions. *Phytoparasitica* 43: 583–595. <https://doi.org/10.1007/s12600-015-0484-z>
- O'Donnell K, Al-Hatmi AMS, Aoki T, Brankovics B, Cano-Lira JF, Coleman JJ, de Hoog GS, Di Pietro A, Frandsen RJN, Geiser DM, Gibas CFC, Guarro J, Kim HS, Kistler HC, Laraba I, Leslie JF, López-Berges MS, Lysøe E, Meis JF, Monod M, Proctor RH, Rep M, Ruiz-Roldán C, Šišić A, Stajich JE, Steenkamp ET, Summerell BA, van der Lee TAJ, van Diepeningen AD, Verweij PE, Waalwijk C, Ward TJ, Wickes BL, Wiederhold NP, Wingfield MJ, Zhang N, Zhang SX (2020) No to *Neocosmospora*: Phylogenomic and practical reasons for continued inclusion of the *Fusarium solani* species complex in the genus *Fusarium*. *MSphere* 5(5): e00810–e00820. <https://doi.org/10.1128/mSphere.00810-20>
- Sandoval-Denis M, Guarnaccia V, Polizzi G, Crous PW (2018) Symptomatic *Citrus* trees reveal a new pathogenic lineage in *Fusarium* and two new *Neocosmospora* species. *Persoonia* 40: 1–25. <https://doi.org/10.3767/persoonia.2018.40.01>
- Santos A, Trindade JVC, Lima CS, Barbosa RDN, da Costa AF, Tiago PV, de Oliveira NT (2019) Morphology, phylogeny, and sexual stage of *Fusarium caatingaense* and *Fusarium pernambucanum*, new species of the *Fusarium incarnatum-equiseti* species complex associated with insects in Brazil. *Mycologia* 111: 244–259. <https://doi.org/10.1080/00275514.2019.1573047>
- Snyder WC, Hansen HN (1940) The species concept in *Fusarium*. *American Journal of Botany* 27(2): 64–67. <https://doi.org/10.1002/j.1537-2197.1940.tb14217.x>
- Suwannarach N, Khuna S, Kumla J, Thitla T, Hongsan S, Nuangmek W, Lumyong S (2023) *Fusarium endophyticum* sp. nov. (Nectriaceae, Hypocreales), a new endophytic fungus from northern Thailand. *Phytotaxa* 606: 43–53. <https://doi.org/10.11646/phytotaxa.606.1.4>
- Toussoun TA, Nelson PE (1968) *Fusarium: A pictorial guide to the identification of Fusarium species according to the taxonomic system of snyder and hansen*. The PaSta. Univ. Press., University Park, London, 51 pp.
- Villani A, Moretti A, De Saeger S, Han Z, Di Mavungu JD, Soares CMG, Proctor RH, Venancio A, Lima N, Stea G, Paciolla C, Logrieco AF, Susca A (2016) A polyphasic approach for characterization of a collection of cereal isolates of the *Fusarium incarnatum-equiseti* species complex. *International Journal of Food Microbiology* 234: 24–35. <https://doi.org/10.1016/j.ijfoodmicro.2016.06.023>



- Wang MM, Chen Q, Diao YZ, Duan WJ, Cai L (2019) *Fusarium incarnatum-equiseti* complex from China. *Persoonia* 43: 70–89. <https://doi.org/10.3767/persoonia.2019.43.03>
- Wang MM, Crous PW, Sandoval-Denis M, Han SL, Liu F, Liang JM, Duan WJ, Cai L (2022) *Fusarium* and allied genera from China: Species diversity and distribution. *Persoonia* 48: 1–53. <https://doi.org/10.3767/persoonia.2022.48.01>
- Wang S, Liu XM, Xiong CL, Gao SS, Xu WM, Zhao LL, Song CY, Liu XY, James TY, Li Z, Zhang XG (2023) ASF1 regulates asexual and sexual reproduction in *Stemphylium eturmiunum* by DJ-1 stimulation of the PI3K/AKT signaling pathway. *Fungal Diversity* 123(1): 159–176. <https://doi.org/10.1007/s13225-023-00528-1>
- Wollenweber HW, Reinking OA (1935) Die Fusarien: Ihre Beschreibung, Schadwirkung und Bekämpfung.
- Xia JW, Sandoval-Denis M, Crous PW, Zhang XG, Lombard L (2019) Numbers to names - restyling the *Fusarium incarnatum-equiseti* species complex. *Persoonia* 43: 186–221. <https://doi.org/10.3767/persoonia.2019.43.05>
- Yin H, Zhou JB, Chen YL, Ren L, Qin N, Xing YL, Zhao XJ (2021) Morphology, phylogeny, and pathogenicity of *Trichothecium*, *Alternaria*, and *Fusarium* species associated with panicle rot on *Chenopodium quinoa* in Shanxi Province, China. *Plant Pathology* 71: 344–360. <https://doi.org/10.1111/ppa.13462>
- Zhang H, Zeng Y, Wei TP, Jiang YL, Zeng XY (2023a) Endophytic *Fusarium* and allied fungi from *Rosa roxburghii* in China. *Mycosphere* 14: 2092–2207. <https://doi.org/10.5943/mycosphere/14/1/25>
- Zhang J, Zhang Z, Li D, Xia J, Li Z (2023b) Three new species of *Microdochium* (Microdochiaceae, Xylariales) on Bambusaceae sp. and saprophytic leaves from Hainan and Yunnan, China. *Journal of Fungi* 9: 1176. <https://doi.org/10.3390/jof9121176>
- Zhang ZX, Shang YX, Zhang MY, Zhang JJ, Geng Y, Xia JW, Zhang XG (2024) Phylogenomics, taxonomy and morphological characters of the Microdochiaceae (Xylariales, Sordariomycetes). *MycKeys* 106: 303–325. <https://doi.org/10.3897/mycokeys.106.127355>

## Supplementary material 1

### GenBank accession numbers of the taxa used in phylogenetic reconstruction

Authors: Congcong Ai, Qiyun Liu, Yaling Wang, Zhaoxue Zhang, Duhua Li, Yun Geng, Xiuguo Zhang, Jiwen Xia

Data type: docx

Copyright notice: This dataset is made available under the Open Database License (<http://opendatacommons.org/licenses/odbl/1.0/>). The Open Database License (ODbL) is a license agreement intended to allow users to freely share, modify, and use this Dataset while maintaining this same freedom for others, provided that the original source and author(s) are credited.

Link: <https://doi.org/10.3897/mycokeys.116.150363.suppl1>

## Supplementary material 2

### Phylogeny of the *Fusarium incarnatum-equiseti* species complex (FIESC) inferred based on the *cal* (a), *rpb2* (b), and *tef1* (c) loci, respectively

Authors: Congcong Ai, Qiyun Liu, Yaling Wang, Zhaoxue Zhang, Duhua Li, Yun Geng, Xiuguo Zhang, Jiwen Xia

Data type: docx

Copyright notice: This dataset is made available under the Open Database License (<http://opendatacommons.org/licenses/odbl/1.0/>). The Open Database License (ODbL) is a license agreement intended to allow users to freely share, modify, and use this Dataset while maintaining this same freedom for others, provided that the original source and author(s) are credited.

Link: <https://doi.org/10.3897/mycokeys.116.150363.supl2>

## Supplementary material 3

### GenBank accession numbers of the taxa used in phylogenetic reconstruction (Supl. material 4)

Authors: Congcong Ai, Qiyun Liu, Yaling Wang, Zhaoxue Zhang, Duhua Li, Yun Geng, Xiuguo Zhang, Jiwen Xia

Data type: docx

Copyright notice: This dataset is made available under the Open Database License (<http://opendatacommons.org/licenses/odbl/1.0/>). The Open Database License (ODbL) is a license agreement intended to allow users to freely share, modify, and use this Dataset while maintaining this same freedom for others, provided that the original source and author(s) are credited.

Link: <https://doi.org/10.3897/mycokeys.116.150363.supl3>

## Supplementary material 4

### Phylogeny inferred based on the combined *cal-rpb2-tef1* sequence dataset with *Fusarium concolor* (NRRL 13459) as the outgroup

Authors: Congcong Ai, Qiyun Liu, Yaling Wang, Zhaoxue Zhang, Duhua Li, Yun Geng, Xiuguo Zhang, Jiwen Xia







Data type: docx

Copyright notice: This dataset is made available under the Open Database License (<http://opendatacommons.org/licenses/odbl/1.0/>). The Open Database License (ODbL) is a license agreement intended to allow users to freely share, modify, and use this Dataset while maintaining this same freedom for others, provided that the original source and author(s) are credited.

Link: <https://doi.org/10.3897/mycokeys.116.150363.supl4>



# Morphological and molecular identification for two new wood-inhabiting species of *Botryobasidium* (Basidiomycota) from China

Xin Li<sup>1,2</sup> , Xin Zhang<sup>1</sup> , Yi-Fei Sun<sup>1</sup> , Zhen-Hao Li<sup>3,4</sup> , An-Hong Zhu<sup>1,5</sup> , Ying-Da Wu<sup>2</sup> 

<sup>1</sup> State Key Laboratory of Efficient Production of Forest Resources, School of Ecology and Nature Conservation, Beijing Forestry University, Beijing 100083, China

<sup>2</sup> Key Laboratory of Forest and Grassland Fire Risk Prevention, Ministry of Emergency Management, China Fire and Rescue Institute, Beijing 102202, China

<sup>3</sup> Zhejiang Key Laboratory of Biological Breeding and Exploitation of Edible and Medicinal Mushrooms, Jinhua 321200, Zhejiang, China

<sup>4</sup> Zhejiang Shouxiangu Pharmaceutical Co., Ltd, Jinhua 321000, Zhejiang, China

<sup>5</sup> Coconut Research Institute, Chinese Academy of Tropical Agricultural Sciences, Wenchang, 571339, China

Corresponding authors: An-Hong Zhu (anhong.zhu@catas.cn); Ying-Da Wu (wydbjfu@163.com)



This article is part of:

**Exploring the Hidden Fungal Diversity:  
Biodiversity, Taxonomy, and Phylogeny of  
Saprobic Fungi**

Edited by Samantha C. Karunarathna,  
Danushka Sandaruwan Tennakoon, Ajay  
Kumar Gautam

Academic editor:

Samantha C. Karunarathna

Received: 5 December 2024

Accepted: 4 March 2025

Published: 9 April 2025

**Citation:** Li X, Zhang X, Sun Y-F, Li Z-H, Zhu A-H, Wu Y-D (2025) Morphological and molecular identification for two new wood-inhabiting species of *Botryobasidium* (Basidiomycota) from China. MycoKeys 116: 73–89. <https://doi.org/10.3897/mycokeys.116.143594>

**Copyright:** © Xin Li et al.  
This is an open access article distributed under  
terms of the Creative Commons Attribution  
License (Attribution 4.0 International – CC BY 4.0).

## Abstract

The wood-inhabiting fungi refer to large basidiomycetes that grow on various woody materials and are distributed in various forest ecosystems, some of which have important economic value. In the present study, two new resupinate, adnate, wood-inhabiting fungal taxa, *Botryobasidium latihyphum* and *B. zhejiangensis*, are introduced based on morphological and molecular characteristics. A molecular phylogenetic study based on sequence data from the internal transcribed spacers (ITS) and the large subunit (nLSU) regions supported the two new species in the genus *Botryobasidium*. Maximum likelihood (ML), maximum parsimony (MP), and Bayesian inference (BI) were employed to perform phylogenetic analyses of these datasets. The new species *B. latihyphum* is characterized by its cream hymenial surface when fresh, olivaceous buff when dry, a monomitic hyphal system with clamp connections, the presence of clavate to tubular cystidia, basidia with six sterigmata, and broadly oval basidiospores measuring 7.9–10.2 × 3.2–4.3 µm. *Botryobasidium zhejiangensis* sp. nov. is characterized by its white to buff-yellow hymenial surface when fresh, cream when dry, a monomitic hyphal system with clamp connections, lacking cystidia, basidia with six sterigmata, and broadly navicular basidiospores measuring 7.9–9.2 × 2.6–3.4 µm. The phylogenetic result inferred from ITS + nLSU sequence data revealed that *B. latihyphum* is closely related to *B. vagum*, *B. laeve*, *B. subincanum*, and *B. incanum*, while *B. zhejiangensis* is closely related to *B. leptocystidiatum*, *B. subcoronatum*, *B. xizangensis*, and *B. intertextum*.

**Key words:** Botryobasidiaceae, new species, phylogeny, taxonomy, wood-rotting fungi

## Introduction

The wood-inhabiting fungi are large basidiomycetes that grow on various woody materials and have a global distribution (Wu et al. 2022a; Bian et al. 2023; Dong et al. 2023; Zhao et al. 2024). The wood-inhabiting fungi play an important role in maintaining the dynamic balance of energy and matter in forest ecosystems, and some of them have important economic values (Dai et al. 2007; Zhao et al. 2012; Dai et al. 2015; Wu et al. 2019; Dai et al. 2021; Yuan et al. 2023;



Zhou et al. 2023a; Dong et al. 2024a). *Botryobasidium* (Botryobasidiaceae, Basidiomycota), typified by *B. subcoronatum* (Höhn. & Litsch.) Donk, is a wood-inhabiting fungal genus with simple macro-morphology. It is characterized by annual, resupinate basidiomata with smooth, pellicular, hypochnoid, or arachnoid hymenophores; a monomitric hyphae system; generative hyphae bearing simple septa or clamp connections, branched mostly at a right angle; basidia with 2–8 sterigmata; smooth or ornamented basidiospores; and causing a white rot (Donk 1964; Langer et al. 2000b; Moncalvo et al. 2006; Xiong et al. 2009).

In the earliest classification system, *Botryobasidium* species were treated in *Corticium* Pers. based on microscopic morphological characteristics; Donk (1931) proposed *Botryobasidium* for the species with four sterigmata on basidia and basidiospores strongly ornamented with rodlets. Many species of *Botryobasidium* in the conidial state belong to the genus *Oidium* Link (Eriksson and Ryvarden 1973). Later, Langer conducted a detailed morphological study, revising the genus based on global samples and identifying 49 species within *Botryobasidium* (Langer et al. 2000a, b). Numerous *Botryobasidium* species exhibited anamorphic stages (Bernicchia and Gorjón 2010). Multiple asexual morph genera viz., *Acladium* Link, *Allescheriella* Henn., *Alysidium* Kunze, *Haplotrichum* Link, *Neoaccladium* P.N. Singh & S.K. Singh, *Physospora* Fr., and *Sporocephalium* Chevall. exhibit congeneric relationships with *Botryobasidium*, prompting their taxonomic reclassification under the genus *Botryobasidium* (Stalpers et al. 2021; Dong et al. 2024b).

Phylogenetically, the genus *Botryobasidium* is a well-supported monophyletic group closely related to *Tulasnella* J. Schröt., *Clavulina* J. Schröt., and *Sistotrema* Fr., but the former differed from the latter three genera by having wider hyphae and lacking oil droplets in basidia and basidiospores (Hibbett et al. 1997; Kotiranta and Saarenoksa 2005; Yuan et al. 2011).

So far, 115 species of *Botryobasidium* have been discovered worldwide (Langer 1994; Parmasto et al. 2004; Ryvarden et al. 2005; Xiong et al. 2009; Bernicchia et al. 2010; Bates et al. 2017; Ram et al. 2021; Stalpers et al. 2021; Zhou et al. 2024a), among them 17 were reported in China (Langer et al. 2000a, 2000b; Xiong et al. 2009; Dong et al. 2024b; Zhou et al. 2024a). During investigations on the diversity of wood-rotting fungi, four *Botryobasidium*-like samples were collected. Phylogenetic analyses based on the ITS and nLSU sequences were carried out to confirm their taxonomic status. Morphological and molecular evidence confirmed that the four examined specimens belong to two distinct new *Botryobasidium* species.

## Materials and methods

### Morphological studies

Fresh fruiting bodies of the fungi were collected from Linzhi of Xizang Autonomous Region and Jinhua of Zhejiang Province, China. After the important collection information was noted (Rathnayaka et al. 2024), the samples were taken to the laboratory at the Institute of Microbiology, Beijing Forestry University (BJFC), in plastic collection boxes. Specimens were dried in a mushroom dryer at 35 °C (Hu et al. 2022), then sealed and stored in an envelope bag. Examined specimens were deposited in the Fungarium of

the Institute of Microbiology, Beijing Forestry University (**BJFC**), Beijing, China. Morphological descriptions were based on field notes and dried specimens. Micro-morphological data were obtained from dried specimens and observed under a compound microscope following Dai (2010) and Li et al. (2014). Sections were studied at a magnification of 1000 × using a Nikon E80i microscope and phase contrast illumination (Nikon, Tokyo, Japan). Line drawings were made with the aid of a drawing tube.

The following abbreviations were used in the descriptions: **KOH** = 5% potassium hydroxide, **IKI** = Melzer's reagent, **IKI–** = neither amyloid nor dextrinoid, **CB** = Cotton Blue, **CB+** = cyanophilous, **CB–** = acyanophilous, **L** = mean spore length (arithmetic average of all spores), **W** = mean basidiospore width (arithmetic average of all spores), **Q** = variation in the L/W ratios between the specimens studied, **n (a/b)** = number of basidiospores (a) measured from the given number of specimens (b). In presenting basidiospore size variation, 5% of measurements were excluded from each end of the range, and these values were given in parentheses. Special color is termed follow Anonymous (1969) and Petersen (1996).

### DNA extraction, polymerase chain reaction amplification, and sequencing

Total genomic DNA from the dried specimens was extracted by a Cetyltrimethyl Ammonium Bromide (**CTAB**) rapid plant genome extraction kit (Aidlab Biotechnologies Company Limited, Beijing, China) according to the manufacturer's instructions with some modifications (Du et al. 2021). ITS locus was amplified using the primer pair ITS4 (TCCTCC GCT TAT TGA TAT GC) and ITS5 (GGA AGT AAA AGT CGT AAC AAG G) (White et al. 1990), while nLSU locus was amplified with primers LR0R (ACC CGC TGA ACT TAA GC) and LR7 (TAC TAC CAC CAA GAT CT) (Vilgalys and Hester 1990).

The polymerase chain reaction (**PCR**) amplification conditions for ITS were an initial denaturation at 95 °C for 3 min, followed by 35 cycles at 94 °C for 40 s, 54 °C for 45 s, and 72 °C for 1 min, and a final extension at 72 °C for 10 min (Zhao et al. 2015), and for nLSU were initial denaturation at 94 °C for 1 min, followed by 35 cycles of denaturation at 94 °C for 30 s, at 48 °C for 1 min, and extension at 72 °C for 1.5 min, and a final extension at 72 °C for 10 min. The PCR products were purified and sequenced in the Beijing Genomics Institute, China, with the same primers used in the PCR reactions.

### Phylogenetic analyses

The species, specimens, and GenBank accession numbers of the sequences used in this study are shown in Table 1.

For the phylogenetic analyses, the combined two-marker dataset (ITS+nLSU) included sequences from 57 samples representing 20 taxa. *Lyomyces allantosporus* Riebesehl et al. and *Lyomyces pruni* (Lasch) Riebesehl & Langer were chosen as the outgroups (Spirin et al. 2015; Riebesehl and Langer 2017; Chen and Zhao 2020). Sequences generated from this study were aligned with additional sequences downloaded from GenBank using BioEdit (Hall 1999) and ClustalX (Thompson et al. 1997). The final ITS and nLSU datasets were subsequently aligned using MAFFT v.7 under the E-INS-i

**Table 1.** List of species, specimens, and GenBank accession numbers of the sequences used in this study. New species are in bold, \* indicates type material, holotype, and - refers to the data unavailability.

Species name	Samples	Country	GenBank Accession no.	
			ITS	nLSU
<i>Botryobasidium acanthosporum</i>	Yuan 17989	China	PP229511	-
<i>B. acanthosporum</i>	Yuan 18083*	China	PP229512	PP218361
<i>B. acanthosporum</i>	Yuan 18128	China	PP229517	-
<i>B. acanthosporum</i>	Yuan 16326	China	PP229497	-
<i>B. asperulum</i>	RAS552	USA	OR471090	OR470959
<i>B. asperulum</i>	RAS578	USA	OR471100	OR470964
<i>B. aureum</i>	RAS571 SV2	USA	OR471099	-
<i>B. aureum</i>	RAS571 SV1	USA	OR471098	-
<i>B. bambusinum</i>	CLZhao 29938	China	PQ539059	PQ539062
<i>B. bambusinum</i>	CLZhao 29936	China	PQ539058	PQ539061
<i>B. bambusinum</i>	CLZhao 29916*	China	PQ539057	PQ539060
<i>B. botryosum</i>	AFTOL-ID 604	USA	DQ267124	DQ089013
<i>B. candicans</i>	UC2022891	USA	KP814227	-
<i>B. candicans</i>	UC2022893	USA	KP814200	-
<i>B. candicans</i>	HFRG_LG230226_1_FRDBI_29580226	UK	OR896129	-
<i>B. coniferarum</i>	LWZ20210928-3*	China	OR557259	OR527282
<i>B. coniferarum</i>	LWZ20171016-15	China	OR557262	OR527286
<i>B. conspersum</i>	AFTOL-ID 1766	USA	DQ911612	DQ521414
<i>B. conspersum</i>	RAS259	USA	OR471145	-
<i>B. gossypirubiginosum</i>	CLZhao 26052*	China	OR668924	OR708665
<i>B. gossypirubiginosum</i>	Dai 26208	China	PQ285750	-
<i>B. incanum</i>	Dai 25375	China	PQ285751	PQ28566
<i>B. incanum</i>	CLZhao 26697	China	OR668923	OR708664
<i>B. indicum</i>	Yuan 18434	China	PP209217	PP218365
<i>B. indicum</i>	hr5326	China	OP806032	-
<i>B. intertextum</i>	UC2022959 18S	USA	KP814540	-
<i>B. laeve</i>	RAS762	USA	OR471128	PP959648
<b><i>B. latihyphum</i></b>	<b>Dai 26858*</b>	<b>China</b>	<b>PQ279526</b>	<b>PQ282521</b>
<b><i>B. latihyphum</i></b>	<b>Yuan 16496</b>	<b>China</b>	<b>PP331854</b>	<b>PP218153</b>
<i>B. leptocystidium</i>	Yuan 17706	China	PP209200	PP218353
<i>B. leptocystidium</i>	Yuan 17708*	China	PP209197	PP218354
<i>B. robustius</i>	CBS:945.69	Czech	MH859491	MH871272
<i>B. robustius</i>	iNaturalist 162067551	USA	PP436446	-
<i>B. rubiginosum</i>	RAS776 taxon1	USA	OR471136	-
<i>B. simile</i>	RAS793	USA	OR471147	-
<i>B. simile</i>	RAS794	USA	OR471146	-
<i>B. subcoronatum</i>	RAS770 SV1	USA	OR471132	-
<i>B. subcoronatum</i>	RAS770 SV2	USA	OR471133	-
<i>B. subovalibasidium</i>	Yuan 16439	China	PP209199	PP218152
<i>B. subovalibasidium</i>	Yuan 18179*	China	PP209196	PP218362
<i>B. subincanum</i>	LWZ20230417-17b	China	PP959661	PP959649
<i>B. subincanum</i>	LWZ20230417-41a	China	PP959660	-
<i>B. tubulicystidium</i>	DK14 139	USA	OL436769	-
<i>B. vagum</i>	LWZ20191016-22	USA	PP959659	PP959648
<i>B. xizangense</i>	LWZ20230722-25a*	China	PP959663	PP959650
<i>B. xizangense</i>	LWZ20230722-16a	China	PP959662	-
<i>B. yunnanense</i>	CLZhao 24877*	China	OR708666	OR668925
<b><i>B. zhejiangensis</i></b>	<b>Dai 25056*</b>	<b>China</b>	<b>PQ279530</b>	<b>PQ282525</b>
<b><i>B. zhejiangensis</i></b>	<b>Dai 24851</b>	<b>China</b>	<b>PQ279529</b>	<b>PQ282524</b>
<i>Lyomyces allantosporus</i>	FR 0249548	France	NR_154135	-
<i>L. pruni</i>	GEL2327	Germany	DQ340312	-

strategy with no cost for opening gaps and equal cost for transformations (command line: `mafft -genafpair -maxiterate 1,000`) (Kato and Standley 2013) and visualized in BioEdit. Alignments were spliced and transformed into formats in Mesquite v.3.2 (Maddison and Maddison 2017). Sequence alignments were deposited at TreeBASE (submission ID 32008, [www.treebase.org](http://www.treebase.org)). The best-fit evolutionary model was estimated using MrModeltest v.2.3 (Posada and Crandall 1998) as GTR + I + G for the combined dataset.

Maximum likelihood (ML) analyses were conducted using RAXML-HPC2 via the CIPRES Science Gateway ([www.phylo.org](http://www.phylo.org); Miller et al. 2010). Branch support (BT) for ML analysis was determined by 1,000 bootstrap replicates. The maximum parsimony (MP) analysis was applied to the ITS+nLSU dataset sequences. The construction was performed in PAUP\* v. 4.0b10 (Swofford 2002). All characters were equally weighted, and gaps were treated as missing data. Trees were inferred using the heuristic search option with TBR branch swapping and 1,000 random sequence additions. Max-trees was set to 5,000, branches of zero length were collapsed, and all parsimonious trees were saved. Clade robustness was assessed by a bootstrap (BT) analysis with 1,000 replicates (Felsenstein 1985). Descriptive tree statistics, i.e., tree length (TL), consistency index (CI), retention index (RI), rescaled consistency index (RC), and homoplasy index (HI), were calculated for each maximum parsimonious tree (MPT) generated. The BI analysis was calculated with MrBayes v.3.1.2 with a general time reversible (GTR) model of DNA substitution and a gamma distribution rate variation across sites (Ronquist and Huelsenbeck 2003). Four Markov chains were run for 2 runs from random starting trees for 2 million generations, and trees were sampled every 100 generations. The first 25% of sampled trees were set as burn-in. A majority rule consensus tree of all remaining trees was calculated. The maximum likelihood bootstrap support value (BS), the maximum parsimony bootstrap support value (BT), and Bayesian posterior probabilities (BPP) simultaneously not less than 50%, 75%, and 0.95, respectively, were shown at the nodes.

## Results

### Phylogenetic analyses

The combined dataset of ITS+nLSU contained sequences from 47 fungal specimens representing 25 *Botryobasidium* taxa (2 new species and another 23 taxa). The combined dataset has an aligned length of 2,027 characters, of which 1,431 characters are constant, 126 are variable and parsimony uninformative, and 470 are parsimony informative. The MP analysis yielded two equally most parsimonious trees (TL = 1,672, CI = 0.587, RI = 0.856, RC = 0.502, HI = 0.413). The Bayesian analysis and MP analysis resulted in a similar topology as the ML analysis. The ML tree is provided in Fig. 1. The average SD of split frequencies in BI analyses is 0.002852 (BI). Two new species, *B. latihyphum* and *B. zhejiangensis*, were proposed based on examining type materials and phylogenetic analyses (Fig. 1).

The top five BLAST results for the ITS of *Botryobasidium latihyphum* on NCBI are *Botryobasidium* sp. (PP229498), *Botryobasidium* sp. (KP814226),



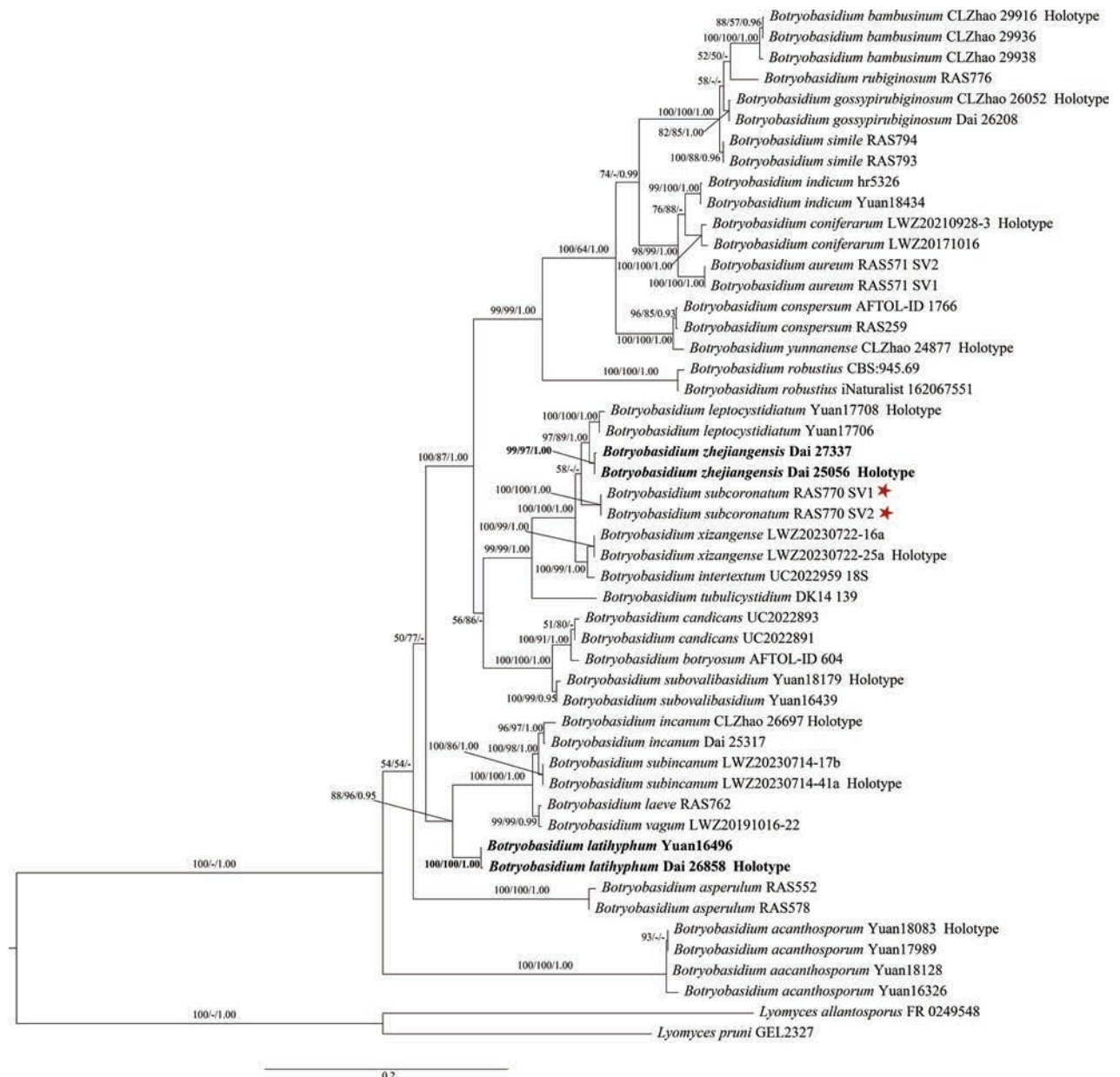


**Figure 1.** Maximum Likelihood tree illustrating the phylogeny of *Botryobasidium* based on combined ITS + nLSU sequence data. Branches are labeled with maximum likelihood bootstrap proportions equal to or higher than 50%, maximum parsimony bootstrap equal to or higher than 75%, and Bayesian posterior probabilities equal to or higher than 0.95. The red star represents the type species. The new species are in bold black.

uncultured Corticiales (FJ475677), *Botryobasidium* sp. (KP814344), and *Botryobasidium* sp. (KP814346); the top five BLAST results for the nLSU of *B. latihyphum* on NCBI are *Botryobasidium* sp. (PP218153), *Botryobasidium* sp. (OR470952), *B. incanum* (OR708664), *B. vagum* (OR470970), and *Botryobasidium* sp. (OR470958); the top five BLAST results for the ITS of *Botryobasidium zhejiangensis* on NCBI are *Botryobasidium* sp. (OR471085), *B. vagum* (OR471082), *B. vagum* (MK809424), *B. subcoronatum* (MK809424), and *B. subcoronatum* (MK795129); and the top five BLAST results for the nLSU of *B. zhejiangensis* on NCBI are *B. subcoronatum* (OM083971), *B. vagum* (OR470953), *B. subcoronatum* (OR470950), *B. subcoronatum* (EU909344), and *B. subcoronatum* (OR470954).

## Taxonomy

***Botryobasidium latihyphum* Xin Li, Y.J. Cui & Y.D. Wu, sp. nov.**

MycoBank No: 856838

Figs 2, 3

**Holotype.** CHINA • Xizang Autonomous Region., Linzhi, Metuo County, the road 219 from Metuo to Bome, on fallen trunk of *Abies*, 25 October 2023, Dai 26858 (BJFC044409).

**Etymology.** *Latihyphum* refers to the characteristic wide subicular hyphae of the new species.

**Description. Basidiomata:** Annual, resupinate, adnate, hypochnoid, difficult to separate from substrate, up to 10 cm long, 4 cm wide, 1 mm thick at center, without odor and taste when fresh and dry; hymenophore white to cream when fresh, smooth, uncracked, cream to olivaceous buff when dry; sterile margin indistinct, thinning out, concolorous with hymenophore.

**Hyphal system:** Monomitic, clamp connections present, generative hyphae CB+, IKI–; tissues unchanged in KOH; subhymenial hyphae slightly thick-walled, smooth, frequently branched at right angles, loosely interwoven, 5–7 µm in diam.; subicular hyphae thick-walled, smooth, frequently branched, 7–10 µm in diam.

**Hymenium:** Cystidia clavate to tubular, infrequent, smooth, thin-walled, colorless, with a basal clamp connection, aseptate, CB+, IKI–, unchanged in KOH, 56–105 × 7–10 µm; basidia slightly barrel-shaped, thin-walled, with six sterigmata and a clamp connection at the base, 17–25 × 6–8.5 µm; basidioles in shape similar to basidia, but slightly smaller.

**Spores:** Basidiospores oval, hyaline, thin-walled, smooth, CB+, IKI–, (7.0–)7.9–10.2(–10.3) × (3.1–)3.2–4.3(–4.4) µm, L = 8.78 µm, W = 3.64 µm, Q = 2.41 (n = 60/2).



**Figure 2.** A basidioma of *Botryobasidium latihyphum* (Dai 26858). Scale bar: 1 cm.



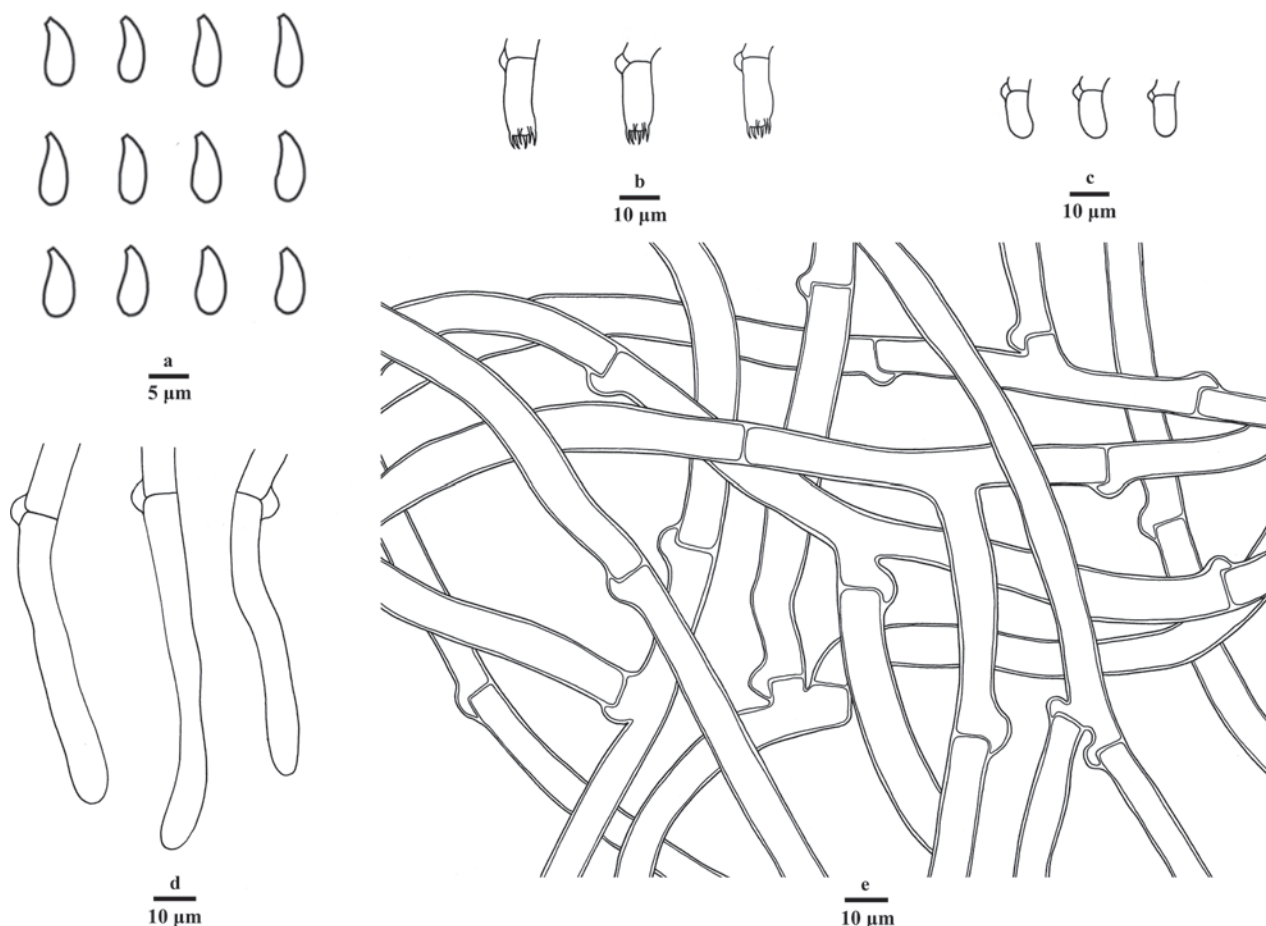


**Figure 3.** Microscopic structures of *Botryobasidium latihyphum* (drawn from the holotype Dai 26858) **a** basidiospores **b** basidia **c** basidioles **d** cystidia **e** subicular hyphae. Scale bars: 5 µm (**a**); 10 µm (**b–e**).

***Botryobasidium zhejiangensis* Xin Li, A.H. Zhu, Yuan Yuan & Y.D. Wu, sp. nov.**

MycoBank No: 856839

Figs 4, 5

**Holotype.** CHINA • Zhejiang Province, Jinhua, Wuyi County, Guodong Village, on rotten wood of *Pinus massoniana*, 18 June 2023, Dai 25056 (BJFC 042609).

**Etymology.** *Zhejiangensis* refers to the type location, Zhejiang Province, East China.

**Description. Basidiomata:** Annual, resupinate, adnate, pellicular, difficult to separate from substrate, up to 11 cm long, 7 cm wide, 1 mm thick, without odor and taste when fresh; hymenophore white to cream, smooth, uncracked, cream to slightly buff when dry; sterile margin indistinct, thinning out, concolorous with hymenophore.

**Hyphal system:** Monomitic, generative hyphae with clamp connections, CB+, IKI–; tissues unchanged in KOH. Subhymenial hyphae hyaline, thin-walled, smooth, frequently branched at right angles, loosely interwoven, 4–6 µm in diam.; subicular hyphae hyaline, slightly thick-walled, smooth, frequently branched, 6–8 µm in diam.

**Hymenium:** Basidia slightly barrel-shaped, hyaline, thin-walled, with six sterigmata and a basal clamp connection, 15–19 × 5–6 µm; basidioles in shape similar to basidia, but smaller.



Figure 4. Basidiomata of *Botryobasidium zhejiangensis* (Dai 25056). Scale bar: 1 cm.

**Spores:** Basidiospores more or less navicular, hyaline, thin-walled, smooth, CB+, IKI–,  $(7.8\text{--}7.9\text{--}9.2\text{--}9.5) \times (2.5\text{--})2.6\text{--}3.4\text{--}3.5) \mu\text{m}$ ,  $L = 8.47 \mu\text{m}$ ,  $W = 3.05 \mu\text{m}$ ,  $Q = 2.78$  ( $n = 60/2$ ).

## Discussion

Prior to this study, 17 *Botryobasidium* species, viz., *B. acanthosporum* L.J. Zhou & H.S. Yuan, *B. arachnoideum* G. Langer, *B. asterosporum*, G. Langer, *B. coniferarum* S.L. Liu & L.W. Zhou, *B. gossypirubiginosum* Qian Zhou & C.L. Zhao, *B. grandisporum* G. Langer, *B. incanum* Qian Zhou & C.L. Zhao, *B. leptocystidium* L.J. Zhou & H.S. Yuan, *B. longisporum* G. Langer, *B. musisporum* G. Langer, *B. subincanum* S.L. Liu & L.W. Zhou, *B. sublaeve* G. Langer, *B. subovalibasidium* L.J. Zhou & H.S. Yuan, *B. tuberculisporum* G. Langer, *B. tubulicystidium* G. Langer, *B. xizangense* S.L. Liu & L.W. Zhou and *B. yunnanense* Qian Zhou & C.L. Zhao were reported from China (Lentz 1967; Jung 1995; Kalinina et al. 2020; Cao et al. 2021; Zhou et al. 2024a). In this study, a large number of specimens were collected from Xizang and Zhejiang provinces in China, and two new species were presented according to morphological and phylogenetic evidence, which further improved the genus diversity of *Botryobasidium* in China.

In the present study, the phylogenetic analyses using the combined ITS + nLSU dataset produced a well-resolved phylogeny (Fig. 1). *Botryobasidium latihyphum* and *B. zhejiangensis* formed two well-supported lineages (100% in ML, 100% in

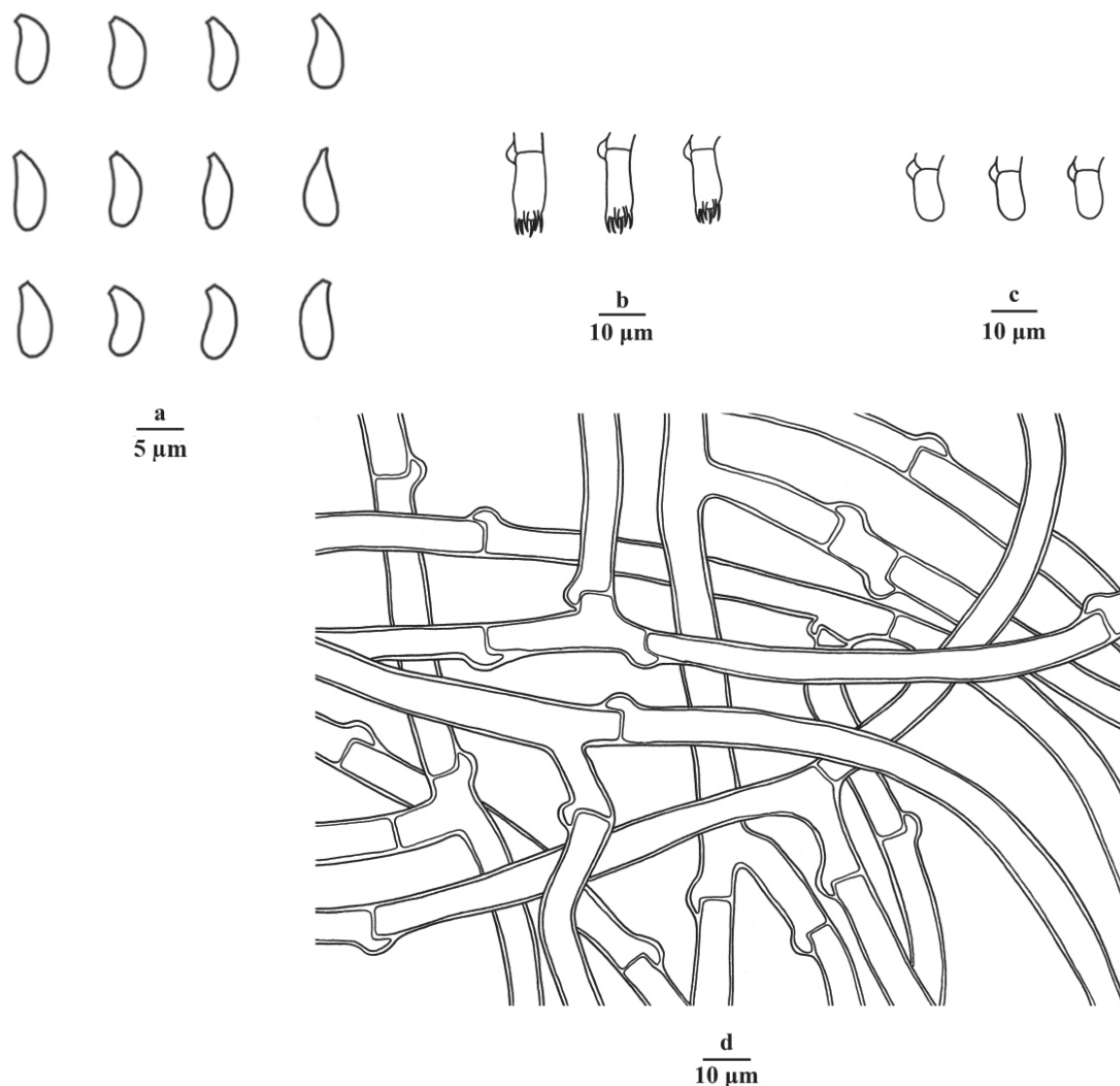


**Figure 5.** Microscopic structures of *Botryobasidium zhejiangensis* (drawn from the holotype Dai 24851) **a** basidiospores **b** basidia **c** basidioles **d** subicular hyphae. Scale bars: 5 µm (**a**); 10 µm (**b–d**).

MP, and 1.00 in BI; 99% in ML, 97% in MP, and 1.00 in BI). The phylogeny analyses revealed that *Botryobasidium latihyphum* is related to *B. vagum* (Berk. & M.A. Curtis) D.P. Rogers, *B. laeve* (J. Erikss.) Parmasto, *B. subincanum*, and *B. incanum* (Figure 1). However, *B. vagum* is readily distinguished from *B. latihyphum* by having reticulate to floccose hymenophore, wider basidiospores (4.5–6 µm vs. 3.2–4.3 µm, Bernicchia and Gorjón 2010), and lacking clamp connection; *B. laeve* differs from *B. latihyphum* by cylindrical basidia and shorter basidiospore (5–8 µm vs. 7.9–10.2 µm); *B. subincanum* differs from *B. latihyphum* by having simple septate hyphae, longer basidia (8–11 µm vs. 6–8.5 µm) and wider basidiospore (4–5 µm vs. 3.2–4.3 µm, Wang et al. 2024a); *B. incanum* differs from *B. latihyphum* by having arachnoid hymenophore, basidia with four sterigmata, and lacking clamp connection (Zhou et al. 2024a). Morphologically, *Botryobasidium danicum* J. Erikss & Hjortstam is similar to *B. latihyphum* by sharing a hypochnoid hymenial surface and subcylindrical basidia with six sterigmata. However, *B. danicum* differs from *B. latihyphum* by having simple septate hyphae and navicular and longer basidiospores (12–14 µm vs. 7.9–10.2 µm, Bernicchia and Gorjón 2010).



In the phylogenetic tree (Fig. 1), *Botryobasidium zhejiangensis* is related to *B. leptocystidiatum*, *B. intertextum* (Schwein.) Jülich & Stalpers, *B. subcoronatum*, and *B. xizangense* (Fig. 1). The ITS region of *B. zhejiangensis* is different from *B. leptocystidiatum* by 7.4%, but *B. leptocystidiatum* differs from *B. zhejiangensis* by having tubular cystidia and shorter basidiospores (6.5–7.8 µm vs. 7.9–9.2 µm, Zhou et al. 2024a); *B. intertextum* differs from *B. zhejiangensis* by subcylindrical basidia and wider basidiospores (1.8–2.8 µm vs. 2.6–3.4 µm); *B. subcoronatum* differs from *B. zhejiangensis* by having yellowish to ochraceous hymenial surface, bigger basidia (20–25 × 7–9 µm vs. 15–19 × 5–6 µm), shorter basidiospores (6–8 µm vs. 7.9–9.2 µm, Bernicchia and Gorjón 2010); *B. xizangense* differs from *B. zhejiangensis* by subcylindrical basidia and wider basidia (6–7 µm vs. 5–6 µm, Wang et al. 2024b). Morphologically, *Botryobasidium zhejiangensis* resembles *B. robustius* Pouzar & Hol-Jech by sharing pellicular hymenial surface and similar basidia with six sterigmata, but *B. robustius* differs from *B. zhejiangensis* by having wider basidia (8–10 µm vs. 5–6 µm, Bernicchia and Gorjón 2010) and a lack of clamp connection.

The wood-inhabiting fungi are a widely studied group of the kingdom fungi, which can promote the material circulation and energy flow of the forest ecosystem and bring great economic value. Further investigation of wood-inhabiting fungi in different forestry habitats will enrich the fungal diversity in China and the world. (Dai et al. 2009; Dai 2010; Wu et al. 2014, 2022b; Cui et al. 2019; Wu et al. 2020; Wijayawardene et al. 2022; Mao et al. 2023; Wang et al. 2023; Zhang et al. 2023; Zhao et al. 2023b; Zhou et al. 2023b; Cui et al. 2024; Qin et al. 2024; Zhou et al. 2024b).

### Key to species of *Botryobasidium* in China

1	Generative hyphae with simple septa .....	2
–	Generative hyphae with clamp connections .....	17
2	Cystidia present .....	<b><i>B. acanthosporum</i></b>
–	Cystidia absent .....	3
3	Chlamydospores present .....	<b><i>B. subovalibasidium</i></b>
–	Chlamydospores absent .....	4
4	Conidia present .....	5
–	Conidia absent .....	6
5	Basidiospores > 13 µm long .....	<b><i>B. robustius</i></b>
–	Basidiospores < 13 µm long .....	<b><i>B. bambusinum</i></b>
6	Basidia with six sterigmata .....	7
–	Basidia with four sterigmata .....	15
7	Basidiospores mostly > 9 µm long .....	8
–	Basidiospores mostly < 9 µm long .....	10
8	Basidia > 20 µm long .....	9
–	Basidia < 20 µm long .....	<b><i>B. danicum</i></b>
9	Basidiomata reticulate to floccose .....	<b><i>B. vagum</i></b>
–	Basidiomata hypochnoid .....	<b><i>B. botryosum</i></b>
10	Basidia obovate .....	<b><i>B. aureum</i></b>
–	Basidia subcylindrical .....	11
11	Basidia > 8 µm wide .....	12
–	Basidia < 8 µm wide .....	13
12	Basidiomata floccose .....	<b><i>B. laeve</i></b>
–	Basidiomata pellicular .....	<b><i>B. subincanum</i></b>

13	Basidiospores navicular.....	14
–	Basidiospores subcylindrical.....	<i>B. conspersum</i>
14	Basal hyphae > 8 µm in diam.....	<i>B. candicans</i>
–	Basal hyphae < 8 µm in diam.....	<i>B. xizangense</i>
15	Basidiomata floccose to cotton .....	<i>B. gossypirubiginosum</i>
–	Basidiomata hypochnoid .....	16
16	Basidiospores > 7 µm wide.....	<i>B. isabellinum</i>
–	Basidiospores < 7 µm wide.....	<i>B. incanum</i>
17	Basidia mostly < 6 µm wide .....	18
–	Basidia mostly > 6 µm wide .....	19
18	Basidiospores > 2.5 µm wide .....	<i>B. zhejiangensis</i>
–	Basidiospores < 2.5 µm wide.....	<i>B. intertextum</i>
19	Basidiospores > 8 µm long .....	<i>B. latihyphum</i>
–	Basidiospores < 8 µm long .....	20
20	Cystidia absent .....	<i>B. subcoronatum</i>
–	Cystidia present.....	<i>B. leptocystidium</i>

## Additional information

### Conflict of interest

The authors have declared that no competing interests exist.

### Ethical statement

No ethical statement was reported.

### Funding

The research is supported by the National Natural Science Foundation of China (Project No. 32300013, 32300002) and the Postdoctoral Fellowship Program (Grade C) of the China Postdoctoral Science Foundation (GZC20230254).

### Author contributions

All authors have contributed equally.


### Author ORCIDs

Xin Li  <https://orcid.org/0009-0001-1625-8589>

Xin Zhang  <https://orcid.org/0009-0005-8363-7852>

Yi-Fei Sun  <https://orcid.org/0000-0003-3997-3662>

Zhen-Hao Li  <https://orcid.org/0000-0001-8279-8981>

An-Hong Zhu  <https://orcid.org/0000-0002-2812-8108>

Ying-Da Wu  <https://orcid.org/0000-0003-1295-4015>

### Data availability

All of the data that support the findings of this study are available in the main text.

## References

Anonymous (1969) Flora of British fungi. Colour identification chart. Her Majesty's Stationery Office, London, 1–3.

- Bates ST, Golday J, Kunnen RL, Pilla NJ (2017) Checklist of Indiana fungi I: Macrofungi. *Proceedings of the Indiana Academy of Sciences* 126: 12–34.
- Bernicchia A, Gorjón SP (2010) Corticiaceae s.l. *Fungi Europaei* n°12. edn. Candusso, Italia.
- Bernicchia A, Langer G, Gorjón SP (2010) *Botryobasidium sassofratinoense* sp. nov. (Cantharellales, Basidiomycota) from Italy. *Mycotaxon* 111: 403–409. <https://doi.org/10.5248/111.403>
- Bian LS, An Q, Wang XH, Chen L, Han ML (2023) Diversity of wood-inhabiting macrofungi in the Taihang Mountains, northern China. *Mycosystema* 42: 2188–2202.
- Cao T, Hu YP, Yu JR, Wei TZ, Yuan HS (2021) A phylogenetic overview of the Hydnaceae (Cantharellales, Basidiomycota) with new taxa from China. *Studies in Mycology* 99(1): 100–121. <https://doi.org/10.1016/j.simyco.2021.100121>
- Chen JZ, Zhao CL (2020) Morphological and molecular identification of four new resupinate species of *Lyomyces* (Hymenochaetales) from southern China. *Mycosystema* 65: 101–118. <https://doi.org/10.3897/mycokeys.65.48660>
- Cui BK, Li HJ, Ji X, Zhou JL, Song J, Si J, Yang ZL, Dai YC (2019) Species diversity, taxonomy and phylogeny of Polyporaceae (Basidiomycota) in China. *Fungal Diversity* 97: 137–392. <https://doi.org/10.1007/s13225-019-00427-4>
- Cui YJ, Wu YD, Jiang YH, Zhu AH, Wu F, Liu HG, Dai YC, Yuan Y (2024) Diversity of macrofungi in southeast Xizang 1. the wood-decay fungi. *Mycology* 26: 1–35. <https://doi.org/10.1080/21501203.2024.2379476>
- Dai YC (2010) Hymenochaetaceae (Basidiomycota) in China. *Fungal Diversity* 45: 131–343. <https://doi.org/10.1007/s13225-010-0066-9>
- Dai YC, Cui BK, Yuan HS, Li BD (2007) Pathogenic wood-decaying fungi in China. *Forest Pathol* 37: 105–120. <https://doi.org/10.1111/j.1439-0329.2007.00485.x>
- Dai YC, Yang ZL, Cui BK, Yu CJ, Zhou LW (2009) Species diversity and utilization of medicinal mushrooms and fungi in China (Re-view). *International Journal of Medicinal Mushrooms* 11: 287–302. <https://doi.org/10.1615/IntJMedMushr.v11.i3.80>
- Dai YC, Wei YL, Zhou LW (2015) Polypore richness along an elevational gradient: A case study in Changbaishan Nature Reserve, Northeastern China. *Fungal Ecology* 13: 226–228. <https://doi.org/10.1016/j.funeco.2014.07.002>
- Dai YC, Yang ZL, Cui BK, Wu G, Yuan HS, Zhou LW, He SH, Ge ZW, Wu F, Wei YL, Yuan Y, Si J (2021) Diversity and systematics of the important macrofungi in Chinese forests. *Mycosystema* 40: 770–805. <https://doi.org/10.13346/j.mycosystema.210036> [in Chinese]
- Dong JH, Gu JY, Zhao CL (2023) Diversity of wood-decaying fungi in Wenshan Area, Yunnan Province, China. *Mycosystema* 42: 638–662.
- Dong JH, Li Q, Yuan Q, Luo YX, Zhang XC, Dai YF, Zhou Q, Deng YL, Zhou HM, Muhammad A, Zhao CL (2024a) Species diversity, taxonomy, molecular systematics and divergence time of wood-inhabiting fungi in Yunnan-Guizhou Plateau, Asia. *Mycosphere* 15(1): 1110–1293. <https://doi.org/10.5943/mycosphere/15/1/10>
- Dong JH, Wang XY, He SY, Zhang JL, Yin HJ, Zhang SH, Zhao CL (2024b) *Botryobasidium bambusinum* (Botryobasidiaceae, Cantharellales): a new species from Yunnan, Southwest China, based on morphology and phylogeny. *New Zealand Journal of Botany*, 1–18. <https://doi.org/10.1080/0028825X.2024.2438181>
- Donk MA (1931) Revisie van de Nederlandse Heterobasidiomycetae en Homobasidiomycetae Aphyllophoraceae 1. Mededengen van de Nederlandse Mycologische Vereeniging 116: 18–20.
- Donk MA (1964) A conspectus of the families of Aphyllophorales. *Persoonia* 3: 199–324.

- Du P, Cao TX, Wu YD, Zhou M, Liu ZB (2021) Two new species of Hymenochaetaceae on *Dracaena cambodiana* from tropical China. *MycKeys* 80: 1–17. <https://doi.org/10.3897/mycokeys.80.63997>
- Eriksson J, Ryvarden L (1973) The Corticiaceae of North Europe Vol. 2, *Aleurodiscus–Confertobasidium*, 60–261.
- Felsenstein J (1985) Confidence intervals on phylogenetics: An approach using bootstrap. *Evolution* 39: 783–791. <https://doi.org/10.2307/2408678>
- Hall TA (1999) Bioedit: A user-friendly biological sequence alignment editor and analysis program for Windows 95/98/NT. *Nucleic Acids Symposium Series* 41: 95–98. <https://doi.org/10.1021/bk-1999-0734.ch008>
- Hibbett DS, Pine EM, Langer E, Langer G, Donoghue MJ (1997) Evolution of gilled mushrooms and puffballs inferred from ribosomal DNA sequences. *Proceedings of the National Academy of Sciences of the United States of America* 94(22): 12002–12006. <https://doi.org/10.1073/pnas.94.22.12002>
- Hu Y, Karunarathna SC, Li H, Galappaththi MC, Zhao CL, Kakumyan P, Mortimer PE (2022) The impact of drying temperature on basidiospore size. *Diversity* 14(4): 239. <https://doi.org/10.3390/d14040239>
- Jung HS (1995) Taxonomic study on Korean Aphyllophorales 1-on some unrecorded genera and species. *The Korean Journal of Mycology* 23(3): 266–274.
- Kalinina BL, Bolshakov SY, Bulyonkova TM (2020) New records of basidiomycetes from the Pskov region in the Polistovskiy State Nature Reserve (Russia). *Nature Conservation Research* 5(3): 9–22. <https://doi.org/10.24189/ncr.2020.024>
- Katoh K, Standley DM (2013) MAFFT multiple sequence alignment software version 7: improvements in performance and usability. *Molecular Phylogenetics and Evolution* 30: 772–780. <https://doi.org/10.1093/molbev/mst010>
- Kotiranta H, Saarenoksa R (2005) *Ceratobasidium* and *Oliveonia* (Basidiomycota, Aphyllophorales) in Finland. *Annales Botanici Fennici* 42: 237–245. <https://doi.org/10.3732/ajb.92.1.179>
- Langer G (1994) Die Gattung *Botryobasidium* Donk (Corticiaceae, Basidiomycetes). *Bibliotheca Mycologica* 158: 1–459.
- Langer G, Langer E, Chen J (2000a) *Botryobasidium musaisporum* sp. nov. collected in Taiwan. *Mycological Research* 104: 510–512. <https://doi.org/10.1017/S0953756299002336>
- Langer G, Langer E, Oberwinkler F, Chen J (2000b) Speciation of *Botryobasidium subcoronatum* (Basidiomycota) collected in Taiwan: morphology, mating tests, and molecular data. *Mycoscience* 41: 201–210. <https://doi.org/10.1007/BF02489672>
- Lentz PL (1967) Delineations of forest fungi: Several species of deuteromycetes and a newly described *Botryobasidium*. *Mycopathologia* 32(1): 1–25. <https://doi.org/10.1007/BF02107032>
- Li HJ, Cui BK, Dai YC (2014) Taxonomy and multi-gene phylogeny of *Datronia* (Polyporales, Basidiomycota). *Persoonia* 32: 170–182. <https://doi.org/10.3767/003158514X681828>
- Maddison WP, Maddison DR (2017) Mesquite: A Modular System for Evolutionary Analysis, Version 3.2. <http://mesquiteproject.org> [accessed October 2020]
- Mao WL, Wu YD, Liu HG, Yuan Y, Dai YC (2023) A contribution to *Porogramme* (Polyporaceae, Agaricomycetes) and related genera. *IMA Fungus* 14: 5. <https://doi.org/10.1186/s43008-023-00110-z>
- Miller MA, Pfeiffer W, Schwartz T (2010) Creating the CIPRES Science Gateway for inference of large phylogenetic trees. *Proceedings of the Gateway Computing Environments Workshop (GCE)*, New Orleans, LA, 1–8. <https://doi.org/10.1109/GCE.2010.5676129>

- Moncalvo JM, Nilsson RH, Koster B, Dunham SM, Bernauer T, Matheny PB, Porter TM, Margaritescu S, Weiss M, Garnica S (2006) The cantharelloid clade: Dealing with incongruent gene trees and phylogenetic reconstruction methods. *Mycologia* 98: 937–948. <https://doi.org/10.1080/15572536.2006.11832623>
- Parmasto E, Nilsson RH, Larsson KH (2004) Cortbase version 2. Extensive updates of a nomenclatural database for corticioid fungi (Hymenomycetes). *Phyloinformatics* 1: 5. <https://doi.org/10.5281/ZENODO.59794>
- Petersen JH (1996) The Danish Mycological Society's colour-chart. Foreningen til Svampekundskabens Fremme, Greve, 1–6.
- Posada D, Crandall KA (1998) Modeltest: Testing the model of DNA substitution. *Bioinformatics* 14: 817–818. <https://doi.org/10.1093/bioinformatics/14.9.817>
- Qin GF, Qin WM, Wang HC, Zhao J, Korhonen K, Chen J, Dai YC, Yuan Y (2024) Phylogeny and species diversity of *Armillaria* in China based on morphological, mating test, and GCPSR criteria. *Mycology*, 1–35. <https://doi.org/10.1080/21501203.2024.2404121>
- Ram E, Singh AP, Kaur R, Gurpaul SD (2021) Four new reports of wood-rotting corticioid fungi from India. *Plant Archives* 21: 85–88. <https://doi.org/10.51470/PLANTARCHIVES.2021.v21.no2.015>
- Rathnayaka AR, Tennakoon DS, Jones GE, Wanasinghe DN, Bhat DJ, Priyashantha AH, Stephenson SL, Tibpromma S, Karunaratna SC (2024) Significance of precise documentation of hosts and geospatial data of fungal collections, with an emphasis on plant-associated fungi. *New Zealand Journal of Botany* 63(2–3): 462–489. <https://doi.org/10.1080/0028825X.2024.2381734>
- Riebesehl J, Langer E (2017) *Hyphodontia* s.l. (Hymenochaetales, Basidiomycota) – 35 new combinations and new keys to currently all 120 species. *Mycological Progress* 16(6): 637–666. <https://doi.org/10.1007/s11557-017-1299-8>
- Ronquist F, Huelsenbeck JP (2003) MRBAYES 3: Bayesian phylogenetic inference under mixed models. *Bioinformatics* 19: 1572–1574. <https://doi.org/10.1093/bioinformatics/btg180>
- Ryvarden L, Hjortstam K, Iturriaga T (2005) Studies in corticioid fungi from *Venezuela* 2 (Basidiomycotina, Aphyllophorales). *Synopsis Fungorum* 20: 42–78.
- Spirin V, Runnel K, Poldmaa K (2015) Studies in the bark-dwelling species of *Hymenochaete* (Hymenochaetales, Basidiomycota) reveal three new species. *Mycologie* 36: 167–176. <https://doi.org/10.7872/crym/v36.iss2.2015.167>
- Stalpers JA, Redhead SA, May TW, Rossman AY, Crouch JA, Cubeta MA, Dai YC, Kirschner R, Langer GJ, Larsson KH, Mack J, Norvell L, Oberwinkler F, Papp V, Roberts P, Rajchenberg M, Seifert GA, Thorn G (2021) Competing sexual-asexual generic names in Agaricomycotina (Basidiomycota) with recommendations for use. *IMA Fungus* 12: 1–31. <https://doi.org/10.1186/s43008-021-00061-3>
- Swofford DL (2002) PAUP\*: Phylogenetic analysis using parsimony (\*and other methods). Version 4.0b 10. Sunderland, MA: Sinauer Associates. <https://doi.org/10.1111/j.0014-3820.2002.tb0019.x>
- Thompson JD, Gibson TJ, Plewniak F, Jeanmagnin F, Thompson JD (1997) The CLUSTAL\_X windows interface: Flexible strategies for multiple sequence alignment aided by quality analysis tools. *Nucleic Acids Research* 25: 4876–4882. <https://doi.org/10.1093/nar/25.24.4876>
- Vilgalys R, and Hester M (1990) Rapid genetic identification and mapping of enzymatically amplified ribosomal DNA from several *Cryptococcus* species. *Journal of Bacteriology* 172(8): 4238–4246. <https://doi.org/10.1128/jb.172.8.4238-4246.1990>



- Wang CG, Zhao H, Liu HG, Zeng GY, Yuan Y, Dai YC (2023) A multi-gene phylogeny clarifies species diversity, taxonomy, and divergence times of *Ceriporia* and other related genera in Irpicaceae (Polyporales, Basidiomycota). *Mycosphere* 14(1): 1665–1729. <https://doi.org/10.5943/mycosphere/14/1/19>
- Wang CG, Dai YC, Kout J, Gates GM, Liu HG, Yuan Y, Vlasák J (2024a) Multi-gene phylogeny and taxonomy of *Physisporinus* (Polyporales, Basidiomycota). *Mycosphere* 15: 1455–1521. <https://doi.org/10.5943/mycosphere/15/1/12>
- Wang K, Liu SL, Liu XZ, Hong P, Wei HW, Wang Y, Dorji P, Zhou LW, Wei TZ (2024b) Catalogue of fungi in China 3. New taxa of macrofungi from southern Xizang, China. *Mycology* 16(1): 91–123. <https://doi.org/10.1080/21501203.2024.2392014>
- White T, Bruns T, Lee S, Taylor FJRM, White T, Lee SH, Taylor L, Shawetaylor J (1990) Amplification and direct sequencing of fungal ribosomal RNA genes for phylogenetics. *PCR Protocols, A guide to methods and applications*. Academic Press, New York, 315–322. <https://doi.org/10.1016/B978-0-12-372180-8.50042-1>
- Wijayawardene NN, Hyde KD, Dai DQ, Sánchez-García M, Goto BT, Saxena RK, Erdoğdu M, Selçuk F, Rajeshkumar KC, Aptroot A, Błaszczowski J, Boonyuen N, da Silva GA, de Souza FA, Dong W, Ertz D, Haelewaters D, Jones EBG, Karunaratna SC, Kirk PM, Kukwa M, Kumla J, Leontyev DV, Lumbsch HT, Maharachchikumbura SSN, Marguno F, Martínez-Rodríguez P, Mešić A, Monteiro JS, Oehl F, Pawłowska J, Pem D, Pfliegler WP, Phillips AJL, Pošta A, He MQ, Li JX, Raza M, Sruthi OP, Suetrong S, Suwannarach N, Tedersoo L, Thiyagaraja V, Tibpromma S, Tkálčec Z, Tokarev YS, Wanasinghe DN, Wijesundara DSA, Wimalaseana SDMK, Madrid H, Zhang GQ, Gao Y, Sánchez-Castro I, Tang LZ, Stadler M, Yurkov A, Thines M (2022) Outline of Fungi and fungus-like taxa – 2021. *Mycosphere* 13: 53–453. <https://doi.org/10.5943/mycosphere/13/1/2>
- Wu G, Feng B, Xu J, Zhu XT, Li YC, Zeng NK, Hosen MI, Yang ZL (2014) Molecular phylogenetic analyses redefine seven major clades and reveal 22 new generic clades in the fungal family Boletaceae. *Fungal Diversity* 69: 93–115. <https://doi.org/10.1007/s13225-014-0283-8>
- Wu F, Zhou LW, Yang ZL, Bau T, Li TH, Dai YC (2019) Resource diversity of Chinese macrofungi: edible, medicinal and poisonous species. *Fungal Diversity* 98: 1–76. <https://doi.org/10.1007/s13225-019-00432-7>
- Wu F, Yuan HS, Zhou LW, Yuan Y, Cui BK, Dai YC (2020) Polypore diversity in south China. *Mycosystema* 39: 653–682. <https://doi.org/10.13346/j.mycosystema.200087>
- Wu F, Man XW, Tohtirjap A, Dai YC (2022a) A comparison of polypore fungi and species composition in forest ecosystems of China, North America, and Europe. *Forest Ecosystems* 9: 100051. <https://doi.org/10.1016/j.fecs.2022.100051>
- Wu F, Zhou LW, Vlasák J, Dai YC (2022b) Global diversity and systematics of Hymenochaetaceae with poroid hymenophore. *Fungal Diversity* 113: 1–192. <https://doi.org/10.1007/s13225-021-00496-4>
- Xiong HX, Dai YC, Wu SH (2009) Three new species of *Hyphodontia* from Taiwan. *Mycological Progress* 8(3): 165–169. <https://doi.org/10.1007/s11557-009-0587-3>
- Yuan HS, Qin WM, Zhou LW (2011) Hydnoaceous fungi of China 3 *Climacodon* (Polyporales, Basidiomycota) in China. *Guihaia* 31: 291–294. <https://doi.org/10.3969/j.issn.1000-3142.2011.05.003>
- Yuan Y, Bian LS, Wu YD, Chen JJ, Wu F, Liu HG, Zeng GY, Dai YC (2023) Species diversity of pathogenic wood-rotting fungi (Agaricomycetes, Basidiomycota) in China. *Mycology* 14: 204–226. <https://doi.org/10.1080/21501203.2023.2238779>
- Zhang QY, Liu HG, Papp V, Zhou M, Dai YC, Yuan Y (2023) New insights into the classification and evolution of *Favolaschia* (Agaricales, Basidiomycota) and its potential

- distribution, with descriptions of eight new species. *Mycosphere* 14: 777–814. <https://doi.org/10.5943/mycosphere/14/1/10>
- Zhao CL, Cui BK, Dai YC (2012) New species and phylogeny of *Perenniporia* based on morphological and molecular characters. *Fungal Diversity* 58: 47–60. <https://doi.org/10.1007/s13225-012-0177-6>
- Zhao CL, Cui BK, Song J, Dai YC (2015) *Fragiliporiaceae*, a new family of Polyporales (Basidiomycota). *Fungal Diversity* 70: 115–126. <https://doi.org/10.1007/s13225-014-0299-0>
- Zhao H, Nie Y, Zong TK, Wang K, Lu ML, Cui YJ, Tohtirjap A, Chen JJ, Zhao CL, Wu F, Cui BK, Yuan Y, Dai YC, Liu XY (2023b) Species diversity, updated classification and divergence times of the phylum Mucoromycota. *Fungal Diversity* 123: 49–157. <https://doi.org/10.1007/s13225-023-00525-4>
- Zhao H, Wu YD, Yang ZR, Liu HG, Wu F, Dai YC, Yuan Y (2024) Polypore fungi and species diversity in tropical forest ecosystems of Africa, America and Asia, and a comparison with temperate and boreal regions of the Northern Hemisphere. *Forest Ecosystems* 11: 100200. <https://doi.org/10.1016/j.fecs.2024.100200>
- Zhou LJ, Geng BB, Zhang GL, Zhang YH, Tian XM (2023a) Diversity and resources of wood-rotting fungi in Shandong Province. *Mycosystema* 42: 2331–2355.
- Zhou M, Dai YC, Vlasák J, Liu HG, Yuan Y (2023b) Updated systematics of *Trichaptum* s.l. (Hymenochaetales, Basidiomycota). *Mycosphere* 14(1): 815–917. <https://doi.org/10.5943/mycosphere/14/1/11>
- Zhou LJ, Li LX, Yuan HS (2024a) Three new wood-inhabiting fungi of *Botryobasidium* (Cantharellales, Basidiomycota) from subtropical forests of Southwestern China. *Mycocokeys* 109: 337–354. <https://doi.org/10.3897/mycokeys.109.133325>
- Zhou Q, Jiang QQ, Yang X, Yang JW, Zhao CL, Zhao J (2024b) Phylogenetic and taxonomic analyses of five new wood-inhabiting fungi of *Botryobasidium*, *Coltricia* and *Coltriciella* (Basidiomycota) from China. *Journal of Fungi* 10(3): 205. <https://doi.org/10.3390/jof10030205>



# Molecular phylogeny and morphology reveal four novel species in Cordycipitaceae in China

Jing Bu<sup>1,2,3</sup>, De-Ping Wei<sup>2,3</sup>, Zheng-Hui Liu<sup>1,2,3</sup>, Yang Yang<sup>4</sup>, Zhong-Liang Liu<sup>1,2,3</sup>,  
 Ji-Chuan Kang<sup>1,2,3</sup>, Xing-Can Peng<sup>2,3,5,6</sup>, Shi-Wen Xie<sup>1,2,3</sup>, He-Gui Zhang<sup>4</sup>, Zhang-Jiang He<sup>1,2,3</sup>,  
 Shi-Ke Huang<sup>2,3,7</sup>, Xian Zhang<sup>2,3,5,6</sup>, Kevin D. Hyde<sup>3,5,6</sup>, Nalin N. Wijayawardene<sup>8</sup>, Ting-Chi Wen<sup>1,2,3</sup>

1 School of Pharmacy, Guizhou University, Guiyang 550025, Guizhou Province, China

2 State Key Laboratory of Green Pesticide, Key Laboratory of Green Pesticide and Agricultural Bioengineering, Ministry of Education, Guizhou University, Guiyang 550025, Guizhou Province, China

3 Engineering Research Center of Southwest Bio-Pharmaceutical Resources, Ministry of Education, Guizhou University, Guiyang 550025, Guizhou Province, China

4 Guizhou Guiwang Biotechnology Co., Ltd, Daozhen 563599, Guizhou Province, China

5 Center of Excellence in Fungal Research, Mae Fah Luang University, Chiang Rai 57100, Thailand

6 School of Science, Mae Fah Luang University, Chiang Rai 57100, Thailand

7 College of Resources and Environment, Zunyi Normal University, Zunyi 563000, Guizhou Province, China

8 Center for Yunnan Plateau Biological Resources Protection and Utilization, College of Biology and Food Engineering, Qujing Normal University, Qujing, 655011, Yunnan Province, China

Corresponding author: Ting-Chi Wen (tingchiwen@yahoo.com)

## Abstract

Cordycipitaceae is a well-known family in Hypocreales, comprising numerous arthropod-pathogenic species. Many taxa in this family have been identified and described through integrated morphological and molecular analyses. In this study, phylogenetic analyses using nrLSU, ITS, nrSSU, 3P\_TEF, *rpb1*, and *rpb2* revealed a new species, *Pleurodesmospora sanduensis*, and a new collection of *Akanthomyces baishanensis*. Additionally, a concatenated 5P\_TEF+3P\_TEF+*rpb1*+MCM7 dataset was employed to clarify interspecific relationships within *Samsoniella*, identifying three new species: *Samsoniella lurida*, *S. subasiatica*, and *S. torquatistipitata*. Detailed morphological descriptions and illustrations are provided for each studied species.

**Key words:** Entomopathogenic fungi, four new species, morphology, phylogeny



Academic editor: Rajesh Jeewon

Received: 17 January 2025

Accepted: 13 March 2025

Published: 9 April 2025

**Citation:** Bu J, Wei D-P, Liu Z-H, Yang Y, Liu Z-L, Kang J-C, Peng X-C, Xie S-W, Zhang H-G, He Z-J, Huang S-K, Zhang X, Hyde KD, Wijayawardene NN, Wen T-C (2025) Molecular phylogeny and morphology reveal four novel species in Cordycipitaceae in China. MycoKeys 116: 91–124. <https://doi.org/10.3897/mycokeys.116.147006>

Copyright: © Jing Bu et al.

This is an open access article distributed under terms of the Creative Commons Attribution License (Attribution 4.0 International – CC BY 4.0).

## Introduction

Cordycipitaceae belongs to Hypocreales (Hypocreomycetidae, Sordariomycetes), and currently it includes 38 genera. Their phylogenetic relationships have been confirmed through molecular and morphological studies (Sung et al. 2001, 2007; Zare and Gams 2016; Kepler et al. 2017; Zhang et al. 2017, 2021; Mongkolsamrit et al. 2018, 2020, 2021, 2022, 2023; Flakus et al. 2019; Wei et al. 2019; Thanakitpipattana et al. 2020, 2022; Wang et al. 2020; Chen et al. 2021a, 2025; Alves et al. 2022; Araújo et al. 2022; Crous et al. 2023a; Guerra-Mateo et al. 2023; Kobmoo et al. 2023; Custódio and Pereira 2024; Hyde et al. 2024; Khonsanit et al. 2024). Most Cordycipitaceae species are known as pathogens of insects and



spiders, while others are reported as hyperparasites on fungi and lichens or are isolated from soil, dung, air, and plant materials (Kepler et al. 2017; Wang et al. 2020; Wei et al. 2022). To adapt to the diverse hosts and habitats, members of Cordycipitaceae have evolved with a wide variety of teleomorphic and anamorphic characteristics (e.g., *Akanthomyces*, *Samsoniella*, and *Pleurodesmospora*).

The genus *Akanthomyces* was introduced by Lebert (1858), typifying with *A. aculeatus* (Mains 1950), and currently 60 epithets are listed in Index Fungorum (<http://www.indexfungorum.org/>, retrieval on 18 March 2025). Species of *Akanthomyces* are characterised by forming superficial, yellow perithecia on mycelial mat covering spider hosts and the filiform, intact ascospores (Boudier 1885; Mongkolsamrit et al. 2018). Later, the morphological diversity of *Akanthomyces* was broadened to include species with isaria-like and lecanicillium-like anamorphs based on phylogenetic evidence (Mongkolsamrit et al. 2018; Vinit et al. 2018; Chen et al. 2020a, b, 2022). The members of the genus have been reported as insect parasites, plant pathogens, fungicolous organisms, and inhabitants of peat, water, and rust (Wang et al. 2024b). Khonsanit et al. (2024) introduced four genera (i.e., *Arachnidicola*, *Lecanicillium*, *Akanthomyces*, and *Kanoksria*) to accommodate *Akanthomyces* species that are not congeneric with *Akanthomyces sensu stricto*.

*Samsoniella* was established by Mongkolsamrit et al. (2018) to accommodate *S. alboaurantium*, *S. aurantia*, and *S. inthanonensis* using both morphological and molecular evidence. *Samsoniella* is characterised by having yellow to orange, fleshy stromata and superficial perithecia and intact ascospores (Mongkolsamrit et al. 2018). Previous researchers have discovered 39 species that are mainly distributed in Asian countries such as China, Thailand, and Vietnam (Wang et al. 2024a). All *Samsoniella* species have been verified with molecular data, and a combination of six genes (ITS-nrSSU-nrLSU-*rpb1-rpb2*-3P-*TEF*) usually was used to study the interspecific relationship (Mongkolsamrit et al. 2018; Wang et al. 2023a, 2024a). However, the taxonomic classification of this genus is considered to be complex due to morphological plasticity, and there is a need to search for new genetic markers with higher resolution (Wang et al. 2023a).

The genus *Pleurodesmospora* was established based on *Pleurodesmospora coccorum*, which is featured with rosetta-like phialidic conidiogenous pegs pasted in erect or procumbent conidiophores (Samson and Gams 1980). *Pleurodesmospora* species are morphologically indistinguishable, emphasising the importance of molecular analysis. Based on DNA phylogeny, Chen et al. (2021a) reported that *Pleurodesmospora* belongs to Cordycipitaceae and demonstrated that the concatenated ITS-3P-*TEF* or ITS-*rpb1-rpb2*-3P-*TEF* datasets were reliable in studying the interspecific relationships of this genus (Chen et al. 2021a; Yeh et al. 2021). Members of *Pleurodesmospora* are known to infect various arthropods, including Araneidae, mites, leafhoppers, and whiteflies (Samson and Gams 1980; Yeh et al. 2021). To date, only five species of this genus have been described: *Pleurodesmospora coccorum*, *P. acaricola*, *P. lemaireae*, *P. lepidopterorum*, and *P. entomophila* (Samson and Gams 1980; Chen et al. 2021a; Yeh et al. 2021; Tan and Shivas 2023, 2024). *Pleurodesmospora acaricola*, *P. coccorum*, and *P. lepidopterorum* (Chen et al. 2021a; Yeh et al. 2021) were reported from China, and *P. lemaireae* and *P. entomophila* were found in Australia (Tan and Shivas 2023, 2024).

During the surveys of entomopathogenic fungi in Guizhou, Liaoning, and Yunnan Provinces, we have collected seven insect specimens (including six Lepidoptera and one Hymenoptera) that were infected by fungi. Based on morphology, five specimens were determined as isaria-like species, one as pleurodesmospora-like, and another one as akanthomyces-like. Further morphology studies herein and molecular phylogenetic analyses revealed four novel species belonging to *Pleurodesmospora* and *Samsoniella* and one known species of *Akanthomyces*. New findings not only enrich the species diversity of these genera but also deepen our understanding of their morphology and ecology.

## Materials and methods

### Sample collection and isolation

A survey was conducted to collect dead insect specimens with fungal infections from Guizhou, Liaoning, and Yunnan provinces (China) from July to November 2023. The specimens were collected from the lower and upper surfaces of living leaves and leaf litter on the ground in evergreen and deciduous forests with less sunlight. The fresh specimens were documented and photographed in the fields using a camera on a mobile phone. Collected specimens were placed in plastic boxes and transported to the laboratory for further examination.

To prevent contamination of fresh specimens by opportunistic fungi in the humid plastic box, fungus isolation was performed on the same day as it was collected. The fresh fruiting bodies were examined using a stereomicroscope (Olympus SZX16). A small mass of conidia on the synnemata or sclerotium inside the insect host bodies was transferred to axenic potato dextrose agar (PDA) plates using a sterile needle. The cultures were incubated at room temperature until the colonies' size attained 2–3 cm. The pure colonies were chopped into tiny bits and stored in sterile water in a centrifuge tube and then submitted to the Kunming Institute of Botany Culture Collection (KUNCC). The fresh specimens were dried with allochroic silica gel and deposited in the Herbarium of Cryptogamic Kunming Institute of Botany Academia Sinica (HKAS), Chinese Academy of Sciences, Kunming, China.

### Morphological studies

The macro-characteristics of the fresh specimens, such as hosts, colour and shape of stroma, and the orientation of perithecia, were recorded and measured using a stereomicroscope (Leica S9E). Micro-morphological characteristics, such as perithecia, asci, ascospores, phialides, and conidia, were removed from the stromata or synnemata and mounted on a glass slide with water, lactic acid cotton blue or congo red solution. A Nikon compound microscope (Nikon ECLIPSE Ni) was used to photograph the above-mentioned microstructures. The axenic PDA plates isolated from fresh specimens were cultured at room temperature for 10–14 days, and the colony characteristics (e.g., size, shape, texture and colour) were recorded. Details of the asexual morphological characteristics from cultures were also documented with a Nikon compound microscope (Nikon ECLIPSE Ni).

### DNA extraction and polymerase chain reaction (PCR) amplification

Total genomic DNA was extracted from axenic living cultures and dry specimens using the DNA extraction kit (Omega Fungus Genomic DNA Extraction Kit, China), following the instructions of the manufacturer. Ten loci, including the internal transcribed spacers 1 and 2 along with the 5.8S rDNA (ITS), partial region of the nuclear ribosomal small subunit (nrSSU) and large subunit (nrLSU), and the largest and second-largest subunits of RNA polymerase II (*rpb1* and *rpb2*), were amplified. Several extra gene regions, including the partial region of the 3' and the 5' end of the translation elongation factor 1-alpha gene (3P\_*TEF* and 5P\_*TEF*), the replication licensing factor 7 (*MCM7*) gene, the actin beta 1 (*ACT*) gene and the beta-tubulin (*TUB*) gene, were amplified for *Samsoniella* species (Table 2). The primer pairs used for amplification were ITS 5 and ITS 4 for ITS (White et al. 1990), NS1 and NS4 for nrSSU (White et al. 1990), LROR and LR5 for nrLSU (Vilgalys and Hester 1990), 983F and 2218R for 3P\_*TEF* (Rehner and Buckley 2005), EF1T and EF2T for 5P\_*TEF* (Rehner and Buckley 2005; Bischoff et al. 2006), CRPB1A and RPB1Cr for *rpb1* (Castlebury et al. 2004), fRPB2-5f and fRPB2-7cR for *rpb2* (Castlebury et al. 2004), Mcm7-709 and Mcm7-1348rev for *MCM7* (Schmitt et al. 2009), Act-1 and Act-4R for *ACT* (Voigt and Wöstemeyer 2000), Bt2a and Bt1b for *TUB* (Glass and Donaldson 1995). All of the PCR was performed in a 25 µl reaction mixture consisting of 12.5 µl of the mixture, 7.5 µl of double distilled water, 1 µl of each primer, and 3 µl of DNA template, using a T100 Thermal Cycler (Bio-Rad). The PCR program for these six loci (nrLSU, ITS, nrSSU, 3P\_*TEF*, *rpb1*, and *rpb2*) was outlined in Wei et al. (2021), while the PCR procedures for the 5P\_*TEF* and *MCM7* genes were respectively given by Bischoff et al. (2006) and Schmitt et al. (2009). The PCR protocols for the *ACT* and *TUB* were respectively referenced from Voigt et al. (1999) and Glass and Donaldson (1995). The PCR products were purified and sequenced at Sangon Biotech Company (Shanghai, China) with the above-mentioned primers. The newly generated sequences were submitted to GenBank for assignment of accession number.

### Sequence alignment and phylogenetic analyses

The quality of the sequence chromatogram generated in this study was examined using BioEdit (Hall et al. 2011). The forward and reverse sequences were assembled using Seqman (Clewley 1995) and verified with those sequence data available in GenBank through the BLAST tool. Taxa used for phylogenetic analyses of Cordycipitaceae were selected following related articles (Chen et al. 2020c; Wang et al. 2020, 2024b) and BLAST research results of the newly generated sequences (Table 1).

In order to investigate the interspecific relationship among *Samsoniella*, a separated phylogenetic analysis based on combined four-gene (5P\_*TEF*+3P\_*TEF*+*rpb1*+*MCM7*) was performed with a larger taxa sampling from this genus (Table 2). The four loci were independently aligned with reference sequences using MAFFT v.7 (<http://mafft.cbrc.jp/alignment/server/>). The alignments of each locus were improved using Trimal v.1.2 (Capella-Gutiérrez et al. 2009) and were concatenated using Sequence Matrix v. 1.7.8 (Vaidya et al. 2011). The final combined dataset was converted to a NEXUS file for Bayesian inference analysis and a FASTA file for maximum likelihood analysis using Aliview (Larsson 2014).

**Table 1.** GenBank accession numbers of the taxa used in this study.

Species	strain	nrLSU	ITS	nrSSU	3P_TEF	rpb1	rpb2	References
<i>Akanthomyces aculeatus</i>	HUA186145 <sup>T</sup>	MF416520			MF416465			Kepler et al. 2017
<i>A. aculeatus</i>	HUA 772	KC519370	KC519371	KC519368	KC519366			Kepler et al. 2017
<i>A. australiensis</i>	BRIP 72630a	OR527524	OR527516	OR512197	OR514840		OR514848	Kepler et al. 2017
<i>A. baishanensis</i>	CGMCC3.25673 <sup>T</sup>	PP179404			PP464678	PP464641	PP464655	Pu et al. 2025
<i>A. baishanensis</i>	CGMCC3.25674	PP179405			PP464679	PP464642	PP464656	Pu et al. 2025
<b><i>A. baishanensis</i></b>	<b>HKAS144393</b>	<b>PQ492341</b>	<b>PQ492702</b>	<b>PQ492709</b>	<b>PQ499067</b>	<b>PQ499073</b>	<b>PQ499080</b>	<b>This study</b>
<i>A. bannaensis</i>	CLZhao 34016 <sup>T</sup>	PP571897	PP571895				PP588774	Zhang et al. 2024
<i>A. buriramensis</i>	BCC 45158	ON008543			ON013546	ON013561		Khonsanit et al. 2024
<i>A. buriramensis</i>	BCC 47939 <sup>T</sup>	ON008545			ON013548	ON013563		Khonsanit et al. 2024
<i>A. fusiformis</i>	BCC 40756 <sup>T</sup>	ON008549			ON013552	ON013567	ON013576	Khonsanit et al. 2024
<i>A. laosensis</i>	YFCC 1910942	OQ509511	OQ509524		OQ506287	OQ511536	OQ511550	Wang et al. 2024b
<i>A. laosensis</i>	YFCC 1910941 <sup>T</sup>	OQ509510	OQ509523		OQ506286	OQ511535	OQ511549	Wang et al. 2024b
<i>A. niveus</i>	BCC 79887 <sup>T</sup>	ON008551			ON013554		ON013578	Khonsanit et al. 2024
<i>A. niveus</i>	BCC 40747	ON008550			ON013553	ON013568	ON013577	Khonsanit et al. 2024
<i>A. noctuidarum</i>	BBH 16595	MT356085	MT356073		MT477979	MT477995	MT478005	Aini et al. 2020
<i>A. noctuidarum</i>	BCC 47498	MT356086	MT356074		MT477980	MT477996	MT477988	Aini et al. 2020
<i>A. noctuidarum</i>	BCC 28571	MT356087	MT356075		MT477981	MT478009	MT478006	Aini et al. 2020
<i>A. noctuidarum</i>	BCC 36265 <sup>T</sup>	MT356084	MT356072		MT477978	MT477994	MT477987	Aini et al. 2020
<i>A. phariformis</i>	BCC 45148 <sup>T</sup>	ON008556			ON013559		ON013583	Khonsanit et al. 2024
<i>A. pseudonoctuidarum</i>	YFCC 1808943 <sup>T</sup>	OQ509512	OQ509525		OQ506288	OQ511537	OQ511551	Khonsanit et al. 2024
<i>A. pseudonoctuidarum</i>	YFCC 1808944	OQ509513	OQ509526		OQ506289	OQ511538	OQ511552	Khonsanit et al. 2024
<i>A. pyralidarum</i>	BCC 32191	MT356092	MT356081		MT477983	MT478001	MT477989	Aini et al. 2020
<i>A. pyralidarum</i>	BCC 40869	MT356093	MT356082		MT477984	MT478002	MT477990	Aini et al. 2020
<i>A. pyralidarum</i>	BCC 28816 <sup>T</sup>	MT356091	MT356080		MT477982	MT478000	MT478007	Aini et al. 2020
<i>Akanthomyces</i> sp.	BCC 76537	ON008557	ON006550		ON013560		ON013584	Aini et al. 2020
<i>A. taiwanicus</i>	NTUPPMCC 20-060	MT974356	MT974202		MW200213	MW200221	MW200230	Chuang et al. 2024
<i>A. tortricidarum</i>	BCC 28583	MT356090	MT356079		MT477986	MT477999	MT477993	Aini et al. 2020
<i>A. tortricidarum</i>	BCC 41868	MT356089	MT356077		MT477985	MT477998	MT478008	Aini et al. 2020
<i>A. tortricidarum</i>	BCC 72638 <sup>T</sup>	MT356088	MT356076		MT478004	MT477997	MT477992	Aini et al. 2020
<i>A. tuberculatus</i>	BCC 16819	GQ249987	GQ250012	GQ249962	GQ250037			Kepler et al. 2017
<i>A. xixiuensis</i>	XX21081764 <sup>T</sup>	OP693480	OP693460	OP693478	OP838887	OP838889	OP838891	Liu et al. 2024
<i>A. xixiuensis</i>	HKAS125851	OP693481	OP693461	OP693479	OP838888	OP838890	OP838892	Liu et al. 2024
<i>Arachnidicola araneicola</i>	GY 29011		MK942435			MK955945	MK955948	Chen et al. 2019
<i>Ara. araneogenus</i>	GZUIF DX1		KU893152			MH978181	MH978184	Chen et al. 2018
<i>Ara. bashanensis</i>	CQ 05621 <sup>T</sup>	OQ300420	OQ300412		OQ325024		OQ349684	Chen et al. 2023a
<i>Ara. bashanensis</i>	CQ 05622	OQ300421	OQ300411		OQ325025		OQ349685	Chen et al. 2023a
<i>Ara. beibeiensis</i>	CQ 05921 <sup>T</sup>	OQ300424	OQ300415		OQ325028		OQ349688	Chen et al. 2023a
<i>Ara. beibeiensis</i>	CQ 05922	OQ300427	OQ300416		OQ325029		OQ349689	Chen et al. 2023a
<i>Ara. coccidioperitheciatus</i>	NHJ 6709	EU369042	JN049865	EU369110	EU369025	EU369067	EU369086	Kepler et al. 2017
<i>Ara. kanyawimiae</i>	TBRC 7242	MF140718	MF140751		MF140838	MF140784	MF140808	Mongkolsamrit et al. 2018
<i>Ara. kanyawimiae</i>	TBRC 7244 <sup>T</sup>	MF140716	MF140752		MF140836			Mongkolsamrit et al. 2018
<i>Ara. kanyawimiae</i>	TBRC 7243	MF140717	MF140750		MF140837	MF140783	MF140807	Mongkolsamrit et al. 2018
<i>Ara. kunmingensis</i>	YFCC 1808940 <sup>T</sup>	OQ509509	OQ509522		OQ506285	OQ511534	OQ511548	Wang et al. 2024b
<i>Ara. kunmingensis</i>	YFCC 1808939	OQ509508	OQ509521		OQ506284	OQ511533	OQ511547	Wang et al. 2024b
<i>Ara. subaraneicola</i>	YFCC 2107937 <sup>T</sup>	OQ509514	OQ509527		OQ506290	OQ511539	OQ511553	Wang et al. 2024b



Species	strain	nrLSU	ITS	nrSSU	3P_TEF	rpb1	rpb2	References
<i>Ara. subaraneicola</i>	YFCC 2107938	OQ509515	OQ509528		OQ506291	OQ511540	OQ511554	Wang et al. 2024b
<i>Ara. sulphureus</i>	TBRC 7248 <sup>T</sup>	MF140722	MF140758		MF140843	MF140787	MF140812	Mongkolsamrit et al. 2018
<i>Ara. thailandicus</i>	TBRC 7245 <sup>T</sup>	MF140719	MF140754		MF140839		MF140809	Mongkolsamrit et al. 2018
<i>Ara. tiankengensis</i>	KY 11571 <sup>T</sup>	ON502825	ON502848		ON525447		ON525446	Chen et al. 2023a
<i>Ara. tiankengensis</i>	KY 11572	ON502827	ON502821		ON525449		ON525448	Chen et al. 2023a
<i>Ara. waltergamsii</i>	TBRC 7252 <sup>T</sup>	MF140714	MF140748		MF140834	MF140782	MF140806	Mongkolsamrit et al. 2018
<i>Beauveria bassiana</i>	ARSEF 1564		HQ880761		HQ880974	HQ880833	HQ880905	Rehner et al. 2011
<i>B. caledonica</i>	ARSEF 2567 <sup>T</sup>	AF339520	HQ880817	NG064865	EF469057	EF469086	HQ880961	Rehner et al. 2011
<i>B. medogensis</i>	BUB 426	MG642846	MG642832	MG642889	MG642904	MG642859	MG642874	Imoulan et al. 2016
<i>B. scarabaeidicola</i>	ARSEF 5689	AF339524	JN049827	AF339574	DQ522335	DQ522380	DQ522431	Kepler et al. 2017
<i>B. sinensis</i>	BUB 504	MG642838	MG642825	MG642880	MG642895	MG642852	MG642865	Chen et al. 2013
<i>Cordyceps amoene-rosea</i>	CBS 107.73 <sup>T</sup>	MF416550	MH860646	AY526464	MF416494	MF416651	MF416445	Wang et al. 2020
<i>C. amoene-rosea</i>	CBS 729.73	MF416551	MH860794	MF416604	MF416495	MF416652	MF416446	Wang et al. 2020
<i>C. coleopterorum</i>	CBS 110.73 <sup>T</sup>	JF415988	AY624177	JF415965	JF416028	JN049903	JF416006	Kepler et al. 2017
<i>C. farinosa</i>	CBS 111113	MF416554	AY624181	AY526474	MF416499	MF416656	MF416450	Kepler et al. 2017
<i>C. fumosorosea</i>	CBS 244.31	MF416557	MH855200	MF416609	MF416503	MF416660	MF416454	Kepler et al. 2017
<i>C. javanica</i>	CBS 134.22	MF416558	MH854719	MF416610	MF416504	MF416661	MF416455	Kepler et al. 2017
<i>C. militaris</i>	OSC 93623	AY184966	JN049825	AY184977	DQ522332	DQ522377		Kepler et al. 2017
<i>C. tenuipes</i>	ARSEF 5135	JF415980	AY624196	MF416612	JF416020	JN049896	JF416000	Kepler et al. 2017
<i>Kanoksria zaquensis</i>	HMAS 246917	MT789696	MT789698	MT789700	MT797811	MT797809		Wang et al. 2023b
<i>Kanoksria zaquensis</i>	HMAS 246915 <sup>T</sup>	MT789697	MT789699	MT789701	MT797812	MT797810		Wang et al. 2023b
<i>Lecanicillium araneosus</i>	KY 11341 <sup>T</sup>	ON502832	ON502826		ON525443		ON525442	Chen et al. 2022
<i>L. araneosus</i>	KY 11342	ON502837	ON502844		ON525445		ON525444	Chen et al. 2022
<i>L. attenuatus</i>	CBS 402.78	AF339565	AJ292434	AF339614	EF468782	EF468888	EF468935	Kepler et al. 2017
<i>L. lecanii</i>	CBS 102067 <sup>T</sup>	KM283795	MH862778	KM283771	KM283818	KM283838	KM283860	Kepler et al. 2017
<i>L. lepidopterorum</i>	SD05152		MT705974				MT727045	Chen et al. 2020a
<i>L. longisporum</i>	CBS 126.27 <sup>T</sup>	KM283797	AJ292385		KM283820	KR064300	KM283862	Kepler et al. 2017
<i>L. muscarius</i>	MFLU 181145	MH497224	MH497223	MH497222	MH511807		MH511806	Kepler et al. 2017
<i>L. neoaraneogenus</i>	GZU1031Lea <sup>T</sup>			KX845705	KX845697	KX845699	KX845701	Shrestha et al. 2019
<i>L. neocoleopterorum</i>	GY11242		MN093297		MN097815	MN097817	MN097814	Shrestha et al. 2019
<i>L. pissodis</i>	CBS 118231 <sup>T</sup>	KM283799		KM283775	KM283822	KM283842	KM283864	Chen et al. 2020a
<i>L. sabanensis</i>	JCh041			KC633263	KC633274			Kepler et al. 2017
<i>Lecanicillium</i> sp.	YFCC 945		OQ509531		OQ506294	OQ511543	OQ511557	Wang et al. 2024b
<i>L. uredinophilum</i>	KACC 44082 <sup>T</sup>	KM283782		KM283758	KM283806	KM283828	KM283848	Wang et al. 2020
<i>L. uredinophilum</i>	KUN 101466	MG948307	MG948305	MG948309	MG948315	MG948311	MG948313	Wang et al. 2020
<i>Pleurodesmospora acaricola</i>	R. Kirschner 4968		MZ435417		LC629776			Yeh et al. 2021
<i>P. coccorum</i>	CBS 460.73	MH872455	MH860743					Yeh et al. 2021
<i>P. entomophila</i>	BRIP 72652a <sup>T</sup>	OR527526	OR527518		OR514842		OR514850	Tan and Shivas 2023
<i>P. lemaireae</i>	BRIP 76543a <sup>T</sup>	PQ792647	PQ806958					Tan and Shivas 2024
<i>P. lepidopterorum</i>	DY10502		MW826577		MW834319		MW834318	Chen et al. 2021a
<i>P. lepidopterorum</i>	DY10501 <sup>T</sup>		MW826576		MW834317	MW834315	MW834316	Chen et al. 2021a
<b><i>P. sanduensis</i></b>	<b>HKAS144399<sup>T</sup></b>	<b>PQ492342</b>	<b>PQ492703</b>	<b>PQ492710</b>	<b>PQ499068</b>	<b>PQ499074</b>	<b>PQ499081</b>	<b>This study</b>
<i>Samsoniella alboaurantium</i>	CBS 262.58 <sup>T</sup>	MG665232	AY624179		JQ425685			Mongkolsamrit et al. 2018
<i>S. alboaurantium</i>	CBS 240.32	JF415979	AY624178		JF416019	JN049895	JF415999	Mongkolsamrit et al. 2018
<i>S. alpina</i>	YFCC 5818	MN576809		MN576753	MN576979	MN576869	MN576923	Wang et al. 2020
<i>S. alpina</i>	YFCC 5831	MN576810		MN576754	MN576980	MN576870	MN576924	Wang et al. 2020

Species	strain	nrLSU	ITS	nrSSU	3P_TEF	rpb1	rpb2	References
<i>S. anhuiensis</i>	RCEF2830 <sup>T</sup>	OM268848		OM268843	OM483864	OM751889		Wang et al. 2024a
<i>S. anhuiensis</i>	RCEF2590	OR978316		OR978313	OR966516	OR989964		Wang et al. 2024a
<i>S. antleroides</i>	YFCC 6113	MN576804		MN576748	MN576974	MN576864	MN576918	Wang et al. 2020
<i>S. antleroides</i>	YFCC 6016 <sup>T</sup>	MN576803		MN576747	MN576973	MN576863	MN576917	Wang et al. 2020
<i>S. aranea</i>	RCEF2831	OM268849		OM268844	OM483865	OM751882	OM802500	Wang et al. 2024a
<i>S. aranea</i>	RCEF2868	OM268850		OM268845	OM483866	OM751883	OM802501	Wang et al. 2024a
<i>S. asiatica</i>	YFCC 869 <sup>T</sup>		OQ476473		OQ506153	OQ506195	OQ506187	Wang et al. 2023a
<i>S. asiatica</i>	YFCC 870		OQ476474		OQ506154	OQ506196	OQ506188	Wang et al. 2023a
<i>S. asiatica</i>	YFCC 871		OQ476475		OQ506155	OQ506197	OQ506189	Wang et al. 2023a
<i>S. aurantia</i>	TBRC 7271	MF140728	MF140764		MF140846	MF140791	MF140818	Mongkolsamrit et al. 2018
<i>S. aurantia</i>	TBRC 7272	MF140727	MF140763		MF140845		MF140817	Mongkolsamrit et al. 2018
<i>S. cardinalis</i>	YFCC 5830	MN576788		MN576732	MN576958	MN576848	MN576902	Wang et al. 2020
<i>S. cardinalis</i>	YFCC 6144 <sup>T</sup>	MN576786		MN576730	MN576956	MN576846	MN576900	Wang et al. 2020
<i>S. coccinellidicola</i>	YFCC 8772 <sup>T</sup>	ON621670		ON563166	ON676514	ON676502	ON568685	Wang et al. 2022
<i>S. coccinellidicola</i>	YFCC 8773	ON621671		ON563167	ON676515	ON676503	ON568686	Wang et al. 2022
<i>S. coleopterorum</i>	A19501 <sup>T</sup>		MT626376		MN101586	MT642600	MN101585	Chen et al. 2020c
<i>S. cristata</i>	YFCC 6023	MN576792	OQ476480	MN576736	MN576962	MN576852	MN576906	Wang et al. 2020
<i>S. cristata</i>	YFCC 7004 <sup>T</sup>	MN576793	OQ476481	MN576737	MN576963	MN576853	MN576907	Wang et al. 2020
<i>S. duyunensis</i>	DY09162	OQ363114	OQ379242		OQ398146			Chen et al. 2023b
<i>S. duyunensis</i>	DY07501	OR263307	OR263188		OR282780	OR282773	OR282776	Chen et al. 2023b
<i>S. duyunensis</i>	DY09502	OR263427	OR263189		OR282781		OR282777	Chen et al. 2023b
<i>S. erucae</i>	KY 11121 <sup>T</sup>	ON502835	ON502828		ON525425		ON525424	Chen et al. 2022
<i>S. erucae</i>	KY 11122	ON502822	ON502847		ON525427		ON525426	Chen et al. 2022
<i>S. farinospora</i>	YFCC 8774 <sup>T</sup>	ON621672		ON563168	ON676516	ON676504	ON568687	Wang et al. 2022
<i>S. farinospora</i>	YFCC 9051	ON621673		ON563169	ON676517	ON676505	ON568688	Wang et al. 2022
<i>S. fusiformispora</i>	RCEF5406	OM268851		OM268846		OM751890		Wang et al. 2024a
<i>S. fusiformispora</i>	RCEF2588 <sup>T</sup>	OR978315		OR978312				Wang et al. 2024a
<i>S. guizhouensis</i>	KY 11161 <sup>T</sup>	ON502830	ON502823		ON525429		ON525428	Chen et al. 2022
<i>S. guizhouensis</i>	KY 11162	ON502846	ON502845		ON525431		ON525430	Chen et al. 2022
<i>S. haniana</i>	YFCC 8769 <sup>T</sup>	ON621674		ON563170	ON676518	ON676506	ON568689	Wang et al. 2022
<i>S. haniana</i>	YFCC 8770	ON621675		ON563171	ON676519	ON676507	ON568690	Wang et al. 2022
<i>S. haniana</i>	YFCC 8771	ON621676		ON563172	ON676520	ON676508	ON568691	Wang et al. 2022
<i>S. hepiali</i>	Cor-4	MN576799		MN576743	MN576969	MN576859	MN576913	Wang et al. 2020
<i>S. hepiali</i>	YFCC 661	MN576795		MN576739	MN576965	MN576855	MN576909	Wang et al. 2020
<i>S. hepiali</i>	ICMM 82-2 <sup>T</sup>	MN576794		MN576738	MN576964	MN576854	MN576908	Wang et al. 2020
<i>S. hymenopterorum</i>	A19521		MN128224		MN101588	MT642603		Chen et al. 2020c
<i>S. hymenopterorum</i>	A19522 <sup>T</sup>		MN128081		MN101591	MN101589		Chen et al. 2020c
<i>S. inthanonensis</i>	TBRC 7915	MF140725	MF140761		MF140849	MF140790	MF140815	Mongkolsamrit et al. 2018
<i>S. kunmingensis</i>	YHH 16002 <sup>T</sup>	MN576802		MN576746	MN576972	MN576862	MN576916	Wang et al. 2020
<i>S. lanmaoa</i>	YFCC 6193	MN576790		MN576734	MN576960	MN576850	MN576904	Wang et al. 2020
<i>S. lanmaoa</i>	YFCC 6148 <sup>T</sup>	MN576789		MN576733	MN576959	MN576849	MN576903	Wang et al. 2020
<i>S. lasiocampidarum</i>	NTUPPMCC 20-061	MT974364	MT974211		MW200220	MW200229		Chuang et al. 2024
<i>S. lasiocampidarum</i>	NTUPPMCC 20-062 <sup>T</sup>	MT974361	MT974208		MW200218	MW200227	MW200236	Chuang et al. 2024
<i>S. lasiocampidarum</i>	NTUPPMCC 20-063	MT974363	MT974210		MW200219		MW200238	Chuang et al. 2024
<i>S. lepidopterorum</i>	DL 10071 <sup>T</sup>		MN128076			MN101592		Chen et al. 2020c
<i>S. lepidopterorum</i>	DL 10072		MN128084					Chen et al. 2020c
<b><i>S. lurida</i></b>	<b>HKAS144387<sup>T</sup></b>	<b>PQ492339</b>	<b>PQ492700</b>	<b>PQ492707</b>	<b>PQ499065</b>		<b>PQ499078</b>	<b>This study</b>
<b><i>S. lurida</i></b>	<b>HKAS144388</b>	<b>PQ492340</b>	<b>PQ492701</b>	<b>PQ492708</b>	<b>PQ499066</b>	<b>PQ499072</b>	<b>PQ499079</b>	<b>This study</b>

Species	strain	nrLSU	ITS	nrSSU	3P_TEF	rpb1	rpb2	References
<i>S. neopupicola</i>	KY 11322	ON502833	ON502834		ON525435		ON525434	Chen et al. 2022
<i>S. neopupicola</i>	KY 11321 <sup>T</sup>	ON502839	ON502843		ON525433		ON525432	Chen et al. 2022
<i>S. pseudogunnii</i>	GY 407202	MZ831865	MZ831863		MZ855234		MZ855240	Chen et al. 2021b
<i>S. pseudogunnii</i>	GY 407201	MZ827010	MZ827470		MZ855233		MZ855239	Chen et al. 2021b
<i>S. pseudotortricidae</i>	YFCC 9052 <sup>T</sup>	ON621677		ON563173	ON676521	ON676509	ON568692	Wang et al. 2022
<i>S. pseudotortricidae</i>	YFCC 9053	ON621678		ON563174	ON676522	ON676510	ON568693	Wang et al. 2022
<i>S. pupicola</i>	DY 101682	MZ827635	MZ827008		MZ855232		MZ855238	Chen et al. 2021b
<i>S. pupicola</i>	DY 101681 <sup>T</sup>	MZ827009	MZ827085		MZ855231		MZ855237	Chen et al. 2021b
<i>S. ramosa</i>	YFCC 6020 <sup>T</sup>	MN576805		MN576749	MN576975	MN576865	MN576919	Wang et al. 2020
<i>S. sanmingense</i>	CGMCC3.25661	PP179392		PP177395	PP482033	PP464664	PP464647	Pu et al. 2025
<i>S. sanmingense</i>	CGMCC3.25662 <sup>T</sup>	PP179393		PP177396	PP482034	PP464665	PP464648	Pu et al. 2025
<i>S. sapaensis</i>	YFCC 873 <sup>T</sup>		OQ476489		OQ506152	OQ506194	OQ506186	Wang et al. 2023a
<i>S. sapaensis</i>	YFCC 872		OQ476488		OQ506151	OQ506193	OQ506185	Wang et al. 2023a
<i>S. sinensis</i>	YFCC 8766 <sup>T</sup>	ON621679		ON563175	ON676523	ON676511	ON568694	Wang et al. 2022
<i>S. sinensis</i>	YFCC 8767	ON621680		ON563176	ON676524	ON676512	ON568695	Wang et al. 2022
<i>S. sinensis</i>	YFCC 8768	ON621681		ON563177	ON676525	ON676513	ON568696	Wang et al. 2022
<b><i>S. subasiatica</i></b>	<b>HKAS144400<sup>T</sup></b>	<b>PQ492343</b>	<b>PQ492704</b>	<b>PQ492711</b>	<b>PQ499069</b>	<b>PQ499075</b>	<b>PQ499082</b>	<b>This study</b>
<i>S. tiankengensis</i>	KY 11741 <sup>T</sup>	ON502838	ON502840		ON525437		ON525436	Chen et al. 2022
<i>S. tiankengensis</i>	KY 11742	ON502841	ON502849		ON525439		ON525438	Chen et al. 2022
<i>S. tortricidae</i>	YFCC 6013	MN576807		MN576751	MN576977	MN576867	MN576921	Wang et al. 2020
<i>S. tortricidae</i>	YFCC 6142	MN576808		MN576752	MN576978	MN576868	MN576922	Wang et al. 2020
<i>S. tortricidae</i>	YFCC 6131 <sup>T</sup>	MN576806		MN576750	MN576976	MN576866	MN576920	Wang et al. 2020
<b><i>S. torquatistipitata</i></b>	<b>HKAS144411<sup>T</sup></b>	<b>PQ492345</b>	<b>PQ492706</b>	<b>PQ492713</b>	<b>PQ499071</b>	<b>PQ499077</b>	<b>PQ499084</b>	<b>This study</b>
<b><i>S. torquatistipitata</i></b>	<b>HKAS144402</b>	<b>PQ492344</b>	<b>PQ492705</b>	<b>PQ492712</b>	<b>PQ499070</b>	<b>PQ499076</b>	<b>PQ499083</b>	<b>This study</b>
<i>S. vallis</i>	DY091092	OR263431	OR263190		OR282783			Chen et al. 2023b
<i>S. vallis</i>	DY091091	OR263428	OR263191		OR282782			Chen et al. 2023b
<i>S. vallis</i>	DY07242	OR263308	OR263186		OR282779		OR282775	Chen et al. 2023b
<i>S. vallis</i>	DY07241 <sup>T</sup>	OR263306	OR263159		OR282778	OR282772	OR282774	Chen et al. 2023b
<i>S. winandae</i>	MY12469.01 <sup>T</sup>	OM491231	OM491228		OM687896	OM687901	OM687899	Crous et al. 2023b
<i>S. yuanzuiensis</i>	NTUPPMCC 20-064 <sup>T</sup>	MT974359	MT974206			MW200225	MW200234	Chuang et al. 2024
<i>S. yuanzuiensis</i>	NTUPPMCC 20-065	MT974360	MT974207		MW200217	MW200226	MW200235	Chuang et al. 2024
<i>S. yunnanensis</i>	YFCC 1527 <sup>T</sup>	MN576812		MN576756	MN576982	MN576872	MN576926	Wang et al. 2020
<i>S. yunnanensis</i>	YFCC 1824	MN576813		MN576757	MN576983	MN576873	MN576927	Wang et al. 2020
<i>S. yunnanensis</i>	YFCC 7282	MN576814		MN576758	MN576984	MN576874	MN576928	Wang et al. 2020
<i>Simplicillium lanosoniveum</i>	CBS 101267	AF339554	AJ292395		DQ522357	DQ522405	DQ522463	Spatafora et al. 2007
<i>Sim. lanosoniveum</i>	CBS 704.86	AF339553			DQ522358	DQ522406	DQ522464	Spatafora et al. 2007

Note: Types are indicated by T. The newly generated sequences in this study were shown in bold.

Maximum likelihood (ML) analysis was performed using IQ-TREE 1.6.12 (Minh et al. 2020) with branch support being estimated from 1000 ultrafast bootstraps. The Bayesian inference (BI) analysis was run on MrBayes on XSEDE (3.2.7a) in the CIPRES Science Gateway. The GTR+I+G model was selected as the best-fit substitution model by MrModeltest 2.3 implemented in MrMTgui v.1.0 (Nylander 2004; Nuin 2007). Four simultaneous Markov chains were run for 100,000,000 generations, and trees were sampled every 1000 generations. Finally, phylogenetic trees were visualised using Figtree v.1.4.0 (Rambaut 2016) and edited using Adobe Illustrator 2020.

**Table 2.** GenBank accession numbers of the *Samsoniella* used in this study.

Species	strain	3P_TEF	5P_TEF	rpb1	MCM7	References
<i>Samsoniella alboaurantium</i>	CBS 240.32	JF416019		JN049895		Mongkolsamrit et al. 2018
<i>S. alboaurantium</i>	CBS 262.58 <sup>T</sup>	MF416497		MF416654		Mongkolsamrit et al. 2018
<i>S. alpina</i>	YFCC 5818 <sup>T</sup>	MN576979	OQ506160	MN576869	OQ506229	Wang et al. 2023a
<i>S. alpina</i>	YFCC 5831	MN576980	OQ506161	MN576870	OQ506230	Wang et al. 2023a
<i>S. antleroides</i>	YFCC 6016 <sup>T</sup>	MN576973	OQ506162	MN576863	OQ506231	Wang et al. 2023a
<i>S. antleroides</i>	YFCC 6113	MN576974	OQ506163	MN576864	OQ506232	Wang et al. 2023a
<i>S. anhuiensis</i>	RCEF2830 <sup>T</sup>	OM483864		OM751889		Wang et al. 2024a
<i>S. anhuiensis</i>	RCEF2590	OR966516		OR989964		Wang et al. 2024a
<i>S. aranea</i>	RCEF2831	OM483865		OM751882		Wang et al. 2024a
<i>S. aranea</i>	RCEF2868	OM483866		OM751883		Wang et al. 2024a
<i>S. asiatica</i>	YFCC 869 <sup>T</sup>	OQ506153	OQ506164	OQ506195	OQ506233	Wang et al. 2023a
<i>S. asiatica</i>	YFCC 870	OQ506154	OQ506165	OQ506196	OQ506234	Wang et al. 2023a
<i>S. asiatica</i>	YFCC 871	OQ506155	OQ506166	OQ506197	OQ506235	Wang et al. 2023a
<i>S. aurantia</i>	TBRC 7271 <sup>T</sup>	MF140846		MF140791		Mongkolsamrit et al. 2018
<i>S. aurantia</i>	YFCC 874	OQ506157	OQ506167	OQ506199	OQ506236	Wang et al. 2023a
<i>S. aurantia</i>	YFCC 880	OQ506156	OQ506168	OQ506198	OQ506237	Wang et al. 2023a
<i>S. cardinalis</i>	YFCC 5830	MN576958	OQ506169	MN576848	OQ506238	Wang et al. 2023a
<i>S. cardinalis</i>	YFCC 6144 <sup>T</sup>	MN576956	OQ506170	MN576846	OQ506239	Wang et al. 2023a
<i>S. coccinellidicola</i>	YFCC 8772 <sup>T</sup>	ON676514		ON676502		Wang et al. 2022
<i>S. coccinellidicola</i>	YFCC 8773	ON676515		ON676503		Wang et al. 2022
<i>S. coleopterorum</i>	A19501 <sup>T</sup>	MN101586		MT642600		Chen et al. 2020c
<i>S. cristata</i>	YFCC 6023	MN576962	OQ506171	MN576852	OQ506240	Wang et al. 2023a
<i>S. cristata</i>	YFCC 7004 <sup>T</sup>	MN576963	OQ506172	MN576853	OQ506241	Wang et al. 2023a
<i>S. duyunensis</i>	DY09162	OQ398146				Chen et al. 2023b
<i>S. duyunensis</i>	DY07501	OR282780		OR282773		Chen et al. 2023b
<i>S. duyunensis</i>	DY09502	OR282781				Chen et al. 2023b
<i>S. erucae</i>	KY11121 <sup>T</sup>	ON525425				Chen et al. 2022
<i>S. erucae</i>	KY11122	ON525427				Chen et al. 2022
<i>S. farinospora</i>	YFCC 8774 <sup>T</sup>	ON676516		ON676504		Wang et al. 2022
<i>S. farinospora</i>	YFCC 9051	ON676517		ON676505		Wang et al. 2022
<i>S. fusiformispora</i>	RCEF5406			OM751890		Wang et al. 2024a
<i>S. guizhouensis</i>	KY11161 <sup>T</sup>	ON525429				Chen et al. 2022
<i>S. guizhouensis</i>	KY11162	ON525431				Chen et al. 2022
<i>S. haniana</i>	YFCC 8769 <sup>T</sup>	ON676518		ON676506		Wang et al. 2022
<i>S. haniana</i>	YFCC 8771	ON676520		ON676508		Wang et al. 2022
<i>S. hepiali</i>	ICMM 82-2 <sup>T</sup>	MN576964	OQ506173	MN576854	OQ506242	Wang et al. 2023a
<i>S. hepiali</i>	YFCC 868	OQ506158	OQ506175	OQ506200	OQ506244	Wang et al. 2023a
<i>S. hepiali</i>	YFCC 2702	MN576966	OQ506174	MN576856	OQ506243	Wang et al. 2023a
<i>S. hymenopterorum</i>	A19521	MN101588		MT642603		Chen et al. 2020c
<i>S. hymenopterorum</i>	A19522 <sup>T</sup>	MN101591		MN101589		Chen et al. 2020c
<i>S. inthanonensis</i>	TBRC 7915 <sup>T</sup>	MF140849		MF140790		Mongkolsamrit et al. 2018
<i>S. kunmingensis</i>	YHH 16002 <sup>T</sup>	MN576972		MN576862		Wang et al. 2023a
<i>S. lanmaoa</i>	YFCC 6148 <sup>T</sup>	MN576959	OQ506176	MN576849	OQ506245	Wang et al. 2023a
<i>S. lanmaoa</i>	YFCC 6193	MN576960	OQ506177	MN576850	OQ506246	Wang et al. 2023a
<i>S. lasiocampidarum</i>	NTUPPMCC 20-061	MW200220		MW200229		Chuang et al. 2024
<i>S. lasiocampidarum</i>	NTUPPMCC 20-062 <sup>T</sup>	MW200218		MW200227		Chuang et al. 2024
<i>S. lasiocampidarum</i>	NTUPPMCC 20-063	MW200219				Chuang et al. 2024

Species	strain	3P_TEF	5P_TEF	rpb1	MCM7	References
<i>S. lepidopterorum</i>	DL 10071 <sup>T</sup>			MN101592		Chen et al. 2020c
<b><i>S. lurida</i></b>	<b>HKAS144387<sup>T</sup></b>	<b>PQ499065</b>				<b>This study</b>
<b><i>S. lurida</i></b>	<b>HKAS144388</b>	<b>PQ499066</b>		<b>PQ499072</b>	<b>PV158406</b>	<b>This study</b>
<i>S. neopupicola</i>	KY11321 <sup>T</sup>	ON525433				Chen et al. 2022
<i>S. neopupicola</i>	KY11322	ON525435				Chen et al. 2022
<i>S. pseudogunii</i>	GY407201 <sup>T</sup>	MZ855233				Chen et al. 2021b
<i>S. pseudogunii</i>	GY407202	MZ855234				Chen et al. 2021b
<i>S. pseudotortricidae</i>	YFCC 9052 <sup>T</sup>	ON676521		ON676509		Wang et al. 2022
<i>S. pseudotortricidae</i>	YFCC 9053	ON676522		ON676510		Wang et al. 2022
<i>S. pupicola</i>	DY101681 <sup>T</sup>	MZ855231				Chen et al. 2021b
<i>S. pupicola</i>	DY101682	MZ855232				Chen et al. 2021b
<i>S. ramosa</i>	YFCC 6020 <sup>T</sup>	MN576975	OQ506178	MN576865		Wang et al. 2023a
<i>S. sanmingense</i>	CGMCC3.25661	PP482033		PP464664		Pu et al. 2025
<i>S. sanmingense</i>	CGMCC3.25662	PP482034		PP464665		Pu et al. 2025
<i>S. sapaensis</i>	YFCC 872	OQ506151	OQ506179	OQ506193	OQ506247	Wang et al. 2023a
<i>S. sapaensis</i>	YFCC 873 <sup>T</sup>	OQ506152	OQ506180	OQ506194	OQ506248	Wang et al. 2023a
<i>S. sinensis</i>	YFCC 8766 <sup>T</sup>	ON676523		ON676511		Wang et al. 2022
<i>S. sinensis</i>	YFCC 8767	ON676524		ON676512		Wang et al. 2022
<b><i>S. subasiatica</i></b>	<b>HKAS144400<sup>T</sup></b>	<b>PQ499069</b>	<b>PV158402</b>	<b>PQ499075</b>	<b>PV158407</b>	<b>This study</b>
<i>S. tiankengensis</i>	KY11741 <sup>T</sup>	ON525437				Chen et al. 2022
<i>S. tiankengensis</i>	KY11742	ON525439				Chen et al. 2022
<i>S. tortricidae</i>	YFCC 6131 <sup>T</sup>	MN576976	OQ506181	MN576866	OQ506249	Wang et al. 2023a
<i>S. tortricidae</i>	YFCC 6142	MN576978	OQ506182	MN576868	OQ506250	Wang et al. 2023a
<b><i>S. torquatistipitata</i></b>	<b>HKAS144411<sup>T</sup></b>	<b>PQ499071</b>		<b>PQ499077</b>	<b>PV158408</b>	<b>This study</b>
<b><i>S. torquatistipitata</i></b>	<b>HKAS144402</b>	<b>PQ499070</b>		<b>PQ499076</b>	<b>PV158409</b>	<b>This study</b>
<i>S. vallis</i>	DY091092	OR282783				Chen et al. 2023b
<i>S. vallis</i>	DY091091	OR282782				Chen et al. 2023b
<i>S. vallis</i>	DY07242	OR282779				Chen et al. 2023b
<i>S. vallis</i>	DY07241 <sup>T</sup>	OR282778		OR282772		Chen et al. 2023b
<i>S. winandae</i>	MY12469.01 <sup>T</sup>	OM687896		OM687901		Crous et al. 2023b
<i>S. yuanzuiensis</i>	NTUPPMCC 20-064 <sup>T</sup>			MW200225		Chuang et al. 2024
<i>S. yuanzuiensis</i>	NTUPPMCC 20-065	MW200217		MW200226		Chuang et al. 2024
<i>S. yunnanensis</i>	YFCC 1527 <sup>T</sup>	MN576982	OQ506183	MN576872	OQ506251	Wang et al. 2020, 2023a
<i>S. yunnanensis</i>	YFCC 1824	MN576983	OQ506184	MN576873	OQ506252	Wang et al. 2020, 2023a
<i>Akanthomyces waltegersii</i>	YFCC 883	OQ506159		OQ506201	OQ506253	Wang et al. 2023a

Note: Types are indicated by T. The newly generated sequences in this study were shown in bold.

## Results

### Phylogenetic analyses

The six-locus dataset (nrLSU, ITS, nrSSU, 3P\_TEF, rpb1, and rpb2) comprises 118 representative taxa sampled from nine genera within Cordycipitaceae, with two strains of *Simplicillium lanosoniveum* (CBS 101267 and CBS 704.86) selected as the outgroup. The ML tree inferred from the six-locus dataset is shown in Fig. 1, in which the seven strains generated in this study belong to three genera: *Akanthomyces*, *Pleurodesmospora* and *Samsoniella*. The isolate HKAS144393 clusters with *Akanthomyces baishanensis* (CGMCC3.25673 and CGMCC3.25674) with strong statistical support (100% SH-aLRT / 100% UFB / 1.00 PP, Fig. 1). The isolate HKAS144399 constitutes a distinct lineage which



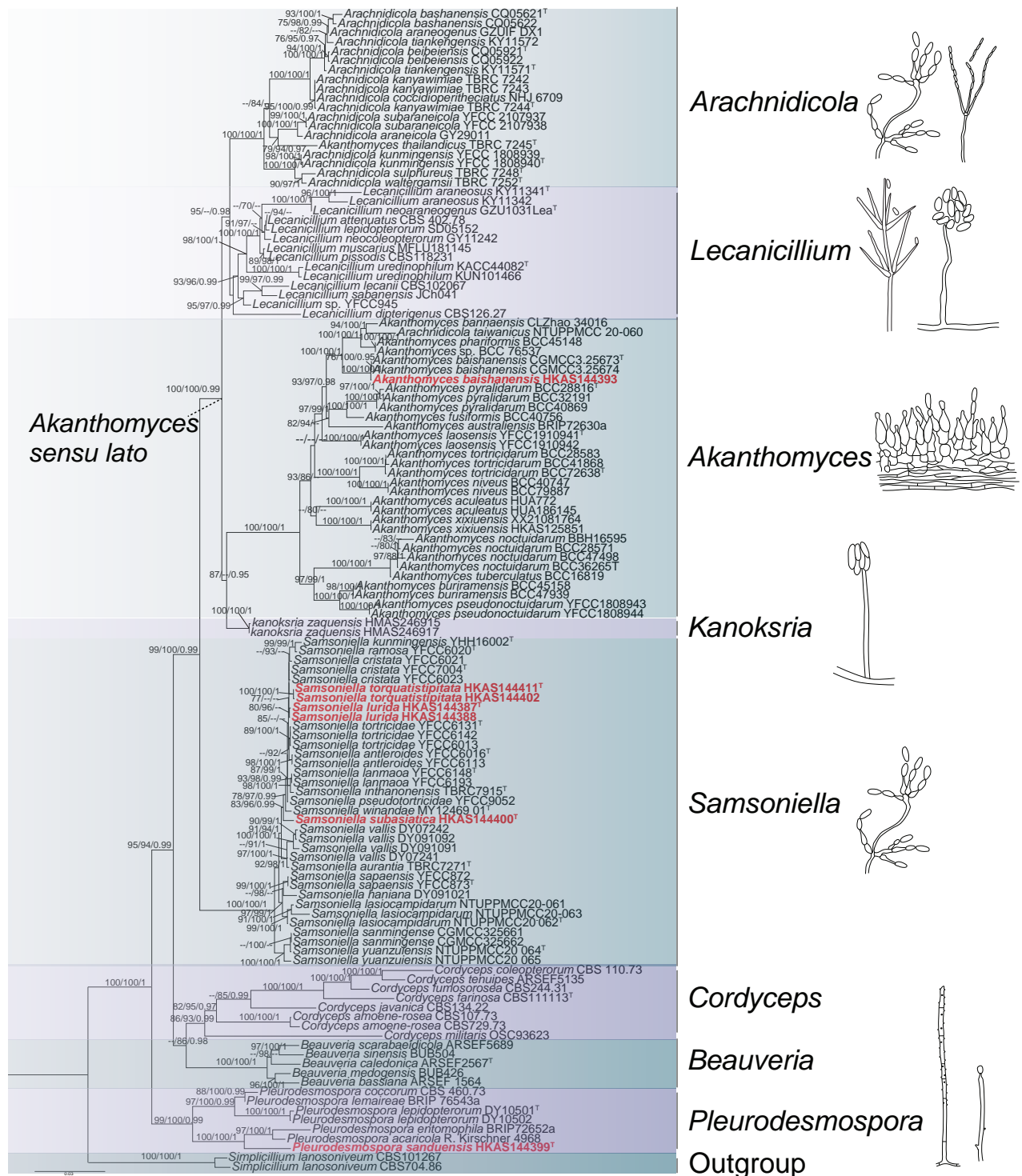


**Figure 1.** Phylogram generated from maximum likelihood analysis of Cordycipitaceae based on a six-locus dataset (nrLSU, ITS, nrSSU, 3P\_TEF, rpb1 and rpb2). SH-aLRT support  $\geq 75\%$ , ultrafast bootstrap support (UFB)  $\geq 75\%$ , and PP values  $\geq 95\%$  are indicated above or below branches. A hyphen (–) indicates values lower than 75% SH-aLRT, 75% UFB, and 95% PP. The isolates in this study are shown in bold red. Generic names are indicated on the right side of the tree. Ex-types are indicated by “T”.

branches off the clade of *Pleurodesmospora acaricola* and *P. entomophila* with maximum support (100% SH-aLRT / 100% UFB / 1.00 PP, Fig. 1). The remaining five strains (HKAS144411, HKAS144402, HKAS144388, HKAS144402, and HKAS144400) group with species of *Samsoniella* with inadequate support.

To clarify the phylogenetic placements of the five specimens of *Samsoniella*, a separated phylogenetic tree based on four genes (5P\_TEF+3P\_TEF+rpb1+MCM7) was constructed with larger taxa sampling from *Samsoniella*. The four-locus dataset included 79 taxa of *Samsoniella* with 3077 bp characters (737 bp for 5P\_TEF, 986 bp for nrSSU, 725 bp for 3P\_TEF, 629 bp for rpb1). *Akanthomyces waltergamsii* YFCC 883 was designated as the out-group taxon. The ML tree (Fig. 2) shows that the isolates HKAS144387 and HKAS144388 are sisters to *S. kunmingensis* and are closely related to *S. tortricidae*, with moderate support (86% SH-aLRT / 89% UFB, Fig. 2). The isolate HKAS144400 shows a sister relationship to *Samsoniella winandae* with significant support (89% SH-aLRT / 94% UFB / 0.99 PP, Fig. 2). The isolates HKAS144411 and HKAS144402 were placed in a clade distantly related to other *Samsoniella* species with strong support (98% SH-aLRT / 100% UFB / 1.00 PP, Fig. 2). The guidelines of Maharachchikumbura et al. (2021) were followed when determining whether species were novel.

## Taxonomy

***Akanthomyces baishanensis*** H.L. Pu & J.Z. Qiu, in Pu, Yang, Keyhani, Yang, Zheng, Qiu, Mao, Shang, Lin, Xiong, Lin, Lai, Huang, Yuan, Liang, Fan, Ma, Qiu & Qiu, *J. Fungi* 11(1, no. 28): 16 (2025)

Index Fungorum: IF903210

Fig. 3

**Description.** Parasitic on moth (Lepidoptera). **Sexual morph.** See Pu et al. (2025). **Asexual morph. Synnemata** arising from the moth body, white, erect, simple, subuliform (2 × 2.7 mm) or subglobose (0.2 × 0.5 mm). **Hyphae** smooth, septate, hyaline, 1.4–2.5 µm ( $\bar{x}$  = 1.8 µm, n = 30) in diam. **Conidiophores** developing from superficial hyphae of synnemata, micronematous, branched, smooth-walled, bearing solitary to clusters of phialides. **Phialides** 6–29.6 × 1.6–3.2 µm ( $\bar{x}$  = 19 × 2.7 µm, n = 30), monophialidic, trimorphic, arising from anastomosing mycelia, slender filiform in shape (Fig. 3G), or arising from conidiophores, cylindrical (Fig. 3E, H, I) or subuliform (Fig. 3F) at basal portion, tapering into a thin neck. **Conidia** 3.2–4.7 × 1.8–2.8 µm ( $\bar{x}$  = 3.9 × 2.2 µm, n = 50), forming on tip of phialides, hyaline, smooth-walled, fusiform, globose or broadly ovoid, gathering in chains.

**Material examined.** CHINA • Liaoning Province, Tieling City (42°17'22.3"N, 123°50'22.2"E), on a dead adult moth (Lepidoptera) on the stem of a plant, 25 August 2023, Ting-Chi Wen, HLJ2023082515 (HKAS144393).

**Notes.** Phylogenetic analysis based on six gene markers revealed that the specimen HKAS144393 and *Akanthomyces baishanensis* (CGMCC3.25673 and CGMCC3.25674) form a robustly supported monophyletic clade (100% SH-aLRT / 100% UFB / 1.00 PP, Fig. 1). Both HKAS144393 and *A. baishanensis* exhibit parasitic relationships with adult moths. Notably, HKAS144393 represents a naturally occurring asexual morph characterised by trimorphic conidiogenous structures, while the asexual morph of *A. baishanensis* described by Pu et al. (2025) was obtained from culture and displayed only a single type of conidiogenous structure. Our observations demonstrate greater morphological plasticity in this species than previously recognised.



**Figure 2.** Phylogram generated from maximum likelihood analysis of *Samsoniella* based on a four-locus dataset (5P\_TEF+3P\_TEF+rpb1+MCM7). SH-aLRT support  $\geq 75\%$ , ultrafast bootstrap support  $\geq 75\%$ , and PP values  $\geq 95\%$  are indicated above or below branches. A hyphen (-) indicates values lower than 75% SH-aLRT, 75% UFB, and 95% PP. The isolates in this study are shown in bold red. Ex-types are indicated by "T".



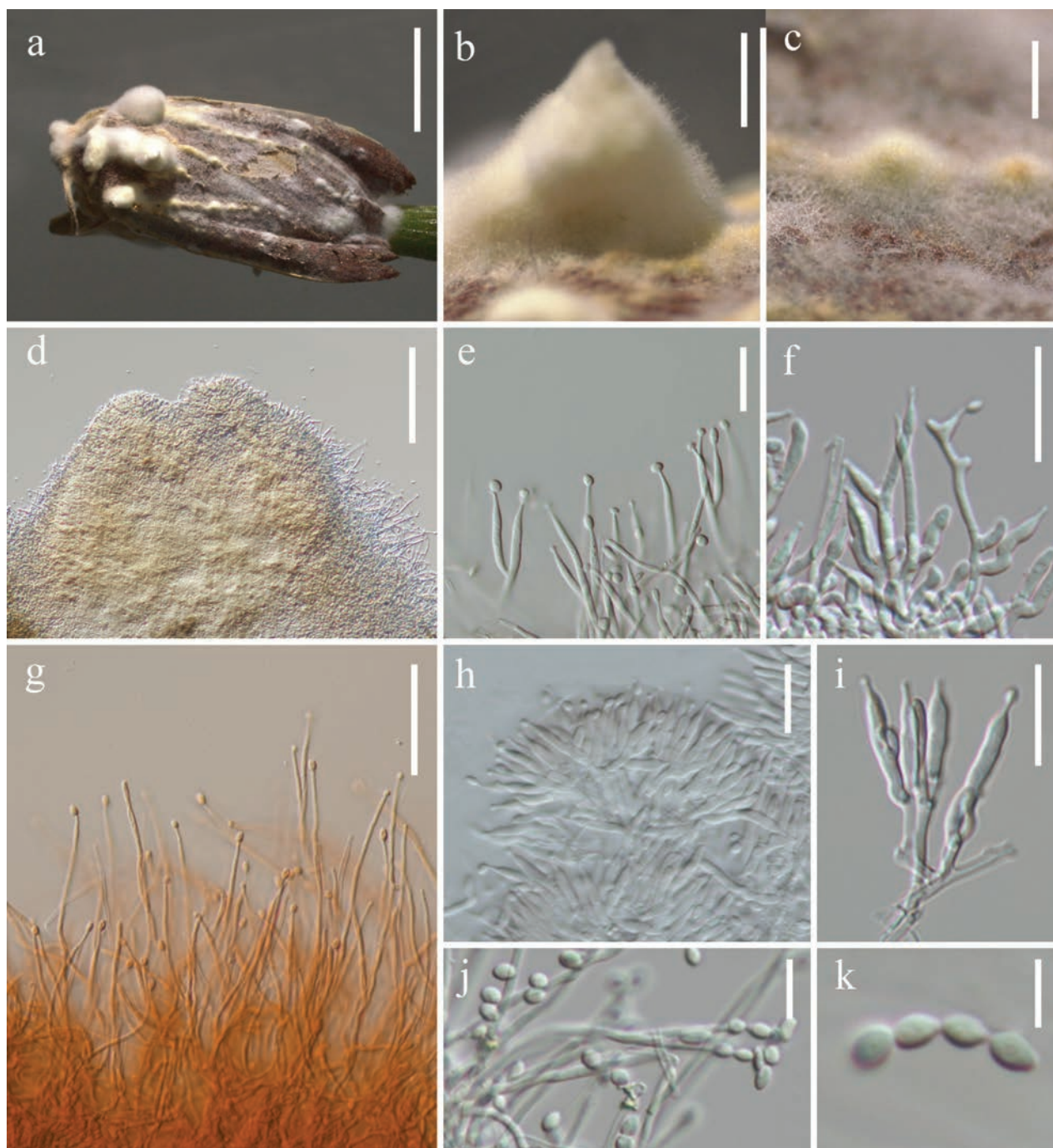


**Figure 3.** *Akanthomyces baishanensis* (HKAS144393) **a** fungus on an adult moth **b–d** synnemata **e–k** phialides and conidia. Scale bars: 5 mm (**a**); 1 mm (**b**); 0.5 mm (**c**); 100 µm (**d**); 30 µm (**g**); 20 µm (**e, f, h, i**); 10 µm (**j**); 5 µm (**k**).

***Pleurodesmospora sanduensis* J. Bu, K.D. Hyde & T.C. Wen, sp. nov.**

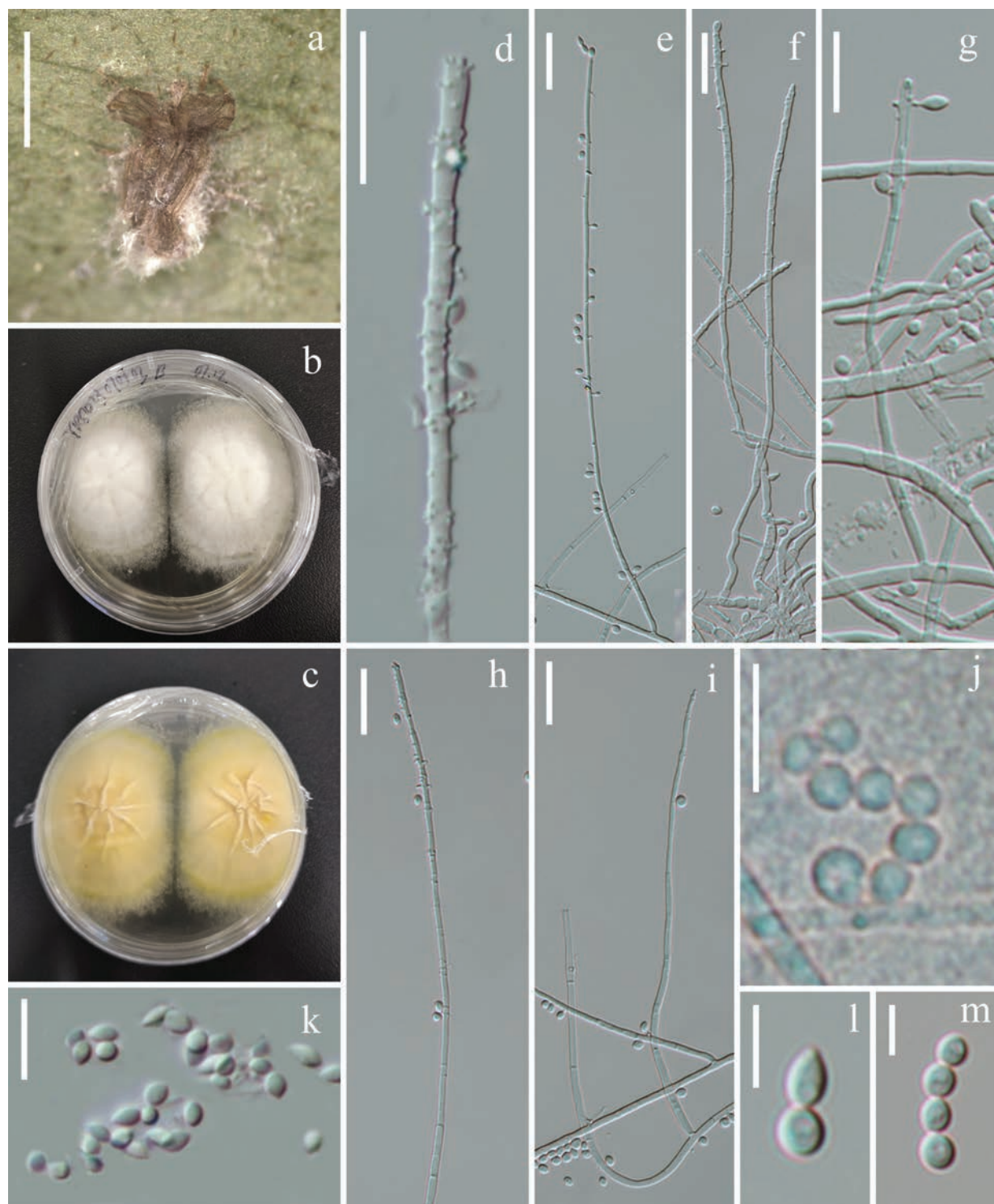
Index Fungorum: IF903211

Fig. 4

**Etymology.** In reference to the location of the type specimen, Sandu County of Guizhou Province, China.

**Description.** Parasitic on adult Lepidoptera. **Sexual morph.** Undetermined.

**Asexual morph. Colonies** on natural specimen white, sparse, only covering the abdomen of host. **Conidiophores** micronematous, cylindrical, erect



**Figure 4.** *Pleurodesmospora sanduensis* (HKAS144399) **a** fungus on host **b, c** obverse (**b**) and reverse (**c**) of colony on PDA **d–i** conidiophore and conidiogenous cells **j, k–m** conidia adhering in a chain. Scale bars: 2 mm (**a**); 20 µm (**d, e, f, h, i**); 10 µm (**g, j, k**); 5 µm (**l, m**).

or procumbent, sparsely branched, smooth, hyaline, septate, ca. 1.3–2.8 µm ( $\bar{x}$  = 2 µm,  $n$  = 30) in width, from the middle part to the distal end densely covered by numerous minute, dentiform pegs, 0.7–1.8 × 0.5–0.8 µm ( $\bar{x}$  = 1 × 0.7 µm,  $n$  = 25). **Conidia** obovoid, globose, smooth-walled, 2.7–4.8 × 1.4–2.5 µm ( $\bar{x}$  = 3.7 × 2 µm,  $n$  = 30), arranged in short chains.



**Culture characteristics.** colonies on PDA reaching a diameter of 42 mm in three weeks at room temperature, white, circular, velvety, flat, edge entire, surface wrinkled, with radially striate, mycelia dense at centre, becoming loose outward, reverse cream-yellow.

**Type.** CHINA • Guizhou Province, Qiannan Buyei and Miao Autonomous Prefecture, Sandu County, the Yaoren Mountain (25°59'41"N, 107°56'41"E, alt. 987.1 m), on a dead adult of Lepidoptera on leaf litter, 08 July 2023, Jing Bu, YRS23070803B (holotype HKAS144399, ex-holotype KUNCC24-18538).

**Notes.** Six-locus phylogenetic analyses show that the *Pleurodesmospora sanduensis* is separated from other species of *Pleurodesmospora* with strong statistical support (100% SH-aLRT / 100% UFB / 1.00 PP, Fig. 1). *Pleurodesmospora sanduensis* is phylogenetically closely related to *P. acaricola* and *P. entomophila*. Pairwise nucleotide differences between *P. sanduensis* and *P. entomophila* (Tan and Shivas 2023) revealed 6 bp in nrLSU, 28 bp in ITS, 25 bp in 3P\_TEF, and 74 bp in rpb2. These molecular divergences support the recognition of *P. sanduensis* as a novel species, consistent with the taxonomic thresholds proposed by Jeewon and Hyde (2016). *Pleurodesmospora sanduensis* is similar to *P. acaricola* in producing loose and white colonies covering the host. However, *Pleurodesmospora sanduensis* differs from *P. acaricola* by its larger conidia ( $2.7\text{--}4.8 \times 1.4\text{--}2.5 \mu\text{m}$  vs.  $2.5\text{--}3 \times 2 \mu\text{m}$ ) in chains, but it is solitary in *P. acaricola* (Yeh et al. 2021). Additionally, chlamydospores are observed in *P. acaricola*, while it is absent in *P. sanduensis*.

***Samsoniella lurida* J. Bu, K.D. Hyde & T.C. Wen, sp. nov.**

Index Fungorum: IF903212

Fig. 5

**Etymology.** Referring to the pale stromata arising from the host, which is different from other species in *Samsoniella*.

**Description.** Parasitic on cocoon of Lepidoptera. **Sexual morph.** **Stromata** 6.4–8.6 mm long, pale orange, cylindrical, unbranched or branched at base, arising from the head and end of the insect cocoon. **Stipe** cylindrical, pale orange, 0.4–0.8 mm wide. **Fertile part** clavate, pale orange,  $2.5\text{--}3.1 \times 0.6\text{--}1 \text{ mm}$ , often with sterile tip (0.5–1.2 mm). The lateral sides had a longitudinal ditch without perithecia. **Perithecia** superficial, crowded, broadly ovoid,  $205\text{--}455 \times 144\text{--}274 \mu\text{m}$  ( $\bar{x} = 319 \times 198 \mu\text{m}$ ,  $n = 15$ ). **Asci** hyaline, cylindrical,  $128\text{--}219 \times 1.4\text{--}3.6 \mu\text{m}$  ( $\bar{x} = 170 \times 2.6 \mu\text{m}$ ,  $n = 20$ ). **Ascus caps** hemispherical, hyaline,  $1.2\text{--}1.8 \times 1.6\text{--}3 \mu\text{m}$  ( $\bar{x} = 1.5 \times 2.5 \mu\text{m}$ ,  $n = 20$ ). **Ascospores** filiform, hyaline, aseptate,  $86\text{--}175 \times 0.4\text{--}1 \mu\text{m}$  ( $\bar{x} = 132 \times 0.7 \mu\text{m}$ ,  $n = 15$ ) wide, do not disarticulate into part-spores. **Asexual morph.** **Synnemata** arising from the middle of the host, erect, single,  $1.2 \times 0.2\text{--}0.35 \text{ mm}$ , producing a mass of floccose conidia at the apex. **Hyphae** smooth-walled, hyaline, septate,  $1.5\text{--}3.6 \mu\text{m}$  ( $\bar{x} = 2.5 \mu\text{m}$ ,  $n = 30$ ) wide. **Conidiophores** smooth-walled, cylindrical, verticillate,  $2.3\text{--}9.1 \times 1.9\text{--}2.9 \mu\text{m}$  ( $\bar{x} = 4.9 \times 2.3 \mu\text{m}$ ,  $n = 15$ ). **Phialides** verticillate, in whorls of two to five, lageniform,  $4.2\text{--}7.3 \mu\text{m}$  ( $\bar{x} = 5.7 \mu\text{m}$ ,  $n = 30$ ) long, basal portion cylindrical, tapering abruptly toward the apex, from  $1.7\text{--}2.5 \mu\text{m}$  ( $\bar{x} = 2.1 \mu\text{m}$ ,  $n = 30$ ) wide (base) to  $0.5\text{--}0.9 \mu\text{m}$  ( $\bar{x} = 0.7 \mu\text{m}$ ,  $n = 30$ ) wide (apex). **Conidia** smooth-walled, hyaline, fusiform,  $1.9\text{--}2.7 \times 1.1\text{--}1.9 \mu\text{m}$  ( $\bar{x} = 2.3 \times 1.4 \mu\text{m}$ ,  $n = 30$ ).

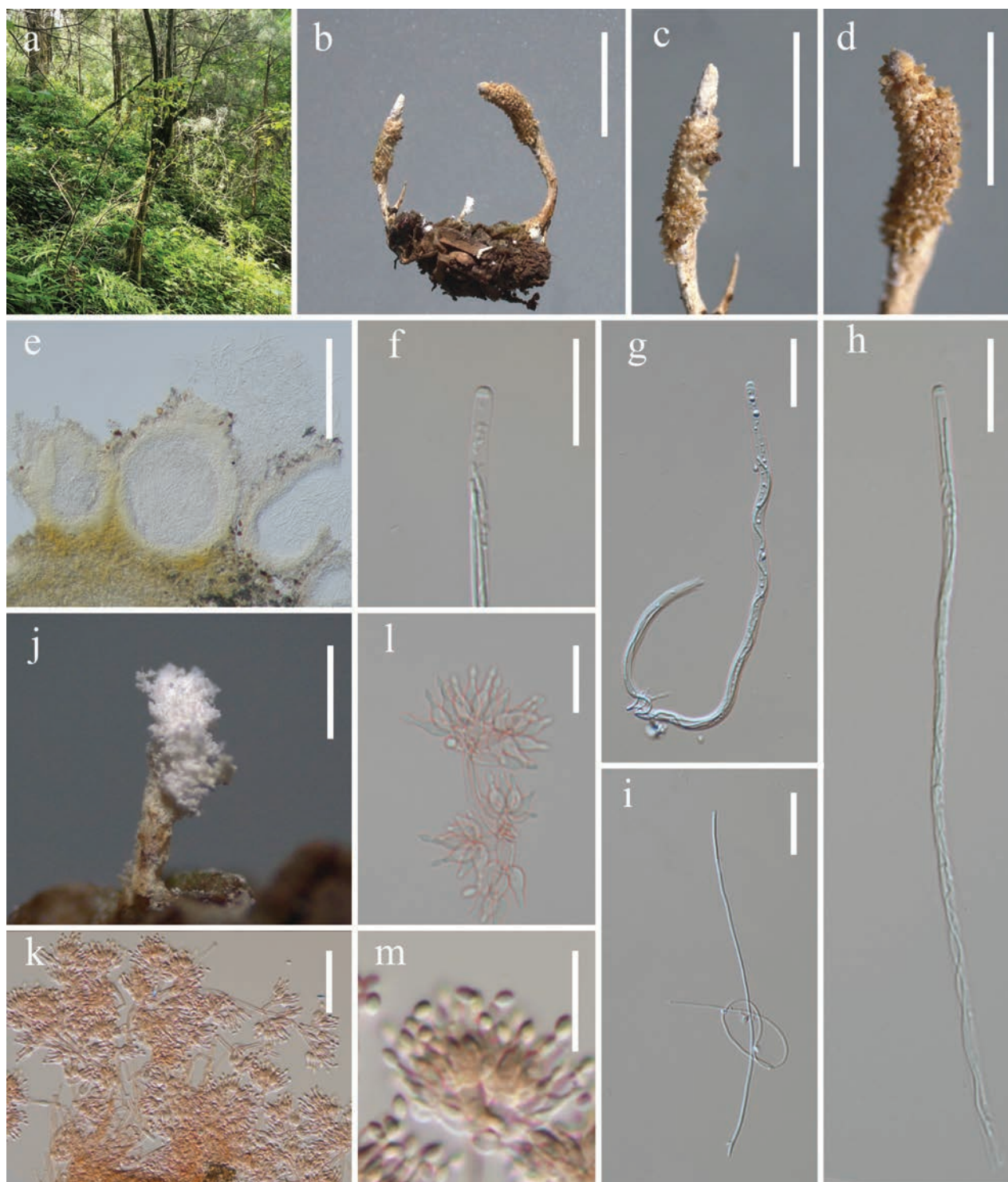


**Figure 5.** *Samsoniella lurida* (HKAS144387) **a** habitat **b** stromata and synnemata arising from host **c, d** fertile part with perithecia **e** vertical section of perithecia **f** ascus cap **g, h** asci **i** ascospore **j** synnema **k–m** conidiophores, phialides and conidia. Scale bars: 5 mm (**b**); 3 mm (**c, d**); 200  $\mu$ m (**e**); 20  $\mu$ m (**f, g, h, i**); 0.5 mm (**j**); 30  $\mu$ m (**k**); 10  $\mu$ m (**l, m**).

**Type.** CHINA • Yunnan Province, Kunming City, Panlong District, the Longchuanqiao Forest Park (25°17'05.26"N, 102°78'07.88"E, alt. 1963.9 m), on a lepidopteran cocoon buried in soil, 20 September 2023, Jing Bu, LCQ2023092034B (holotype HKAS144387).

**Additional materials examined.** CHINA • Yunnan Province, Kunming, Xishan District, Tuanjie Country (25°08'61.38"N, 102°46'11.71"E, alt. 1971.2 m) on lepidopteran larva buried in soil, 17 October 2023, Jing Bu, MLSX2023101741B (HKAS144388, living culture KUNCC24-18534).

**Notes.** Phylogenetic analyses revealed that two specimens of *Samsoniella lurida* (HKAS144387 and HKAS144388) are closely related to *S. kunmingensis* and *S. tortricidae* (Fig. 2). Morphological comparisons demonstrate distinct characteristics among these species. *S. kunmingensis* and *S. tortricidae* produce larger, brightly coloured, multi-branched stromata with oblong-ovate to fusiform perithecia; *S. lurida* is characterised by pallid stromata and broadly ovoid perithecia (Table 3). Furthermore, *S. lurida* possesses a unique sterile tip, a feature not observed in other known *Samsoniella* species. Sequence comparisons between *S. lurida* and *S. kunmingensis* showed that there are 8 bp differences within 943 bp 3P\_*TEF* and 12 bp differences within 979 bp *rpb2*. *S. lurida* differs from *S. tortricidae* by 10 bp within 943 bp 3P\_*TEF* and 11 bp within 979 bp *rpb2*. Both morphological characters and molecular analyses support this fungus as a new species in *Samsoniella* (Jeewon and Hyde 2016).

**Table 3.** Comparison between the sexual morphs in *Samsoniella*. The data generated in this study are shown in bold.

Species	Host	Stromata (mm)	Fertile Part (mm)	Perithecia (µm)	Asci (µm)	Ascospores (µm)	References
<i>S. cristata</i>	Lepidopteran pupa	solitary or two, 25–40 long, crista-like	crista-like or subulate, 3.1–18.5 × 0.9–8.0	superficial, narrowly ovoid, 370–485 × 150–245	cylindrical, 8-spored, 180–356 × 3.0–4.8	bola-shaped, septate, 155–290 × 1.0–1.3	Wang et al. 2020
<i>S. inthanonensis</i>	Lepidopteran larva	gregarious, 20–50 long, 1–1.5 broad, cylindrical to clavate	clavate, 8–15 × 1.5–2	superficial, ovoid, 417.5–474.5 × 205–260	cylindrical, 8-spored, 300 × 2–2.5	bola-shaped, 3 or 4 septate, 221.5–267 × 0.5–1	Mongkolsamrit et al. 2018
<i>S. kunmingensis</i>	Lepidopteran pupa	solitary, 23 long, cylindrical to clavate	clavate, 3.3–4.2 × 0.8–1.2	superficial, narrowly ovoid to fusiform, 330–395 × 110–185	cylindrical, 8-spored, 150–297 × 3.0–4.6	bola-shaped, septate, 127–190 × 0.8–1.5	Wang et al. 2020
<i>S. lanmaoa</i>	Lepidopteran pupa	two to five, 38–69 long, palmately branched	clavate, 8.5–11.2 × 0.6–2.3	superficial, narrowly ovoid to fusiform, 360–467 × 124–210	cylindrical, 8-spored, 160–325 × 3.3–4.8	bola-shaped, septate, 135–260 × 0.9–1.4	Wang et al. 2020
<b><i>S. lurida</i></b>	<b>Lepidopteran pupa</b>	<b>6.4–8.6 long, cylindrical</b>	<b>clavate, 2.5–3.1 × 0.6–1.0, sterile tip 0.5–1.2 wide</b>	<b>superficial, broadly ovoid, 205–455 × 144–274</b>	<b>cylindrical, 128–219 × 1.4–3.6</b>	<b>filiform, aseptate, 86.1–174.7 × 0.4–1.0</b>	<b>This study</b>
<i>S. pseudotortricidae</i>	Lepidopteran pupa	solitary to several, 20–65 long, clavate	clavate to subulate, 10–17 × 1.5–4.2	superficial, narrowly ovoid to fusiform, 285.7–313.2 × 149.2–154.9	/	/	Wang et al. 2022
<b><i>S. torquatistipitata</i></b>	<b>Coleoptera</b>	<b>solitary, 4.4 × 0.1–0.3, clavate</b>	<b>clavate, 1.5 × 0.4</b>	<b>superficial, lageniform, 263–353 × 174–238</b>	<b>cylindrical, 8-spored, up to 114–173 × 1.6–3.3</b>	<b>filiform, 86.2–125.7 × 0.3–0.6</b>	<b>This study</b>
<i>S. tortricidae</i>	Lepidopteran cocoon	gregarious, 25–60	clavate to subulate, 5–15 × 1.2–2.3	superficial, narrowly ovoid to fusiform, 350–468 × 140–225	cylindrical, 8-spored, 170–285 × 2.8–4.0	bola-shaped, septate, 120–235 × 0.8–1.3	Wang et al. 2020
<i>S. winandae</i>	Lepidopteran cocoon	multiple, 8–20 long and 0.5–2 broad, cylindrical to enlarging apically	clavate, 2–8 × 2–3	superficial, narrowly ovoid, 500–570 × 135–180	cylindrical, 8-spored, 300 × 4–5	bola shaped, 3 or 5 septate, 200–265 × 0.5–1	Crous et al. 2023b

***Samsoniella torquatistipitata* J. Bu, K.D. Hyde & T.C. Wen, sp. nov.**

Index Fungorum: IF903213

Fig. 6

**Etymology.** From the Latin “torqu”, referring to the stipe of stroma, is torsional rather than cylindrical.

**Description.** Parasitic on ant (Hymenopteran). **Sexual morph.** **Stroma** arising from head of ant, orange, single, simple,  $4.4 \times 0.1\text{--}0.3$  mm. **Stipe** fleshy, torsional, reddish-orange, up to 2.7 mm long. **Fertile part** cylindrical, becoming acuminate toward the end, reddish-orange,  $1.7 \times 0.4$  mm. **Perithecia** lageniform, superficial,  $255\text{--}368 \times 163\text{--}244$   $\mu\text{m}$  ( $\bar{x} = 288 \times 190$   $\mu\text{m}$ ,  $n = 5$ ), growing on one side of fertile part. **Asci** cylindrical, hyaline, 8-spored,  $114\text{--}173 \times 1.6\text{--}3.3$   $\mu\text{m}$  ( $\bar{x} = 135 \times 2.4$   $\mu\text{m}$ ,  $n = 20$ ), with hemispherical cap,  $1.7\text{--}2.5 \times 1.1\text{--}1.8$   $\mu\text{m}$  ( $\bar{x} = 2.2 \times 1.4$   $\mu\text{m}$ ,  $n = 20$ ). **Ascospores** filiform, aseptate, hyaline,  $86\text{--}125 \times 0.3\text{--}0.6$   $\mu\text{m}$  ( $\bar{x} = 98.6 \times 0.5$   $\mu\text{m}$ ,  $n = 15$ ), non-disarticulating. **Asexual morph.** produced on the cultures, hyphomycetous. **Hyphae** smooth, septate, hyaline,  $1.2\text{--}2.0$   $\mu\text{m}$  ( $\bar{x} = 1.6$   $\mu\text{m}$ ,  $n = 30$ ) in diam. **Conidiophores** smooth-walled, cylindrical or elongated ellipsoid, verticillate with phialides in whorls of two to five or singly along the hyphae,  $4.4\text{--}18.4 \times 1.7\text{--}3.9$   $\mu\text{m}$  ( $\bar{x} = 8.4 \times 2.7$   $\mu\text{m}$ ,  $n = 30$ ). **Phialides** lageniform,  $6.1\text{--}10.7$   $\mu\text{m}$  ( $\bar{x} = 8.0$   $\mu\text{m}$ ,  $n = 30$ ) long, basal portion inflated,  $1.8\text{--}3.5$   $\mu\text{m}$  ( $\bar{x} = 2.6$   $\mu\text{m}$ ,  $n = 30$ ) wide, tapering abruptly into a thin neck,  $0.7\text{--}1.4$   $\mu\text{m}$  ( $\bar{x} = 0.9$   $\mu\text{m}$ ,  $n = 30$ ) wide. **Conidia** subglobose, hyaline,  $1.8\text{--}2.8$   $\mu\text{m}$  ( $\bar{x} = 2.3$   $\mu\text{m}$ ,  $n = 50$ ) in diam.

**Culture characteristics.** colonies on PDA reaching 40 mm in 14 days at room temperature, circular, flat, edge entire, mycelia dense, cottony, creamy yellow at centre, becoming white outward, with concentric rings, sporulation, reverse creamy yellow, with radially striate.

**Type.** CHINA • Yunnan Province, Puer City, Simao District, Plum Lake Park ( $22^{\circ}72'66.83''\text{N}$ ,  $100^{\circ}97'83.57''\text{E}$ , alt. 1354.5 m), on an adult ant (Hymenoptera) buried in soil, 25 October 2023, Jing Bu, DSSZ20231025110B (holotype HKAS144411, ex-holotype KUNCC24-18535).

**Additional materials examined.** CHINA • Yunnan Province, Puer, Simao District, Plum Lake Park ( $22^{\circ}75'14.29''\text{N}$ ,  $100^{\circ}97'73.13''\text{E}$ , alt. 1338.8 m), on lepidopteran cocoon buried in soil, 26 October 2023, Jing Bu, MZH20231025119B (paratype HKAS144402, ex-paratype KUNCC24-18536).

**Notes.** The phylogenetic tree (Fig. 2) showed that *Samsoniella torquatistipitata* constitutes a distinct clade distantly related to *S. cristata*, *S. kunmingensis*, *S. lurida*, and *S. tortricidae*. A pairwise comparison of *3P\_TEF*, *rpb1*, *MCM7*, and *rpb2* showed that *S. torquatistipitata* differs from *S. cristata*, *S. kunmingensis*, *S. lurida*, and *S. tortricidae* in 1–6 bp, 3–4 bp, 6–9 bp, and 4–16 bp, respectively. *Samsoniella torquatistipitata* is characterised by the small, single stroma (4.4 mm long), reddish-orange, cylindrical fertile part, superficial, lageniform perithecia, and the association with adult ants. Morphological comparisons of the novel taxa with closely related *Samsoniella* species are provided in Table 3. Both morphological characteristics and molecular analyses support this fungus as a new species in *Samsoniella* (Jeewon and Hyde 2016).



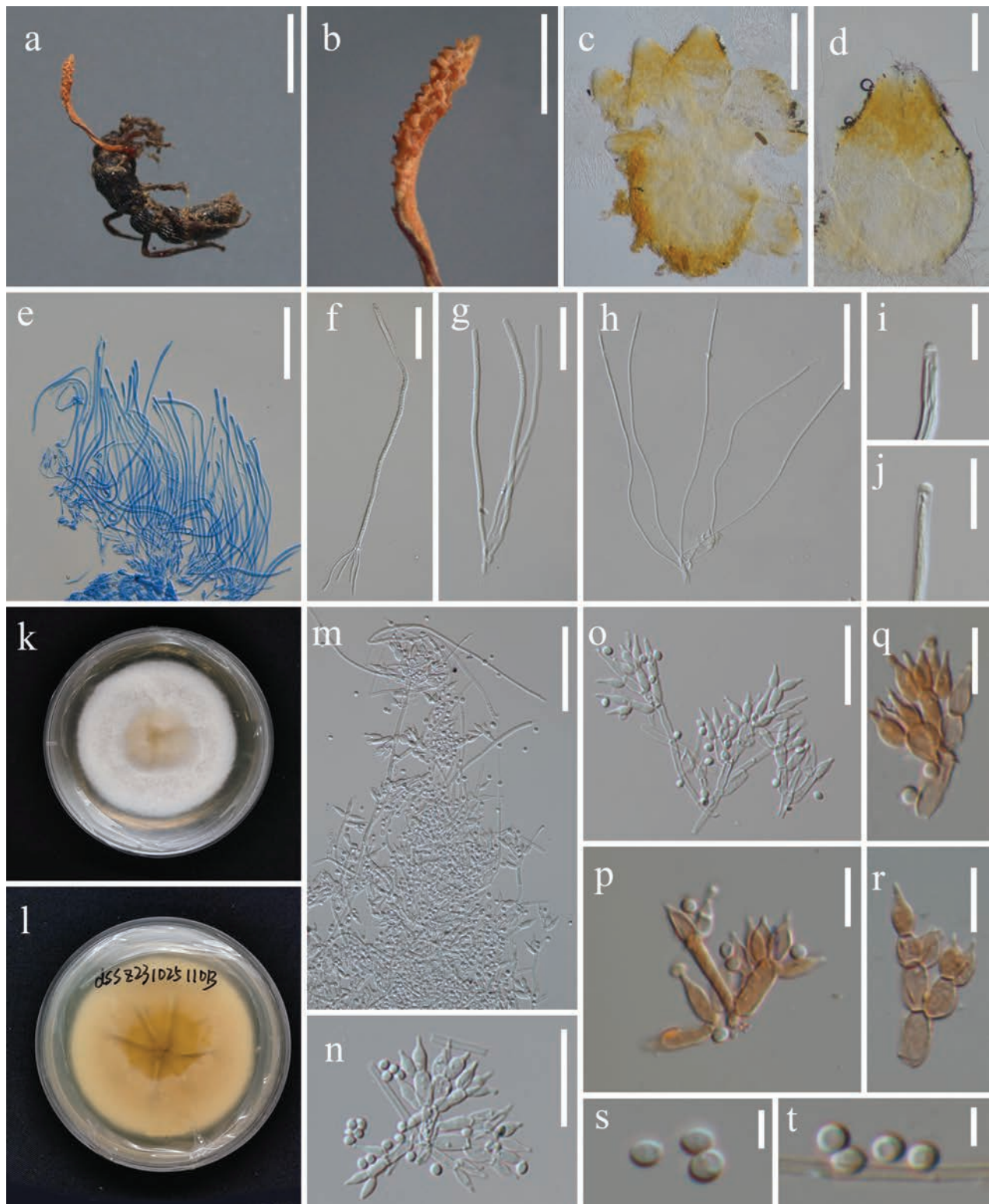


**Figure 6.** *Samsoniella torquatistipitata* (HKAS144411) **a** fungus on the adult ant **b** fertile part **c** vertical section of stroma **d** perithecium **e–g** asci **h** ascospore **i, j** ascus cap **k, l** obverse (**k**) and reverse (**l**) of colony on PDA; **m–r** conidiophores and phialides; **s, t** conidia. Scale bars: 3 mm (**a**); 1 mm (**b**); 200 µm (**c**); 100 µm (**d**); 50 µm (**e, m**); 30 µm (**f, g, h**); 20 µm (**n, o**); 10 µm (**i, j, p, q, r**); 3 µm (**s, t**).

***Samsoniella subasiatica* J. Bu, K.D. Hyde & T.C. Wen, sp. nov.**

Index Fungorum: IF903214

Fig. 7

**Etymology.** Referring to the morphology similar to *Samsoniella asiatica*.

**Description.** Parasitic on pupa of Lepidoptera. **Sexual morph.** Undetermined.

**Asexual morph. Synnema** arising from middle part of pupa, solitary, erect, flexuous, unbranched,  $2.8 \times 0.2$  mm. **Stipe** cylindrical, pale orange. **Hyphae** smooth-walled, septate, hyaline  $1.3\text{--}2.8\text{ }\mu\text{m}$  ( $\bar{x} = 2.0\text{ }\mu\text{m}$ ,  $n = 50$ ). **Conidiophores** grouped together at the apex of synnema and the head of pupa, verticillate  $3.6\text{--}7.4 \times 2\text{--}3\text{ }\mu\text{m}$  ( $\bar{x} = 5.2 \times 2.4\text{ }\mu\text{m}$ ,  $n = 20$ ). **Phialides** lageniform, usually in whorls of two to five,  $4.2\text{--}6.8\text{ }\mu\text{m}$  ( $\bar{x} = 5.6\text{ }\mu\text{m}$ ,  $n = 50$ ) long, globose at basal portion, tapering gradually toward the apex, from  $1.8\text{--}2.4\text{ }\mu\text{m}$  ( $\bar{x} = 2.1\text{ }\mu\text{m}$ ,  $n = 50$ ) wide (base) to  $0.6\text{--}1\text{ }\mu\text{m}$  ( $\bar{x} = 0.8\text{ }\mu\text{m}$ ,  $n = 50$ ) wide (apex). **Conidia** single, smooth-walled, hyaline, fusiform to oval,  $1.9\text{--}2.9 \times 1.4\text{--}1.8\text{ }\mu\text{m}$  ( $\bar{x} = 2.4 \times 1.6\text{ }\mu\text{m}$ ,  $n = 50$ ).

**Culture characteristics.** Colonies on PDA reaching a diameter of 27–29 mm in two weeks at room temperature, white, circular, velvety, mycelia dense, becoming loose in the outmost ring, reverse brightly yellow.

**Type.** CHINA • Guizhou Province, Qiannan Buyei and Miao Autonomous Prefecture, Anlong County ( $24^{\circ}99'08.43''\text{N}$ ,  $105^{\circ}59'76.06''\text{E}$ , alt. 1395.6 m), on lepidopteran pupa on leaf litter, 07 September 2023, Jing Bu, AI2023090717B (holotype HKAS144400, ex-holotype KUNCC24-18537).

**Notes.** *Samsoniella subasiatica* morphologically resembles *S. asiatica* (Wang et al. 2023a) by producing a flexuous synnema, pale orange stipe, with a mass of conidia at the apex. However, *S. subasiatica* differs from *S. asiatica* in having simple synnema and larger conidia ( $1.9\text{--}2.9\text{ }\mu\text{m}$  vs.  $1.1\text{--}1.8\text{ }\mu\text{m}$ ) (Table 4). The synnema of *S. asiatica* is branched at the base (Wang et al. 2023a). Furthermore, phylogenetic analysis based on four loci revealed that *S. subasiatica* is sister to *S. winandae*, with moderate statistical support (89% SH-aLRT / 94% UFB / 0.99 PP; Fig. 2). However, *S. subasiatica* can be distinguished from *S. winandae* by its significantly smaller synnemata and phialides ( $4.2\text{--}6.8 \times 1.8\text{--}2.4\text{ }\mu\text{m}$  vs.  $5\text{--}12 \times 2\text{--}3\text{ }\mu\text{m}$ ) (Table 4). Additionally, a comparison of nucleotide sequences between *S. subasiatica* and *S. winandae* indicated that there are 6 bp differences in *3P\_TEF*, 14 bp in *rpb1*, and 8 bp in *rpb2*. Based on the recommendations made by Jeewon and Hyde (2016), we determined this fungus as a novel species.

## Discussion

### Morphology-phylogeny of *Akanthomyces sensu lato*

*Akanthomyces sensu lato* is a monophyletic lineage, and it was segregated into four genera, including *Akanthomyces sensu stricto*, *Arachnidicola*, *Lecanicillium* and *Kanoksria*, corresponding to their morphological and ecological traits (Khonsanit et al. 2024; Wang et al. 2024b, Fig. 1). *Akanthomyces sensu stricto* comprises seventeen species pathogenic to moths, characterised by white to creamy synnemata with cylindrical, papillate phialides and catenulate conidia (Aini et al. 2020; Khonsanit et al. 2024). *Arachnidicola* comprises twelve species primarily pathogenic to spiders, displaying isaria-like anamorphs (Mongkolsamrit et al. 2018; Chen et al. 2022; 2023a; Wang et al. 2024b), except for



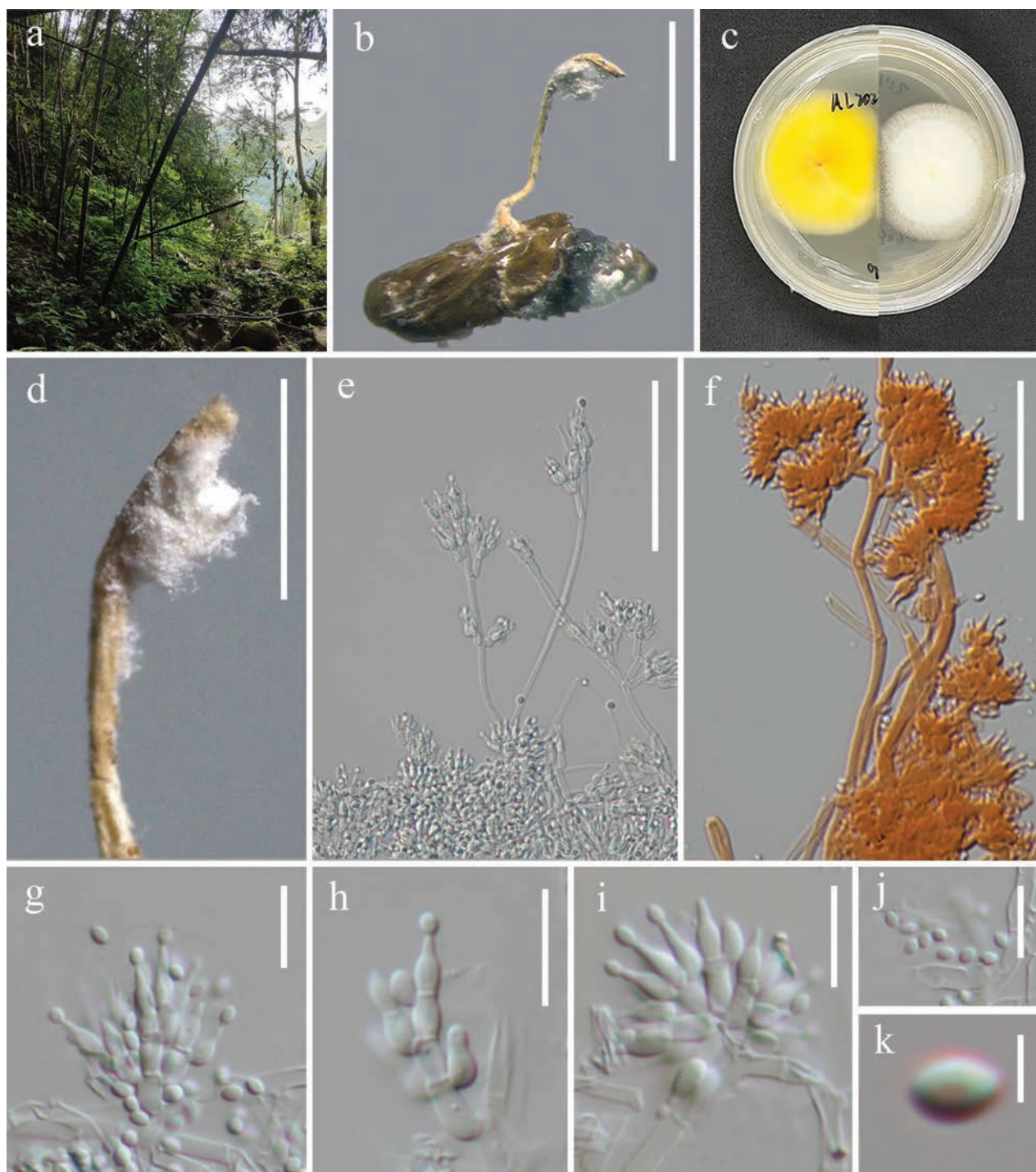


**Figure 7.** *Samsoniella subasiatica* (HKAS144400) **a** habitat **b** synnema arising from pupa **c** lower and upper view of the colony on PDA **d** synnema **e**, **f** conidiophores **g–i** phialides **j**, **k** conidia. Scale bars: 2 mm (**b**); 1 mm (**d**); 50  $\mu$ m (**e**); 30  $\mu$ m (**f**); 10  $\mu$ m (**g**, **h**, **i**, **j**); 2  $\mu$ m (**k**).

*Akanthomyces thailandicus*, which has a lecanicillium-like anamorph (Mongkol-samrit et al. 2018). *Lecanicillium* includes twelve species pathogenic to diverse hosts (e.g., Lepidoptera, Coleoptera, Hemiptera, spiders) with acremonium-like and verticillium-like anamorphs (Chiriví-Salomón et al. 2015; Chen et al. 2017, 2020a, 2020b, 2022; Manfrino et al. 2022). *Kanoksria*, a monotypic genus basal to the others, exhibits simplicillium-like anamorphs and is a hyperparasite on *Ophiocordyceps sinensis* (Wang et al. 2023b).

**Table 4.** Comparison between the asexual morphs in *Samsoniella*. The data generated in this study are shown in bold.

Species	Host	Synnemata (mm)	Conidiophores (μm)	Phialides	Phialides Size (μm)	Conidia (μm)	References
<i>S. aurantia</i>	Lepidopteran larva	25–75 × 1–1.5	150 × 2–3	/	(5–)7.5(–9) × 2–3	fusiform, oval with pointed ends, (2–)2.5(–3) × 1–2	Mongkolsamrit et al. 2018
<i>S. asiatica</i>	Lepidopteran pupa	4–26 × 0.4–1.5	4.6–10.3 × 0.8–1.9	verticillate, in whorls of two to four, or solitary on hyphae	2.7–8.6 × 0.7–1.7, 0.6–1.1 wide at apex	fusiform or oval, 1.1–1.8 × 0.8–1.2	Wang et al. 2023a
<i>S. cristata</i>	Lepidopteran pupa	/	3.6–11.5 × 1.7–2.5	verticillate, in whorls of two to five, or solitary on hyphae	4.5–23.2 × 1.6–2.7, 0.5–1.1 wide at apex	fusiform or oval, 2.4–3.2 × 1.6–2.3	Wang et al. 2020
<i>S. inthanonensis</i>	Lepidopteran larva	/	2–3 wide	verticillate, in whorls of two to five, cylindrical basal portion	basal (4–)6.5–10(–12) × (1–)1.5–2(3), neck (1–)2.5(–4) × 0.5–1	fusiform, (2–)3(–3.5) × 1.5–2	Mongkolsamrit et al. 2018
<i>S. lanmaoa</i>	Lepidopteran pupa	/	3.8–13.3 × 1.5–2.1	verticillate, in whorls of two to six, usually solitary on hyphae	3.5–20.7 × 1.7–2.6, 0.5–1.1 wide at apex	fusiform or oval, 1.9–2.7 × 1.4–2.0	Wang et al. 2020
<i>S. lurida</i>	Lepidopteran pupa	<b>1.2 × 0.2–0.35</b>	<b>2.3–9.1 × 1.9–2.9</b>	<b>verticillate, in whorls of two to five</b>	<b>4.2–7.3 × 1.7–2.5, 0.5–0.9 wide at apex</b>	<b>fusiform, 1.9–2.7 × 1.1–1.9</b>	<b>This study</b>
<i>S. pseudotortricidae</i>	Lepidopteran pupa	/	6.6–26.5 × 1.1–2.5	verticillate, in whorls of two to five, usually solitary on hyphae	5.4–6.9 × 1.0–1.6, 0.5–0.8 wide at apex	fusiform or oval, 0.9–1.5 × 0.8–1.3	Wang et al. 2022
<i>S. subasiatica</i>	Lepidopteran pupa	<b>2.8 × 0.2</b>	<b>3.6–7.4 × 2–3</b>	<b>verticillate, in whorls of two to five</b>	<b>4.2–6.8 × 1.8–2.4, 0.6–1.0 wide at apex</b>	<b>fusiform to oval, 1.9–2.9 × 1.4–1.8</b>	<b>This study</b>
<i>S. torquatistipitata</i>	Coleopteran adult	/	<b>4.4–18.4 × 1.7–3.9</b>	/	<b>6.1–10.7 × 1.8–3.5, 0.7–1.4 wide at apex</b>	<b>subglobose, up to 1.8–2.8 in diameter</b>	<b>This study</b>
<i>S. vallis</i>	Lepidopteran pupa	/	11.3–22.1 × 1.3–1.4	single phialide or whorls of two to four	7.2–8.1 × 2.8–3.2	fusiform to ellipsoidal, 2.3–3.1 × 1.5–2.1	Chen et al. 2023b
<i>S. winandae</i>	Lepidopteran pupa and cocoon	12 × 2	/	verticillate, in whorls of two to five	5–12 × 2–3	ellipsoidal, 1.5–3 × 1–2	Crous et al. 2023b

In this study, we identified a moth-pathogenic species, *Akanthomyces bais-hanensis*, which exhibits the typical phialide characteristics of *Akanthomyces sensu stricto*, along with previously undescribed phialide types within this clade. Although molecular data provide precise taxonomic evidence, morphological and ecological traits remain indispensable. An integrated taxonomy approach is necessary for resolving these complex fungal groups. Furthermore, ecological features may also provide valuable insights for the identification and discovery of novel *Akanthomyces* species.

### The molecular phylogeny and morphology of *Samsoniella*

Sexual morphs of *Samsoniella* share similarities in producing yellowish to reddish-orange, fleshy, simple to branched stromata; superficial, ovoid to fusiform perithecia; cylindrical asci with thickened apex and filiform, multiseptate, non-disarticulating ascospores (Mongkolsamrit et al. 2018). Species of this genus are indistinguishable solely based on sexual morphology. However, they can be divided into two types based on their stroma size: **Type Ia** includes nine species with a length of stromata more than 25 mm and is pathogenic to lepidopteran hosts (Mongkolsamrit et al. 2018; Wang et al. 2020, 2022, 2023b); **Type IIa** includes six species with a length of stromata lower than 25 mm and are pathogenic to lepidopteran and hymenopteran hosts or hyperparasitic to



*Cordyceps* species (Wang et al. 2020; Crous et al. 2023b) (Table 5). In this study, we introduce two new species in this group, namely, *Samsoniella lurida* and *S. torquatistipitata*, based on their sexual and asexual morphs. It is worth noting that *S. torquatistipitata* is pathogenic to an adult ant and has a very small, solitary, simple, reddish-orange stroma (4.4 mm in length). This is the first time to report the sexual typified species from an adult ant and contribute to the morphological diversity of *Samsoniella*.

The asexual morphs of *Samsoniella* have been known from 39 species. Macromorphologically, they can be categorised into two types: **Type Ib** includes 16 species which have well-developed stromata and are pathogenic to Lepidoptera, Coleoptera, Hymenoptera and *Cordyceps* sp. (Mongkolsamrit et al. 2018; Wang et al. 2020, 2022, 2023a; Chen et al. 2022, 2023b; Crous et al. 2023b; Chuang et al. 2024); **Type IIb** includes 15 species which form white colonies on the host surface and are pathogenic to Lepidoptera, Coleoptera, Hymenoptera, and spiders (Chen et al. 2020c, 2021b, 2022; Wang et al. 2020, 2022, 2024a). Our new species *S. subasiatica* was known only from its asexual morphs. This species has well-developed stroma covered with a white, powdery conidia mass, extremely resembling *S. asiatica*. However, these two species are phylogenetically distant, indicating that characteristics of asexual morphs have less taxonomic significance in interspecific demarcation.

Collectively, taxonomic inferences from phylogenetic analyses do not align with the morphological categories outlined in Table 5. The morphological plasticity of *Samsoniella* species limits their utility in taxonomy, necessitating molecular analyses for accurate species delineation (Mongkolsamrit et al. 2018). The six-locus (nrLSU+ITS+nrSSU+3P\_*TEF*+*rpb1*+*rpb2*) phylogeny effectively resolves genetically distant species, while it struggles with closely related taxa, particularly due to the limited resolution of the ITS regions. In contrast, the four-gene (5P\_*TEF*+3P\_*TEF*+*rpb1*+*MCM7*, Wang et al. 2023a) dataset provides superior resolution, highlighting its importance in refining the taxonomy of *Samsoniella*.

**Table 5.** Morphological synopsis of *Samsoniella* species.

Type	Species	Morphological characteristics	Host	References
Type Ia	<i>S. antleroides</i> , <i>S. aurantia</i> , <i>S. cristata</i> , <i>S. inthanonensis</i> , <i>S. lanmaoa</i> , <i>S. pseudotortricidae</i> , <i>S. ramosa</i> , <i>S. sapaensis</i> , <i>S. tortricidae</i> .	Stromata orange, fleshy, solitary to gregarious, simple or branched, more than 25 mm in length	Lepidoptera	Mongkolsamrit et al. 2018; Wang et al. 2020, 2022, 2023b
Type IIa	<i>S. cardinalis</i> , <i>S. hepiali</i> , <i>S. kunmingensis</i> , <b><i>S. lurida</i></b> , <b><i>S. torquatistipitata</i></b> , <i>S. winandae</i> .	Stromata orange, fleshy, solitary to gregarious, usually unbranched, less than 25 mm in length	<i>Cordyceps</i> sp., Lepidoptera	Wang et al. 2020; Crous et al. 2023b
Type Ib	<i>S. asiatica</i> , <i>S. aurantia</i> , <i>S. coccinellidicola</i> , <i>S. duyunensis</i> , <i>S. erucae</i> , <i>S. haniana</i> , <i>S. lasiocampidarum</i> , <i>S. ramosa</i> , <i>S. sapaensis</i> , <i>S. sinensis</i> , <b><i>S. subasiatica</i></b> , <i>S. tiankengensis</i> , <i>S. vallis</i> , <i>S. winandae</i> , <i>S. yuanzuiensis</i> , <i>S. yunnanensis</i> .	Synnemata erect, terminal irregularly branched, with conidial mass at the subterminal region of synnemata, conidial mass powdery and floccose	Lepidoptera, Coleoptera, Hymenoptera, <i>Cordyceps</i> sp.	Mongkolsamrit et al. 2018; Wang et al. 2020, 2022, 2023a; Chen et al. 2022, 2023b; Crous et al. 2023b; Chuang et al. 2024
Type IIb	<i>S. alpina</i> , <i>S. anhuiensis</i> , <i>S. aranea</i> , <i>S. coleopterorum</i> , <i>S. farinospora</i> , <i>S. formicae</i> , <i>S. fusiformispora</i> , <i>S. guizhouensis</i> , <i>S. hepiali</i> , <i>S. hymenopterorum</i> , <i>S. lepidopterorum</i> , <i>S. neopupicola</i> , <i>S. pupicola</i> , <i>S. pseudogunnii</i> , <i>S. sanmingense</i> .	White colonies surround the host surface without synnemata	Lepidoptera, Coleoptera, Hymenoptera, Spider.	Chen et al. 2020c, 2021b, 2022; Wang et al. 2020, 2022, 2024a; Pu et al. 2025

## Acknowledgements

We would like to thank Shaun Pennycook for checking the Latin diagnosis of the new species.

## Additional information

### Conflict of interest

The authors have declared that no competing interests exist.

### Ethical statement

No ethical statement was reported.

### Funding

This work was supported by the National Natural Science Foundation of China (No. 31760014) and the Science and Technology Foundation of Guizhou Province (No. [2019]2451-3). Shi-Ke Huang acknowledges the Department of Education of Guizhou Province (No: [2022]310).

### Author contributions

Investigation: SWX, SKH, XZ, ZHL, ZLL, YY. Resources: JCK, HGZ, ZJH, KDH. Writing - original draft: JB. Writing - review and editing: DPW, TCW, NNW, XCP.

### Author ORCIDs

Jing Bu  <https://orcid.org/0009-0006-6861-7770>

De-Ping Wei  <https://orcid.org/0000-0002-6576-2239>

Zheng-Hui Liu  <https://orcid.org/0000-0001-7022-4075>

Zhong-Liang Liu  <https://orcid.org/0009-0007-9519-1418>

Ji-Chuan Kang  <https://orcid.org/0000-0002-6294-5793>

Xing-Can Peng  <https://orcid.org/0000-0002-7271-7639>

Zhang-Jiang He  <https://orcid.org/0000-0002-7120-1227>

Shi-Ke Huang  <https://orcid.org/0000-0002-2936-396X>

Xian Zhang  <https://orcid.org/0009-0008-0919-4303>

Kevin D. Hyde  <https://orcid.org/0000-0002-2191-0762>

Nalin N. Wijayawardene  <https://orcid.org/0000-0003-0522-5498>

Ting-Chi Wen  <https://orcid.org/0000-0003-1744-5869>

### Data availability

All of the data that support the findings of this study are available in the main text or Supplementary Information.

## References

- Aini AN, Mongkolsamrit S, Wijanarka W, Thanakitpipattana D, Luangsa-ard JJ, Budiharjo A (2020) Diversity of *Akanthomyces* on moths (Lepidoptera) in Thailand. *MycoKeys* 71: 1–22. <https://doi.org/10.3897/mycokeys.71.55126>
- Alves VCS, Lira RA, Lima JMS, Barbosa RN, Bento DM, Barbier E, Bernard E, Souza-Motta CM, Bezerra JDP (2022) Unravelling the fungal darkness in a tropical cave: Richness

- and the description of one new genus and six new species. *Fungal Systematics and Evolution* 10(1): 139–167. <https://doi.org/10.3114/fuse.2022.10.06>
- Araújo JPM, Lebert BM, Vermeulen S, Brachmann A, Ohm RA, Evans HC, de Bekker C (2022) Masters of the manipulator: Two new hypocrealean genera, *Niveomyces* (Cordycipitaceae) and *Torrubiellomyces* (Ophiocordycipitaceae), parasitic on the zombie ant fungus *Ophiocordyceps camponoti-floridani*. *Persoonia* 49(1): 171–194. <https://doi.org/10.3767/persoonia.2022.49.05>
- Bischoff JF, Rehner SA, Humber RA (2006) *Metarhizium frigidum* sp. nov.: A cryptic species of *M. anisopliae* and a member of the *M. flavoviride* complex. *Mycologia* 98(5): 737–745. <https://doi.org/10.1080/15572536.2006.11832645>
- Boudier E (1885) Note sur un nouveau genre et quelques nouvelles especes des Pyrenomycetes. *Revue Mycologique Toulouse* 7: 224–227.
- Capella-Gutiérrez S, Silla-Martínez JM, Gabaldón T (2009) trimAl: A tool for automated alignment trimming in large-scale phylogenetic analyses. *Bioinformatics* 25(15): 1972–1973. <https://doi.org/10.1093/bioinformatics/btp348>
- Castlebury LA, Rossman AY, Sung GH, Hyten AS, Spatafora JW (2004) Multigene phylogeny reveals new lineage for *Stachybotrys chartarum*, the indoor air fungus. *Mycological Research* 108(8): 864–872. <https://doi.org/10.1017/S0953756204000607>
- Chen MJ, Huang B, Li ZZ, Spatafora JW (2013) Morphological and genetic characterisation of *Beauveria sinensis* sp. nov. from China. *Mycotaxon* 124(1): 301–308. <https://doi.org/10.5248/124.301>
- Chen WH, Han YF, Liang ZQ, Jin D (2017) *Lecanicillium araneogenum* sp. nov., a new araneogenous fungus. *Phytotaxa* 305(1): 29–34. <https://doi.org/10.11646/phytotaxa.305.1.4>
- Chen WH, Liu C, Han YF, Liang JD, Liang ZQ (2018) *Akanthomyces araneogenum*, a new Isaria-like araneogenous species. *Phytotaxa* 379(1): 66–72. <https://doi.org/10.11646/phytotaxa.379.1.6>
- Chen WH, Liu C, Han YF, Liang JD, Tian WY, Liang ZQ (2019) *Akanthomyces araneicola*, a new araneogenous species from Southwest China. *Phytotaxa* 409(4): 227–232. <https://doi.org/10.11646/phytotaxa.409.4.5>
- Chen WH, Han YF, Liang JD, Liang ZQ (2020a) *Akanthomyces lepidopterorum*, a new lecanicillium-like species. *Phytotaxa* 459(2): 117–123. <https://doi.org/10.11646/phytotaxa.459.2.3>
- Chen WH, Han YF, Liang JD, Liang ZQ (2020b) *Akanthomyces neocoleopterorum*, a new verticillium-like species. *Phytotaxa* 432(2): 119–124. <https://doi.org/10.11646/phytotaxa.432.2.2>
- Chen WH, Han YF, Liang JD, Tian WY, Liang ZQ (2020c) Morphological and phylogenetic characterisations reveal three new species of *Samsoniella* (Cordycipitaceae, Hypocreales) from Guizhou, China. *MycKeys* 74: 1–15. <https://doi.org/10.3897/mycokeys.74.56655>
- Chen WH, Han YF, Liang JD, Tian WY, Liang ZQ (2021a) Multi-gene phylogenetic evidence indicates that *Pleurodesmospora* belongs in Cordycipitaceae (Hypocreales, Hypocreomycetidae) and *Pleurodesmospora lepidopterorum* sp. nov. on pupa from China. *MycKeys* 80: 45–55. <https://doi.org/10.3897/mycokeys.80.66794>
- Chen WH, Liang J, Ren X, Zhao J, Han Y, Liang ZQ (2021b) Cryptic diversity of *Isaria*-like species in Guizhou, China. *Life* 11(10): 1093. <https://doi.org/10.3390/life11101093>
- Chen WH, Liang JD, Ren XX, Zhao JH, Han YF, Liang ZQ (2022) Species diversity of *Cordyceps*-like fungi in the Tiankeng Karst region of China. *Microbiology Spectrum* 10: e01975–e22. <https://doi.org/10.1128/spectrum.01975-22>

- Chen WH, Liang JD, Ren XX, Zhao JH, Han YF (2023a) Study on species diversity of *Akanthomyces* (Cordycipitaceae, Hypocreales) in the Jinyun Mountains, Chongqing, China. *MycKeys* 98: 299–315. <https://doi.org/10.3897/mycokeys.98.106415>
- Chen WH, Liang JD, Ren XX, Zhao JH, Han YF (2023b) Two new species of *Samsoniella* (Cordycipitaceae, Hypocreales) from the Mayao River Valley, Guizhou, China. *MycKeys* 99: 209–226. <https://doi.org/10.3897/mycokeys.99.109961>
- Chen WH, Li D, Shu HL, Liang JD, Zhao JH, Tian WY, Han YF (2025) Four new araneogenous species and a new genus in Hypocreales (Clavicipitaceae, Cordycipitaceae) from the karst region of China. *MycKeys* 112: 335–359. <https://doi.org/10.3897/mycokeys.112.140799>
- Chiriví-Salomón JS, Danies G, Restrepo S, Sanjuan T (2015) *Lecanicillium sabanense* sp. nov. (Cordycipitaceae) a new fungal entomopathogen of coccids. *Phytotaxa* 234(1): 63–74. <https://doi.org/10.11646/phytotaxa.234.1.4>
- Chuang WY, Lin YC, Shrestha B, Luangsa-ard JJ, Stadler M, Tzean SS, Wu S, Ko CC, Hsieh SY, Wu ML, Wang SC, Shen TL, Ariyawansa HA (2024) Phylogenetic diversity and morphological characterization of cordycipitaceous species in Taiwan. *Studies in Mycology* 109(1): 1–56. <https://doi.org/10.3114/sim.2024.109.01>
- Clewley JP (1995) Macintosh sequence analysis software: DNASTar's LaserGene. *Molecular Biotechnology* 3: 221–224. <https://doi.org/10.1007/BF02789332>
- Crous PW, Costa MM, Kandemir H, Vermaas M, Vu D, Zhao L, Arumugam E, Flakus A, Jurjević Ž, Kaliyaperumal M, Mahadevakumar S, Murugadoss R, Shivas RG, Tan YP, Wingfield MJ, Abell SE, Marney TS, Danteswari C, Darmostuk V, Denchev CM, Denchev TT, Etayo J, Gené J, Gunaseelan S, Hubka V, Illescas T, Jansen GM, Kezo K, Kumar S, Larsson E, Mufeeda KT, Pitek M, Rodriguez-Flakus P, Sarma PVSRN, Stryjak-Bogacka M, Torres-Garcia D, Vauras J, Acal DA, Akulov A, Alhudaib K, Asif M, Balashov S, Baral H-O, Baturo-Cieniewska A, Begerow D, Beja-Pereira A, Bianchinotti MV, Bilaski P, Chandranayaka S, Chellappan N, Cowan DA, Custódio FA, Czachura P, Delgado G, Desilva NI, Dijksterhuis J, Dueñas M, Eisvand P, Fachada V, Fournier J, Fritsche Y, Fuljer F, Ganga KGG, Guerra MP, Hansen K, Hywel-Jones N, Ismail AM, Jacobs CR, Jankowiak R, Karich A, Kemler M, Kisło K, Klofac W, Krisai-Greilhuber I, Latha KPD, Lebeuf R, Lopes ME, Lumyong S, Maciá-Vicente JG, Maggs-Köling G, Magistà D, Manimohan P, Martín MP, Mazur E, Mehrabi-Koushki M, Miller AN, Mombert A, Ossowska EA, Patejuk K, Pereira OL, Piskorski S, Plaza M, Podile AR, Polhorský A, Pusz W, Raza M, Ruszkiewicz-Michalska M, Saba M, Sánchez RM, Singh R, Liwa L, Smith ME, Stefenon VM, Strašitáková D, Suwannarach N, Szczepaska K, Telleria MT, Tennakoon DS, Thines M, Thorn RG, Urbaniak J, Vandervegte M, Vasan V, Vila-Viçosa C, Voglmayr H, Wrzosek M, Zappellini J, Groenewald JZ (2023a) Fungal Planet description sheets: 1550–1613. *Persoonia* 51(1): 280–417. <https://doi.org/10.3767/persoonia.2023.51.08>
- Crous PW, Osieck ER, Shivas RG, Tan YP, Bishop-Hurley SL, Esteve-Raventós F, Larsson E, Luangsa-ard JJ, Pancorbo F, Balashov S, Baseia IG, Boekhout T, Chandranayaka S, Cowan DA, Cruz RHSF, Czachura P, De La Peña-Lastra S, Dovana F, Drury B, Fell J, Flakus A, Fotedar R, Jurjević Ž, Kolecka A, Mack J, Maggs-Köling G, Mahadevakumar S, Mateos A, Mongkolsamrit S, Noisripoom W, Plaza M, Overy DP, Pitek M, Sandoval-Denis M, Vauras J, Wingfield MJ, Abell SE, Ahmadpour A, Akulov A, Alavi F, Alavi Z, Altés A, Alvarado P, Anand G, Ashtekar N, Assyov B, Banc-Prandi G, Barbosa KD, Barreto GG, Bellanger JM, Bezerra JL, Bhat DJ, Bilański P, Bose T, Bozok F, Chaves J, Costa-Rezende DH., Danteswari C, Darmostuk V, Delgado G, Denman S, Eichmeier A, Etayo J, Eyssartier G, Faulwetter S, Ganga KGG, Ghosta Y, Goh J, Góis JS, Gramaje D, Granit L, Groenewald M, Gulden G, Gusmão LFP, Hammerbacher A, Heidarian Z, Hywel-Jones N, Jankowiak R, Kaliyaperumal M,



- Kaygusuz O, Kezo K, Khonsanit A, Kumar S, Kuo CH, Laessøe T, Latha KPD, Loizides M, Luo SM, Maciá-Vicente JG, Manimohan P, Marbach PAS, Marinho P, Marney TS., Marques G, Martín MP, Miller AN, Mondello F, Moreno G, Mufeeda KT, Mun HY, Nau T, Nkomo T, Okraśińska A, Oliveira JPAF, Oliveira RL, Ortiz DA, Pawłowska J, Pérez-De-Gregorio MA, Podile AR, Portugal A, Privitera N, Rajeshkumar KC, Rauf I, Rian B, Rigueiro-Rodríguez A, Rivas-Torres GF, Rodríguez-Flakus P, Romero-Gordillo M, Saar I, Saba M, Santos CD, Sarma PVSRN, Siquier JL, Sleiman S, Spetik M, Sridhar KR, Stryjak-Bogacka M, Szczepańska K, Taşikn H, Tennakoon DS, Thanakitpipattana D, Trovão J., Türkeul A, Van Iperen AL, Van 'T Hof P, Vasquez G, Visagie CM, Wingfield BD, Wong PTW, Yang WX, Yazar M, Yarden O, Yilmaz N, Zhang N, Zhu YN, Groenewald JZ (2023b) Fungal Planet description sheets: 1478–1549. *Persoonia* 50(1): 158–310. <https://doi.org/10.3767/persoonia.2023.50.05>
- Custódio FA, Pereira OL (2024) New treasures in Cordycipitaceae: Fungicolous fungi associated with *Pseudocercospora fijiensis* and *P. musae* in Brazil, including *Matutiniella* gen. nov. *Fungal Systematics and Evolution* 15(1): 133–152. <https://doi.org/10.3114/fuse.2025.15.06>
- Flakus A, Etayo J, Miadlikowska J, Lutzoni F, Kukwa M, Matura N, Rodríguez-Flakus P (2019) Biodiversity assessment of ascomycetes inhabiting *Lobariella* lichens in Andean cloud forests led to one new family, three new genera and 13 new species of lichenicolous fungi. *Plant and Fungal Systematics* 64(2): 283–344. <https://doi.org/10.2478/pfs-2019-0022>
- Glass NL, Donaldson GC (1995) Development of primer sets designed for use with the PCR to amplify conserved genes from filamentous ascomycetes. *Applied and Environmental Microbiology* 61(4): 1323–1330. <https://doi.org/10.1128/aem.61.4.1323-1330.1995>
- Guerra-Mateo D, Gené J, Baulin V, Cano-Lira JF (2023) Phylogeny and taxonomy of the genus *Amphichorda* (Bionectriaceae): An Update on *Beauveria*-like Strains and Description of a Novel Species from Marine Sediments. *Diversity* 15(7): 795. <https://doi.org/10.3390/d15070795>
- Hall T, Biosciences I, Carlsbad C (2011) BioEdit: An important software for molecular biology. *GERF Bulletin of Biosciences* 2(1): 60–61.
- Hyde KD, Noorabadi MT, Thiagaraja V, He MQ, Johnston PR, Wijesinghe SN, Armand A, Biketova AY, Chethana KWT, Erdoğan M, Ge ZW, Groenewald JZ, Hongsanan S, Kušan I, Leontyev DV, Li DW, Lin CG, Liu NG, Maharachchikumbura SSN, Matočec N, May TW, McKenzie EHC, Mešić A, Perera RH, Phukhamsakda C, Piątek M, Samarakoon MC, Selcuk F, Senanayake IC, Tanney JB, Tian Q, Vizzini A, Wanasinghe DN, Wannasawang N, Wijayawardene NN, Zhao RL, Abdel-Wahab MA, Abdollahzadeh J, Abeywickrama PD, Abhinav, Absalan S, Acharya K, Afshari N, Afshan NS, Afzalnia S, Ahmadpour SA, Akulov O, Alizadeh A, Alizadeh M, Al-Sadi AM, Alves A, Alves VCS, Alves-Silva G, Antonín V, Aouali S, Aptroot A, Apurillo CCS, Arias RM, Asgari, B, Asghari R, Assis DMA, Assyov B, Atienza V, Aumentado HDR, Avasthi S, Azevedo E, Bakhshi M, Bao DF, Baral HO, Barata M, Barbosa KD, Barbosa RN, Barbosa FR, Baroncelli R, Barreto GG, Baschien C, Bennett RM, Bera I, Bezerra JDP, Bhunjun CS, Bianchinotti MV, Błaszowski J, Boekhout T, Bonito GM, Boonmee S, Boonyuen N, Bortnikov FM, Bregant C, Bundhun D, Burgaud G, Buyck B, Caeiro MF, Cabarroi-Hernández M, Cai M Feng, Cai L, Calabon MS, Calaça FJS, Callalli M, Câmara MPS, Cano-Lira J, Cao B, 5162 Carlavilla JR, Carvalho A, Carvalho TG, Castañeda-Ruiz RF, Catania MDV, Cazabonne J, Cedeño-Sánchez M, Chaharmiri-Dokhaharani S, Chaiwan N, Chakraborty N, Cheewankoon R, Chen C, Chen J, Chen Q, Chen YP, Chinaglia S, Coelho-Nascimento CC, Coleine C, CostaRezende DH, Cortés-Pérez A, Crouch, JA, Crous PW, Cruz RHSF, Czachura P, Damm U, Darmostuk V, Daroodi Z, Das K, Das K, Davoodian N, Davydov EA, da Silva GA, da Silva IR, da Silva RMF, da Silva Santos AC, Dai DQ, Dai YC, de Groot Michiel

D, De Kesel A, De Lange R, de Medeiros EV, de Souza CFA, de Souza FA, dela Cruz TEE, Decock C, Delgado G, Denchev CM, Denchev TT, Deng YL, Dentinger BTM, Devadatha B, Dianese JC, Dima B, Doilom M, Dissanayake AJ, Dissanayake DMLS, Dissanayake LS, Diniz AG, Dolatabadi S, Dong JH, Dong W, Dong ZY, Drechsler-Santos ER, Druzhinina IS, Du TY, Dubey MK, Dutta AK, Elliott TF, Elshahed MS, Egidi E, Eisvand P, Fan L, Fan X, Fan XL, Fedosova AG, Ferro LO, Fiuza PO, Flakus A, W. Fonseca EO, Fryar SC, Gabaldón T, Gajanayake AJ, Gannibal PB, Gao F, GarcíaSánchez D, García-Sandoval R, Garrido-Benavent I, Garzoli L, Gasca-Pineda J, Gautam AK, Gené J, Ghobad-Nejhad M, Ghosh A, Giachini AJ, Gibertoni TB, Gentekaki E, Gmoshinskiy VI, GóesNeto A, Gomdola D, Gorjón SP, Goto BT, Granados-Montero MM, Griffith GW, Groenewald M, Grossart H-P, Gu ZR, Gueidan C, Gunarathne A, Gunaseelan S, Guo SL, Gusmão LFP, Gutierrez AC, Guzmán-Dávalos L, Haelewaters D, Haituk H, Halling RE, He SC, Heredia G, HernándezRestrepo M, Hosoya T, Hoog SD, Horak E, Hou CL, Houbraken J, Htet ZH, Huang SK, Huang WJ, Hurdeal VG, Hustad VP, Inácio CA, Janik P, Jayalal RGU, Jayasiri SC, Jayawardena RS, Jeewon R, Jerônimo GH, Jin J, Jones EBG, Joshi Y, Jurjević Ž, Justo A, Kakishima M, Kaliyaperumal M, Kang GP, Kang JC, Karimi O, Karunarathna SC, Karpov SA, Kezo K, Khalid AN, Khan MK, Khuna S, Khyaju S, Kirchmair M, Klawonn I, Kraisitudomsook N, Kukwa M, Kularathnage ND, Kumar S, Lachance MA, Lado C, Latha KPD, Lee HB, Leonardi M, Lestari AS, Li C, Li H, Li J, Li Q, Li Y, Li YC, Li YX, Liao CF, Lima JLR, Lima JMS, Lima NB, Lin L, Linaldeddu BT, Linn MM, Liu F, Liu JK, Liu JW, Liu S, Liu SL, Liu XF, Liu XY, Longcore JE, Luangharn T, Luangsa-ard JJ, Lu L, Lu YZ, Lumbsch HT, Luo L, Luo M, Luo ZL, Ma J, Madagammana AD, Madhushan A, Madrid H, Magurno F, Magyar D, Mahadevakumar S, Malosso E, Malysch JM, Mamarabadi M, Manawasinghe IS, Manfrino RG, Manimohan P, Mao N, Mapook A, Marchese P, Marasinghe DS, Mardones M, Marin-Felix Y, Masigol H, Mehrabi M, MehrabiKoushki M, Meiras-Ottoni A de, Melo RFR, Mendes-Alvarenga RL, Mendieta S, Meng QF, Menkis A, Menolli Jr N, Mikšík M, Miller SL, Moncada B, Moncalvo JM, Monteiro JS, Monteiro M, Mora-Montes HM, Moroz EL, Moura JC, Muhammad U, Mukhopadhyay S, Nagy GL, Najam ul Sehar A, Najafiniya M, Nanayakkara CM, Naseer A, Nascimento ECR, Nascimento SS, Neuhauser S, Neves MA, Niazi AR, Nie Yong, Nilsson RH, Nogueira PTS, Novozhilov YK, Noordeloos M, Norphanphoun C, Nuñez Otaño N, O'Donnell RP, Oehl F, Oliveira JA, Oliveira Junior I, Oliveira NVL, Oliveira PHF, Orihara T, Oset M, Pang KL, Papp V, Pathirana LS, Peintner U, Pem D, Pereira OL, Pérez-Moreno J, Pérez-Ortega S, Péter G, Pires-Zottarelli CLA, Phonemany M, Phongeun S, Pošta A, Prazeres JFSA, Quan Y, Quandt CA, Queiroz MB, Radek R, Rahnama K, Raj KNA, Rajeshkumar KC, Rajwar Soumyadeep, Ralaiveloarisoa AB, Rămă T, Ramírez-Cruz V, Rambold G, Rathnayaka AR, Raza M, Ren GC, Rinaldi AC, Rivas-Ferreiro M, Robledo GL, Ronikier A, Rossi W, Rusevska K, Ryberg M, Safi A, Salimi F, Salvador-Montoya CA, Samant B, Samaradiwakara NP, Sánchez-Castro I, Sandoval-Denis M, Santiago ALCMA, Santos ACDS, Santos LA dos, Sarma VV, Sarwar S, Savchenko A, Savchenko K, Saxena RK, Schoutteten N, Selbmann L, Ševčíková H, Sharma A, Shen HW, Shen YM, Shu YX, Silva HF, Silva-Filho AGS, Silva VSH, Simmons DR, Singh R, Sir EB, Sohrabi M, Souza FA, Souza-Motta CM, Sriindrasutdhi V, Sruthi OP, Stadler M, Stemler J, Stephenson SL, Stoyneva-Gaertner MP, Strasser JFH, Stryjak-Bogacka M, Su H, Sun YR, Svantesson S, Sysouphanthong P, Takamatsu S, Tan TH, Tanaka K, Tang C, Tang X, Taylor JE, Taylor PWJ, Tennakoon DS, Thakshila SAD, Thambugala KM, Thamodini GK, Thilanga D, Thines M, Tiago PV, Tian XG, Tian WH, Tibpromma S, Tkáčec Z, Tokarev YS, Tomšovský M, Torruella G, Tsurykau A, Udayanga D, Ulukapi M, Untereiner WA, Usman M, Uzunov BA, Vadthanarat S, Valenzuela R, Van den Wyngaert S, Van Vooren N, Velez P, Verma RK, Vieira LC, Vieira WAS, Vinzelj JM, Tang AMC, Walker A, Walker AK, Wang QM, Wang Y, Wang XY, Wang ZY, Wannathes N, Wartchow F, Weerakoon G, Wei DP, Wei X,

- White JF, Wijesundara DSA, Wisitrassameewong K, Worobiec G, Wu HX, Wu N, Xiong YR, Xu B, Xu JP, Xu R, Xu RF, Xu RJ, Yadav S, Yakovchenko LS, Yang HD, Yang X, Yang YH, Yang Y, Yang YY, Yoshioka R, Youssef Noha H, Yu FM, Yu ZF, Yuan LL, Yuan Q, Zabin DA, Zamora JC, Zapata CV, Zare R, Zeng M, Zeng XY, Zhang JF, Zhang JY, Zhang S, Zhang XC, Zhao CL, Zhao H, Zhao Q, Zhao H, Zhao HJ, Zhou HM, Zhu XY, Zmitrovich IV, Zucchini L, Zvyagina E (2024) The 2024 Outline of Fungi and fungus-like taxa. *Mycosphere* 15(1): 5146–6239. <https://doi.org/10.5943/mycosphere/15/1/25>
- Imoulan A, Wu HJ, Lu WL, Li Y, Li BB, Yang RH, Wang WJ, Wang XL, Kirk PM, Yao YJ (2016) *Beauveria medogensis* sp. nov., a new fungus of the entomopathogenic genus from China. *Journal of Invertebrate Pathology* 139: 74–81. <https://doi.org/10.1016/j.jip.2016.07.006>
- Jeewon R, Hyde KD (2016) Establishing species boundaries and new taxa among fungi: Recommendations to resolve taxonomic ambiguities. *Mycosphere : Journal of Fungal Biology* 7(11): 1669–1677. <https://doi.org/10.5943/mycosphere/7/11/4>
- Kepler RM, Luangsa-ard JJ, Hywel-Jones NL, Quandt CA, Sung G-H, Rehner SA, Aime MC, Henkel TW, Sanjuan T, Zare R, Chen M, Li Z, Rossman AY, Spatafora JW, Shrestha B (2017) A phylogenetically-based nomenclature for Cordycipitaceae (Hypocreales). *IMA Fungus* 8(2): 335–353. <https://doi.org/10.5598/ima fungus.2017.08.02.08>
- Khonsanit A, Thanakitpipattana D, Mongkolsamrit S, Kobmoo N, Phosrithong N, Samson RA, Crous PW, Luangsa-ard JJ (2024) A phylogenetic assessment of *Akanthomyces sensu lato* in Cordycipitaceae (Hypocreales, Sordariomycetes): Introduction of new genera, and the resurrection of *Lecanicillium*. *Fungal Systematics and Evolution* 14(1): 271–305. <https://doi.org/10.3114/fuse.2024.14.17>
- Kobmoo N, Tasanathai K, Araújo JPM, Noisripoom W, Thanakitpipattana D, Mongkolsamrit S, Himaman W, Houbraken J, Luangsa-Ard JJ (2023) New mycoparasitic species in the genera *Niveomyces* and *Pseudoniveomyces* gen. nov. (Hypocreales : Cordycipitaceae), with sporothrix-like asexual morphs, from Thailand. *Fungal Systematics and Evolution* 12(1): 91–110. <https://doi.org/10.3114/fuse.2023.12.07>
- Larsson A (2014) AliView: A fast and lightweight alignment viewer and editor for large datasets. *Bioinformatics* 30(22): 3276–3278. <https://doi.org/10.1093/bioinformatics/btu531>
- Lebert H (1858) Ueber einige neue oder unvollkommen gekannte Krankheiten der Insekten, welche durch Entwicklung niederer Pflanzen im lebenden Körper entstehen. *Zeitschrift für Wissenschaftliche Zoologie* 9: 439–453.
- Liu SL, Wang XW, Li GJ, Deng CY, Rossi W, Leonardi M, Liimatainen K, Kekki T, Niskanen T, Smith ME, Ammirati J, Bojantchev D, Abdel-Wahab MA, Zhang M, Tian EJ, Lu YZ, Zhang JY, Ma J, Dutta AK, Acharya K, Du TY, Xu J, Kim JS, Lim YW, Gerlach A, Zeng NK, Han YX, Razaghi P, Raza M, Cai L, Calabon MS, Jones EBG, Saha R, Kumar TKA, Krishnapriya K, Thomas A, Kaliyaperumal M, Kezo K, Gunaseelan S, Singh SK, Singh PN, Lagashetti AC, Pawar KS, Jiang SH, Zhang C, Zhang H, Qing Y, Bau T, Peng XC, Wen TC, Ramirez NA, Niveiro N, Li MX, Yang ZL, Wu G, Tarafder E, Tennakoon DS, Kuo CH, Silva TM, Souza-Motta CM, Bezerra JDP, He G, Ji XH, Suwannarach N, Kumla J, Lumyong S, Wannathes N, Rana S, Hyde KD, Zhou LW (2024) Fungal diversity notes. 1717–1817: Taxonomic and phylogenetic contributions on genera and species of fungal taxa. *Fungal Diversity* 124(1): 1–216. <https://doi.org/10.1007/s13225-023-00529-0>
- Maharachchikumbura SSN, Chen Y, Ariyawansa HA, Hyde KD, Haelewaters D, Perera RH, Samarakoon MC, Wanasinghe DN, Bustamante DE, Liu J, Lawrence DP, Cheewangkoon R, Stadler M (2021) Integrative approaches for species delimitation in Ascomycota. *Fungal Diversity* 109(1): 155–179. <https://doi.org/10.1007/s13225-021-00486-6>

- Mains EB (1950) Entomogenous Species of *Akanthomyces*, *Hymenostilbe* and *Insecticola* in North America. *Mycologia* 42(4): 566–589. <https://doi.org/10.1080/00275514.1950.12017861>
- Manfrino R, Gutierrez A, Diez Del Valle F, Schuster C, Ben Gharsa H, López Lastra C, Leclercque A (2022) First Description of *Akanthomyces uredinophilus* comb. nov. from Hemipteran Insects in America. *Diversity* 14(12): 1118. <https://doi.org/10.3390/d14121118>
- Minh BQ, Schmidt HA, Chernomor O, Schrempf D, Woodhams MD, von Haeseler A, Lanfear R (2020) IQ-TREE 2: New Models and Efficient Methods for Phylogenetic Inference in the Genomic Era. *Molecular Biology and Evolution* 37(5): 1530–1534. <https://doi.org/10.1093/molbev/msaa015>
- Mongkolsamrit S, Noisriboom W, Thanakitpipattana D, Wutikhun T, Spatafora JW, Luangsa-ard JJ (2018) Disentangling cryptic species with *isaria*-like morphs in Cordycipitaceae. *Mycologia* 110(1): 230–257. <https://doi.org/10.1080/00275514.2018.1446651>
- Mongkolsamrit S, Noisriboom W, Tasanathai K, Khonsanit A, Thanakitpipattana D, Himaman W, Kobmoo N, Luangsa-ard JJ (2020) Molecular phylogeny and morphology reveal cryptic species in *Blackwellomyces* and *Cordyceps* (Cordycipitaceae) from Thailand. *Mycological Progress* 19(9): 957–983. <https://doi.org/10.1007/s11557-020-01615-2>
- Mongkolsamrit S, Noisriboom W, Pumiputikul S, Boonlarppradab C, Samson RA, Stadler M, Becker K, Luangsa-ard JJ (2021) *Ophiocordyceps flavida* sp. nov. (Ophiocordycipitaceae), a new species from Thailand associated with *Pseudogibellula formicarum* (Cordycipitaceae), and their bioactive secondary metabolites. *Mycological Progress* 20(4): 477–492. <https://doi.org/10.1007/s11557-021-01683-y>
- Mongkolsamrit S, Noisriboom W, Tasanathai K, Kobmoo N, Thanakitpipattana D, Khonsanit A, Petcharad B, Sakolrak B, Himaman W (2022) Comprehensive treatise of *Hevansia* and three new genera *Jenniferia*, *Parahevansia* and *Polystromomyces* on spiders in Cordycipitaceae from Thailand. *MycKeys* 91: 113–149. <https://doi.org/10.3897/mycokeys.91.83091>
- Mongkolsamrit S, Sandargo B, Ebada SS, Noisriboom W, Jaiyen S, Luangsa-ard JJ, Stadler M (2023) *Bhushaniella* gen. nov. (Cordycipitaceae) on spider eggs sac: A new genus from Thailand and its bioactive secondary metabolites. *Mycological Progress* 22(9): 64. <https://doi.org/10.1007/s11557-023-01915-3>
- Nuin P (2007) MrMTgui. v 1.0. MrModelTest/ModelTest Graphical interface for Windows/Linux.
- Nylander J (2004) MrModeltest Version 2. Program distributed by the author. <https://github.com/nylander/MrModeltest2>
- Pu HL, Yang J, Keyhani NO, Yang LX, Zheng MH, Qiu CH, Mao YC, Shang JY, Lin YS, Xiong CJ, Lin LB, Lai PY, Huang YB, Yuan X, Liang HL, Fan LF, Ma XL, Qiu CJ, Qiu JZ (2025) Molecular phylogenetics and estimation of evolutionary divergence and biogeography of the family Cordycipitaceae (Ascomycota, Hypocreales). *Journal of Fungi* 11(1): 1–29. <https://doi.org/10.3390/jof11010028>
- Rambaut A (2016) FigTree version 1.4. 0. <http://tree.bio.ed.ac.uk/software/figtree> [Accessed 11 Sep. 2023]
- Rehner SA, Buckley E (2005) A *Beauveria* phylogeny inferred from nuclear ITS and EF1- $\alpha$  sequences: Evidence for cryptic diversification and links to *Cordyceps* teleomorphs. *Mycologia* 97(1): 84–98. <https://doi.org/10.3852/mycologia.97.1.84>
- Rehner SA, Minnis AM, Sung GH, Luangsa-ard JJ, Devotto L, Humber RA (2011) Phylogeny and systematics of the anamorphic, entomopathogenic genus *Beauveria*. *Mycologia* 103(5): 1055–1073. <https://doi.org/10.3852/10-302>



- Samson RA, Gams W (1980) *Pleurodesmospora*, a new genus for the entomogenous hyphomycete gonorrhodiella coccorum. *Persoonia* 11(1): 65–69.
- Schmitt I, Crespo A, Divakar PK, Fankhauser JD, Herman-Sackett E, Kalb K, Nelsen MP, Nelson NA, Rivas-Plata E, Shimp AD, Widhelm T, Lumbsch HT (2009) New primers for promising single-copy genes in fungal phylogenetics and systematics. *Persoonia* 23(1): 35–40. <https://doi.org/10.3767/003158509X470602>
- Shrestha B, Kubátová A, Tanaka E, Oh J, Yoon DH, Sung JM, Sung GH (2019) Spider-pathogenic fungi within Hypocreales (Ascomycota): Their current nomenclature, diversity, and distribution. *Mycological Progress* 18(8): 983–1003. <https://doi.org/10.1007/s11557-019-01512-3>
- Spatafora JW, Sung GH, Sung JM, Hywel-Jones NL, White Jr J (2007) Phylogenetic evidence for an animal pathogen origin of ergot and the grass endophytes. *Molecular Ecology* 16(8): 1701–1711. <https://doi.org/10.1111/j.1365-294X.2007.03225.x>
- Sung GH, Spatafora JW, Zare R, Hodge KT, Gams W (2001) A revision of *Verticillium* sect. Prostrata. II. Phylogenetic analyses of SSU and LSU nuclear rDNA sequences from anamorphs and teleomorphs of the Clavicipitaceae. *Nova Hedwigia* 72(3–4): 311–328. <https://doi.org/10.1127/nova.hedwigia/72/2001/311>
- Sung GH, Hywel-Jones NL, Sung JM, Luangsa-ard JJ, Shrestha B, Spatafora JW (2007) Phylogenetic classification of *Cordyceps* and the clavicipitaceous fungi. *Studies in Mycology* 57: 5–59. <https://doi.org/10.3114/sim.2007.57.01>
- Tan YP, Shivas R (2023) Nomenclatural novelties. *Index of Australian Fungi* 15:1–11. <https://doi.org/10.5281/zenodo.8327643>
- Tan YP, Shivas R (2024) Nomenclatural novelties. *Index of Australian Fungi* 49: 1–16. <https://doi.org/10.5281/zenodo.14561830>
- Thanakitpipattana D, Tasanathai K, Mongkolsamrit S, Khonsanit A, Lamlerththong S, Luangsa-ard JJ (2020) Fungal pathogens occurring on *Orthoptera* in Thailand. *Persoonia* 44(1): 140–160. <https://doi.org/10.3767/persoonia.2020.44.06>
- Thanakitpipattana D, Mongkolsamrit S, Khonsanit A, Himaman W, Luangsa-ard JJ, Pornputtapong N (2022) Is *Hyperdermium* congeneric with *Ascopolyporus*? Phylogenetic relationships of *Ascopolyporus* spp. (Cordycipitaceae, Hypocreales) and a new genus *Neohyperdermium* on scale insects in Thailand. *Journal of Fungi* 8(5): 516. <https://doi.org/10.3390/jof8050516>
- Vaidya G, Lohman DJ, Meier R (2011) SequenceMatrix: Concatenation software for the fast assembly of multi-gene datasets with character set and codon information. *Cladistics* 27(2): 171–180. <https://doi.org/10.1111/j.1096-0031.2010.00329.x>
- Vilgalys R, Hester M (1990) Rapid genetic identification and mapping of enzymatically amplified ribosomal DNA from several *Cryptococcus* species. *Journal of Bacteriology* 172(8): 4238–4246. <https://doi.org/10.1128/jb.172.8.4238-4246.1990>
- Vinit K, Doilom M, Wanasinghe DN, Bhat DJ, Brahmanage RS, Jeewon R, Xiao Y, Hyde KD (2018) Phylogenetic placement of *Akanthomyces muscarius*, a new endophyte record from *Nypa fruticans* in Thailand. *Current Research in Environmental & Applied Mycology* 8(3): 404–417. <https://doi.org/10.5943/cream/8/3/10>
- Voigt K, Wöstemeyer J (2000) Reliable amplification of actin genes facilitates deep-level phylogeny. *Microbiological Research* 155(3): 179–195. [https://doi.org/10.1016/S0944-5013\(00\)80031-2](https://doi.org/10.1016/S0944-5013(00)80031-2)
- Voigt K, Cigelnik E, O'donnell K (1999) Phylogeny and PCR identification of clinically important Zygomycetes based on nuclear ribosomal-DNA sequence data. *Journal of Clinical Microbiology* 37(12): 3957–3964. <https://doi.org/10.1128/JCM.37.12.3957-3964.1999>

- Wang YB, Wang Y, Fan Q, Duan DE, Zhang GD, Dai RQ, Dai YD, Zeng WB, Chen ZH, Li DD, Tang DX, Xu ZH, Sun T, Nguyen TT, Tran NL, Dao VM, Zhang CM, Huang LD, Liu YJ, Zhang XM, Yang DR, Sanjuan T, Liu XZ, Yang ZL, Yu H (2020) Multigene phylogeny of the family Cordycipitaceae (Hypocreales): New taxa and the new systematic position of the Chinese cordycipitoid fungus *Paecilomyces hepiali*. Fungal Diversity 103: 1–46. <https://doi.org/10.1007/s13225-020-00457-3>
- Wang ZQ, Wang Y, Dong Q, Fan Q, Dao VM, Yu H (2022) Morphological and phylogenetic characterization reveals five new species of *Samsoniella* (Cordycipitaceae, Hypocreales). Journal of Fungi 8(7): 747. <https://doi.org/10.3390/jof8070747>
- Wang Y, Wang ZQ, Thanarut C, Dao VM, Wang YB, Yu H (2023a) Phylogeny and species delimitations in the economically, medically, and ecologically important genus *Samsoniella* (Cordycipitaceae, Hypocreales). MycoKeys 99: 227–250. <https://doi.org/10.3897/mycokeys.99.106474>
- Wang YH, Wang WJ, Wang K, Dong CH, Hao JR, Kirk PM, Yao YJ (2023b) *Akanthomyces zaquensis* (Cordycipitaceae, Hypocreales), a new species isolated from both the stroma and the sclerotium of *Ophiocordyceps sinensis* in Qinghai, China. Phytotaxa 579(3): 198–208. <https://doi.org/10.11646/phytotaxa.579.3.5>
- Wang T, Li J, Chang X, Li Z, Hywel-Jones NL, Huang B, Chen M (2024a) Morphology and multigene phylogeny reveal three new species of *Samsoniella* (Cordycipitaceae, Hypocreales) from spiders in China. MycoKeys 101: 329–346. <https://doi.org/10.3897/mycokeys.101.111882>
- Wang Y, Wang ZQ, Luo R, Souvannachit S, Thanarut C, Dao VM, Yu H (2024b) Species diversity and major host/substrate associations of the genus *Akanthomyces* (Hypocreales, Cordycipitaceae). MycoKeys 101: 113–141. <https://doi.org/10.3897/mycokeys.101.109751>
- Wei DP, Wanasinghe DN, Hyde KD, Mortimer PE, Xu J, Xiao YP, Bhunjun CS, To-anun C (2019) The genus *Simplicillium*. MycoKeys 60: 69–92. <https://doi.org/10.3897/mycokeys.60.38040>
- Wei DP, Wanasinghe DN, Xu JC, To-Anun C, Mortimer PE, Hyde KD, Elgorban AM, Madawala S, Suwannarach N, Karunarathna SC, Tibpromma S, Lumyong S (2021) Three Novel Entomopathogenic Fungi From China and Thailand. Frontiers in Microbiology 11: e608991. <https://doi.org/10.3389/fmicb.2020.608991>
- Wei DP, Gentekaki E, Wanasinghe DN, Tang SM, Hyde KD (2022) Diversity, molecular dating and ancestral characters state reconstruction of entomopathogenic fungi in Hypocreales. Mycosphere 13(2): 281–351. <https://doi.org/10.5943/mycosphere/si/1f/8>
- White TJ, Bruns T, Lee S, Taylor J (1990) Amplification and direct sequencing of fungal ribosomal RNA genes for phylogenetics. PCR protocols: a guide to methods and applications 18: 315–322. <https://doi.org/10.1016/B978-0-12-372180-8.50042-1>
- Yeh YW, Huang YM, Hsieh CM, Kirschner R (2021) *Pleurodesmospora acaricola* sp. nov. and a new record of *Pleurodesmospora coccorum* (Cordycipitaceae, Ascomycota) in Taiwan. Taiwania 66(4): 517–525. <https://doi.org/10.6165/tai.2021.66.517>
- Zare R, Gams W (2016) More white *verticillium*-like anamorphs with erect conidiophores. Mycological Progress 15(10): 993–1030. <https://doi.org/10.1007/s11557-016-1214-8>
- Zhang ZF, Liu F, Zhou X, Liu XZ, Liu SJ, Cai L (2017) Culturable mycobiota from Karst caves in China, with descriptions of 20 new species. Persoonia 39(1): 1–31. <https://doi.org/10.3767/persoonia.2017.39.01>
- Zhang ZF, Zhou SY, Eurwilaichitr L, Ingsriswang S, Raza M, Chen Q, Zhao P, Liu F, Cai L (2021) Culturable mycobiota from Karst caves in China II, with descriptions of 33 new species. Fungal Diversity 106: 29–136. <https://doi.org/10.1007/s13225-020-00453-7>

Zhang X, Fu Z, Lu F, Song J, Zhao C (2024) Morphological characteristics and phylogenetic analyses revealed a new invertebrate-pathogenic fungus *Akanthomyces bannaensis* (Cordycipitaceae, Ascomycota), in China. *Phytotaxa* 666(1): 17–30. <https://doi.org/10.11646/phytotaxa.666.1.2>

## Supplementary material 1

### Alignment of Cordycipitaceae tree-six locus

Authors: Jing Bu

Data type: fas

Explanation note: The alignment of Cordycipitaceae tree that based on six locus (nrLSU, ITS, nrSSU, tef-1 $\alpha$ , rpb1 and rpb2).

Copyright notice: This dataset is made available under the Open Database License (<http://opendatacommons.org/licenses/odbl/1.0/>). The Open Database License (ODbL) is a license agreement intended to allow users to freely share, modify, and use this Dataset while maintaining this same freedom for others, provided that the original source and author(s) are credited.

Link: <https://doi.org/10.3897/mycokeys.116.147006.suppl1>

## Supplementary material 2

### Alignment of Samsoniella tree-five locus

Authors: Jing Bu

Data type: fas

Explanation note: The alignment of Samsoniella tree based on five locus (nrLSU, nrSSU, tef-1 $\alpha$ , rpb1 and rpb2).

Copyright notice: This dataset is made available under the Open Database License (<http://opendatacommons.org/licenses/odbl/1.0/>). The Open Database License (ODbL) is a license agreement intended to allow users to freely share, modify, and use this Dataset while maintaining this same freedom for others, provided that the original source and author(s) are credited.

Link: <https://doi.org/10.3897/mycokeys.116.147006.suppl2>

## Supplementary material 3

### Legend for supplementary figures of single gene tree


Authors: Jing Bu

Data type: docx

Copyright notice: This dataset is made available under the Open Database License (<http://opendatacommons.org/licenses/odbl/1.0/>). The Open Database License (ODbL) is a license agreement intended to allow users to freely share, modify, and use this Dataset while maintaining this same freedom for others, provided that the original source and author(s) are credited.

Link: <https://doi.org/10.3897/mycokeys.116.147006.suppl3>

# Four new species of *Beltraniella* (Amphisphaeriales, Beltraniaceae) revealed by morphology and phylogenetic analyses from China

Wen-Wen Liu<sup>1</sup>, Chang-Zhun Yin<sup>1</sup>, Zhao-Xue Zhang<sup>2</sup>, Xing-Sheng Wang<sup>1</sup>, Zhe Meng<sup>1</sup>, Xiu-Guo Zhang<sup>1,2</sup>, Shi Wang<sup>1</sup>

<sup>1</sup> College of Life Sciences, Shandong Normal University, Jinan, 250358, China

<sup>2</sup> Shandong Provincial Key Laboratory for Biology of Vegetable Diseases and Insect Pests, College of Plant Protection, Shandong Agricultural University, Taian, 271018, China

Corresponding author: Shi Wang (wangssdau@126.com)

## Abstract

*Beltraniella* is a widely-distributed genus on Earth, although its abundance is relatively limited in relation to other dematiaceous hyphomycetes. In the present study, diseased leaves of *Myristica fragrans* and decaying leaves were collected from Hainan and Sichuan Province. Fungal DNA was amplified and sequenced using two barcodes, the internal transcribed spacer (ITS) and large subunit of ribosomal RNA (LSU), and phylogenetic analyses were conducted through maximum likelihood (ML) and Bayesian inference (BI) algorithms. Four new species of *Beltraniella*, *B. dujiangyanensis*, *B. jianfengensis*, *B. myristicae*, and *B. xinglongensis* are identified through phylogenetic analyses and morphological comparison during a survey of fungal diversity in Hainan and Sichuan Provinces, China. Detailed descriptions of the morphological characteristics of these four new species are provided and illustrated with figures.

**Key words:** Dematiaceous hyphomycetes, novel taxa, phylogeny, Sordariomycetes, taxonomy



Academic editor: Xinlei Fan

Received: 29 October 2024

Accepted: 20 March 2025

Published: 9 April 2025

**Citation:** Liu W-W, Yin C-Z, Zhang Z-X, Wang X-S, Meng Z, Zhang X-G, Wang S (2025) Four new species of *Beltraniella* (Amphisphaeriales, Beltraniaceae) revealed by morphology and phylogenetic analyses from China. MycoKeys 116: 125–144. <https://doi.org/10.3897/mycokeys.116.140506>

Copyright: © Wen-Wen Liu et al.

This is an open access article distributed under terms of the Creative Commons Attribution License (Attribution 4.0 International – CC BY 4.0).

## Introduction

*Beltraniella* was proposed by Subramanian in 1952, and he selected *B. odinae* as the type species (Subramanian 1952). Currently, a total of 33 epithet records of *Beltraniella* have been documented in the Index Fungorum (<http://www.indexfungorum.org/>, accessed on 14 February 2025). *Beltraniella* belongs to the Sordariomycetes, Amphisphaeriales, Beltraniaceae (Hyde et al. 2024). *Beltraniella* was characterized by sterile setae, which were extensions of conidiophores, or were present among conidiophores and arising from radially lobed basal cells. Conidiophores were branched, often with setae-shaped apices, and they originated from radially lobulated basal cells. Conidiogenous cells were polyblastic and sympodial; Conidia were turbinate or biconical. The distinction between setae and conidiophores lies in their apex; setae gradually narrow to a sharp point, whereas conidiophores may sometimes be reduced to conidiogenous cells (Hyde et al. 2020b). Furthermore, *Beltraniella* is a genus of dematiaceous hyphomycetes that play a crucial ecological role in natural ecosystems



by breaking down lignin and cellulose, recycling matter and energy, and maintaining ecosystem balance.

*Beltraniella* typically inhabits decaying leaves and other natural substrates on the ground, maintaining the balance of natural ecosystems, and aiding in the decomposition of diseased or decaying leaves (Dighton et al. 1985). Shirouzu et al. (2010) isolated and identified *B. botryospora* Shirouzu & Tokum, a fungus frequently reported on both live and deciduous leaves of *Quercus aspera*, suggesting a close relationship with this species. Hyde et al. (2020a) reported a new species, *B. ramosiphora* C.G. Lin & K.D. Hyde, found in decomposing organic matter on decaying leaves, while Tan and Roger (2022) reported *B. hesseae* Y.P. Tan, Bishop-Hurley & R.G on the leaves of *Digitaria ciliaris*. The principal methodology employed in studying this fungus encompasses a synthesis of traditional morphological taxonomy and molecular systematics. Crous et al. (2014) isolated and characterized *B. endiandrae* Crous & Summerell, reporting that its conidia were solitary, light brown, and smooth, with hyaline transverse bands. They also demonstrated the colony color variation of *B. endiandrae* on three distinct media. The frontal and reverse sides appeared iron-gray on PDA medium; the light olive-gray patches appeared on OA medium, while the frontal side was light olive-gray and the reverse side was yellowish-brown on MEA medium. Tibpromma et al. (2018) reported two new species, *B. pandanicola* Tibpromma & K.D. Hyde and *B. thailandica* Tibpromma & K.D. Hyde [as '*thailandicus*'], and described their morphological characteristics in detail. In addition, they provided a detailed description of *Pandanus* growing on withered leaves, whereas Crous et al. (2016) employed the ITS sequence to conduct a phylogenetic analysis of *Beltraniella*. Recently, Liu et al. (2024) identified a new species named *B. jiangxiensis* P. Razaghi, Raza & L. Cai, through phylogenetic analysis based on ITS and LSU sequences, combined with morphological analysis. This method is currently widely accepted as the identification method for *Beltraniella*.

The primary objective of this study is to identify putative new strains of *Beltraniella* through morphological comparison and phylogenetic analysis. Four new species of *Beltraniella* were identified and thoroughly characterized, with their differences from closely related species compared and discussed, thereby enriching the species diversity of the genus.

## Materials and methods

### Sample collection and treatment

Samples of diseased or decaying leaves were collected in Hainan and Sichuan provinces from June 2023 to March 2024. Upon collection, they were numbered by time, location and plant type, and then photographed and recorded. Flatter leaves were chosen for photography. The processed samples were returned to the kraft bag for the next step. For each sample, 4–7 diseased or decaying leaves were cut into squares (5 × 5 mm) and placed in sterile containers. These were then sterilized on a clean bench. Pour in 75% alcohol, soak the leaves thoroughly for 1 minute to sterilize their surfaces. Use a disposable syringe to remove the alcohol, rinse with sterile water, then remove the sterile water and add 5% sodium hypochlorite to sterilize the leaf surface again for

30 seconds. Rinse the leaves three times with sterile water, then place them on sterilized filter paper to dry using sterilized tweezers. Once dry, clip the leaves with the diseased spot pointing downward and place 3–5 samples of them on each PDA medium (PDA: 14 g agar, 20 g dextrose, 200 g potato, 1000 mL distilled water, pH 7.0). The medium with leaves was securely wrapped with sealing film and placed in a constant temperature incubator at 25 °C for incubation. The growth of the fungus was observed every day, and after 2–3 days of incubation, the agar with fungal growth was transferred from the PDA medium to a new PDA medium for purification.

### **Morphological and cultural characterization**

The single colonies that were isolated and purified were photographed on the 7<sup>th</sup> and 14<sup>th</sup> day of growth, using a digital camera (Canon Powershot G7X; Beijing, China), on both the surface and reverse of the PDA medium. A stereo microscope (Olympus SZX10; Beijing, China) was used to observe whether conidia were produced. If conidia were observed, a temporary mount was prepared to examine the morphology of the fungal conidia under a microscope (Olympus BX53). Subsequently, fungal structures, including conidia and conidiogenous cells, were photographed using a high-definition digital camera (Olympus DP80). All strains were stored in a 4 °C thermostat using sterilized 10% glycerol test tubes. Voucher specimens have been carefully preserved in two herbariums: the Herbarium of the Department of Plant Pathology at Shandong Agricultural University in Taian, China (HSAUP), and the Herbarium Mycologicum Academiae Sinicae at the Institute of Microbiology, Chinese Academy of Sciences in Beijing, China (HMAS). Additionally, living cultures derived from the holotype have been safeguarded in the Shandong Agricultural University Culture Collection (SAUCC). The morphological description and taxonomic characters of the new species have been uploaded to MycoBank (<http://www.mycobank.org>).

### **DNA extraction, PCR amplification, and sequencing**

The method of extracting fungal DNA involves using CTAB (cetyl trimethyl ammonium bromide) (Wang et al. 2023). When the mycelium has grown to a certain degree in the PDA medium, use a sterilized scalpel to scrape approximately 0.2 g of mycelium into a 1.5 mL centrifugal tube, add precipitating CTAB lysate to the tube, pulverize the mycelium using a grinder, and then place the tube in a water bath at 65 °C for 2 hours. After pulverization, centrifuge the sample to extract the supernatant, add chloroform (and other precipitate agents) to the supernatant to isolate the genomic DNA. Further centrifuge the supernatant, and then add chloroform: isoamyl alcohol (24:1) to precipitate the DNA (Doyle and Doyle 1990; Guo et al. 2000). PCR (Polymerase Chain Reaction) amplification of the extracted fungal DNA is performed using ITS and LSU (White et al. 1990; Glass and Donaldson 1995). Each sterilized PCR tube contains a total of 25 µL reaction mixture, which includes 9.5 µL of ddH<sub>2</sub>O, 12.5 µL of 2 × Taq Plus Master Mix (Shanghai, China) (with dye) (Yeasn Biotechnology, Shanghai, China, Cat No. 10154ES03), 1 µL of forward primer, and 1 µL of reverse primer. The products of PCR amplification were

detected by electrophoresis in a 2% agarose gel. After electrophoresis, the gel was removed and observed under UV light, where the presence of DNA was indicated by fluorescent bands (Zhang et al. 2022). PCR primer synthesis and DNA sequencing were completed by Tsingke Biotechnology Co., Ltd. (Qingdao, China). Once sequencing was completed, MAGE7 (Kumar et al. 2016) was utilized for sequence comparison and splicing of the sequencing results. The gene sequences of the four new species were uploaded to the GenBank. Subsequently, the most recent article was downloaded by searching for '*Beltraniella*' on Index Fungorum (<https://indexfungorum.org/Names/Names.asp>, accessed on 14 February 2025). The GenBank table mentioned in the article was found, and the results were presented in Table 1.

### Phylogenetic analyses

Nucleic acid sequences of *Beltraniella* were downloaded from the National Center for Biotechnology Information (<https://www.ncbi.nlm.nih.gov/>, accessed on 14 February 2025), and GenBank accession numbers were obtained from the latest version of the article (Zhang et al. 2000). Nucleic acid sequences of the four new species were aligned with reference sequences from the literature using MAFFT 7 (<http://mafft.cbrc.jp/alignment/server/>, accessed on 14 February 2025) (Kato et al. 2019). Data from the completed sequence alignments were systematically analyzed using the maximum likelihood (ML) and Bayesian inference (BI) methods. BI and ML analyses were conducted separately through registering on the CIPRES website (Miller et al. 2012). For the ML analysis, RAxML-HPC2 v.8.2.12 was used on XSEDE with 1000 rapid bootstrap replications and the GTRGAMMA model (Stamatakis 2014). MrModeltest v.2.3 (Nylander 2004) software was utilized to screen for optimal evolutionary models, while BI was conducted using MrBayes 3.2.7a (on XSEDE) (Huelsenbeck and Ronquist 2001; Ronquist and Huelsenbeck 2003; Ronquist et al. 2012). FigTree v1.4.3 (<http://tree.bio.ed.ac.uk/software/figtree/>, accessed on 14 February 2025) was used to open the successfully obtained topology and reroot the tree with the outgroup. The final phylogenetic tree was created with Adobe Illustrator CC 2019. In the final phylogenetic tree output, the names and strain numbers of the new species are marked in red.

## Results

### Phylogenetic analyses

Interspecific relationships of the genus *Beltraniella* were identified by phylogenetic analyses. These analyses were based on downloaded sequences and newly acquired sequences of new species, using *Beltrania pseudorhombica* Crous & Y. Zhang CBS 138003 and *B. querna* Harkn CBS 126097 as outgroups. The concatenated sequence matrix comprised 27 sequences with a total of 1295 characters (the combined dataset: ITS: 1–502, LSU: 503–1295). There were 1192 constant characters, 33 variable but parsimony non-informative, and 70 parsimony informative characters. The topologies of the evolutionary trees obtained using the maximum likelihood (ML) and

**Table 1.** GenBank numbers used in the phylogenetic analysis of *Beltraniella*.

Species	Strains	Country	GenBank accession numbers	
			ITS	LSU
<i>Beltrania querna</i>	CBS 126097	Spain	MH864016	MH875474
<i>Beltrania pseudorhombica</i>	CBS 138003*	China	MH554124	NG_058667
<i>Beltraniella acaciae</i>	CPC 29498*	USA	NR_147685	KY173483
<i>Beltraniella botryospora</i>	TMQa1A18	Japan	N/A	AB496426
<i>Beltraniella brevis</i>	DS 2-23	China	MN252876	MN252883
<i>Beltraniella carolinensis</i>	9502 (IFO)	N/A	N/A	DQ810233
<b><i>Beltraniella dujiangyanensis</i></b>	<b>SAUCC427003*</b>	<b>China</b>	<b>PP301351</b>	<b>PP301362</b>
<b><i>Beltraniella dujiangyanensis</i></b>	<b>SAUCC427004</b>	<b>China</b>	<b>PP301352</b>	<b>PP301363</b>
<i>Beltraniella endiandrae</i>	CBS 137976*	Australia	NR_148073	KJ869185
<i>Beltraniella endiandrae</i>	CBS 137976	Australia	KJ869128	MH878615
<i>Beltraniella fertilis</i>	MFLUCC 20-0119	Thailand	MT835158	MT835156
<i>Beltraniella fertilis</i>	MRC 3BEL	Thailand	MF580247	MF580254
<i>Beltraniella hesseae</i>	BRIP 72433a*	Australia	OP023124	OP023141
<i>Beltraniella humicola</i>	CBS 203.64	India	MH858416	MH870044
<b><i>Beltraniella jianfengensis</i></b>	<b>SAUCC639001*</b>	<b>China</b>	<b>PP301353</b>	<b>PP301364</b>
<b><i>Beltraniella jianfengensis</i></b>	<b>SAUCC639002</b>	<b>China</b>	<b>PP301354</b>	<b>PP301365</b>
<i>Beltraniella jiangxiensis</i>	CGMCC 3.23486*	N/A	OP022178	OP022174
<b><i>Beltraniella myristicae</i></b>	<b>SAUCC638601*</b>	<b>China</b>	<b>PP301355</b>	<b>PP301366</b>
<b><i>Beltraniella myristicae</i></b>	<b>SAUCC638602</b>	<b>China</b>	<b>PP301356</b>	<b>PP301367</b>
<i>Beltraniella pandanicola</i>	MFLUCC 18-0121*	Thailand	MH275049	MH260281
<i>Beltraniella podocarp</i>	CPC 36783*	South Africa	MT373370	NG_074446
<i>Beltraniella portoricensis</i>	CBS 856.70	N/A	MH859981	MH871777
<i>Beltraniella pseudoportoricensis</i>	CBS 145547*	South Africa	NR_165552	NG_067875
<i>Beltraniella ramosiphora</i>	MFLU 17-2649*	Thailand	NR_171732	NG_073615
<i>Beltraniella thailandica</i>	MFLUCC 16-0377*	Thailand	NR_168175	NG_068824
<i>Beltraniella xinglongensis</i>	SAUCC737701*	China	PQ325612	PQ325618
<i>Beltraniella xinglongensis</i>	SAUCC737702	China	PQ325613	PQ325619

Notes: New species established in this study are shown in bold. Those marked “\*” in the table are represented as ex-type or ex-epitype strains. N/A: Not available.

Bayesian inference (BI) algorithms are essentially similar. Fig. 1 shows the best-scoring maximum likelihood (ML) evolutionary tree, where maximum likelihood bootstrap analyses and Bayesian posterior probabilities (MLBS/BPP) are labeled at node positions. Eight new strains of *Beltraniella* were incorporated into the phylogenetic analysis presented in the ML tree. The eight new strains introduced in this study were divided into four monophyletic branches in the phylogenetic tree, representing four new species of *Beltraniella*, *B. dujiangyanensis*, *B. jianfengensis*, *B. myristicae*, and *B. xinglongensis*. The strains of *Beltraniella dujiangyanensis* form a distinct clade sister to *B. xinglongensis* with good bootstrap support (ML/BI = 90/0.99); *B. thailandica* forms a high-support clade (ML/BI = 89/1.00) alongside the lineage consisting of *B. dujiangyanensis* and *B. xinglongensis*; *B. myristicae* forms a high-support clade (ML/BI = 94/1.00) with *B. brevis*; and *B. jianfengensis* forms a high-support clade (ML/BI = 81/0.98) with the lineage consisting of *B. brevis* and *B. myristicae*.



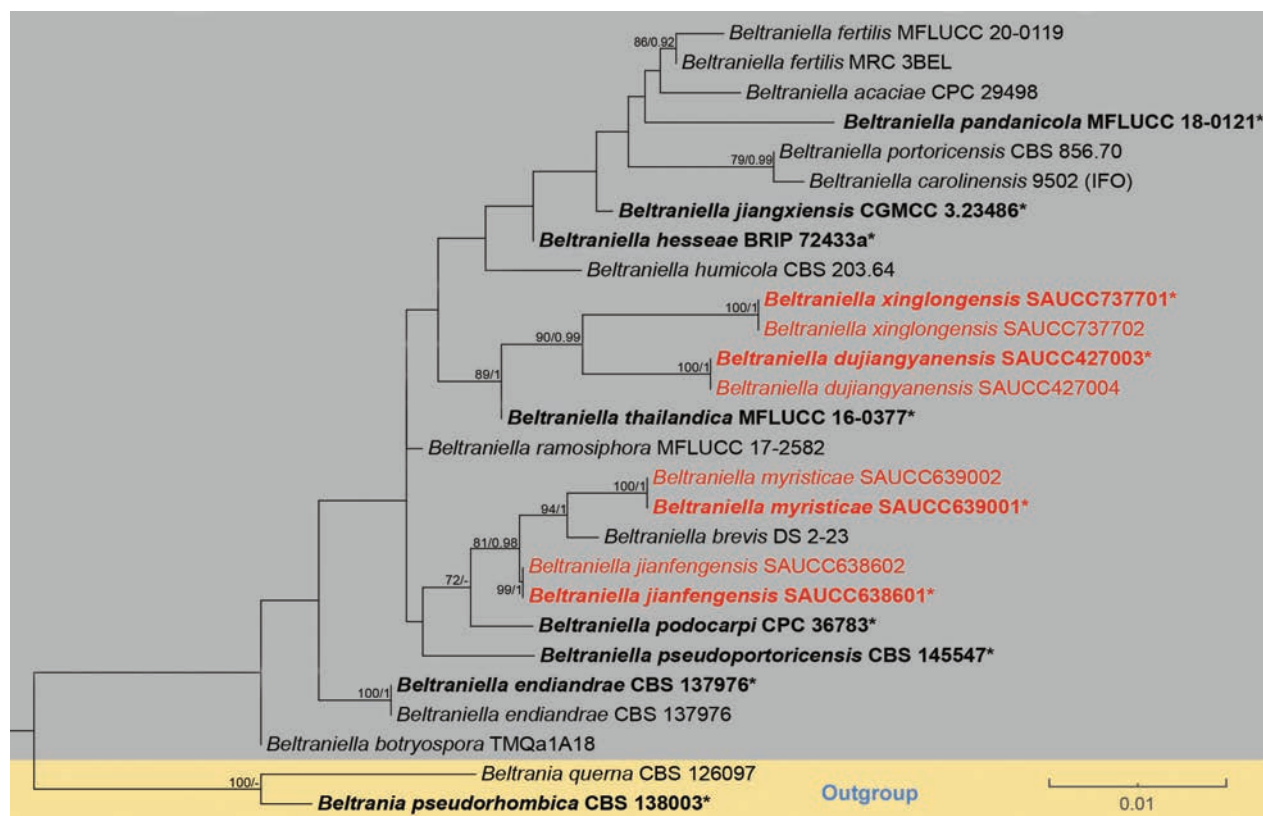


**Figure 1.** Phylogenetic tree of *Beltraniella* based on combined ITS and LSU sequences. Bootstrap support values exceeding 70% (ML) and 0.90 (BI) are indicated by MLBS/BPP, and new species are highlighted in red. Branches separated by gray and yellow indicate different species of *Beltraniella* and *Beltrania*. The lines in the lower right-hand corner represent changes of 0.01 nucleotides per site.

## Taxonomy

***Beltraniella dujiangyanensis*** W.W. Liu, C.Z. Yin, Z.X. Zhang & X.G. Zhang, sp. nov.

MycoBank No: MB853427

Fig. 2

**Holotype.** CHINA • Sichuan Province, Dujiangyan City, 30°57'53"N, 103°35'13"E, on decaying leaves, 24 June 2023, W.W. Liu, holotype HMAS 352921, ex-type living culture SAUCC427003.

**Etymology.** The epithet "*dujiangyanensis*" denotes the geographical origin of the strains, namely, Dujiangyan City.

**Description.** Parasitic on decaying leaves. Asexual morph: Setae unbranched, straight or flexuous, single, dark brown, subulate, thick-walled, tapering to a pointed apex, 9–10-septate, verrucose, dark brown, swollen, arising from a radially lobed basal cell, 83.9–150.2 × 3.0–5.4 µm. Conidiophores hyaline, presenting two distinct forms: long and short. Long conidiophores arise from lobed basal cells, macronematous, erect, straight or slightly curved, either simple or rarely branched, septate, verrucose, dark-brown, apical part lighter, arising from basal cells of setae or from separate cells, 113.1–259.9 × 3.1–5.8 µm. Short conidiophores hyaline, septate, smooth edges, simple or branched, 13.1–31.9 × 3.2–5.7 µm. Conidiogenous cells polyblastic, integrated, determinate, cylindrical, smooth, terminal, geniculate, denticulate, hyaline



**Figure 2.** *Beltraniella dujiangyanensis* (holotype: HMAS 352921) **a, b** colony front and back after 7 days culture on PDA **c** setae **d** long conidiophores **e** short conidiophores **f** separating cells and conidia. Scale bars: 10 µm (**c–f**).

to subhyaline,  $5.5\text{--}10.9 \times 2.9\text{--}4.7$  µm. Separating cells ellipsoid to subglobose, smooth, subhyaline, single, denticle at each end,  $9.7\text{--}12.3 \times 3.1\text{--}5.3$  µm. Conidia originate directly from the conidiogenous cells in the long conidiophores and from the separating cells in the short ones. Conidia arise directly from conidiogenous cells or from separating cells, simple, teardrop-shaped, sometimes verrucose, narrow-tipped, terminal, hyaline, smooth, straight, rostrate to pointed at proximal end, truncate at distal end,  $16.5\text{--}21.1 \times 4.2\text{--}8.5$  µm. Sexual morph: Inconclusive.

**Culture characteristics.** On PDA medium, after seven days of dark incubation in a 25 °C incubator, colonies reached 68 mm in diameter with a growth rate of 9.2–10.2 mm/day. Colonies on PDA medium were concentric, flatter, white, moderately dense, granular surface, sparse aerial mycelia, with mycelium in the middle portion aggregated into a circle and mycelium on the edges dispersed to form a fluffy shape; reverse, pale yellow to white, fluffy edges.

**Additional material studied.** CHINA • Sichuan Province, Dujiangyan City, 30°57'53"N, 103°35'13"E, on decaying leaves, 24 June 2023, W.W. Liu, HSAUP 427004, living culture SAUCC427004.

**Notes.** Based on the phylogenetic tree constructed using ITS and LSU sequence data, *Beltraniella dujiangyanensis* was identified as the closest relative to *B. xinglongensis* sp. nov., with 90% MLBS and 0.99 BPP support values (Fig. 1). Additionally, there is a disparity of 16/502 bp between their ITS sequences. Morphologically, *B. dujiangyanensis* differed from *B. xinglongensis* in having shorter long conidiophores (*B. dujiangyanensis*: 113.1–259.9 × 3.1–5.8 µm vs. *B. xinglongensis*: 232.5–298.6 × 2.4–4.9 µm) and fewer septa (*B. dujiangyanensis*: 9–10 septa vs. *B. xinglongensis*: 13–15 septa), shorter in short conidiophores (*B. dujiangyanensis*: 13.1–31.9 × 3.2–5.7 µm vs. *B. xinglongensis*: 21.2–47.8 × 3.2–6.4 µm), shorter separating cells (*B. dujiangyanensis*: 9.7–12.3 × 3.1–5.3 µm vs. *B. xinglongensis*: 13.6–17.6 × 2.3–5.4 µm) and shorter conidia (*B. dujiangyanensis*: 16.5–21.1 × 4.2–8.5 µm vs. *B. xinglongensis*: 21.9–28.7 × 5.0–9.5 µm). As a result, *B. dujiangyanensis* was identified as a new species of *Beltraniella* by phylogenetic analysis and morphological comparison.

***Beltraniella jianfengensis* W.W. Liu, C.Z. Yin, Z.X. Zhang & X.G. Zhang, sp. nov.**

MycoBank No: MB853429

Fig. 3

**Holotype.** CHINA • Hainan Province, Ledong County, Jianfengling National Forest Park, 18°44'25"N, 108°51'32"E, on decaying leaves, 14 October 2023, W.W. Liu, holotype HMAS 352923, ex-type living culture SAUCC639001.

**Etymology.** The epithet "*jianfengensis*" signifies the geographical location of the holotype, specifically Jianfengling National Forest Park.

**Description.** Parasitic on decaying leaves. Asexual morph: Setae subulate, emerging from lobed basal cells, upright, straight or slightly curved, simple, septate, verrucose, dark-brown, swollen, radially lobed basal cell, 84.3–254.4 × 2.9–4.9 µm. Conidiophores macronematous, mononematous, occurring in two distinct forms: long and short. Long conidiophores arise from lobed basal cells and have a setiform appearance, upright, straight to slightly curved, simple or rarely branched, septate, verrucose, dark brown, swollen at the base, with a lighter apical region, arising from basal cells of setae or from separate ones, without a hyaline transverse band, 171.8–254.9 × 2.6–4.9 µm. Short conidiophores solitary or grouped, smoother, pale brown, smaller, 20.1–57.2 × 3.3–6.5 µm. Conidiogenous cells cylindrical, polyblastic, integrating sympodially, denticulate surface, 9.2–15.3 × 2.2–5.0 µm. Separating cells ellipsoid to subglobose, smooth, subhyaline, denticle at each end, 10.7–14.7 × 2.8–5.5 µm. Conidia originate directly from the conidiogenous cells on long conidiophores and from





**Figure 3.** *Beltraniella jianfengensis* (holotype: HMAS 352923) **a, b** colony front and back after 7 days culture on PDA **c** setae **d** long conidiophores and short conidiophores **e** conidia **f** separating cells and conidia. Scale bars: 10 µm (**c–f**).

the separating cells on short conidiophores, turbinated, obovate to obpyriform, subhyaline, simple, smooth, straight, terminal,  $17.1\text{--}23.6 \times 3.6\text{--}9.5$  µm. Sexual morph: Inconclusive.

**Culture characteristics.** On PDA medium, after seven days of dark incubation in a 25 °C incubator, colonies reached 90 mm in diameter with a growth rate of 12.5–13.1 mm/day. Colonies on PDA, cottony, moderately dense, sparse aerial mycelia, steel-blue gray, granular surface, with gray exudates, flatter, smooth edge; reverse steel-blue gray, smooth edge.



**Additional material studied.** CHINA • Hainan Province, Ledong County, Jianfengling National Forest Park, 18°44'25"N, 108°51'32"E, on decaying leaves, 14 October 2023, W.W. Liu, HSAUP 639002, living culture SAUCC639002.

**Notes.** Based on the phylogenetic tree of ITS and LSU sequences, *Beltraniella jianfengensis* emerged as a cluster with *B. brevis* and *B. myristicae*. However, a significant discrepancy was noted in the ITS sequence, with a disparity of 6/502 bp between *B. jianfengensis* and *B. brevis*; and a disparity of 4/496 bp between *B. jianfengensis* and *B. myristicae*. Furthermore, a substantial difference was observed in their LSU sequences. Morphologically, *B. jianfengensis* was different from *B. brevis* by having narrower setae (*B. jianfengensis*:  $84.3\text{--}254.4 \times 2.9\text{--}4.9$  vs. *B. brevis*:  $89\text{--}251 \times 4.5\text{--}10.5$   $\mu\text{m}$ ), and shorter conidia (*B. jianfengensis*:  $17.1\text{--}23.6 \times 3.6\text{--}9.5$  vs. *B. brevis*:  $20\text{--}26.5 \times 4.5\text{--}7.2$   $\mu\text{m}$ ) (Hyde et al. 2020b), and there were also differences in conidial shape: *B. brevis* exhibited diamond-shaped conidia with a hyaline supraequatorial transverse band, whereas *B. myristicae* had teardrop-shaped conidia lacking a hyaline transverse band. Additionally, *B. jianfengensis* was different from *B. myristicae* by having longer and wider separating cells (*B. jianfengensis*:  $9.2\text{--}15.3 \times 2.8\text{--}5.5$  vs. *B. myristicae*:  $8.7\text{--}12.5 \times 2.5\text{--}5.4$ ), and there were also differences in separating cells' shape: *B. jianfengensis* features two distinct transverse projections on its surface, whereas *B. myristicae* boasts a smoother exterior devoid of such projections. Consequently, *B. jianfengensis* was classified as a new species within the genus *Beltraniella*, through a combination of phylogenetic analysis and morphological comparisons.

***Beltraniella myristicae* W.W. Liu, C.Z. Yin, Z.X. Zhang & X.G. Zhang, sp. nov.**

MycoBank No: MB853428

Fig. 4

**Holotype.** CHINA • Hainan Province, Ledong County, Jianfengling National Forest Park, 18°44'25"N, 108°51'32"E, on diseased leaves of *Myristica fragrans* (Myristicaceae), 14 October 2023, W.W. Liu, holotype HMAS 352922, ex-type living culture SAUCC638601.

**Etymology.** The epithet "*myristicae*" is derived from the name of the host plant, *Myristica fragrans*.

**Description.** Associated with diseased leaves of *Myristica fragrans*, the surface of the leaf blade shows black irregular protrusions, marked with black circles and arrows in Fig. 4. Asexual morph: Setae dark-brown, simple, subulate, verrucose,  $80.5\text{--}99.8 \times 2.7\text{--}5.5$   $\mu\text{m}$ . Conidiophores present two distinct forms: long and short. Long conidiophores emerge from lobed basal cells, macronematous, setiform, upright, straight or gently curved, simple, septate, verrucose, subhyaline to pale olivaceous, swollen at the base, arising from basal cells of setae or from separate,  $74.4\text{--}150.5 \times 2.9\text{--}5.3$   $\mu\text{m}$ . Short conidiophores hyaline, septate, smooth edges, simple or branched,  $18.3\text{--}45.0 \times 2.7\text{--}5.8$   $\mu\text{m}$ . Conidiogenous cell polyblastic, ovoid, hyaline,  $5.5\text{--}12.5 \times 2.0\text{--}4.9$   $\mu\text{m}$ . Separating cells ellipsoid to subglobose, smooth,  $7.0\text{--}12.8 \times 2.5\text{--}5.4$   $\mu\text{m}$ . Conidia originate directly from the conidiogenous cells in the long conidiophores and from the separating cells in the short ones, aggregated, dry, straight, teardrop-shaped, truncate at distal end, narrow-tipped, terminal, hyaline, smooth, diaphragm, without a hyaline transverse band,  $13.6\text{--}22.2 \times 3.9\text{--}9.8$   $\mu\text{m}$ . Sexual morph: Inconclusive.



**Figure 4.** *Beltraniella myristicae* (holotype: HMAS 352922) **a** leaf of host plant *Myristica fragrans*, black circle and arrow indicate the location of fungal infestation **b, c** colony front and back after 7 days culture on PDA **d** setae **e** long conidiophores **f** short conidiophores **g** separating cells and conidia **h** conidia. Scale bars: 10 µm (**d–h**).

**Culture characteristics.** On PDA medium, after seven days of dark incubation in a 25 °C incubator, colonies reached 68 mm in diameter with a growth rate of 9.2–10.2 mm/day. Colonies on PDA raised, concentric, white, flatter, velutinous edge, with mycelium in the middle portion aggregated into a circle; reverse pale yellow, velutinous edge.

**Additional material studied.** CHINA • Hainan Province, Ledong County, Jianfengling National Forest Park, 18°44'25"N, 108°51'32"E, on diseased leaves of

*Myristica fragrans*, 14 October 2023, W.W. Liu, HSAUP 638602, living culture SAUCC638602.

**Notes.** Based on the phylogenetic tree constructed using ITS and LSU sequences, *Beltraniella myristicae* emerged as the closest to *B. brevis* DS 2-23 with 94% MLBS and 1.00 BPP support values (Fig. 1). However, a significant discrepancy was observed in the ITS sequence, with a disparity of 7/548 bp between *B. myristicae* and *B. brevis*. Morphologically, *B. myristicae* differed from *B. brevis* by having shorter setae (*B. myristicae*:  $80.5\text{--}99.8 \times 2.7\text{--}5.5$  vs. *B. brevis*:  $89\text{--}251 \times 4.5\text{--}10.5$   $\mu\text{m}$ ), shorter separating cells (*B. myristicae*:  $7.0\text{--}12.8 \times 2.5\text{--}5.4$  vs. *B. brevis*:  $11\text{--}18 \times 3.4\text{--}4.1$   $\mu\text{m}$ ), and shorter conidia (*B. myristicae*:  $13.6\text{--}22.2 \times 3.9\text{--}9.8$  vs. *B. brevis*:  $20\text{--}26.5 \times 4.5\text{--}7.2$   $\mu\text{m}$ ); differences in conidia (*B. brevis*: diamond-shaped, with a hyaline supraequatorial transverse band; *B. myristicae*: teardrop-shaped, without a hyaline transverse band). Consequently, *B. myristicae* was classified as a new species within the genus *Beltraniella*, based on a combination of phylogenetic analysis and morphological comparisons

***Beltraniella xinglongensis* W.W. Liu, C.Z. Yin, Z.X. Zhang & X.G. Zhang, sp. nov.**

MycoBank No: MB856046

Fig. 5

**Holotype.** CHINA • Hainan Province, Wanning City, Xinglong tropical botanical garden,  $18^{\circ}43'59''\text{N}$ ,  $110^{\circ}11'55''\text{E}$ , on decaying leaves, 24 April 2024, W.W. Liu, holotype HMAS 353196, ex-type living culture SAUCC737701.

**Etymology.** The epithet “*xinglongensis*” refers to the name of the location, Xinglong tropical botanical garden where the holotype was collected.

**Description.** Parasitic on decaying leaves. Asexual morph: Setae dark-brown, unbranched, tapering to a pointed apex, upright, single or in small groups, septate, straight or gently flexuous, emerging from radially lobed basal cells,  $75.9\text{--}195.9 \times 2.5\text{--}6.1$   $\mu\text{m}$ . Conidiophores septate, occasionally reduced to conidiogenous cells, smooth, swollen at the base, subhyaline to pale brown, present two distinct forms: long and short. Long conidiophores emerging from lobed basal cells, upright, straight or gently curved, simple or branched at apical regions,  $13\text{--}15$  septate, verrucose, swollen at the base, olivaceous to dark-brown, arising from basal cells of setae or from separate,  $232.5\text{--}298.6 \times 2.4\text{--}4.9$   $\mu\text{m}$ . Short conidiophores hyaline, septate, smooth,  $21.2\text{--}47.8 \times 3.2\text{--}6.4$   $\mu\text{m}$ . Conidiogenous cells ovoid, polyblastic, cylindrical, hyaline to subhyaline, integrated, denticulate, terminal, smooth,  $6.5\text{--}9.7 \times 2.8\text{--}5.4$   $\mu\text{m}$ . Separating cells fusiform, ellipsoid to subglobose, smooth,  $13.6\text{--}17.6 \times 2.3\text{--}5.4$   $\mu\text{m}$ . Conidia originate directly from the conidiogenous cells in the long conidiophores and from the separating cells in the short ones, teardrop-shaped, narrow-tipped, aggregated, terminal, simple, dry, straight, hyaline, smooth and integrated, without a hyaline transverse band,  $21.9\text{--}28.7 \times 5.0\text{--}9.5$   $\mu\text{m}$ . Sexual morph: Inconclusive.

**Culture characteristics.** On PDA medium, after seven days of dark incubation in a  $25^{\circ}\text{C}$  incubator, colonies reached a diameter of 90 mm with a growth rate of  $12.5\text{--}13.1$  mm/day. Colonies on PDA raised, cottony, white, flatter, with gray exudates, sparse aerial mycelia, undulate margin; reverse white, with an undulate margin, abundant gray exudates.



**Figure 5.** *Beltraniella xinglongensis* (holotype: HMAS 353196) **a, b** colony front and back after 7 days culture on PDA **c** setae **d–f** long conidiophores **g** short conidiophores **h** separating cells and conidia **i** conidia. Scale bars: 10  $\mu\text{m}$  (**d–i**).

**Additional material studied.** CHINA • Hainan Province, Wanning City, Xinglong tropical botanical garden, 18°43'59"N, 110°11'55"E, on decaying leaves, 24 April 2024, W.W. Liu, HSAUP 737701, living culture SAUCC737701.

**Notes.** Based on the phylogenetic tree constructed with ITS and LSU sequence, *Beltraniella dujiangyanensis* was the closest relative to *B. xinglongensis*, with a gap of 16/502 bp between their comparative ITS sequences. Morphologically, *B. xinglongensis* differed from *B. dujiangyanensis* in having longer long conidiophores (*B. xinglongensis*: 232.5–298.6  $\times$  2.4–4.9  $\mu\text{m}$  vs.



*B. dujiangyanensis*: 113.1–259.9 × 3.1–5.8 µm) and more septa (*B. xinglongensis*: 13–15 septa vs. *B. dujiangyanensis*: 9–10 septa), longer in short conidiophores (*B. xinglongensis*: 21.2–47.8 × 3.2–6.4 µm vs. *B. dujiangyanensis*: 13.1–31.9 × 3.2–5.7 µm), longer separating cells (*B. xinglongensis*: 13.6–17.6 × 2.3–5.4 µm vs. *B. dujiangyanensis*: 9.7–12.3 × 3.1–5.3 µm) and longer conidia (*B. xinglongensis*: 21.9–28.7 × 5.0–9.5 µm vs. *B. dujiangyanensis*: 16.5–21.1 µm). Consequently, *B. xinglongensis* was identified as a new *Beltraniella* species through phylogenetic analysis and morphological comparison

## Discussion

With the increasing number of reported species within this genus, the classification of *Beltraniella* has encountered significant challenges. The observed striking similarity in spore structures, characterized by turbinate or biconic shapes, often with caudate appendages, as documented in early studies, accounts for this phenomenon (Hudson and Ellis 1972). Consequently, elucidating interspecific relationships within the genus using traditional morphological identification methods has been exceedingly challenging. We employed ITS and LSU to procure fungal DNA sequences, followed by the evaluation of phylogenetic relationships using maximum likelihood (ML) and Bayesian inference (BI) methods. To achieve a comprehensive and accurate classification, we complemented our analysis with morphological assessments (Miller et al. 2010; Stamatakis 2006; Stamatakis et al. 2008). In this investigation, four new species of fungi were identified and reported, namely *Beltraniella dujiangyanensis*, *B. jianfengensis*, *B. myristicae*, and *B. xinglongensis*. Based on DNA sequence analysis, these four new species were initially identified as *Beltraniella*. Subsequent phylogenetic analyses with other *Beltraniella* species confirmed their phylogenetic placement with high confidence (Ronquist and Huelsenbeck 2003; Crous et al. 2017; Liu et al. 2019). Subsequently, morphological assessments were conducted to discern the similarities and distinctions among *B. dujiangyanensis*, *B. jianfengensis*, *B. myristicae*, *B. xinglongensis*, and additional *Beltraniella* species within the same clade. The four species, *B. dujiangyanensis*, *B. jianfengensis*, *B. myristicae*, and *B. xinglongensis* were validated as new species within the genus *Beltraniella* based on conventional morphological analysis and molecular phylogenetic analysis. The *Beltraniella* taxon is minute, and a previous study employed phylogenetic analysis integrating ITS and LSU sequences with morphological analysis. The understanding of interspecific relationships has been enriched by the addition of supplementary morphological descriptions. Index Fungorum (<https://indexfungorum.org/Names/Names.asp>, accessed on 14 February 2025) listed 33 species, of which 25 were recorded in the National Center for Biotechnology Information (NCBI) (<https://www.ncbi.nlm.nih.gov/>, accessed on 14 February 2025). To ensure data reliability, all pertinent sequences of these 25 species were incorporated.

*Beltraniella* demonstrates a global distribution, supported by the GlobalFungi database (<https://globalfungi.com/>, accessed on 14 February 2025) comprising 1098 samples and 1626 sequences. Specifically, *Beltraniella* was detected in Asia (57.92%), South America (19.31%), North America (9.11%), Africa (7.1%), Australia (4.28%), Europe (1.73%), Pacific Ocean (0.27%), Antarctica (0.18%), and Indian Ocean (0.09%). The samples used in this study originated from

Sichuan and Hainan Provinces, which are characterized by the Central Sub-tropical Monsoon Humid Climate and the Tropical Rainforest Climate, respectively. These regions are characterized by abundant precipitation, a humid climate, diverse vegetation, and a rich assortment of fungi, including *Beltraniella*. In addition, *Beltraniella* is recognized as an invasive fungus affecting a broad spectrum of plants and has been observed parasitizing diverse plant leaves. For instance, two *Beltraniella* species, *B. botryospora* and *B. portoricensis*, were detected on the deciduous leaves of representative plants from the Atlantic Forest (*Inga thibaudiana*, *Myrcia splendens*, and *Pera glabrata*) (dos Santos et al. 2014). Furthermore, the presence of *B. endiandrae* was verified on the fallen leaves of a Lauraceae plant in Nightcap National Park, New South Wales, Australia. (Crous et al. 2014). Our analysis of *Beltraniella*'s sequence and morphological characteristics revealed its parasitism on diseased leaves of *Myristica fragrans* and decaying leaves. Specifically, *B. dujiangyanensis*, *B. jianfengensis* and *B. xinglongensis* were identified as parasites on decaying leaves, whereas *B. myristicae* was observed to parasitize diseased leaves of *Myristica fragrans*. These findings indicate the potential existence of additional host species of *Beltraniella* among these two hosts (Hyde et al. 2007). Therefore, we expect to discover additional species of *Beltraniella* fungi through the collection of diseased leaves of *Myristica fragrans* and decaying leaves in Hainan and Sichuan Provinces. Ultimately, this research enhances our understanding of fungal diversity in Hainan and Sichuan provinces and expands the known species range of *Beltraniella* fungi.

## Conclusions

In this study, a wide range of new fungal species were isolated from a large collection of diseased and decaying leaves gathered from Sichuan and Hainan provinces, China. Through rigorous phylogenetic analysis and examination of morphological characteristics, we successfully identified four new species within the genus *Beltraniella*. The pathogenicity and host associations of these newly reported *Beltraniella* fungi are relatively underexplored, necessitating further research. Building on the insights from this study, we anticipate that a more targeted collection of diseased and decaying leaves will expedite the isolation and characterization of further potential *Beltraniella* fungi.

## Additional information

### Conflict of interest

The authors have declared that no competing interests exist.

### Ethical statement

No ethical statement was reported.


### Funding

This research was funded by National Natural Science Foundation of China (nos. 32300011, 32170012, 32470004), Ji'nan City's 'New University 20 Policies' Initiative for Innovative Research Teams Project (202228028), Innovative Agricultural Application Technology Project of Jinan City (CX202210), and Key Technological Innovation Program of Shandong Province, China (2022CXGC020710).

## Author contributions

Conceptualization: W.-W. Liu; Data curation: W.-W. Liu and X.-S. Wang; Formal analysis: C.-Z. Yin; Funding acquisition: S. Wang; Investigation: W.-W. Liu; Methodology: W.-W. Liu; Project administration: S. Wang; Resources: S. Wang; Software: W.-W. Liu; Supervision: Z.-X. Zhang and X.-G. Zhang; Validation: C.-Z. Yin; Visualization: W.-W. Liu; Writing – original draft: W.-W. Liu; Writing–review and editing: W.-W. Liu and Z. Meng.

## Author ORCIDs

Wen-Wen Liu  <https://orcid.org/0009-0009-3477-194X>

Chang-Zhun Yin  <https://orcid.org/0009-0000-0034-2199>

Zhao-Xue Zhang  <https://orcid.org/0000-0002-4824-9716>

Xing-Sheng Wang  <https://orcid.org/0009-0005-1127-7368>

Shi Wang  <https://orcid.org/0000-0002-7376-7638>

## Data availability

All of the data that support the findings of this study are available in the main text or Supplementary Information.

## References

- Crous PW, Shivas RG, Quaedvlieg W, van der Bank M, Zhang Y, Summerell BA, Guarro J, Wingfield MJ, Wood AR, Alfenas AC, Braun U, Cano-Lira JF, García D, Marin-Felix Y, Alvarado P, Andrade JP, Armengol J, Assefa A, den Breejën A, Camele I, Cheewangkoon R, De Souza JT, Duong TA, Esteve-Raventós F, Fournier J, Frisullo S, García-Jiménez J, Gardiennet A, Gené J, Hernández-Restrepo M, Hirooka Y, Hospenthal DR, King A, Lechat C, Lombard L, Mang SM, Marbach PAS, Marincowitz S, Marin-Felix Y, Montaña-Mata NJ, Moreno G, Perez CA, Pérez Sierra AM, Robertson JL, Roux J, Rubio E, Schumacher RK, Stchigel AM, Sutton DA, Tan YP, Thompson EH, Vanderlinde E, Walker AK, Walker DM, Wickes BL, Wong PTW, Groenewald JZ (2014) Fungal Planet Description Sheets: 214–280. *Persoonia* 32(1): 183–306. <https://doi.org/10.3767/003158514X682395>
- Crous PW, Wingfield MJ, Burgess TI, Hardy GE, Crane C, Barrett S, Cano-Lira JF, Le Roux JJ, Thangavel R, Guarro J, Stchigel AM, Martín MP, Alfredo DS, Barber PA, Barreto RW, Baseia IG, Cano-Canals J, Cheewangkoon R, Ferreira RJ, Gené J, Lechat C, Moreno G, Roets F, Shivas RG, Sousa JO, Tan YP, Wiederhold NP, Abell SE, Accioly T, Albizu JL, Alves JL, Antonielli ZI, Aplin N, Araújo J, Arzanlou M, Bezerra JD, Bouchara JP, Carlavilla JR, Castillo A, Castroagudín VL, Ceresini PC, Claridge GF, Coelho G, Coimbra VR, Costa LA, da Cunha KC, da Silva SS, Daniel R, de Beer ZW, Dueñas M, Edwards J, Enwistle P, Fiuza PO, Fournier J, García D, Gibertoni TB, Giraud S, Guevara-Suarez M, Gusmão LF, Haituk S, Heykoop M, Hirooka Y, Hofmann TA, Houbraken J, Hughes DP, Kautmanová I, Koppel O, Koukol O, Larsson E, Latha KP, Lee DH, Lisboa DO, Lisboa WS, López-Villalba Á, Maciel JL, Manimohan P, Manjón JL, Marincowitz S, Marney TS, Meijer M, Miller AN, Olariaga I, Paiva LM, Piepenbring M, Poveda-Molero JC, Raj KN, Raja HA, Rougeron A, Salcedo I, Samadi R, Santos TA, Scarlett K, Seifert KA, Shuttleworth LA, Silva GA, Silva M, Siqueira JP, Souza-Motta CM, Stephenson SL, Sutton DA, Tamakeaw N, Telleria MT, Valenzuela-Lopez N, Viljoen A, Visagie CM, Vizzini A, Wartchow F, Wingfield BD, Yurchenko E, Zamora JC, Groenewald JZ (2016) Fungal Planet description sheets: 469–557. *Persoonia* 37(1): 218–403. <https://doi.org/10.3767/003158516X694499>

- Crous PW, Wingfield MJ, Burgess TI, Carnegie AJ, Hardy GESJ, Smith D, Summerell BA, Cano-Lira JF, Guarro J, Houbraken J, Lombard L, Martín MP, Sandoval-Denis M, Alexandrova AV, Barnes CW, Baseia IG, Bezerra JDP, Guarnaccia V, May TW, Hernández-Restrepo M, Stchigel AM, Miller AN, Ordoñez ME, Abreu VP, Accioly T, Agnello C, Agustin Colmán A, Albuquerque CC, Alfredo DS, Alvarado P, Araújo-Magalhães GR, Arauzo S, Atkinson T, Barili A, Barreto RW, Bezerra JL, Cabral TS, Camello Rodríguez F, Cruz RHSF, Daniëls PP, da Silva BDB, de Almeida DAC, de Carvalho Júnior AA, Decock CA, Delgat L, Denman S, Dimitrov RA, Edwards J, Fedosova AG, Ferreira RJ, Firmino AL, Flores JA, García D, Gené J, Giraldo A, Góis JS, Gomes AAM, Gonçalves CM, Gouliamova DE, Groenewald M, Guéorguiev BV, Guevara-Suarez M, Gusmão LFP, Hosaka K, Hubka V, Huhndorf SM, Jadan M, Jurjević Ž, Kraak B, Kučera V, Kumar TKA, Kušan I, Lacerda SR, Lamlerthton S, Lisboa WS, Loizides M, Luangsa-Ard JJ, Lysková P, Mac Cormack WP, Macedo DM, Machado AR, Malysheva EF, Marinho P, Matočec N, Meijer M, Mešić A, Mongkolsamrit S, Moreira KA, Morozova OV, Nair KU, Nakamura N, Noisripoom W, Olariaga I, Oliveira RJV, Paiva LM, Pawar P, Pereira OL, Peterson SW, Prieto M, Rodríguez-Andrade E, Rojo De Blas C, Roy M, Santos ES, Sharma R, Silva GA, Souza-Motta CM, Takeuchi-Kaneko Y, Tanaka C, Thakur A, Smith MT, Tkalčec Z, Valenzuela-Lopez N, van der Kleij P, Verbeken A, Viana MG, Wang XW, Groenewald JZ (2017) Fungal Planet description sheets: 625–715. *Persoonia* 39: 270–467. <https://doi.org/10.3767/persoonia.2017.39.11>
- Dighton J, Cooke RC, Rayner ADM (1985) Ecology of Saprotrophic Fungi. *Journal of Applied Ecology* 22(2): 604. <https://doi.org/10.2307/2403197>
- dos Santos MVO, Barbosa FR, Magalhães DMA, Luz EDMN, Bezerra JL (2014) *Beltraniella* species associated with leaf litter of the atlantic forest in southern bahia, brazil. *Mycotaxon* 129(1): 1–6. <https://doi.org/10.5248/129.1>
- Doyle JJ, Doyle JL (1990) Isolation of plant DNA from fresh tissue. *Focus* (San Francisco, Calif.) 12: 13–15.
- Glass NL, Donaldson GC (1995) Development of primer sets designed for use with the PCR to amplify conserved genes from filamentous ascomycetes. *Applied and Environmental Microbiology* 61(4): 1323–1330. <https://doi.org/10.1128/aem.61.4.1323-1330.1995>
- Guo LD, Hyde KD, Liew ECY (2000) Identification of endophytic fungi from *Livistona chinensis* based on morphology and rDNA sequences. *The New Phytologist* 147(3): 617–630. <https://doi.org/10.1046/j.1469-8137.2000.00716.x>
- Hudson HJ, Ellis MB (1972) Transactions of the British Mycological Society. *Transactions of the British Mycological Society* 58(3): 534. [https://doi.org/10.1016/S0007-1536\(72\)80113-X](https://doi.org/10.1016/S0007-1536(72)80113-X)
- Huelsenbeck JP, Ronquist F (2001) MRBAYES: Bayesian inference of phylogeny. *Bioinformatics* (Oxford, England) 17(8): 754–755. <https://doi.org/10.1093/bioinformatics/17.8.754>
- Hyde KD, Bussaban B, Paulus B, Crous PW, Lee S, Mckenzie EHC, Photita W, Lumyong S (2007) Diversity of saprobic microfungi. *Biodiversity and Conservation* 16(1): 7–35. <https://doi.org/10.1007/s10531-006-9119-5>
- Hyde KD, Norphanphoun C, Maharachchikumbura SSN, Bhat DJ, Jones EBG, Bundhun D, Chen YJ, Bao DF, Boonmee S, Calabon MS, Chaiwan N, Chethana KWT, Dai DQ, Dayarathne MC, Devadatha B, Dissanayake AJ, Dissanayake LS, Doilom M, Dong W, Fan XL, Goonasekara ID, Hongsanana S, Huang SK, Jayawardena RS, Jeewon R, Karunarathna A, Konta S, Kumar V, Lin CG, Liu JK, Liu NG, Luangsa-ard J, Lumyong S,



- Luo ZL, Marasinghe DS, McKenzie EHC, Niego AGT, Niranjana M, Perera RH, Phukham-sakda C, Rathnayaka AR, Samarakoon MC, Samarakoon SMBC, Sarma VV, Senan-ayake IC, Shang QJ, Stadler M, Tibpromma S, Wanasinghe DN, Wei DP, Wijayawar-dene NN, Xiao YP, Yang J, Zeng XY, Zhang SN, Xiang MM (2020a) Refined families of Sordariomycetes. *Mycosphere: Journal of Fungal Biology* 11(1): 1058. <https://www.mycosphere.org/volume-11-2020/>
- Hyde KD, de Silva NI, Jeewon R, Bhat DJ, Phookamsak R, Doilom M, Boonmee S, Jay-awardena RS, Maharachchikumbura SSN, Senanayake IC, Manawasinghe IS, Liu NG, Abeywickrama PD, Chaiwan N, Karunarathna A, Pem D, Lin CG, Sysouphan-thong P, Luo ZL, Wei DP, Wanasinghe DN, Norphanphoun C, Tennakoon DS, Sa-marakoon MC, Jayasiri SC, Jiang HB, Zeng XY, Li JF, Wijesinghe SN, Devadatha B, Goonasekara ID, Brahmanage RS, Yang EF, Aluthmuhandiram JVS, Dayarathne MC, Marasinghe DS, Li WJ, Dissanayake LS, Dong W, Huanraluek N, Lumyong S, Liu JK, Karunarathna SC, Jones EBG, Al-Sadi AM, Xu JC, Harishchandra D, Sar-ma VV (2020b) New records and collections of fungi: 1–100. *Asian Journal of Mycology* 3(1): 22–294. <https://www.asianjournalofmycology.org/volume-3-january-2020-december-2020/>
- Hyde KD, Noorabadi MT, Thiyagaraja V, He MQ, Johnston PR, Wijesinghe SN, Armand A, Biketova AY, Chethana KWT, Erdoğan M, Ge ZW, Groenewald JZ, Hongsanan S, Kušan I, Leontyev DV, Li DW, Lin CG, Liu NG, Maharachchikumbura SSN, Ma-točec N, et al. (2024) The 2024 Outline of Fungi and fungus-like taxa. *Mycosphere: Journal of Fungal Biology* 15(1): 5146–6239. <https://doi.org/10.5943/myco-sphere/15/1/25>
- Katoh K, Rozewicki J, Yamada KD (2019) MAFFT online service: Multiple sequence alignment, interactive sequence choice and visualization. *Briefings in Bioinformatics* 20(4): 1160–1166. <https://doi.org/10.1093/bib/bbx108>
- Kumar S, Stecher G, Tamura K (2016) MEGA7: Molecular Evolutionary Genetics Analysis Version 7.0 for Bigger Datasets. *Molecular Biology and Evolution* 33(7): 1870–1874. <https://doi.org/10.1093/molbev/msw054>
- Liu G, Bonthond JZ, Groenewald L, Cai PW, Crous PW (2019) Sporocadaceae, a family of coelomycetous fungi with appendage-bearing conidia. *Studies in Mycology* 92(1): 287–415. <https://doi.org/10.1016/j.simyco.2018.11.001>
- Liu SL, Wang XW, Li GJ, Deng C-Y, Rossi W, Leonardi M, Liimatainen K, Kekki T, Niskanen T, Smith ME, Ammirati J, Bojantchev D, Abdel-Wahab MA, Zhang M, Tian E, Lu Y-Z, Zhang J-Y, Ma J, Dutta AK, Acharya K, Du T-Y, Xu J, Kim JS, Lim YW, Gerlach A, Zeng N-K, Han Y-X, Razaghi P, Raza M, Cai L, Calabon MS, Jones EBG, Saha R, Kumar TKA, Krishnapriya K, Thomas A, Kaliyaperumal M, Kezo K, Gunaseelan S, Singh SK, Singh PN, Lagashetti AC, Pawar KS, Jiang S, Zhang C, Zhang H, Qing Y, Bau T, Peng X-C, Wen T-C, Ramirez NA, Niveiro N, Li M-X, Yang ZL, Wu G, Tarafder E, Tennakoon DS, Kuo C-H, da Silva TM, Souza-Motta CM, Bezerra JDP, He G, Ji X-H, Suwannarach N, Kumla J, Lumyong S, Wannathes N, Rana S, Hyde KD, Zhou L-W (2024) Fungal diversity notes 1717–1817: Taxonomic and phylogenetic contributions on genera and species of fungal taxa. *Fungal Diversity* 124(1): 1–216. <https://doi.org/10.1007/s13225-023-00529-0>
- Miller MA, Pfeiffer W, Schwartz T (2010) Creating the CIPRES Science Gateway for inference of large phylogenetic trees. *Proceedings of the Gateway Computing Envi-ronments Workshop (GCE)*, New Orleans, LA, USA 14: 1–8. <https://doi.org/10.1109/GCE.2010.5676129>

- Miller MA, Pfeiffer W, Schwartz T (2012) The CIPRES science gateway: Enabling high-impact science for phylogenetics researchers with limited resources. *ACM* 39: 1–8. <https://doi.org/10.1145/2335755.2335836>
- Nylander JAA (2004) MrModelTest v. 2. Program distributed by the author. Evolutionary Biology Centre, Uppsala University.
- Ronquist F, Huelsenbeck JP (2003) MrBayes 3: Bayesian Phylogenetic Inference under Mixed Models. *Bioinformatics* (Oxford, England) 19(12): 1572–1574. <https://doi.org/10.1093/bioinformatics/btg180>
- Ronquist F, Teslenko M, van der Mark P, Ayres DL, Darling A, Höhna S, Larget B, Liu L, Suchard MA, Huelsenbeck JP (2012) MrBayes 3.2: Efficient Bayesian phylogenetic inference and model choice across a large model space. *Systematic Biology* 61(3): 539–542. <https://doi.org/10.1093/sysbio/sys029>
- Shirouzu T, Hirose D, Tokumasu S, To-Anun C, Maekawa N (2010) Host affinity and phylogenetic position of a new anamorphic fungus *Beltraniella botryospora* from living and fallen leaves of evergreen oaks. *Fungal Diversity* 43(1): 85–92. <https://doi.org/10.1007/s13225-010-0037-1>
- Stamatakis A (2006) RAXML-VI-HPC: Maximum likelihood-based phylogenetic analyses with thousands of taxa and mixed models. *Bioinformatics* (Oxford, England) 22: 2688–2690. <https://doi.org/10.1093/bioinformatics/btl446>
- Stamatakis A (2014) RAXML Version 8: A tool for phylogenetic analysis and post-analysis of large phylogenies. *Bioinformatics* (Oxford, England) 30(9): 1312–1313. <https://doi.org/10.1093/bioinformatics/btu033>
- Stamatakis A, Hoover P, Rougemont JA (2008) rapid bootstrap algorithm for the RAXML Web servers. *Systematic Biology* 57: 758–771. <https://doi.org/10.1080/10635150802429642>
- Subramanian CV (1952) Fungi imperfecti from Madras—III. *Beltraniella* gen. nov. *Proceedings of the Indian Academy of Sciences. Section B, Biological Sciences* 36: 223–228. <https://doi.org/10.1007/BF03050466>
- Tan YPT, Roger GS (2022) Index of Australian Fungi No. 3. *Index of Australian Fungi* 3 13: 3.
- Tibpromma S, Hyde KD, McKenzie EHC, Bhat DJ, Phillips AJL, Wanasinghe DN, Samarakoon MC, Jayawardena RS, Dissanayake AJ, Tennakoon DS, Doilom M, Phookamsak R, Tang AMC, Xu J, Mortimer PE, Promputtha I, Maharachchikumbura SSN, Khan S, Karunarathna SC (2018) Micro-fungi associated with Pandanaceae. *Fungal Diversity* 93(1): 840–928. <https://doi.org/10.1007/s13225-018-0408-6>
- Wang S, Liu X, Xiong C, Gao S, Xu W, Zhao L, Song C, Liu X, James TY, Li Z, Zhang X (2023) ASF1 regulates asexual and sexual reproduction in *Stemphylium eturmiurnum* by DJ-1 stimulation of the PI3K/AKT signaling pathway. *Fungal Diversity* 123(1): 159–176. <https://doi.org/10.1007/s13225-023-00528-1>
- White TJ, Bruns TD, Lee SB, Taylor JM (1990) Amplification and direct sequencing of fungal ribosomal rna genes for phylogenetics. *PCR – Protocols and Applications – A Laboratory Manual*, 315–322. <https://doi.org/10.1016/B978-0-12-372180-8.50042-1>
- Zhang Z, Schwartz S, Wagner L, Miller WA (2000) A greedy algorithm for aligning DNA sequences. *Journal of Computational Biology* 7(1–2): 203–214. <https://doi.org/10.1089/10665270050081478>
- Zhang ZX, Liu RY, Liu SB, Mu TC, Zhang XG, Xia JW (2022) Morphological and phylogenetic analyses reveal two new species of Sporocadaceae from Hainan, China. *MycKeys* 88: 171–192. <https://doi.org/10.3897/mycokeys.88.82229>

## Supplementary material 1

### DNA sequences

Authors: Wen-Wen Liu, Chang-Zhun Yin, Zhao-Xue Zhang, Xing-Sheng Wang, Zhe Meng, Xiu-Guo Zhang, Shi Wang

Data type: fas

Copyright notice: This dataset is made available under the Open Database License (<http://opendatacommons.org/licenses/odbl/1.0/>). The Open Database License (ODbL) is a license agreement intended to allow users to freely share, modify, and use this Dataset while maintaining this same freedom for others, provided that the original source and author(s) are credited.

Link: <https://doi.org/10.3897/mycokeys.116.140506.suppl1>

# Five new species of *Cortinarius* (Cortinariaceae) from Yunnan, China, based on molecular and morphological evidence

Liu-Kun Jia<sup>1,2,3\*</sup>, Zi-Rui Wang<sup>1,2,3,4\*</sup>, Zhu-Liang Yang<sup>1,2</sup>

<sup>1</sup> State Key Laboratory of Phytochemistry and Natural Medicines, Kunming Institute of Botany, Chinese Academy of Sciences, Kunming, 650201, China

<sup>2</sup> Yunnan Key Laboratory for Fungal Diversity and Green Development, Kunming Institute of Botany, Chinese Academy of Sciences, Kunming, 650201, China

<sup>3</sup> College of Life Sciences, University of Chinese Academy of Sciences, Beijing, 101408, China

<sup>4</sup> School of Ecology and Environmental Science, Yunnan University, Kunming, 650500, China

Corresponding author: Zhu-Liang Yang ([fungi@mail.kib.ac.cn](mailto:fungi@mail.kib.ac.cn))

## Abstract

*Cortinarius* is a globally distributed, exceptionally species-rich genus of Cortinariaceae, serving as important ectomycorrhizal fungi. Yunnan province, located in southwestern China, boasts a vast array of environmental conditions and fungal resources, with numerous new *Cortinarius* species yet to be discovered. Based on morphological evidence and phylogenetic inference using a two-locus dataset, five novel species have been identified within the genus, namely *C. brunneoverrucosus*, *C. coriaceus*, *C. fusco-candidus*, *C. neodisjungendus*, and *C. sinoconfirmatus*. Notably, two of these species (*C. brunneoverrucosus* and *C. neodisjungendus*) occur in subtropical areas, while the other three species (*C. coriaceus*, *C. fusco-candidus*, and *C. sinoconfirmatus*) inhabit sub-alpine temperate areas. Taxonomic descriptions for these five species are provided.

**Key words:** Diversity, morphology, new taxa, phylogeny, taxonomy



Academic editor: Kentaro Hosaka

Received: 14 January 2025

Accepted: 27 March 2025

Published: 14 April 2025

**Citation:** Jia L-K, Wang Z-R, Yang Z-L (2025) Five new species of *Cortinarius* (Cortinariaceae) from Yunnan, China, based on molecular and morphological evidence.

MycoKeys 116: 145–166. <https://doi.org/10.3897/mycokeys.116.146710>

Copyright: © Liu-Kun Jia et al.

This is an open access article distributed under terms of the Creative Commons Attribution License (Attribution 4.0 International – CC BY 4.0).

## Introduction

*Cortinarius* (Pers.) Gray, belonging to the order Agaricales, is the most species-rich genus within the family Cortinariaceae. Currently, over 2,000 species have been formally described (Liimatainen et al. 2022). It is widely distributed across tropical to subpolar areas in both the Northern and Southern Hemispheres, holding irreplaceable ecological, research, and economic value (Kirk et al. 2008; Soop et al. 2019; Liimatainen et al. 2020, 2022). Based on recent genomic and multi-locus sequence data, *Cortinarius* sensu lato has been split into ten genera, with the core groups within *Cortinarius* s. l. being transferred to *Cortinarius* sensu stricto, emended in Liimatainen et al. (2022).

*Cortinarius* s.s., typified by *C. violaceus* (L.) Gray, has several distinguishing features. These include a pileus adorned with fibrillose squamules, a fibrillose cortina, a negative KOH reaction, and rusty brown basidiospores with weakly to strongly verrucose ornamentations. Additionally, it features a duplex pileipellis with a hypoderm that is variably developed. The basidiomata vary widely in size, ranging from very small to large, and can be dry to glutinous in texture.

\* These authors contributed equally to this work.



They exhibit a diverse array of colors, with brown being the most common (Bidaud et al. 2000, 2012; Liimatainen et al. 2015, 2017, 2020, 2022; Soop et al. 2019; Ammirati et al. 2021; Zhou et al. 2023; Long et al. 2024). Liimatainen et al. (2022) identified 11 recognized subgenera under *Cortinarius* s.s., including subgen. *Cortinarius*, subgen. *Dermocybe* (Fr.) Trog, subgen. *Illumini* Liimat., Niskanen & Kytö, subgen. *Leprocycbe* M.M. Moser, subgen. *Iodolentes* Niskanen & Liimat., subgen. *Orellani* (M.M. Moser) Gasparini, subgen. *Telamonia* (Fr.) Trog, subgen. *Infracti* Niskanen & Liimat, subgen. *Camphorati* Liimat., Niskanen & Ammirati, subgen. *Myxadium* (Fr.) Trog, and subgen. *Paramyxadium* M.M. Moser & E. Horak.

The research on the genus *Cortinarius* primarily originated and has remained concentrated in Europe, North America, and Oceania (Peintner et al. 2002a, 2002b, 2004; Garnica et al. 2003, 2005; Liimatainen et al. 2014, 2015, 2017, 2020, 2022; Niskanen 2014, 2020; Soop et al. 2019), whereas studies in East Asia are still insufficient. Since the reporting of *C. testaceus* Cooke in China by Teng and Ou (1937), numerous Chinese mycologists have described *Cortinarius* species across various areas, including northeast, north, east, south, and southwestern parts of China (Deng 1963; Li 1980; Mao and Zong 1988; Ying and Zang 1994; Zang 1996; Mao 2000, 2009). However, most of these species' names recorded by the aforementioned studies are based on those from Europe, North America, and Oceania, and their distinctiveness in China awaits confirmation through molecular evidence. Recently, based on a combination of morphological and molecular systematic evidence, 26 new *Cortinarius* species from China have been published (Wei and Yao 2013; Xie et al. 2019, 2020, 2021a, 2021b, 2022, 2023; Yuan et al. 2020; Luo and Bau 2021; Zhang et al. 2023; Zhou et al. 2023; Long et al. 2024), indicating that the species diversity of *Cortinarius* in China is high, and potential undiscovered species may exist within the genus.

In this study, five *Cortinarius* species new to science were identified in Yunnan, southwestern China. Based on a combination of morphological observations and phylogenetic analysis, we provide descriptions of these species.

## Materials and methods

### Specimens and morphological description

Macro-morphological characteristics were described based on fresh basidiomata, detailed field notes, and photographs taken in situ. Colors in the descriptions were coded following Kornerup and Wanscher (1981). The basidiomata size, determined by pileus width, was categorized as tiny (< 1.5 cm), small (1.5–3 cm), medium-sized (3–5 cm), or large (> 5 cm). Additionally, 'L' refers to the number of lamellae reaching the stipe, while 'l' denotes the number of lamellulae located between two lamellae.

Microscopic structures were observed with light microscopy under a ZEISS Axiostar Plus microscope. Dried specimens were sectioned and mounted in a 5% KOH solution or Melzer's reagent. Congo Red staining was applied when necessary. For observing basidiospore ornamentations, small hymenophoral fragments were taken from dried specimens, mounted on aluminum stubs with double-sided adhesive tape, coated with gold-palladium, and then observed under a ZEISS Sigma 300 scanning electron microscope (SEM) at the Kunming Institute of Botany, Chinese Academy of Sciences.

In the descriptions of basidiospores, the abbreviation [n/m/p] indicates that 'n' basidiospores were measured from 'm' basidiomata of 'p' collections. Dimensions are presented in the form (a–)b–c(–d), where the range 'b–c' includes a minimum of 90% of the measured values, with extreme values "a" or 'd' given in parentheses. The ratio of basidiospore length to width in side view is represented by Q. The mean values and average Q of basidiospores, along with standard deviations, are indicated as "av." and 'Qav.', respectively. Basidiospore shapes were determined based on descriptions by Bas (1969) and Kirk et al. (2008).

The studied collections were deposited in the Cryptogamic Herbarium of Kunming Institute of Botany, Chinese Academy of Sciences (KUN-HKAS).

### DNA extraction, polymerase chain reaction (PCR), and sequencing

Total genomic DNA was extracted from dried specimens using an Ezup Column Fungi Genomic DNA Purification Kit (Sangon Biotech, Shanghai, China). The ITS region was amplified using the primers ITS1F/ITS4. For older specimens, primer combinations ITS1F/ITS2 and ITS3/ITS4 were also employed (White et al. 1990; Gardes and Bruns 1993). The ribosomal large subunit 28S region (nrLSU) was amplified using the primers LROR/LR5 (Vilgalys and Hester 1990; Hopple and Vilgalys 1994).

PCR reactions were conducted using an ABI 2720 Thermal Cycler, Veriti™ Dx 96-Well Thermal Cycler, or SimpliAmp™ Thermal Cycler (Applied Biosystems, Foster City, CA, USA). The PCR settings for the ITS1F/ITS4 were 94 °C for 5 min, followed by 35 cycles of 94 °C for 40 s, 52 °C for 40 s, and 72 °C for 1 min, with a final extension at 72 °C for 8 min. For the LROR/LR5 primers, the settings were 94 °C for 5 min, followed by 35 cycles of 94 °C for 40 s, 50 °C for 40 s, and 72 °C for 1 min, with a final extension at 72 °C for 8 min.

The PCR products were purified using a Gel Extraction and PCR Purification Combo Kit (Spin-column) (Bioteke, Beijing, China). After purification, the products were sequenced on an ABI-3730-XL DNA Analyzer (Applied Biosystems, Foster City, CA, USA) using the same primer combinations as those used for the PCR.

### Phylogenetic analysis

Forward and reverse sequences were assembled and edited with SeqMan (DNA STAR package; DNASTar Inc., Madison, WI, USA). The ITS sequences were used to infer related taxa through a BLASTn search in GenBank (<https://blast.ncbi.nlm.nih.gov/Blast.cgi>). The top hits in the BLASTn results confirmed that our specimens belonged to the genus *Cortinarius*. Related species were selected for the phylogenetic analyses based on BLASTn results (> 90% identity) and references from publications by Soop et al. (2019), Liimatainen et al. (2017, 2020), and Ammirati et al. (2021). A total of 64 collections representing 57 species were included in this study, with five species from the sect. *Leprocybe* selected as outgroups.

Alignments were constructed using MAFFT v7.3.10 (Katoh and Standley 2013) and optimized using BioEdit v7.2.5 (Hall 1999). The final alignments have been submitted to TreeBASE (<http://purl.org/phylo/treebase/phylows/study/TB2:S31924>).

Phylogenetic analyses were conducted using maximum likelihood (ML) and Bayesian inference (BI) methods, implemented in IQ-TREE v2.2.0 (Nguyen et al. 2015) and MrBayes 3.2.7 (Ronquist et al. 2012). The best-fit substitution model for ML analyses using the ITS+nrLSU matrix was determined with the 'MFP'

**Table 1.** DNA substitution models selected for phylogenetic analysis based on the ITS-nrLSU matrix.

Loci	Models for maximum likelihood (IQ-TREE)	Models for Bayesian inference (MrBayes)
ITS	TIM2+F+I+R2	lset applyto = (ITS) nst = 6 rates = Invgamma
nrLSU	TN+F+I	lset applyto = (nrLSU) nst = 2 rates = Propinv prset applyto = (all) statefreqpr = Dirichlet(1,1,1,1)

option in IQ-TREE v2.2.0 (Kalyaanamoorthy et al. 2017) based on the Akaike Information Criterion (AIC) (Table 1). For ML analyses, 1,000 replicates of the Shimodaira-Hasegawa-like aLRT test (SH-aLRT) (Guindon et al. 2010) and 1,000 replicates of the ultrafast bootstrap (UFB) (Hoang et al. 2018) were set. The ‘-p’ option was used for reading the partition file (ITS: 1–744; nrLSU: 745–1627), while other parameters remained at default settings. For BI analyses, substitution models were selected based on IQ-TREE v2.2.0 outputs (Table 1). Four Markov chains were run twice from random starting trees for 10 million generations, with sampling every 100<sup>th</sup> generation. The stop value (stopval) was set to 0.001. Parameters and sampled trees were summarized after discarding the first 25% of trees as burn-in using the ‘sump’ and ‘sumt’ commands in MrBayes 3.2.7.

## Results

### Molecular analyses

The dataset comprised a total of 78 sequences, including 24 newly generated and 54 downloaded sequences (64 ITS, 14 nrLSU) from 64 collections representing 57 species (Table 2). The concatenated dataset (ITS-nrLSU) consisted of 1,627 positions after excluding poorly aligned regions. Accession numbers for all the sequences used for molecular analyses are provided in Table 2. Both ML and BI trees exhibited the same topology; therefore, only the ML tree, with the SH-aLRT support values, UFB values, and Bayesian posterior probabilities (BPP), is shown (Fig. 1).

### Taxonomy

***Cortinarius brunneoverrucosus* Zhu L. Yang, Liu K. Jia & Zi R. Wang, sp. nov.**

MycoBank No: 857350

Fig. 2

**Etymology.** The epithet “*brunneoverrucosus*” (Lat.) refers to the pileus with brown verrucose squamules of this species.

**Holotype.** CHINA • Yunnan Province: Pu’er City, Jingdong Yi Autonomous County Ailao Mountain Subtropical Forest Ecosystem Research Station, Chinese Academy of Sciences, in a subtropical broad-leaved forest with trees of *Lithocarpus*, 24°32.57’N, 101°1.62’E, elevation 2,491 m, 23 July 2013, Yang-Yang Cui 32 (KUN-HKAS 79712). GenBank: ITS: PQ772212, nrLSU: PQ772224.

**Diagnosis.** *Cortinarius brunneoverrucosus* is sister to *C. corrugatus* Peck but differs by its yellowish brown to brown pileus with brown verrucose squamules, more robust stipe, relatively wider basidiospores, and exclusive occurrence in subtropical broad-leaved forest with trees of *Lithocarpus* and *Quercus* (Peck 1872; Phillips 2010; Kuo 2020).

**Table 2.** Voucher information, GenBank accession numbers of the samples used in the phylogenetic analysis.

Taxa	voucher	Status	Locations	Section	GenBank Accession No.		Sequence origin
					ITS	nrLSU	
<i>Cortinarius</i> aff. <i>leucophaeatus</i>	S: CFP536		Sweden	<i>Telamonia</i>	KC608590	in ITS	Liimatainen et al. 2020
<i>C. aff. tenebricus</i>	G: 056		France	<i>Verni</i>	MT935483	-	Liimatainen et al. 2020
<i>C. albolens</i>	PC: A. Bidaud 97-10-368	Holotype	France	<i>Hinnulei</i>	MT934855	in ITS	Liimatainen et al. 2020
<i>C. ammophiloides</i>	BP: 57443	Holotype	Hungary	<i>Verni</i>	NR_171309	-	Liimatainen et al. 2020
<i>C. badioflavidus</i>	WTU: JFA13668	Holotype	USA	<i>Hinnulei</i>	KU041723	in ITS	Liimatainen et al. 2020
<i>C. boulderensis</i>	MICH: AHS17461	Holotype	USA	<i>Boulderenses</i>	DQ499466	in ITS	Liimatainen et al. 2020
<i>C. brunneofibrillosus</i>	WTU: JFA13654	Holotype	USA	<i>Leprocye</i>	MW009188	-	Ammirati et al. 2021
<b><i>C. brunneoverrucosus</i></b>	<b>KUN-HKAS 79712</b>	<b>Holotype</b>	<b>China</b>	<b><i>Dulciolentes</i></b>	<b>PQ772212</b>	<b>PQ772224</b>	<b>This study</b>
<b><i>C. brunneoverrucosus</i></b>	<b>KUN-HKAS 145321</b>		<b>China</b>	<b><i>Dulciolentes</i></b>	<b>PQ772211</b>	<b>PQ772223</b>	<b>This study</b>
<i>C. claroplaniusculus</i>	PC: RH2334	Holotype	France	<i>Disjungendi</i>	NR_131844	-	Liimatainen et al. 2020
<i>C. confirmatus</i>	PC: RH84/159		Italy	<i>Saturnini</i>	KX964440	in ITS	Liimatainen et al. 2017
<i>C. confirmatus</i>	PC: RH3195	Holotype	France	<i>Saturnini</i>	KX964438	in ITS	Liimatainen et al. 2017
<b><i>C. coriaceus</i></b>	<b>KUN-HKAS 145314</b>		<b>China</b>	<b><i>Telamonia</i></b>	<b>PQ772201</b>	<b>PQ772213</b>	<b>This study</b>
<b><i>C. coriaceus</i></b>	<b>KUN-HKAS 145315</b>		<b>China</b>	<b><i>Telamonia</i></b>	<b>PQ772203</b>	<b>PQ772215</b>	<b>This study</b>
<b><i>C. coriaceus</i></b>	<b>KUN-HKAS 145316</b>	<b>Holotype</b>	<b>China</b>	<b><i>Telamonia</i></b>	<b>PQ772202</b>	<b>PQ772214</b>	<b>This study</b>
<i>C. corrugatus</i>	IB: 2000544		North America	<i>Dulciolentes</i>	AF325611	in ITS	Soop et al. 2019
<i>C. disjungendus</i>	H: IK98-861	Holotype	Sweden	<i>Disjungendi</i>	NR_131838	-	Liimatainen et al. 2020
<i>C. disjungendus</i>	H: PAK4370	Holotype	Finland	<i>Disjungendi</i>	KP013190	in ITS	Liimatainen et al. 2020
<i>C. dulciolens</i>	PDD: 68471	Holotype	New Zealand	<i>Dulciolentes</i>	NR_157914	-	Soop et al. 2019
<i>C. flavifolius</i>	EH230	Epitype	USA	<i>Leprocye</i>	MW009217	in ITS	Ammirati et al. 2021
<i>C. fructuodorus</i>	H: 7001104	Holotype	USA	<i>Telamonia</i>	NR_131827	in ITS	Liimatainen et al. 2020
<i>C. fulvopaludosus</i>	H: 6033460	Holotype	Finland	<i>Hinnulei</i>	MG136823	in ITS	Liimatainen et al. 2020
<b><i>C. fuscocandidus</i></b>	<b>KUN-HKAS 69792</b>		<b>China</b>	<b><i>Hinnulei</i></b>	<b>PQ772209</b>	<b>PQ772221</b>	<b>This study</b>
<b><i>C. fuscocandidus</i></b>	<b>KUN-HKAS 70198</b>	<b>Holotype</b>	<b>China</b>	<b><i>Hinnulei</i></b>	<b>PQ772210</b>	<b>PQ772222</b>	<b>This study</b>
<i>C. fuscovelatus</i>	H: IK00-036	Holotype	Sweden	<i>Boulderenses</i>	NR_131888	-	Liimatainen et al. 2020
<i>C. hinnuleus</i>	TUB: 011905		Sweden	<i>Hinnulei</i>	AY669667	in ITS	Liimatainen et al. 2020
<i>C. hughesiae</i>	WTU: JFA13086	Holotype	USA	<i>Leprocye</i>	MW009224	in ITS	Ammirati et al. 2021
<i>C. imbutus</i>	H: IK97-1162	Neotype	Finland	<i>Saturnini</i>	KX964498	in ITS	Liimatainen et al. 2017
<i>C. ionophyllus</i>	IB: MM1949-0052	Holotype	Austria	<i>Telamonia</i>	MT935168	-	Liimatainen et al. 2020
<i>C. leproleptopus</i>	PC: RH84-109	Holotype	France	<i>Leprocye</i>	MW009226	in ITS	Ammirati et al. 2021
<i>C. leucophaeatus</i>	H: IK97-138		Finland	<i>Telamonia</i>	MT935196	in ITS	Liimatainen et al. 2020
<i>C. lucorum</i>	S: CFP490	Neotype	Norway	<i>Saturnini</i>	KX964585	in ITS	Liimatainen et al. 2017
<i>C. malachius</i>	G: 452		France	<i>Malachii</i>	MT934962	-	Liimatainen et al. 2020
<i>C. melanotus</i>	S: CFP1101	Epitype	France	<i>Leprocye</i>	MW009230	-	Ammirati et al. 2021
<i>C. montebelloensis</i>	H: TN10-149	Holotype	Canada	<i>Disjungendi</i>	KP114459	in ITS	Liimatainen et al. 2020
<b><i>C. neodisjungendus</i></b>	<b>KUN-HKAS 145322</b>	<b>Holotype</b>	<b>China</b>	<b><i>Cinnabarini</i></b>	<b>PQ772207</b>	<b>PQ772219</b>	<b>This study</b>
<b><i>C. neodisjungendus</i></b>	<b>KUN-HKAS 145323</b>		<b>China</b>	<b><i>Cinnabarini</i></b>	<b>PQ772208</b>	<b>PQ772220</b>	<b>This study</b>
<i>C. niveotraganus</i>	H: IK98-033	Holotype	Finland	<i>Telamonia</i>	NR_131842	-	Liimatainen et al. 2020
<i>C. odoritraganus</i>	H: 7057490	Holotype	Canada	<i>Telamonia</i>	MT112154	-	Liimatainen et al. 2020
<i>C. odoritraganus</i>	MICH: 10398/G: 00121		USA	<i>Telamonia</i>	NR_170852	MK277857	Liimatainen et al. 2020
<i>C. olididisjungendus</i>	H: 7000854	Holotype	Canada	<i>Disjungendi</i>	NR_131839	-	Liimatainen et al. 2020
<i>C. orasericeus</i>	PC: RH70239	Holotype	France	<i>Disjungendi</i>	KP013203	in ITS	Liimatainen et al. 2020
<i>C. peraurantiacus</i>	PDD: 70818		New Zealand	<i>Dulciolentes</i>	KC520543	in ITS	Soop et al. 2019
<i>C. piceidisjungendus</i>	H: TN11-443	Holotype	USA	<i>Disjungendi</i>	NR_131840	-	Liimatainen et al. 2020
<i>C. pisciodorus</i>	PDD: 27062/JAC 13813	Holotype	New Zealand	<i>Dulciolentes</i>	MN492664	MH108417	Soop et al. 2019
<i>C. psammocola</i>	H: IK99-722	Holotype	Finland	<i>Verni</i>	MG136821	-	Liimatainen et al. 2020
<i>C. pseudobovinus</i>	IB: MM1989-0300	Holotype	USA	<i>Boulderenses</i>	DQ499465	in ITS	Liimatainen et al. 2020
<i>C. roseonudipes</i>	G: 37	Holotype	France	<i>Hinnulei</i>	MT935391	-	Liimatainen et al. 2020
<i>C. rubrovioleipes</i>	GK: 13271/635a		Switz	<i>Boulderenses</i>	MT934924	in ITS	Liimatainen et al. 2020
<i>C. saturninus</i>	S: CFP514	Neotype	Sweden	<i>Saturnini</i>	KX964584	in ITS	Liimatainen et al. 2017
<i>C. semiodoratus</i>	TUB: 011512		-	<i>Hinnulei</i>	AY669665	in ITS	Liimatainen et al. 2020
<b><i>C. sinoconfirmatus</i></b>	<b>KUN-HKAS 145318</b>		<b>China</b>	<b><i>Saturnini</i></b>	<b>PQ772206</b>	<b>PQ772218</b>	<b>This study</b>
<b><i>C. sinoconfirmatus</i></b>	<b>KUN-HKAS 145319</b>		<b>China</b>	<b><i>Saturnini</i></b>	<b>PQ772204</b>	<b>PQ772216</b>	<b>This study</b>
<b><i>C. sinoconfirmatus</i></b>	<b>KUN-HKAS 145320</b>	<b>Holotype</b>	<b>China</b>	<b><i>Saturnini</i></b>	<b>PQ772205</b>	<b>PQ772217</b>	<b>This study</b>
<i>C. suberi</i>	S: F16406	Holotype	Sweden	<i>Malachii</i>	MT935480	-	Liimatainen et al. 2020
<i>C. suberi</i>	S: F14331		Sweden	<i>Malachii</i>	MT934927	in ITS	Liimatainen et al. 2020



Taxa	voucher	Status	Locations	Section	GenBank Accession No.		Sequence origin
					ITS	nrLSU	
<i>C. subionophyllus</i>	H: TN06-050	Holotype	Norway	<i>Telamonia</i>	MF379634	-	Liimatainen et al. 2020
<i>C. subpulchrifolius</i>	MICH: 10419	Lectotype	USA	<i>Telamonia</i>	NR_170855	in ITS	Liimatainen et al. 2020
<i>C. tigrinipes</i>	G: 874	Holotype	France	<i>Telamonia</i>	MT935549	in ITS	Liimatainen et al. 2020
<i>C. torvus</i>	S: CFP778	Epitype	Sweden	<i>Telamonia</i>	MT935556	in ITS	Liimatainen et al. 2020
<i>C. veneto-occidentalis</i>	H: TN11-051	Holotype	USA	<i>Leprocye</i>	MW009243	in ITS	Ammirati et al. 2021
<i>C. vernus</i>	BP:58132		Hungary	<i>Verni</i>	MT935033	in ITS	Liimatainen et al. 2020
<i>C. vernus</i>	CHEV 3130-T		France	<i>Verni</i>	FN429003	-	Suárez-Santiago et al. 2009
<i>C. venustus</i>	H: PAK3234	Holotype	Finland	<i>Telamonia</i>	MT935132	in ITS	Liimatainen et al. 2020

Newly generated sequences were marked in bold.

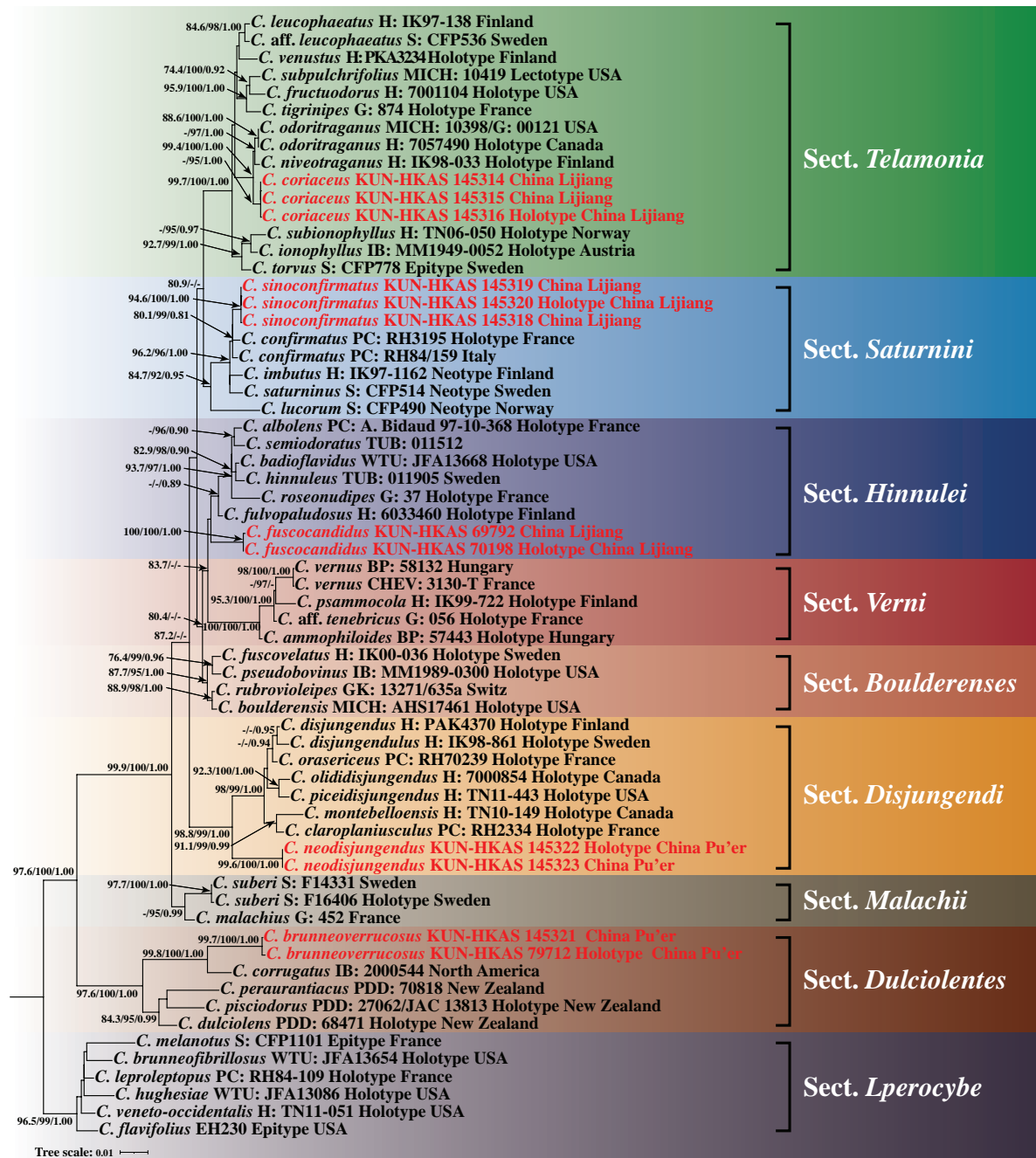


**Figure 1.** Maximum-likelihood phylogenetic tree of *Cortinarius* inferred from the concatenated ITS-nrLSU matrix. SH-aLRT support values  $\geq 80\%$ , UFB values  $\geq 90\%$  for ML, and BPP values  $\geq 0.80$  for BI are shown above the nodes as SH-aLRT/UFB/BPP. Sequences generated in this study are highlighted in red.

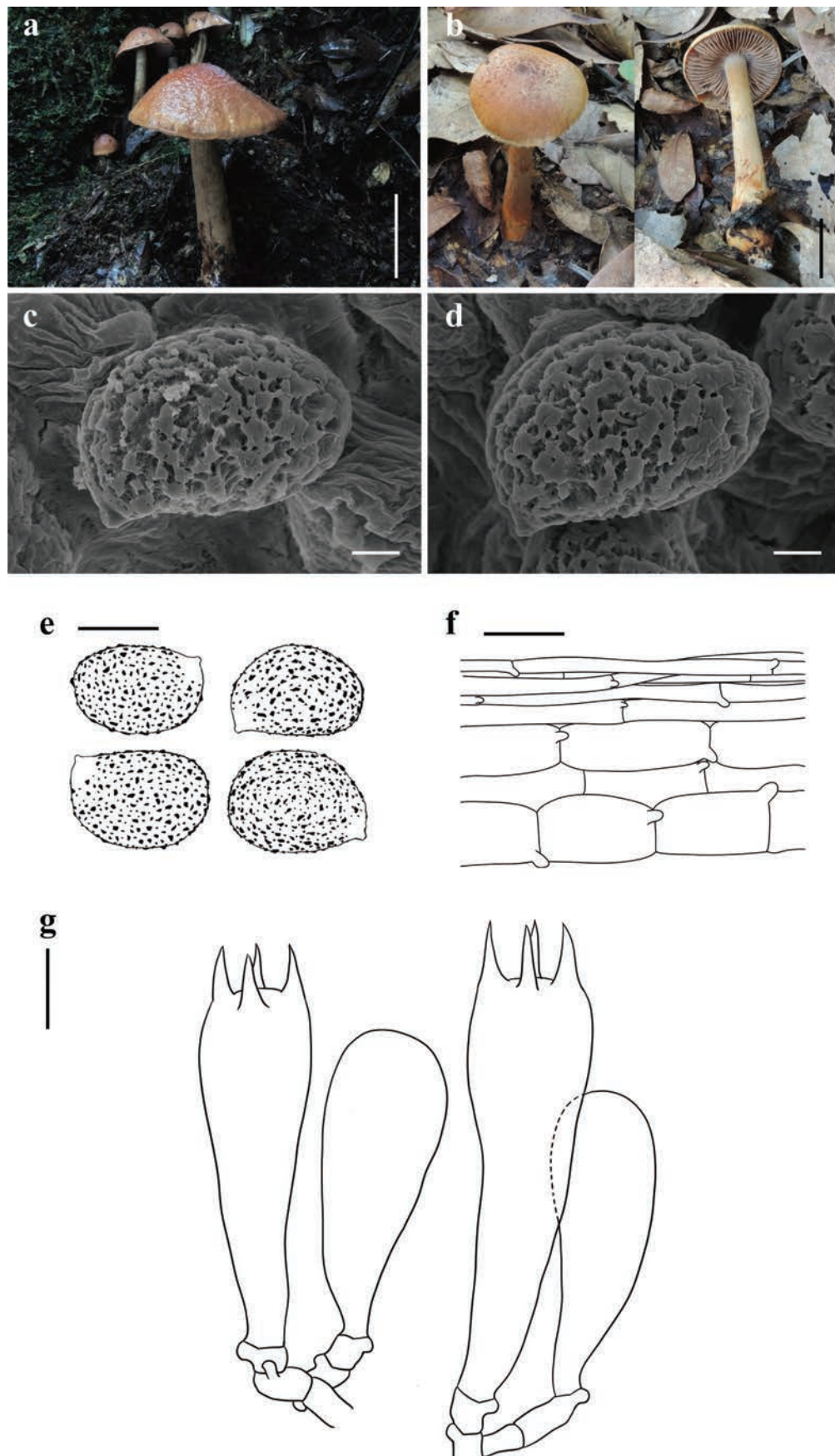


**Figure 2.** *Cortinarius brunneoverrucosus* (**a, c–g** KUN-HKAS 79712, Holotype **b** KUN-HKAS 145321) **a, b** basidiomata **c–e** basidiospores **f** pileipellis **g** basidia; and marginal sterile cells. Scale bars: 5 cm (**a, b**); 2  $\mu\text{m}$  (**c, d**); 10  $\mu\text{m}$  (**e**); 20  $\mu\text{m}$  (**f, g**).

**Description.** *Basidioma* large. *Pileus* 8–10.5 cm diam, hemispherical, viscid, verrucose; yellow-brown to brown (5B7–5C7), darker towards the center (5D8), paler towards the margin (5B3–5B5); covered with brown (5C7) to dark brown (5D8–5E8) verrucose to floccose squamules; margin with innate radial stripes, occasionally with pale yellow (4A2) floccose squamules; context of pileus white (1A1). *Lamellae* adnate with decurrent tooth, crowded (L = 64–73, l = 33–38), pale brown (6A2–6A4) with a faint pale pinkish (12A2) tint. *Stipe* 8.5–18 × 1.2–2 cm, tapering upwards, pale brown (6A2–6A4) to pale yellow (3A2–3A4), covered with brown (6C4) to orange-brown (5A8) fibrillose squamules; context of stipe white (1A1); basal mycelium white (1A1) with a faint pale pinkish (12A2) tint.

*Basidiospores* [60/2/2] (12.5–)15–16.5(–17.5) × (10–)11.5–12.5(–15) µm, Q = 1.2–1.5(–1.75), av. = 15.64 ± 1.61 × 12.31 ± 1.48 µm, Qav. = 1.27 ± 0.12, broadly ellipsoid to broadly amygdaliform, strongly verrucose, inamyloid. *Basidia* 37.5–50 × 7.5–10 µm, 4-spored, clavate. *Trama of lamellae* regular, composed of colorless to yellowish, smooth hyphae 10–12.5 µm wide. *Cystidia* absent. *Pileipellis* duplex: epicutis weakly developed, 12–15 µm thick, composed of only 3–5 layers of interwoven to parallel, colorless to yellowish, smooth, thin-walled, long-celled hyphae 2.5–4 µm wide; hypocutis composed of parallel, colorless to yellowish brown, cylindrical, thin-walled hyphae 12.5–20 µm wide. *Clamp connections* common in all parts of basidioma.

**Habitat/host.** Summer to autumn. Solitary on soil in subtropical broad-leaved forests with trees of Fagaceae.

**Distribution.** Currently known from southwestern China.

**Additional specimen examined.** CHINA • Yunnan Province: Pu'er City, Jingdong Yi Autonomous County, Ailao Mountain Subtropical Forest Ecosystem Research Station, Chinese Academy of Sciences, in a subtropical broad-leaved forest with trees of *Quercus*, 24°32.57'N, 101°1.62'E, elevation 2,424 m, 8 October 2021, Jian-Wei Liu 2440 (KUN-HKAS 145321).

**Notes.** *Cortinarius brunneoverrucosus* is characterized by its hemispherical, viscid, verrucose pileus, pale brown lamellae with a slightly pale pinkish tint, and relatively larger, broadly ellipsoid to ellipsoid basidiospores.

*Cortinarius brunneoverrucosus* is sister to *C. corrugatus* Peck, originally described from the highlands in the United States, under *Aalmia latifolia*, but *C. brunneoverrucosus* is only found in subtropical China, under trees of *Lithocarpus* or *Quercus*. Moreover, *C. corrugatus* differs from *C. brunneoverrucosus* by its convex to broadly convex pileus with distinctively corrugated-wrinkled, thinner stipe, amygdaliform, relatively narrower basidiospores (12–15 × 8–10 µm) (Peck 1872; Phillips 2010; Kuo 2020).

*Cortinarius brunneoverrucosus* belongs to sect. *Dulciolentes* Soop, a small section that has previously included only seven species, mainly distributed in Australia, inhabiting forests with Fagaceae, Nothofagaceae, and Myrtaceae (Soop et al. 2019). However, excluding *C. corrugatus*, which is from North America and is agaricoid, as mentioned earlier, three other species from Oceania, *C. peraurantiacus* Peintner & M.M. Moser, *C. pisciodorus* (E. Horak) Peintner & M.M. Moser, and *C. dulciolens* E. Horak, M.M. Moser, Peintner & Vilgalys, are all sequestrate (Moser 1983; Peintner et al. 2002a, 2002b; Soop et al. 2019). The discovery of *C. brunneoverrucosus* represents the first species of sect. *Dulciolentes* in China and the second agaricoid taxon within the section.



***Cortinarius coriaceus* Zhu L. Yang, Liu K. Jia & Zi R. Wang, sp. nov.**

MycoBank No: 857351

Fig. 3

**Etymology.** The epithet “*coriaceus*” (Lat.) refers to the brown pileus with a leathery texture of this species.

**Holotype.** CHINA • Yunnan Province: Lijiang City, Yulong Naxi Autonomous County, Lijiang Alpine Botanical Garden, in a subalpine temperate broad-leaved and coniferous mixed forest with trees of *Quercus* and *Pinus*, 27°0.21'N, 100°10.71'E, elevation 3,340 m, 7 August 2023, Dong-Mei Li 299 (KUN-HKAS 145316). GenBank: ITS: PQ772202, nrLSU: PQ772214.

**Diagnosis.** *Cortinarius coriaceus* looks like *C. odoritriganus* Niskanen, Liimat. & Ammirati, but differs in its emarginate lamellae, cylindrical stipe, and relatively larger basidiospores (Niskanen 2020).

**Description.** **Basidioma** medium-sized to large. **Pileus** 3 cm diam when young, 4.5–7 cm diam when mature, initially slightly campanulate, becoming plano-convex, occasionally with slightly subumbonate center, viscid, with a leathery texture; brown (6C4–6C7), paler (6A2–6A4) towards the center, covered with white (1A1) fibrillose squamules when young; pale brown to brown (6A4–6C4), pale brown (6A2), or dark brown (6D4–6D6) towards the center when mature; margin incurved, with innate radial brownish (6C2–6C3) stripes when young; context of pileus pale brown to brown (6A3–6B3, 6C6). **Lamellae** emarginate, medium-spaced ( $L = 38–52$ ,  $I = 27–36$ ), pale brown (6A4) with a faint pinkish (12A2) tint when young, later brown (6C4–6C7). **Stipe** 4.5–6 × 0.7–1.2 cm, cylindrical, dirty white (1A1–1B1) and pale violaceous (16A2–16A4), with more and more violaceous (16A4) tint towards the stipe apex when young, later dirty white (1A1–1B1), pale brown (6B2–6B4), covered with brown (6C6) to dark brown (6D6) fibrillose squamules; annulus cortinate; context of stipe dirty white (1A1–1B1) with brown (6C6); basal mycelium white (1A1).

**Basidiospores** [60/3/3]  $(10–)11.5–12.5(–14) \times (5–)7.5–10 \mu\text{m}$ ,  $Q = 1.25–1.43(–1.66)$ ,  $av. = 12.06 \pm 0.85 \times 8.33 \pm 1.48 \mu\text{m}$ ,  $Q_{av.} = 1.48 \pm 0.24$ , ellipsoid to amygdaliform, moderately to strongly verrucose, inamyloid. **Basidia** 37.5–43 × 7.5–10  $\mu\text{m}$ , 4-spored, clavate. **Trama of lamellae** regular, composed of colorless to yellowish, smooth hyphae 12.5–15  $\mu\text{m}$  wide. **Cystidia** absent. **Pileipellis** duplex: epicutis weakly developed, 15–20  $\mu\text{m}$  thick, composed of only 2–3 layers of interwoven to parallel, colorless, smooth, thin-walled, long-celled hyphae 3–7.5  $\mu\text{m}$  wide; hypocutis composed of interwoven to parallel, colorless, cylindrical, thin-walled hyphae 12.5–17.5  $\mu\text{m}$  wide. **Clamp connections** common in all parts of basidioma.

**Habitat/host.** Summer. Solitary or gregarious on soil in subalpine temperate broad-leaved and coniferous mixed forests with trees of *Quercus* and *Pinus*.

**Distribution.** Currently known from southwestern China.

**Additional specimens examined.** CHINA • Yunnan Province: Lijiang City, Yulong Naxi Autonomous County, Lijiang Alpine Botanical Garden, in a subalpine temperate broad-leaved and coniferous mixed forest with trees of *Quercus* and *Pinus*, 27°0.21'N, 100°10.71'E, elevation 3,340 m, 7 August 2023, Guan-Rui Li 328 (KUN-HKAS 145314), same place and date, Guan-Rui Li 333 (KUN-HKAS 145315).

**Notes.** *Cortinarius coriaceus* is characterized by its brown, leathery-wrinkled pileus, pinkish-tinted lamellae, and relatively larger basidiospores.



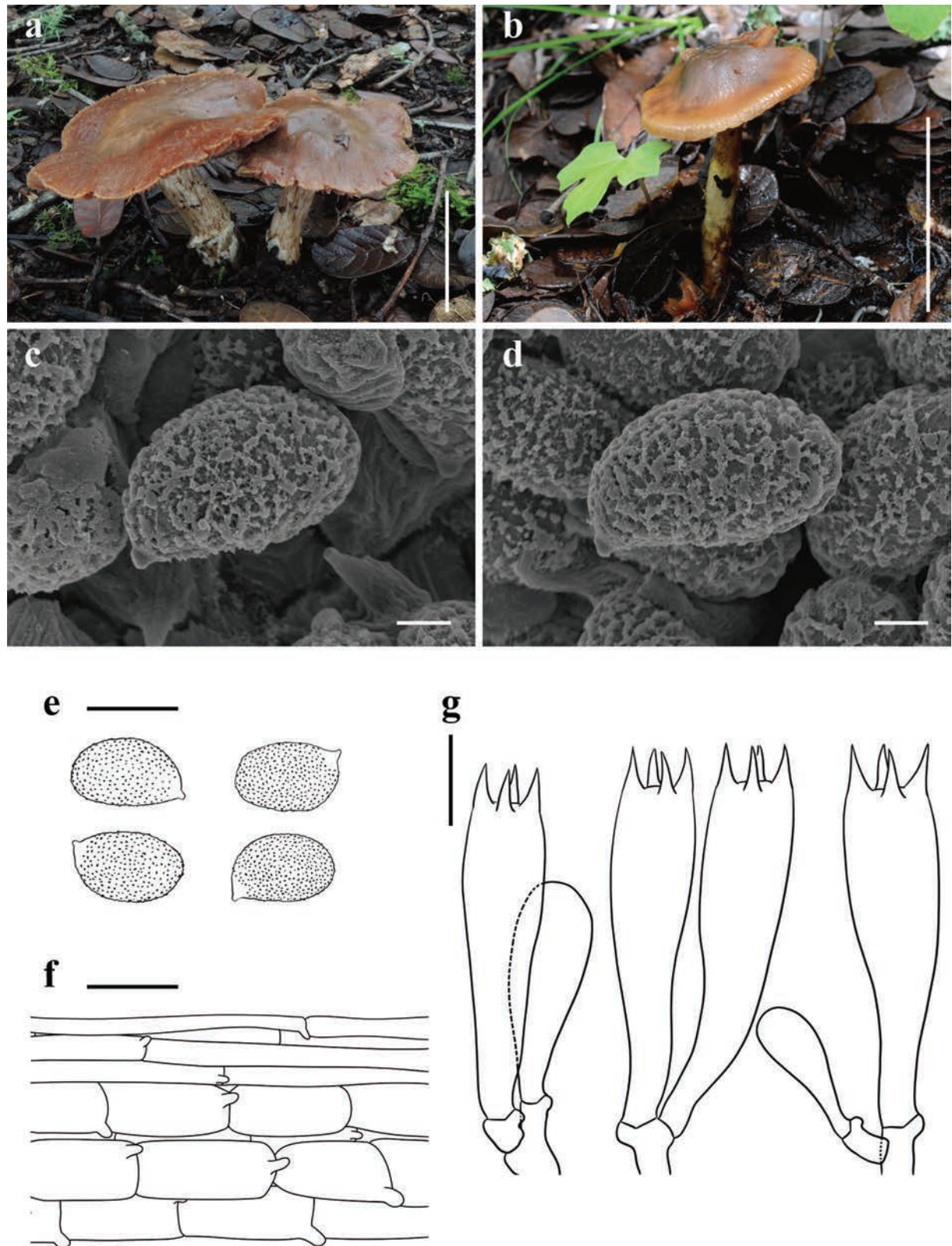


**Figure 3.** *Cortinarius coriaceus* (a, c–g KUN-HKAS 145136, Holotype b KUN-HKAS 145314) a, b basidiomata c–e basidiospores f pileipellis g basidia; and marginal sterile cells. Scale bars: 5 cm (a, b); 2 μm (c, d); 10 μm (e); 20 μm (f, g).

*Cortinarius coriaceus* is phylogenetically closely related to and morphologically similar to *C. odoritraganus*, known from Eastern North America and Costa Rica, in mixed temperate forest with *Abies* and *Betula* or mountain *Quercus* forest.

However, *C. odoritranganus* differs in its paler pileus, adnexed, purple-brown to brown lamellae, longer and thicker stipe (5–10 × 1–2 cm), and relatively smaller basidiospores (9.5–11.5 × 6–7.5 µm) (Niskanen 2020). *Cortinarius niveotraganus* Kytöv., Niskanen & Liimat., another related species, is distinguished by its hemispherical to broadly convex pileus, initially white to greyish white lamellae with bluish tints, clavate stipe, relatively smaller basidiospores (8.6–10.9 × 5.2–6.3 µm), and occurrence in planted *Betula* forests (Niskanen 2014).

***Cortinarius fuscocandidus* Zhu L. Yang, Liu K. Jia & Zi R. Wang, sp. nov.**

MycoBank No: 857352

Fig. 4

**Etymology.** The epithet “*fuscocandidus*” (Lat.) refers to the dark brown pileus with a white margin of this species.

**Holotype.** CHINA • Yunnan Province: Lijiang City, Ninglang Yi Autonomous County, Xinyingpan Township, in a subalpine temperate broad-leaved and coniferous mixed forest with trees of *Quercus* and *Pinus*, 27°9.9'N, 100°55.63'E, elevation 2,700 m, 7 August 2011, Qing Cai 602 (KUN-HKAS 70198). GenBank: ITS: PQ772210, nrLSU: PQ772222.

**Diagnosis.** *Cortinarius fuscocandidus* resembles *C. fulvopaludosus* Kytöv., Niskanen & Liimat. (Liimatainen 2017), but differs in its white margin, more robust stipe, and broadly ellipsoid to amygdaliform basidiospores.

**Description.** **Basidioma** small. **Pileus** 1.8–2 cm diam, applanate to plano-convex with a papilla, viscid; dark brown (6E7); margin white (1A1), sparsely covered with brown (6C6) fibrillose squamules; context of pileus brown (6D7). **Lamellae** emarginate with decurrent tooth, medium-spaced (L = 25–33, I = 9–12), pale brown (6B4) with a somewhat pale violaceous (16A2) tint. **Stipe** 5–7 × 0.3–0.6 cm, cylindrical, white (1A1) with a somewhat pale violaceous (16A2) tint, pale brown (6B2–6B4) when damaged; annulus cortinate; context of stipe not observed; basal mycelium white (1A1) with a somewhat pale violaceous (16A2) tint.

**Basidiospores** [60/2/2] 7.5–10.5 × (5–)7–10 µm, Q = 1.07–1.5(–1.65), av. = 8.19 ± 1.24 × 6.99 ± 1.26 µm, Qav. = 1.29 ± 0.18, broadly ellipsoid to amygdaliform, occasionally subglobose, strongly verrucose, inamyloid. **Basidia** 20–22.5 × 7.5–10 µm, 4-spored, clavate. **Trama of lamellae** regular, composed of colorless, smooth hyphae 7.5–10 µm wide. **Cystidia** absent. **Pileipellis** duplex: epicutis weakly developed, 11–15 µm thick, gelatinous, composed of interwoven to parallel, colorless, smooth, thin-walled, long-celled hyphae 2.5–5 µm wide, with brownish incrustation; hypocutis composed of only 3–5 layers of interwoven to parallel, colorless, cylindrical, thin-walled hyphae 7.5–15 µm wide. **Clamp connections** common in all parts of basidioma.

**Habitat/host.** Summer. Gregarious on soil in subalpine temperate broad-leaved and coniferous mixed forests with trees of *Quercus* and *Pinus*.

**Distribution.** Currently known from southwestern China.

**Additional specimen examined.** CHINA • Yunnan Province: Lijiang City, Gu-cheng District, Jinshan Township, in a subalpine temperate broad-leaved and coniferous mixed forest with trees of *Quercus* and *Pinus*, 26°54.55'N, 100°18.44'E, elevation 2,145 m, 28 July 2011, Li-Ping Tang 1331 (KUN-HKAS 69792).



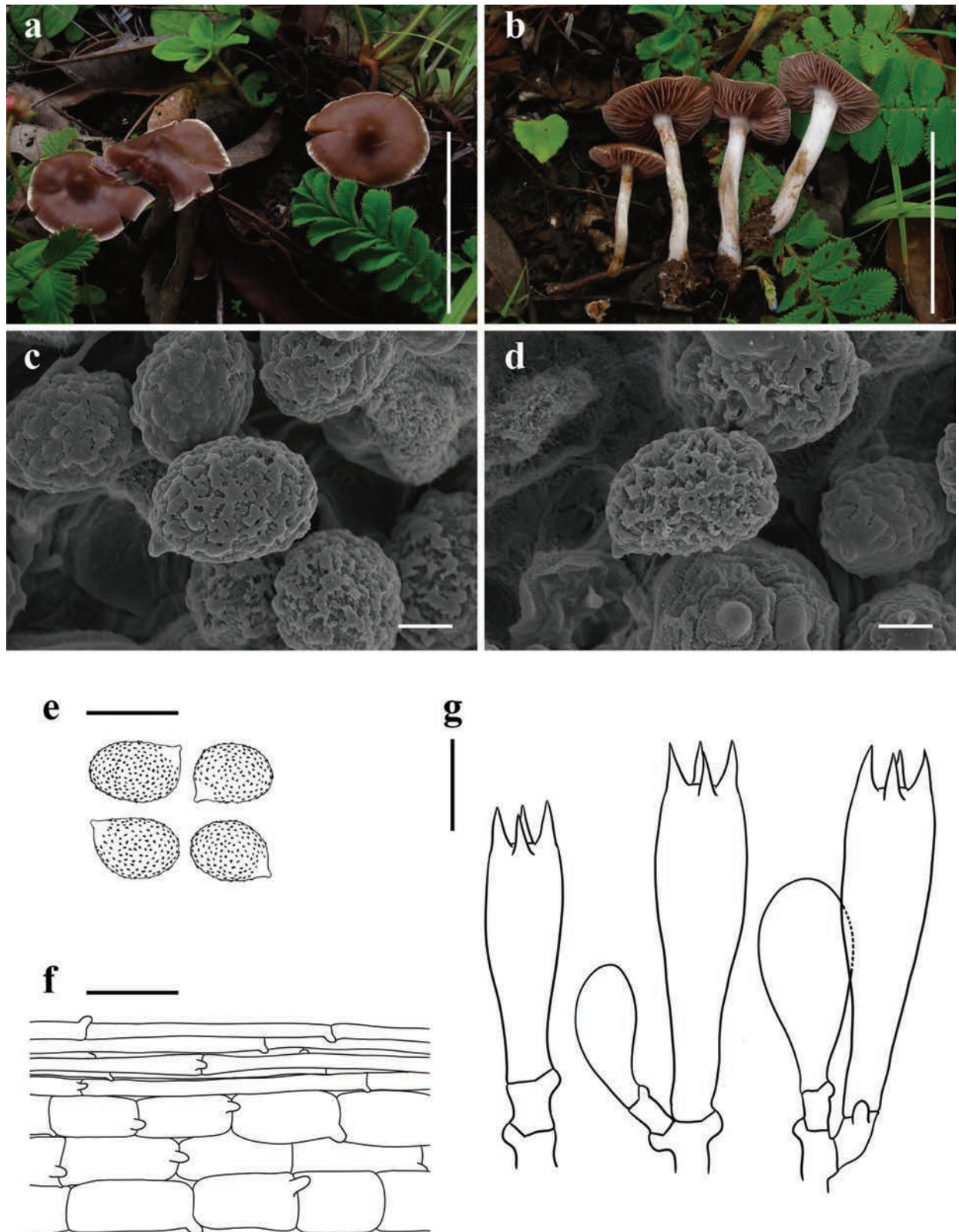


**Figure 4.** *Cortinarius fuscocandidus* (a–g KUN-HKAS 70198, Holotype) **a, b** basidiomata **c–e** basidiospores **f** pileipellis **g** basidia; and marginal sterile cells. Scale bars: 5 cm (**a, b**); 2  $\mu\text{m}$  (**c, d**); 10  $\mu\text{m}$  (**e**); 20  $\mu\text{m}$  (**f, g**).

**Notes.** *Cortinarius fuscocandidus* is characterized by its dark brown, papillate pileus with a white margin, pale brown lamellae with a somewhat pale violaceous tint, and broadly ellipsoid basidiospores.

Phylogenetically, *C. fuscocandidus* belongs to sect. *Hinnulei* and is closely related to *C. fulvopaludosus*. However, the phylogenetic tree shows low support between these two similar species, which can only be distinguished by their margin coloration and basidiospore size (Liimatainen 2017).

Morphologically, *C. fuscocandidus* looks like a typical member of sect. *Hinnulei* (Fries 1838; Bidaud et al. 2012; Li et al. 2016; Liimatainen et al. 2017; 2020), where the overall coloration of the pileus is brown to dark brown. However, the white margin, somewhat pale violaceous lamellae, and broadly ellipsoid basidiospores ( $7.5\text{--}10.5 \times (5\text{--})7\text{--}10\ \mu\text{m}$ ) differentiate it from the most similar species, *C. badioflavidus* Ammirati et al., which has brown to rich brown lamellae and narrower basidiospores ( $8.1\text{--}10.5 \times 5.8\text{--}6.5\ \mu\text{m}$ ) (Li et al. 2016).

***Cortinarius neodisjungendus* Zhu L. Yang, Liu K. Jia & Zi R. Wang, sp. nov.**

MycoBank No: 857353

Fig. 5

**Etymology.** The epithet “*neodisjungendus*” (Lat.) refers to its similarity to *C. disjungendus*.

**Holotype.** CHINA • Yunnan Province: Pu’er City, Jingdong Yi Autonomous County Ailao Mountain Subtropical Forest Ecosystem Research Station, Chinese Academy of Sciences, in a subtropical broad-leaved forest with trees of *Quercus*,  $24^{\circ}32.57'\text{N}$ ,  $101^{\circ}1.62'\text{E}$ , elevation 2,532 m, 8 October 2021, Jian-Wei Liu 2505 (KUN-HKAS 145322). GenBank: ITS: PQ772207, nrLSU: PQ772219.

**Diagnosis.** *Cortinarius neodisjungendus* differs from other species within sect. *Disjungendi* by its plano-convex pileus with an umbo, pale brown coloration, and relatively larger basidiospores (Karsten 1893; Niskanen 2014; Liimatainen et al. 2015).

**Description.** **Basidioma** medium-sized. **Pileus** 3.5–4.2 cm diam, applanate to plano-convex with an umbonate center, viscid with hygrophanous streaks; pale brown to brown (6D3–6D4), dark brown (6E6) towards the center, white (1A1) to pale brown (6B2) towards the margin, sparsely covered with white (1A1) fibrillose squamules; context not observed. **Lamellae** emarginate, crowded ( $L = 52\text{--}61$ ,  $I = 48\text{--}53$ ), pale brown (6B4) to brown (6D6). **Stipe** 8–10  $\times$  0.5–0.8 cm, cylindrical with a subbulbous base 1–1.5 cm wide, white (1A1) to pale brown (6B2–6B4), base sparsely covered with brown (6C5) fibrillose squamules; basal mycelium white (1A1).

**Basidiospores**  $[60/2/2]$   $11\text{--}13.5(-15) \times (5\text{--})7.5\text{--}9\ \mu\text{m}$ ,  $Q = 1.43\text{--}1.71(-2)$ ,  $av. = 12.73 \pm 0.93 \times 7.52 \pm 0.96\ \mu\text{m}$ ,  $Q_{av.} = 1.71 \pm 0.2$ , broadly amygdaliform, strongly verrucose, inamyloid. **Basidia**  $32.5\text{--}40 \times 7.5\text{--}10\ \mu\text{m}$ , 4-spored, clavate. **Trama of lamellae** regular, composed of colorless to brownish, smooth hyphae  $10\text{--}12.5\ \mu\text{m}$  wide. **Cystidia** absent. **Pileipellis** duplex: epicutis weakly developed,  $8.5\text{--}15\ \mu\text{m}$  thick, composed of only 3–5 layers of interwoven to parallel, colorless to brownish, smooth, thin-walled, long-celled hyphae  $2.5\text{--}5\ \mu\text{m}$  wide; hypocutis composed of interwoven to parallel, colorless to pale brownish, cylindrical, thin-walled hyphae  $12.5\text{--}15\ \mu\text{m}$  wide. **Clamp connections** common in all parts of basidioma.

**Habitat/host.** Autumn. Solitary on soil in subtropical broad-leaved forests with trees of *Quercus*.

**Distribution.** Currently known from southwestern China.



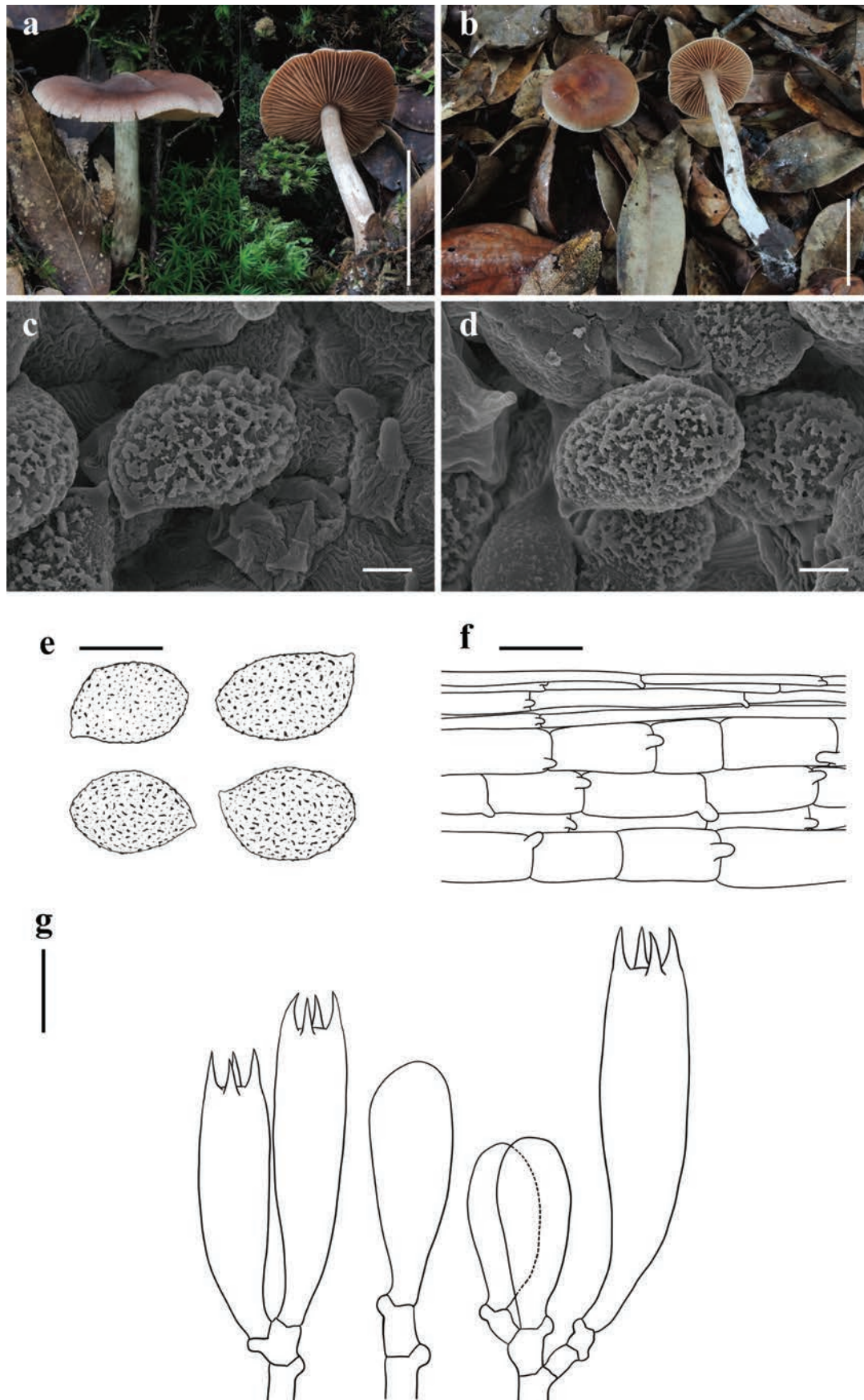


**Figure 5.** *Cortinarius neodisjungendus* (**a, c–g** KUN-HKAS 145322, Holotype **b** KUN-HKAS 145323) **a, b** basidiomata **c–e** basidiospores **f** pileipellis **g** basidia; and marginal sterile cells. Scale bars: 5 cm (**a, b**); 2  $\mu$ m (**c, d**); 10  $\mu$ m (**e**); 20  $\mu$ m (**f, g**).

**Additional specimen examined.** CHINA • Yunnan Province: Pu'er City, Jingdong Yi Autonomous County Ailao Mountain Subtropical Forest Ecosystem Research Station, Chinese Academy of Sciences, in a subtropical broad-leaved forest with trees of *Quercus*, 24°32.57'N, 101°1.62'E, elevation 2,532 m, 8 October 2021, Jian-Wei Liu 2529 (KUN-HKAS 145323).

**Notes.** *Cortinarius neodisjungendus* is characterized by its hygrophanous, pale brown to brown pileus with a whitish margin, whitish stipe, and relatively larger basidiospores. All other species in sect. *Disjungendi* have a brownish pileus lacking a white margin, a brown stipe, and smaller basidiospores (range from 9–11 µm long, 6–7 µm wide) (Karsten 1893; Niskanen 2014; Liimatainen et al. 2015, 2020).

***Cortinarius sinoconfirmatus* Zhu L. Yang, Liu K. Jia & Zi R. Wang, sp. nov.**

MycoBank No: 857354

Fig. 6

**Etymology.** The epithet “*sinoconfirmatus*” (Lat.) refers to the species in China that is similar to *C. confirmatus*.

**Holotype.** CHINA • Yunnan Province: Lijiang City, Yulong Naxi Autonomous County, Taian Township, in a subalpine temperate coniferous forest with trees of *Pinus*, 26°48.91'N, 100°5.96'E, elevation 2,633 m, 9 August 2023, Zi-Rui Wang 160 (KUN-HKAS 145320). GenBank: ITS: PQ772205, nrLSU: PQ772217.

**Diagnosis.** *Cortinarius sinoconfirmatus* looks like *C. confirmatus* Rob. Henry, but differs in its dark brown pileus center, more brown lamellae, thinner stipe, and larger basidiospores (Henry 1983; Mahiques et al. 2001; Ortega et al. 2007; Liimatainen et al. 2017).

**Description.** **Basidioma** medium-sized. **Pileus** 1.2 cm diam when young, 3–4.3 cm diam when mature, hemispherical when young, later convex, viscid; pale brown (6B2–6B4) to brown (5C6–5C7), covered with white (1A1) fibrillose squamules when young; brown (6C4–6C6), pale brown (6B2–6B4) towards the margin, dark brown (6E7) towards the center when mature; margin covered with brown (6C7) fibrillose squamules; context of pileus gelatinous, pale brown (6B2–6B4) to brown (6C7). **Lamellae** emarginate, crowded (L = 74–95, l = 46–52), pale brown (6B2–6B3) with a faint pinkish (12A2) tint when young, later brown (6B6–6C6). **Stipe** 5–7 × 0.5–0.7 cm, cylindrical, dirty white (1A1–1B1), pale brown (6B2–6B3) to brown (6C6), with a pale violaceous (16A2–16A3) tint at the stipe apex when young, later the upper 1/2 stipe dirty white, pale brown (6B2–6B3) to brown (6C6) with a pale violaceous (16A2–16A3) tint, covered with brown (7C4) fibrillose squamules, the lower 1/2 brown to dark brown (7B4–7E4); context of stipe dirty white (1A1–1B1) and brown (7C6); basal mycelium white (1A1).

**Basidiospores** [60/3/3] 7.5–11.5 × 4–5(6) µm, Q = (1.5–)2–3.13, av. = 9.92 ± 1.19 × 4.85 ± 0.59 µm, Qav. = 2.06 ± 0.28, ellipsoid to narrowly ellipsoid, moderately to strongly verrucose, inamyloid. **Basidia** 27.5–35 × 5–7.5 µm, 4-spored, clavate. **Trama of lamellae** regular, composed of pale yellowish, smooth hyphae 12.5–15 µm wide. **Cystidia** absent. **Pileipellis** duplex: epicutis weakly developed, 10–14 µm thick, gelatinous, composed of only 2–4 layers of interwoven to parallel, colorless to pale yellow, smooth, thin-walled, long-celled hyphae 2.5–5 µm wide; hypocutis composed of interwoven to parallel, colorless, cylindrical, thin-walled hyphae 12.5–17.5 µm wide. **Clamp connections** common in all parts of basidioma.



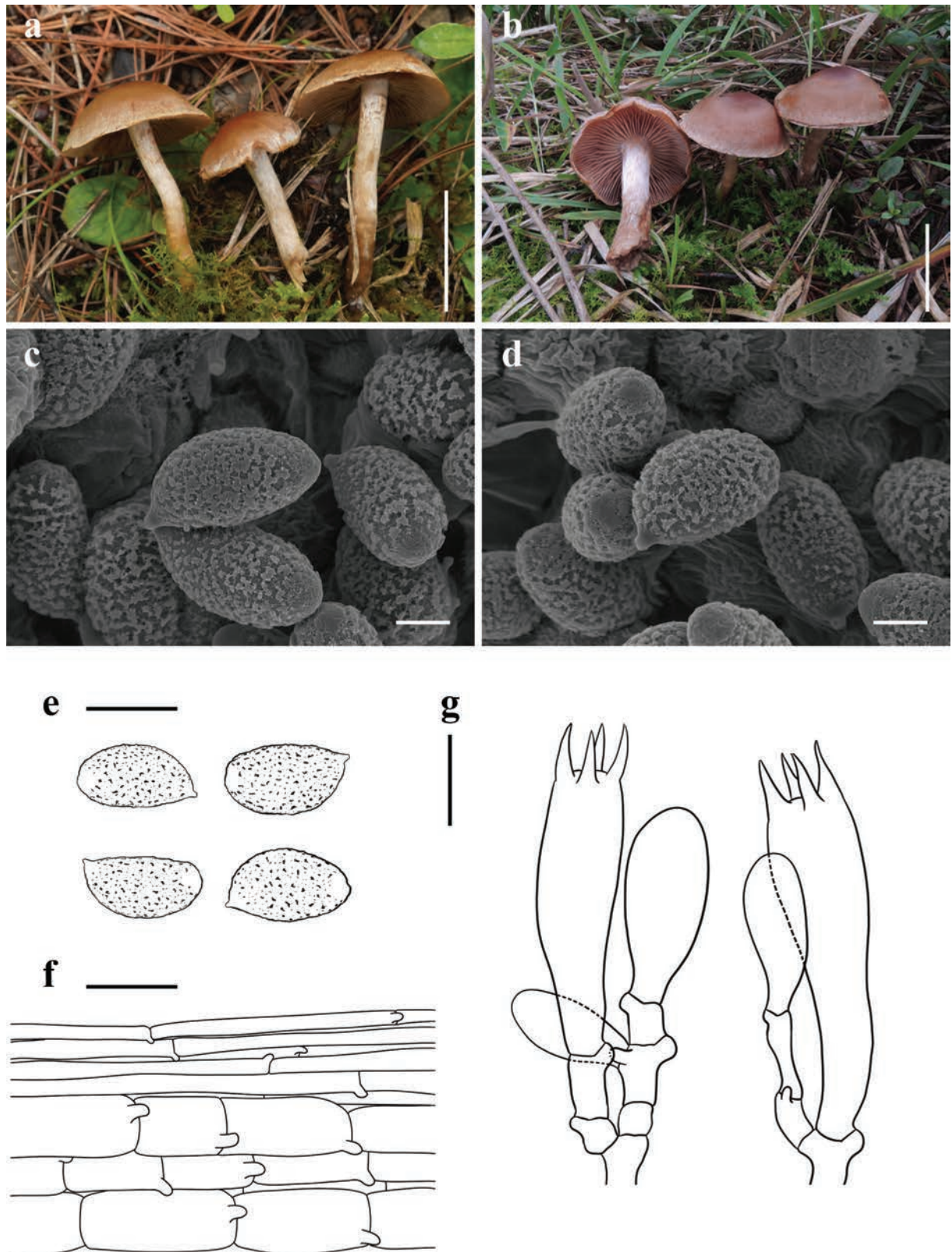


Figure 6. *Cortinarius sinoconfirmatus* (a, c–g KUN-HKAS 145320, Holotype b KUN-HKAS 145318) a, b basidiomata c–e basidiospores f pileipellis g basidia; and marginal sterile cells. Scale bars: 5 cm (a, b); 2  $\mu$ m (c, d); 10  $\mu$ m (e); 20  $\mu$ m (f, g).

**Habitat/host.** Summer. Gregarious on soil in subalpine temperate coniferous forests with trees of *Pinus*.

**Distribution.** Currently known from southwestern China.

**Additional specimens examined.** CHINA • Yunnan Province: Lijiang City, Yulong Naxi Autonomous County, Taian Township, in a subalpine temperate coniferous forest with trees of *Pinus*, 26°48.91'N, 100°5.96'E, elevation 2,633 m, 9 August 2023, Zi-Rui Wang 154 (KUN-HKAS 145319); same Township and date, 26°48.32'N, 100°4.35'E, elevation 2,700 m, Dong-Mei Li 331 (KUN-HKAS 145318).

**Notes.** *Cortinarius sinoconfirmatus* is closely related to *C. confirmatus*, but the latter differs from the former by its paler pileus with vinaceous or violaceous tints, paler, adnate lamellae, more robust stipe, and narrower basidiospores ( $8.8\text{--}10 \times 5.2\text{--}5.6\ \mu\text{m}$ ,  $Q = 1.55\text{--}1.9$ ) (Henry 1983; Mahiques et al. 2001; Ortega et al. 2007; Liimatainen et al. 2017). *Cortinarius sinoconfirmatus* is also closely related to *C. imbutus* Fr. and *C. saturninus* (Fr.) Fr. However, *C. imbutus* differs from *C. sinoconfirmatus* by its pale yellow pileus and whitish stipe with somewhat violaceous tint at the stipe apex (Fries 1838), and *C. saturninus* differs from *C. sinoconfirmatus* by its dark reddish brown pileus, violet stipe with purplish red squamules (Fries 1838).

Morphologically, *C. sinoconfirmatus* looks like *C. lucorum* (Fr.) E. Berger, but the latter differs from the former by its pileus with marble-like stripes and more prominent bulbous stipe base (Bidaud et al. 2000; Matheny and Ammirati 2006).

## Discussion

### Phylogenetics of five new species within *Cortinarius*

In this study, five species of *Cortinarius* are described as new to science based on phylogenetic evidence and morphological characteristics. Our phylogenetic tree reveals that four of these species—*C. coriaceus*, *C. fuscocandidus*, *C. neodisjungendus*, and *C. sinoconfirmatus*—belong to subgen. *Telamonia*, while the relationships between *C. coriaceus* and *C. niveotraganus*, as well as *C. sinoconfirmatus* and *C. confirmatus*, have been resolved (Fig. 1). The phylogenetic position of *C. fuscocandidus* remains uncertain. Additionally, *C. brunneoverrucosus* is assigned to sect. *Dulciolentes* (Fig. 1), a small section not yet placed in any subgenus of *Cortinarius* (Liimatainen et al. 2022). *Cortinarius neodisjungendus* forms a strongly sister clade (98.8/99/1.00) with other species within sect. *Disjungendi*, but differs by its whitish margin and whitish stipe (Karsten 1893; Liimatainen et al. 2015, 2020).

### Ecological distribution of five new species within *Cortinarius*

Ecologically, the five species fall into two categories: *Cortinarius coriaceus*, *C. fuscocandidus*, and *C. sinoconfirmatus* inhabit subalpine temperate areas, whereas *C. brunneoverrucosus* and *C. neodisjungendus* are restricted to subtropical areas. Notably, within sect. *Dulciolentes*, three sequestrate species—*C. peraurantiacus*, *C. pisciodorus*, and *C. dulciolens*—are known only from Oceania, while the agaricoid *C. corrugatus* occurs in North America (Peck 1872; Moser 1983; Peintner et al. 2002a, 2002b; Phillips 2010; Soop et al. 2019; Kuo 2020). The discovery of *C. brunneoverrucosus* in China represents the first record of sect. *Dulciolentes* in East Asia. Furthermore, the agaricoid basidioma of *C. brunneoverrucosus* provides evidence of biogeographic linkages between North America and East Asia.



## Acknowledgments

The authors thank Dr. Li-Ping Tang, Dr. Qing Cai, Dr. Yang-Yang Cui, Dr. Jian-Wei Liu, Ms. Dong-Mei Li, and Ms. Guan-Rui Li (Kunming Institute of Botany, Chinese Academy of Sciences) for providing valuable specimens on loan, and Mr. Zhi-Jia Gu (Kunming Institute of Botany) for assistance with SEM. The authors are grateful to Ms. Xue Xiao (Yunnan Agricultural University) and Mr. Jing-Jie Chen (Yunnan University) for experimental support and contributions to phylogenetic analyses.

## Additional information

### Conflict of interest

The authors have declared that no competing interests exist.

### Ethical statement

No ethical statement was reported.

### Funding

This study was supported by the Yunnan Revitalization Talent Support Program: Science & Technology Champion Project (202305AB350004) and the Joint Funds of the National Natural Science Foundation of China and Yunnan Provincial Government (U2202205).

### Author contributions

Zhu L. Yang conceived and designed the study. Liu-Kun Jia and Zi-Rui Wang collected specimens from China and generated the DNA sequence data. Zhu L. Yang, Liu-Kun Jia, and Zi-Rui Wang analyzed the data and checked issues related to nomenclatural articles. Liu-Kun Jia and Zi-Rui Wang wrote the manuscript draft. Zhu L. Yang, Liu-Kun Jia, and Zi-Rui Wang revised the draft.

### Author ORCIDs

Liu-Kun Jia  <https://orcid.org/0000-0002-3180-5077>

Zi-Rui Wang  <https://orcid.org/0000-0003-4564-1904>

Zhu-Liang Yang  <https://orcid.org/0000-0001-9745-8453>

### Data availability

Sequence alignments were deposited in TreeBASE (Study ID: TB2:S31924; URL: <http://purl.org/phylo/treebase/phyloids/study/TB2:S31924>). DNA sequences (Table 2) are available in GenBank (<https://www.ncbi.nlm.nih.gov/genbank/>).

## References

- Ammirati J, Liimatainen K, Bojantchev D, Peintner U, Kuhnert-Finkernagel R, Cripps C, Dentinger B, Niskanen T (2021) *Cortinarius* subgenus *Leprocybe*, unexpected diversity and significant differences in species compositions between western and eastern North America. *Persoonia* 46: 216–239. <https://doi.org/10.3767/persoonia.2021.46.08>
- Bas C (1969) Morphology and subdivision of *Amanita* and a monograph of its section *Lepidella*. *Persoonia* 5(4): 285–573. <https://api.semanticscholar.org/CorpusID:83338510>
- Bidaud A, Carteret X, Patrick R, Moënné-Loccoz P, Eyssartier G, Henry R (2000) Atlas des Cortinaires. Fédération Mycologique et Botanique Dauphiné-Savoie, Marlioz, France, 399 pp.

- Bidaud A, Carteret X, Patrick R, Moënné-Loccoz P (2012) Atlas des Cortinaires. Fédération Mycologique et Botanique Dauphiné-Savoie, Marlioz, France, 1573 pp.
- Deng SQ (1963) Fungi of China. Science Press, Beijing, China.
- Fries EM (1838) *Epicrisis systematis mycologici, seu synopsis hymenomycetum*. Upsaliae, 296–306.
- Gardes M, Bruns TD (1993) ITS primers with enhanced specificity for basidiomycetes-application to the identification of mycorrhizae and rusts. *Molecular Ecology* 2(2): 113–118. <https://doi.org/10.1111/j.1365-294X.1993.tb00005.x>
- Garnica S, Weiss M, Oberwinkler F (2003) Morphological and molecular phylogenetic studies in South American *Cortinarius* species. *Mycological Research* 107(10): 1143–1156. <https://doi.org/10.1017/S0953756203008414>
- Garnica S, Weiß M, Oertel B, Oberwinkler FA (2005) framework for a phylogenetic classification in the genus *Cortinarius* (Basidiomycota, Agaricales) derived from morphological and molecular data. *Canadian Journal of Botany* 83(11): 1457–1477. <https://doi.org/10.1139/b05-107>
- Guindon S, Dufayard JF, Lefort V, Anisimova M, Hordijk W, Gascuel O (2010) New algorithms and methods to estimate maximum-likelihood phylogenies: Assessing the performance of PhyML3.0. *Systematic Biology* 59: 307–321. <https://doi.org/10.1093/sysbio/syq010>
- Hall TA (1999) BioEdit: A user-friendly biological sequence alignment editor and analysis program for Windows 95/98/NT. *Nucleic Acids Symposium Series* 41: 95–98. <https://doi.org/10.1021/bk-1999-0734.ch008>
- Henry R (1983) Cortinaires rares ou nouveaux. *Bulletin de la Société Mycologique de France* 99(1): 5–92.
- Hoang DT, Chernomor O, Haeseler AV, Minh BQ, Vinh LS (2018) UFBoot2: Improving the ultrafast bootstrap approximation. *Molecular Biology and Evolution* 35: 518–522. <https://doi.org/10.1093/molbev/msx281>
- Hopple JS, Vilgalys R (1994) Phylogenetic relationships among coprinoid taxa and allies based on data from restriction site mapping of nuclear rDNA. *Mycologia* 86(1): 96–107. <https://doi.org/10.1080/00275514.1994.12026378>
- Kalyaanamoorthy S, Minh BQ, Wong TKF, von Haeseler A, Jermini LS (2017) ModelFinder: Fast model selection for accurate phylogenetic estimates. *Nature Methods* 14: 587–589. <https://doi.org/10.1038/nmeth.4285>
- Karsten PA (1893) *Symbolae ad mycologiam fennicam. pars XXXII*. *Acta Soc Fauna Flora Fenn* 9: 1–11.
- Katoh K, Standley DM (2013) MAFFT multiple sequence alignment software version 7: Improvements in performance and usability. *Molecular Biology and Evolution* 30(4): 772–780. <https://doi.org/10.1093/molbev/mst010>
- Kirk PM, Cannon PF, Minter DW, Stalpers JA (2008) *Dictionary of the Fungi*, 10<sup>th</sup> edn. CABI Europe, Woking, United Kingdom.
- Kornerup A, Wanscher JH (1981) *Taschenlexikon der Farben: 1440 Farbnuancen Und 600 Farbnamen*, 3<sup>rd</sup> edn. Muster-Schmidt Verlag, Göttingen, Germany.
- Kuo M (2020) *Cortinarius corrugatus*. MushroomExpert.Com Web site. [https://www.mushroomexpert.com/cortinarius\\_corrugatus.html](https://www.mushroomexpert.com/cortinarius_corrugatus.html) [Access date: 1-12-2025]
- Li RG (1980) Useful and harmful fungi of Jilin Province. Jilin People's Press, Jilin, China.
- Li GJ, Hyde KD, Zhao RL, Hongsanan S, Abdel-Aziz FA, Abdel-Wahab MA, Alvarado P, Alves-Silva G, Ammirati JF, Ariyawansa HA, Baghela A, Bahkali AH, Beug M, Bhat DJ, Bojantchev D, Boonpratuang T, Bulgakov TS, Camporesi E, Boro MC, Ceska O, Chakraborty D, Chen JJ, Chethana KWT, Chomnunti P, Consiglio G, Cui BK, Dai DQ, Dai YC, Daranagama DA, Das K, Dayarathne MC, De Crop E, De Oliveira RJV, de Souza CAF, de Souza JI, Dentinger

- BTM, Dissanayake AJ, Doilom M, Drechsler-Santos ER, Ghobad-Nejhad M, Gilmore SP, Góes-Neto A, Gorczak M, Haitjema CH, Hapuarachchi KK, Hashimoto A, He MQ, Henske JK, Hirayama K, Iribarren MJ, Jayasiri SC, Jayawardena RS, Jeon SJ, Jerônimo GH, Jesus AL, Jones EBG, Kang JC, Karunarathna SC, Kirk PM, Konta S, Kuhnert E, Langer E, Lee HS, Lee HB, Li WJ, Li XH, Liimatainen K, Lima DX, Lin CG, Liu JK, Liu XZ, Liu ZY, Luangsa JJ-ard, Lücking R, Lumbsch HT, Lumyong S, Leaño EM, Marano AV, Matsumura M, McKenzie EHC, Mongkolsamrit S, Mortimer PE, Nguyen TTT, Niskanen T, Norphanphoun C, MA O'Malley, Parnmen S, Pawłowska J, Perera RH, Phookamsak R, Phukhamsakda C, Pires-Zottarelli CLA, Raspé O, Reck MA, Rocha SCO, de Santiago ALCMA, Senanayake IC, Setti L, Shang QJ, Singh SK, Sir EB, Solomon KV, Song J, Srikitikulchai P, Stadler M, Suetrong S, Takahashi H, Takahashi T, Tanaka K, Tang LP, Thambugala KM, Thanakitpipattana D, Theodorou MK, Thongbai B, Thummarukcharoen T, Tian Q, Tibpromma S, Verbeken A, Vizzini A, Vlasák J, Voigt K, Wanasinghe DN, Wang Y, Weerakoon G, Wen HA, Wen TC, Wijayawardene NN, Wongkanoun S, Wrzosek M, Xiao YP, Xu JC, Yan JY, Yang J, Yang SD, Hu Y, Zhang JF, Zhao J, Zhou LW, Peršoh D, Phillips AJL, Maharachchikumbura SSN (2016) Fungal diversity notes 253–366: Taxonomic and phylogenetic contributions to fungal taxa. *Fungal Diversity* 78: 1–237. <https://doi.org/10.1007/s13225-016-0366-9>
- Liimatainen K (2017) Index Fungorum no. 344. <https://www.indexfungorum.org/Publications/Index%20Fungorum%20no.344.pdf>
- Liimatainen K, Niskanen T, Dima B, Kytövuori I, Ammirati JF, Frøslev TG (2014) The largest type study of Agaricales species to date: Bringing identification and nomenclature of *Phlegmacium* (*Cortinarius*) into the DNA era. *Persoonia* 33(1): 98–140. <https://doi.org/10.3767/003158514X684681>
- Liimatainen K, Niskanen T, Ammirati JF, Kytövuori I, Dima B (2015) *Cortinarius*, subgenus *Telamonia*, section *Disjungendi*, cryptic species in North America and Europe. *Mycological Progress* 14: 1–8. <https://doi.org/10.1007/s11557-014-1016-9>
- Liimatainen K, Carteret X, Dima B, Kytövuori I, Bidaud A, Reumaux P, Niskanen T, Ammirati JF, Bellanger JM (2017) *Cortinarius* section *Bicolores* and section *Saturnini* (Basidiomycota, Agaricales), a morphogenetic overview of European and North American species. *Persoonia* 10(39): 175–200. <https://doi.org/10.3767/persoonia.2017.39.08>
- Liimatainen K, Niskanen T, Dima B, Ammirati JF, Kirk PM, Kytövuori I (2020) Mission impossible completed: Unlocking the nomenclature of the largest and most complicated subgenus of *Cortinarius*, *Telamonia*. *Fungal Diversity* 104: 291–331. <https://doi.org/10.1007/s13225-020-00459-1>
- Liimatainen K, Kim JT, Pokorny L, Kirk PM, Dentinger B, Niskanen T (2022) Taming the beast: A revised classification of Cortinariaceae based on genomic data. *Fungal Diversity* 112: 89–170. <https://doi.org/10.1007/s13225-022-00499-9>
- Long P, Zhou SY, Li SN, Liu FF, Chen ZH (2024) Three new species of *Cortinarius* section *Delibuti* (Cortinariaceae, Agaricales) from China. *MycKeys* 101: 143–162. <https://doi.org/10.3897/mycokeys.101.114705>
- Luo YX, Bau T (2021) *Cortinarius jiaoheensis* (Cortinariaceae), a new species of *Cortinarius* subgenus *Telamonia* section *Flexipedes*, from northeast China. *Phytotaxa* 494(1): 113–121. <https://doi.org/10.11646/phytotaxa.494.1.7>
- Mahiques R, Ortega A, Bidaud A (2001) *Cortinarius assiduus* (*Telamonia*, *Firmiores*), nouvelle espece de la zone mediterraneenne de la peninsule Iberique. *Bulletin de la Fédération Mycologique Dauphiné-Savoie* 162: 41–47.
- Mao XL (2000) The macrofungi in China. Henan Science and Technology Press, Zhengzhou, China.
- Mao XL (2009) Mushroom China. Science Press, Beijing, China.

- Mao XL, Zong YC (1988) The Mushroom Checklist of Mangshan, Hunan. *Edible Fungi* 4: 7–8.
- Matheny PB, Ammirati JF (2006) *Cortinarius lucorum* (Fr.) Karst., a *Populus* associate from North America. *Pacific Northwest Fungi* 1(4): 1–10. <https://doi.org/10.2509/pnwf.2006.001.004>
- Moser MM (1983) Keys to Agarics and Boleti (Polyporales, Boletales, Agaricales, Russulales). In: Kibby G (Ed.) *Plant S* (transl.). Roger Phillips, London, United Kingdom, 535 pp.
- Nguyen L, Schmidt HA, von Haeseler A, Minh BQ (2015) IQ-TREE: A fast and effective stochastic algorithm for estimating maximum-likelihood phylogenies. *Molecular Biology and Evolution* 32: 268–274. <https://doi.org/10.1093/molbev/msu300>
- Niskanen T (2014) Index Fungorum: Published Numbers 186: 1–2. <https://www.indexfungorum.org/Publications/Index%20Fungorum%20no.186.pdf>
- Niskanen T (2020) Index Fungorum: Published Numbers 6(438). <https://www.indexfungorum.org/Publications/Index%20Fungorum%20no.438.pdf>
- Ortega A, Vila J, Bidaud A, Mahiques R, Marco C (2007) Notes on four mediterranean *Cortinarius* fruiting in sclerophilous and heliophilous plant ecosystems. *Mycotaxon* 101: 137–147. <http://www.mycotaxon.com/vol/abstracts/101/101-137>
- Peck CH (1872) *Fungi*. In: Pruyn JVL, Corning E, Hoffman JT, et al. (Eds) *Twenty-fourth annual report of the New York State Museum of Natural History*. The Argus Company, Albany, United States, 59–108.
- Peintner U, Moser M, Vilgalys R (2002a) *Thaxterogaster* is a taxonomic synonym of *Cortinarius*: New combinations and new names. *Mycotaxon* 81: 177–184. <https://api.semanticscholar.org/CorpusID:89389682>
- Peintner U, Horak E, Moser M, Vilgalys R (2002b) *Rozites*, *Cuphocybe* and *Rapacea* are taxonomic synonyms of *Cortinarius*: New combinations and new names. *Mycotaxon* 83: 447–452. <http://www.mycotaxon.com/vol/abstracts/83/83.447>
- Peintner U, Moncalvo JM, Vilgalys R (2004) Toward a better understanding of the infrageneric relationships in *Cortinarius* (Agaricales, Basidiomycota). *Mycologia* 96(5): 1042–1058. <https://doi.org/10.1080/15572536.2005.11832904>
- Phillips R (2010) *Mushrooms and other fungi of North America*. Firefly Books, Richmond Hill, Canada, 319 pp.
- Ronquist F, Teslenko M, van der Mark P, Ayres DL, Darling A, Höhna S, Larget B, Liu L, Suchard MA, Huelsenbeck JP (2012) MrBayes 3.2: Efficient Bayesian phylogenetic inference and model choice across a large model space. *Systematic Biology* 61(3): 539–542. <https://doi.org/10.1093/sysbio/sys029>
- Soop K, Dima B, Cooper JA, Park D, Oertel B (2019) A phylogenetic approach to a global supraspecific taxonomy of *Cortinarius* (Agaricales) with an emphasis on the southern mycota. *Persoonia* 42(1): 261–290. <https://doi.org/10.3767/persoonia.2019.42.10>
- Suárez-Santiago VN, Ortega A, Peintner U, López-Flores I (2009) Study on *Cortinarius* subgenus *Telamonia* section *Hydrocybe* in Europe, with especial emphasis on Mediterranean taxa. *Mycological Research* 113(10): 1070–1090. <https://doi.org/10.1016/j.mycres.2009.07.006>
- Teng SC, Ou SH (1937) Additional fungi from China VII. *Sinensia* 8: 411–444.
- Vilgalys R, Hester M (1990) Rapid genetic identification and mapping of enzymatically amplified ribosomal DNA from several *Cryptococcus* species. *Journal of Bacteriology* 172(8): 4238–4246. <https://doi.org/10.1128/jb.172.8.4238-4246.1990>
- Wei TZ, Yao YJ (2013) *Cortinarius korffii*, a new species from China. *Junwu Xuebao* 32(3): 557–562. <https://manu40.magtech.com.cn/Jwx/b/EN/Y2013/V32/I3/557>



- White TJ, Bruns T, Lee S, Taylor J (1990) Amplification and direct sequencing of fungal ribosomal RNA genes for phylogenetics. In: Innis MA, Gelfand DH, Sninsky JJ, White TJ (Eds) PCR protocols: a guide to methods and applications. Academic Press, New York, United States, 315–322. <https://doi.org/10.1016/B978-0-12-372180-8.50042-1>
- Xie ML, Li D, Wei SL, Ji RQ, Li Y (2019) *Cortinarius subcaesiobrunneus* sp. nov., (Cortinariaceae, Agaricales) a new species from northwest China. *Phytotaxa* 392(3): 217–224. <https://doi.org/10.11646/phytotaxa.392.3.4>
- Xie ML, Wei TZ, Fu YP, Li D, Qi LL, Xing PJ, Cheng GH, Ji RQ, Li Y (2020) Three new species of *Cortinarius* subgenus *Telamonina* (Cortinariaceae, Agaricales) from China. *Mycoclaves* 14(69): 91–109. <https://doi.org/10.3897/mycokeys.69.49437>
- Xie ML, Wei TZ, Dima B, Fu YP, Ji RQ, Li Y (2021a) *Cortinarius khinganensis* (Agaricales), a new species of section *Illumini* from Northeast China. *Phytotaxa* 500: 1–10. <https://doi.org/10.11646/phytotaxa.500.1.1>
- Xie ML, Chen JL, Phukhamsakda C, Dima B, Fu YP, Ji RQ, Wang K, Wei TZ, Li Y (2021b) *Cortinarius subsalor* and *C. tibeticisalor* spp. nov., two new species from the section *Delibuti* from China. *PeerJ* 9: e11982. <https://doi.org/10.7717/peerj.11982>
- Xie ML, Phukhamsakda C, Wei TZ, Li JP, Wang K, Wang Y, Ji RQ, Li Y (2022) Morphological and phylogenetic evidence reveal five new *Telamonioideae* species of *Cortinarius* (Agaricales) from East Asia. *Journal of Fungi* 8(3): 257. <https://doi.org/10.3390/jof8030257>
- Xie ML, Li Y, Wang K, Ji RQ, Wei TZ (2023) *Cortinarius liyui* sp. nov., a new species of *Cortinarius* sect. *Liyuorum* sect. nov. from China. *Mycosystema* 42(1): 244–251. <https://doi.org/10.13346/j.mycosystema.220421>
- Ying JZ, Zang M (1994) Large Economic Fungi in Southwest China. Science Press, Beijing, China.
- Yuan HS, Lu X, Dai YC, Hyde KD, Kan YH, Kušan I, He SH, Liu NG, Sarma VV, Zhao CL, Cui B-K, Yousaf N, Sun G, Liu S-Y, Wu F, Lin C-G, Dayarathne MC, Gibertoni TB, Conceição LB, Garibay-Orijel R, Villegas-Ríos M, Salas-Lizana R, Wei T-Z, Qiu J-Z, Yu Z-F, Phookamsak R, Zeng M, Paloi S, Bao D-F, Abeywickrama PD, Wei D-P, Yang J, Manawasinghe IS, Harishchandra D, Brahmanage RS, de Silva NI, Tennakoon DS, Karunarathna A, Gafforov Y, Pem D, Zhang S-N, de Azevedo Santiago ALCM, Bezerra JDP, Dima B, Acharya K, Alvarez-Manjarrez J, Bahkali AH, Bhatt VK, Brandrud TE, Bulgakov TS, Camporesi E, Cao T, Chen Y-X, Chen Y-Y, Devadatha B, Elgorban AM, Fan L-F, Du X, Gao L, Gonçalves CM, Gusmão LFP, Huanraluek N, Jadan M, Jayawardena RS, Khalid AN, Langer E, Lima DX, de Lima NC-Júnior, de Lira CRS, Liu J-K(J), Liu S, Lumyong S, Luo Z-L, Matočec N, Niranjana M, JRC Oliveira-Filho, Papp V, E P-Pazos, Phillips AJL, Qiu P-L, Ren Y, RFC Ruiz, Semwal KC, Soop K, de Souza CAF, Souza-Motta CM, Sun L-H, Xie M-L, Yao Y-J, Zhao Q, Zhou L-W (2020) Fungal diversity notes 1277–1386: Taxonomic and phylogenetic contributions to fungal taxa. *Fungal Diversity* 104: 1–266. <https://doi.org/10.1007/s13225-020-00461-7>
- Zang M (1996) Fungi of the Hengduan Mountains. Science Press, Beijing, China.
- Zhang QY, Jin C, Zhou HM, Ma ZY, Zhang YZ, Liang JQ, Si J, Li HJ (2023) Enlargement of the knowledge of *Cortinarius* section *Anomali* (Agaricales, Basidiomycota): Introducing three new species from China. *Frontiers in Cellular and Infection Microbiology* 13: 1–15. <https://doi.org/10.3389/fcimb.2023.1215579>
- Zhou SY, Long P, Yang ZL (2023) Three new species and a new record of *Cortinarius* section *Camphorati* from southwestern China. *Mycologia* 115(6): 904–917. <https://doi.org/10.1080/00275514.2023.2251365>

# Three novel species of *Alternaria* (Pleosporales, Pleosporaceae) from cereal crops (Poaceae) in China

Hai-Feng Liu<sup>1,2\*</sup>, Feng-Yin Liu<sup>1\*</sup>, Hai-Yan Ke<sup>1</sup>, Qing-Xiao Shi<sup>1</sup>, Jian-Xin Deng<sup>1</sup>, Hyunkyu Sang<sup>2</sup>

<sup>1</sup> Department of Plant Protection, College of Agriculture, Yangtze University, Jingzhou 434025, China

<sup>2</sup> Department of Integrative Food, Bioscience and Biotechnology, Chonnam National University, Gwangju, 61186, Republic of Korea

Corresponding authors: Jian-Xin Deng (djxin555@yangtzeu.edu.cn); Hyunkyu Sang (hksang@jnu.ac.kr)

## Abstract

The genus *Alternaria* (Pleosporales, Pleosporaceae) comprises saprophytes and pathogens that are widespread around the world. Currently, more than 400 species are recognized within this genus and are classified into 29 sections. In this study, *Alternaria* strains were isolated from diseased leaves of two cereal crops, rice (*Oryza sativa*) and maize (*Zea mays*) in China. These *Alternaria* spp. were characterized by morphological characterization and phylogenetic analysis using maximum likelihood and Bayesian inference with multiple loci (ITS, *GAPDH*, *RPB2*, *TEF1*, *Alt a 1*, *EndoPG*, and OPA10-2). Based on the above analyses, three novel species of *Alternaria* section *Alternaria* were introduced, namely *A. oryzicola* **sp. nov.**, *A. poae* **sp. nov.**, and *A. zeae* **sp. nov.** This study expands the species diversity of *Alternaria* associated with Poaceae plants in China.

**Key words:** Dematiaceous hyphomycetes, maize and rice diseases, morphology, new taxa, multigene phylogeny, taxonomy



## Academic editor:

Rungtiwa Phookamsak

Received: 31 December 2024

Accepted: 17 March 2025

Published: 16 April 2025

**Citation:** Liu H-F, Liu F-Y, Ke H-Y, Shi Q-X, Deng J-X, Sang H (2025) Three novel species of *Alternaria* (Pleosporales, Pleosporaceae) from cereal crops (Poaceae) in China. MycoKeys 116: 167–183. <https://doi.org/10.3897/mycokeys.116.145681>

**Copyright:** © Hai-Feng Liu et al.

This is an open access article distributed under terms of the Creative Commons Attribution License (Attribution 4.0 International – CC BY 4.0).

## Introduction

The genus *Alternaria* consists of more than 400 species of dematiaceous hyphomycetes (Li et al. 2022, Gou et al. 2023, Liao et al. 2023, Hyde et al. 2024). Species in this genus have been mainly described as saprophytes, endophytes, or phytopathogens and currently accommodated in the family Pleosporaceae (Hyde et al. 2024). Historically, taxonomy of *Alternaria* has gone through different stages since it was first established by Nees in 1816 (Lawrence et al. 2016). In brief, *Alternaria* and related genera, especially *Macrosporium* and *Stemphylium*, were confused in earlier stages. Although attempts were made by researchers to determine their taxonomic status, issues in nomenclature and generic boundaries persisted for a long time. Afterwards, a complete revision of taxa related to *Alternaria* based on sporulation patterns and conidial morphology was undertaken by Simmons (Simmons 2007), which accelerated the establishment of order in the nomenclature of alternarioid hyphomycetes.

Nowadays, a DNA-based molecular approach has been used to better understand taxonomy of *Alternaria* (Lawrence et al. 2016). A variety of loci have been used in the classification of this genus, such as the internal transcribed spacer

\* These authors contributed equally to this work and share first authorship.

(ITS) of the rDNA region, small subunit ribosomal RNA gene (SSU), large subunit ribosomal RNA gene (LSU), glyceraldehyde-3-phosphate dehydrogenase (*GAPDH*), second largest subunit of the RNA polymerase (*RPB2*), translation elongation factor 1- $\alpha$  (*TEF1*), *Alternaria* major allergen (*Alt a 1*), endopolygalacturonase gene (*EndoPG*), an anonymous genomic region (OPA10-2), calmodulin (*CAM*), and the plasma membrane ATPase gene (*ATP*). Based on multi-locus phylogenetic analysis, this genus consists of 29 sections (Gannibal et al. 2022, Li et al. 2023). Currently, both morphology and multi-locus phylogeny are crucial for the taxonomy of *Alternaria* spp. and have been widely employed in charactering novel species (Aung et al. 2024; He et al. 2024; Nwe et al. 2024; Bessadat et al. 2025).

*Alternaria* spp. have been associated with more than 4,000 host plants, ranking the genus 10<sup>th</sup> among the 100 most cited fungal genera (Lawrence et al. 2013; Woudenberg et al. 2013, 2015; Pinto and Patriarca 2017; Li et al. 2022; Bhunjun et al. 2024). Collectively, certain *Alternaria* spp. cause diseases that lead to economic losses in agricultural crops, including cereals, oil crops, fruits, and vegetables (Li et al. 2022; Haituk et al. 2023; Alasadi 2024). Cereal crops (Poaceae), such as wheat (*Triticum aestivum*), maize (*Zea mays*), and rice (*Oryza sativa*), have been widely cultivated and consumed since they are popular staple foods with most of the world's population. Infections on cereal crops caused by *Alternaria* spp. occur constantly and have attracted increasing attention worldwide (Tralamazza et al. 2018; Orina et al. 2021; Zhong et al. 2022). For instance, wheat black point is an important disease mainly caused by different *Alternaria* species (*A. alternata*, *A. infectoria*, and *A. tenuissima*), with *A. alternata* being isolated more frequently (Pinto and Patriarca 2017; Tralamazza et al. 2018). In addition, *A. triticina* has been considered as another important pathogen causing leaf blight on wheat (Mercado Vergnes et al. 2006; Amatulli et al. 2013). Recently, *A. alternata*, *A. tenuissima*, *A. burnsii*, and an unclassified species *Alternaria* sp. were identified as causal agents of leaf blight on maize in China (Xu et al. 2022). In rice, *A. padwickii* (Syn *Trichoconis padwickii*) has been frequently detected as a seed pathogen (Gutiérrez et al. 2010). Moreover, *A. arborescens* and *A. gaisen* were also reported as leaf spot pathogens of rice in Pakistan (Akhtar et al. 2014a, 2014b).

In this study, *Alternaria* spp. were isolated from symptomatic leaves of rice and maize in Guangxi Province and in Hainan Province in China, respectively. The aim of this study was to characterize these species taxonomically using morphological traits and multi-locus phylogenetic analysis.

## Materials and methods

### Isolation

In 2023, diseased maize (*Zea mays*) and rice (*Oryza sativa*) leaves exhibiting leaf spot and blight symptoms were collected in Guangxi and Hainan provinces, respectively. Leaf tissues were cut into small pieces with sterile blades and placed in petri dishes containing wet filter papers. After incubation at 25 °C for 1–2 days, fungal development on tissue samples were observed with a stereo microscope. Spores of *Alternaria* spp. developed from the edge of the leave tissues were singly picked using sterile glass needles and inoculated onto PDA

(potato dextrose agar, Difco, Montreal, Canada). Pure cultures were deposited in the Fungi Herbarium of Yangtze University in Jingzhou, China. Dried cultures of the strains were also preserved in the herbarium for long-term storage.

## Morphology

Colony characteristics of strains of *Alternaria* spp. were observed and recorded following 7 days of incubation at 25 °C on 90-mm PDA plates under dark conditions. To determine their conidial morphology, the strains were grown on potato carrot agar (PCA) and V8 juice agar (V8A) at 25 °C for 7 days under a photoperiod of 8 hours of light per day. Conidia of the strains were observed and imaged with an ECLIPSE Ni-U optical microscope (Nikon, Tokyo, Japan). The dimensions of the conidia were measured (n = 50). Conidial morphology was determined based on sporulation pattern and conidial characteristics.

## PCR amplification

Fresh mycelia of the fungal strains grown on PDA were harvested and used for genomic DNA extraction following the procedures described by Watanabe et al. (2010). DNA solutions were then used to amplify fragments from several gene regions, including ITS, *GAPDH*, *RPB2*, *TEF1*, *Alt a 1*, *EndoPG*, and OPA10-2. Polymerase chain reaction (PCR) amplification of the above-mentioned regions was performed by a Bio-Rad T100™ Thermal Cycler with primer pairs ITS5/ITS4 (White et al. 1990), *gpd1/gpd2* (Berbee et al. 1999), EF1-728F/EF1-986R (Carbone and Kohn 1999), *RPB2-5F/RPB2-7cR* (Liu et al. 1999), *Alt-for/Alt-rev* (Hong et al. 2005), *PG3/PG2b* (Andrew et al. 2009), and OPA10-2L/OPA10-2R (Andrew et al. 2009), respectively. Reaction conditions for the PCR amplification were referred to previous studies (Woudenberg et al. 2015, Nwe et al. 2024). Successful amplification products were sent to TSINGKE (Beijing, China) for purification and Sanger sequencing in both directions. Sequences obtained from the company were manually examined with BioEdit v7.0.9 (Hall 1999) and then trimmed using MEGA X (Kumar et al. 2018). Consensus sequences were deposited in GenBank (<https://www.ncbi.nlm.nih.gov/>) with accession numbers shown in Table 1. New species are established based on the recommendations outlined by Jeewon and Hyde (2016).

## Phylogenetic analysis

Nucleotide sequences generated in this study were subjected to BLASTn (<https://blast.ncbi.nlm.nih.gov/Blast.cgi>, accessed on 31 October 2024) for similarity searches against the NCBI nucleotide database. Reference sequences of *Alternaria* spp. used for phylogenetic analysis were obtained based on recent publications (Woudenberg et al. 2015; Li et al. 2022, 2023; Romain et al. 2022; Aung et al. 2024; Nwe et al. 2024). Phylogenetic analysis was performed using the OFPT (One-click Fungal Phylogenetic Tool) program developed by Zeng et al. (2023). In brief, sequences of each genetic region were aligned by MAFFT v7.307 online version (Katoh and Standley 2013; Katoh et al. 2019) and then trimmed using TrimAl (Capella-Gutiérrez et al. 2009). Subsequently, nucleotide substitution models of each dataset were tested by ModelFinder (Kalyaanamoorthy et



**Table 1.** GenBank accession numbers of *Alternaria* spp. used for phylogenetic analysis.

Species	Strain	ITS	Alt a 1	GAPDH	RPB2	TEF1	OPA10-2	EndoPG
<i>A. alstroemeriae</i>	CBS 118808	KP124296	KP123845	KP124153	KP124764	KP125071	KP124601	KP123993
<i>A. alstroemeriae</i>	CBS 118809 <sup>T</sup>	KP124297	–	KP124154	KP124765	KP125072	KP124602	KP123994
<i>A. alternantherae</i>	CBS 124392	KC584179	KP123846	KC584096	KC584374	KC584633	–	–
<i>A. alternata</i>	CBS 916.96 <sup>T</sup>	AF347031	AY563301	AY278808	KC584375	KC584634	KP124632	JQ811978
<i>A. alternata</i>	CBS 112249	KP124338	KP123886	KP124192	KP124806	KP125114	KP124648	KP124039
<i>A. arborescens</i>	CBS 119544 <sup>T</sup>	KP124408	KP123955	JQ646321	KP124878	KP125186	KP124722	KP124112
<i>A. arborescens</i>	CBS 102605 <sup>T</sup>	AF347033	AY563303	AY278810	KC584377	KC584636	KP124712	AY295028
<i>A. arctoseptata</i>	MFLUCC 21-0139 <sup>T</sup>	–	OK236755	OK236702	OK236655	OK236608	–	–
<i>A. baoshanensis</i>	MFLUCC 21-0124 <sup>T</sup>	MZ622003	OK236760	OK236706	OK236659	OK236613	–	–
<i>A. betae-kenyensis</i>	CBS 118810 <sup>T</sup>	KP124419	KP123966	KP124270	KP124888	KP125197	KP124733	KP124123
<i>A. brevicongiophora</i>	MFLUCC 21-0786 <sup>T</sup>	MZ621997	OK236751	OK236698	OK236651	OK236604	–	–
<i>A. burnsii</i>	CBS 118816	KP124423	KP123970	KP124273	KP124892	KP125201	KP124737	KP124127
<i>A. burnsii</i>	CBS 118817	KP124424	KP123971	KP124274	KP124893	KP125202	KP124738	KP124128
<i>A. burnsii</i>	CBS 107.38 <sup>T</sup>	KP124420	KP123967	JQ646305	KP124889	KP125198	KP124734	KP124124
<i>A. burnsii</i>	CBS 879.95	KP124422	KP123969	KP124272	KP124891	KP125200	KP124736	KP124126
<i>A. burnsii</i>	CBS 130264	KP124425	KP123972	KP124275	KP124894	KP125203	KP124739	KP124129
<i>A. burnsii</i>	CBS 110.50	KP124421	KP123968	KP124271	KP124890	KP125199	KP124735	KP124125
<i>A. burnsii</i>	CBS 108.27	KC584236	KP123850	KC584162	KC584468	KC584727	KP124605	KP123997
<i>A. eichhorniae</i>	CBS 489.92 <sup>T</sup>	KC146356	KP123973	KP124276	KP124895	KP125204	KP124740	KP124130
<i>A. ellipsoidialis</i>	MFLUCC 21-0132	MZ621989	OK236743	OK236690	OK236643	OK236596	–	–
<i>A. eupatoriicola</i>	MFLUCC 21-0122	MZ621982	OK236736	OK236683	OK236636	OK236589	–	–
<i>A. falcate</i>	MFLUCC 21-0123	MZ621992	OK236746	OK236693	OK236649	OK236599	–	–
<i>A. gaisen</i>	CBS 118488 <sup>R</sup>	KP124427	KP123975	KP124278	KP124897	KP125206	KP124743	KP124132
<i>A. gaisen</i>	CBS 632.93 <sup>R</sup>	KC584197	KP123974	KC584116	KC584399	KC584658	KP124742	AY295033
<i>A. gossypina</i>	CBS 104.32 <sup>T</sup>	KP124430	JQ646395	JQ646312	KP124900	KP125209	KP124746	KP124135
<i>A. gossypina</i>	CBS 102601	KP124433	KP123979	KP124282	KP124903	KP125212	KP124749	KP124138
<i>A. iridialustralis</i>	CBS 118487	KP124436	KP123982	KP124285	KP124906	KP125215	KP124752	KP124141
<i>A. iridialustralis</i>	CBS 118486 <sup>T</sup>	KP124435	KP123981	KP124284	KP124905	KP125214	KP124751	KP124140
<i>A. jacinthicola</i>	CBS 878.95	KP124437	KP123983	KP124286	KP124907	KP125216	KP124753	KP124142
<i>A. jacinthicola</i>	CPC 25267	KP124439	KP123985	KP124288	KP124909	KP125218	KP124755	KP124144
<i>A. jacinthicola</i>	CBS 133751 <sup>T</sup>	KP124438	KP123984	KP124287	KP124908	KP125217	KP124754	KP124143
<i>A. jingzhouensis</i>	YZU 221144 <sup>T</sup>	OR883772	OR887694	OR887690	OR887688	OR887686	OR887684	OR887692
<i>A. koreana</i>	SPL2-1 <sup>T</sup>	LC621613	LC631831	LC621647	LC621681	LC621715	LC631857	LC631844
<i>A. lathyri</i>	MFLUCC 21-0140 <sup>T</sup>	MZ621974	OK236728	OK236675	OK236628	OK236581	–	–
<i>A. lijiangensis</i>	YZU 221458 <sup>T</sup>	OQ679970	OQ686781	OQ686785	OQ686789	OQ686783	OQ686787	OQ686779
<i>A. longipes</i>	CBS 540.94 <sup>R</sup>	AY278835	AY563304	AY278811	KC584409	KC584667	KP124758	KP124147
<i>A. longipes</i>	CBS 121332 <sup>R</sup>	KP124443	KP123989	KP124292	KP124913	KP125222	KP124760	KP124149
<i>A. longiensis</i>	YZU 221221 <sup>T</sup>	OQ534546	OQ473629	OQ512732	OQ543009	OQ512726	OQ543003	OQ512720
<i>A. lycopersici</i>	YZU 221185 <sup>T</sup>	OQ519795	OQ473633	OQ512736	OQ543013	OQ512730	OQ543007	OQ512724
<i>A. macilenta</i>	MFLUCC 21-0138 <sup>T</sup>	MZ621972	OK236726	OK236673	OK236626	OK236579	–	–
<i>A. macroconidia</i>	MFLUCC 21-0134 <sup>T</sup>	MZ622001	OK236757	OK236704	OK236657	OK236610	–	–
<i>A. minimispora</i>	MFLUCC 21-0127 <sup>T</sup>	MZ621980	OK236734	OK236681	OK236634	OK236587	–	–
<i>A. momordicae</i>	YZU 161378 <sup>T</sup>	OR883774	OR887695	OR887691	OR887689	OR887687	OR887685	OR887693
<i>A. muriformispora</i>	MFLUCC 21-0784 <sup>T</sup>	MZ621976	OK236730	OK236677	OK236630	OK236583	–	–
<i>A. myanmarensis</i>	YZU 231736 <sup>T</sup>	OR897031	OR979657	OR963612	PP508256	OR963615	PP034184	OR979663
<i>A. oblongoellipsoidea</i>	MFLUCC 22-0074 <sup>T</sup>	MZ621967	OK236721	OK236668	OK236621	OK236574	–	–
<i>A. obpyricnidia</i>	MFLUCC 21-0121 <sup>T</sup>	MZ621978	OK236732	OK236680	OK236633	OK236585	–	–
<i>A. orobanches</i>	MFLUCC 21-0137 <sup>T</sup>	MZ622007	OK236763	OK236710	–	–	–	–
<b><i>A. oryzicola</i> sp. nov.</b>	<b>YZU 231199<sup>T</sup></b>	<b>PQ812549</b>	<b>PV155522</b>	<b>PV155536</b>	<b>PV155548</b>	<b>PV155528</b>	<b>PV155542</b>	<b>–</b>
<i>A. ovoidea</i>	MFLUCC 21-0782 <sup>T</sup>	MZ622005	–	OK236708	OK236661	OK236614	–	–
<i>A. phragmiticola</i>	MFLUCC 21-0125 <sup>T</sup>	MZ621994	OK236749	OK236696	OK236649	OK236602	–	–
<b><i>A. poae</i> sp. nov.</b>	<b>YZU 231197<sup>T</sup></b>	<b>PQ812551</b>	<b>PV155524</b>	<b>PV155538</b>	<b>PV155550</b>	<b>PV155530</b>	<b>PV155544</b>	<b>PV155532</b>
<b><i>A. poae</i> sp. nov.</b>	<b>YZU 231198</b>	<b>PQ812550</b>	<b>PV155523</b>	<b>PV155537</b>	<b>PV155549</b>	<b>PV155529</b>	<b>PV155543</b>	<b>PV155531</b>
<i>A. rostroconidia</i>	MFLUCC 21-0136 <sup>T</sup>	MZ621969	OK236723	OK236670	OK236623	OK236576	–	–
<i>A. salicicola</i>	MFLUCC 22-0072 <sup>T</sup>	MZ621999	OK236753	OK236700	OK236653	OK236606	–	–
<i>A. solanicola</i>	YZU 221189 <sup>T</sup>	OQ534548	OQ473631	OQ512734	OQ543011	OQ512728	OQ543005	OQ512722
<i>A. tomato</i>	CBS 103.30	KP124445	KP123991	KP124294	KP124915	KP125224	KP124762	KP124151
<i>A. tomato</i>	CBS 114.35	KP124446	KP123992	KP124295	KP124916	KP125225	KP124763	KP124152
<i>A. torilis</i>	MFLUCC 14-0433 <sup>T</sup>	MZ621988	OK236741	OK236688	OK236641	OK236594	–	–
<i>A. yamethinensis</i>	YZU 231739 <sup>T</sup>	OR889008	OR979655	OR963610	PP179253	OR963614	PP034182	OR979661
<b><i>A. zeae</i> sp. nov.</b>	<b>YZU 231602<sup>T</sup></b>	<b>PQ812548</b>	<b>PV155521</b>	<b>PV155535</b>	<b>PV155547</b>	<b>PV155527</b>	<b>PV155541</b>	<b>–</b>
<b><i>A. zeae</i> sp. nov.</b>	<b>YZU 231638</b>	<b>PQ812547</b>	<b>PV155520</b>	<b>PV155534</b>	<b>PV155546</b>	<b>PV155526</b>	<b>PV155540</b>	<b>–</b>
<b><i>A. zeae</i> sp. nov.</b>	<b>YZU 231640</b>	<b>PQ812546</b>	<b>PV155519</b>	<b>PV155533</b>	<b>PV155545</b>	<b>PV155525</b>	<b>PV155539</b>	<b>–</b>

al. 2017) and the best-fit model for each dataset was selected based on the Bayesian information criterion (BIC). All the datasets were concatenated with partition information and then used for maximum likelihood (ML) and Bayesian phylogenetic analyses with software IQ-TREE (Nguyen et al. 2015) and MrBayes 3.2.7 (Ronquist et al. 2012), respectively. In the ML analysis, 1,000 replicates were performed using bootstrap approximation. In the Bayesian inference (BI) analysis, a Markov Chain Monte Carlo (MCMC) algorithm was employed, involving four MCMC chains running for 50,000,000 generations with sampling every 100 generations. Posterior probabilities (PP) were estimated after discarding the first 25% of sampled tree as burn-in. The consensus BI tree was generated once the average standard deviation of split frequencies fell below 0.01.

## Results

### Phylogenetic analysis

A total of 63 strains (including 6 strains from this study) of *Alternaria* species in section *Alternaria*, were used for phylogenetic analysis. The concatenated sequence matrix consisted of seven loci, with a total length of 3608 bp, including 514 bp from ITS, 566 bp from *GAPDH*, 753 bp from *RPB2*, 234 bp from *TEF1*, 472 bp from *Alt a 1*, 448 bp from *EndoPG*, and 621 bp from OPA10-2. The best-fit evolutionary models for each gene were as follows: JC for ITS, TNe+G4 for *RPB2*, TIMe+I for *EndoPG*, TNe+R2 for OPA10-2, and K2P+G4 for *GAPDH*, *Alt a 1* and *TEF1*. In phylogenetic analyses, similar topologies were obtained from maximum likelihood and Bayesian methods. Additionally, the six strains examined in this study were placed within *Alternaria* section *Alternaria*, clustering into three distinct clades. Specifically, strains YZU 231602, YZU 231638, and YZU 231640 (isolated from *Z. mays*) formed one clade supported with a bootstrap (BS) value of 81% and a Bayesian posterior probability (PP) of 1.00 (Fig. 1). This clade was positioned close to another clade composed of strains YZU 231197 and YZU 231198 (isolated from *O. sativa*). These two clades were relatively close to *A. burnsii* with BS/PP support values of 69%/0.73 (Fig. 1). Strain YZU 231199 isolated from *O. sativa* formed a single clade sister to strains of *A. tomato* (CBS 103.30 and CBS 114.35), supported with BS/PP values of 72%/0.80 (Fig. 1). The phylogenetic placements of these strains indicated that they represent three novel species in the genus *Alternaria* section *Alternaria*.

### Taxonomy

#### ***Alternaria oryzicola* H.F. Liu & J.X. Deng, sp. nov.**

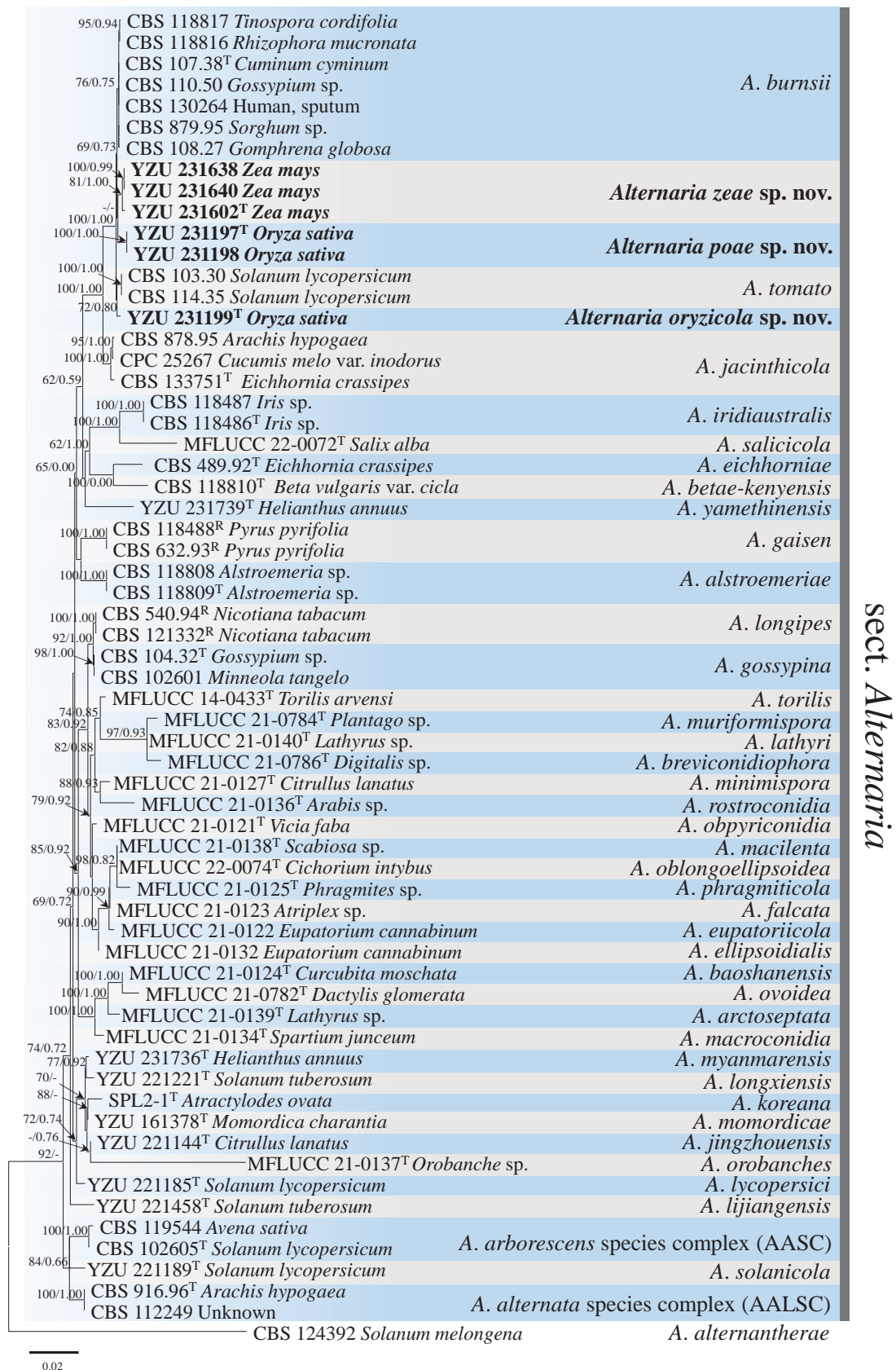
MycoBank No: 857595

Fig. 2

**Etymology.** Name refers to its host *Oryza sativa*.

**Type.** CHINA • Hainan Province, Lingshui County, diseased leaves of *Oryza sativa*, July 2023, J.L. Yin, holotype YZU-H-2023056A (permanently preserved in a metabolically inactive state), ex-type culture YZU 231199.

**Description.** **Colonies** on PDA sub-circular, velvety to fluffy, white to greyish-green, darker at the center, reverse side pale yellow to light brown, 61–63 mm



**Figure 1.** Phylogenetic tree constructed using the maximum likelihood method based on concatenated sequences of ITS, GAPDH, RPB2, TEF1, Alt a 1, EndoPG, and OPA10-2 from *Alternaria* spp. Bootstrap support values (BS) and Bayesian posterior or probability (PP) are given at the nodes (BS/PP). The strains from this study are marked in bold. Ex-type strains are indicated with 'T', representative strains are indicated with 'R'. *Alternaria alternantherae* CBS 124392 is used as the outgroup taxon.

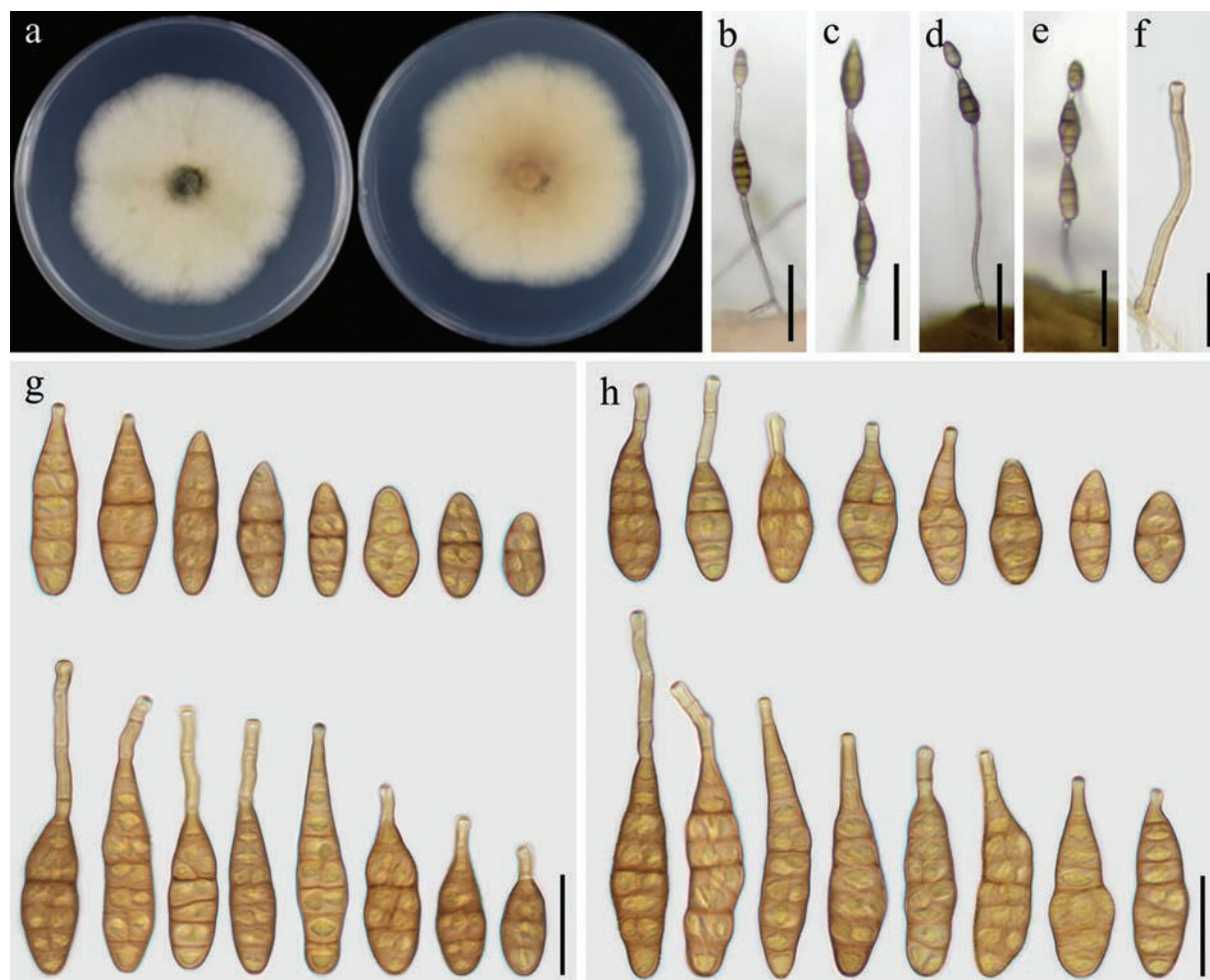


**Figure 2.** Morphology of *Alternaria oryzicola* sp. nov. (YZU 231199) **a** colony on PDA for 7 days at 25 °C **b, c** sporulation on PCA **d, e** sporulation on V8A **f** conidiophore and conidiogenous cell **g** conidia on PCA **h** conidia on V8A. Scale bars: 50 µm (**b, c, d, e**); 15 µm (**f**); 25 µm (**g, h**).

in diameter (Fig. 2a). On PCA, **conidiophores**, erect or curved, unbranched, sometimes slightly expanded at the apex,  $32\text{--}105 \times 3\text{--}4$  µm in size, with 1–6 septa (Fig. 2f). **Conidiogenous cells** integrated, terminal, smooth, cylindrical, apically doliiform,  $5\text{--}14 \times 3\text{--}4$  µm, with 1 conidiogenous locus. **Conidia** borne in chain, 1–3 units per chain, unbranched, mostly narrow-obclavate, obclavate, or long ellipsoid,  $20\text{--}48 \times 9\text{--}16$  µm in dimension, 1–4 transverse septa, apical beak  $4\text{--}39 \times 2.5\text{--}4$  µm (Fig. 2b, c, g). On V8A, **conidiophores** unbranched,  $20\text{--}67 \times 3\text{--}4$  µm, with 1–5 septa. **Conidia** solitary or in chain with 2–3 units per chain, narrow-obclavate, obclavate, or long ellipsoid,  $18\text{--}56 \times 9\text{--}16$  µm in size, with 2–6 transverse septa, apical beak  $4\text{--}39$  µm in length,  $3\text{--}4$  µm in width (Fig. 2d, e, h).

**Notes.** Based on phylogenetic analysis using combined dataset of multiple regions, strain YZU 231199 was relatively close to strains of *Alternaria tomato* (CBS 103.30 and CBS 114.35). Comparative analysis of nucleotide sequences revealed that strain YZU 231199 differed from representative strain of *A. tomato* (CBS 103.30) at four regions: 3 bp differences in *GAPDH* with 1 gap; 4 bp differences in *RPB2*, 1 bp difference in *TEF1*, and 1 bp difference in *OPA10-2*. Morphologically, the present fungus (YZU 231199) was also different with *A. tomato* in having smaller body size, less septa, and shorter beak (Table 2). Therefore, strain YZU 231199 was introduced as a novel species *A. oryzicola* sp. nov. in this study.



***Alternaria poae* H.F. Liu & J.X. Deng, sp. nov.**

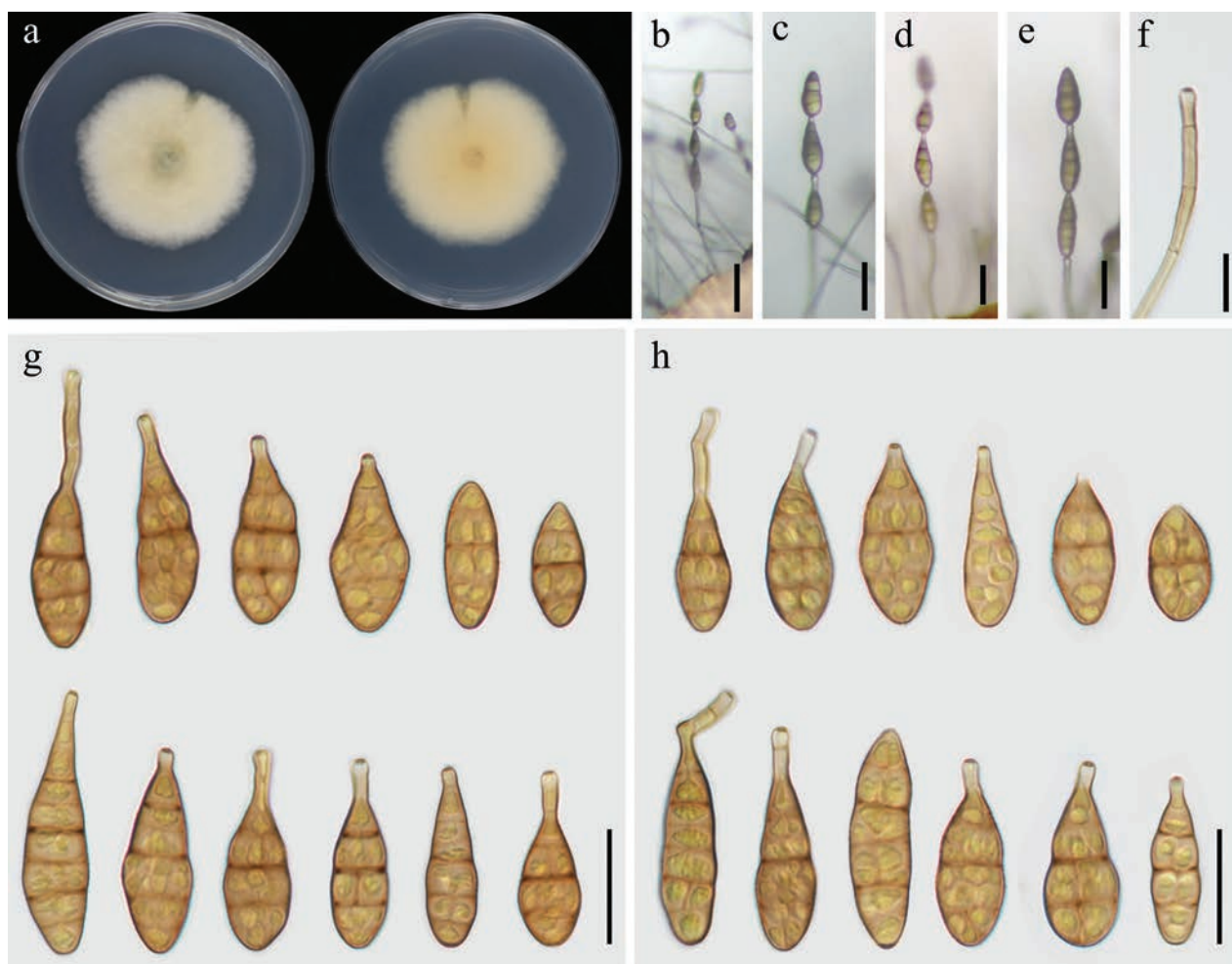
MycoBank No: 857596

Fig. 3

**Etymology.** Name refers to its host family Poaceae.

**Type.** CHINA • Hainan Province, Lingshui County, diseased leaves of *Oryza sativa*, July 2023, J.L. Yin, holotype YZU-H-2023056B (permanently preserved in a metabolically inactive state), ex-type culture YZU 231197.

**Description.** On PDA, **colonies** sub-rounded, fluffy, cottony, white to pale green or yellow-green, reverse side pale yellow to light yellow, 55–56 mm in diameter (Fig. 3a). On PCA, **conidiophores** unbranched, curved or straight, 15–77 × 3–4 µm in size, with 1–5 septa (Fig. 3f). **Conidiogenous cells** 5–9 × 3–4 µm, integrated, terminal, cylindrical, thin-walled, smooth, apically doliiform, with 1 conidiogenous locus. **Conidia** borne single or in chain with at least 2–4 conidia per chain, unbranched, narrow-ovoid, subellipsoid, or obclavate, smooth, 20–42 × 10–19 µm, with 1–4 transverse septa. basal rounded, apical beak 6–26 × 3–4 µm (Fig. 3b, c, g). On V8A, **conidiophores** unbranched, smooth, 30–96 × 3–4 µm, with 2–7 septa. **Conidia** produced in chain with at least 2–4 conidia



**Figure 3.** Morphology of *Alternaria poae* sp. nov. (YZU 231197) **a** colony on PDA for 7 days at 25 °C **b, c** sporulation on PCA **d, e** sporulation on V8A **f** conidiophore and conidiogenous cell **g** conidia on PCA **h** conidia on V8A. Scale bars: 50 µm (**b, c, d, e**); 15 µm (**f**); 25 µm (**g, h**).

per chain, subellipsoid, obclavate, or narrow-ovoid,  $20\text{--}45 \times 10\text{--}17 \mu\text{m}$ , 1–4 transverse septa, beak  $5\text{--}17 \times 3\text{--}4 \mu\text{m}$  (Fig. 3d, e, h).

**Additional isolated examined.** CHINA • Hainan Province, Lingshui County, diseased leaves of *Oryza sativa*, July 2023, J.L. Yin, living culture YZU 231198.

**Notes.** In phylogenetic analysis using concatenated sequences of ITS, *GAPDH*, *RPB2*, *TEF1*, *Alt a 1*, *EndoPG*, and OPA10-2, strains of *Alternaria poae* (YZU 231197 and YZU 231198) fell into a separate clade close to clades of *A. zeae* and *A. burnsii*. Based on nucleotide sequences, *A. poae* differs from *A. zeae* in five loci (3 bp in *GAPDH* with 1 gap, 5 bp in *RPB2*, 3 bp in *TEF1*, 3 bp in *Alt a 1*, and 7 bp in OPA10-2), and differs from *A. burnsii* in six loci (2 bp in *GAPDH*, 2 bp in *RPB2*, 3 bp in *TEF1*, 2 bp in *Alt a 1*, 2 bp in *EndoPG*, and 4 bp in OPA10-2). In morphology, *A. poae* can be distinguished from *A. zeae* by its shorter beak length, and from *A. burnsii* by its wider conidia bodies (Table 2).

### ***Alternaria zeae* H.F. Liu & J.X. Deng, sp. nov.**

MycoBank No: 857597

Fig. 4

**Etymology.** Name refers to its host *Zea mays*.

**Type.** CHINA • Guangxi Province, Liuzhou City, diseased leaves of *Zea mays*, September 2023, F.Y. Liu, holotype YZU-H-2023150A (permanently preserved in a metabolically inactive state), ex-type culture YZU 231602.

**Description.** **Colonies** on PDA round, fluffy, cottony, greenish-gray, white at the margin, reverse side pale yellow, 58–59 mm in diameter (Fig. 4a). The conidial morphology on PDA and PCA was similar, with only slight differences. On PCA, **conidiophores** straight or curved, unbranched,  $25\text{--}123 \times 2.5\text{--}4.5 \mu\text{m}$ , with 1–8 septa (Fig. 4d). **Conidia** borne singly or in chain with 2–4 conidia per chain, ovate, ellipsoid or obclavate, with 3–6 transverse septa,  $26\text{--}46 \times 10\text{--}18 \mu\text{m}$  in size, mostly with septate apical beak,  $9\text{--}93 \times 2.5\text{--}4 \mu\text{m}$  in size (Fig. 4b, e). On V8A, **conidiophores** straight or curved, unbranched,  $38\text{--}118 \times 2.5\text{--}4 \mu\text{m}$ , with 1–7 septa. **Conidiogenous cells**  $5\text{--}14 \times 3\text{--}5 \mu\text{m}$ , integrated, apical, cylindrical, light brown, smooth, apically doliiform, with 1 conidiogenous locus. **Conidia** solitary or produced in chain with 2–4 conidia, ovate, ellipsoid or obclavate, with 3–6 transverse septa,  $26\text{--}45 \times 10\text{--}17 \mu\text{m}$ , apical beak  $4.5\text{--}65 \times 2.5\text{--}4 \mu\text{m}$ , with 0–4 septa (Fig. 4c, f).

**Additional isolates examined.** CHINA • Guangxi Province, Liuzhou City, diseased leaves of *Zea mays*, September 2023, F.Y. Liu, living culture YZU 231638 and YZU 231640.

**Notes.** Strains of *Alternaria zeae* (YZU 231602, YZU 231638 and YZU 231640) formed a distinct clade in the multi-locus phylogenetic analysis. *Alternaria poae* and *A. burnsii* were genetically close to *A. zeae*. In nucleotide sequences, *A. zeae* differs from *A. poae* at five loci: 3 bp in *GAPDH* with 1 gap, 5 bp differences in *RPB2*, 3 bp in *TEF1*, 3 bp in *Alt a 1*, and 7 bp in OPA10-2. Nucleotide sequence differences were also observed between *A. zeae* and *A. burnsii* (3 bp in *GAPDH* with 1 gap, 2 bp in *RPB2*, 1 bp in *Alt a 1*, and 1 bp in OPA10-2). Morphologically, *A. zeae* has obviously longer beak than *A. poae* and *A. burnsii* (Table 2). In addition, conidia bodies of *A. zeae* are also wider than those of *A. burnsii* (Simmons 2007).

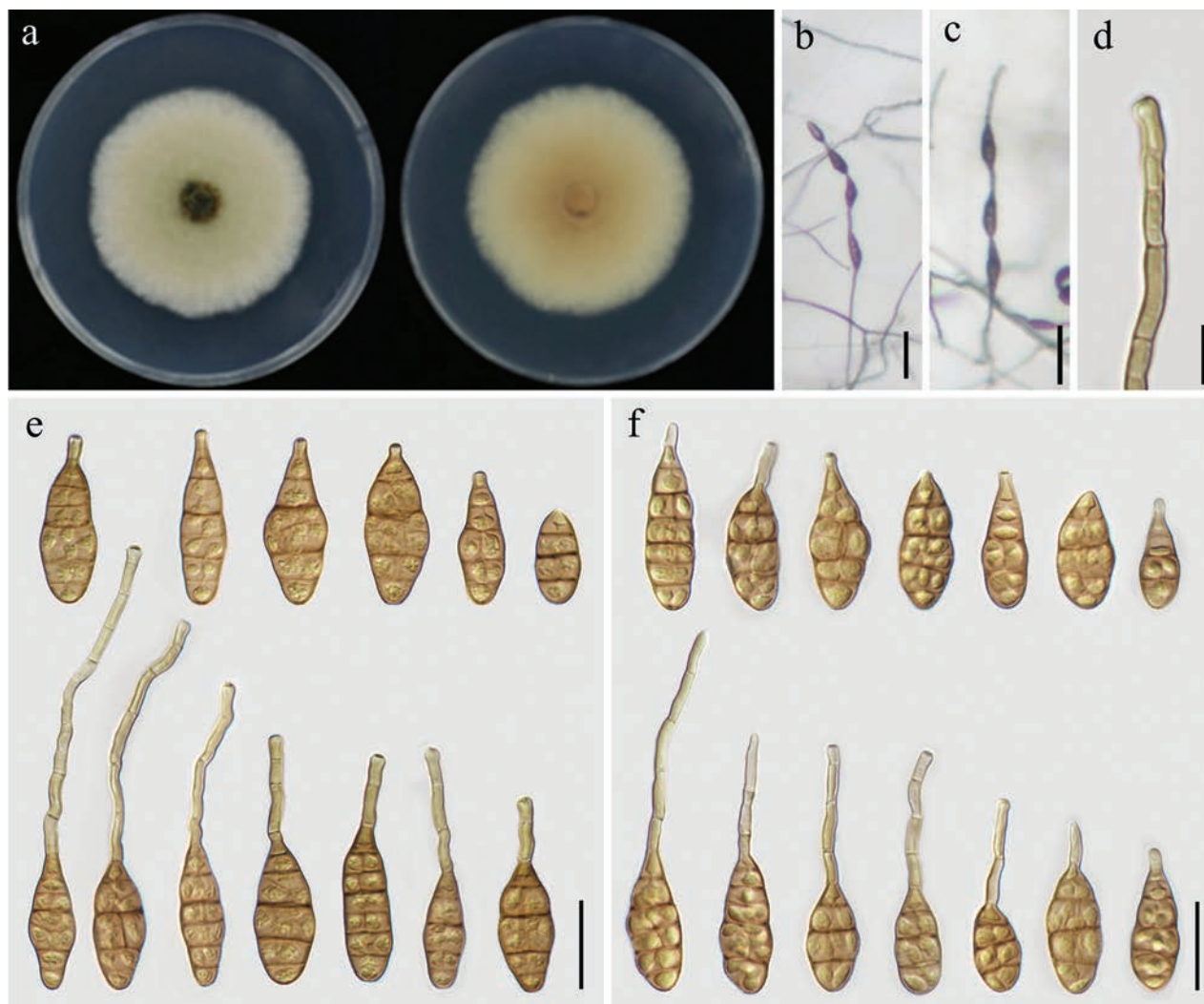


**Figure 4.** Morphology of *Alternaria zeae* sp. nov. (YZU 231602) **a** colony on PDA for 7 days at 25 °C **b, c** sporulation on PCA **d** conidiophore and conidiogenous cell **e** conidia on PCA **f** conidia on V8A. Scale bars: 50 µm (**b, c**); 15 µm (**d**); 25 µm (**e, f**).

## Discussion

Based on integrated analyses of morphological characterization and multi-locus phylogenetic study, three novel species of *Alternaria* (*A. oryzicola* sp. nov., *A. poae* sp. nov., and *A. zeae* sp. nov.) from two different cereal crops (*O. sativa* and *Z. mays*) were described in this study. These findings contribute to the understanding of the diversity of *Alternaria* spp. on cereal crops in China.

In phylogenetic analysis using concatenated sequences of ITS, *GAPDH*, *RPB2*, *TEF1*, *Alt a 1*, *EndoPG*, and OPA10-2, all of the three novel species were assigned to distinct clades in *Alternaria* section *Alternaria*. This section contains most of the small-spored species, which include important plant, human and postharvest pathogens (Woudenberg et al. 2015). Phylogenetically, species *A. zeae* sp. nov. and *A. poae* sp. nov. were relatively close to *A. burnsii* and *A. oryzicola* sp. nov. was relatively close to *A. tomato*. These species were located at the top of the phylogenetic tree of section *Alternaria*. In terms of morphology, the three species from this study were distinguished from their related species (*A. burnsii* and *A. tomato*) based on conidial characteristics, such as conidia size, septa, and beak size, as shown in Table 2. Therefore, both

**Table 2.** Conidial morphology of *Alternaria* spp. from this study and previous publication.

Species	Conidia				Conidia per chain	Substrate	Reference
	Shape	Body size (µm)	Septa	Beak size (µm)			
<i>Alternaria burnsii</i>	ovoid or ellipsoid	30–50 × 9–13	5–8	–	Short chain	Host	Simmons (2007)
	narrow-ovoid or narrow-ellipsoid	30–40 × 8–14	3–7	–	–	PCA, V8A	Simmons (2007)
<i>A. oryzicola</i> sp. nov.	narrow-obclavate, obclavate, or long ellipsoid	20–48 × 9–16	1–4	4–39 × 2.5–4	1–3	PCA	This study
		18–56 × 9–16	2–6	4–39 × 3–4	1–3	V8A	This study
<i>A. poae</i> sp. nov.	subellipsoid, obclavate, or narrow-ovoid	20–42 × 10–19	1–4	6–26 × 3–4	1–4	PCA	This study
		20–45 × 10–17	2–7	5–17 × 3–4	1–4	V8A	This study
<i>A. tomato</i>	ellipsoid to long-ovoid	39–65 × 13–22	6–9	60–105 × 2	Solitary	Host	Simmons (2007)
<i>A. zeae</i> sp. nov.	ovate, ellipsoid or obclavate	26–46 × 10–18	3–6	9–93 × 2.5–4	1–4	PCA	This study
		26–45 × 10–17	3–6	4.5–65 × 2.5–4	1–4	V8A	This study

morphological and phylogenetic approaches provide evidence supporting the novelty of the species identified in this study.

In addition, the host is one of the important factors in the description of *Alternaria* species (Zhang 2003). According to fungus-host distribution in the USDA Fungal Databases (<https://fungi.ars.usda.gov>, accessed on 31 October 2024) and related publications, *A. burnsii* and *A. tomato* have been associated with different sources, but most are not from Poaceae plants. For example, *A. burnsii* was found on *Cuminum cyminum* (Simmons 2007; Woudenberg et al. 2015), *Tinospora cordifolia* (Woudenberg et al. 2015), *Rhizophora mucronata* (Woudenberg et al. 2015), *Gossypium* sp. (Woudenberg et al. 2015; El Gobashy et al. 2018), *Gomphrena globosa* (Woudenberg et al. 2015), *Sorghum* sp. (Kim et al. 2020), human sputum (Woudenberg et al. 2015), *Helianthus annuus* (Nwe et al. 2024), *Allium cepa* (Htun et al. 2022), *Apium graveolens* (Zhuang 2005), *Bunium persicum* (Mondal et al. 2002), *Cucurbita maxima* (Paul et al. 2015), *Pandanus* sp. (Hyde et al. 2018), and *Zea mays* (Xu et al. 2022). *Alternaria tomato* was reported on several plants, including *Solanum lycopersicum* (Simmons 2007), *Helianthus annuus* (Poudel et al. 2019), *Nopalea cochenillifera* (Infante et al. 2021), and *Phaseolus vulgaris* (Allen 1995). In the present study, the three novel species were isolated from two cereal crops (*Z. mays* and *O. sativa*), suggesting an increasing association of *Alternaria* species with Poaceae plants. According to previous studies, *Alternaria* spp. have been reported as predominant mycobiota in cereal grains (Kulik et al. 2015; Puvača et al. 2020; Orina et al. 2021). Most of these *Alternaria* species were predominantly classified in sections *Alternaria* and *Infectoriae* (Gannibal 2018), whereas some were sporadically found in section *Pseudoalternaria* (Gannibal 2018, Poursafar et al. 2018). Much attention has been devoted to detecting *Alternaria* spp. capable of producing mycotoxins (Orina et al. 2021). On cereal grains, several mycotoxins produced by *Alternaria* spp., such as AOH, AME, TEN, and TeA, were detected (Orina et al. 2021), posing potential risks to food safety. The ability of the three species in this study (*A. oryzicola* sp. nov., *A. poae* sp. nov., and *A. zeae* sp. nov.) to produce mycotoxins warrants further investigation. Since these three species were all isolated from diseased leaves of cereal crops, they could be potential pathogens. Furthermore, they are phylogenetically closely related to *A. burnsii* and *A. tomato*, which have recently been isolated and identified as pathogens of a cereal crop, wheat (Al-Nadabi et al. 2018).



Overall, this study characterized three novel species of *Alternaria* from two cereal crops, rice and maize, through morphological and molecular approaches. The potential interactions between these novel species and their host plants merit further investigation to uncover their ecological and agricultural impacts.

## Additional information

### Conflict of interest

The authors have declared that no competing interests exist.

### Ethical statement

No ethical statement was reported.

### Funding

This study was funded by the National Natural Science Foundation of China (32270022).

### Author contributions

Hai-Feng Liu: methodology, data curation, writing - original draft. Feng-Yin Liu: methodology, investigation, data curation. Hai-Yan Ke: methodology. Qing-Xiao Shi: methodology. Jian-Xin Deng: conceptualization, writing – review & editing, supervision, project administration. Hyunkyu Sang: writing – review & editing, supervision.

### Author ORCIDs

Hai-Feng Liu  <https://orcid.org/0000-0002-9733-9240>

Feng-Yin Liu  <https://orcid.org/0000-0003-3114-603X>

Jian-Xin Deng  <https://orcid.org/0000-0001-7304-5603>

Hyunkyu Sang  <https://orcid.org/0000-0002-7459-5217>

### Data availability

All of the data that support the findings of this study are available in the main text.

## References

- Akhtar N, Bashir U, Mushtaq S (2014a) First report of leaf spot of rice caused by *Alternaria arborescens* in Pakistan. Plant Disease 98: 846–846. <https://doi.org/10.1094/PDIS-09-13-0969-PDN>
- Akhtar N, Hafeez R, Awan ZA (2014b) First report of rice leaf spot by *Alternaria gaisen* from Pakistan. Plant Disease 98: 1440–1440. <https://doi.org/10.1094/PDIS-05-14-0477-PDN>
- Al-Nadabi HH, Maharachchikumbura SSN, Agrama H, Al-Azri M, Nasehi A, Al-Sadi AM (2018) Molecular characterization and pathogenicity of *Alternaria* species on wheat and date palms in Oman. European Journal of Plant Pathology 152: 577–588. <https://doi.org/10.1007/s10658-018-1550-4>
- Alasadi RMS (2024) *Alternaria alternata*: The most common pathogen on date palm. Studies in Fungi 9: 0–0. <https://doi.org/10.48130/sif-0024-0012>
- Allen DJ (1995) An annotated list of diseases, pathogens and associated fungi of the common bean (*Phaseolus vulgaris*) in eastern and southern Africa. Centro Internacional de Agricultura Tropical (CIAT); CAB International, Wallingford, 42 pp.

- Amatulli MT, Fanelli F, Moretti A, Mule G, Logrieco AF (2013) *Alternaria* species and mycotoxins associated to black point of cereals. *Mycotoxins* 63: 39–46. <https://doi.org/10.2520/myco.63.39>
- Andrew M, Peever TL, Pryor BM (2009) An expanded multilocus phylogeny does not resolve morphological species within the small-spored *Alternaria* species complex. *Mycologia* 101: 95–109. <https://doi.org/10.3852/08-135>
- Aung SLL, Liu F-Y, Gou Y-N, Nwe ZM, Yu Z-H, Deng J-X (2024) Morphological and phylogenetic analyses reveal two new *Alternaria* species (Pleosporales, Pleosporaceae) in *Alternaria* section from Cucurbitaceae plants in China. *MycKeys* 107: 125–139. <https://doi.org/10.3897/mycokeys.107.124814>
- Berbee ML, Pirseyedi M, Hubbard S (1999) Cochliobolus phylogenetics and the origin of known, highly virulent pathogens, inferred from ITS and glyceraldehyde-3-phosphate dehydrogenase gene sequences. *Mycologia* 91: 964–977. <https://doi.org/10.1080/00275514.1999.12061106>
- Bessadat N, Bataillé-Simoneau N, Colou J, Hamon B, Mabrouk K, Simoneau P (2025) New members of *Alternaria* (pleosporales, pleosporaceae) collected from apiaceae in algeria. *MycKeys* 113: 169–192. <https://doi.org/10.3897/mycokeys.113.138005>
- Bhunjun CS, Chen YJ, Phukhamsakda C, Boekhout T, Groenewald JZ, McKenzie EHC, Francisco EC, Frisvad JC, Groenewald M, Hurdeal VG, Luangsa-ard J, Perrone G, Visagie CM, Bai FY, Błaszowski J, Braun U, De Souza FA, De Queiroz MB, Dutta AK, Gonkhom D, Goto BT, Guarnaccia V, Hagen F, Houbraken J, Lachance MA, Li JJ, Luo KY, Magurno F, Mongkolsamrit S, Robert V, Roy N, Tibpromma S, Wanasinghe DN, Wang DQ, Wei DP, Zhao CL, Aiphuk W, Ajayi-Oyetunde O, Arantes TD, Araujo JC, Begerow D, Bakhshi M, Barbosa RN, Behrens FH, Bensch K, Bezerra JDP, Bilański P, Bradley CA, Bubner B, Burgess TI, Buyck B, Čadež N, Cai L, Calaça FJS, Campbell LJ, Chaverri P, Chen YY, Chethana KWT, Coetzee B, Costa MM, Chen Q, Custódio FA, Dai YC, Damm U, Santiago ALCMA, De Miccolis Angelini RM, Dijksterhuis J, Dissanayake AJ, Doilom M, Dong W, Álvarez-Duarte E, Fischer M, Gajanayake AJ, Gené J, Gomdola D, Gomes AAM, Hausner G, He MQ, Hou L, Iturrieta-González I, Jami F, Jankowiak R, Jayawardena RS, Kandemir H, Kiss L, Kobmoo N, Kowalski T, Landi L, Lin CG, Liu JK, Liu XB, Loizides M, Luangharn T, Maharachchikumbura SSN, Makhathini Mkhwanazi GJ, Manawasinghe IS, Marin-Felix Y, McTaggart AR, Moreau PA, Morozova OV, Mostert L, Osiewacz HD, Pem D, Phookamsak R, Pollastro S, Pordel A, Poyntner C, Phillips AJL, Phonemany M, Promputtha I, Rathnayaka AR, Rodrigues AM, Romanazzi G, Rothmann L, Salgado-Salazar C, Sandoval-Denis M, Saupe SJ, Scholler M, Scott P, Shivas RG, Silar P, Silva-Filho AGS, Souza-Motta CM, Spies CFJ, Stchigel AM, Sterflinger K, Summerbell RC, Svetasheva TY, Takamatsu S, Theelen B, Theodoro RC, Thines M, Thongklang N, Torres R, Turchetti B, Van Den Brule T, Wang XW, Wartchow F, Welti S, Wijesinghe SN, Wu F, Xu R, Yang ZL, Yilmaz N, Yurkov A, Zhao L, Zhao RL, Zhou N, Hyde KD, Crous PW (2024) What are the 100 most cited fungal genera? *Studies in Mycology*. <https://doi.org/10.3114/sim.2024.108.01>
- Capella-Gutiérrez S, Silla-Martínez JM, Gabaldón T (2009) trimAl: A tool for automated alignment trimming in large-scale phylogenetic analyses. *Bioinformatics (Oxford, England)* 25: 1972–1973. <https://doi.org/10.1093/bioinformatics/btp348>
- Carbone I, Kohn LM (1999) A method for designing primer sets for speciation studies in filamentous ascomycetes. *Mycologia* 91: 553–556. <https://doi.org/10.1080/00275514.1999.12061051>
- El Gobashy SF, Mikhail WZA, Ismail AM, Zekry A, Moretti A, Susca A, Soliman ASH (2018) Phylogenetic, toxigenic and virulence profiles of *Alternaria* species causing leaf blight

- of tomato in Egypt. *Mycological Progress* 17: 1269–1282. <https://doi.org/10.1007/s11557-018-1442-1>
- Gannibal PhB (2018) Factors affecting *Alternaria* appearance in grains in European Russia. *Selskokhozyaistvennaya Biologiya* 53: 605–615. <https://doi.org/10.15389/agrobiology.2018.3.605eng>
- Gannibal PB, Orina AS, Gasich EL (2022) A new section for *Alternaria helianthiinficiens* found on sunflower and new asteraceous hosts in Russia. *Mycological Progress* 21: 34. <https://doi.org/10.1007/s11557-022-01780-6>
- Gou Y, Aung SLL, Guo Z, Li Z, Shen S, Deng J (2023) Four new species of small-spored *Alternaria* isolated from *solanum tuberosum* and *S. lycopersicum* in China. *Journal of Fungi* (Basel, Switzerland) 9: 880. <https://doi.org/10.3390/jof9090880>
- Gutiérrez SA, Carmona MA, Reis EM (2010) Methods for detection of *Alternaria padwickii* in rice seeds. *Journal of Phytopathology* 158: 523–526. <https://doi.org/10.1111/j.1439-0434.2009.01651.x>
- Haituk S, Pakdeeniti P, Withee P, Karunarathna A, Literatus IC, Kumla J, Cheewangkoon R, Suwannamanee J, Nguanhom J (2023) Biological control of brassicales ring spot disease caused by *Alternaria brassicicola* using antagonistic yeasts. *Warasan Khana Witthayasat Maha Witthayalai Chiang Mai* 50: 1–17. <https://doi.org/10.12982/CMJS.2023.016>
- Hall TA (1999) BioEdit: A user-friendly biological sequence alignment editor and analysis program for windows 95/98/NT. *Nucleic acids symposium series*. Oxford, 95–98.
- He J, Li D-W, Cui W-L, Huang L (2024) Seven new species of *Alternaria* (Pleosporales, Pleosporaceae) associated with Chinese fir, based on morphological and molecular evidence. *MycKeys* 101: 1–44. <https://doi.org/10.3897/mycokeys.101.115370>
- Hong SG, Cramer RA, Lawrence CB, Pryor BM (2005) Alt a 1 allergen homologs from *Alternaria* and related taxa: Analysis of phylogenetic content and secondary structure. *Fungal Genetics and Biology* 42: 119–129. <https://doi.org/10.1016/j.fgb.2004.10.009>
- Htun AA, Liu HF, He L, Xia ZZ, Aung SLL, Deng JX (2022) New species and new record of *Alternaria* from onion leaf blight in Myanmar. *Mycological Progress* 21: 59–69. <https://doi.org/10.1007/s11557-021-01765-x>
- Hyde KD, Norphanphoun C, Chen J, Dissanayake AJ, Doilom M, Hongsanan S, Jayawardena RS, Jeewon R, Perera RH, Thongbai B, Wanasinghe DN, Wisitrassameewong K, Tibpromma S, Stadler M (2018) Thailand’s amazing diversity: Up to 96% of fungi in northern Thailand may be novel. *Fungal Diversity* 93: 215–239. <https://doi.org/10.1007/s13225-018-0415-7>
- Hyde KD, Noorabadi MT, Thiyagaraja V, He MQ, Johnston PR, Wijesinghe SN, Armand A, Biketova AY, Chethana KWT, Erdoğdu M, Ge ZW, Groenewald JZ, Hongsanan S, Kušan I, Leontyev DV, Li DW, Lin CG, Liu NG, Maharachchikumbura SSN, Matočec N, May TW, McKenzie EHC, Mešić A, Perera RH, Phukhamsakda C, Piątek M, Samarakoon MC, Selcuk F, Senanayake IC, Tanney JB, Tian Q, Vizzini A, Wanasinghe DN, Wannasawang N, Wijayawardene NN, Zhao RL, Abdel-Wahab MA, Abdollahzadeh J, Abeywickrama PD, Abhinav, Absalan S, Acharya K, Afshari N, Afshan NS, Afzalnia S, Ahmadpour SA, Akulov O, Alizadeh A, Alizadeh M, Al-Sadi AM, Alves A, Alves VCS, Alves-Silva G, Antonín V, Aouali S, Aptroot A, Apurillo CCS, Arias RM, Asgari B, Asghari R, Assis DMA, Assyov B, Atienza V, Aumentado HDR, Avasthi S, Azevedo E, Bakhshi M, Bao DF, Baral HO, Barata M, Barbosa KD, Barbosa RN, Barbosa FR, Baroncelli R, Barreto GG, Baschien C, Bennett RM, Bera I, Bezerra JDP, Bhunjun CS, Bianchinotti MV, Błaszowski J, Boekhout T, Bonito GM, Boonmee S, Boonyuen N, Bortnikov FM, Bregant C, Bundhun D, Burgaud G, Buyck B, Caeiro MF, Cabarroi-Hernández M, Cai

- MF, Cai L, Calabon MS, Calaça FJS, Callalli M, Câmara MPS, Cano-Lira J, Cao B, Carlavilla JR, Carvalho A, Carvalho TG, Castañeda-Ruiz RF, Catania MDV, Cazabonne J, Cedeño-Sanchez M, Chaharmiri-Dokhaharani S, Chaiwan N, Chakraborty N, Cheewankoon R, Chen C, Chen J, Chen Q, Chen YP, Chinaglia S, Coelho-Nascimento CC, Celine C, CostaRezende DH, Cortés-Pérez A, Crouch JA, Crous PW, Cruz RHSF, Czachura P, Damm U, Darmostuk V, Daroodi Z, Das K, Davoodian N, Davydov EA, da Silva GA, da Silva IR, da Silva RMF, da Silva Santos AC, Dai DQ, Dai YC, de Groot MD, De Kesel A, De Lange R, de Medeiros EV, de Souza CFA, de Souza FA, dela Cruz TEE, Decock C, Delgado G, Denchev CM, Denchev TT, Deng YL, Dentinger BTM, Devadatha B, Dianese JC, Dima B, Doilom M, Dissanayake AJ, Dissanayake DMLS, Dissanayake LS, Diniz AG, Dolatabadi S, Dong JH, Dong W, Dong ZY, Drechsler-Santos ER, Druzhinina IS, Du TY, Dubey MK, Dutta AK, Elliott TF, Elshahed MS, Egidi E, Eisvand P, Fan L, Fan X, Fan XL, Fedosova AG, Ferro LO, Fiuza PO, Flakus AW, Fonseca EO, Fryar SC, Gabaldón T, Gajanayake AJ, Gannibal PB, Gao F, García-Sánchez D, García-Sandoval R, Garrido-Benavent I, Garzoli L, Gasca-Pineda J, Gautam AK, Gené J, Ghobad-Nejhad M, Ghosh A, Giachini AJ, Gibertoni TB, Gentekaki E, Gmoshinskiy VI, Góes-Neto A, Gomdola D, Gorjón SP, Goto BT, Granados-Montero MM, Griffith GW (2024) The 2024 outline of fungi and fungus-like taxa. *Mycosphere: Journal of Fungal Biology* 15: 5146–6239.
- Infante NB, Da Silva GCS, Feijó FM, Da Silva SJC, Assunção IP, De Andrade Lima GS (2021) *Alternaria* species associated with cladode brown spot in cactus prickly pear (*Nopalea cochenillifera*). *European Journal of Plant Pathology* 160: 215–226. <https://doi.org/10.1007/s10658-021-02236-5>
- Jeewon R, Hyde K (2016) Establishing species boundaries and new taxa among fungi: Recommendations to resolve taxonomic ambiguities. *Mycosphere: Journal of Fungal Biology* 7: 1669–1677. <https://doi.org/10.5943/mycosphere/7/11/4>
- Kalyaanamoorthy S, Minh BQ, Wong TKF, Von Haeseler A, Jermini LS (2017) ModelFinder: Fast model selection for accurate phylogenetic estimates. *Nature Methods* 14: 587–589. <https://doi.org/10.1038/nmeth.4285>
- Katoh K, Standley DM (2013) MAFFT multiple sequence alignment software version 7: Improvements in performance and usability. *Molecular Biology and Evolution* 30: 772–780. <https://doi.org/10.1093/molbev/mst010>
- Katoh K, Rozewicki J, Yamada KD (2019) MAFFT online service: Multiple sequence alignment, interactive sequence choice and visualization. *Briefings in Bioinformatics* 20: 1160–1166. <https://doi.org/10.1093/bib/bbx108>
- Kim W-G, Ryu J-T, Choi H-W (2020) Black mold on tomato fruits caused by *Alternaria alternata* in Korea. *The Korean Journal of Mycology* 48: 369–379. <https://doi.org/10.4489/KJM.20200036>
- Kulik T, Treder K, Załuski D (2015) Quantification of *Alternaria*, *Cladosporium*, *Fusarium* and *Penicillium verrucosum* in conventional and organic grains by qPCR. *Journal of Phytopathology* 163: 522–528. <https://doi.org/10.1111/jph.12348>
- Kumar S, Stecher G, Li M, Knyaz C, Tamura K (2018) MEGA X: Molecular evolutionary genetics analysis across computing platforms. *Molecular Biology and Evolution* 35: 1547–1549. <https://doi.org/10.1093/molbev/msy096>
- Lawrence DP, Gannibal PB, Peever TL, Pryor BM (2013) The sections of *Alternaria*: Formalizing species-group concepts. *Mycologia* 105: 530–546. <https://doi.org/10.3852/12-249>
- Lawrence DP, Rotondo F, Gannibal PB (2016) Biodiversity and taxonomy of the pleomorphic genus *Alternaria*. *Mycological Progress* 15: 3. <https://doi.org/10.1007/s11557-015-1144-x>





- Li J, Phookamsak R, Jiang H, Bhat DJ, Camporesi E, Lumyong S, Kumla J, Hongsanan S, Mortimer PE, Xu J, Suwannarach N (2022) Additions to the inventory of the genus *Alternaria* section *Alternaria* (Pleosporaceae, Pleosporales) in Italy. *Journal of Fungi* (Basel, Switzerland) 8: 898. <https://doi.org/10.3390/jof8090898>
- Li J-F, Jiang H-B, Jeewon R, Hongsanan S, Bhat DJ, Tang S-M, Lumyong S, Mortimer PE, Xu J-C, Camporesi E, Bulgakov TS, Zhao G-J, Suwannarach N, Phookamsak R (2023) *Alternaria*: Update on species limits, evolution, multi-locus phylogeny, and classification. *Studies in Fungi* 8: 1–61. <https://doi.org/10.48130/SIF-2023-0001>
- Liao Y-C-Z, Cao Y-J, Wan Y, Li H, Li D-W, Zhu L-H (2023) *Alternaria arborescens* and *A. italica* causing leaf blotch on *Celtis julianae* in China. *Plants* 12: 3113. <https://doi.org/10.3390/plants12173113>
- Liu YJ, Whelen S, Hall BD (1999) Phylogenetic relationships among ascomycetes: Evidence from an RNA polymerase II subunit. *Molecular Biology and Evolution* 16: 1799–1808. <https://doi.org/10.1093/oxfordjournals.molbev.a026092>
- Mercado Vergnes D, Renard M-E, Duveiller E, Maraite H (2006) Identification of *Alternaria* spp. on wheat by pathogenicity assays and sequencing. *Plant Pathology* 55: 485–493. <https://doi.org/10.1111/j.1365-3059.2006.01391.x>
- Mondal KK, Rana SS, Sood P, Singh Y (2002) Kalazira: A new host for *Alternaria burnsii*. *Indian Phytopathology* 55: 532–533.
- Nguyen L-T, Schmidt HA, Von Haeseler A, Minh BQ (2015) IQ-TREE: A fast and effective stochastic algorithm for estimating maximum-likelihood phylogenies. *Molecular Biology and Evolution* 32: 268–274. <https://doi.org/10.1093/molbev/msu300>
- Nwe ZM, Htut KN, Aung SLL, Gou Y-N, Huang C-X, Deng J-X (2024) Two novel species and a new host record of *Alternaria* (Pleosporales, Pleosporaceae) from sunflower (Compositae) in Myanmar. *MycKeys* 105: 337–354. <https://doi.org/10.3897/mycokeys.105.123790>
- Orina AS, Gavrilova OP, Gogina NN, Gannibal PB, Gagkaeva TYu (2021) Natural occurrence of *Alternaria* fungi and associated mycotoxins in small-grain cereals from the urals and west siberia regions of Russia. *Toxins* 13: 681. <https://doi.org/10.3390/toxins13100681>
- Paul NC, Deng JX, Lee HB, Yu S-H (2015) Characterization and pathogenicity of *Alternaria burnsii* from seeds of *Cucurbita maxima* (Cucurbitaceae) in Bangladesh. *Mycobiology* 43: 384–391. <https://doi.org/10.5941/MYCO.2015.43.4.384>
- Pinto VEF, Patriarca A (2017) *Alternaria* species and their associated mycotoxins. In: Moretti A, Susca A (Eds) *Mycotoxigenic fungi. Methods in molecular biology*. Springer New York, New York, NY, 13–32. [https://doi.org/10.1007/978-1-4939-6707-0\\_2](https://doi.org/10.1007/978-1-4939-6707-0_2)
- Poudel B, Velázquez-del Valle MG, Hernández-Lauzardo AN, Zhang S (2019) First report of *Alternaria tomato* causing leaf spot on sunflower in Mexico. *Plant Disease* 103: 1029–1029. <https://doi.org/10.1094/PDIS-07-18-1173-PDN>
- Poursafar A, Ghosta Y, Orina AS, Gannibal PB, Javan-Nikkhah M, Lawrence DP (2018) Taxonomic study on *Alternaria* sections *Infectoriae* and *Pseudoalternaria* associated with black (sooty) head mold of wheat and barley in Iran. *Mycological Progress* 17: 343–356. <https://doi.org/10.1007/s11557-017-1358-1>
- Puvača N, Bursić V, Vuković G, Budakov D, Petrović A, Merkuri J, Avantaggiato G, Cara M (2020) Ascomycete fungi (*Alternaria* spp.) characterization as major feed grains pathogens. *Journal of Agronomy, Technology and Engineering Management* 3: 499–505.
- Romain BBND, Hassan O, Kim JS, Chang T (2022) *Alternaria koreana* sp. nov., a new pathogen isolated from leaf spot of ovate-leaf atractylodes in south Korea. *Molecular Biology Reports* 49: 413–420. <https://doi.org/10.1007/s11033-021-06887-9>

- Ronquist F, Teslenko M, Van Der Mark P, Ayres DL, Darling A, Höhna S, Larget B, Liu L, Suchard MA, Huelsenbeck JP (2012) MrBayes 3.2: Efficient Bayesian phylogenetic inference and model choice across a large model space. *Systematic Biology* 61: 539–542. <https://doi.org/10.1093/sysbio/sys029>
- Simmons EG (2007) *Alternaria: An identification manual*. CBS Biodiversity Series 6. Centraalbureau voor Schimmelcultures, Utrecht.
- Tralamazza SM, Piacentini KC, Iwase CHT, Rocha LDO (2018) Toxigenic *Alternaria* species: Impact in cereals worldwide. *Current Opinion in Food Science* 23: 57–63. <https://doi.org/10.1016/j.cofs.2018.05.002>
- Watanabe M, Lee K, Goto K, Kumagai S, Sugita-Konishi And Y, Hara-Kudo Y (2010) Rapid and effective DNA extraction method with bead grinding for a large amount of fungal DNA. *Journal of Food Protection* 73: 1077–1084. <https://doi.org/10.4315/0362-028X-73.6.1077>
- White TJ, Bruns T, Lee S, Taylor J (1990) Amplification and direct sequencing of fungal ribosomal RNA genes for phylogenetics. In: Innis MA, Gelfand DH, Sninsky JJ, White TJ (Eds) *PCR protocols: a guide to methods and applications*. Academic Press, San Diego, 315–322. <https://doi.org/10.1016/B978-0-12-372180-8.50042-1>
- Woudenberg JHC, Groenewald JZ, Binder M, Crous PW (2013) *Alternaria* redefined. *Studies in Mycology* 75: 171–212. <https://doi.org/10.3114/sim0015>
- Woudenberg JHC, Seidl MF, Groenewald JZ, De Vries M, Stielow JB, Thomma BPHJ, Crous PW (2015) *Alternaria* section *Alternaria*: Species, *formae speciales* or pathotypes? *Studies in Mycology* 82: 1–21. <https://doi.org/10.1016/j.simyco.2015.07.001>
- Xu X, Zhang L, Yang X, Cao H, Li J, Cao P, Guo L, Wang X, Zhao J, Xiang W (2022) *Alternaria* spp. associated with leaf blight of maize in Heilongjiang Province, China. *Plant Disease* 106: 572–584. <https://doi.org/10.1094/PDIS-06-21-1151-RE>
- Zeng X, Tan T, Tian F, Wang Y, Wen T (2023) OFPT: A one-stop software for fungal phylogeny. *Mycosphere: Journal of Fungal Biology* 14: 1730–1741. <https://doi.org/10.5943/mycosphere/14/1/20>
- Zhang TY (2003) *Flora fungorum sinicorum, Alternaria*, vol. 16. Science Press, Beijing, China.
- Zhong FT, Liu YL, Zheng DF, Lu SL (2022) First report of *Alternaria alternata* causing brown leaf spot on wild rice (*oryza rufipogon*) in China. *Plant Disease* 106: 324. <https://doi.org/10.1094/PDIS-05-21-1024-PDN>
- Zhuang W-Y (2005) *Fungi of northwestern China*. Mycotaxon, Ltd., Ithaca, NY, 430 pp.



# Species of *Diaporthe* (Diaporthaceae, Diaporthales) associated with *Alnus nepalensis* leaf spot and branch canker diseases in Xizang, China

JiETING LI<sup>1,2</sup>, YI LI<sup>1,2</sup>, JIANGRONG LI<sup>1,2</sup>, NING JIANG<sup>3</sup>

<sup>1</sup> Institute of Xizang Plateau Ecology, Key Laboratory of Forest Ecology in Xizang Plateau (Xizang Agricultural and Animal Husbandry University), Ministry of Education, Linzhi, Xizang 860000, China

<sup>2</sup> National Forest Ecosystem Observation & Research Station of Linzhi Xizang, Linzhi, Xizang 860000, China

<sup>3</sup> Key Laboratory of Forest Protection of National Forestry and Grassland Administration, Ecology and Nature Conservation Institute, Chinese Academy of Forestry, Beijing 100091, China

Corresponding authors: Jiangrong Li (ljrong06@xza.edu.cn); Ning Jiang (n.jiang@caf.ac.cn)

## Abstract

*Alnus nepalensis* is an important tree species in the Himalayas with significant ecological and economic roles. During disease surveys in Xizang, China, we observed leaf spot and branch canker symptoms on this tree. Fungal isolates associated with these diseases were collected and identified based on morphological characteristics and phylogenetic analysis of ITS, *cal*, *his3*, *tef1*, and *tub2* sequences. As a result, *Diaporthe alnicola* sp. nov. and *D. amygdali* were identified from the leaf spots, while *D. linzhiensis* was identified to be associated with the cankered branches. This study identifies pathogenic species from alder trees, providing a foundation for future disease management and forest health research.

**Key words:** Alder, molecular phylogeny, novel taxa, plant disease, Sordariomycetes, taxonomy



Academic editor: Nattawut Boonyuen

Received: 26 November 2024

Accepted: 31 March 2025

Published: 23 April 2025

**Citation:** Li J, Li Y, Li J, Jiang N (2025) Species of *Diaporthe* (Diaporthaceae, Diaporthales) associated with *Alnus nepalensis* leaf spot and branch canker diseases in Xizang, China. MycoKeys 116: 185–204. <https://doi.org/10.3897/mycokeys.116.142750>

Copyright: © JiETING Li et al.

This is an open access article distributed under terms of the Creative Commons Attribution License (Attribution 4.0 International – CC BY 4.0).

## Introduction

*Alnus nepalensis* (Nepalese alder) is a tree species of significant ecological and economic importance, particularly in the temperate and subtropical regions of the Himalayas, including Xizang, Nepal, and northern India (Sharma et al. 1998; Xia et al. 2023). This plant fulfills a crucial role in maintaining the ecological balance of forest ecosystems (Tobita et al. 2016; Sen et al. 2022). Beyond its ecological importance, *A. nepalensis* also has considerable economic value (Saxena et al. 2016). Given its critical role in both ecosystem function and local economies, any threats to *A. nepalensis* populations, such as leaf spot and canker diseases, could have severe consequences for forest health.

*Diaporthe* is a pathogenic fungal genus in the Diaporthaceae (Diaporthales, Sordariomycetes, Ascomycota) (Udayanga et al. 2012; Dissanayake et al. 2017; Jiang et al. 2025). Species of this genus are commonly associated with plant diseases, acting as pathogens, endophytes, or saprobes (Dissanayake et al. 2020; Dong et al. 2021; Jiang et al. 2021). For example, *D. hsinchuensis* and five other



species have been shown to cause leaf spots on *Camellia sinensis* (Ariyawansa et al. 2021). Several other *Diaporthe* species were shown to be associated with branch canker, dieback, and stem blight diseases (Guarnaccia et al. 2020; Guo et al. 2020; Bai et al. 2023). Additionally, *D. biconispora* and 15 other species from this genus were described as endophytes in *Citrus* (Huang et al. 2015).

*Diaporthe* is a species-rich genus with nearly 1,300 epithets listed in Index Fungorum (<https://www.indexfungorum.org/>). Over the past decade, many new species of this genus have been described based on both morphological characteristics and molecular phylogeny (Udayanga et al. 2014, 2015; Guarnaccia and Crous 2017; Yang et al. 2017, 2020, 2021; Fan et al. 2018; Manawasinghe et al. 2019; Huang et al. 2021; Sun et al. 2021; Cao et al. 2022; Lambert et al. 2023; Zhu et al. 2023, 2024; Liu et al. 2024). However, the species concepts of several taxa have been re-evaluated in recent years using the genealogical concordance phylogenetic species recognition (GCPSR) principle and coalescence-based models, such as the General Mixed Yule-Coalescent (GMYC) and Poisson Tree Processes (PTP). These re-evaluations have led to the synonymization of several species (Hilário et al. 2021a, 2021b; Dissanayake et al. 2024). For example, recent studies demonstrated that what was once thought to be a complex of nine species (*Diaporthe amygdali* species complex) is actually a single species (Hilário et al. 2021a, 2021b).

Dissanayake et al. (2024) divided the genus *Diaporthe* into seven sections and 15 species complexes based on phylogenetic analysis of all available type isolates of this genus, such as section Rudis and the *D. virgiliae* species complex. This classification has simplified phylogenetic analysis during species identification. In the present study, a survey of alder diseases was conducted in Xizang, China, with the aim of identifying the fungal species associated with leaf spots and branch cankers through a combination of morphological and molecular approaches.

## Materials and methods

### Sample collection, isolation, and morphology

Disease investigations were conducted from June to October in 2024 in Bayi District and Bomi County, Linzhi City, Xizang, China. Branch canker and leaf spot symptoms were observed, with canker being relatively rare and leaf spots more commonly encountered (Fig. 1). Infected branches exhibited sunken, discolored lesions, along with the presence of conidiomata of the fungal pathogen. Diseased leaves displayed small, rounded, or irregularly shaped spots, characterized by dark brown margins. Branch and leaf samples were collected and placed in paper envelopes for further analysis.

Sample branches and leaves were washed with sterile water and dried using refined absorbent cotton. Tissue fragments (5 × 5 mm) from both healthy and diseased samples were cut with a sterilized surgical knife, then immersed in 75% alcohol for 1 min, subsequently washed three times for 30 seconds each in sterile water, and dried with refined absorbent cotton. These tissue fragments were then transferred to the surface of Potato Dextrose Agar (PDA) plates. Hyphal tips grown from the tissue fragments on PDA were observed under a stereomicroscope (Discovery v8, Zeiss, Oberkochen, Germany). The fragments were then subcultured onto fresh PDA plates to obtain pure cultures.

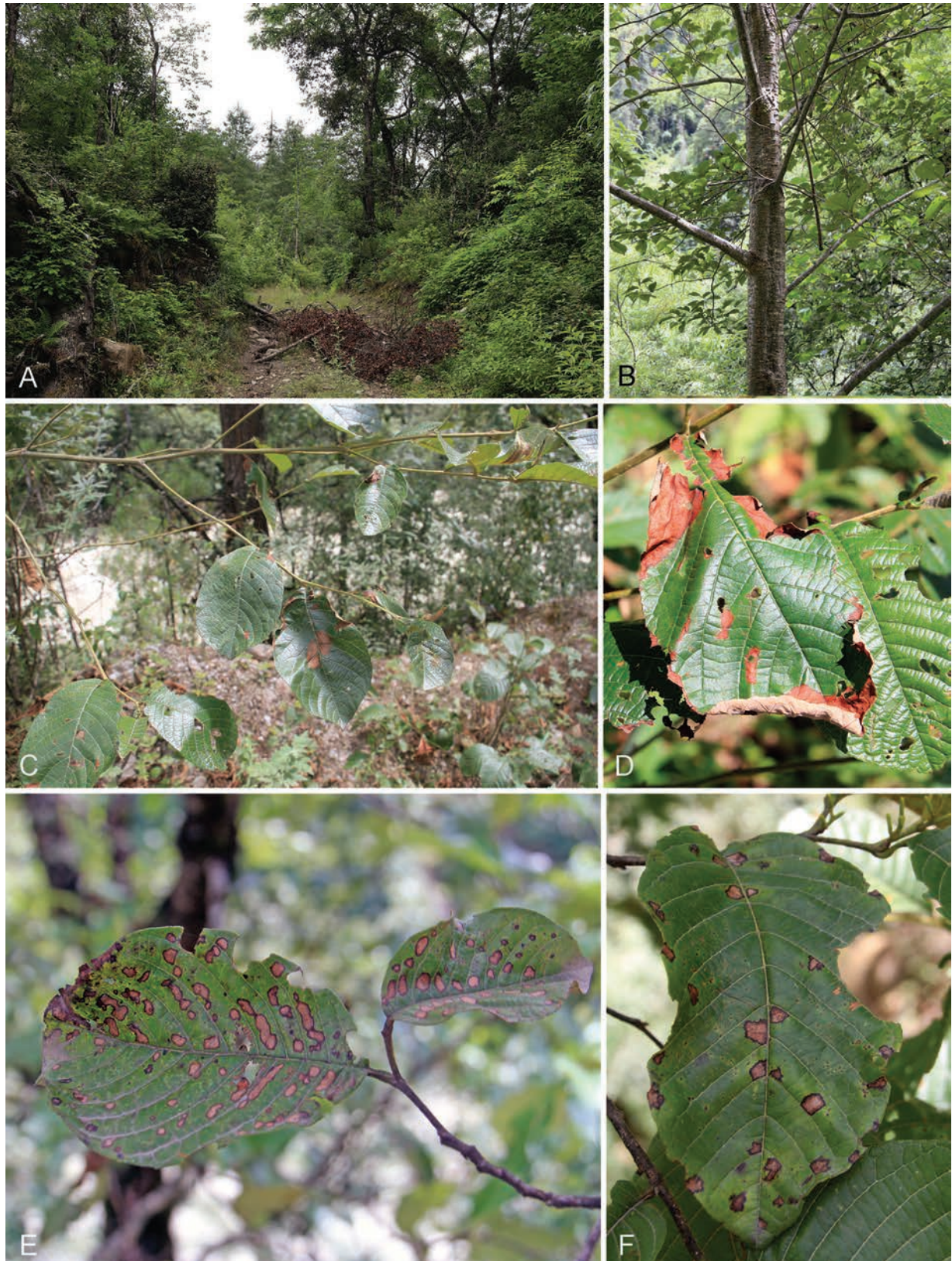


Figure 1. A, B sampling site C–F leaf spot symptoms of *Alnus nepalensis*.

Type specimens were deposited in the herbarium of the Chinese Academy of Forestry (CAF), and ex-type isolates were stored in the China Forestry Culture Collection Center (CFCC, <https://cfcc.caf.ac.cn/>).



Cultures were grown on PDA, malt extract agar (MEA), and synthetic nutrient agar (SNA) plates for observation. Conidiomata formed on the culture plates and branches were studied. The conidiomata were carefully sectioned using a double-edged blade, and fungal structures were observed under a Zeiss Discovery v8 stereomicroscope. Conidiophores, conidiogenous cells, and conidia were further examined and photographed using an Olympus BX51 microscope (Tokyo, Japan).

## Phylogenetic analyses

The genomic DNA of the *Diaporthe* isolates obtained in this study was extracted from young colonies grown on PDA plates following the protocol of Doyle and Doyle (1990). The internal transcribed spacer (ITS) region of rDNA, along with fragments of the calmodulin (*cal*), histone H3 (*his3*), translation elongation factor 1- $\alpha$  (*tef1*), and partial beta-tubulin (*tub2*) genes, was amplified using the primers and protocols outlined in Table 1. The PCR products were subjected to electrophoresis on 2% agarose gels for analysis, followed by sequencing using the same primers as those employed in the PCR amplification. The sequencing service was provided by Ruibo Xingke Biotechnology Co., Ltd. (Beijing, China).

The ITS, *cal*, *his3*, *tef1*, and *tub2* gene sequences obtained in this study were queried against the GenBank nucleotide database located at the National Center for Biotechnology Information (NCBI) to identify closely related sequences and determine the associated species. Sequence data for related taxa were retrieved from Dissanayake et al. (2024) and downloaded from NCBI (Table 2). The sequences were aligned using the MAFFT v.7 online server (<http://mafft.cbrc.jp/alignment/server/index.html>, Katoh et al. 2019) with default settings.

The isolates described in this study were shown to belong to the *Diaporthe* Section Rudis and the *D. virgiliae* species complex, respectively. Maximum likelihood (ML) phylogenetic analysis was conducted using the CIPRES Science Gateway platform (Miller et al. 2010), with RAXMLHPC2 on XSEDE (v. 8.2.10) under the GTR substitution model and 1000 non-parametric bootstrap replicates. Bayesian analysis was performed with MrBayes v. 3.2.6, utilizing four simultaneous Markov chain runs for 1,000,000 generations. The resulting trees were visualized using FigTree v. 1.4.0 (Rambaut 2012).

The pairwise homoplasy index test was employed to confirm the new species status using SplitsTree v.4.16.1 (Huson and Bryant 2006). Incongruence among the ITS-*cal*-*his3*-*tef1*-*tub2* genealogies was used as a criterion to identify hypothesized “species” and infer the occurrence of sexual recombination (Bruen et al. 2006). Results of the  $\Phi$ w-statistic below a 0.05 threshold ( $p$ -value < 0.05)

**Table 1.** Primers and PCR protocols.

Gene Regions	Primers	PCR conditions	References
ITS	ITS1/ITS4	95 °C for 4 min, 35 cycles of 94 °C for 45 s, 48 °C for 1 min, and 72 °C for 2 min, 72 °C for 10 min	White et al. 1990
<i>cal</i>	CAL228F/CAL737R	95 °C for 4 min, 35 cycles of 94 °C for 45 s, 54 °C for 1 min, and 72 °C for 2 min, 72 °C for 10 min	Carbone and Kohn 1999
<i>his3</i>	CYLH3F/H3-1b	95 °C for 5 min, 35 cycles of 95 °C for 1 min, 57 °C, 1.25 min, and 72 °C for 2 min, 72 °C for 10 min	Crous et al. 2004; Glass and Donaldson 1995
<i>tef1</i>	EF1-728F/EF1-986R	94 °C for 3 min, 35 cycles of 94 °C for 30 s, 54 °C for 50 s, and 72 °C for 2 min, 72 °C for 10 min	Carbone and Kohn 1999
<i>tub2</i>	T1(Bt2a)/Bt2b	95 °C for 4 min, 35 cycles of 94 °C for 45 s, 54 °C for 1 min, and 72 °C for 2 min, 72 °C for 10 min	Glass and Donaldson 1995; O'Donnell and Cigelnik 1997

**Table 2.** GenBank accession numbers used in the phylogenetic analyses.

Species	Strain	GenBank accession numbers					References
		ITS	<i>tef1</i>	<i>tub2</i>	<i>cal</i>	<i>his3</i>	
<i>Diaporthe acaciigena</i>	CBS 129521	KC343005	KC343731	KC343973	KC343247	KC343489	Gomes et al. 2013
<b><i>D. alnicola</i></b>	<b>CFCC 70997*</b>	<b>PQ636515</b>	<b>PQ635059</b>	<b>PQ635065</b>	<b>PQ635047</b>	<b>PQ635053</b>	<b>In this study</b>
<b><i>D. alnicola</i></b>	<b>CFCC 70998*</b>	<b>PQ636516</b>	<b>PQ635060</b>	<b>PQ635066</b>	<b>PQ635048</b>	<b>PQ635054</b>	<b>In this study</b>
<i>D. amygdali</i>	CBS 126679	KC343022	KC343748	KC343990	KC343264	KC343506	Gomes et al. 2013
<i>D. amygdali</i>	CBS 111811	KC343019	KC343745	KC343987	KC343261	KC343503	Gomes et al. 2013
<i>D. amygdali</i>	CBS 115620	KC343020	KC343746	KC343988	KC343262	KC343504	Gomes et al. 2013
<i>D. amygdali</i>	CBS 120840	KC343021	KC343747	KC343989	KC343263	KC343505	Gomes et al. 2013
<i>D. amygdali</i> syn. <i>D. chongqingensis</i>	CGMCC 3.19603	MK626916	MK654866	MK691321	MK691209	MK726257	Guo et al. 2020
<i>D. amygdali</i> syn. <i>D. chongqingensis</i>	PSCG 435	MK626916	MK654866	MK691321	MK691209	MK726257	Guo et al. 2020
<i>D. amygdali</i> syn. <i>D. chongqingensis</i>	PSCG 436	MK626917	MK654867	MK691322	MK691208	MK726256	Guo et al. 2020
<i>D. amygdali</i> syn. <i>D. chongqingensis</i>	PSCG 436-2	MK626917	MK654867	MK691322	MK691208	MK726256	Guo et al. 2020
<i>D. amygdali</i> syn. <i>D. fusicola</i>	CGMCC 3.17087	KF576281	KF576256	KF576305	KF576233	NA	Gao et al. 2015
<i>D. amygdali</i> syn. <i>D. fusicola</i>	CGMCC 3.17088	KF576263	KF576238	KF576287	KF576221	NA	Gao et al. 2015
<i>D. amygdali</i> syn. <i>D. garethjonesii</i>	MFLUCC 12-0542	KT459423	KT459457	KT459441	KT459470	NA	Gao et al. 2015
<i>D. amygdali</i> syn. <i>D. kadsurae</i>	CFCC 52586	MH121521	MH121563	MH121600	MH121439	MH121479	Yang et al. 2018
<i>D. amygdali</i> syn. <i>D. kadsurae</i>	CFCC 52587	MH121522	MH121564	MH121601	MH121440	MH121480	Yang et al. 2018
<i>D. amygdali</i> syn. <i>D. mediterranea</i>	CBS 146754	MT007496	MT006996	MT006693	MT006768	MT007102	León et al. 2020
<i>D. amygdali</i> syn. <i>D. ovoicola</i>	CGMCC 3.17092	KF576264	KF576239	KF576288	KF576222	NA	Gao et al. 2015
<i>D. amygdali</i> syn. <i>D. ovoicola</i>	CGMCC 3.17093	KF576265	KF576240	KF576289	KF576223	NA	Gao et al. 2015
<i>D. amygdali</i> syn. <i>D. ovoicola</i>	CGMCC 3.17094	KF576266	KF576241	KF576290	KF576224	NA	Gao et al. 2015
<i>D. amygdali</i> syn. <i>D. ovoicola</i>	ACJY62	MW578711	MW597404	MW598141	MW598161	MW598183	Gao et al. 2015
<i>D. amygdali</i> syn. <i>D. sterilis</i>	CBS 136969	KJ160579	KJ160611	KJ160528	KJ160548	MF418350	Lombard et al. 2014
<i>D. amygdali</i> syn. <i>D. sterilis</i>	CPC 20580	KJ160582	KJ160614	KJ160531	KJ160551	NA	Lombard et al. 2014
<i>D. amygdali</i> syn. <i>D. ternstroemia</i>	CGMCC 3.15183	KC153098	KC153089	NA	NA	NA	Gao et al. 2014
<i>D. amygdali</i> syn. <i>D. ternstroemia</i>	CGMCC 3.15184	KC153099	KC153090	NA	NA	NA	Gao et al. 2014
<b><i>D. amygdali</i></b>	<b>CFCC 70999</b>	<b>PQ636517</b>	<b>PQ635061</b>	<b>PQ635067</b>	<b>PQ635049</b>	<b>PQ635055</b>	<b>In this study</b>
<b><i>D. amygdali</i></b>	<b>Q3B</b>	<b>PQ636518</b>	<b>PQ635062</b>	<b>PQ635068</b>	<b>PQ635050</b>	<b>PQ635056</b>	<b>In this study</b>
<i>D. araucanorum</i>	CBS 145285	MN509711	MN509733	MN509722	NA	NA	Zapata et al. 2020
<i>D. araucanorum</i>	CBS 145283	MN509709	MN509731	MN509720	NA	NA	Zapata et al. 2020
<i>D. beckhausii</i>	CBS 138.27	KC343041	KC343767	KC344009	KC343283	KC343525	Gomes et al. 2013
<i>D. benedicti</i>	BPI 893190	KM669929	KM669785	NA	KM669862		Lawrence et al. 2015
<i>D. brevicongiophora</i>	CGMCC 3.24298	OP056725	OP150564	OP150641	OP150718	OP150794	Dissanayake et al. 2024
<i>D. brevicongiophora</i>	GZCC 22-0030	OP056725	OP150564	OP150641	OP150718	OP150794	Dissanayake et al. 2024
<i>D. cassines</i>	CPC 21916	KF777155	KF777244	NA	NA	NA	Crous et al. 2013
<i>D. celticola</i>	CFCC 53074	MK573948	MK574623	MK574643	MK574587	MK574603	Cao et al. 2022
<i>D. celticola</i>	CFCC 53075	MK573949	MK574624	MK574644	MK574588	MK574604	Cao et al. 2022
<i>D. crousii</i>	CAA823	MK792311	MK828081	MK837932	MK883835	MK871450	Hilário et al. 2020
<i>D. crousii</i>	CAA820	MK792300	MK828072	MK837923	MK883828	MK871441	Hilário et al. 2020
<i>D. eres</i>	AR5193	KJ210529	KJ210550	KJ420799	KJ434999	KJ420850	Udayanga et al. 2014
<i>D. eres</i>	DLR12a	KJ210518	KJ210542	KJ420783	KJ434996	KJ420833	Udayanga et al. 2014
<i>D. foikelawen</i>	CBS 145289	MN509713	MN509735	MN509724	NA	NA	Zapata et al. 2020
<i>D. foikelawen</i>	CBS 145287	MN509714	MN509736	MN509725	NA	NA	Zapata et al. 2020
<i>D. grandifori</i>	SAUCC 194.84	MT822612	MT855924	MT855809	MT855691	MT855580	Sun et al. 2021
<i>D. guizhouensis</i>	GZCC 20-0338	OM060254	OL961761	OL961762	OL961763	NA	Bhunjun et al. 2022
<i>D. guizhouensis</i>	GZCC 22-0027	OP056683	OP150522	OP150600	OP150679	OP150754	Bhunjun et al. 2022
<i>D. guizhouensis</i>	GZCC 22-0045	OP056684	OP150523	OP150601	OP150680	OP150755	Bhunjun et al. 2022
<i>D. heterophyllae</i>	CBS 143769	MG600222	MG600224	MG600226	MG600218	MG600220	Marín-Félix et al. 2019
<i>D. heveae</i>	B23	KR812219	NA	NA	NA	NA	Dos Santos et al. 2015
<b><i>D. linzhiensis</i></b>	<b>CFCC 71057*</b>	<b>PQ636519</b>	<b>PQ635063</b>	<b>PQ635069</b>	<b>PQ635051</b>	<b>PQ635057</b>	<b>In this study</b>
<b><i>D. linzhiensis</i></b>	<b>N266C*</b>	<b>PQ636520</b>	<b>PQ635064</b>	<b>PQ635070</b>	<b>PQ635052</b>	<b>PQ635058</b>	<b>In this study</b>
<i>D. nothofagi</i>	BRIP 54801	JX862530	JX862536	KF170922	NA	NA	Tan et al. 2013
<i>D. obtusifoliae</i>	CBS 143449	MG386072	NA	NA	NA	MG386137	Crous et al. 2017
<i>D. ocoteae</i>	CPC 26217	KX228293	NA	KX228388	NA	NA	Crous et al. 2013



Species	Strain	GenBank accession numbers					References
		ITS	<i>tef1</i>	<i>tub2</i>	<i>cal</i>	<i>his3</i>	
<i>D. penetrитеum</i>	LC3353	KP714505	KP714517	KP714529	NA	KP714493	Gao et al. 2016
<i>D. pustulata</i>	CBS 109742	KC343185	KC343911	KC344153	KC343427	KC343669	Gomes et al. 2013
<i>D. pustulata</i>	CBS 109784	KC343187	KC343913	KC344155	KC343429	KC343671	Gomes et al. 2013
<i>D. rudis</i>	AR3422	KC843331	KC843090	KC843177	KC843146	NA	Udayanga et al. 2014
<i>D. rudis</i>	AR3654	KC843338	KC843097	KC843184	KC843153	NA	Udayanga et al. 2014
<i>D. rudis</i>	DA244	KC843334	KC843093	KC843180	KC843149	NA	Udayanga et al. 2014
<i>D. rudis</i>	ICMP 16419	KC145904	KC145976	NA	NA	NA	Udayanga et al. 2014
<i>D. rudis</i>	ICMP 7025	KC145885	KC145995	NA	NA	NA	Udayanga et al. 2014
<i>D. rudis</i>	CBS 113201	MH862916	KC343960	KC344202	KC343476	KC343718	Vu et al. 2019
<i>D. rudis</i> syn. <i>D. australafricana</i>	CBS 111886	KC343038	KC343764	KC344006	KC343280	KC343522	Gomes et al. 2013
<i>D. rudis</i> syn. <i>D. australafricana</i>	CBS 113487	KC343039	KC343765	KC344007	KC343281	KC343523	Gomes et al. 2013
<i>D. rudis</i> syn. <i>D. cynaroidis</i>	CBS 122676	KC343058	KC343784	KC344026	KC343300	KC343542	Gomes et al. 2013
<i>D. rudis</i> syn. <i>D. patagonica</i>	CBS 145291	MN509717	MN509739	MN509728	NA	NA	Zapata et al. 2020
<i>D. rudis</i> syn. <i>D. patagonica</i>	CBS 145755	MN509718	MN509740	MN509729	NA	NA	Zapata et al. 2020
<i>D. rudis</i> syn. <i>D. salicicola</i>	BRIP 54825	JX862531	JX862537	KF170923	NA	NA	Tan et al. 2013
<i>D. rudis</i> syn. <i>D. subcylindrospora</i>	KUMCC 17-0151	MG746629	MG746630	MG746631	NA	NA	Hyde et al. 2018
<i>D. shennongjiaensis</i>	CNUCC 201905	MN216229	MN224672	MN227012	MN224551	MN224559	Zhou and Hou 2019
<i>D. shennongjiaensis</i>	CNUCC 201906	MN216228	MN224673	MN227013	MN224552	MN224561	Zhou and Hou 2019
<i>D. silvicola</i>	CFCC 54191	MZ727041	MZ816347	MZ753491	MZ753472	MZ753481	Jiang et al. 2021
<i>D. silvicola</i>	M79	MZ727042	MZ816348	MZ753492	MZ753473	MZ753482	Jiang et al. 2021
<i>D. torilicola</i>	MFLUCC 17-1051	KY964212	KY964168	KY964096	KY964127		Dissanayake et al. 2017
<i>D. toxica</i>	CBS 534.93	KC343220	KC343946	KC344188	KC343462	KC343704	Gomes et al. 2013
<i>D. toxica</i>	CBS 546.93	KC343222	KC343948	KC344190	KC343464	KC343706	Gomes et al. 2013
<i>D. virgiliae</i>	CMW 40755	KP247573	NA	KP247582	NA	NA	Machingambi et al. 2015
<i>D. virgiliae</i>	CMW 40748	KP247566	NA	KP247575	NA	NA	Machingambi et al. 2015
<i>D. zaofenghuang</i>	CGMCC 3.20271	MW477883	MW480871	MW480875	MW480867	MW480863	Wang et al. 2021
<i>D. zaofenghuang</i>	TZFH3	MW477884	MW480872	MW480876	MW480868	MW480864	Wang et al. 2021

**Note:** "NA" indicates unavailable sequences; sequences produced in the current study are in bold, and \* means ex-type strains from new species in this study.

indicated significant recombination. A phylogenetic network based on the combined dataset of five loci was constructed using the NeighborNet algorithm to assess the impact of recombination.

## Results

### Phylogenetic analyses

For the analysis of *Diaporthe* Section *Rudis*, the combined dataset of ITS, *cal*, *his3*, *tef1*, and *tub2* comprised 67 strains, with *D. eres* (AR5193 and DLR12a) used as the outgroup taxa. The final alignment included 2,691 characters (ITS: 451, *cal*: 702, *his3*: 410, *tef1*: 596, *tub2*: 532), including gaps. The final ML optimization likelihood value of the best RAxML tree was -17019.93, and the matrix contained 1,257 distinct alignment patterns, with 32.15% undetermined characters or gaps. The estimated base frequencies were A = 0.216951, C = 0.313266, G = 0.235799, T = 0.233984; substitution rates were AC = 1.028567, AG = 3.157223, AT = 1.223911, CG = 0.822997, CT = 4.362405, GT = 1.0; and the gamma distribution shape parameter  $\alpha$  = 0.386104. Both the RAxML and Bayesian analyses produced similar tree topologies, which were consistent with those of previous studies (Norphanphoun et al. 2022; Dissanayake et al. 2024). Isolates from this study (CFCC 70999 and Q3B) clustered together with other *Diaporthe amygdali* strains, showing strong support (Fig. 2), thus confirming their identification as *D. amygdali*.

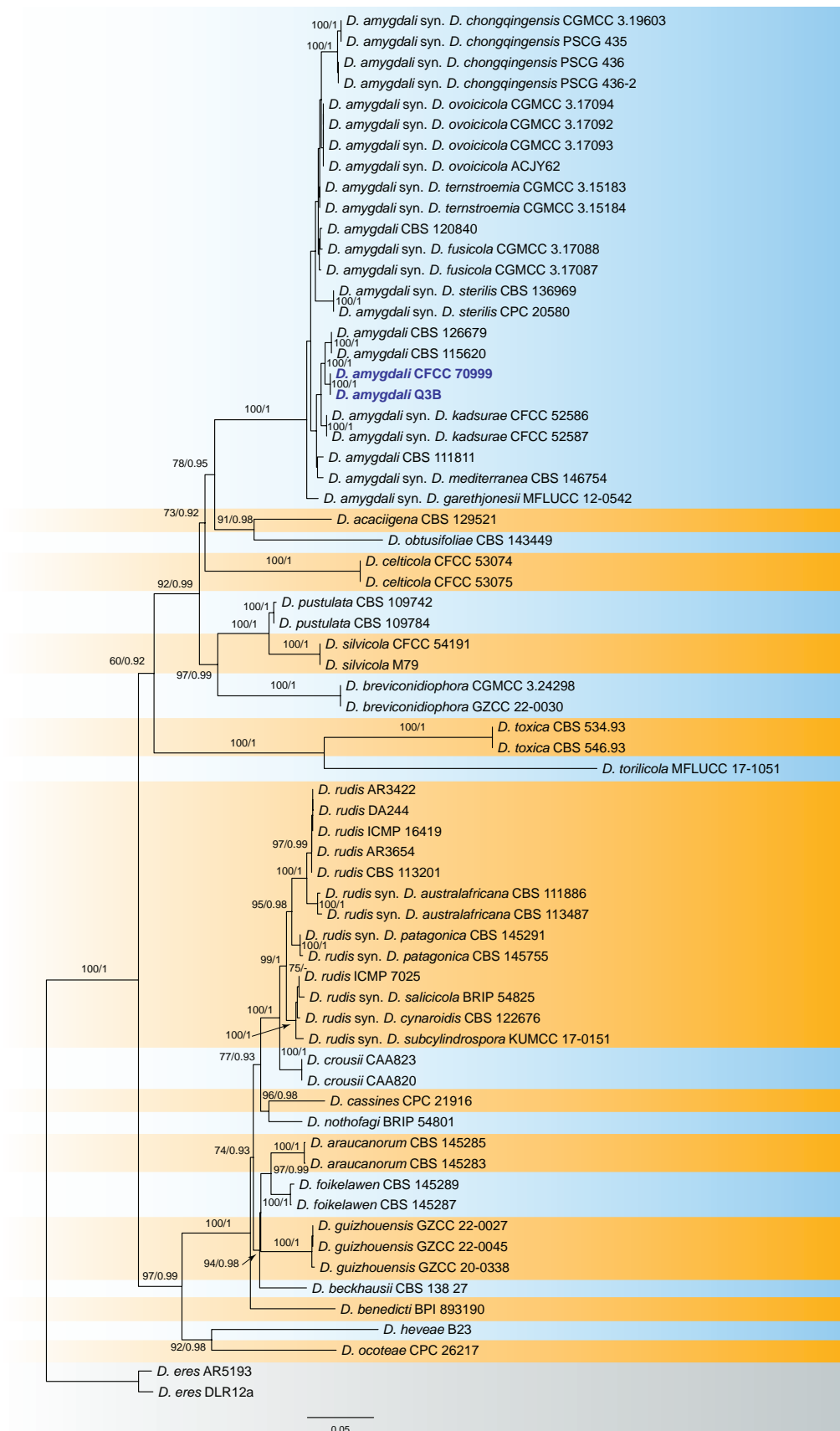


**Figure 2.** Maximum likelihood tree of *Diaporthe* Section Rudis generated from combined ITS, *cal*, *his3*, *tef1*, and *tub2* sequence data. Bootstrap support values  $\geq 50\%$  and Bayesian posterior probabilities  $\geq 0.90$  are demonstrated at the branches. Isolates from the present study are indicated in blue.

In the *Diaporthe virgiliae* species complex, the combined dataset of ITS, *cal*, *his3*, *tef1*, and *tub2* included 13 strains, with *D. shennongjiaensis* (CUNCC 201905 and CUNCC 201906) as the outgroup taxa. The final alignment contained 2,598 characters (ITS: 593, *cal*: 421, *his3*: 466, *tef1*: 331, *tub2*: 787), including gaps. The final ML optimization likelihood value of the best RAXML tree was -5834.44, and the matrix had 346 distinct alignment patterns, with 20.11% undetermined characters or gaps. The estimated base frequencies were A = 0.212455, C = 0.329026, G = 0.238268, T = 0.220251; substitution rates were AC = 1.111868, AG = 2.843163, AT = 1.775735, CG = 0.816784, CT = 3.662621, GT = 1.0; and the gamma distribution shape parameter  $\alpha$  = 0.047755. Both RAXML and Bayesian analyses produced similar tree topologies, which closely matched those of prior publications (Norphanphoun et al. 2022; Dissanayake et al. 2024). Four isolates from this study formed two new clades distinct from any lineage and are hence accommodated as two novel species: *D. alnicola* (CFCC 70997 and CFCC 70998) and *D. linzhiensis* (CFCC 71057 and N266C).

The network relationships within the *D. virgiliae* species complex are depicted in Fig. 4, indicating no significant recombination based on the PHI test ( $p$  = 0.9624). Furthermore, based on the relative distances between species and the structure of the phylogenetic network, isolates within the *D. virgiliae* complex represent seven different species.

## Taxonomy

### *Diaporthe alnicola* Ning Jiang, sp. nov.

MycoBank No: 856742

Fig. 5

**Etymology.** “*Alni*” refers to the host genus *Alnus*, and “-cola” means inhabiting.

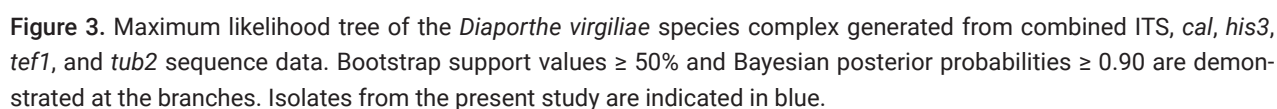
**Description.** Associated with leaf spot disease of *Alnus nepalensis*.

**Teleomorph:** Undetermined. **Anamorph:** Conidiomata formed on PDA pycnidial, scattered, erumpent, pulvinate to subglobose, dark brown, 150–350  $\mu$ m diam. Conidiophores indistinct, usually reduced to conidiogenous cells. Conidiogenous cells cylindrical, attenuate towards the apex, hyaline, phialidic, 9.5–33  $\times$  2–3  $\mu$ m. Alpha conidia aseptate, hyaline, smooth, guttulate, cylindrical, straight, base truncate, (6–)6.5–7(–7.5)  $\times$  (2–)2.5–3(–3.5)  $\mu$ m ( $\bar{x}$  = 6.8  $\times$  2.6  $\mu$ m,  $n$  = 50), L/W = 2–3.4. Beta conidia aseptate, hyaline, smooth, guttulate, filiform, tapering towards both ends, curved, (13–)14.5–22(–24)  $\times$  1.5–2.5  $\mu$ m ( $\bar{x}$  = 18.3  $\times$  2.1  $\mu$ m,  $n$  = 50), L/W = 5.9–12.5. Gamma conidia not observed.

**Culture characteristics.** Colonies on PDA at 25 °C are spreading, flocculent, forming abundant aerial mycelium and an undulate margin, initially white, turning mouse gray and reaching a diameter of 90 mm after 10 d, developing dark brown conidiomata with orange conidial masses after 20 d. Colonies on MEA at 25 °C are flat, spreading, feathery, with a smooth entire margin, white, reaching a diameter of 90 mm after 15 d, sterile. Colonies on SNA at 25 °C are flat, spreading with a smooth entire margin, white, reaching 90 mm in diameter after 20 d, developing dark brown conidiomata with orange conidial masses after 30 d.

**Materials examined.** CHINA • Xizang Autonomous Region (Tibet), Linzhi City, Bayi District, Pailong Town, 30°4'22"N, 95°8'2"E, 2192 m, from leaf spots of

**Notes.** *Diaporthe alnicola*, identified from leaf spots on *Alnus nepalensis* in this study, is phylogenetically closely related to *D. virgiliae*, which originates from the rot root of *Virgilia oroboides* in South Africa (Fig. 3). Morphologically, *D. alnicola* is similar to *D. virgiliae* in terms of the size of alpha and beta conidia (alpha conidia:  $6.5\text{--}7 \times 2.5\text{--}3 \mu\text{m}$  in *D. alnicola* vs.  $5.2\text{--}8 \times 1.1\text{--}3.5 \mu\text{m}$  in *D. virgiliae*; beta conidia:  $14.5\text{--}22 \times 1.5\text{--}2.5 \mu\text{m}$  in *D. alnicola* vs.  $17.1\text{--}25.4 \times 1\text{--}1.8 \mu\text{m}$  in *D. virgiliae*). However, they can be distinguished by the size of their conidiogenous cells ( $9.5\text{--}33 \times 2\text{--}3 \mu\text{m}$  in *D. alnicola* vs.  $12.3\text{--}21.3 \times 0.7\text{--}1.5 \mu\text{m}$  in *D. virgiliae*) (Machingambi et al. 2015). Furthermore, *D. alnicola* differs from *D. virgiliae* at the nucleotide level (ITS, 11/432; *tub2*, 7/743).





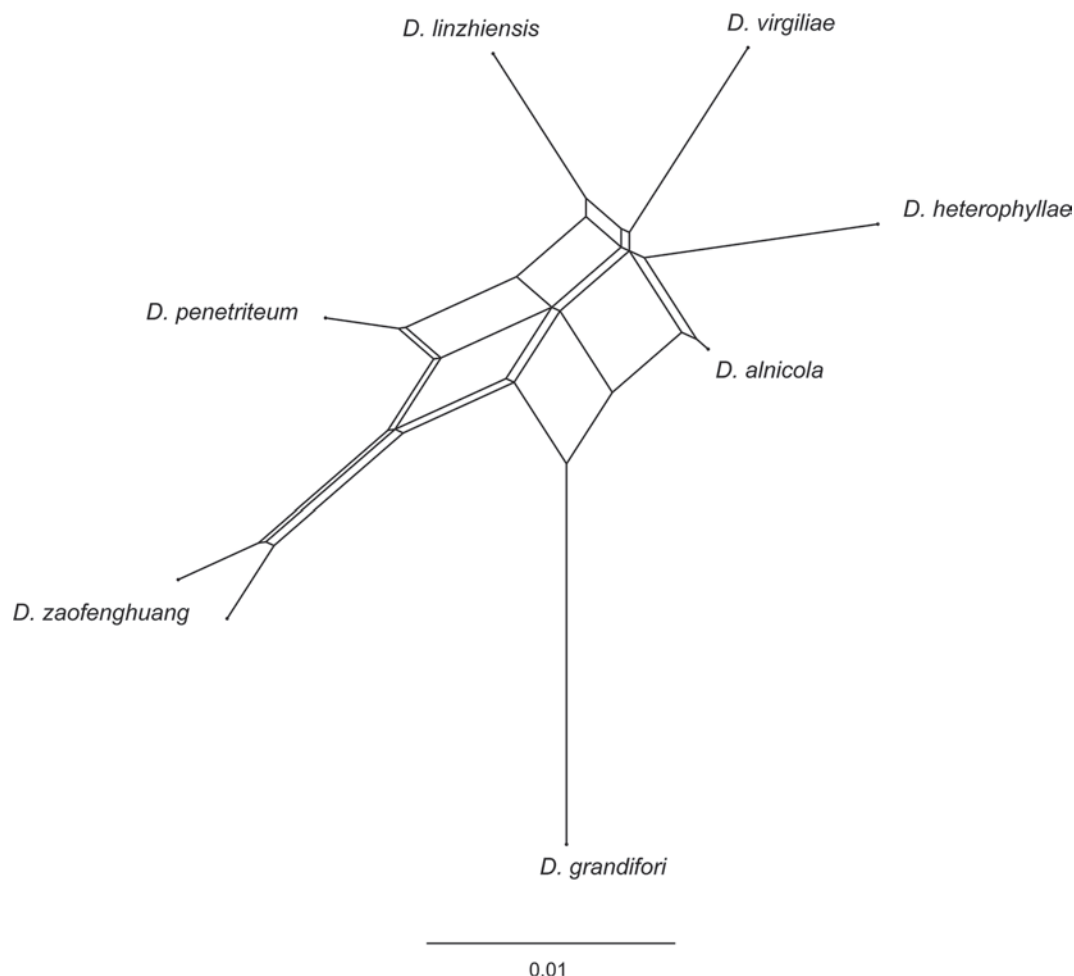


**Figure 4.** Phylogenetic network from concatenated data (ITS, *cal*, *his3*, *tef1*, and *tub2*) representing the structure of the *Diaporthe virgiliae* species complex, based on LogDet transformation and the NeighborNet algorithm, inferred by SplitsTree ( $p = 0.9624$ ). The scale bar represents the expected number of substitutions per nucleotide position.

***Diaporthe amygdali* (Delacr.) Udayanga, Crous & K.D. Hyde, Fungal Diversity 56(1): 166. 2012**

Fig. 6

**Description.** Associated with leaf spot disease of *Alnus nepalensis*. **Teleomorph:** Undetermined. **Anamorph:** Conidiomata formed on PDA pycnidial, scattered, erumpent, subglobose, dark brown, 700–2250  $\mu\text{m}$  diam. Conidiophores indistinct, usually reduced to conidiogenous cells. Conidiogenous cells cylindrical, attenuate towards the apex, hyaline, phialidic, 16.5–34  $\times$  1.5–3  $\mu\text{m}$ . Alpha conidia not observed. Beta conidia aseptate, hyaline, smooth, guttulate, filiform, tapering towards both ends, straight or slightly curved, (27.5–)30–35(–40.5)  $\times$  1.5–2  $\mu\text{m}$  ( $\bar{x} = 32.6 \times 1.6 \mu\text{m}$ ,  $n = 50$ ), L/W = 15.8–23.1. Gamma conidia not observed.

**Culture characteristics.** Colonies on PDA at 25 °C are flocculent, forming concentric zones with undulate margins, initially white, turning pale brownish, and reaching a diameter of 90 mm after 10 d, developing dark brown conidiomata with white conidial masses after 25 d. Colonies on MEA at 25 °C are flat, spreading, with a smooth entire margin, white, reaching a diameter of 80 mm after 20 d, sterile. Colonies on SNA at 25 °C are flat, spreading with a feathery margin, white, reaching 80 mm in diameter after 20 d, sterile.

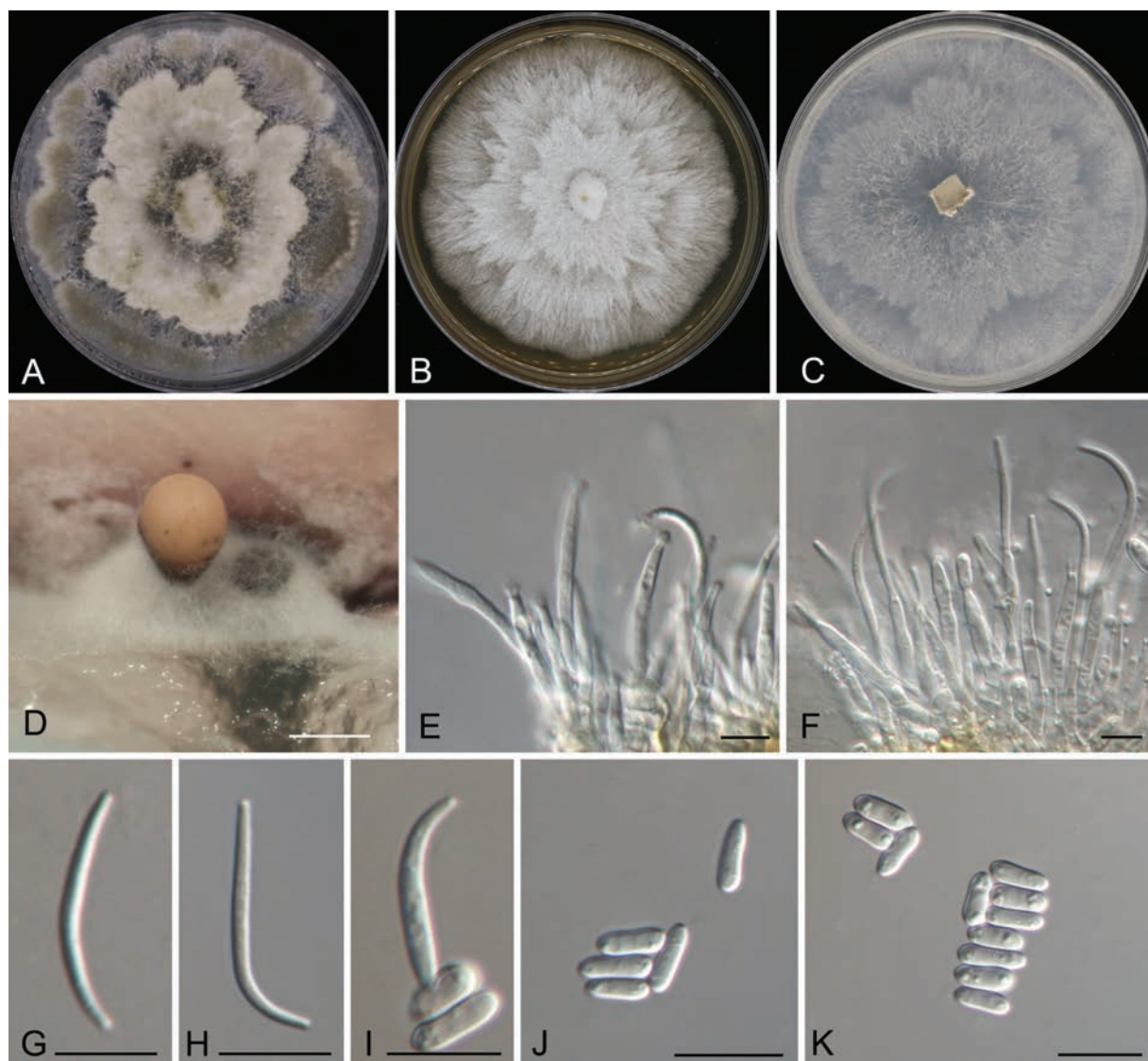


**Figure 5.** Morphology of *Diaporthe alnicola* **A** colony on PDA after 15 d **B** Colony on MEA after 15 d **C** colony on SNA after 15 d **D** conidioma formed on PDA **E, F** conidiogenous cells **G–K** alpha and beta conidia. Scale bars: 500 µm (**D**); 10 µm (**E–K**).

**Materials examined.** CHINA • Xizang Autonomous Region (Tibet), Linzhi City, Bayi District, Pailong Town, 30°4'22"N, 95°8'2"E, 2192 m, from leaf spots of *Alnus nepalensis*, 9 Jul. 2024, Ning Jiang, JiETING LI & Haoyin Zhang (cultures CFCC 70999 and Q3B).

**Notes.** The species concept of *Diaporthe amygdali* has been revised in recent studies using phylogenetic analysis, GCPSR, and coalescence-based models (Hilário et al. 2021b; Dissanayake et al. 2024). Currently, *D. amygdali* is considered synonymous with *D. chongqingensis*, *D. fusicola*, *D. garethjonesii*, *D. kadsurae*, *D. mediterranea*, *D. ovoicicola*, *D. sterilis*, and *D. ternstroemia* (Hilário et al. 2021b; Dissanayake et al. 2024). This fungus is widely distributed, inhabiting a range of plant hosts, including *Acer* spp., *Camellia sinensis*, *Lithocarpus glabra*, *Prunus dulcis*, *Prunus persica*, *Prunus salicina*, *Pyrus pyrifolia*, *Ternstroemia gymnanthera*, *Vaccinium corymbosum*, and *Vitis vinifera* (Hilário et al. 2021b). In this study, two isolates from leaf spots of *Alnus nepalensis* clustered with strains of *D. amygdali* with high support values (Fig. 2). Therefore, these two isolates were identified as *D. amygdali*, which led us to describe *Alnus nepalensis* as a new host for this fungus.

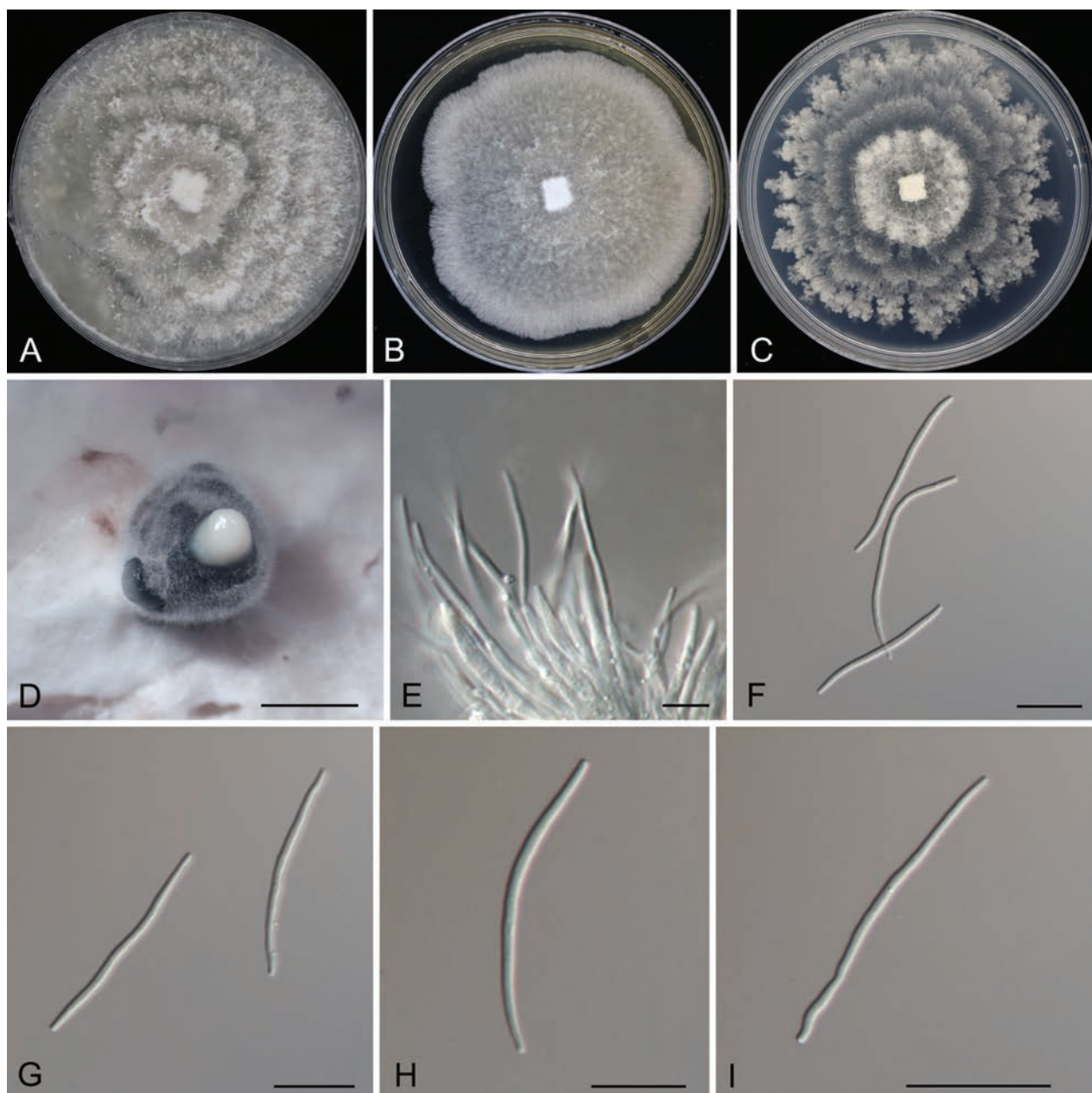


**Figure 6.** Morphology of *Diaporthe amygdali* **A** colony on PDA after 15 d **B** colony on MEA after 15 d **C** colony on SNA after 15 d **D** conidioma formed on PDA **E** conidiogenous cells **E–I** beta conidia. Scale bars: 800 µm (**D**); 10 µm (**E–I**).

***Diaporthe linzhiensis* Ning Jiang, sp. nov.**

MycoBank No: 856743

Fig. 7

**Etymology.** Named after the collection site of the type specimen, Linzhi City.

**Description.** Associated with branch canker disease of *Alnus nepalensis*.

**Teleomorph:** Undetermined. **Anamorph:** Conidiomata pycnidial, immersed in bark, scattered, erumpent through the bark surface, conical, with a solitary locule, 300–500 µm diam., 250–400 µm high. Conidiophores reduced to conidiogenous cells. Conidiogenous cells cylindrical, attenuate towards the apex, hyaline, phialidic, straight or slightly curved,  $5.5\text{--}16 \times 1.5\text{--}3$  µm. Alpha conidia not



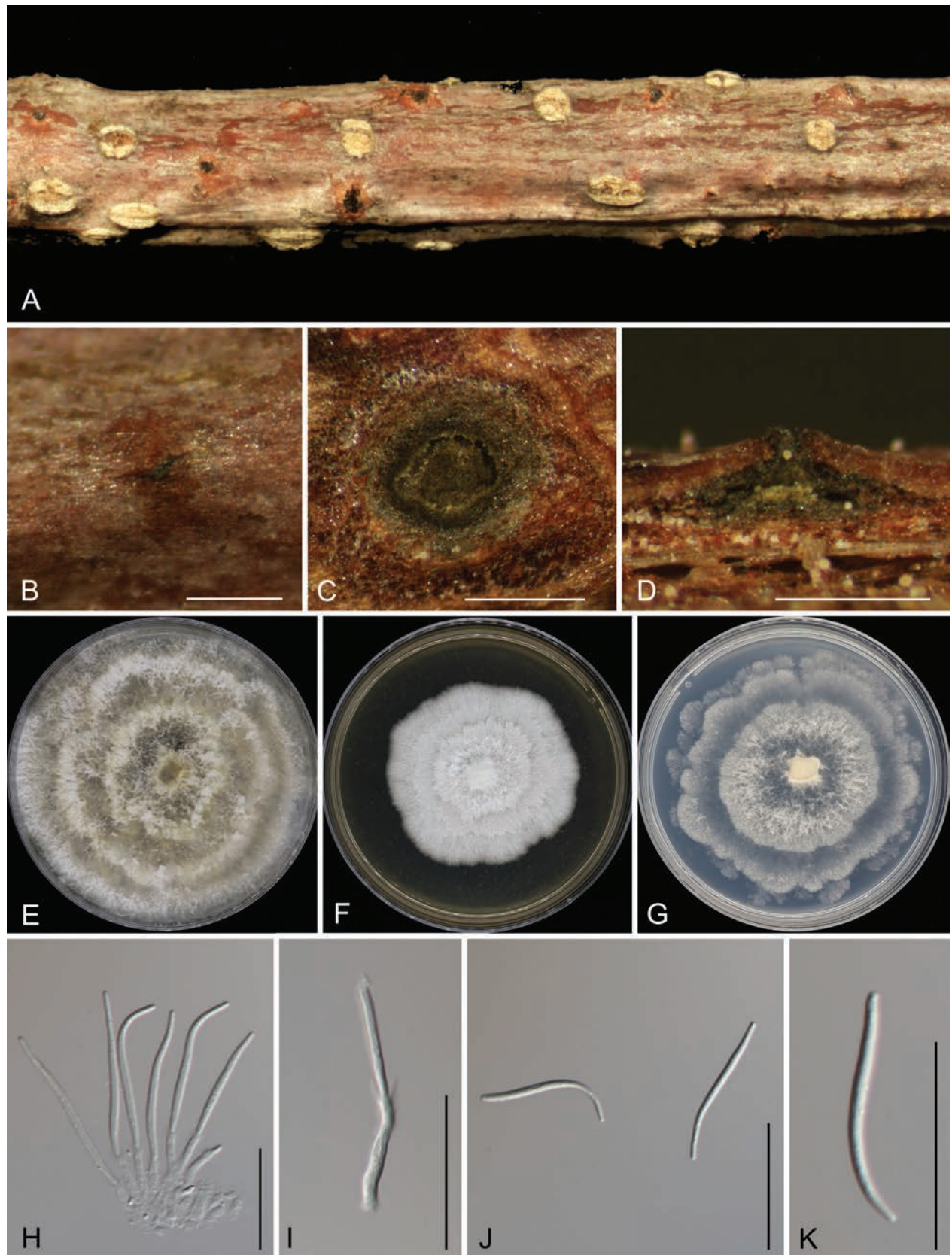


**Figure 7.** Morphology of *Diaporthe linzhiensis* **A, B** conidiomata formed on twigs of *Alnus nepalensis* **C** transverse section through a conidioma **D** longitudinal section through a conidioma **E** colony on PDA after 15 d **F** colony on MEA after 15 d **G** colony on SNA after 15 d **H, I** conidiogenous cells **J, K** beta conidia. Scale bars: 500  $\mu$ m (**B–D**); 20  $\mu$ m (**H–K**).



observed. Beta conidia aseptate, hyaline, smooth, guttulate, filiform, tapering towards both ends, straight or slightly curved,  $(23.5\text{--}24.5\text{--}29\text{--}30) \times 1.5\text{--}2\text{ }\mu\text{m}$  ( $\bar{x} = 26.6 \times 1.8\text{ }\mu\text{m}$ ,  $n = 50$ ),  $L/W = 12.4\text{--}19.4$ . Gamma conidia not observed.

**Culture characteristics.** Colonies on PDA at 25 °C are spreading, flocculent, forming abundant aerial mycelium and concentric zones with an undulate margin, initially white, turning pale luteous, and reaching a diameter of 90 mm after 10 d, sterile. Colonies on MEA at 25 °C are flat, spreading, with a smooth entire margin, white, reaching a diameter of 60 mm after 20 d, sterile. Colonies on SNA at 25 °C are flat, spreading, forming concentric zones with undulate margins, white, reaching 80 mm in diameter after 20 d, sterile.

**Materials examined.** CHINA • Xizang Autonomous Region (Tibet), Linzhi City, Bomi County, Tongmai Town, 30°5'53"N, 95°3'49"E, 2055 m, from branches of *Alnus nepalensis*, 9 Jul. 2024, Ning Jiang, JiETING LI & Haoyin Zhang (**holotype** CAF800101, ex-paratype cultures CFCC 71057 and N266C).

**Notes.** *Diaporthe linzhiensis* is phylogenetically closely related to *D. alnicola*, *D. heterophyllae*, and *D. virgiliae* (Fig. 2). Both *D. linzhiensis* and *D. alnicola* infect *Alnus nepalensis* in China, while *D. heterophyllae* is found on *Acacia heterophylla* in France, and *D. virgiliae* inhabits *Virgilia oroboides* in South Africa (Machingambi et al. 2015; Marín-Felix et al. 2019). Morphologically, *D. linzhiensis* shares a similar conidiogenous cell size with *D. alnicola* and *D. heterophyllae*, which is wider than that of *D. virgiliae* ( $5.5\text{--}16 \times 1.5\text{--}3\text{ }\mu\text{m}$  in *D. linzhiensis* vs.  $9.5\text{--}33 \times 2\text{--}3\text{ }\mu\text{m}$  in *D. alnicola* vs.  $6\text{--}9 \times 1\text{--}2\text{ }\mu\text{m}$  in *D. heterophyllae* vs.  $12.3\text{--}21.3 \times 0.7\text{--}1.5\text{ }\mu\text{m}$  in *D. virgiliae*). Additionally, *D. linzhiensis* has longer beta conidia compared to the other species ( $24.5\text{--}29 \times 1.5\text{--}2\text{ }\mu\text{m}$  in *D. linzhiensis* vs.  $14.5\text{--}22 \times 1.5\text{--}2.5\text{ }\mu\text{m}$  in *D. alnicola* vs.  $17\text{--}24 \times 1\text{--}2\text{ }\mu\text{m}$  in *D. heterophyllae* vs.  $17.1\text{--}25.4 \times 1\text{--}1.8\text{ }\mu\text{m}$  in *D. virgiliae*) (Machingambi et al. 2015; Marín-Felix et al. 2019). At the nucleotide level, *D. linzhiensis* also differs from *D. alnicola* (ITS, 23/547; *cal*, 2/382; *his3*, 6/469; *tef1*, 4/349; *tub2*, 6/778), *D. heterophyllae* (ITS, 28/560; *cal*, 11/420; *his3*, 6/447; *tef1*, 12/326; *tub2*, 3/406), and *D. virgiliae* (ITS, 16/434; *tub2*, 7/743).

## Discussion

This study enhances the understanding of *Diaporthe* species on alder by revealing two previously undescribed species and a new host association, viz. *Diaporthe alnicola* sp. nov., *D. linzhiensis* sp. nov., and *D. amygdali* on *Alnus nepalensis*. *Diaporthe* is a morphologically distinct genus characterized by the production of alpha, beta, and gamma conidia. The alpha conidia are typically aseptate, hyaline, guttulate, and cylindrical to fusiform, while the beta conidia are aseptate, hyaline, and filiform (Farr et al. 2002; Udayanga et al. 2015; Guarnaccia and Crous 2017; Manawasinghe et al. 2019; Huang et al. 2021; Sun et al. 2021; Lambert et al. 2023). However, species within the genus usually share the same host genera and are morphologically similar, often exhibiting overlapping sizes of conidia or ascospores. As a result, it is relatively easy to identify specimens at the generic level, but more challenging to distinguish them at the species level (Yang et al. 2020, 2021; Zhu et al. 2023, 2024; Liu et al. 2024). In this study, we present novel findings from Xizang, China, which indicate the potential existence of numerous undescribed species in unexplored or minimally investigated regions worldwide.

*Diaporthe alnicola* and *D. amygdali* are here reported to be associated with leaf spot disease of *Alnus nepalensis*, which is a common disease in Linzhi,

Xizang, China. Among these pathogens, *D. alnicola* is a novel species and may be the primary pathogen associated with *A. nepalensis*. In contrast, *D. amygdali* is a generalist fungus that infects a wide range of plant hosts, including *Acer* spp., *Camellia sinensis*, *Lithocarpus glabra*, *Prunus dulcis*, *Pr. persica*, *Pr. salicina*, *Pyrus pyrifolia*, *Ternstroemia gymnanthera*, *Vaccinium corymbosum*, and *Vitis vinifera* (Hilário et al. 2021b). This suggests that *D. amygdali* may be a secondary pathogen to *A. nepalensis*. For successful disease management, it will be of paramount importance, albeit challenging, to effectively interrupt the infection cycle of *A. nepalensis* maintained by the occurrence of leaf spots caused by and due to the broad host range of *D. amygdali*. Therefore, future investigations need to focus on identifying other hosts of *D. amygdali* in Linzhi City.

## Additional information

### Conflict of interest

The authors have declared that no competing interests exist.

### Ethical statement

No ethical statement was reported.

### Funding

This research was funded by the Science and Technology Project of Nyingchi City, Tibet Autonomous Region (SYQ2024-14), the Key Laboratory of Forest Ecology in Xizang Plateau (Xizang Agricultural and Animal Husbandry University), Ministry of Education, Grant numbers XZAJYBSYS-202401 and XZAJYBSYS-202404, the Science and Technology Project of the Department of Science and Technology of Tibet Autonomous Region (XZ202301JD0001G), and the National Microbial Resource Center of the Ministry of Science and Technology of the People's Republic of China (NMRC-2024-7).

### Author contributions

Conceptualization: JTL, JRL, NJ. Methodology: JRL, NJ. Formal analysis: JTL, YL. Investigation: JTL, JRL, NJ. Data curation: JTL, JRL, NJ. Writing-original draft: JTL. Writing-review and editing: JRL, NJ. Visualization: NJ.

### Author ORCIDs

Jieting Li  <https://orcid.org/0009-0001-8984-7261>

Yi Li  <https://orcid.org/0009-0004-0656-9799>

Jiangrong Li  <https://orcid.org/0000-0002-6679-5227>

Ning Jiang  <https://orcid.org/0000-0002-9656-8500>

### Data availability

All of the data that support the findings of this study are available in the main text.

## References

Ariyawansa HA, Tsai I, Wang JY, Withee P, Tanjira M, Lin SR, Suwannarach N, Kumla J, Elgorban AM, Cheewangkoon R (2021) Molecular phylogenetic diversity and biological characterization of *Diaporthe* species associated with leaf spots of *Camellia sinensis* in Taiwan. *Plants* 10(7): 1434. <https://doi.org/10.3390/plants10071434>

- Bai Y, Lin L, Pan M, Fan XL (2023) Studies of *Diaporthe* (Diaporthaceae, Diaporthales) species associated with plant cankers in Beijing, China, with three new species described. *MycKeys* 98: 59–86. <https://doi.org/10.3897/mycokeys.98.104156>
- Bhunjun CS, Niskanen T, Suwannarach N, Wannathes N, Chen YJ, McKenzie EH, Lumyong S (2022) The numbers of fungi: Are the most speciose genera truly diverse? *Fungal Diversity* 114(1): 387–462. <https://doi.org/10.1007/s13225-022-00501-4>
- Bruen TC, Philippe H, Bryant D (2006) A simple and robust statistical test for detecting the presence of recombination. *Genetics* 172(4): 2665–2681. <https://doi.org/10.1534/genetics.105.048975>
- Cao L, Luo D, Lin W, Yang Q, Deng X (2022) Four new species of *Diaporthe* (Diaporthaceae, Diaporthales) from forest plants in China. *MycKeys* 91: 25–47. <https://doi.org/10.3897/mycokeys.91.84970>
- Carbone I, Kohn LM (1999) A method for designing primer sets for speciation studies in filamentous ascomycetes. *Mycologia* 3(3): 553–556. <https://doi.org/10.1080/00275514.1999.12061051>
- Crous PW, Groenewald JZ, Rissède JM, Simoneau P, Hywel-Jones NL (2004) *Calonectria* species and their *Cylindrocladium* anamorphs: Species with sphaeropedunculate vesicles. *Studies in Mycology* 50: 415–430.
- Crous PW, Wingfield MJ, Guarro J, Cheewangkoon R, van der Bank M, Swart WJ, Stchigel AM, Cano-Lira JF, Roux J, Madrid H, Damm U, Wood AR, Shuttleworth LA, Hodges CS, Munster M, de Jesús Yáñez-Morales M, Zúñiga-Estrada L, Cruywagen EM, De Hoog GS, Silvera C, Najafzadeh J, Davison EM, Davison PJN, Barrett MD, Barrett RL, Manamgoda DS, Minnis AM, Kleczewski NM, Flory SL, Castlebury LA, Clay K, Hyde KD, Maússe-Sitoe SND, Chen Shuaifei, Lechat C, Hairaud M, Lesage-Meessen L, Pawłowska J, Wilk M, Śliwińska-Wyrzychowska A, Mętrak M, Wrzosek M, Pavlic-Zupanc D, Maleme HM, Slippers B, Mac Cormack WP, Archuby DI, Grünwald NJ, Tellería MT, Dueñas M, Martín MP, Marincowitz S, de Beer ZW, Perez CA, Gené J, Marin-Felix Y, Groenewald J Z (2013) Fungal Planet description sheets: 154–213. *Persoonia* 31(1): 188–296. <https://doi.org/10.3767/003158513X675925>
- Crous PW, Wingfield MJ, Burgess TI, Carnegie AJ, Hardy GE, Smith D, Summerell BA, Cano-Lira JF, Guarro J, Houbraken J, Lombard L, Martín MP, Sandoval-Denis M, Alexandrova AV, Barnes CW, Baseia IG, Bezerra JDP, Guarnaccia V, May TW, Hernández-Restrepo M, Stchigel AM, Miller AN, Ordoñez ME, Abreu VP, Accioly T, Agnello C, Agustincolmán A, Albuquerque CC, Alfredo DS, Alvarado P, Araújo-Magalhães GR, Arauzo S, Atkinson T, Barili A, Barreto RW, Bezerra JL, Cabral TS, Rodríguez F Camello, Cruz RHSF, Daniëls PP, da Silva BDB, de Almeida DAC, de Carvalho Júnior AA, Decock CA, Delgat L, Denman S, Dimitrov RA, Edwards J, Fedosova AG, Ferreira RJ, Firmino AL, Flores JA, García D, Gené J, Giraldo A, Góis JS, Gomes AAM, Gonçalves CM, Gouliamova DE, Groenewald M, Guéorguiev BV, Guevara-Suarez M, Gusmão LFP, Hosaka K, Hubka V, Huhndorf SM, Jadan M, Jurjevi, Kraak B, Kuera V, Kumar TKA, Kušan I, Lacerda SR, Lamertthton S, Lisboa WS, Loizides M, Luangsa-Ard JJ, Lysková P, McCormack WP, Macedo DM, Machado AR, Malysheva EF, Marinho P, Matoec N, Meijer M, Meši A, Mongkolsamrit S, Moreira KA, Morozova OV, Nair KU, Nakamura N, Noisripoom W, Olariaga I, Oliveira RJV, Paiva LM, Pawar P, Pereira OL, Peterson SW, Prieto M, Rodríguez-Andrade E, Rojodeblas C, Roy M, Santos ES, Sharma R, Silva GA, Souza-Motta CM, Takeuchi-Kaneko Y, Tanaka C, Thakur A, Smith MTH, Tkalec Z, Valenzuela-Lopez N, Vanderkleij P, Verbeken A, Viana MG, Wang XW, Groenewald JZ (2017) Fungal Planet description sheets: 625–715. *Persoonia* 39: 270–467. <https://doi.org/10.3767/persoonia.2017.39.11>

- Dissanayake AJ, Phillips AJL, Hyde KD, Yan JY, Li XH (2017) The current status of species in *Diaporthe*. *Mycosphere* 8: 1106–1156. <https://doi.org/10.5943/mycosphere/8/5/5>
- Dissanayake AJ, Chen YY, Liu JK (2020) Unravelling *Diaporthe* species associated with woody hosts from karst formations (Guizhou) in China. *Journal of Fungi* 6(4): 251. <https://doi.org/10.3390/jof6040251>
- Dissanayake AJ, Zhu JT, Chen YY, Maharachchikumbura SS, Hyde KD, Liu JK (2024) A re-evaluation of *Diaporthe*: Refining the boundaries of species and species complexes. *Fungal Diversity* 126(1): 1–125. <https://doi.org/10.1007/s13225-024-00538-7>
- Dong Z, Manawasinghe IS, Huang Y, Shu Y, Phillips AJL, Dissanayake AJ, Hyde KD, Xiang M, Luo M (2021) Endophytic *Diaporthe* associated with *Citrus grandis* cv. *to-mentosa* in China. *Frontiers in Microbiology* 11: e3621. <https://doi.org/10.3389/fmicb.2020.609387>
- Dos Santos RBM, Silva A, Alvarez MR, de Oliveira TB, Rodrigues A (2015) Fungal communities in gardens of the leafcutter ant *Atta cephalotes* in forest and cabruca agrosystems of southern Bahia State (Brazil). *Fungal Biology* 119(12): 1170–1178. <https://doi.org/10.1016/j.funbio.2015.09.001>
- Doyle JJ, Doyle JL (1990) Isolation of plant DNA from fresh tissue. *Focus* 12: 13–15.
- Fan XL, Yang Q, Bezerra JDP, Alvarez LV, Tian CM (2018) *Diaporthe* from walnut tree (*Juglans regia*) in China, with insight of *Diaporthe eres* complex. *Mycological Progress*: 1–13. <https://doi.org/10.1007/s11557-018-1395-4>
- Farr DF, Castlebury LA, Rossman AY (2002) Morphological and molecular characterization of *Phomopsis vaccinii* and additional isolates of *Phomopsis* from blueberry and cranberry in the eastern United States. *Mycologia* 94(3): 494–504. <https://doi.org/10.1080/15572536.2003.11833214>
- Gao YH, Sun W, Su YY, Cai L (2014) Three new species of *Phomopsis* in Gutianshan nature reserve in China. *Mycological Progress* 13: 111–121. <https://doi.org/10.1007/s11557-013-0898-2>
- Gao Y, Su Y, Sun W, Cai L (2015) *Diaporthe* species occurring on *Lithocarpus glabra* in China, with descriptions of five new species. *Fungal Biology* 119(5): 295–309. <https://doi.org/10.1016/j.funbio.2014.06.006>
- Gao Y, Liu F, Cai L (2016) Unravelling *Diaporthe* species associated with *Camellia*. *Systematics and Biodiversity* 14(1): 102–117. <https://doi.org/10.1080/14772000.2015.1101027>
- Glass NL, Donaldson GC (1995) Development of primer sets designed for use with the PCR to amplify conserved genes from filamentous ascomycetes. *Applied and Environmental Microbiology* 61(4): 1323–1330. <https://doi.org/10.1128/aem.61.4.1323-1330.1995>
- Gomes RR, Glienke C, Videira SIR, Lombard L, Groenewald JZ, Crous PW (2013) *Diaporthe*: A genus of endophytic, saprobic and plant pathogenic fungi. *Persoonia* 31: 1–41. <https://doi.org/10.3767/003158513X666844>
- Guarnaccia V, Crous PW (2017) Emerging citrus diseases in Europe caused by *Diaporthe* spp. *IMA Fungus* 8: 317–334. <https://doi.org/10.5598/imafungus.2017.08.02.07>
- Guarnaccia V, Martino I, Tabone G, Brondino L, Gullino ML (2020) Fungal pathogens associated with stem blight and dieback of blueberry in northern Italy. *Phytopathologia Mediterranea* 59(2): 229–245. <https://doi.org/10.14601/Phyto-11278>
- Guo YS, Crous PW, Bai Q, Fu M, Yang MM, Wang XH, Du YM, Hong N, Xu WX, Wang GP (2020) High diversity of *Diaporthe* species associated with pear shoot canker in China. *Persoonia* 45: 132–162. <https://doi.org/10.3767/persoonia.2020.45.05>
- Hilário S, Amaral IA, Gonçalves MF, Lopes A, Santos L, Alves A (2020) *Diaporthe* species associated with twig blight and dieback of *Vaccinium corymbosum* in Portugal, with









- p>description of four new species.
- Mycologia*
- 112(2): 293–308.
- <https://doi.org/10.1080/00275514.2019.1698926>
- Hilário S, Micael FM, Artur A (2021a) Using genealogical concordance and coalescent-based species delimitation to assess species boundaries in the *Diaporthe eres* complex. *Journal of Fungi* 7: 507. <https://doi.org/10.3390/jof7070507>
- Hilário S, Santos L, Alves A (2021b) *Diaporthe amygdali*, a species complex or a complex species? *Fungal Biology* 125(7): 505–518. <https://doi.org/10.1016/j.funbio.2021.01.006>
- Huang F, Udayanga D, Wang X, Hou X, Mei X, Fu Y, Hyde KD, Li HY (2015) Endophytic *Diaporthe* associated with *Citrus*: A phylogenetic reassessment with seven new species from China. *Fungal Biology* 119: 331–347. <https://doi.org/10.1016/j.funbio.2015.02.006>
- Huang ST, Xia JW, Zhang XG, Sun WX (2021) Morphological and phylogenetic analyses reveal three new species of *Diaporthe* from Yunnan, China. *MycKeys* 78: 49–77. <https://doi.org/10.3897/mycokeys.78.60878>
- Huson DH, Bryant D (2006) Application of phylogenetic networks in evolutionary studies. *Molecular Biology and Evolution* 23(2): 254–267. <https://doi.org/10.1093/molbev/msj030>
- Hyde KD, Chaiwan N, Norphanphoun C, Boonmee S, Camporesi E, Chethana KWT, Dayarathne MC, de Silva NI, Dissanayake AJ, Ekanayaka AH, Hongsanan S, Huang SK, Jayasiri SC, Jayawardena RS, Jiang HB, Karunarathna A, Lin CG, Liu JK, Liu NG, Lu YZ, Luo ZL, Maharachchimbura SSN, Manawasinghe IS, Pem D, Perera RH, Phukham-sakda C, Samarakoon MC, Senwanna C, Shang QJ, Tennakoon DS, Thambugala KM, Tibpromma S, Wanasinghe DN, Xiao YP, Yang J, Zeng XY, Zhang JF, Zhang SN, Bulgakov TS, Bhat DJ, Cheewangkoon R, Goh TK, Jones EBG, Kang JC, Jeewon R, Liu ZY, Lumyong S, Kuo CH, McKenzie EHC, Wen TC, Yan JY, Zhao Q (2018) *Mycosphere* notes 169–224. *Mycosphere* 9(2): 271–430. <https://doi.org/10.5943/mycosphere/9/2/8>
- Jiang N, Voglmayr H, Piao CG, Li Y (2021) Two new species of *Diaporthe* (Diaporthaceae, Diaporthales) associated with tree cankers in the Netherlands. *MycKeys* 85: 31–56. <https://doi.org/10.3897/mycokeys.85.73107>
- Jiang N, Xue H, Li Y (2025) Novel genus and species of Diaporthostomataceae (Diaporthales) in China. *IMA Fungus* 16: e145422. <https://doi.org/10.3897/ima fungus.16.145422>
- Katoh K, Rozewicki J, Yamada KD (2019) MAFFT online service: Multiple sequence alignment, interactive sequence choice and visualisation. *Briefings in Bioinformatics* 20: 1160–1166. <https://doi.org/10.1093/bib/bbx108>
- Lambert C, Schweizer L, Kemkuignou BM, Anoumedem EGM, Kouam SF, Marin-Felix Y (2023) Four new endophytic species of *Diaporthe* (Diaporthaceae, Diaporthales) isolated from Cameroon. *MycKeys* 99: 319–362. <https://doi.org/10.3897/mycokeys.99.110043>
- Lawrence DP, Travadon R, Baumgartner K (2015) Diversity of *Diaporthe* species associated with wood cankers of fruit and nut crops in northern California. *Mycologia* 107(5): 926–940. <https://doi.org/10.3852/14-353>
- León M, Berbegal M, Rodríguez-Reina JM, Elena G, Abad-Campos P, Ramón-Albalat A, Armengol J (2020) Identification and characterization of *Diaporthe* spp. associated with twig cankers and shoot blight of almonds in Spain. *Agronomy* 10(8): 1062. <https://doi.org/10.3390/agronomy10081062>
- Liu HY, Luo D, Huang HL, Yang Q (2024) Two new species of *Diaporthe* (Diaporthaceae, Diaporthales) associated with *Camellia oleifera* leaf spot disease in Hainan Province, China. *MycKeys* 102: 225–243. <https://doi.org/10.3897/mycokeys.102.113412>

- Lombard L, van Leeuwen G, Guarnaccia V, Polizzi G, van Rijswijk P, Rosendahl K, Crous P (2014) *Diaporthe* species associated with *Vaccinium*, with specific reference to Europe. *Phytopathologia Mediterranea* 53(2): 287–299. [https://doi.org/10.14601/Phytopathol\\_Mediterr-12361](https://doi.org/10.14601/Phytopathol_Mediterr-12361)
- Machingambi NM, Dreyer LL, Oberlander KC, Roux J, Roets F (2015) Death of endemic *Virgilia oroboides* trees in South Africa caused by *Diaporthe virgiliae* sp. nov. *Plant Pathology* 64(5): 1149–1156. <https://doi.org/10.1111/ppa.12341>
- Manawasinghe IS, Dissanayake AJ, Li X, Liu M, Wanasinghe DN, Xu J, Zhao W, Zhang W, Zhou Y, Hyde KD, Brooks S, Yan J (2019) High genetic diversity and species complexity of *Diaporthe* associated with grapevine dieback in China. *Frontiers in Microbiology* 10: 1936. <https://doi.org/10.3389/fmicb.2019.01936>
- Marín-Felix Y, Hernández-Restrepo M, Wingfield MJ, Akulov A, Carnegie AJ, Cheewangkoon R, Crous PW (2019) Genera of phytopathogenic fungi: GOPHY 2. *Studies in Mycology* 92: 47–133. <https://doi.org/10.1016/j.simyco.2018.04.002>
- Miller MA, Pfeiffer W, Schwartz T (2010) Creating the CIPRES Science Gateway for inference of large phylogenetic trees. *Gateway Computing Environments Workshop, GCE 2010*: 1–8. <https://doi.org/10.1109/GCE.2010.5676129>
- Norphanphoun C, Gentekaki E, Hongsanan S, Jayawardena R, Senanayake IC, Manawasinghe IS, Hyde KD (2022) *Diaporthe*: Formalizing the species-group concept. *Mycosphere* 13: 752–819. <https://doi.org/10.5943/mycosphere/13/1/9>
- O'Donnell K, Cigelnik E (1997) Two divergent intragenomic rDNA ITS2 types within a monophyletic lineage of the fungus *Fusarium* are nonorthologous. *Molecular Phylogenetics and Evolution* 7(1): 103–116. <https://doi.org/10.1006/mpev.1996.0376>
- Rambaut A (2012) FigTree, version 1.4.2. University of Edinburgh, Edinburgh.
- Saxena A, Yadav D, Mohanty S, Cheema HS, Gupta MM, Darokar MP, Bawankule DU (2016) Diarylheptanoids rich fraction of *Alnus nepalensis* attenuates malaria pathogenesis: In-vitro and in-vivo study. *Phytotherapy Research* 30(6): 940–948. <https://doi.org/10.1002/ptr.5596>
- Sen G, Sarkar I, Chhettri S, Kar P, Roy A, Sen A, Bhattacharya M (2022) Rhizospheric soil metabarcoding analysis of *Alnus nepalensis* from Darjeeling hills reveals the abundance of nitrogen-fixing symbiotic microbes. *Journal of Forest Research* 27(2): 106–112. <https://doi.org/10.1080/13416979.2022.2037813>
- Sharma E, Sharma R, Pradhan M (1998) Ecology of Himalayan alder (*Alnus nepalensis* D. Don). *Proceedings-Indian National Science Academy Part B* 64: 59–78.
- Sun W, Huang S, Xia J, Zhang X, Li Z (2021) Morphological and molecular identification of *Diaporthe* species in south-western China, with description of eight new species. *MycKeys* 77: 65–95. <https://doi.org/10.3897/mycokeys.77.59852>
- Tan YP, Edwards J, Grice KR, Shivas RG (2013) Molecular phylogenetic analysis reveals six new species of *Diaporthe* from Australia. *Fungal Diversity* 61(1): 251–260. <https://doi.org/10.1007/s13225-013-0242-9>
- Tobita H, Yazaki K, Harayama H, Kitao M (2016) Responses of symbiotic N<sub>2</sub> fixation in *Alnus* species to the projected elevated CO<sub>2</sub> environment. *Trees (Berlin)* 30: 523–537. <https://doi.org/10.1007/s00468-015-1297-x>
- Udayanga D, Liu X, Crous PW, McKenzie EH, Chukeatirote E, Chukeatirote E, Hyde KD (2012) A multi-locus phylogenetic evaluation of *Diaporthe* (*Phomopsis*). *Fungal Diversity* 56(1): 157–171. <https://doi.org/10.1007/s13225-012-0190-9>
- Udayanga D, Castlebury LA, Rossman AY, Chukeatirote E, Hyde KD (2014) Insights into the genus *Diaporthe*: Phylogenetic species delimitation in the *D. eres* species complex. *Fungal Diversity* 67(1): 203–229. <https://doi.org/10.1007/s13225-014-0297-2>

- Udayanga D, Castlebury LA, Rossman AY, Chukeatirote E, Hyde KD (2015) The *Diaporthe sojae* species complex: Phylogenetic re-assessment of pathogens associated with soybean, cucurbits and other field crops. *Fungal Biology* 119(5): 383–407. <https://doi.org/10.1016/j.funbio.2014.10.009>
- Vu D, Groenewald M, De Vries M, Gehrman T, Stielow B, Eberhardt U, Verkley GJM (2019) Large-scale generation and analysis of filamentous fungal DNA barcodes boosts coverage for kingdom fungi and reveals thresholds for fungal species and higher taxon delimitation. *Studies in Mycology* 92(1): 135–154. <https://doi.org/10.1016/j.simyco.2018.05.001>
- Wang X, Guo Y, Du Y, Yang Z, Huang X, Hong N, Wang G (2021) Characterization of *Diaporthe* species associated with peach constriction canker, with two novel species from China. *MycKeys* 80: 77–90. <https://doi.org/10.3897/mycokeys.80.63816>
- White TJ, Bruns T, Lee S, Taylor J (1990) Amplification and direct sequencing of fungal ribosomal RNA genes for phylogenetics. In: Innis MA, Gelfand DH, Sninsky JJ, White TJ (Eds) *PCR protocols: a guide to methods and applications*. Academic Press, San Diego, 315–322. <https://doi.org/10.1016/B978-0-12-372180-8.50042-1>
- Xia C, Zhao W, Wang J, Sun J, Cui G, Zhang L (2023) Progress on geographical distribution, driving factors and ecological functions of Nepalese alder. *Diversity* 15(1): 59. <https://doi.org/10.3390/d15010059>
- Yang Q, Fan XL, Du Z, Tian CM (2017) *Diaporthe* species occurring on *Senna bicapsularis* in southern China, with descriptions of two new species. *Phytotaxa* 302: 145–155. <https://doi.org/10.11646/phytotaxa.302.2.4>
- Yang Q, Fan XL, Guarnaccia V, Tian CM (2018) High diversity of *Diaporthe* species associated with dieback diseases in China, with twelve new species described. *MycKeys* 39: 97–149. <https://doi.org/10.3897/mycokeys.39.26914>
- Yang Q, Jiang N, Tian CM (2020) Three new *Diaporthe* species from Shaanxi Province, China. *MycKeys* 67: 1–18. <https://doi.org/10.3897/mycokeys.67.49483>
- Yang Q, Jiang N, Tian CM (2021) New species and records of *Diaporthe* from Jiangxi Province, China. *MycKeys* 77: 41–64. <https://doi.org/10.3897/mycokeys.77.59999>
- Zapata M, Palma MA, Aninat MJ, Piontelli E (2020) Polyphasic studies of new species of *Diaporthe* from native forest in Chile, with descriptions of *Diaporthe araucanorum* sp. nov., *Diaporthe foikelawen* sp. nov. and *Diaporthe patagonica* sp. nov. *International Journal of Systematic and Evolutionary Microbiology* 70(5): 3379–3390. <https://doi.org/10.1099/ijsem.0.004183>
- Zhou H, Hou CL (2019) Three new species of *Diaporthe* from China based on morphological characters and DNA sequence data analyses. *Phytotaxa* 422(2): 157–174. <https://doi.org/10.11646/phytotaxa.422.2.3>
- Zhu YQ, Ma CY, Xue H, Piao CG, Li Y, Jiang N (2023) Two new species of *Diaporthe* (Diaporthaceae, Diaporthales) in China. *MycKeys* 95: 209–228. <https://doi.org/10.3897/mycokeys.95.98969>
- Zhu YQ, Ma L, Xue H, Li Y, Jiang N (2024) New species of *Diaporthe* (Diaporthaceae, Diaporthales) from *Bauhinia variegata* in China. *MycKeys* 108: 317–335. <https://doi.org/10.3897/mycokeys.108.128983>

# Three new species of *Apiospora* (Apiosporaceae, Amphisphaeriales) associated with diseased bamboo in China

Xiaoyun Chang<sup>1</sup>, Yuanyuan Wang<sup>1</sup>, Tao Xu<sup>1</sup>, Guangshuo Li<sup>2</sup>, Xianghua Yue<sup>3</sup>, Mingjun Chen<sup>1</sup>

<sup>1</sup> Anhui Province Key Laboratory of Green Control for Major Forestry Pests, Anhui Agricultural University, Hefei 230036, China

<sup>2</sup> Key Laboratory of Biology and Sustainable Management of Plant Diseases and Pests of Anhui Higher Education Institutes, School of Plant Protection, Anhui Agricultural University, Hefei 230036, China

<sup>3</sup> International Centre for Bamboo and Rattan, Sanya Research Base, Sanya 572000, China

Corresponding authors: Mingjun Chen (mjchen@ahau.edu.cn); Xianghua Yue (yuexianghua@icbr.ac.cn)

## Abstract

*Apiospora* is widely distributed worldwide, primarily comprising pathogens, endophytes, and saprobes associated with plants, and most of its hosts are Poaceae. In this study, 37 pathogenic strains of *Apiospora* were isolated from diseased bamboo collected in the provinces of Hunan and Guizhou, China. Multilocus phylogenetic analysis using combined ITS, LSU, *TUB2*, and *TEF1* sequence data, along with morphological assessments, identified three new species: *A. bambusiparasitica* **sp. nov.**, *A. qiannanensis* **sp. nov.**, and *A. xiangxiense* **sp. nov.** Descriptions, illustrations, and phylogenetic trees for the newly discovered species are provided and compared with closely related *Apiospora* species to enhance our understanding of the genus *Apiospora*. The pathogenicity test results demonstrated that the three new species could cause bamboo culm diseases, providing valuable information for the diagnosis and management of bamboo culm diseases.

**Key words:** Bambusicolous fungi, morphology, new taxa, phylogeny, taxonomy



Academic editor: Thorsten Lumbsch

Received: 20 November 2024

Accepted: 1 April 2025

Published: 23 April 2025

**Citation:** Chang X, Wang Y, Xu T, Li G, Yue X, Chen M (2025) Three new species of *Apiospora* (Apiosporaceae, Amphisphaeriales) associated with diseased bamboo in China. MycoKeys 116: 205–226. <https://doi.org/10.3897/mycokeys.116.142263>

**Copyright:** © Xiaoyun Chang et al.  
This is an open access article distributed under terms of the Creative Commons Attribution License (Attribution 4.0 International – CC BY 4.0).

## Introduction

The genus *Apiospora* (Amphisphaeriales, Apiosporaceae) was established and described by Saccardo in 1875, with *Apiospora montagnei* (Saccardo 1875) designated as the type species. The ongoing development of fungal taxonomy and phylogeny has led to multiple revisions of the taxonomic status of the genus *Apiospora*. Before 2021, the phylogenetic relationship between *Arthrinium* and *Apiospora* remained unclear. Molecular phylogenetic studies initially placed both genera in the family Apiosporaceae (Hyde et al. 1998). Subsequently, Crous and Groenewald (2013) proposed synonymizing *Arthrinium* with *Apiospora* and prioritized the former as per the “one fungus, one name” policy (Hawksworth et al. 2011; Réblová et al. 2016), despite a lack of data on the type species *Arthrinium caricicola*. However, Pintos and Alvarado’s (2021) study showed that genetic, morphological, and ecological differences between *Apiospora* and *Arthrinium* were considered sufficient to support the taxonomic separation of the two genera. Furthermore, Pintos and Alvarado (2022) refined the identity of *Apiospora montagnei* as the type species and delineated



its phylogenetic boundaries. Additionally, many species from *Arthrimum* were transferred to *Apiospora* (Pintos and Alvarado 2021; Tian et al. 2021). As of March 2025, there are 206 epithets listed in Index Fungorum.

Morphologically, *Apiospora* and *Arthrimum* share many similarities, particularly in their asexual characteristics (Yuan et al. 2020). However, most *Apiospora* conidia are nearly spherical from the front view and lenticular from the side, while *Arthrimum* often produces conidia of various shapes, including angular, spherical, curved, boat-shaped, fusiform, and polygonal (Crous and Groenewald 2013; Pintos and Alvarado 2021, 2022; Li et al. 2023; Ai et al. 2024; Liu et al. 2024).

Ecologically, *Apiospora* is mainly associated with Poaceae or other plant hosts in tropical and subtropical regions (Liao et al. 2023; Liu et al. 2023; Zhang et al. 2023), while *Arthrimum* primarily occurs on Cyperaceae or Juncaceae hosts in temperate, cold, or alpine habitats (Sharma et al. 2014; Kwon et al. 2021; Pintos and Alvarado 2022). Current fungal taxonomy also emphasizes the correlation between host specificity and geographic location. All these pieces of evidence support the taxonomic separation of the two genera.

Bamboo is a vital non-wood bioresource, playing an irreplaceable role in economic, ecological, medicinal, and societal development (Shukla et al. 2016; Borowski et al. 2022). However, the intensification of bamboo cultivation has heightened its vulnerability to infectious diseases. Among fungal pathogens associated with bamboo, obligate pathogens such as *Phyllachora*, *Physopella*, *Puccinia*, *Stereostromum*, and *Uredo* predominantly infect bamboo leaves, while sporadic pathogens, including *Apiospora*, *Meliola*, *Fusarium*, and *Sclerotium*, target both leaves and culms (Hyde et al. 2002; Yang et al. 2019). The pathogenicity of *Apiospora* species on bamboo has garnered increasing attention. For instance, Li et al. (2016) identified *A. phaeospermum* as the causative agent of culm rot in *Phyllostachys viridis* in China. Subsequently, Yang et al. (2019) reported *A. yunnanum* as the pathogen responsible for bamboo blight in *Phyllostachys heteroclada*. More recently, Zheng et al. (2022) confirmed that *A. arundinis* caused culm rhomboid rot in Moso bamboo (*Phyllostachys edulis*). Beyond their pathogenic roles, several *Apiospora* species are recognized as endophytes, contributing to the microbial diversity of bamboo (Wang et al. 2018).

In this study, we isolated several *Arthrimum*-like taxa from diseased culms of bamboo in China. To clarify their taxonomic status, we used a dataset composed of nuclear ribosomal DNA internal transcribed spacer (ITS), large sub-unit ribosomal DNA (LSU),  $\beta$ -tubulin (*TUB2*), and translation elongation factor 1- $\alpha$  (*TEF1*). Based on morphological characteristics and multi-gene phylogenetic analyses, we identified and described three new *Apiospora* species.

## Materials and methods

### Plant material

In this study, diseased bamboo samples were collected from Jiuyi Mountain in Ningyuan County, Xiangxi Tujia and Miao Autonomous Prefecture, Hunan, and from Libo County, Qiannan Buyi and Miao Autonomous Prefecture, Guizhou, China. The International Center for Bamboo and Rattan provided the specimens. Samples were deposited in the Research Center for Entomogenous Fungi (RCEF) of Anhui Agricultural University.

## Pathogen isolation

Pure cultures of all fungal isolates were obtained by the single hyphal tip isolation method. For pathogen isolation, lesion margin specimens were excised into 5 × 5 mm fragments, surface-sterilized in 2% sodium hypochlorite for 2 min, followed by immersion in 75% ethanol for 1 min, and rinsed three times consecutively with sterile water (Zheng et al. 2022). The sterilized pieces were wiped dry with sterilized filter paper and then placed into Petri dishes containing potato dextrose agar (PDA) (three pieces per dish) amended with 50 µg/mL of benzylpenicillin potassium (Cai et al. 2009). The plates were incubated at 25 °C under a 12 h light/dark photoperiod. Hyphal tips from the leading edge of fungal colonies emerging from the tissues were transferred to fresh PDA after two days to obtain pure cultures, which were subsequently maintained at 25 °C. Living cultures were stored in a metabolically inactive state at the Research Center for Entomogenous Fungi (RCEF) of Anhui Agricultural University. The MycoBank number for the newly described species is referenced as outlined in Robert et al. (2013).

## Morphological characterization

For morphological identification, the purified isolated strains were incubated on PDA (fresh diced potato 200 g/L, dextrose 20 g/L, agar 20 g/L) and MEA (malt extract 20 g/L and 20 g/L agar) at 25 °C. Incubate at 25 °C in alternating light and dark (12 h for each); colony growth was observed daily, and the morphology, color, texture of colonies, and the diameter of colonies were recorded. Asexual reproductive structures were observed based on cultures on PDA, following synoptic keys for *Apiospora* species identification. In the morphological analysis, the fungi were mounted in a drop of lactophenol solution on glass slides. The microstructures, such as mycelium, conidiogenous cells, and conidia, were observed using an optical microscope (ZEISS Axiolab 5) and microphotographed. Forty conidiogenous cells and conidia were measured and examined. The colors of fresh specimens and cultures were recorded by referring to the Methuen Handbook of Color (Kornerup and Wanscher 1978).

## DNA extraction and PCR amplification

The genomic DNA of the isolates was extracted from mycelium that was cultured on a PDA plate and incubated for 3–5 days at 25 °C. DNA extraction was performed according to the CTAB method (Spatafora et al. 1998).

Polymerase chain reaction (PCR) amplification was applied to amplify four gene fragments, including ITS, LSU, *TUB2*, and *TEF1*. The following primer pairs were used: ITS1/ITS4 for ITS (White et al. 1990), LR0R/LR5 for LSU (Rehner and Samuels 1995), EF1-728F/EF2 for *TEF1* (O'Donnell et al. 1998; Carbone and Kohn 1999), and T1/Bt2b for *TUB2* (Glass and Donaldson 1995; O'Donnell and Cigelnik 1997). The PCR amplification system consisted of 2 min at 94 °C, followed by 35 cycles of 30 s at 94 °C, 30 s at 48 °C (ITS), and 45 s at 72 °C, and a final step of 2 min at 72 °C. Different annealing temperatures were used according to the genomic region to be amplified: 56 °C for *TEF1* and LSU, 58 °C for *TUB2*. The final product was detected by agarose gel electrophoresis and sent to Beijing Liuhe Huada Gene Technology Company. The resulting sequences were submitted to GenBank for sequencing.

## Molecular and phylogenetic analysis

Newly generated sequences from each isolate were blasted against the GenBank database, and searches were restricted to type materials for the initial determination of the closest matching species and species complex. Related gene sequences (ITS, LSU, *TUB2*, *TEF1*) of *Apiospora* spp. from recent publications were downloaded from GenBank (Table 1) (Yan and Zhang 2024). Manual adjustments of sequences were carried out using BioEdit (Hall et al. 2011) to maximize homology.

The DNA sequences were aligned using the MAFFT v7 with the G-INS-I option (Kato et al. 2019). Sequences were manually edited as necessary using BioEdit v7.1.9 (Hall 1999). The combined loci were analyzed using maximum likelihood (ML) and Bayesian inference (BI) methods. Combined sequences of ITS-LSU-*TUB2*-*TEF1* were performed in SequenceMatrix v1.7.8 (Vaidya et al. 2011). The ML analysis was conducted using the TNe+I+R4 model and 1000 bootstrap replicates. The ML analysis was designed with IQ-TREE (Trifinopoulos et al. 2016). In Bayesian inference analysis, the best-fit substitution models for different datasets were estimated using MrModeltest v2.3 based on the implementation of the Akaike information criterion (AIC) (Nylander 2004). Posterior probabilities (PP) were determined by Markov Chain Monte Carlo sampling (MCMC) under the estimated model of evolution (Zhaxybayeva and Gogarten 2002). Four simultaneous Markov chains were run for 20 million generations, and trees were sampled every 1000 generations. The run was stopped automatically when the average standard deviation of split frequencies fell below 0.01. The first 25% trees, which represented the burn-in phase of the analyses, were discarded, and the remaining trees were used for calculating PP in the majority rule consensus tree. Phylogenetic trees were subsequently visualized and refined using the Interactive Tree of Life (iTOL) online platform (Letunic and Bork 2019).

## Pathogenicity assay

Fresh bamboo samples were collected from the campus of Anhui Agricultural University in Anhui Province, China, to validate Koch's postulates. Bamboo culms were cut into 30 cm sections, sterilized with 75% ethanol spray, and wounded using sterile drills. Mycelial plugs (5 mm in diameter) from the edge of each isolate colony were placed onto the artificial wounds, while control pieces received PDA plugs without fungal inoculum (Zheng et al. 2022). All treated culms were placed in moisture chambers with sterile wet cotton to maintain humidity and incubated at 25 °C under a 12-hour light/12-hour dark cycle. Symptom development was observed daily, and each treatment was replicated six times.

## Results

### Disease symptoms and isolation of the pathogen

From the field survey, disease symptoms developed on the culm of the bamboo. The typical symptoms: (I) started with brown spots and irregular shapes that gradually enlarged, with dark edges and spread around, sometimes forming symmetrical or lobed patterns (Fig. 1A–C). (II) started with black spots and irregular shapes; each spot remained relatively small and did not expand significantly. In the later stages,

**Table 1.** Species of Apiosporaceae used in the phylogenetic analyses. Notes: Strains in this study are marked in bold. “T” indicates a type culture. NA = not available.

Strain	Code	Host and Substrates	Locality	GenBank accession numbers			
				ITS	LSU	TUB2	TEF1
<i>Apiospora acutiapica</i>	KUMCC 20-0209	<i>Bambusa bambos</i>	China	MT946342	MT946338	MT947365	MT947359
<i>A. adinandrae</i>	SAUCC 1282B-1 <sup>T</sup>	Diseased leaves of <i>Adinandra glischroloma</i>	China	OR739431	OR739572	OR757128	OR753448
<i>A. agari</i>	KUC21333 <sup>T</sup>	<i>Agarum cribrosum</i>	South Korea	MH498520	MH498440	MH498478	MH544663
<i>A. aquatica</i>	S-642 <sup>T</sup>	Submerged wood	China	MK828608	MK835806	NA	NA
<i>A. arctoscopi</i>	KUC21331 <sup>T</sup>	Eggs of <i>Arctoscopus japonicus</i>	South Korea	MH498529	MH498449	MH498487	MN868918
<i>A. armeniaca</i>	SAUCC DL1831 <sup>T</sup>	Leaves of <i>Prunus armeniaca</i>	China	OQ592540	OQ615269	OQ613285	OQ613313
<i>A. arundinis</i>	CBS 124788	Living leaves of <i>Fagus sylvatica</i>	Switzerland	KF144885	KF144929	KF144975	KF145017
<i>A. aseptata</i>	KUNCC 23-14169 <sup>T</sup>	Living roots of <i>Dicranopteris pedata</i>	China	OR590341	OR590335	OR634943	OR634949
<i>A. aurea</i>	CBS 244.83 <sup>T</sup>	Air	Spain	AB220251	KF144935	KF144981	KF145023
<i>A. babylonica</i>	SAUCC DL1841 <sup>T</sup>	Diseased leaves of <i>Salix babylonica</i>	China	OQ592538	OQ615267	OQ613283	OQ613311
<i>A. balearica</i>	AP24118 <sup>T</sup>	Poaceae plant	Spain	MK014869	MK014836	MK017975	MK017946
<i>A. bambusicola</i>	MFLUCC 20-0144 <sup>T</sup>	<i>Schizostachyum brachycladum</i>	Thailand	MW173030	MW173087	NA	MW183262
<b><i>A. bambusiparasitica</i></b>	<b>RCEF20000</b>	<b>Diseased culms of bamboo</b>	<b>China</b>	<b>OR687309</b>	<b>PQ530552</b>	<b>OR712912</b>	<b>PQ538537</b>
<b><i>A. bambusiparasitica</i></b>	<b>RCEF20003<sup>T</sup></b>	<b>Diseased culms of bamboo</b>	<b>China</b>	<b>OR687306</b>	<b>PQ530551</b>	<b>OR712906</b>	<b>OR712911</b>
<i>A. bawanglingensis</i>	SAUCC BW0444 <sup>T</sup>	Leaves of <i>Indocalamus longiauritus</i>	China	OR739429	OR739570	OR757126	OR753446
<i>A. bawanglingensis</i>	SAUCC 0443	Diseased leaves of <i>Indocalamus longiauritus</i>	China	OQ592552	OQ615281	OQ613303	OQ613325
<i>A. bawanglingensis</i>	SAUCC 0444	Diseased leaves of <i>Indocalamus longiauritus</i>	China	OQ592551	OQ615280	OQ613302	OQ613324
<i>A. biserialis</i>	CGMCC 3.20135 <sup>T</sup>	Bamboo	China	MW481708	MW478885	MW522955	MW522938
<i>A. camelliae-sinensis</i>	LC5007 <sup>T</sup>	<i>Camellia sinensis</i>	China	KY494704	KY494780	KY705173	KY705103
<i>A. cannae</i>	ZHKUCC 22-0139	Leaves of <i>Canna</i> sp.	China	OR164902	OR164949	OR166322	OR166286
<i>A. chiangraiense</i>	MFLU 21-0046	Dead culms of bamboo	Thailand	MZ542520	MZ542524	MZ546409	NA
<i>A. chromolaenae</i>	MFLUCC 17-1505 <sup>T</sup>	<i>Chromolaena odorata</i>	Thailand	MT214342	MT214436	NA	MT235802
<i>A. cordylines</i>	GUCC 10026	<i>Cordylina fruticosa</i>	China	MT040105	NA	MT040147	MT040126
<i>A. coryli</i>	CFCC 58978 <sup>T</sup>	Dead plant culms of <i>Corylus yunnanensis</i>	China	OR125564	OR133586	OR139978	OR139974
<i>A. cyclobalanopsidis</i>	GZCC 20-0103	<i>Cyclobalanopsidis glauca</i>	China	MW481714	MW478893	MW522963	MW522946
<i>A. dematiacea</i>	KUNCC 23-14202 <sup>T</sup>	Healthy leaf <i>Dicranopteris ampla</i>	China	OR590346	OR590339	OR634948	OR634953
<i>A. dendrobii</i>	MFLUCC 14-0152 <sup>T</sup>	Roots of <i>Dendrobium harveyanum</i>	Thailand	MZ463151	MZ463192	NA	NA
<i>A. descalsii</i>	AP31118A <sup>T</sup>	<i>Ampelodesmos mauritanicus</i>	Spain	MK014870	MK014837	MK017976	MK017947
<i>A. dichotomanthi</i>	LC4950 <sup>T</sup>	<i>Dichotomanthes tristaniicarpa</i>	China	KY494697	KY494773	KY705167	KY705096
<i>A. dicranopteridis</i>	KUNCC23-14171 <sup>T</sup>	Living stems of <i>Dicranopteris pedata</i>	China	OR590342	OR590336	OR634944	OR634950
<i>A. dongyingensis</i>	SAUCC 0302 <sup>T</sup>	Leaves of bamboo	China	OP563375	OP572424	OP573270	OP573264
<i>A. elliptica</i>	ZHKUCC 22-0131 <sup>T</sup>	Dead stems of unknown plant	China	OR164905	OR164952	OR166323	OR166284
<i>A. endophytica</i>	ZHKUCC 23-0006 <sup>T</sup>	Living leaves of <i>Wurfbainia villosa</i>	China	OQ587996	OQ587984	OQ586075	OQ586062
<i>A. esporiensis</i>	AP16717	<i>Phyllostachys aurea</i>	Spain	MK014878	MK014845	MK017983	MK017954
<i>A. euphorbiae</i>	IMI 285638b	<i>Bambusa</i> sp.	Bangladesh	AB220241	AB220335	AB220288	NA
<i>A. fermenti</i>	KUC21289 <sup>T</sup>	Seaweeds	South Korea	MF615226	MF615213	MF615231	MH544667
<i>A. gaoyouensis</i>	CFCC 52301 <sup>T</sup>	<i>Phragmites australis</i>	China	MH197124	NA	NA	MH236793
<i>A. gaoyouensis</i>	CFCC 52302	<i>Phragmites australis</i>	China	MH197125	NA	NA	MH236794
<i>A. garethjonesii</i>	SICAUC 22-0027	Bamboo	China	ON228603	ON228659	ON237651	NA
<i>A. gelatinosa</i>	GZAAS 20-0107	Bamboo	China	MW481707	MW478889	NA	MW522942
<i>A. globosa</i>	KUNCC 23-14210 <sup>T</sup>	Living stems of <i>Dicranopteris linearis</i>	China	OR590347	OR590340	NA	OR634954
<i>A. gongcheniae</i>	GDMCC 3.1045 <sup>T</sup>	Stems of <i>Oryza meyeriana</i> subsp. <i>granulata</i>	China	PP033259	PP034691	PP033102	PP034683
<i>A. gongcheniae</i>	YNE00565	Stems of <i>Oryza meyeriana</i> subsp. <i>granulata</i>	China	PP033260	PP034692	PP033103	PP034684
<i>A. guangdongensis</i>	ZHKUCC 23-0004 <sup>T</sup>	<i>Wurfbainia villosa</i>	China	OQ587994	OQ587982	OQ586073	OQ586060
<i>A. guizhouensis</i>	LC5318	Air in karst cave	China	KY494708	KY494784	KY705177	KY705107
<i>A. hainanensis</i>	SAUCC 1681 <sup>T</sup>	Leaves of bamboo	China	OP563373	OP572422	OP573268	OP573262



Strain	Code	Host and Substrates	Locality	GenBank accession numbers			
				ITS	LSU	TUB2	TEF1
<i>A. hispanica</i>	IMI 326877 <sup>†</sup>	Beach sands	Spain	AB220242	AB220336	AB220289	NA
<i>A. hydei</i>	CBS 114990 <sup>†</sup>	Culms of <i>Bambusa tuldoidea</i> s	China	KF144890	KF144936	KF144982	KF145024
<i>A. hyphopodii</i>	SICAUCC 22-0034	Bamboo	China	ON228605	ON228661	ON237653	NA
<i>A. hysteryna</i>	AP12118	<i>Phyllostachys aurea</i>	Spain	MK014877	KM014844	MK017982	MK017953
<i>A. iberica</i>	AP10118 <sup>†</sup>	<i>Arundo donax</i>	Portugal	MK014879	MK014846	MK017984	MK017955
<i>A. intestini</i>	CBS 135835	Gut of grasshopper	India	KR011352	MH877577	KR011350	KR011351
<i>A. italica</i>	AP29118	<i>Arundo donax</i>	Italy	MK014881	MK014848	MK017986	NA
<i>A. jatrophae</i>	MMI00052 <sup>†</sup>	Living <i>Jatropha podagrica</i>	India	JQ246355	NA	NA	NA
<i>A. jiangxiensis</i>	LC4577 <sup>†</sup>	<i>Maesa</i> sp.	China	KY494693	KY494769	KY705163	KY705092
<i>A. jiangxiensis</i>	LC4578	Camellia sinensis	China	KY494694	KY494770	KY705164	KY705093
<i>A. jinanensis</i>	SAUCC DL1981 <sup>†</sup>	Diseased leaves of Bambusaceae sp.	China	OQ592544	OQ615273	OQ613289	OQ613317
<i>A. kogelbergensis</i>	CBS 113332	<i>Cannomois virgata</i>	South Africa	KF144891	KF144937	KF144983	KF145025
<i>A. koreana</i>	KUC21332 <sup>†</sup>	Eggs of <i>Arctoscopus japonicus</i>	South Korea	MH498524	MH498444	MH498482	MH544664
<i>A. lageniformis</i>	KUC21686 <sup>†</sup>	Culms of <i>Phyllostachys nigra</i>	South Korea	ON764022	ON787761	ON806636	ON806626
<i>A. lageniformis</i>	KUC21687	Culms of <i>Phyllostachys nigra</i>	South Korea	ON764023	ON787764	ON806637	ON806627
<i>A. locuta-pollinis</i>	LC11683 <sup>†</sup>	<i>Brassica campestris</i>	China	MF939595	NA	MF939622	MF939616
<i>A. longistroma</i>	MFLUCC11-0481 <sup>†</sup>	Dead culms of bamboo	Thailand	KU940141	KU863129	NA	NA
<i>A. lophatheri</i>	CFCC 58975 <sup>†</sup>	Diseased leaves of <i>Lophatherum gracile</i>	China	OR125566	OR133588	OR139980	OR139970
<i>A. machili</i>	SAUCC 1175A-4 <sup>†</sup>	Diseased leaves of <i>Machilus nanmu</i>	China	OR739433	OR739574	OR757130	OR753450
<i>A. machili</i>	SAUCC 1175	Diseased leaves of <i>Machilus nanmu</i>	China	OQ592560	OQ615289	OQ613307	OQ613333
<i>A. machili</i>	SAUCC 1176	Diseased leaves of <i>Machilus nanmu</i>	China	OQ592559	OQ615288	OQ613306	OQ613332
<i>A. malaysiana</i>	CBS 102053 <sup>†</sup>	<i>Macaranga hullettii</i>	Malaysia	KF144896	KF144942	KF144988	KF145030
<i>A. marianiae</i>	AP18219 <sup>†</sup>	Dead stems of <i>Phleum pratense</i>	Spain	ON692406	ON692422	ON677186	ON677180
<i>A. marii</i>	CBS 497.90 <sup>†</sup>	Beach sands	Spain	AB220252	KF144947	KF144993	KF145035
<i>A. marina</i>	KUC21328 <sup>†</sup>	Seaweeds	South Korea	MH498538	MH498458	MH498496	MH544669
<i>A. mediterranea</i>	IMI 326875 <sup>†</sup>	Air	Spain	AB220243	AB220337	AB220290	NA
<i>A. minutispora</i>	1.70E-42 <sup>†</sup>	Mountain soils	South Korea	LC517882	NA	LC518888	LC518889
<i>A. montagnei</i>	AP301120 <sup>†</sup>	<i>Arundo micrantha</i>	Spain	ON692408	ON692424	ON677188	ON677182
<i>A. mori</i>	MFLU 18-2514 <sup>†</sup>	<i>Morus australis</i>	China	MW114313	MW114393	NA	NA
<i>A. mukdahanensis</i>	MFLUCC 22-0056 <sup>†</sup>	Dead leaves of bamboo	Thailand	OP377735	OP377742	NA	NA
<i>A. mytilomorpha</i>	DAOM 214595	Dead blades of <i>Andropogon</i> sp.	India	KY494685	NA	NA	NA
<i>A. neobambusae</i>	LC7106 <sup>†</sup>	Leaves of bamboo	China	KY494718	KY494794	KY705186	KY806204
<i>A. neochinense</i>	CFCC 53036 <sup>†</sup>	<i>Fargesia qinlingensis</i>	China	MK819291	NA	MK818547	MK818545
<i>A. neosubglobosa</i>	JHB 007 <sup>†</sup>	Bamboo	China	KY356090	KY356095	NA	NA
<i>A. obovata</i>	LC4940 <sup>†</sup>	<i>Lithocarpus</i> sp.	China	KY494696	KY494772	KY705166	KY705095
<i>A. obovata</i>	LC8177	<i>Lithocarpus</i> sp.	China	KY494757	KY494833	KY705225	KY705153
<i>A. oenotherae</i>	CFCC 58972	Diseased leaves of <i>Oenothera biennis</i>	China	OR125568	OR133590	OR139982	OR139972
<i>A. olivata</i>	CGMCC 3.25514 <sup>†</sup>	soil	China	OR680531	OR680598	OR843234	OR858925
<i>A. olivata</i>	ZY 22.053	soil	China	OR680532	OR680599	OR843235	OR858926
<i>A. ovata</i>	CBS 115042 <sup>†</sup>	<i>Arundinaria hindsii</i>	China	KF144903	KF144950	KF144995	KF145037
<i>A. pallidesporae</i>	ZHKUCC 22-0129 <sup>†</sup>	Dead wood of unknown host	China	OR164903	OR164950	NA	NA
<i>A. paraphaeosperma</i>	KUC21488	Culms of bamboo	South Korea	ON764024	ON787763	ON806638	ON806628
<i>A. phragmitis</i>	CPC 18900 <sup>†</sup>	<i>Phragmites australis</i>	Italy	KF144909	KF144956	KF145001	KF145043
<i>A. phyllostachydis</i>	MFLUCC 18-1101 <sup>†</sup>	<i>Phyllostachys heteroclada</i>	China	MK351842	MH368077	MK291949	MK340918
<i>A. piptatheri</i>	SAUCC BW0455	Diseased leaves of <i>Indocalamus longiauritus</i>	China	OR739430	OR739571	OR757127	OR753447
<i>A. pseudohyphopodii</i>	KUC21680 <sup>†</sup>	Culms of <i>Phyllostachys pubescens</i>	South Korea	ON764026	ON787765	ON806640	ON806630
<i>A. pseudomarii</i>	GUCC 10228 <sup>†</sup>	Leaves of <i>Aristolochia debilis</i>	China	MT040124	NA	MT040166	MT040145
<i>A. pseudoparenchymatica</i>	LC7234 <sup>†</sup>	Leaves of bamboo	China	KY494743	KY494819	KY705211	KY705139
<i>A. pseudorasikravindrae</i>	KUMCC 20-0208 <sup>†</sup>	<i>Bambusa dolichoclada</i>	China	MT946344	NA	MT947367	MT947361
<i>A. pseudosinensis</i>	SAUCC 0221	Leaves of bamboo	China	OP563377	OP572426	OP573272	OP573266
<i>A. pseudospegazzinii</i>	CBS 102052 <sup>†</sup>	<i>Macaranga hullettii</i>	Malaysia	KF144911	KF144958	KF145002	KF145045
<i>A. pterosperma</i>	CPC 20193 <sup>†</sup>	<i>Lepidosperma gladiatum</i>	Australia	KF144913	KF144960	KF145004	KF145046

Strain	Code	Host and Substrates	Locality	GenBank accession numbers			
				ITS	LSU	TUB2	TEF1
<i>A. pusillisperma</i>	KUC21321 <sup>†</sup>	Seaweeds	South Korea	MH498533	MH498453	MH498491	MN868930
<b><i>A. qiannanensis</i></b>	<b>RCEF7610</b>	<b>Diseased culms of bamboo</b>	<b>China</b>	<b>PQ526600</b>	<b>PQ530550</b>	<b>PQ538539</b>	<b>PQ538535</b>
<b><i>A. qiannanensis</i></b>	<b>RCEF7611<sup>†</sup></b>	<b>Diseased culms of bamboo</b>	<b>China</b>	<b>PQ526599</b>	<b>PQ530549</b>	<b>PQ538538</b>	<b>PQ538536</b>
<i>A. qinlingensis</i>	CFCC 52303 <sup>†</sup>	<i>Fargesia qinlingensis</i>	China	MH197120	NA	NA	MH236795
<i>A. rasikravindrae</i>	LC8179	Brassica rapa	China	KY494759	KY494835	KY705227	KY705155
<i>A. sacchari</i>	CBS 372.67	Air	Not mentioned	KF144918	KF144964	KF145007	KF145049
<i>A. saccharicola</i>	CBS 191.73	Air	Netherlands	KF144920	KF144966	KF145009	KF145051
<i>A. sargassi</i>	KUC21232	Seaweeds	South Korea	KT207750	NA	KT207648	MH544676
<i>A. sasae</i>	CPC 38165 <sup>†</sup>	Dead culms of <i>Sasa veitchii</i>	Netherlands	MW883402	MW883797	MW890120	MW890104
<i>A. septata</i>	GZCC 20-0109	Bamboo Food	China	MW481712	MW478891	MW522961	MW522944
<i>A. serenensis</i>	IMI 326869 <sup>†</sup>	Excipients, atmosphere and home dust	Spain	AB220250	AB220344	AB220297	NA
<i>A. setariae</i>	CFCC 54041 <sup>†</sup>	Decaying culms of <i>Setaria viridis</i>	China	MT492004	NA	MT497466	MW118456
<i>A. setostroma</i>	KUMCC 19-0217	Dead branches of bamboo	China	MN528012	MN528011	NA	MN527357
<i>A. sichuanensis</i>	HKAS 107008 <sup>†</sup>	Dead culms of Poaceae	China	MW240648	MW240578	MW775605	MW759536
<i>Apiospora</i> sp.	SAUCC 1429	NA	China	OQ592558	OQ615287	OQ613305	OQ613331
<i>Apiospora</i> sp.	SAUCC 1430	NA	China	OQ592557	OQ615286	OQ613304	OQ613330
<i>A. sphaerosperma</i>	CBS 114315	Leaves of <i>Hordeum vulgare</i>	Iran	KF144905	KF144952	KF144997	KF145039
<i>A. stipae</i>	CPC 38101 <sup>†</sup>	Dead culms of <i>Stipa gigantea</i>	Spain	MW883403	MW883798	MW890121	MW890082
<i>A. subglobosa</i>	MFLUCC 11-0397 <sup>†</sup>	Dead culms of bamboo	Thailand	KR069112	KR069113	NA	NA
<i>A. subrosea</i>	LC7291	Leaves of bamboo	China	KY494751	KY494827	KY705219	KY705147
<i>A. taeanensis</i>	KUC21359	Seaweeds	South Korea	MH498513	NA	MH498471	MN868935
<i>A. thailandica</i>	MFLUCC 15-0202 <sup>†</sup>	Dead culms of bamboo	Thailand	KU940145	KU863133	NA	NA
<i>A. tropica</i>	MFLUCC 21-0056	Dead culms of Bambusoideae	Thailand	OK491657	OK491653	NA	NA
<i>A. vietnamensis</i>	IMI 99670 <sup>†</sup>	<i>Citrus sinensis</i>	Vietnam	KX986096	KX986111	KY019466	NA
<i>A. wurfbainiae</i>	ZHKUCC 23-0009	<i>Wurfbainia villosa</i>	China	OQ587999	OQ587987	OQ586078	OQ586065
<i>A. xenocordella</i>	CBS 478.86 <sup>†</sup>	Soils from roadway	Zimbabwe	KF144925	KF144970	KF145013	KF145055
<b><i>A. xiangxiense</i></b>	<b>RCEF20001<sup>†</sup></b>	<b>Diseased culms of bamboo</b>	<b>China</b>	<b>OR687308</b>	<b>PQ530553</b>	<b>OR712910</b>	<b>OR712909</b>
<b><i>A. xiangxiense</i></b>	<b>RCEF20002</b>	<b>Diseased culms of bamboo</b>	<b>China</b>	<b>OR687307</b>	<b>PQ530548</b>	<b>OR712908</b>	<b>OR712907</b>
<i>A. xishuangbannaensis</i>	KUMCC 21-0696	<i>Rhinolophus pusillus</i>	China	ON426833	OP363249	OR025931	OR025970
<i>A. yunnana</i>	DDQ 00281	Phyllostachys nigra	China	KU940148	KU863136	NA	NA
<i>A. yunnanensis</i>	ZHKUCC 23-0014 <sup>†</sup>	Dead stems of grass	China	OQ588004	OQ587992	OQ586083	OQ586070
<i>Arthrinium caricicola</i>	AP23518	<i>Carex ericetorum</i>	China	MK014871	MK014838	MK017977	MK017948
<i>Arthrinium caricicola</i>	CBS 145903	Dead and attached leaves	Germany	MN313782	MN317266	MN313861	NA

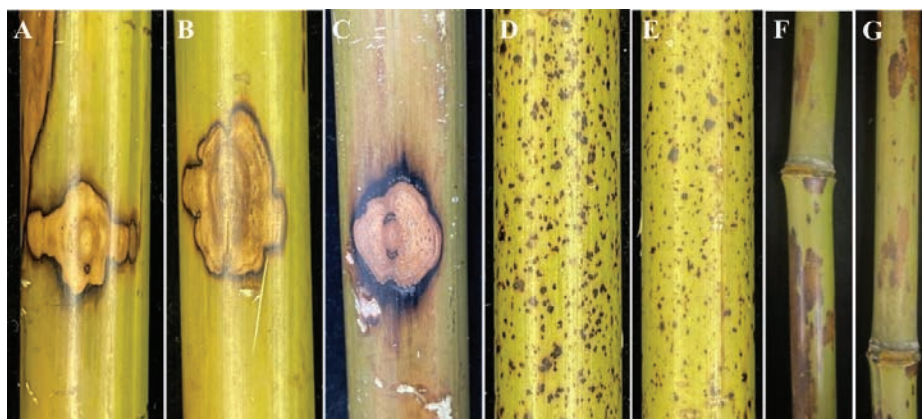


Figure 1. Symptoms of disease in naturally infected bamboo in the field.

they densely covered bamboo culm and exhibited chlorosis in the bamboo culms (Fig. 1D, E). (III) Irregular brownish lesions spread extensively, sometimes coalescing into large patches, covering a significant area of the bamboo culm (Fig. 1F, G).

A total of 37 isolates were obtained on PDA. As the colony morphology of the isolates was uniform, two representative isolates from each group were selected for further analysis: (I). RCEF20001 and RCEF20002; (II). RCEF20000 and RCEF20003; (III). RCEF7610 and RCEF7611.

### Phylogenetic analysis

A comprehensive dataset integrating ITS, LSU, *TUB2*, and *TEF1* sequences was constructed from 131 strains, including six newly sequenced isolates, with *Arthrrium caricicola* (CBS 145903 and AP23518) designated as the outgroup. Multi-locus sequences contained 2,544 characters, including gaps with ITS (1-433), LSU (434-1229), *TUB2* (1230-1678), and *TEF1* (1679-2544).

The phylogenetic trees derived from ML and BI analyses exhibited consistent topologies, with the ML tree, including MLBP and BIPP values, depicted in Fig. 2. Phylogenetic analysis revealed that the six strains represented three new species lineages, which are now recognized as *A. bambusiparasitica*, *A. qiannanensis*, and *A. xiangxiense*.

### Taxonomy

#### *Apiospora bambusiparasitica* X.Y. Chang & M.J. Chen, sp. nov.

MycoBank No: 851766

Fig. 3

**Etymology.** The name refers to the species that is capable of infecting the culm of bamboo.

**Typification.** CHINA • Hunan Province, Xiangxi Tujia and Miao Autonomous Prefecture, Ningyuan County, Jiuyi Mountain (25°24'N, 111°58'E), on diseased culms of bamboo, November 2022; X.H. Yue, holotype H5, ex-type RCEF20003.

**Description. Asexual morph:** Hyphae 1.5–5.0 µm diam, hyaline, branched, septate. **Conidiogenous cells** hyaline to pale brown, smooth, erect or flexuous, scattered or aggregated in clusters on hyphae, ampulliform to clavate, 7.0–17.0 × 2.0–4.5 µm ( $\bar{x}$  = 9.6 ± 2.6 × 2.7 ± 0.7, n = 40), apical neck 6.0–10.0 µm long, basal part 3.0–6.0 µm long. **Conidia** 7.0–11.5 × 6.0–10.5 µm ( $\bar{x}$  = 9.2 ± 0.9 × 8.1 ± 1.1, n = 40), brown, smooth to finely roughened, granular, globose to ellipsoid in surface view, usually with a longitudinal, hyaline, germ-slit. **Sexual morph:** Undetermined.

**Culture characteristics.** Colonies on PDA fluffy, spreading, margin irregular, with abundant aerial mycelia, surface and reverse white to grey, reaching 9 cm in 8 d at 25 °C. On MEA, the colony is thick in the middle and thin at the edges. The margin is irregular, the surface white, and the central color on the colony's reverse side is characterized by a deeper, brownish-yellow tone that extends towards the periphery and transitions to a lighter, pale yellow shade.

**Additional specimens examined.** CHINA • Hunan Province, Ningyuan County, diseased on culms of bamboo, November 2022, other living culture RCEF20000.

**Note.** Phylogenetic analyses confirmed that *A. bambusiparasitica* formed an independent clade (1.0 BIPP and 100% MLBS), exhibiting a close evolutionary relationship with *A. arctoscopi* and *A. obovata*. Based on a BLASTN

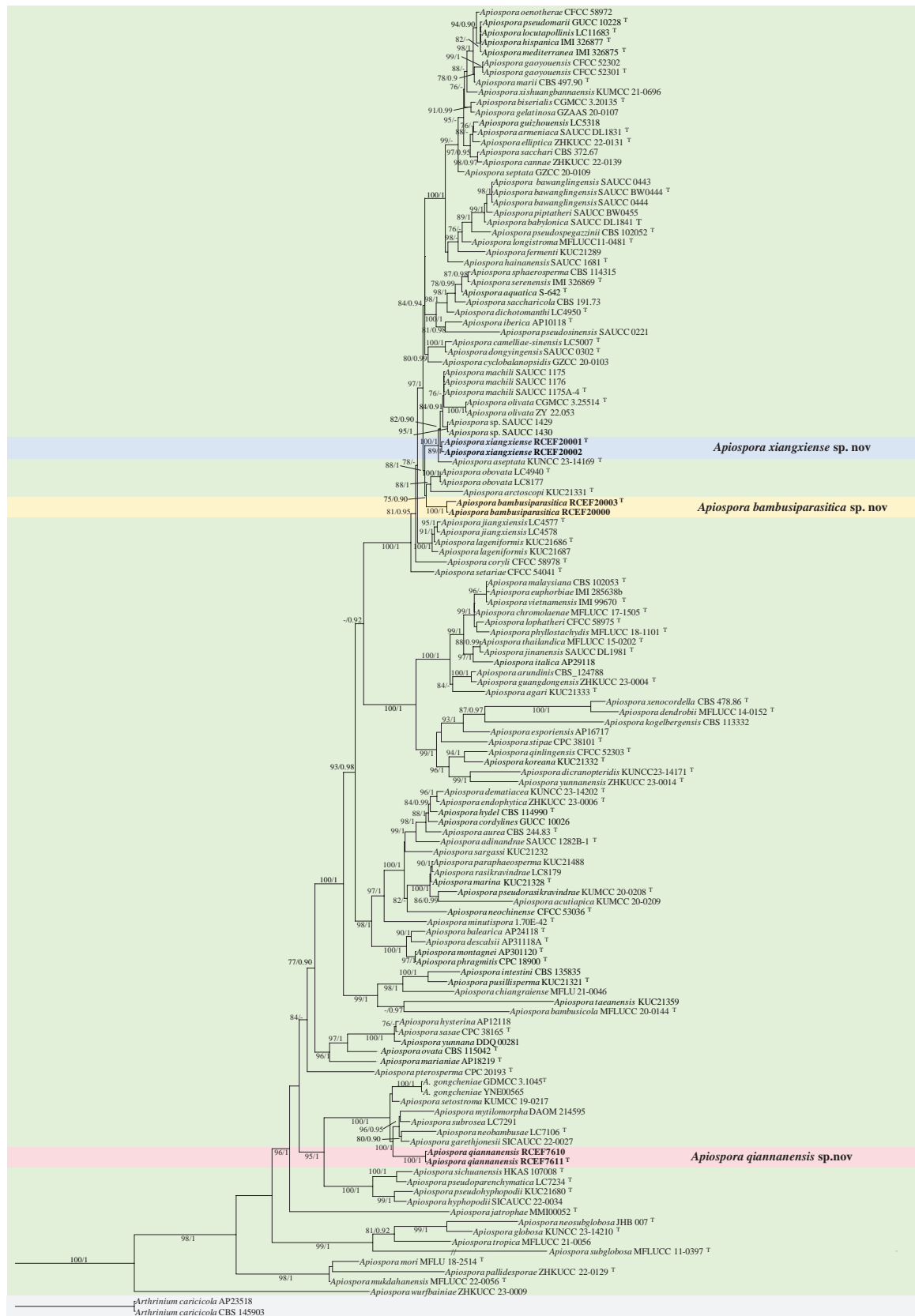


**Figure 2.** Phylogenetic tree of *Apiospora* based on a concatenated data matrix of ITS, LSU, TUB2, and TEF1. Bootstrap support values (> 75%) and posterior probabilities (> 0.9) are given at the nodes (ML/PP). The tree is rooted with *Arthrinium caricicola* CBS 145903 and AP23518. The novel species were highlighted. "T" indicates a type culture.



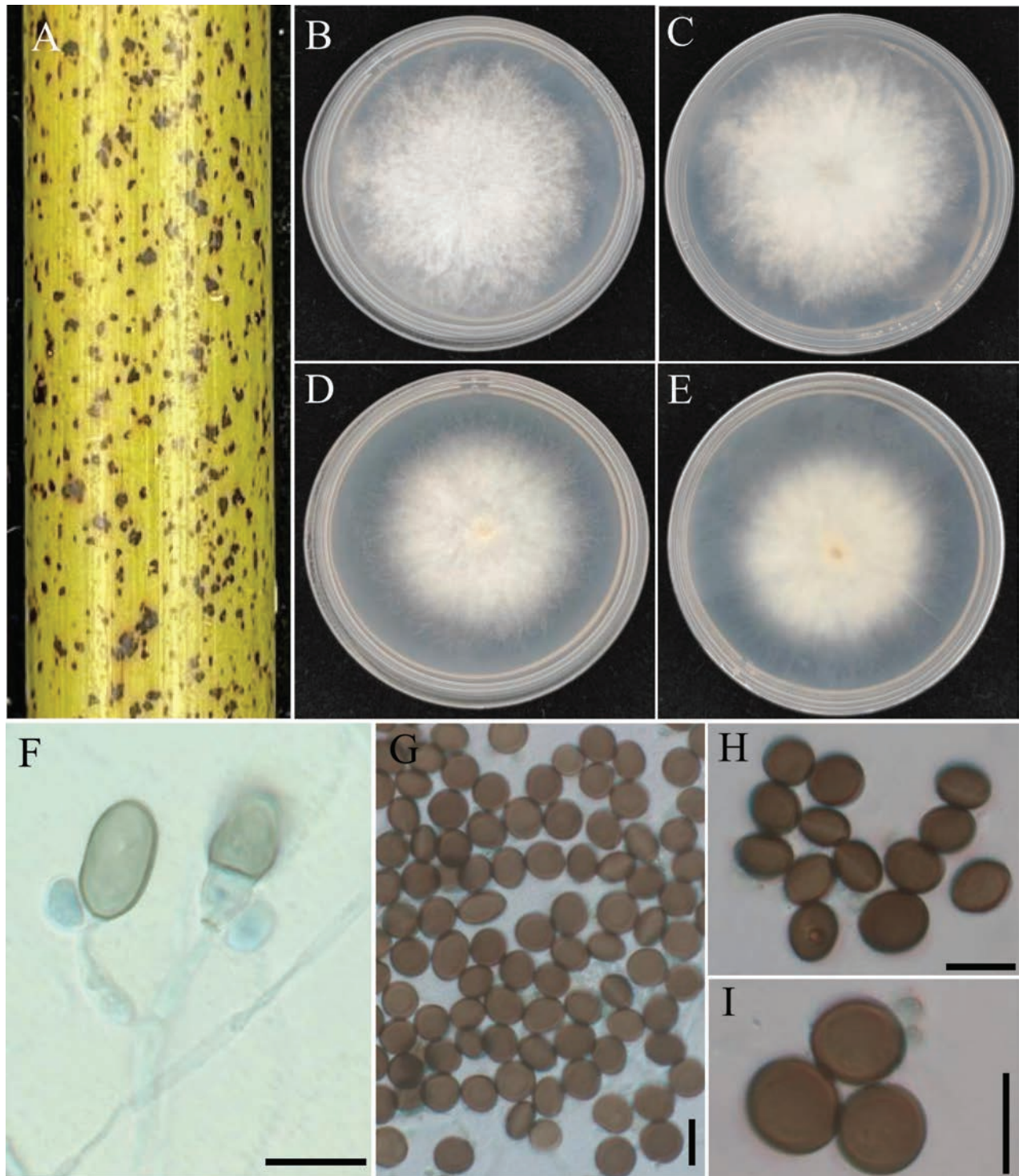


**Figure 3.** *Apiospora bambusiparasitica* (from ex-type living cultures RCEF20003) **A** diseased culms of bamboo **B, C** upper view and reverse view of culture on PDA **D, E** upper view and reverse view of culture on MEA **F** conidiogenous cells giving rise to conidia **G–I** conidia with pale germ slit. Scale bars: 10 µm.

search of the GenBank database, it was found that *A. bambusiparasitica* shares high similarities with the following strains: *A. arctoscopi* strain KUC21331 (86.48% in ITS, 98.9% in LSU, 92.2% in *TEF1*, 92.91% in *TUB2*); *A. obovata* strain LC4940 (90.03% in ITS, 95.77% in LSU, 93.42% in *TEF1*, 95.27% in *TUB2*); strain LC8177 (90.15% in ITS, 95.77% in LSU, 93.42% in *TEF1*, 95.27% in *TUB2*).

**Table 2.** Synopsis of morphological characteristics of *A. bambusiparasitica* and its closely related species.

Species	Isolation source	Country	Colony morphology (on PDA)	Conidia		References
				Shape	Diam (µm)	
<i>A. obovata</i>	<i>Lithocarpus</i> sp.	China	White to olivaceous-grey; Reaching 9 cm in 7 days	a. Roughened, globose to subglobose; b. obovoid, occasionally elongated to ellipsoidal.	a. 11.0–16.5; b. 16.0–31.0 × 9.0–16.0	Wang et al. (2018)
<i>A. arctoscopi</i>	Egg masses of <i>Arctoscopus japonicus</i>	Korea	Creamy white; 5–7 cm in 5 days	globose to elongate ellipsoid	9.5–13 × 7.5–12	Kwon et al. (2021)
<i>A. bambusiparasitica</i>	Diseased culms of Bamboo	China	White to grey; Reaching 9 cm in 8 days	globose to elongate ellipsoid	8.6–15.4 × 6.7–10.2	<b>This study</b>

Morphologically, *A. bambusiparasitica* and *A. obovata* show distinct differences. *Apiospora obovata* forms darker colonies and produces significantly longer, ellipsoidal conidia, measuring 16.0–31.0 × 9.0–16.0 µm, whereas *A. bambusiparasitica* has spherical to oval conidia, measuring 8.6–15.4 × 6.7–10.2 µm. *Apiospora bambusiparasitica* and *A. arctoscopi* are morphologically similar, with conidia of comparable size and overlapping dimensions. However, *A. arctoscopi* forms thicker colonies with more developed hyphae. Additionally, the two species exhibit significant ecological differences in host association, as *A. arctoscopi* is associated with *Arctoscopus japonicus*, while *A. bambusiparasitica* is associated with bamboo. Current fungal taxonomy emphasizes the importance of host association. For details, see Table 2. Thus, both morphological and molecular evidence support *A. bambusiparasitica* as a new species.

#### ***Apiospora qiannanensis* X.Y. Chang & M.J. Chen, sp. nov.**

MycoBank No: 856457

Fig. 4

**Etymology.** The name refers to the locality where the type specimens were collected, Qiannan Buyi and Miao Autonomous Prefecture, Guizhou Province, China.

**Typification.** CHINA • Guizhou Province, Qiannan Buyi and Miao Autonomous Prefecture, Libo County (25°25'N, 107°53'E), on diseased culms of bamboo, May. 2023, X.H. Yue, holotype GZ15, ex-type RCEF7610.

**Description. Asexual morph:** Hyphae 1.5–6.0 µm diam, hyaline to pale brown, branched, septate. **Conidiophores** hyaline to pale brown, smooth, erect or ascending, simple, flexuous, subcylindrical, and grouped together. **Conidiophores** aggregated in brown sporodochia, smooth, hyaline to brown, up to 30 µm long, 3.0–4.0 µm width. **Conidiogenous cells** 9.5–23.0 × 3.0–5.5 µm ( $\bar{x}$  = 15.0 ± 4.50 × 4.3 ± 0.9, n = 40), pale brown, smooth, doliform to subcylindrical. **Conidia** 16.5–20.8 µm ( $\bar{x}$  = 18.5 µm, n = 40), pale brown to dark brown, smooth, globose to subglobose. **Sexual morph:** Undetermined.

**Culture characteristics.** Colonies on PDA are fluffy, spreading, and circular, with moderate aerial mycelia, flocculent cotton, surface, and reverse white to grey, reaching 60 mm in 7 d at 25 °C. On MEA, surface grey-white with abundant mycelia, reverse greyish without patches.

**Additional specimens examined.** CHINA • Hunan Province, Ningyuan County, diseased on culms of bamboo, May 2023, other living culture RCEF7611.

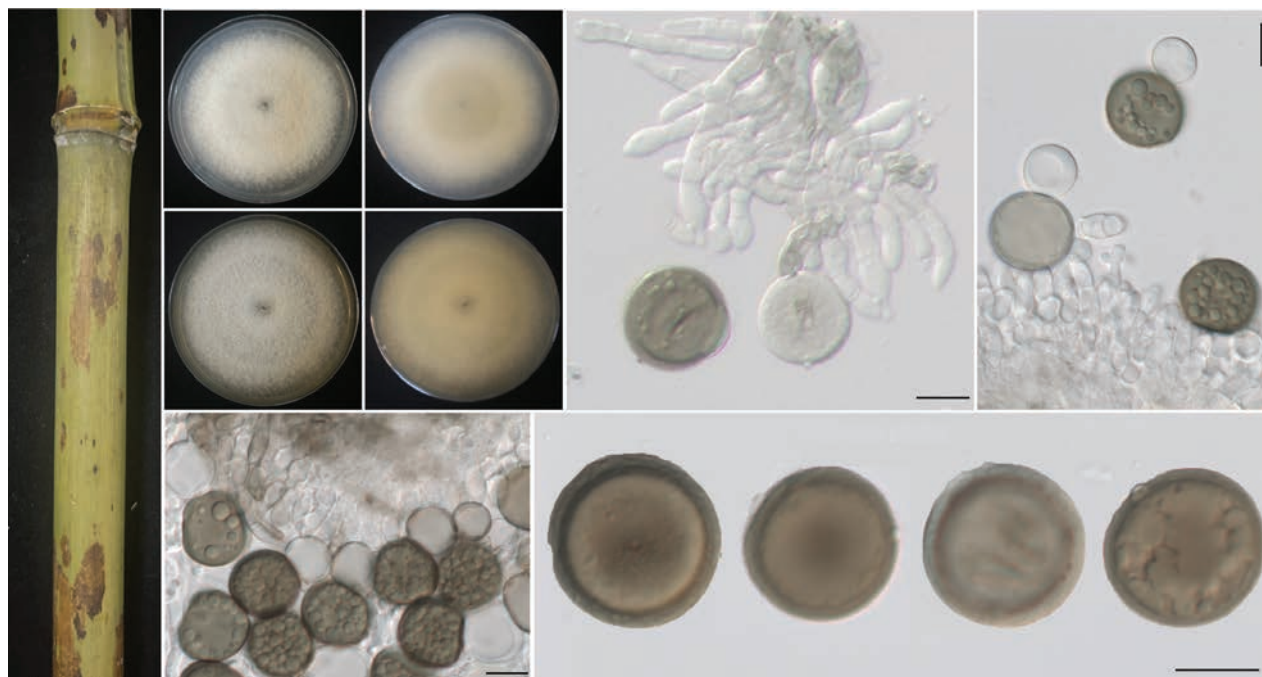


**Figure 4.** *Apiospora qiannanensis* (from ex-holotype strain RCEF7610) **A** diseased culms of bamboo **B, C** upper view and reverse view of culture on PDA **D, E** upper view and reverse view of culture on MEA **F–H** conidiogenous cells giving rise to conidia **I** conidia. Scale bars: 10 µm.

**Note.** Phylogenetic analyses confirmed that *A. qiannanensis* formed an independent clade (1.0 BIPP and 100% MLBS), exhibiting a close evolutionary relationship with *A. setostroma*, *A. mytilomorpha*, *A. subrosea*, *A. neobambusae*, and *A. Garethjonesii*. Based on a BLASTN search of the GenBank database, it was found that *A. qiannanensis* exhibits some differences in the ITS, LSU, *TUB2*, and *TEF1* sequences compared to closely related species: *A. setostroma* strain KUMCC 19-0217 (92.65% in ITS, 99.16% in LSU, 95.01% in *TEF1*); *A. mytilomorpha* strain DAOM 2145955 (96.28% in ITS); *A. subrosea* strain LC7291 (90.33% in ITS, 99.02% in LSU, 94.38% in *TEF1*, 99.25% in *TUB2*); *A. neobambusae* strain LC7106 (89.16% in ITS, 99.16% in LSU, 95.22% in *TEF1*, 91.94% in *TUB2*); *A. Garethjonesii* strain SICAUCC 22-0027 (93.65% in ITS, 99.29% in LSU, 94.50% in *TUB2*); *A. gongcheniae* strain GDMCC 3.1045 (95.44% in ITS, 99.41% in LSU, 93.14% in *TEF1*, 91.77% in *TUB2*).

Morphologically, colony characteristics of *A. mytilomorpha* are lacking, and the asexual morphology of *A. Garethjonesii* has not been described. We compared the existing morphological data and found that these closely related species have certain differences. *A. setostroma* and *A. subrosea* produce pigments in the later stages of colonies, while the others do not. *Apiospora qiannanensis*, *A. mytilomorpha*, and *A. neobambusae* differ in conidia shape (globose to subglobose vs. fusiform or boat-shaped vs. subglobose to ellipsoid) and size (16.5–20.8 µm vs. 20–30 × 6–8.5 µm vs. 11.5–15.5 × 7.0–14.0 µm). In addition, *A. qiannanensis* differs from *A. gongcheniae* in having larger conidia (16.5–20.8 µm) compared to *A. gongcheniae* (8.0–17.0 × 6.8–16.1 µm). Although some morphological features overlap among these taxa, significant genetic divergence is evident, underscoring their distinct species boundaries. For details, see Table 3. Based on molecular and morphological evidence, we propose *A. qiannanensis* as a new species.



**Table 3.** Synopsis of morphological characteristics of *A. qiannanensis* and its closely related species.

Species	Isolation source	Country	Colony morphology (on PDA)	Conidia		References
				Shape	Diam (µm)	
<i>A. qiannanensis</i>	Diseased culms of bamboo	China	White to grey; Reaching 60 mm in 7 days	Globose to subglobose	16.5–20.8	This study
<i>A. gongcheniae</i>	Stems of <i>Oryza meyeriana</i> subsp. <i>granulata</i>	China	Greyish, reverse light orange; Reaching 90 mm in 7 days	Globose to subglobose	8.0–17.0 × 6.8–16.1	Yan and Zhang (2024)
<i>A. setostroma</i>	Dead branches of bamboo	China	Initially white, becoming greyish, reverse reddish; Reaching 35 mm in 7 days	Subglobose to obovoid, 0–1-septate	18–20 × 15–19	Jiang et al. (2019)
<i>A. mytilomorpha</i>	Dead blades of <i>Andropogon</i>	India	Undetermined	Fusiform or boat-shaped	20–30 × 6–8.5	Bhat and Kendrick (1993)
<i>A. subrosea</i>	Bamboo	China	Initially white, becoming light pink on surface, reverse peach-puff; Reaching 10 cm in 8 days	Globose to subglobose or ellipsoidal	12.0–17.5 × 9.0–16.0	Wang et al. (2018)
<i>A. neobambusae</i>	Leaf of bamboo	China	White to grey	Subglobose to ellipsoid	11.5–15.5 × 7.0–14.0	Wang et al. (2018)
<i>A. garethjonesii</i>	Dead culms of bamboo	China	White; Reaching 40 cm in 7 days	Undetermined	Undetermined	Dai et al. (2016)

***Apiospora xiangxiense* X.Y. Chang & M.J. Chen, sp. nov.**

MycoBank No: 851765

Fig. 5

**Etymology.** The name refers to the locality where the type specimens were collected, Xiangxi Tujia and Miao Autonomous Prefecture, Hunan Province, China.

**Typification.** CHINA • Hunan Province, Xiangxi Tujia and Miao Autonomous Prefecture, Ningyuan County, Jiuyi Mountain (25°24'N, 111°58'E), on diseased culms of bamboo, November 2022, X.H. Yue, holotype H2 (stored in a metabolically inactive state), ex-type living cultures RCEF20001.

**Description.** **Asexual morph:** Hyphae 1.5–5.0 µm diam, hyaline, branched, septate. **Conidiogenous cells** 2.0–15.5 × 1.4–3.9 µm ( $\bar{x}$  = 8.1 ± 3.9 × 2.4 ± 0.7, n = 40), aggregated in clusters on hyphae or solitary, at first hyaline, becoming pale brown, basauxic, polyblastic, sympodial, erect, cylindrical. **Conidia** 8.6–15.4 × 6.7–10.2 µm ( $\bar{x}$  = 10.3 ± 1.5 × 8.3 ± 1.0, n = 40), brown, smooth to granular, globose to elongate ellipsoid in surface view, lenticular in side view, pale equatorial slit, with a central scar, 3.5 to 5.5 µm diam. Sterile cells forming on solitary loci on hyphae, brown, finely roughened, subcylindrical to clavate.

**Sexual morph:** Undetermined.

**Culture characteristics.** Colonies on PDA are fluffy, spreading, circular, with abundant aerial mycelia, surface and reverse white to grey, sometimes with pale yellow, reaching 9 cm in 8 d at 25 °C. On MEA, slower growth, surface white, reverse white, and slightly yellowish.

**Additional specimens examined.** CHINA • Hunan Province, Ningyuan County, diseased on culms of bamboo, November 2022, other living culture RCEF20002.

**Note.** Phylogenetic analyses confirmed that *A. xiangxiense* formed an independent clade, exhibiting a close evolutionary relationship with *A. aseptata*, *A. olivata*, and *A. machili* (1.0 BIPP and 100% MLBS).

However, *A. xiangxiense* differs from *A. aseptata* in several key aspects, including conidial size (8.6–15.4 × 6.7–10.2 µm vs. 7–9.5 (–13) µm). Based on nucleotide comparisons, *A. xiangxiense* differs from *A. aseptata* by 0.69% in ITS, 0.16% in LSU, 2.36% in *TUB2*, and 0.49% in *TEF1*. *Apiospora xiangxiense* also differs from *A. machili* by having longer conidia (8.6–15.4 × 6.7–10.2 µm vs. 7.1–9.5 ×



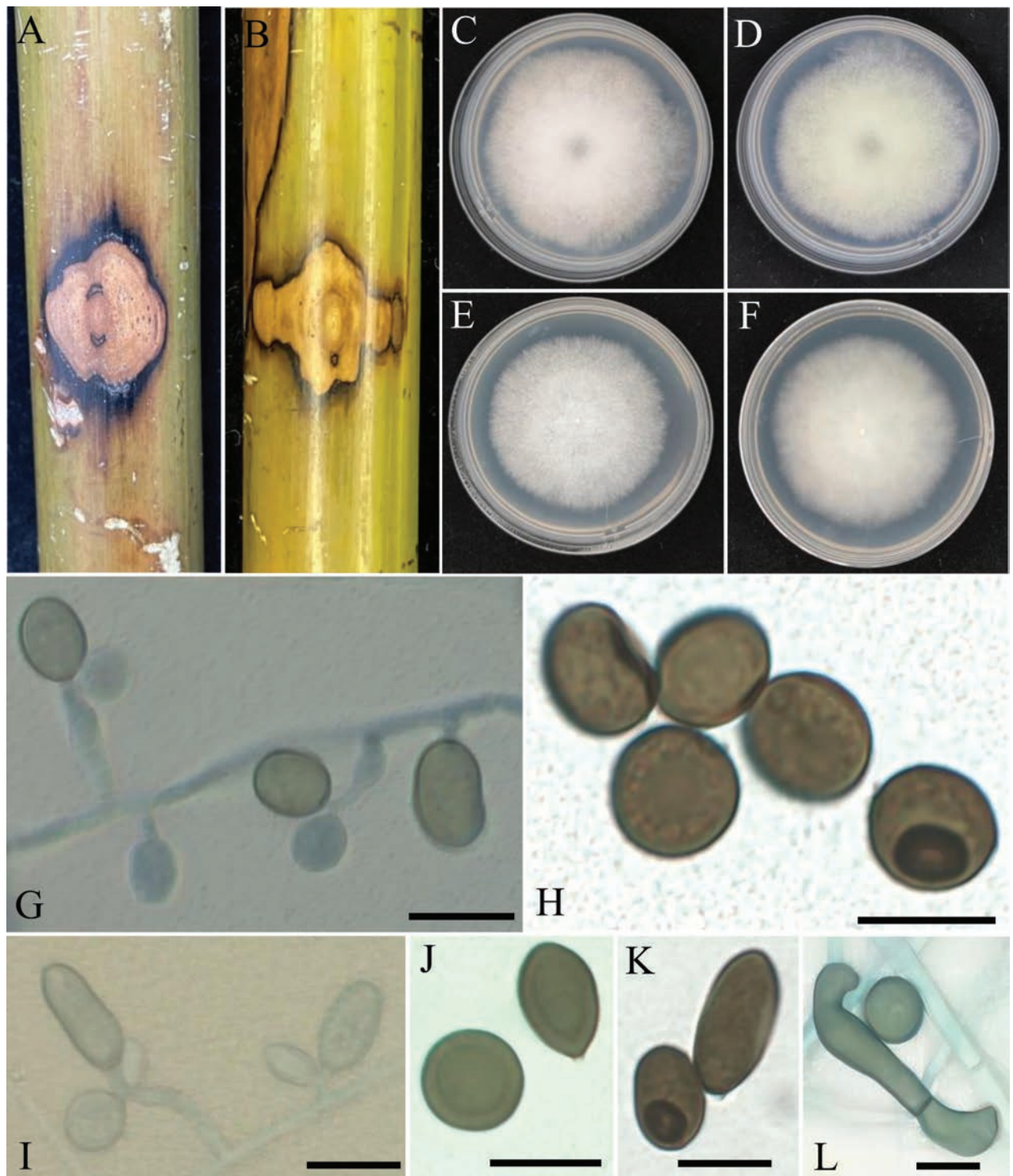


**Figure 5.** *Apiospora xiangxiense* (from ex-type living cultures RCEF20001) **A, B** diseased culms of bamboo **C, D** upper view and reverse view of culture on PDA **E, F** upper view and reverse view of culture on MEA **G, H** conidiogenous cells giving rise to conidia **I–K** conidia **L** sterile cells and conidia. Scale bars: 10 µm.

5.6–8.8 µm) and more elongated conidiogenous cells (2.0–15.5 × 1.4–3.9 µm vs. 6.0–8.0 × 2.5–4.0 µm). *Apiospora xiangxiense* differs from *A. olivata* by having longer conidia (8.6–15.4 × 6.7–10.2 µm) compared to *A. olivata* (8–12 × 5.5–8 µm), with sequence differences of 7.52% in ITS, 1.22% in LSU, and 1.94% in *TUB2*. Furthermore, their isolation sources are different.

**Table 4.** Synopsis of morphological characteristics of *A. xiangxiense* and its closely related species.

Species	Isolation source	Country	Colony morphology (on PDA)	Conidia		References
				Shape	Diam (µm)	
<i>A. aseptata</i>	Healthy leaf of <i>Dicranopteris pedata</i>	China	Grey-brown; 5 cm in 10 days	Globose or sub globose	7–9.5 (–13)	Zhang et al. (2023)
<i>A. machili</i>	Diseased leaves of <i>Machilus nanmu</i>	China	Ivory; 69.7–78.8 mm cm in 7 days	Globose to subglobose	7.1–9.5 × 5.6–8.8	Liu et al. (2024)
<i>A. olivata</i>	Green belt soil	China	initially white, becoming curry on the surface; reverse pale green; more than 90 mm in 14 days	a. olivary; b. subglobose to globose	a. 8–12 × 5.5–8 µm; b. 8–11.5 µm	Zhang et al. (2024)
<i>A. xiangxiense</i>	Diseased culms of Bamboo	China	white to grey, sometimes with pale yellow; Reaching 9 cm in 8 days	globose to elongate ellipsoid	8.6–15.4 × 6.7–10.2	<b>This study</b>

For details, see Table 4. Thus, both morphological and molecular evidence support *A. xiangxiense* as a new species.

### Pathogenicity tests

To determine the pathogenicity of the three new species isolates, three representative strains (RCEF20001, RCEF20000, and RCEF7611) were selected and inoculated onto fresh bamboo culms using a wound inoculation method. All three isolates were able to induce necrotic lesions. Inoculation with *A. xiangxiense* RCEF20001 resulted in the formation of gray-brown diamond-shaped lesions at the wound site after three days. Upon removing the epidermis, the internal lesions exhibited regular hollow black-brown diamond-shaped spots, which were larger than those observed on the surface (Fig. 6A–C). Inoculation with *A. bambusiparasitica* RCEF20000 caused rotting, diamond-shaped lesions at the wound site, with internal lesions displaying elliptical to scattered black-brown spots after the epidermis was scraped off (Fig. 6D–F). Inoculation with *A. qiannanensis* RCEF7611 resulted in gray-brown oval to diamond-shaped lesions at the wound site after three days. Scraping off the epidermis revealed hollow black-brown diamond-shaped spots, which were smaller than those seen on the surface (Fig. 6H, I). The control group was subjected to the same wound treatment as the experimental groups, but without pathogen inoculation, and no visible symptoms were observed in the control group (Fig. 6J). The symptoms observed were similar to those of naturally infected bamboo. Furthermore, the same fungus was consistently recovered from the experimentally inoculated bamboo. Deposits of the isolates are maintained at the Research Center for Entomogenous Fungi (RCEF), Anhui Agricultural University, Anhui Province, China.

### Discussion

In this study, 37 isolates of *Apiospora* (Apiosporaceae, Amphisphaeriales, Sordariomycetes) were obtained from diseased culms of bamboo in China (Hunan and Guizhou Provinces). Based on morphological and culture characteristics and phylogenetic analyses of combined ITS, LSU, *TUB2*, and *TEF1* sequence data, three novel species were identified, namely *Apiospora bambusiparasitica*, *A. xiangxiense*, and *A. qiannanensis*. These findings were confirmed through both morphological and molecular characterization, verifying the taxonomic classification of the three species.

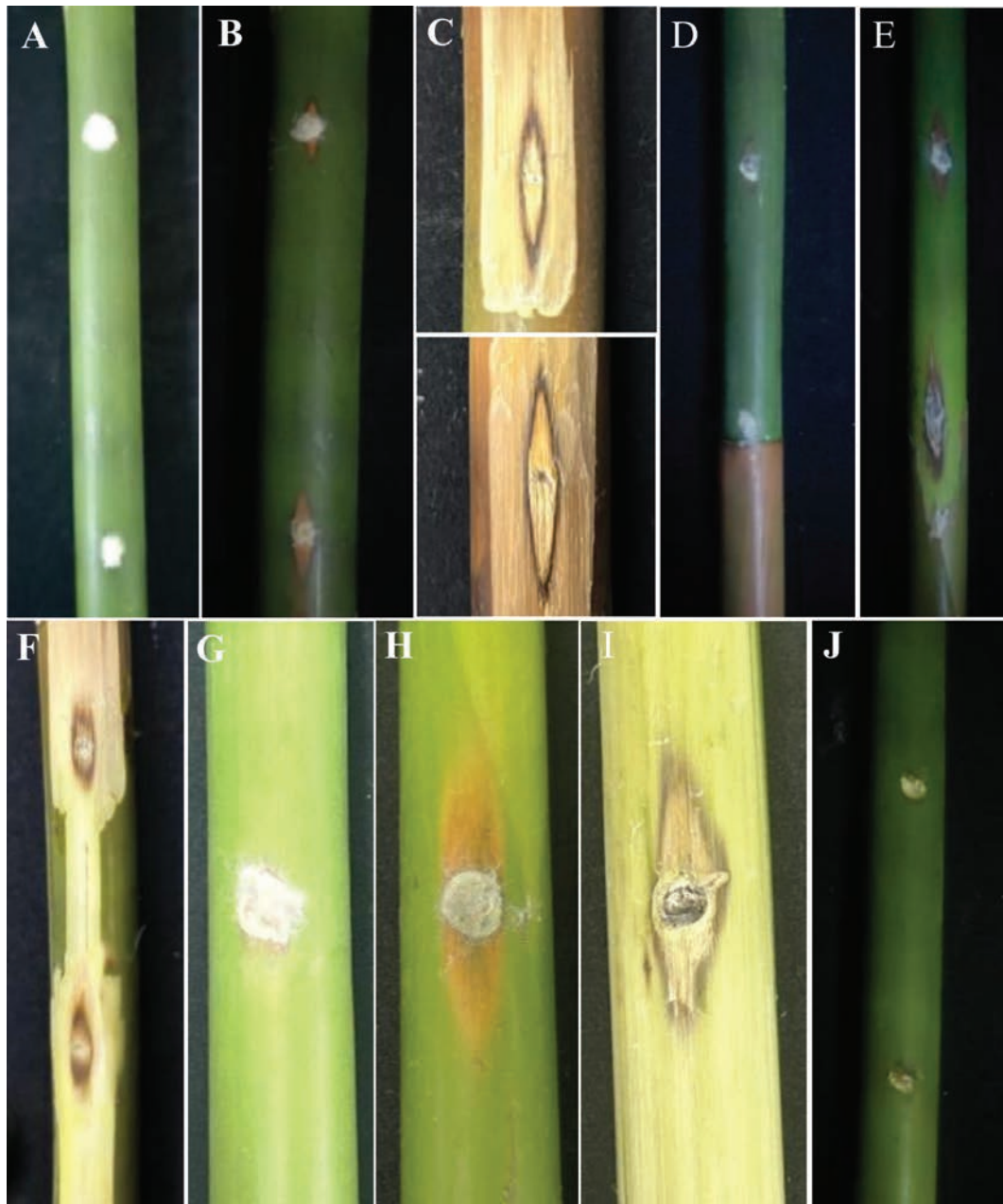


**Figure 6.** Pathogenicity test **A** symptoms on bamboo culm inoculated with the isolate *A. xiangxiense* RCEF20001 after 3 days **B** inoculation with RCEF20001 strain after 5 days **C** details under the diseased tissues **D** symptoms on bamboo culm inoculated with the isolate *A. bambusiparasitica* RCEF20000 after 3 days **E** inoculation with RCEF20000 strain after 5 days **F** details under the diseased tissues **G** symptoms on bamboo culm inoculated with the isolate *A. qiannanensis* RCEF7611 after 3 days **H** inoculation with RCEF7611 strain after 5 days **I** details under the diseased tissues **J** bamboo inoculated with PDA plug.

*Apiospora* is a cosmopolitan genus distributed across tropical, subtropical, and temperate climates, primarily associated with Poaceae, but also known to colonize a wide range of other hosts (Pintos and Alvarado 2021; Yan and Zhang 2024; Zhang et al. 2024). The strains analyzed in this study were isolated from bamboo in the subtropical regions of China (Guizhou and Hunan), further validating the previously described ecological characteristics of the genus.



According to data from Index Fungorum (accessed on October 28, 2024), the genus *Apiospora* has been recognized to have 196 species. Among them, many species of *Apiospora* are known to be associated with various living and decaying plant materials, and several *Apiospora* species act as plant pathogens. Such as *A. marii*, which causes olive tree dieback in Italy (Gerin et al. 2020); *A. phaeospermum*, which causes leaf necrosis in the olive crop in Sicily (Lo Piccolo et al. 2014); *A. arundinis*, which causes kernel blight of barley in the USA, *Phyllostachys praecox* brown culm streak disease in Nanjing, leaf blight on tea plants in China, leaf edge spot of peach in China, and culm rhomboid rot of Moso Bamboo (Martínez-Cano et al. 1992; Chen et al. 2014; Thangaraj et al. 2019; Ji et al. 2020; Zheng et al. 2022). The three species in this study were isolated from diseased culms of bamboo, and we verified their pathogenicity to bamboo under laboratory conditions. In the field, the disease symptoms caused by these fungi typically manifest as brown or black lesions of irregular shape on bamboo culms. These lesions may expand, coalesce, and in some cases, lead to extensive necrotic patches, resembling what we refer to as bamboo culm piebald-spot disease. Our pathogenicity tests confirmed that the three newly described species can induce similar symptoms under laboratory conditions, providing a theoretical basis for future research on bamboo disease management and control strategies.

In terms of biological applications, numerous *Apiospora* species produce bioactive secondary metabolites, potentially offering a promising source for pharmacological and medicinal research. For instance, *Apiospora* has shown strong antifungal activity against various plant pathogens (Hong et al. 2015). *A. saccharicola*, isolated from *Miscanthus* sp., is known to produce enzymes of industrial significance (Shrestha et al. 2015). *A. rasikravindrae*, isolated from *Coleus amboinicus*, exhibits notable cytotoxicity against WiDr cells and displays effective antibacterial activity against *Staphylococcus aureus* and *Escherichia coli* (Astuti et al. 2021). Metabolites from *A. arundinis*, isolated from *Aconitum brevicalcaratum*, show cytotoxic effects on breast cancer cell lines (Shu et al. 2022), while *A. arundinis* MA30, derived from sea anemones, demonstrates significant anti-inflammatory activity (Lee et al. 2024). Whole-genome sequencing with antiSMASH analysis identified six and ten NR-PKS gene clusters in *A. malaysianum* and *A. koreana*, respectively, which may encode known or novel quinone compounds with notable biological functions (Christiansen et al. 2021). *Apiospora* holds substantial potential for synthesizing diverse secondary metabolites. However, many novel species, including new species in this study, remain underexplored. Future research necessitates further exploration of the biological applications of both known and newly discovered *Apiospora* species to comprehensively elucidate their biological properties.

In conclusion, this study provides a detailed account of three new species of *Apiospora* from China and emphasizes the importance of integrating morphological and molecular data for accurate species identification. Given their potential ecological and economic impacts on bamboo, further research is warranted. Comprehensive taxonomic and ecological investigations will offer valuable insights for potential biotechnological applications and enhance our understanding of this genus and its broader ecological and medicinal significance.



## Additional information

### Conflict of interest

The authors have declared that no competing interests exist.

### Ethical statement

No ethical statement was reported.


### Funding

This study was supported by the Scientific Research Projects in Higher Education Institutions in Anhui Province (Key Project), China (No. 2024AH050480), and the National Key R&D Program of China (2021YFD2200501).

### Author contributions

Conceptualization: Xiaoyun Chang and Mingjun Chen; Data curation: Xiaoyun Chang, Yuanyuan Wang, and Tao Xu; Funding acquisition: Xianghua Yue and Mingjun Chen; Investigation: Xianghua Yue; Project administration: Mingjun Chen; Resources: Xianghua Yue and Mingjun Chen; Supervision: Mingjun Chen, Xianghua Yue, and Guangshuo Li; Writing—original draft: Xiaoyun Chang; Writing—review and editing: Mingjun Chen, Guangshuo Li, Xianghua Yue, Yuanyuan Wang, and Tao Xu. All authors have read and agreed to the published version of the manuscript.

### Author ORCIDs

Xiaoyun Chang  <https://orcid.org/0000-0002-0093-9582>

Yuanyuan Wang  <https://orcid.org/0009-0007-1801-3984>

Tao Xu  <https://orcid.org/0009-0009-0028-6508>

Guangshuo Li  <https://orcid.org/0000-0002-7285-0712>

Xianghua Yue  <https://orcid.org/0000-0003-2165-7653>

Mingjun Chen  <https://orcid.org/0000-0002-1439-7796>

### Data availability

All of the data that support the findings of this study are available in the main text.

## References

- Ai C, Dong Z, Yun J, Zhang Z, Xia J, Zhang X (2024) Phylogeny, Taxonomy and Morphological Characteristics of *Apiospora* (Amphisphaeriales, Apiosporaceae). *Microorganisms* 12(7): 1372. <https://doi.org/10.3390/microorganisms12071372>
- Astuti P, Pratoko DK, Rollando R, Nugroho G-W, Wahyuono S, Hertiani T, Nurrochmad A (2021) Bioactivities of A Major Compound from *Arthrinium rasikravindrae* An Endophytic Fungus of *Coleus amboinicus* Lour. *Fabad Journal of Pharmaceutical Sciences* 46: 23–30.
- Bhat D, Kendrick B (1993) Twenty-five new conidial fungi from the Western Ghats and the Andaman Islands (India). *Mycotaxon* 49: 19–90. <https://doi.org/10.2337/dc15-er04b>
- Borowski PF, Patuk I, Bandala ER (2022) Innovative industrial use of bamboo as key “Green” material. *Sustainability* 14: 1955. <https://doi.org/10.3390/su14041955>
- Cai L, Hyde K, Taylor P, Weir B, Waller J, Abang M, Zhang J, Yang Y, Phoulivong S, Liu Z (2009) A polyphasic approach for studying *Colletotrichum*. *Fungal Diversity* 39: 183–204.

- Carbone I, Kohn L-M (1999) A method for designing primer sets for speciation studies in filamentous ascomycetes. *Mycologia* 91: 553–556. <https://doi.org/10.1080/00275514.1999.12061051>
- Chen K, Wu XQ, Huang MX, Han YY (2014) First report of brown culm streak of *Phyllostachys praecox* caused by *Arthrinium arundinis* in Nanjing, China. *Plant Disease* 98: 1274–1274. <https://doi.org/10.1094/PDIS-02-14-0165-PDN>
- Christiansen JV, Isbrandt T, Petersen C, Sondergaard TE, Nielsen MR, Pedersen TB, Sørensen JL, Larsen TO, Frisvad JC (2021) Fungal quinones: Diversity, producers, and applications of quinones from *Aspergillus*, *Penicillium*, *Talaromyces*, *Fusarium*, and *Arthrinium*. *Applied Microbiology and Biotechnology*: 1–37. <https://doi.org/10.1007/s00253-021-11597-0>
- Crous PW, Groenewald J-Z (2013) A phylogenetic re-evaluation of *Arthrinium*. *IMA Fungus* 4: 133–154. <https://doi.org/10.5598/ima fungus.2013.04.01.13>
- Dai DQ, Jiang HB, Tang LZ, Bhat DJ (2016) Two new species of *Arthrinium* (Apiosporaceae, Xylariales) associated with bamboo from Yunnan, China. *Mycosphere* 7: 1332–1345. <https://doi.org/10.5943/mycosphere/7/9/7>
- Gerin D, Nigro F, Faretra F, Pollastro S (2020) Identification of *Arthrinium marii* as causal agent of olive tree dieback in Apulia (southern Italy). *Plant Disease* 104: 694–701. <https://doi.org/10.1094/PDIS-03-19-0569-RE>
- Glass NL, Donaldson GC (1995) Development of primer sets designed for use with the PCR to amplify conserved genes from filamentous ascomycetes. *Applied and Environmental Microbiology* 61: 1323–1330. <https://doi.org/10.1128/aem.61.4.1323-1330.1995>
- Hall TA (1999) BioEdit: a user-friendly biological sequence alignment editor and analysis program for Windows 95/98/NT. *Oxford*, 95–98.
- Hall T, Biosciences I, Carlsbad C (2011) BioEdit: An important software for molecular biology. *GERF Bulletin of Biosciences* 2: 60–61.
- Hawksworth DL, Crous PW, Redhead SA, Reynolds DR, Samson RA, Seifert KA, Taylor JW, Wingfield MJ, Abaci Ö, Aime C, Asan A, Bai F-Y, de Beer ZW, Begerow D, Berikten D, Boekhout T, Buchanan PK, Burgess T, Buzina W, Cai L, Cannon PF, Crane JL, Damm U, Daniel H-M, van Diepeningen AD, Druzhinina I, Dyer PS, Eberhardt U, Fell JW, Frisvad JC, Geiser DM, Geml J, Glienke C, Gräfenhan T, Groenewald JZ, Groenewald M, de Gruyter J, Guého-Kellermann E, Guo L-D, Hibbett DS, Hong S-B, de Hoog GS, Houbraken J, Huhndorf SM, Hyde KD, Ismail A, Johnston PR, Kadaifciler DG, Kirk PM, Kõljalg U, Kurtzman CP, Lagneau P-E, Lévesque CA, Liu X, Lombard L, Meyer W, Miller A, Minter DW, Najafzadeh MJ, Norvell L, Ozerskaya SM, Öziç R, Pennycook SR, Peterson SW, Pettersson OV, Quaedvlieg W, Robert VA, Ruibal C, Schnürer J, Schroers H-J, Shivas R, Slippers B, Spierenburg H, Takashima M, Taşkın E, Thines M, Thrane U, Uztan AH, van Raak M, Varga J, Vasco A, Verkley G, Videira SIR, de Vries RP, Weir BS, Yilmaz N, Yurkov A, Zhang N (2011) The Amsterdam declaration on fungal nomenclature. *IMA Fungus* 2: 105–111. <https://doi.org/10.5598/ima fungus.2011.02.01.14>
- Hong J-H, Jang S, Heo YM, Min M, Lee H, Lee Y-M, Lee H, Kim J-J (2015) Investigation of marine-derived fungal diversity and their exploitable biological activities. *Marine Drugs* 13: 4137–4155. <https://doi.org/10.3390/md13074137>
- Hyde K, Fröhlich J, Taylor J (1998) Fungi from palms. XXXVI. Reflections on unitunicate ascomycetes with apiospores.
- Hyde K, Zhou D, Dalisay T (2002) Bambusicolous fungi: A review. *Fungal Diversity* 9: 1–14.
- Ji Z, Zhang S, Zhu F, Wan B, Liang R (2020) First report of *Arthrinium arundinis* causing leaf edge spot of peach in China. *Plant Disease* 104: 3077. <https://doi.org/10.1094/PDIS-12-19-2666-PDN>


- Jiang H, Hyde K, Doilom M, Karunarathna S, Xu J, Phookamsak R (2019) *Arthrinium setostromum* (Apiosporaceae, Xylariales), a novel species associated with dead bamboo from Yunnan, China. *Asian Journal of Mycology* 2: 254–268. <https://doi.org/10.5943/ajom/2/1/16>
- Katoh K, Rozewicki J, Yamada KD (2019) MAFFT online service: Multiple sequence alignment, interactive sequence choice and visualization. *Briefings in Bioinformatics* 20: 1160–1166. <https://doi.org/10.1093/bib/bbx108>
- Kornerup A, Wanscher JH (1978) *Methuen Handbook of Colour*.
- Kwon SL, Park MS, Jang S, Lee YM, Heo YM, Hong J-H, Lee H, Jang Y, Park J-H, Kim C (2021) The genus *Arthrinium* (Ascomycota, Sordariomycetes, Apiosporaceae) from marine habitats from Korea, with eight new species. *IMA Fungus* 12: 13. <https://doi.org/10.1186/s43008-021-00065-z>
- Lee Y-S, Wu H-C, Huang S-J, Hsiao G, Chi W-C, Lee T-H (2024) Anti-inflammatory constituents from a sea anemone-derived fungus *Arthrinium arundinis* MA30. *Phytochemistry* 219: 113998. <https://doi.org/10.1016/j.phytochem.2024.113998>
- Letunic I, Bork P (2019) Interactive Tree Of Life (iTOL) v4: Recent updates and new developments. *Nucleic Acids Research* 47: W256–W259. <https://doi.org/10.1093/nar/gkz239>
- Li B, Liu P, Jiang Y, Weng Q, Chen Q (2016) First report of culm rot caused by *Arthrinium phaeospermum* on *Phyllostachys viridis* in China. *Plant Disease* 100: 1013–1013. <https://doi.org/10.1094/PDIS-08-15-0901-PDN>
- Li S, Peng C, Yuan R, Tian C (2023) Morphological and phylogenetic analyses reveal three new species of *Apiospora* in China. *MycKeys* 99: 297. <https://doi.org/10.3897/mycokeys.99.108384>
- Liao C, Senanayake I-C, Dong W, Thilini Chethana K-W, Tangtrakulwanich K, Zhang Y, Doilom M (2023) Taxonomic and phylogenetic updates on *Apiospora*: Introducing four new species from *Wurfbainia villosa* and grasses in China. *Journal of Fungi* 9: 1087. <https://doi.org/10.3390/jof9111087>
- Liu R, Li D, Zhang Z, Liu S, Liu X, Wang Y, Zhao H, Liu X, Zhang X, Xia J (2023) Morphological and phylogenetic analyses reveal two new species and a new record of *Apiospora* (Amphisphaeriales, Apiosporaceae) in China. *MycKeys* 95: 27. <https://doi.org/10.3897/mycokeys.95.96400>
- Liu X, Zhang Z, Wang S, Zhang X (2024) Three New Species of *Apiospora* (Amphisphaeriales, Apiosporaceae) on *Indocalamus longiauritus*, *Adinandra glischroloma* and *Machilus nanmu* from Hainan and Fujian, China. *Journal of Fungi* 10: 74. <https://doi.org/10.3390/jof10010074>
- Lo Piccolo S, Mondello V, Giambra S, Conigliaro G, Torta L, Burruano S (2014) *Arthrinium phaeospermum*, *Phoma cladoniicola* and *Ulocladium consortiale*, new olive pathogens in Italy. *Journal of Phytopathology* 162: 258–263. <https://doi.org/10.1111/jph.12179>
- Martínez-Cano C, Grey W, Sands D (1992) First report of *Arthrinium arundinis* causing kernel blight on barley. *Plant Disease* 76(10): 1077B. <https://doi.org/10.1094/PD-76-1077B>
- Nylander J (2004) MrModeltest v2. Program distributed by the author. Evolutionary Biology Centre, Uppsala University. *ampignons de l'Équateur* (Pugillus IV). *Bull L'Herb Boissier* 3: 53–74.
- O'Donnell K, Cigelnik E (1997) Two divergent intragenomic rDNA ITS2 types within a monophyletic lineage of the fungus *Fusarium* are nonorthologous. *Molecular Phylogenetics and Evolution* 7: 103–116. <https://doi.org/10.1006/mpev.1996.0376>
- O'Donnell K, Kistler H-C, Cigelnik E, Ploetz R-C (1998) Multiple evolutionary origins of the fungus causing Panama disease of banana: Concordant evidence from nuclear and

- mitochondrial gene genealogies. *Proceedings of the National Academy of Sciences of the United States of America* 95: 2044–2049. <https://doi.org/10.1073/pnas.95.5.2044>
- Pintos Á, Alvarado P (2021) Phylogenetic delimitation of *Apiospora* and *Arthrinium*. *Fungal Systematics and Evolution* 7: 197–221. <https://doi.org/10.3114/fuse.2021.07.10>
- Pintos Á, Alvarado P (2022) New studies on *Apiospora* (Amphisphaeriales, Apiosporaceae): Epitypification of *Sphaeriaapiospora*, proposal of *Ap. marianiae* sp. nov. and description of the asexual morph of *Ap. sichuanensis*. *MycKeys* 92: 63. <https://doi.org/10.3897/mycokeys.92.87593>
- Réblová M, Miller A-N, Rossman A-Y, Seifert K-A, Crous P-W, Hawksworth D-L, Abdel-Wahab M-A, Cannon P-F, Daranagama D-A, De Beer Z-W (2016) Recommendations for competing sexual-asexually typified generic names in Sordariomycetes (except Diaporthales, Hypocreales, and Magnaporthales). *IMA Fungus* 7: 131–153. <https://doi.org/10.5598/ima fungus.2016.07.01.08>
- Rehner SA, Samuels GJ (1995) Molecular systematics of the Hypocreales: A teleomorph gene phylogeny and the status of their anamorphs. *Canadian Journal of Botany* 73: 816–823. <https://doi.org/10.1139/b95-327>
- Robert V, Vu D, Amor A, Wiele N, Brouwer C, Jabas B, Szoke S, Dridi A, Triki M, Daoud S, Chouchen O, Vaas L, Cock A, Stalpers J, Stalpers D, Verkley G, Groenewald M, Borges dos Santos F, Crous P (2013) MycoBank gearing up for new horizons. *IMA Fungus* 4: 371–379. <https://doi.org/10.5598/ima fungus.2013.04.02.16>
- Saccardo PA (1875) *Conspectus generum pyrenomycetum italicorum additis speciebus fungorum Venetorum novis vel criticis, systemate carpologico dispositorum*. *Atti della Società Veneto-Trentina di Scienze Naturali* 4: 77–100.
- Sharma R, Kulkarni G, Sonawane MS, Shouche YS (2014) A new endophytic species of *Arthrinium* (Apiosporaceae) from *Jatropha podagrica*. *Mycoscience* 55: 118–123. <https://doi.org/10.1016/j.myc.2013.06.004>
- Shrestha P, Ibáñez AB, Bauer S, Glassman SI, Szaro TM, Bruns TD, Taylor JW (2015) Fungi isolated from *Miscanthus* and sugarcane: Biomass conversion, fungal enzymes, and hydrolysis of plant cell wall polymers. *Biotechnology for Biofuels* 8: 1–14. <https://doi.org/10.1186/s13068-015-0221-3>
- Shu Y, Wang JP, Li BX, Gan JL, Ding H, Liu R, Cai L, Ding ZT (2022) Bioactive cytochalasans from the fungus *Arthrinium arundinis* DJ-13. *Phytochemistry* 194: 113009. <https://doi.org/10.1016/j.phytochem.2021.113009>
- Shukla A, Singh A, Tiwari D, Ahirwar BK (2016) Bambusicolous fungi: A reviewed documentation. *International Journal of Pure & Applied Bioscience* 4: 304–310. <https://doi.org/10.18782/2320-7051.2268>
- Spatafora JW, Volkmann-Kohlmeyer B, Kohlmeyer J (1998) Independent terrestrial origins of the Halosphaeriales (marine Ascomycota). *American Journal of Botany* 85: 1569–1580. <https://doi.org/10.2307/2446483>
- Thangaraj K, Cheng LL, Deng C, Deng WW, Zhang ZZ (2019) First report of leaf blight caused by *Arthrinium arundinis* on tea plants in China. *Plant Disease* 103: 3282. <https://doi.org/10.1094/PDIS-06-19-1324-PDN>
- Tian X, Karunarathna SC, Mapook A, Promputtha I, Xu J, Bao D, Tibpromma S (2021) One new species and two new host records of *Apiospora* from bamboo and maize in northern Thailand with thirteen new combinations. *Life (Chicago, Ill.)* 11: 1071. <https://doi.org/10.3390/life11101071>
- Trifinopoulos J, Nguyen LT, von Haeseler A, Minh BQ (2016) W-IQ-TREE: A fast online phylogenetic tool for maximum likelihood analysis. *Nucleic Acids Research* 44: W232–W235. <https://doi.org/10.1093/nar/gkw256>



- Vaidya G, Lohman DJ, Meier R (2011) SequenceMatrix: Concatenation software for the fast assembly of multi-gene datasets with character set and codon information. *Cladistics* 27: 171–180. <https://doi.org/10.1111/j.1096-0031.2010.00329.x>
- Wang M, Tan XM, Liu F, Cai L (2018) Eight new *Arthrinium* species from China. *MycKeys* 34: 1–24. <https://doi.org/10.3897/mycokeys.34.24221>
- White TJ, Bruns T, Lee S, Taylor J (1990) Amplification and direct sequencing of fungal ribosomal RNA genes for phylogenetics. *PCR protocols: a guide to methods and applications* 18: 315–322. <https://doi.org/10.1016/B978-0-12-372180-8.50042-1>
- Yan XN, Zhang CL (2024) Three new endophytic *Apiospora* species (Apiosporaceae, Amphisphaeriales) from China. *MycKeys* 105: 295–316. <https://doi.org/10.3897/mycokeys.105.122583>
- Yang C, Xu X, Liu Y, Xu X (2019) First report of bamboo blight disease caused by *Arthrinium yunnanum* on *Phyllostachys heteroclada* in Sichuan, China. *Plant Disease* 103: 1026–1026. <https://doi.org/10.1094/PDIS-10-18-1740-PDN>
- Yuan H-S, Lu X, Dai Y-C, Hyde KD, Kan Y-H, Kušan I, He S-H, Liu N-G, Sarma VV, Zhao C-L, Cui B-K, Yousaf N, Sun G, Liu S-Y, Wu F, Lin C-G, Dayarathne MC, Gibertoni TB, Conceição LB, Garibay-Orijel R, Villegas-Ríos M, Salas-Lizana R, Wei T-Z, Qiu J-Z, Yu Z-F, Phookamsak R, Zeng M, Paloi S, Bao D-F, Abeywickrama PD, Wei D-P, Yang J, Manawasinghe IS, Harishchandra D, Brahmanage RS, de Silva NI, Tennakoon DS, Karunarathna A, Gafforov Y, Pem D, Zhang S-N, de Azevedo Santiago ALCM, Bezerra JDP, Dima B, Acharya K, Alvarez-Manjarrez J, Bahkali AH, Bhatt VK, Brandrud TE, Bulgakov TS, Camporesi E, Cao T, Chen Y-X, Chen Y-Y, Devadatha B, Elgorban AM, Fan L-F, Du X, Gao L, Gonçalves CM, Gusmão LFP, Huanraluek N, Jadan M, Jayawardena RS, Khalid AN, Langer E, Lima DX, de Lima-Júnior NC, de Lira CRS, Liu J-K, Liu S, Lumyong S, Luo Z-L, Matošec N, Niranjana M, Oliveira-Filho JRC, Papp V, Pérez-Pazos E, Phillips AJL, Qiu P-L, Ren Y, Ruiz RFC, Semwal KC, Soop K, de Souza CAF, Souza-Motta CM, Sun L-H, Xie M-L, Yao Y-J, Zhao Q, Zhou L-W (2020) Fungal diversity notes 1277–1386: Taxonomic and phylogenetic contributions to fungal taxa. *Fungal Diversity* 104: 1–266. <https://doi.org/10.1007/s13225-020-00461-7>
- Zhang J-Y, Chen M-L, Boonmee S, Wang Y-X, Lu Y-Z (2023) Four new endophytic *Apiospora* species isolated from three *Dicranopteris* species in Guizhou, China. *Journal of Fungi* 9: 1096. <https://doi.org/10.3390/jof9111096>
- Zhang Z, Pan H, Tao G, Li X, Han Y, Feng Y, Tong S, Ding C (2024) Culturable Mycobiota from Guizhou Wildlife Park in China. *Mycosphere* 15: 654–763. <https://doi.org/10.5943/mycosphere/15/1/5>
- Zhaxybayeva O, Gogarten JP (2002) Bootstrap, Bayesian probability and maximum likelihood mapping: Exploring new tools for comparative genome analyses. *BMC Genomics* 3: 1–15. <https://doi.org/10.1186/1471-2164-3-4>
- Zheng S, Zhang Q, Song Z, Zhou H, Liao Y, Zhang F (2022) *Arthrinium arundinis*, a novel causal agent of moso bamboo (*Phyllostachys edulis*) culm rhomboid rot and its sensitivity to fungicides. *Forests* 13: 1616. <https://doi.org/10.3390/f13101616>

# Biotrophic and saprophytic fungi from the *Rhodocybe-Clitopilus* clade (Entolomataceae): two new species and one new record in subtropical China

Sipeng Jian<sup>1</sup>, Xia Chen<sup>2</sup>, Tianwei Yang<sup>1</sup>, Xinjing Xu<sup>1</sup>, Feng Gao<sup>1</sup>, Yiwei Fang<sup>1</sup>, Jing Liu<sup>1</sup>, Chunxia Zhang<sup>1</sup>

<sup>1</sup> Yunnan Institute of Tropical Crops, Jinghong, Yunnan, 666100, China

<sup>2</sup> The Administration Bureau of Dr. Sun Yat-sen's Mausoleum, Nanjing, Jiangsu, 210014, China

Corresponding author: Chunxia Zhang (zhangchunxia7084@163.com)



This article is part of:

**Exploring the Hidden Fungal Diversity: Biodiversity, Taxonomy, and Phylogeny of Saprobic Fungi**

Edited by Samantha C. Karunarathna,  
Danushka Sandaruwan Tennakoon,  
Ajay Kumar Gautam

Academic editor: Ajay Kumar Gautam

Received: 5 February 2025

Accepted: 28 March 2025

Published: 24 April 2025

**Citation:** Jian S, Chen X, Yang T, Xu X, Gao F, Fang Y, Liu J, Zhang C (2025) Biotrophic and saprophytic fungi from the *Rhodocybe-Clitopilus* clade (Entolomataceae): two new species and one new record in subtropical China. MycoKeys 116: 227–254. <https://doi.org/10.3897/mycokeys.116.148775>

Copyright: © Sipeng Jian et al.

This is an open access article distributed under terms of the Creative Commons Attribution License (Attribution 4.0 International – CC BY 4.0).

## Abstract

This study proposes two new species and a new record in the *Rhodocybe-Clitopilus* clade, based on comprehensive morphological and molecular analyses. The nuc rDNA internal transcribed spacer region ITS1-5.8S-ITS2 (ITS), the large subunit ribosomal RNA gene (LSU), the RNA polymerase II second largest subunit (*RPB2*) and the translation elongation factor 1-alpha gene (*TEF1*), were employed to elucidate the relationships of *Clitopilus* and *Rhodocybe*. The first species, *Clitopilus parasiticus*, is capable of infecting the leaves of host plants in the genera *Dryopteris* and *Oplismenus*, exhibiting typical biotrophic behaviour while also demonstrating saprophytic growth on soil. Intraspecific comparisons were conducted, examining environmental factors as well as macro- and microscopic characteristics amongst individuals found on different plant hosts. Furthermore, this study reports the new saprophytic species, *Rhodocybe zijinshanensis* and provides a detailed description of *Clitopilus baronii*, a newly-recorded species in China.

**Key words:** Biotrophic species, Entolomataceae, morphology, multigene phylogeny, plant pathogens, taxonomy

## Introduction

In nature, numerous fungi are well-known for their parasitic relationships, enabling them to thrive in dynamic environments. For example, the ergot (*Claviceps purpurea* (Fr.) Tul.) and corn smut (*Mycosarcoma maydis* (DC.) Bref.) are recognised as pathogenic fungi affecting cultivated plants (*Triticum aestivum* L. and *Zea mays* L., respectively) (Tudzynski and Scheffer 2004; McTaggart et al. 2016). Additionally, several special form genera, such as *Asterophora* Ditmar, *Squamanita* Imbach and *Hypomyces* (Fr.) Tul. & C. Tul., exhibit fungicolous parasitism or mycoparasitic behaviour (Rogerson and Samuels 2018; Elkhateeb and Daba 2021; Liu et al. 2021). However, parasitic forms are relatively rare in Agaricales Underw., particularly for biotrophic parasitism.

Saprophytic and symbiotic modes of nutrition are predominant amongst fungi in Basidiomycetes, but some fungi also employ parasitic nutrition as a strategy for survival and reproduction (Pölme et al. 2021; Shi et al. 2023). Thereinto,

biotrophic parasitism is an intriguing and unique phenomenon in fungi, defined as a nutritional strategy where fungi derive nutrients from a living host while keeping it alive, often causing restricted damage to the host plant (Luttrell 1974; Kemen and Jones 2012). Species within the Agaricales that exhibit distinct biotrophic capabilities often also possess saprophytic abilities, indicating that they are not obligate parasites. For example, Zhang et al. (2022) identified a new species, viz. *Crepidotus herbaceus* T. Bau & Y.P. Ge, which is not only parasitic on the leaves or stems of *Oreocnide frutescens* (Thunb.) Miq. and *Alpinia japonica* (Thunb.) Miq., but is also found on the plant debris or humus.

In the family Entolomataceae Kotl. & Pouzar, there are two main clades: *Entoloma* (Fr.) P. Kumm. and *Rhodocybe-Clitopilus* (Co-David et al. 2009; Baroni and Matheny 2011; Kluting et al. 2014). The *Rhodocybe-Clitopilus* clade differs from the *Entoloma* clade by its basidiospores, which are characterized by either longitudinal ridges or scattered, finely to distinctly pustulate ornamentations (Baroni 1981; Singer 1986; Kluting et al. 2014). Within the *Rhodocybe-Clitopilus* clade, most species are primarily regarded as saprophytic (Sanchez-Garcia and Matheny 2017). However, a few species, such as *Rhodophana stangliana* (Bresinsky & Pfaff) Vizzini, *Clitopilus passeckerianus* (Pilát) Sing., *C. fasciculatus* Noordel. and *C. daamsii* Noordel., also appear mycoparasite (Noordeloos 1984, 1993; Læssøe and Rosendahl 1994; Czederpiltz et al. 2001). Notably, *C. hobsonii* (Berk.) P.D. Orton has been reported to grow on stumps, fallen logs, twigs and living herbaceous leaves and stems (Orton 1960; Noordeloos 1984), highlighting its saprophytic and biotrophic capacities.

In the current study, several specimens gathered from Jiangsu Province are examined carefully. Three samples closely resembled *Pleurotus* (Fr.) P. Kumm., *Crepidotus* (Fr.) Staude and *Omphalotus* Fayod. Upon microscopic examination, they were all confirmed to the *Rhodocybe-Clitopilus* clade, respectively. Furthermore, two new species and one new record species were identified, based on the multi-gene phylogenetic tree. Therefore, all three species are described herein.

## Materials and methods

### Sample collections and morphological observations

The collection information of voucher specimens and the sequences used in phylogenetic analyses are shown in Table 1. The colour codes (hex triplets) from ColorHexa (<https://www.colorhexa.com>) were employed to depict the colour of basidiomata. These codes consist of characters ranging from a to f and 0 to 9, with each pair corresponding to the red, green and blue components of the colour. The general description of basidiomata, including both macro- and microscopic features, as well as the morphological classification rules in *Clitopilus* and *Rhodocybe* Maire were based on the work of Baroni (1981) and Jian et al. (2020a). All voucher specimens have been deposited at the Cryptogamic Herbarium of the Herbaria of Kunming Institute of Botany, Chinese Academy of Sciences (KUN-HKAS).

Sections of dried basidiomata were rehydrated in purified water and 5% potassium hydroxide (KOH) and were occasionally stained with 1% Congo Red to enhance visibility. The notation “[*n*/*m*/*p*]” indicates *n* basidiospores from *m* basidiomata of *p* specimens. The measurements of basidiospores are presented in the format (a–)b–c(–d), where the range b–c includes at least 90% of the measured values, while a and d (given in parentheses) represent the extreme values.

The average length and width of basidiospore ( $\pm$  standard deviation) are denoted as  $L_m$  and  $W_m$ , respectively. The term  $Q$  refers to the “length/width ratio” of a basidiospore in side view, with  $Q_{avg}$  representing the average  $Q$  across all specimens ( $\pm$  standard deviation). Fragments isolated from specimens were attached to aluminium stubs using double-sided adhesive tape, and then coated with gold/palladium. Finally, a ZEISS EVO LS10 (Germany) scanning electron microscope (SEM) was used to observe the ornamentation of the basidiospores.

The genetic names appeared in this study are abbreviated as follows: *Clitopilus* = “C.”, *Rhodocybe* = “R.”.

## Molecular phylogenetic analyses

In this study, we utilised two sequences of non-protein-coding and two protein-coding genes: the nuc rDNA internal transcribed spacer region ITS1-5.8S-ITS2 (ITS), the large subunit ribosomal RNA gene (LSU), the RNA polymerase II second largest subunit (*RPB2*) and the translation elongation factor 1- $\alpha$  gene (*TEF1*). The ITS and LSU genes were selected for their availability of universal primers (White et al. 1990), while the *RPB2* and *TEF1* genes were chosen due to their relatively high number of informative sites and sufficient nucleotide variation, which are essential for inferring evolutionary relationships within the Entolomataceae (Matheny et al. 2007; Co-David et al. 2009; Kluting et al. 2014). All the sequences were submitted to the National Center for Biotechnology Information (NCBI) and detailed information regarding each gene was provided in Table 1.

Genomic DNA was extracted from collected materials and herbarium specimens using the CTAB (cetyltrimethylammonium bromide) procedure outlined by Doyle and Doyle (1987). The PCR protocol followed the touchdown method described by Kluting et al. (2014), with detailed data provided in Table 2. Gel extraction and PCR (polymerase chain reaction) were conducted to purify the PCR products, which were then sequenced on an ABI-3730-XL sequence analyser (Applied Biosystems, Foster City, CA) using the same primers as in the PCR. The new sequences generated from this study are highlighted in bold in Table 1.

For the sequence alignments, Sequencher 4.1.4 (Gene Code Corp., Ann Arbor, MI) was used to concatenate sequences obtained from both direction (5′–3′ & 3′–5′), to remove regions with heavy peaks and to merge degenerate bases. The sequences were then aligned using MAFFT 7.526 (Kato et al. 2005) and manually checked in BioEdit 7.7.1 (Hall 1999). Separate single-gene analyses were performed to exclude conflicts amongst topologies using Maximum Likelihood and Bayesian Inference. Subsequently, Phyutility 2.2 (Smith and Dunn 2008) was employed to combine all the separate single-gene datasets. Any deficiencies in the DNA fragment sequences were treated as missing data in the subsequent analyses. A super-matrix was generated by combining sequences of all four loci.

Under the Akaike Information Criterion (AIC), the best-fitted substitution model for each dataset was determined with MrModelTest 2.3 (Nylander 2004). Phylogenetic analyses were conducted using Maximum Likelihood (ML) with RAxML 7.2.6 (Stamatakis 2006) and Bayesian Inference (BI) with MrBayes 3.2.6 (Ronquist and Huelsenbeck 2003). In view of the close kinship amongst *Lulesia* Singer & *Clitopilus*, as well as *Clitopilopsis* Maire & *Rhodocybe*, *Lulesia umbrinomarginata* Y.Q. Xiao et al. and *Lulesia orientalis* (S.P. Jian & Zhu L. Yang) Vizzini et al. were selected as outgroups for the phylogenetic tree of *Clitopilus*.



**Table 1.** Sequencing primers and the best annealing temperature for ITS, LSU, *RPB2* and *TEF1*.

Primer name	Nucleotide sequence 5'-3'	PCR annealing temperature (°C)
ITS4	TCC TCC GCT TAT TGA TAT GC	52
ITS5	GGA AGT AAA AGT CGT AAC AAG G	
LR0R	ACC CGC TGA ACT TAA GC	52
LR5	TCC TGA GGG AAA CTT CG	
EF1-983F	GCY CCY GGH CAY CGT GAY TTY AT	56/touchdown*
EF1-1953R	CCR GCR ACR GTR TGT CTC AT	
bRPB2-6F	TGG GGY ATG GTN TGY CCY GC	52
bRPB2-7.1R	CCC ATR GCY TGY TTM CCC ATD GC	

Notes: \* the details of the touchdown method refer to Kluting et al. (2014).

Similarly, *Clitopilopsis albida* S.P. Jian & Zhu L. Yang and *Clitopilopsis hirneola* (Fr.) Kühner were chosen as outgroups for the phylogenetic tree of *Rhodocybe*.

For ML analyses, the GTRGAMMAI model was applied to the combined dataset, with statistical support for internodes obtained through non-parametric bootstrapping with 1000 replications. For the BI analyses of the combined dataset, a partitioned mixed model was implemented, defining the sequences of ITS, LSU, *RPB2* and *TEF1* as four independent partitions, with each gene estimated using different model parameters. The best-selected model was employed and the Markov Chain Monte Carlo (MCMC) chain was run for four million generations. The STOPRULE command was set with STOPVAL = 0.01 and trees were sampled every 100 generations. We verified chain convergence using Tracer 1.5 (<http://tree.bio.ed.ac.uk/software/tracer>) to ensure sufficiently large effective sample size (ESS) values greater than 200. The combined tree was summarised using the sump and sumt commands with a 25% burn-in.

## Results

### Phylogenetic analyses

No topological inconsistency was detected between the ML and BI analyses, both for the individual genes and the multigene data. The phylogenetic tree inferred from the ML strategy is presented, with statistical results from both ML (Bootstrap Supports, BS) and BI (Posterior Probabilities, PP) displayed on the branches (see Figs 1, 2). The best-fit model for ML and BI analyses was the GTR+I+R model. In the multigene matrix for *Clitopilus*, we assembled a total of 131 sequences from four genes: 96 for ITS, 89 for LSU, 110 for *RPB2* and 78 for *TEF1*. Analogously, the multigene matrix for *Rhodocybe* included 120 sequences derived from the same four genes, with 72 for ITS, 48 for LSU, 55 for *RPB2* and 37 for *TEF1*. Finally, the dataset for *Clitopilus* included 3664 sites in total, with 788 from ITS, 957 from LSU, 784 from *RPB2* and 1135 from *TEF1*. Similarly, the dataset for *Rhodocybe* included 3881 sites, with 960 from ITS, 985 from LSU, 799 from *RPB2* and 1137 from *TEF1*.

In the phylogenetic tree of *Clitopilus* (Fig. 1), species with parasitic abilities are clustered together in *Clitopilus* sect. *Scyphoides* Singer, representing a new species. The species collected from rotten wood are positioned close to *C. baronii* Consiglio & Setti. Furthermore, the phylogenetic tree of *Rhodocybe* (Fig. 2) shows that other species collected from rotten wood are clustered within *Rhodocybe* sect. *Rufobrunnea* Singer ex T.J. Baroni, also signifying a new species.

**Table 2.** Collection information of voucher specimen and GenBank accession numbers for sequences used in phylogenetic analyses. H in parentheses means the holotype specimen.

Species	Collection or collector no.	Location and year	GenBank accession numbers				References
			ITS	LSU	RPB2	TEF1	
<i>C. abprunulus</i>	KUN-HKAS 107040 <sup>a</sup>	Macedonia 2019	NR_172792	NG_074438	MT349666	MT349670	Jian et al. (2020b)
<i>C. abprunulus</i>	KUN-HKAS 107041 <sup>a</sup>	Macedonia 2019	MT345049	MT345054	MT349667	MT349671	Jian et al. (2020b)
<i>C. abprunulus</i>	KUN-HKAS 107042 <sup>a</sup>	Macedonia 2019	MT345047	MT345052	MT349665	MT349669	Jian et al. (2020b)
<i>C. abprunulus</i>	MEN 2003-09-14 <sup>b</sup>	Belgium 2003	KR261096	GQ289149	GQ289221	–	Co-David et al. (2009)
<i>C. albidus</i>	CAL 1319 <sup>c</sup>	Kerala State, India 2001	MF926596	MF926595	MF946579	–	Raj and Manimohan (2018)
<i>C. amygdaliformis</i>	KUN-HKAS 60406 <sup>a</sup>	Yunnan, China 2008	MN061292	–	MN148120	–	Jian et al. (2020a)
<i>C. amygdaliformis</i>	KUN-HKAS 81125 <sup>a</sup>	Yunnan, China 2014	NR_172768	MN065681	MN148119	MN166231	Jian et al. (2020a)
<i>C. amygdaliformis</i>	KUN-HKAS 87950 <sup>a</sup>	Yunnan, China 2014	MN061290	MN065680	MN148118	MN166230	Jian et al. (2020a)
<i>“C. cf. argentinus”</i>	MTB 4804/2 <sup>d</sup>	Germany 2011	–	–	KC816907	KC816823	Kluting et al. (2014)
<i>C. austroprunulus</i>	MEN2009001 <sup>e</sup>	Tahune, Australia 2009	KC139084	–	–	–	Crous et al. (2012)
<i>C. austroprunulus</i>	MEN2009062 <sup>e</sup>	Tasmania, Australia 2009	KC139085	–	–	–	Crous et al. (2012)
<b><i>C. baronii</i></b>	<b>KUN-HKAS 145333</b>	<b>Jiangsu, China 2023</b>	<b>PQ793166</b>	<b>PQ781610</b>	<b>PQ788395</b>	<b>PQ788402</b>	<b>This study</b>
<b><i>C. baronii</i></b>	<b>KUN-HKAS 145334</b>	<b>Jiangsu, China 2023</b>	<b>PQ793167</b>	<b>PQ781611</b>	<b>PQ788396</b>	<b>PQ788403</b>	<b>This study</b>
<i>C. baronii</i>	K(M)179703 <sup>f</sup>	UK 2012	MN855362	–	MN856160	–	Consiglio and Setti (2019)
<i>C. baronii</i>	AMB 18359 <sup>g</sup>	Mantova, Italy 2006	MN855365	–	MN856163	MN856174	Consiglio and Setti (2019)
<i>C. baronii</i>	AMB 18362 <sup>g</sup>	Ferrara, Italy 2007	MN855368	–	MN856166	MN856176	Consiglio and Setti (2019)
<i>C. baronii</i>	AMB 18363 <sup>g</sup>	Mantova, Italy 2007	NR_176131	–	MN856167	MN856177	Consiglio and Setti (2019)
<i>C. baronii</i>	AMB 18378 <sup>g</sup>	Pisa, Italy 2007	MN855370	–	MN856168	MN856178	Consiglio and Setti (2019)
<i>C. brunneiceps</i>	KUN-HKAS 73123 <sup>a</sup>	Yunnan, China 2011	MN061294	MN065683	MN148122	MN166233	Jian et al. (2020a)
<i>C. brunneiceps</i>	KUN-HKAS 80211 <sup>a</sup>	Hubei, China 2013	MN061293	MN065682	MN148121	MN166232	Jian et al. (2020a)
<i>C. brunneiceps</i>	KUN-HKAS 104510 <sup>a</sup>	Yunnan, China 2018	NR_172769	MN065684	MN148123	MN166234	Jian et al. (2020a)
<i>C. brunneiceps</i>	HMJAU 23509 <sup>h</sup>	Neimenggu, China 2013	MN061296	MN065685	MN148115	–	Jian et al. (2020a)
<i>C. chichawatniensis</i>	LAH37431 <sup>i</sup>	Punjab, Pakistan 2019	ON980767	ON980764	–	–	Fatima et al. (2022)
<i>C. chichawatniensis</i>	LAH37432 <sup>i</sup>	Punjab, Pakistan 2020	ON980766	ON980763	–	–	Fatima et al. (2022)
<i>C. chrischonensis</i>	TO HG1994 <sup>j</sup>	Basilea, Switzerland 2008	HM623128	HM623131	–	–	Vizzini et al. (2011)
<i>“C. cinerascens”</i>	8024 TJB <sup>d</sup>	Florida, USA 1996	–	GU384613	KC816908	KC816824	Kluting et al. (2014)
<i>“C. cinerascens”</i>	8133 TJB <sup>d</sup>	Louisiana, USA 1996	–	–	KC816909	KC816825	Kluting et al. (2014)
<i>C. cretoalbus</i>	LAH37017 <sup>i</sup>	Punjab, Pakistan 2020	OM935685	OM934826	–	–	Izhar et al. (2023)
<i>C. cretoalbus</i>	LAH35709 <sup>j</sup>	Punjab, Pakistan 2017	ON117610	ON229505	–	–	Izhar et al. (2023)
<i>C. crispus</i>	9982 TJB <sup>d</sup>	Chiang Mai, Thailand 2006	–	–	KC816910	KC816826	Kluting et al. (2014)
<i>C. crispus</i>	10027 TJB <sup>d</sup>	Chiang Mai, Thailand 2006	–	–	KC816911	KC816827	Kluting et al. (2014)
<i>C. crispus</i>	KUN-HKAS 84667 <sup>a</sup>	Yunnan, China 2014	MN061314	MN065705	MN148142	MN166254	Jian et al. (2020a)
<i>C. crispus</i>	KUN-HKAS 87018 <sup>a</sup>	Yunnan, China 2014	MN061315	MN065706	MN148143	MN166255	Jian et al. (2020a)
<i>C. crispus</i>	KUN-HKAS 90506 <sup>a</sup>	Yunnan, China 2015	MN061312	MN065702	MN148139	MN166251	Jian et al. (2020a)
<i>C. crispus</i>	KUN-HKAS 90508 <sup>a</sup>	Yunnan, China 2015	–	MN065703	MN148140	MN166252	Jian et al. (2020a)
<i>C. crispus</i>	KUN-HKAS 97509 <sup>a</sup>	Yunnan, China 2016	MN061318	MN065708	MN148145	MN166258	Jian et al. (2020a)
<i>C. crispus</i>	KUN-HKAS 102670 <sup>a</sup>	Yunnan, China 2017	MN061313	MN065704	MN148141	MN166253	Jian et al. (2020a)
<i>C. crispus</i>	KUN-HKAS 104507 <sup>a</sup>	Yunnan, China 2017	MN061316	MN065707	MN148144	MN166256	Jian et al. (2020a)
<i>C. cystidiatus</i>	MEN 200350	Slovakia 2003	–	GQ289147	GQ289220	–	Co-David et al. (2009)
<i>C. fasciculatus</i>	MO#297071	California, USA 2017	MG551863	–	–	–	Direct submission
<i>C. fusiformis</i>	SAAS 1038 <sup>k</sup>	Yunnan, China 2015	KY385634	–	KY385632	–	Wang et al. (2017)
<i>C. fusiformis</i>	SAAS 1892 <sup>k</sup>	Yunnan, China 2015	NR_158328	–	KY385633	–	Wang et al. (2017)
<i>C. fusiformis</i>	KUN-HKAS 104513 <sup>a</sup>	Yunnan, China 2018	MN061297	MN065686	MN148124	MN166235	Jian et al. (2020a)
<i>C. fusiformis</i>	KUN-HKAS 104514 <sup>a</sup>	Yunnan, China 2018	MN061298	MN065687	MN148125	MN166236	Jian et al. (2020a)
<i>C. fusiformis</i>	KUN-HKAS 104515 <sup>a</sup>	Yunnan, China 2018	MN061300	MN065690	MN148128	MN166239	Jian et al. (2020a)
<i>C. fusiformis</i>	KUN-HKAS 104516 <sup>a</sup>	Yunnan, China 2018	MN061299	MN065688	MN148126	MN166237	Jian et al. (2020a)
<i>C. fusiformis</i>	KUN-HKAS 104517 <sup>a</sup>	Yunnan, China 2018	–	MN065689	MN148127	MN166238	Jian et al. (2020a)
<i>C. giovanellae</i>	S.F.14368 <sup>l</sup>	Trento, Italy 1888	EF413030	EF413027	–	–	Moreno et al. (2007)
<i>C. giovanellae</i>	AH 19780 <sup>m</sup>	Spain 1998	–	EF413026	–	–	Moreno et al. (2007)
<i>C. highlandensis</i>	KUN-HKAS 68389 <sup>a</sup>	Yunnan, China 2010	MN061310	MN065700	MN148137	MN166249	Jian et al. (2020a)
<i>C. highlandensis</i>	KUN-HKAS 117632 <sup>a</sup>	Yunnan, China 2021	ON999061	ON999062	OP006563	OP006564	Jian et al. (2023)
<i>C. hobsonii</i>	K(M) 167650 <sup>f</sup>	UK 2010	MN855371	–	MN856169	–	Consiglio and Setti (2019)
<i>C. hobsonii</i>	K(M) 122842 <sup>f</sup>	UK 2004	NR_182819	–	MN856170	–	Consiglio and Setti (2019)
<i>C. hobsonii</i>	K(M) 199928 <sup>f</sup>	UK 2015	MN855373	–	MN856171	–	Consiglio and Setti (2019)
<i>“C. hobsonii”</i>	QYL10	–	OK652826	OK655769	MN092372	MN092373	Peng et al. (2021)
<i>“C. hobsonii”</i>	DLL 9779	Queensland, Australia 2010	–	–	KC816916	KC816831	Kluting et al. (2014)

Species	Collection or collector no.	Location and year	GenBank accession numbers				References
			ITS	LSU	RPB2	TEF1	
<i>"C. hobsonii"</i>	5967 TJB <sup>d</sup>	New York, USA 1988	–	–	KC816917	–	Kluting et al. (2014)
<i>"C. hobsonii"</i>	DLL 9586	Queensland, Australia 2009	–	KJ021698	KC816912	KC816828	Kluting et al. (2014)
<i>"C. hobsonii"</i>	DLL 9635	Queensland, Australia 2009	–	–	KC816913	KC816829	Kluting et al. (2014)
<i>"C. hobsonii"</i>	DLL 9643	Queensland, Australia 2009	–	–	KC816914	–	Kluting et al. (2014)
<i>"C. hobsonii"</i>	DLL 9746	Queensland, Australia 2010	–	–	KC816915	KC816830	Kluting et al. (2014)
<i>"C. hobsonii" grp."</i>	7051 TJB <sup>d</sup>	North Carolina, USA 1993	–	–	KC816918	–	Kluting et al. (2014)
<i>C. aff. hobsonii</i>	K:M195388 <sup>f</sup>	UK 2014	MN855375	–	MN856172	MN856179	Consiglio and Setti (2019)
<i>"C. aff. hobsonii"</i>	UC 1860830 <sup>n</sup>	California, USA 2011	–	–	KC816928	KC816841	Kluting et al. (2014)
<i>C. cf. kamaka</i>	KA12-0364 <sup>e</sup>	South Korea 2012	KR673433	–	–	–	Kim et al. (2015)
<i>C. kamaka</i>	PDD 96106 <sup>p</sup>	New Zealand 2010	NR_137867	–	–	–	Cooper (2014)
<i>C. lampangensis</i>	SDBR-CMUJK 0147 <sup>q</sup>	Lampang, Thailand 2018	NR_175631	MK764935	MK784129	–	Kumla et al. (2019)
<i>C. lampangensis</i>	SDBR-CMUNK 0047 <sup>q</sup>	Lampang, Thailand 2018	MK764934	MK773856	MK784128	–	Kumla et al. (2019)
<i>C. orientalis</i>	CAL 1613 <sup>c</sup>	Kerala State, India 2011	MG345134	MG321558	MG321559	–	Raj and Manimohan (2018)
<b><i>C. parasiticus</i></b>	<b>KUN-HKAS 145335<sup>a</sup></b>	<b>Jiangsu, China 2023</b>	<b>PQ793168</b>	<b>PQ781612</b>	<b>PQ788397</b>	<b>PQ788404</b>	<b>This study</b>
<b><i>C. parasiticus</i> (H)</b>	<b>KUN-HKAS 145336<sup>a</sup></b>	<b>Jiangsu, China 2024</b>	<b>PQ793169</b>	<b>PQ781613</b>	<b>PQ788398</b>	<b>–</b>	<b>This study</b>
<b><i>C. parasiticus</i></b>	<b>KUN-HKAS 145337<sup>a</sup></b>	<b>Jiangsu, China 2024</b>	<b>PQ793170</b>	<b>PQ781614</b>	<b>PQ788399</b>	<b>PQ788405</b>	<b>This study</b>
<i>C. passeckerianus</i>	CBS:299.35 <sup>r</sup>	Austria –	MH855682	MH867198	–	–	Vu et al. (2019)
<i>C. passeckerianus</i>	P73	South Korea 2015	KY962489	KY963073	–	–	Direct submission
<i>C. passeckerianus</i>	P78	South Korea 2015	KY962494	KY963078	–	–	Direct submission
<i>C. passeckerianus</i>	K:M134571 <sup>f</sup>	UK 2005	MN855376	–	MN856173	–	Consiglio and Setti (2019)
<i>C. paxilloides</i>	5809 TJB <sup>d</sup>	California, USA 1987	–	–	KC816919	KC816832	Kluting et al. (2014)
<i>"C. peri"</i>	10040 TJB <sup>d</sup>	Chiang Mai, Thailand 2006	–	–	KC816921	KC816834	Kluting et al. (2014)
<i>"C. peri"</i>	10033 TJB <sup>d</sup>	Chiang Mai, Thailand 2006	–	–	KC816920	KC816833	Kluting et al. (2014)
<i>"C. peri"</i>	10041 TJB <sup>d</sup>	Chiang Mai, Thailand 2006	–	–	KC816922	KC816835	Kluting et al. (2014)
<i>C. pinsitus</i>	CBS 623.70 <sup>r</sup>	England, UK –	MH859879	MH871665	–	–	Vu et al. (2019)
<i>C. pinsitus</i>	G. Immerzeel 1990-11	Netherlands 1990	–	GQ289148	–	–	Co-David et al. (2009)
<i>"C. prunulus"</i>	CORT:11CA012 <sup>d</sup>	California, USA 2011	–	–	KC816926	KC816839	Kluting et al. (2014)
<i>C. prunulus</i>	REH8456 <sup>d</sup>	Novgorod Region, Russia 2003	–	–	KC816923	KC816836	Kluting et al. (2014)
<i>"C. prunulus"</i>	6805 TJB <sup>d</sup>	New York, USA 1992	–	–	KC816924	KC816837	Kluting et al. (2014)
<i>"C. prunulus"</i>	TJB 9425 <sup>d</sup>	Dominican Republic 2002	–	–	MN893320	MN893330	Baroni et al. (2020)
<i>"C. prunulus"</i>	AFTOL522, TJB6838 <sup>d</sup>	USA –	DQ202272	AY700181	–	–	Direct submission
<i>"C. prunulus"</i>	TB8229 <sup>d</sup>	New York, USA 1996	–	GU384615	GU384650	–	Baroni et al. (2011)
<i>"C. prunulus"</i>	TB9663 <sup>d</sup>	–	–	GU384614	GU384648	–	Baroni et al. (2011)
<i>C. prunulus</i>	KUN-HKAS 96158 <sup>a</sup>	Austria 2016	MN061301	MN065691	MN148129	MN166240	Jian et al. (2020a)
<i>C. prunulus</i>	KUN-HKAS 123138 <sup>a</sup>	France –	OP626992	OP646418	OP939970	OP687894	He et al. (2023)
<i>C. prunulus</i>	HMJAU 4521 <sup>s</sup>	Kirov, Russia 2006	MN061302	MN065692	MN148117	MN166241	Jian et al. (2020a)
<i>C. cf. prunulus</i>	KUN-HKAS 75845 <sup>a</sup>	California, USA 2011	MN061303	MN065693	MN148130	MN166242	Jian et al. (2020a)
<i>C. rarus</i>	KUN-HKAS 107043 <sup>a</sup>	Yunnan, China 2019	MT345050	MT345055	MT349668	MT349672	Jian et al. (2020b)
<i>C. reticulosporus</i>	WU27150 <sup>b</sup>	Vienna, Austria 2004	KC885966	HM164412	HM164416	–	Morgado et al. (2016)
<i>C. rugosiceps</i>	KUN-HKAS 57003 <sup>a</sup>	Yunnan, China 2009	MN061304	MN065694	MN148131	MN166243	Jian et al. (2020a)
<i>C. rugosiceps</i>	KUN-HKAS 59455 <sup>a</sup>	Yunnan, China 2009	–	MN065696	MN148133	MN166245	Jian et al. (2020a)
<i>C. rugosiceps</i>	KUN-HKAS 73232 <sup>a</sup>	Yunnan, China 2011	NR_172771	MN065695	MN148132	MN166244	Jian et al. (2020a)
<i>C. rugosiceps</i>	KUN-HKAS 107044 <sup>a</sup>	Yunnan, China 2019	MT345046	MT345051	–	–	Jian et al. (2020b)
<i>C. rugosiceps</i>	KUN-HKAS 115921 <sup>a</sup>	Yunnan, China 2017	MZ855871	MZ853557	MZ826364	MZ826362	He and Yang (2022)
<i>C. scyphoides</i>	CBS 127.47 <sup>r</sup>	France –	MH856181	MH867707	–	–	Vu et al. (2019)
<i>C. cf. scyphoides</i>	KUN-HKAS 104511 <sup>a</sup>	Gansu, China 2016	MN061329	MN065720	MN148157	MN166268	Jian et al. (2020a)
<i>C. sinoapalus</i>	KUN-HKAS 77037 <sup>a</sup>	Jiangxi, China 2012	MN061321	MN065713	MN148149	–	Jian et al. (2020a)
<i>C. sinoapalus</i>	KUN-HKAS 82230 <sup>a</sup>	Guangzhou, China 2013	MN061320	MN065712	MN148148	–	Jian et al. (2020a)
<i>C. sinoapalus</i>	KUN-HKAS 83831 <sup>a</sup>	Yunnan, China 2014	–	MN065714	MN148150	–	Jian et al. (2020a)
<i>C. sinoapalus</i>	KUN-HKAS 101191 <sup>a</sup>	Yunnan, China 2017	NR_172773	MN065711	MN148151	MN166261	Jian et al. (2020a)
<i>C. sinoapalus</i>	KUN-HKAS 102737 <sup>a</sup>	Yunnan, China 2017	–	MN065709	MN148146	MN166259	Jian et al. (2020a)
<i>C. sinoapalus</i>	KUN-HKAS 102807 <sup>a</sup>	Yunnan, China 2017	MN061319	MN065710	MN148147	MN166260	Jian et al. (2020a)
<i>C. subalbidus</i>	GDGM 72219 <sup>t</sup>	Guangdong, China 2018	NR_198267	NG_243733	ON959185	ON959190	Jian et al. (2023)
<i>C. subalbidus</i>	GDGM 72229 <sup>t</sup>	Guangdong, China 2018	ON963952	ON963946	ON959186	–	Jian et al. (2023)
<i>C. subscyphoides</i>	CAL 1325 <sup>c</sup>	Kerala State, India 2011	MF927542	MF946580	MF946581	–	Raj and Manimohan (2018)
<i>C. subscyphoides</i>	GDGM 72195 <sup>t</sup>	Guangdong, China 2018	–	–	ON959188	–	Jian et al. (2023)

Species	Collection or collector no.	Location and year	GenBank accession numbers				References
			ITS	LSU	RPB2	TEF1	
<i>C. subscyphoides</i>	GDGM 72683 <sup>t</sup>	Guangdong, China 2018	ON963953	ON963947	–	–	Jian et al. (2023)
<i>C. subscyphoides</i>	GDGM 73056 <sup>t</sup>	Guangdong, China 2018	ON963954	ON963948	ON959187	ON959191	Jian et al. (2023)
<i>C. umbilicatus</i>	KUN-HKAS 80289 <sup>a</sup>	Hunan, China 2013	MN061323	MN065715	MN148152	MN166262	Jian et al. (2020a)
<i>C. umbilicatus</i>	KUN-HKAS 80310 <sup>a</sup>	Anhui, China 2013	MN061324	MN065716	MN148153	MN166263	Jian et al. (2020a)
<i>C. umbilicatus</i>	KUN-HKAS 80370 <sup>a</sup>	Fujian, China 2013	MN061325	MN065717	MN148154	MN166264	Jian et al. (2020a)
<i>C. umbilicatus</i>	KUN-HKAS 80945 <sup>a</sup>	Anhui, China 2013	MN061326	MN065718	MN148155	MN166265	Jian et al. (2020a)
<i>C. umbilicatus</i>	KUN-HKAS 104509 <sup>a</sup>	Yunnan, China 2017	MN061327	MN065719	MN148156	MN166266	Jian et al. (2020a)
<i>C. velutinus</i>	CORT 014618 <sup>d</sup>	Dominican Republic 2015	MN784991	–	MN893321	MN893331	Baroni et al. (2020)
<i>C. venososulcatus</i>	8111 TJB <sup>d</sup>	Louisiana, USA 1996	–	–	KC816930	–	Kluting et al. (2014)
<i>C. yunnanensis</i>	KUN-HKAS 59712 <sup>a</sup>	Yunnan, China 2009	MN061307	–	MN148135	–	Jian et al. (2020a)
<i>C. yunnanensis</i>	KUN-HKAS 82076 <sup>a</sup>	Yunnan, China 2012	MN061306	MN065697	MN148134	MN166246	Jian et al. (2020a)
<i>C. yunnanensis</i>	KUN-HKAS 104518 <sup>a</sup>	Yunnan, China 2018	MN061308	MN065698	MN148136	MN166247	Jian et al. (2020a)
<i>C. yunnanensis</i>	HMJAU 24677 <sup>s</sup>	Sichuan, China 2013	MN061309	MN065699	MN148116	MN166248	Jian et al. (2020a)
<i>“Clitopilus sp.”</i>	7130 TJB <sup>d</sup>	New York, USA 1993	–	–	KC816929	–	Kluting et al. (2014)
<i>Clitopilus</i> sp.	TB8067 <sup>d</sup>	Florida, USA 1996	–	GU384612	GU384649	–	Baroni et al. (2011)
<i>Clitopilus</i> sp.	KUN-HKAS 104508 <sup>a</sup>	Yunnan, China 2017	MN061311	MN065701	MN148138	MN166250	Jian et al. (2020a)
<i>Clitopilus</i> sp.	KUN-HKAS 104512 <sup>a</sup>	Yunnan, China 2018	MN061330	MN065721	MN148158	MN166269	Jian et al. (2020a)
<i>R. alutacea</i>	5726 TJB <sup>d</sup>	North Carolina, USA 1987	–	–	KC816931	KC816842	Kluting et al. (2014)
<i>R. asanii</i>	KATO 3659 <sup>u</sup>	Turkey 2015	KX834263	KX834264	–	–	Sesli and Vizzini (2017)
<i>R. asanii</i>	KATO 3657 <sup>u</sup>	Turkey 2015	KX834265	–	–	–	Sesli and Vizzini (2017)
<i>R. asanii</i>	NA13102020	East Sussex, UK 2020	MW375030	–	–	–	Aplin et al. (2022)
<i>R. asyae</i>	KATO 3640 <sup>u</sup>	Trabzon, Turkey 2015	KX834266	KX834267	–	–	Sesli and Vizzini (2017)
<i>R. asyae</i>	KATO 3653 <sup>u</sup>	Trabzon, Turkey 2015	KX834268	–	–	–	Sesli and Vizzini (2017)
<i>R. asyae</i>	NA131019 <sup>v</sup>	East Sussex, UK 2019	MN840644	–	–	–	Aplin et al. (2022)
<i>R. aureicystidiata</i>	PBM 1902 <sup>w</sup>	Washington, USA –	–	AY380407	AY337412	–	Matheny (2005)
<i>R. brunneoaurantiaca</i>	CAL 1825 <sup>c</sup>	West Bengal, India 2019	MW031906	MW031916	–	–	Dutta et al. (2021)
<i>R. brunneoaurantiaca</i>	CUH AM720 <sup>a</sup>	West Bengal, India 2019	MW023201	MW023223	–	–	Dutta et al. (2021)
<i>R. brunnescens</i>	TENN 056140 <sup>v</sup>	Tennessee, USA 1985	NR_119914	NG_058820	–	–	Baroni et al. (2011)
<i>R. brunnescens</i>	TENN 056140-2 <sup>v</sup>	Tennessee, USA 1987	HQ222033	JF706313	–	–	Baroni et al. (2011)
<i>R. byssisedoides</i>	AG 2004-04-27	Jena, Germany 2004	–	GQ289212	GQ289279	–	Co-David et al. (2009)
<i>R. caelata</i>	511	Germany 2005	–	GQ289208	–	–	Co-David et al. (2009)
<i>“R. caelata”</i>	6919 TJB <sup>d</sup>	North Carolina, USA 1992	–	–	KC816933	KC816843	Kluting et al. (2014)
<i>R. caelata</i>	J. Parkin <sup>d</sup>	Ontario, Canada 1988	–	–	KC816934	–	Kluting et al. (2014)
<i>R. caelata</i>	REH3569 <sup>d</sup>	Jurmala, Latvia 1982	–	–	KC816932	–	Kluting et al. (2014)
<i>R. caelata</i>	TB5890 <sup>d</sup>	–	–	AF261282	–	–	Moncalvo et al. (2002)
<i>“R. caelata”</i>	TB6995 <sup>d</sup>	–	–	GU384625	GU384652	–	Baroni et al. (2011)
<i>R. cistetorum</i>	KATO 4260 <sup>u</sup>	Trabzon, Turkey 2019	NR_176724	MT252601	–	–	Sesli (2021)
<i>R. collybioides</i>	10417 TJB <sup>d</sup>	Jujuy, Argentina 2011	–	–	KC816935	KC816844	Kluting et al. (2014)
<i>R. dominicana</i>	ANGE 464	Dominican Republic 2014	–	–	MN893322	MN893332	Baroni et al. (2020)
<i>R. dominicana</i>	ANGE 473	Dominican Republic 2014	–	–	MN893323	MN893333	Baroni et al. (2020)
<i>R. formosa</i>	1061015-6 <sup>d</sup>	Catalonia, Spain 2006	KU862856	–	KC816939	KC816849	Kluting et al. (2014)
<i>R. formosa</i>	12/198	Latium, Italy 2012	KU862857	–	–	–	Vizzini et al. (2016)
<i>R. formosa</i>	12/208	Latium, Italy 2012	KU862858	–	–	–	Vizzini et al. (2016)
<i>R. formosa</i>	1071101-4 <sup>d</sup>	Catalonia, Spain 2007	KU862860	–	KC816947	KC816857	Kluting et al. (2014)
<i>R. formosa</i>	K(M): 158060 <sup>f</sup>	England, UK 2006	MZ159381	–	KC816978	KC816885	Direct submission
<i>R. fuliginea</i>	E537 <sup>d</sup>	Tasmania, Australia 1999	–	–	KC816940	KC816850	Kluting et al. (2014)
<i>R. fumanellii</i>	HFRG_PC200928_1	Buckinghamshire, UK 2020	MW401761	–	–	–	Aplin et al. (2022)
<i>R. fumanellii</i>	BOLGH_22122001	Tuscany, Italy 2022	OR831361	–	–	–	Direct submission
<i>R. fumanellii</i>	MCVE 29550 <sup>c</sup>	Veneto, Italy 2017	MH399225	MH399226	–	–	Vizzini et al. (2018)
<i>R. fusipes</i>	DLK 587 <sup>aa</sup>	Amazonas, Brazil 2012	MN306209	–	–	–	Silva-Filho et al. (2020)
<i>R. fusipes</i>	DLK 298 <sup>aa</sup>	Amazonas, Brazil 2012	MN306210	–	–	–	Silva-Filho et al. (2020)
<i>R. gemina</i>	GZ 2003-09-14	Belgium 2003	–	–	GQ289277	–	Co-David et al. (2009)
<i>“R. gemina”</i>	MEN 2001119	– 2001	–	HM164411	–	–	Morgado et al. (2016)
<i>R. gemina</i>	CBS 604.76 <sup>c</sup>	–	–	AF223168	–	–	Vu et al. (2019)
<i>R. gemina</i>	KATO 2658 <sup>u</sup>	Turkey 2009	–	KX834269	–	–	Sesli and Vizzini (2017)
<i>R. gemina</i>	CBS 482.50 <sup>c</sup>	–	EF421110	AF223167	EF421019	KP255478	Baroni et al. (2011)
<i>R. griseoaurantia</i>	CAL 1324 <sup>c</sup>	Kerala, India 2011	NR_154435	KX083574	KX083568	–	Hyde et al. (2016)
<i>R. griseonigrella</i>	1081204 <sup>ab</sup>	Barcelona, Spain 2008	KU862859	–	–	–	Vizzini et al. (2016)
<i>R. hondensis</i>	6103 TJB <sup>d</sup>	California, US 1988	–	–	KC816941	KC816851	Kluting et al. (2014)
<i>R. incarnata</i>	REH5369	Venezuela 1987	MT254071	–	–	–	Silva-Filho et al. (2020)



Species	Collection or collector no.	Location and year	GenBank accession numbers				References
			ITS	LSU	RPB2	TEF1	
<i>R. indica</i>	CAL 1323 <sup>c</sup>	Kerala, India 2013	KX083569	NG_060166	KX083566	–	Hyde et al. (2016)
<i>R. lateritia</i>	Co-David 418	–	–	HM164410	–	–	Morgado et al. (2016)
<i>R. lateritia</i>	E1589 <sup>d</sup>	Tasmania, Australia 2002	–	–	KC816942	KC816852	Kluting et al. (2014)
<i>R. luteobrunnea</i>	CAL 1322 <sup>c</sup>	Kerala, India 2010	NR_154434	NG_060167	KX083567	–	Hyde et al. (2016)
<i>R. luteocinnamomea</i>	GUA241 <sup>d</sup>	Guana Island, UK 1999	–	–	KC816943	KC816853	Kluting et al. (2014)
<i>R. luteocinnamomea</i> var. <i>fulva</i>	ANGE 169	Dominican Republic 2013	–	–	MN893324	MN893334	Baroni et al. (2020)
<i>R. matesina</i>	MCVE 29262 <sup>z</sup>	Campania, Italy 2012	KY629961	KY629963	–	–	Crous et al. (2017)
<i>R. matesina</i>	MCVE 29261 <sup>z</sup>	Campania, Italy 2016	KY629962	KY629964	–	–	Crous et al. (2017)
<i>R. matesina</i>	F3-2	Fnaydek, Lebanon 2018	MZ088085	–	–	–	Sleiman et al. (2021)
<i>“R. mellea”</i>	ANGE 893	Dominican Republic 2016	MN784993	–	MN893326	–	Baroni et al. (2020)
<i>“R. mellea”</i>	TJB 9823 <sup>d</sup>	Belize 2004	MN784994	–	–	–	Baroni et al. (2020)
<i>R. mellea</i>	NYBG815044	Costa Rica 1986	MN784995	–	–	–	Baroni et al. (2020)
<i>“R. mellea”</i>	6883 TJB <sup>d</sup>	Florida, USA 1992	–	MG702608	KC816944	KC816854	Kluting et al. (2014)
<i>“R. mellea”</i>	TJB 9805 <sup>d</sup>	Dominican Republic 2003	MN784992	–	MN893325	–	Baroni et al. (2020)
<i>R. mellea</i> var. <i>depressa</i>	FW 08/2019	Brazil 2019	MT408926	OL687341	–	–	Xavier et al. (2022)
<i>R. nuciolens</i>	WTU-F-074620	Washington, USA 2017	OP828513	–	–	–	Direct submission
<i>R. nuciolens</i>	TENN:076696 <sup>y</sup>	Washington, USA 2021	ON478246	–	–	–	Direct submission
<i>R. nuciolens</i>	iN147673878	California, USA 2023	OR162504	–	–	–	Direct submission
<i>R. nuciolens</i>	iN147466901	California, USA 2023	OR168848	–	–	–	Direct submission
<i>R. pakistanica</i>	LAH37947 <sup>i</sup>	Punjab, Pakistan 2022	OR606543	OR606541	–	–	Khan and Khalid (2024)
<i>R. pakistanica</i>	LAH37948 <sup>i</sup>	Punjab, Pakistan 2022	OR606544	OR606542	–	–	Khan and Khalid (2024)
<i>R. pallidogrisea</i>	CORT 013944 <sup>d</sup>	Australia –	NR_154437	–	–	–	Direct submission
<i>R. pallidogrisea</i>	118	Tasmania, Australia 2004	–	GQ289216	GQ289283	–	Co-David et al. (2009)
<i>R. pallidogrisea</i>	E652 <sup>d</sup>	Tasmania, Australia 1999	–	–	KC816968	KC816875	Kluting et al. (2014)
<i>R. paurii</i>	JM99/233	Uttaranchal, India 1999	–	AY286004	–	–	Moncalvo et al. (2004)
<i>R. paurii</i>	JM99/233-2	Uttaranchal, India 1999	–	–	KC816969	KC816876	Kluting et al. (2014)
<i>R. praesidentialis</i>	MCVE 21991 <sup>z</sup>	Italy –	EF679793	–	–	–	Consiglio et al. (2007)
<i>R. pruinosostipitata</i>	MCA1492	Guyana –	–	GU384627	GU384653	–	Baroni et al. (2011)
<i>R. pseudoalutacea</i>	TJB 9466 <sup>d</sup>	Dominican Republic 2003	–	–	MN893327	MN893335	Baroni et al. (2020)
<i>R. pseudoalutacea</i>	TJB 9507 <sup>d</sup>	Dominican Republic 2003	–	–	MN893328	MN893336	Baroni et al. (2020)
<i>R. pseudopiperita</i>	E1159 <sup>d</sup>	Tasmania, Australia 2001	–	–	KC816979	KC816886	Kluting et al. (2014)
<i>R. pseudopiperita</i>	162	Tasmania, Australia 2004	–	GQ289217	GQ289284	–	Co-David et al. (2009)
<i>R. reticulata</i>	E2183 <sup>d</sup>	Tasmania, Australia 2005	–	–	KC816980	KC816887	Kluting et al. (2014)
<i>R. rhizogena</i>	5551 TJB <sup>d</sup>	North Carolina, USA 1987	–	–	KC816981	KC816888	Kluting et al. (2014)
<i>R. roseiavellanea</i>	8130 TJB <sup>d</sup>	Louisiana, USA 1996	–	KR869930	KC816982	KC816889	Kluting et al. (2014)
<i>R. roseiavellanea</i>	PBM4056	Tennessee, USA –	MF686525	–	–	–	Direct submission
<i>R. roseiavellanea</i>	ANGE 947	Dominican Republic 2017	–	–	MN893329	MN893337	Baroni et al. (2020)
<i>R. rubrobrunnea</i>	CAL 1387 <sup>c</sup>	Kerala, India 2014	KX951452	–	–	–	Crous et al. (2016)
<i>Rhodocybe</i> sp.	DLL9851	New South Wales, Australia 2010	–	–	KC816986	KC816893	Kluting et al. (2014)
<i>Rhodocybe</i> sp.	DLL9846	New South Wales, Australia 2010	–	–	KC816985	KC816892	Kluting et al. (2014)
<i>Rhodocybe</i> sp.	DLL9860	New South Wales, Australia 2010	–	–	KC816987	KC816894	Kluting et al. (2014)
<i>Rhodocybe</i> sp.	DLL9952	New South Wales, Australia 2010	–	–	KC816988	KC816895	Kluting et al. (2014)
<i>Rhodocybe</i> sp.	DLL9957	New South Wales, Australia 2010	–	–	KC816989	KC816896	Kluting et al. (2014)
<i>Rhodocybe</i> sp.	DLL10218	New South Wales, Australia 2011	–	–	KC816990	KC816897	Kluting et al. (2014)
<i>Rhodocybe</i> sp.	DLL10032	Queensland, Australia 2011	–	–	KC816991	KC816898	Kluting et al. (2014)
<i>Rhodocybe</i> sp.	KUN-HKAS 89081 <sup>a</sup>	Yunnan, China 2023	MZ675559	MZ675570	MZ681892	MZ681870	He and Yang (2022)
<i>Rhodocybe</i> sp.	MEL:2382939	Palmerston, Australia 2014	KP012803	–	–	–	Direct submission
<i>Rhodocybe</i> sp.	MEL:2382705	Australia 2014	KP012885	–	–	–	Direct submission
<i>Rhodocybe</i> sp.	KS-RE53	New Zealand –	–	MK277733	–	–	Varga et al. (2019)
<i>Rhodocybe</i> sp.	Buyck 99.152	Madagascar –	–	MK278564	–	–	Varga et al. (2019)

Species	Collection or collector no.	Location and year	GenBank accession numbers				References
			ITS	LSU	RPB2	TEF1	
<i>Rhodocybe</i> sp.	Sulzbacher 340	Brazil –	LT594979	–	–	–	Sulzbacher et al. (2017)
<i>Rhodocybe</i> sp.	Sulzbacher 413	Brazil –	LT594984	–	–	–	Sulzbacher et al. (2017)
<i>Rhodocybe</i> sp.	HFRG_EJ171117_1	Hampshire, UK 2017	MW397197	MW397521	–	–	Aplin et al. (2022)
<i>Rhodocybe</i> sp.	iN130319090	Indiana, USA 2022	OP749482	–	–	–	Direct submission
<i>Rhodocybe</i> sp.	iN129753148	Indiana, USA 2022	OP749140	–	–	–	Direct submission
<i>Rhodocybe</i> sp.	iN130020200	Indiana, USA 2022	OP643320	–	–	–	Direct submission
<i>Rhodocybe</i> sp.	AD5 (TENN) <sup>†</sup>	Tennessee, USA 2011	MF773647	–	–	–	Direct submission
<i>R. stipitata</i>	5523 TJB <sup>d</sup>	Tennessee, USA 1987	–	–	KC816993	–	Kluting et al. (2014)
<i>R. spongiosa</i>	MCA2129		–	GU384628	GU384657	–	Baroni et al. (2011)
<i>R. subasyae</i>	HMJAU56921-1 <sup>s</sup>	Jilin, China 2020	MW298803	–	–	–	Sun and Bau (2023)
<i>R. subasyae</i>	HMJAU56921-2 <sup>s</sup>	Jilin, China 2020	MW298804	–	–	–	Sun and Bau (2023)
<i>R. subasyae</i>	HMJAU56921-3 <sup>s</sup>	Jilin, China 2020	MW298805	–	–	–	Sun and Bau (2023)
<i>R. tugrulii</i>	KATO 3340 <sup>u</sup>	Trabzon, Turkey 2014	KX271751	KX271754	–	–	Vizzini et al. (2016)
<i>R. tugrulii</i>	MSNG3938	Italy –	KY945354	–	–	–	Direct submission
<i>R. tugrulii</i>	CORT:14755 <sup>d</sup>	New York, USA 2018	MZ322093	–	–	–	Direct submission
<i>R. tugrulii</i>	IMG-7316 <sup>d</sup>	New York, USA 2017	MG050105	MG050111	–	–	Direct submission
<i>R. tugrulii</i>	WU-MYC 0010084 <sup>b</sup>	Burgenland, Austria 1991	OP363995	–	–	–	Vizzini et al. (2023)
<i>R. tugrulii</i>	WU-MYC 0022202 <sup>b</sup>	Niederösterreich, Austria 2002	OP363994	OP363999	OP381082	OP381084	Vizzini et al. (2023)
<i>R. tugrulii</i>	WU-MYC 0006178 <sup>b</sup>	Niederösterreich, Austria 1987	–	OP364000	–	–	Vizzini et al. (2023)
<i>R. tugrulii</i>	WU-MYC 0006320 <sup>b</sup>	Niederösterreich, Austria 1987	OP363992	OP363997	OP381080	OP381083	Vizzini et al. (2023)
<i>R. tugrulii</i>	WU-MYC 0004222 <sup>b</sup>	Niederösterreich, Austria 1984	OP363991	–	–	–	Vizzini et al. (2023)
<i>R. tugrulii</i>	WU-MYC 0003753 <sup>b</sup>	Niederösterreich, Austria 1984	OP363993	OP363998	OP381081	–	Vizzini et al. (2023)
<i>R. tugrulii</i>	GB-013 1395	Skaane, Sweden 1983	OP363996	OP364001	–	–	Vizzini et al. (2023)
<b><i>R. zjinshanensis</i> (H)</b>	<b>KUN-HKAS 145338<sup>a</sup></b>	<b>Jiangsu, China 2024</b>	<b>PQ793171</b>	<b>PQ781615</b>	<b>PQ788400</b>	<b>PQ788406</b>	<b>This study</b>
<b><i>R. zjinshanensis</i></b>	<b>KUN-HKAS 145339<sup>a</sup></b>	<b>Jiangsu, China 2024</b>	<b>PQ793172</b>	<b>PQ781616</b>	<b>PQ788401</b>	<b>PQ788407</b>	<b>This study</b>
<i>Lulesia umbrinomarginata</i>	MHHNU 20023-2	Guangdong, China 2023	PP060632	PP059607	PP158704	PP158696	Xiao et al. (2024)
<i>Lulesia orientalis</i>	KUN-HKAS 75548 <sup>a</sup>	Hubei, China 2012	MN061333	MN065727	MN148164	MN166275	Jian et al. (2020a)
<i>Clitopilopsis albida</i>	KUN-HKAS 104520 <sup>a</sup>	Yunnan, China 2018	MN061336	MN065731	MN148168	MN166279	Jian et al. (2020a)
<i>Clitopilopsis himaeola</i>	MEN 199956	Italy –	KC710132	GQ289211	GQ289278	–	Co-David et al. (2009)

<sup>a</sup> The Cryptogamic Herbarium of Kunming Institute of Botany, the Chinese Academy of Sciences, Kunming, China (KUN-HKAS)

<sup>b</sup> Herbarium, Institute of Botany, University of Vienna, Austria (WU)

<sup>c</sup> Central National Herbarium, Kolkata, India (CAL)

<sup>d</sup> State University of New York College at Cortland Herbarium, Cortland, New York, USA (CORT)

<sup>e</sup> The Leiden Herbarium of Naturalis Biodiversity Center, Leiden, Netherland (L)

<sup>f</sup> The Royal Herbarium, Royal Botanic Garden, Kew, Richmond, Surrey, England, UK (KEW)

<sup>g</sup> Associazione Micologica Bresadola, Trento, Italy (AMB)

<sup>h</sup> The Herbarium of Mycology, Jilin Agricultural University, Changchun, Jilin, China (HMJAU)

<sup>i</sup> The Lahore, Institute of Botany, University of the Punjab, Pakistan (LAH)

<sup>j</sup> Herbarium generale del Dipartimento di Biologia Vegetale, Università degli Studi di Torino, Italy (TO)

<sup>k</sup> The Herbarium of Soil and Fertilizer Institute, Sichuan Academy of Agricultural Sciences, Sichuan, China (SAAS)

<sup>l</sup> The Swedish Museum of Natural History, Stockholm, Sweden (S)

<sup>m</sup> The Herbarium of the University of Alcalá, Madrid, Spain (AH)

<sup>n</sup> Jepson Herbarium, University of California, Berkeley, California, USA (JEPS)

<sup>o</sup> The Herbarium of Korea National Arboretum, Gyeonggi-do, Republic of Korea (KH)

<sup>p</sup> New Zealand Fungal Herbarium, Auckland, New Zealand (PDD)

<sup>q</sup> The Herbarium of the Sustainable Development of Biological Resources Laboratory, Chiang Mai University, Thailand (SDBR-CMU)

<sup>r</sup> Centraalbureau voor Schimmelcultures, Utrecht, Netherland (CBS)

<sup>s</sup> The Herbarium of Mycology, Jilin Agricultural University, Changchun, Jilin, China (HMJAU)

<sup>t</sup> The Mycological Herbarium of the Guangdong Institute of Microbiology, Guangdong Academy of Sciences, Guangzhou, China (GDGM)

<sup>u</sup> Karadeniz Technical University Faculty of Forestry Herbarium, Trabzon, Turkey (KATO)

<sup>v</sup> United States National Arboretum, USDA-ARS, Washington, USA (NA)

<sup>w</sup> The Herbarium of Mahidol University, Nakhon Pathom, Thailand (PBM)

<sup>x</sup> The Calcutta University Herbarium, Kolkata, West Bengal, India (CUH)

<sup>y</sup> The Herbarium of University of Tennessee – Knoxville, Tennessee, USA (TENN)

<sup>z</sup> New Herbarium of Museo di Storia Naturale di Venezia, Venezia, Italy (MCVE)

<sup>aa</sup> Herbário of Instituto Nacional de Pesquisas da Amazônia, Amazonas, Brazil (INPA)

<sup>ab</sup> Herbar of Université de Lille, Lille, France (LIP)

(Newly-generated information of specimens and sequences are in bold).

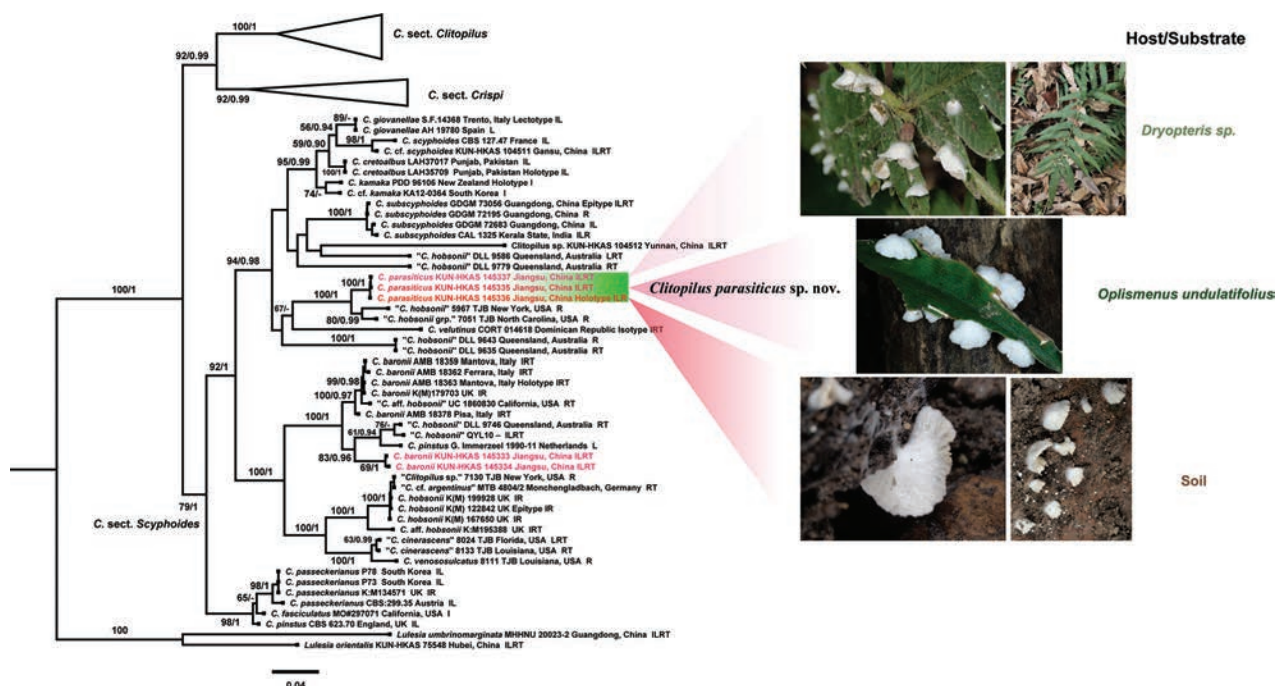


**Figure 1.** Phylogenetic relationships amongst representative species of *Clitopilus* were inferred from a multigene dataset (ITS-LSU-RPB2-TEF1) using both ML and BI methods (only shown the ML tree). Supported branches indicate bootstrap supports (BS > 50%) and posterior probabilities (PP > 0.90). Sequences from type specimens (holotype, epitype or isotype) are marked with an asterisk, while new and new record taxa are highlighted in red. The abbreviations ILRT stand for: I = ITS, L = LSU, R = RPB2 and T = TEF1.

## Morphological observations and SEM

The images of fresh basidiomata, substrate and habitats of the collected specimens are shown in Fig. 3. Scanning Electron Microscopy revealed that the ornamentation of basidiospores provides some extra valuable information (Fig. 4). The basidiospores of *Clitopilus* exhibit several classical longitudinal ridges (Fig. 4a–f), while those of *Rhodocybe* are characterised by undulate-pustulate walls (Fig. 4g–h). In addition, crystals on the pileus hyphae of the new species in *Clitopilus* was also identified (Fig. 4i).

## Taxonomy

### *Clitopilus parasiticus* S.P. Jian, X. Chen & Z.H. Zhang, sp. nov.

Mycobank No: 857348

Figs 1, 3e–h, 4d–f, 5a–c

**Holotype.** CHINA • Jiangsu Province, Nanjing City, Zijinshan, E 118.83, N 32.08, alt. 32 m, scattered on soil, in the mixed broadleaf (i.e. *Quercus variabilis*, *Robinia pseudoacacia*, *Osmanthus fragrans*, *Broussonetia papyrifera*, *Ilex latifolia* and *Yulania* sp.) forest, 15 August 2024, collected by X. Chen and Z.H. Zhang, CX 966 (KUN-HKAS 145336). GenBank: ITS = PQ793169; LSU = PQ781613; RPB2 = PQ788398.

**Etymology.** “*parasiticus*” is proposed by its biotrophic behaviour.

**Diagnosis.** *Clitopilus parasiticus* is similar to *C. hobsonii*, but differs by the tomentose pileus, explanate margin and smaller basidiospores.



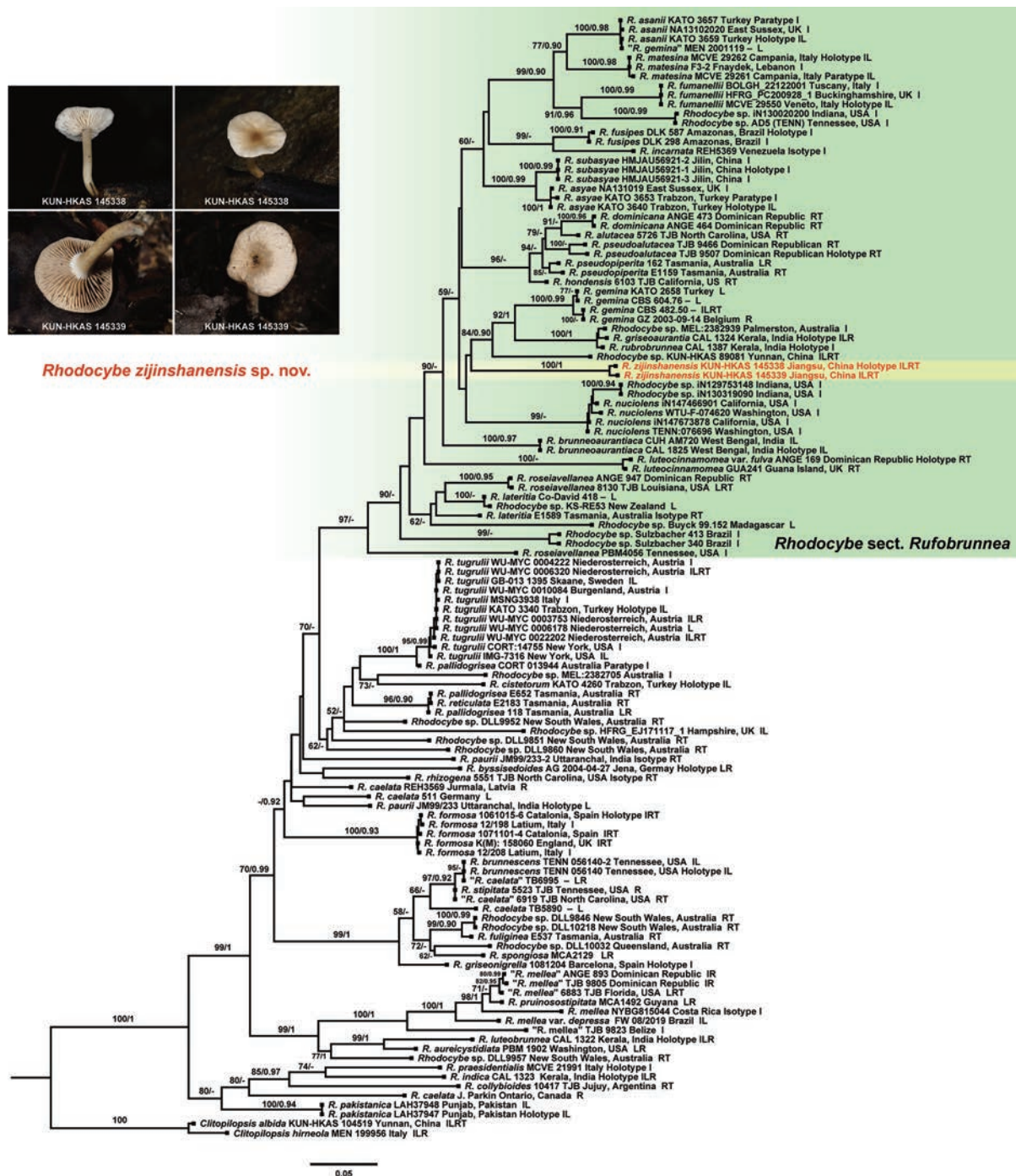


**Figure 2.** Phylogenetic relationships amongst representative species of *Rhodocybe* were inferred from a multigenic dataset (ITS-LSU-RPB2-TEF1) using both ML and BI methods (only shown the ML tree). Supported branches indicate bootstrap supports (BS > 50%) and posterior probabilities (PP > 0.90). Sequences from type specimens (holotype, paratype or isotype) are marked, while new and new record taxa are highlighted in red. The abbreviations ILRT stand for: I = ITS, L = LSU, R = RPB2 and T = TEF1.

**Description.** Basidiomata pleurotoid to conchoid, small size. Pileus 2–8 mm, convex; surface whitish (#b4c4cb) to chalk white (#e3edf3), with fine tomentose texture usually extending beyond the margin and densely woolly-tomentose at the base; margin typically applanate; context less than 1 mm thick. Lamellae meeting at an excentric point, whitish (#c6d4d3) to yellowish-white (#d3dad4) to yellowish (#dac7ac), slightly dense or crowded, edges entire and



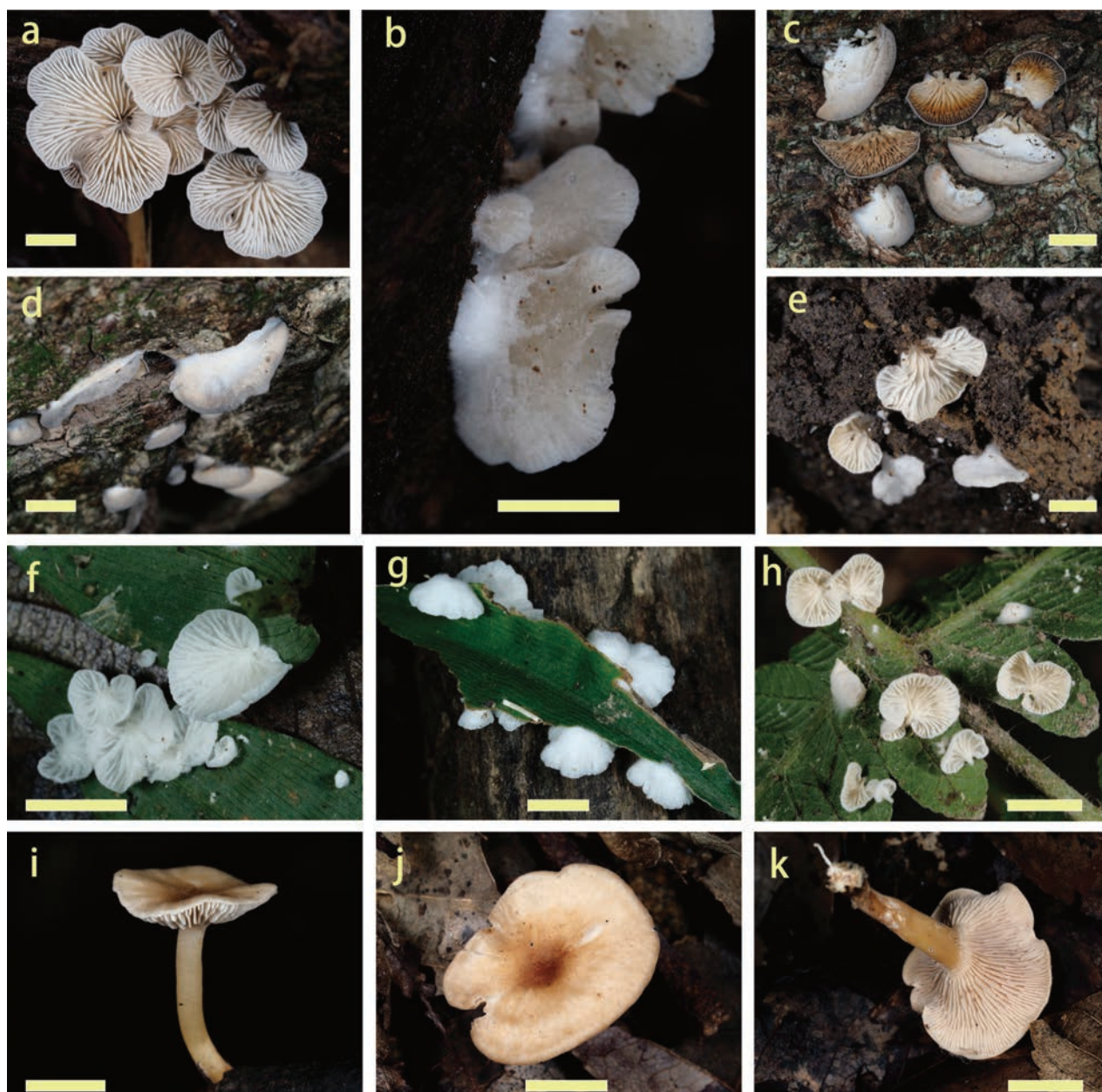


**Figure 3.** Basidiomata of *Clitopilus* and *Rhodocybe* **a–d** *Clitopilus baronii* (**a, b** KUN-HKAS 145333; **c, d** KUN-HKAS 145334) **e–h** *Clitopilus parasiticus* (**e** KUN-HKAS 145336, holotype; **f, g** KUN-HKAS 145335; **h** KUN-HKAS 145337) **i–k** *Rhodocybe zijinshanensis* (KUN-HKAS 145338, holotype). Scale bar: 5 mm.

concolorous, lamellulae numerous. Stipe absent or very short, eccentric to lateral, measuring  $1\text{--}2 \times 0.2\text{--}0.5$  mm, concolorous with lamellae. The base with white (#ddddd) mycelium. Odour none.

Basidiospores (5)  $5.5\text{--}8.5 \times 3.5\text{--}5.0$  ( $5.5$ )  $\mu\text{m}$ ,  $L_m \times W_m = 6.6 (\pm 0.63) \times 4.2 (\pm 0.34) \mu\text{m}$ ,  $Q = 1.20\text{--}1.90$  ( $Q_{\text{avg}} = 1.55 \pm 0.13$ ) [186/9/3], hyaline, ellipsoid to broadly fusiform, subovoid in profile and face view, slightly angled in polar view, with 7–9 inconspicuous or obscure longitudinal ridges in total. Basidia  $16\text{--}23 \times 6\text{--}9.5 \mu\text{m}$ , clavate, hyaline, 4-spored, rarely 2-spored; sterigmata  $2\text{--}3 \mu\text{m}$ . Lamellar trama subregular, composed of thin-walled, hyaline, cylindrical hyphae with a diameter of  $2.5\text{--}9 \mu\text{m}$ . Lamellae edges fertile. Pleurocystidia and cheilocystidia absent. Pileipellis a cutis composed of sparsely arranged, thin-walled,

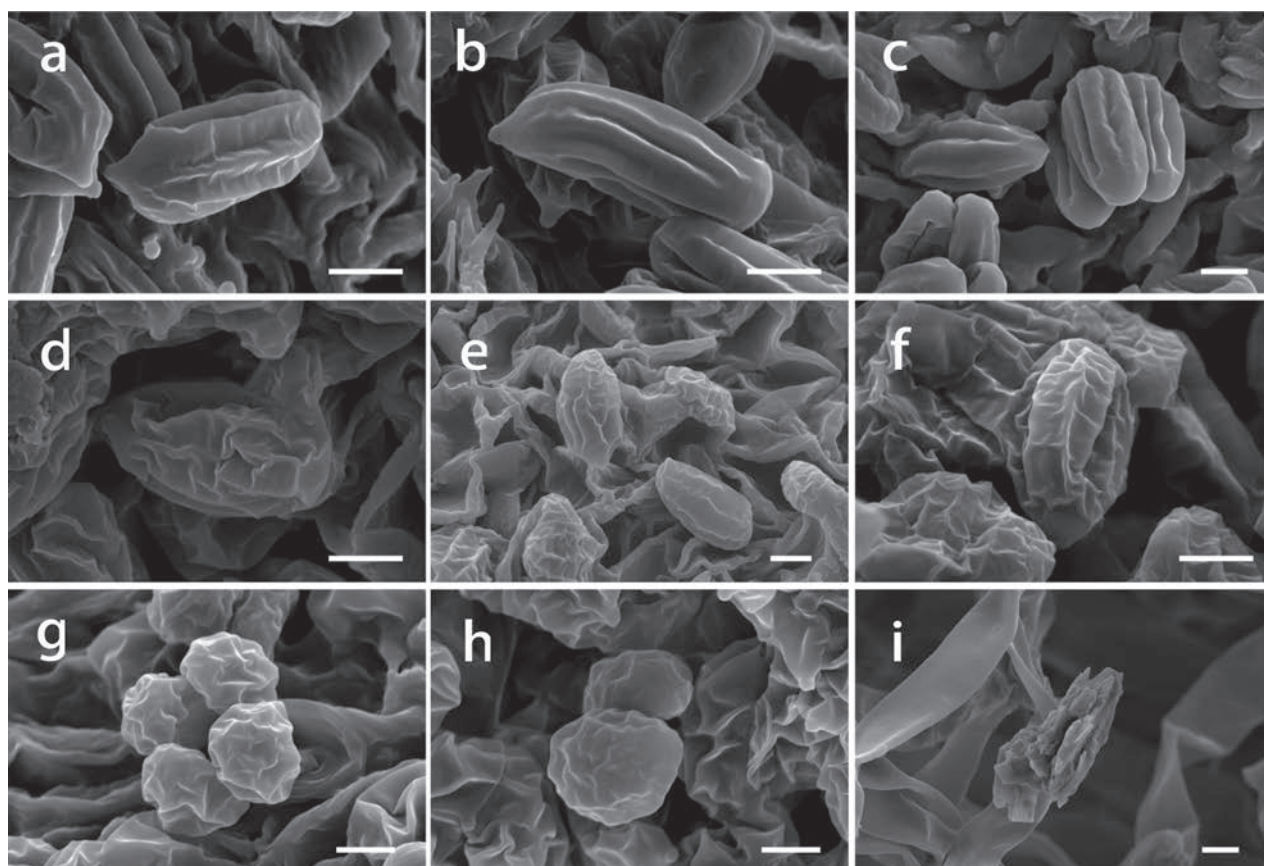


**Figure 4.** Basidiospores and crystals of *Clitopilus* and *Rhodocybe* reveal by SEM **a–c** *Clitopilus baronii* (KUN-HKAS 145334) **d–f** *Clitopilus parasiticus* (KUN-HKAS 145336, holotype) **g, h** *Rhodocybe zijinshanensis* (KUN-HKAS 145338, holotype) **i** the crystals around the hyphae in pileipellis of *Clitopilus parasiticus* (KUN-HKAS 145336, holotype). Scale bar: 2  $\mu\text{m}$ .

hyaline, smooth, interwoven, cylindrical hyphae with a diameter of 3–5  $\mu\text{m}$ , sometimes featuring erect hyphae; crystals present around the hyphae, square to subsquare, measuring 3  $\times$  3  $\mu\text{m}$  to 14  $\times$  15  $\mu\text{m}$  in area; pileal trama subregular, composed of hyaline, filamentous, thin-walled hyphae, with a diameter of 3–7.5  $\mu\text{m}$ . Clamp connections absent.

**Ecology and distribution.** Solitary, scattered on soil, lignicolous or gregariously living on leaves of plants (*Dryopteris* sp. and *Oplismenus undulatifolius*) in the mixed broadleaf forest, distributed in Jiangsu Province, China, in August.

**Additional specimens examined.** CHINA • Jiangsu Province, Nanjing City, Zijinshan, alt. 48 m, dispersedly or gregariously lignicolous or living on twigs or leaves of *Oplismenus undulatifolius*, in the mixed broadleaf (i.e. *Quercus variabilis*, *Quercus aliena*, *Cunninghamia lanceolata*, *Symplocos tanakana*, *Celtis sinensis* and *Ilex cornuta*) forest, 16 August 2023, collected by X. Chen and Z.H. Zhang, CX 628 (KUN-HKAS 145335); same places, alt. 48 m, dispersedly or gregariously living on leaves of *Dryopteris* sp., 16 August 2024, collected by X. Chen and Z.H. Zhang, CX 967 (KUN-HKAS 145337).

**Notes.** *Clitopilus parasiticus* belongs to *Clitopilus* sect. *Scyphoides* (Fig. 1). This new taxon is similar to *C. hobsonii*, *C. daamsii*, *C. passeckerianus*, *C. pinsitus* and *C. baronii*. *Clitopilus hobsonii* was originally described from Britain and exhibits both saprophytic and parasitic abilities. It resembles *C. parasiticus* in its living habits and the shape of its basidiomata, but differs from the latter by its involute or inflexed margins of the pileus and larger basidiospores ( $L_m \times W_m = 7.5 \times 5 \mu\text{m}$ )



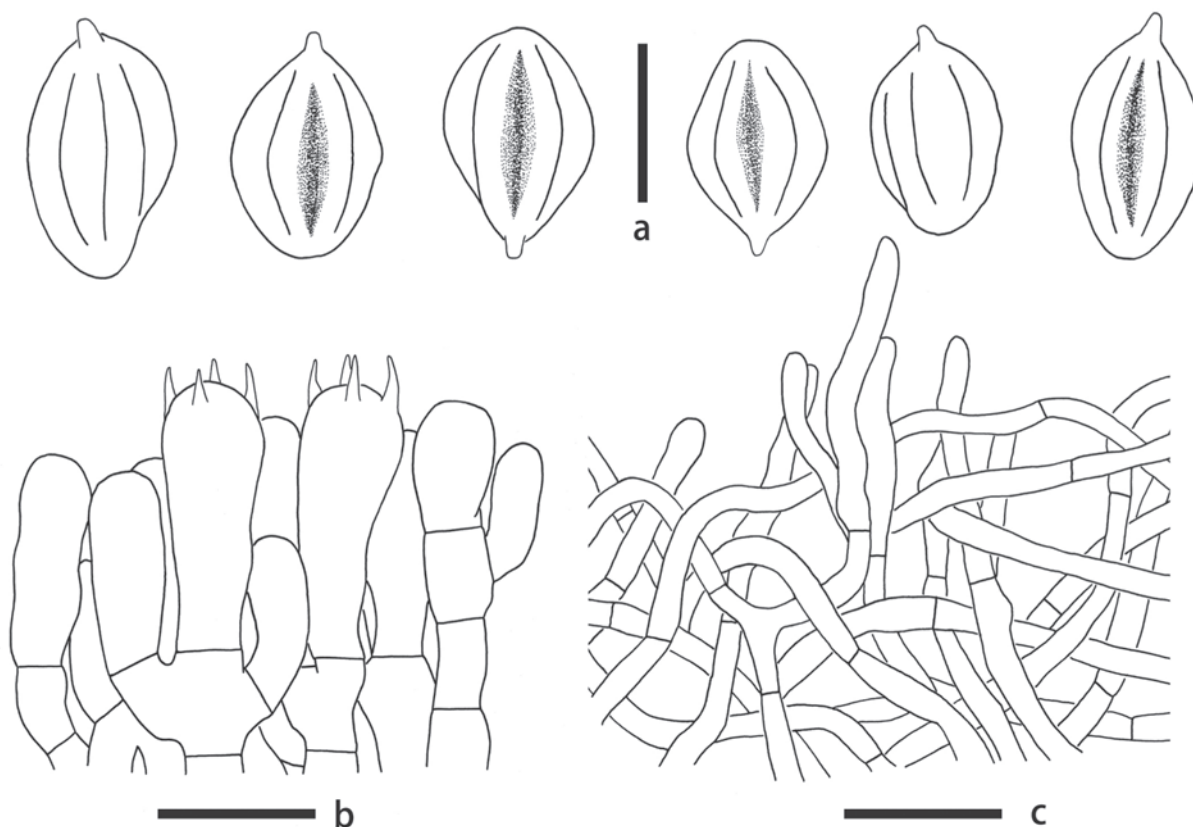


**Figure 5.** Microscopic features of *Clitopilus parasiticus* (KUN-HKAS 145336, holotype) **a** basidiospores **b** hymenium and subhymenium **c** pileipellis. Scale bars: 5 µm (**a**); 10 µm (**b**); 20 µm (**c**).

(Orton 1960; Noordeloos 1984; Noordeloos 1988). Meanwhile, *C. daamsii* was also similar to *C. parasiticus* in outline; however, it differs due to its xylogenous or mycoparasitic behaviour, involute margin of pileus and larger basidiospores ( $8\text{--}11.5 \times 4.8\text{--}6.6$  µm) (Noordeloos 1984). Another closely-related species is *C. passeckerianus*, which has sessile basidiomata and a white pileus. However, the habit of growing on mushroom-beds, basidiomata size (8–40 mm), the reniform to spatulate shape of the pileus and larger basidiospores ( $7\text{--}9 \times 4\text{--}5$  µm) of *C. passeckerianus* significantly differs from *C. parasiticus* (Pilát 1935; Noordeloos 1993). *Clitopilus pinsitus* was first collected from Sweden and was found growing on the trunk of *Quercus*. This species is characterised by its spatulate, white pileus (15–40 mm) and ellipsoidal to amygdaliform basidiospores ( $7.5\text{--}9 \times 4.6\text{--}5.3$  µm) with 7–8 obscure longitudinal ridges (Josserand 1937; Singer 1946a). Lastly, *C. baronii*, recently described by Consiglio and Setti (2019) in Marmirolo, Italy, resembles *C. parasiticus*, but can be differentiated by its larger pileus (5–40 mm) and basidiospores ( $L_m \times W_m = 7.6 \times 5.0$  µm), as well as its lageniform cheilocystidia.

***Clitopilus baronii* Consiglio & Setti, Index Fungorum 427: 1. 2019.**

Figs 3a–d, 4a–c, 6a–c

**Description.** Basidiomata pleurotoid to crepidotoid, small size. Pileus 3–15 mm wide, convex then expanded; surface yellowish-white (#9a8a7a), greyish (#a6a39f) to bluish-grey (#6a757b), usually subtly woolly-tomentose

at the base then reduced to border; margin slightly incurved, even, sometimes faintly striated; context less than 1 mm thick. Lamellae whitish (#a9a7a8) to yellowish (#9d896d), sometimes hygrophanous, slightly dense or crowded, edges entire and concolorous, lamellulae numerous. Stipe absent; the base with white (#e9ebed) mycelium. Odour none.

Basidiospores (6)  $6.5\text{--}9.5$  (11)  $\times$   $4\text{--}5$  (5.5)  $\mu\text{m}$ ,  $L_m \times W_m = 7.5 (\pm 1.01) \times 4.5 (\pm 0.35)$   $\mu\text{m}$ ,  $Q = 1.4\text{--}1.98$  ( $Q_{\text{avg}} = 1.66 \pm 0.14$ ) [43/2/2], hyaline, ellipsoid to fusiform, subovoid in profile and face view, slightly angled in polar view with 8–10 inconspicuous or obscure longitudinal ridges in total. Basidia  $17.5\text{--}24 \times 6.5\text{--}9$   $\mu\text{m}$ , clavate, hyaline, 2- or 4-spored; sterigmata 3–5.5  $\mu\text{m}$ . Lamellar trama subregular, composed of thin-walled, hyaline, cylindrical hyphae with a diameter of 2.5–9  $\mu\text{m}$ . Lamellae edges fertile. Pleurocystidia and cheilocystidia absent, but occasionally forming a few cylindrical tramal hyphae with a diameter of 2–3  $\mu\text{m}$  over the edge. Pileus context about 150–200  $\mu\text{m}$  thick. Pileipellis a cutis composed of compactly arranged, thin-walled, hyaline, smooth, cylindrical hyphae with a diameter of 3.5–9  $\mu\text{m}$ , featuring sparsely arranged and erect hyphae with a diameter of 2–3  $\mu\text{m}$ ; pileal trama subregular or irregular, composed of hyaline, filamentous, thin-walled hyphae, with a diameter of 2.5–8.5  $\mu\text{m}$ . Clamp connections absent.

**Ecology and distribution.** Lignicolous, scattered or gregarious on rotten wood in the mixed broadleaf forest, distributed in Jiangsu Province, China, in May.

**Additional specimens examined.** CHINA • Jiangsu Province, Nanjing City, Zijinshan, alt. 42 m, scattered or gregarious on rotten wood (*Quercus* sp.), in the mixed broadleaf (i.e. *Quercus acutissima*, *Quercus aliena*, *Celtis sinensis*, *Liquidambar formosana* and *Cunninghamia lanceolata*) forest, 7 May 2023, collected by X. Chen, CX 119 (KUN-HKAS 145333); same places, alt. 38 m, scattered on rotten wood (*Quercus* sp.), in the mixed broadleaf (*Quercus glauca*, *Pterocarya stenoptera*, *Ilex chinensis*, *Cunninghamia lanceolata*, *Ilex cornuta*, *Liquidambar formosana* and *Ligustrum lucidum*) forest, 9 May 2023, collected by X. Chen, CX 134 (KUN-HKAS 145334).

**Notes.** *Clitopilus baronii* belongs to *C.* sect. *Scyphoides* (Fig. 1). In the original description, this species was found growing on a decaying trunk of *Quercus* sp. It is characterised by its sessile basidiomata, orbicular to conchate white pileus, cream-rose lamellae, ellipsoidal to subamygdaliform basidiospores with 8–10 obscure longitudinal ridges and lageniform cheilocystidia. The macro- and microscopic features of our specimens (KUN-HKAS 145333 & 145334) closely match those described in the primary literature (Consiglio and Setti 2019). However, we did not observe any lageniform cheilocystidia in our specimens; we only identified a few thin cylindrical tramal hyphae over the edge. This observation aligns with findings by Noordeloos (1984) regarding *C. daamsii*, particularly in some older specimens. In our previous study, we also noted this phenomenon of thin cylindrical tramal hyphae at the edge in *C. crispus* Pat. However, this occurrence was generally casual and rare.

In the phylogenetic tree of *Clitopilus*, we could discover some unusual results regarding *C. baronii*. In the combined multigene analyses (ITS-LSU-RPB2-TEF1), our specimens were found to separate from the clades of *C. baronii* and grouped (BS/PP = 69/1) closer to *C. pinatus* (G. Immerzeel 1990-11). When we compared the different genes separately between our samples and holotype of *C. baronii* (AMB 18363), we found that our samples exhibited over 99% similarity in ITS region. However, the similarity was only about 90% for both RPB2



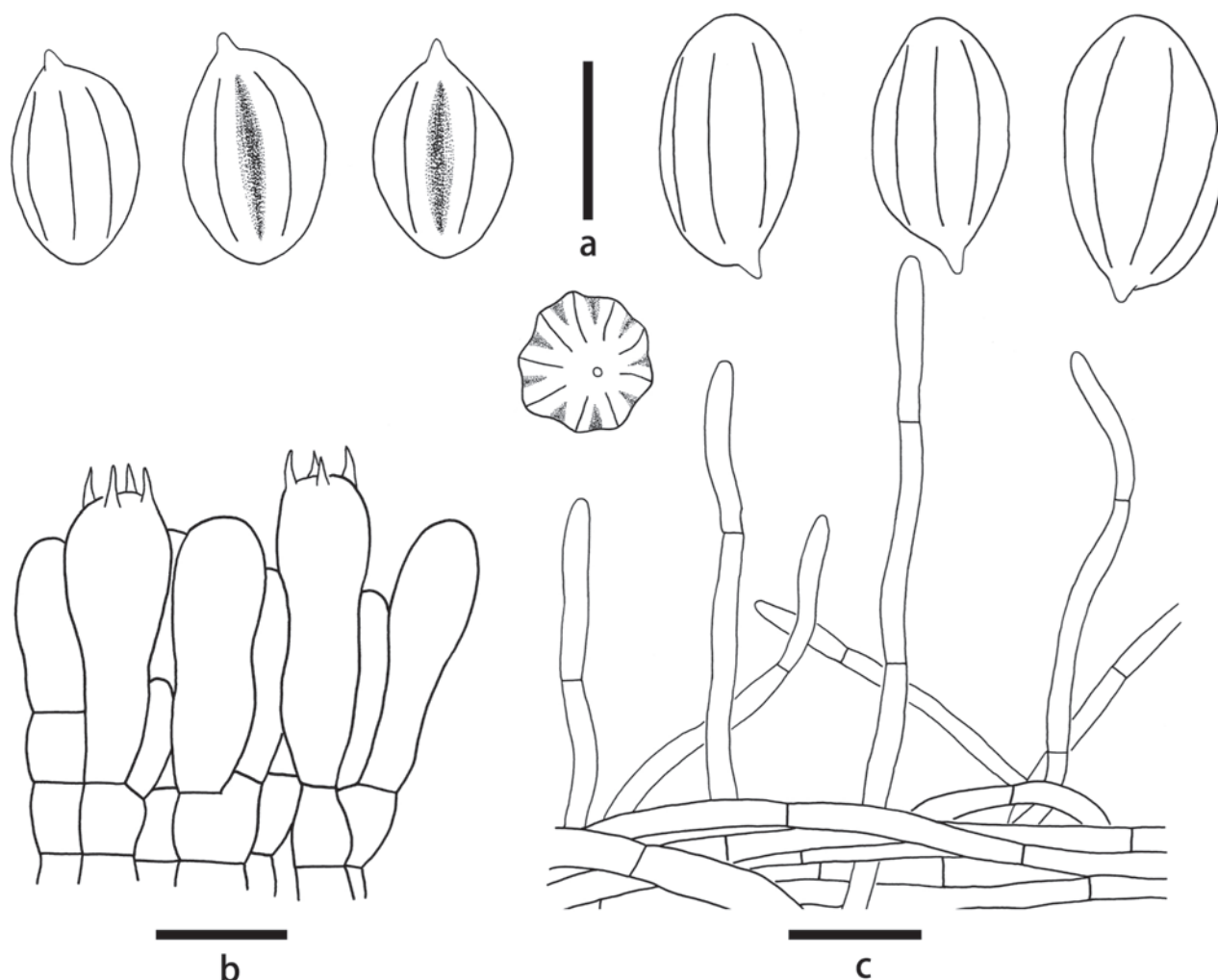


**Figure 6.** Microscopic features of *Clitopilus baronii* (KUN-HKAS 145334) **a** hymenium and subhymenium **b** basidiospores **c** pileipellis. Scale bars: 5 µm (**a**); 10 µm (**b**); 20 µm (**c**).

and *TEF1*. For ITS, we have tested them several times in different companies, but all yielded consistent results. Regarding *RPB2* and *TEF1*, we did not detect any issues with the original data; all sequences were bidirectionally sequenced to ensure unimodality and were matched by hand in software. Considering the macro- and microscopic features, we tentatively classified our specimens as *Clitopilus baronii*. More samples are needed to resolve our uncertainties regarding both the presence of cheilocystidia and the phylogenetic relationship.

***Rhodocybe zijingshanensis* S.P. Jian & X. Chen, sp. nov.**

MycoBank No: 857349

Figs 2, 3i–k, 4g–h, 7a–c

**Holotype.** CHINA • Jiangsu Province, Nanjing City, Zijingshan, E 118.87, N 32.06, alt. 99 m, solitary on rotten wood, in mixed broadleaf (i.e. *Quercus acutissima*, *Quercus aliena*, *Aphananthe aspera*, *Osmanthus fragrans*, *Liquidambar formosana*, *Photinia serratifolia* and *Ilex chinensis*) forest, 30 August 2024, collected by X. Chen, CX 664 (KUN-HKAS 145338). GenBank: ITS = PQ793171; LSU = PQ781615; *RPB2* = PQ788400; *TEF1* = PQ788406.

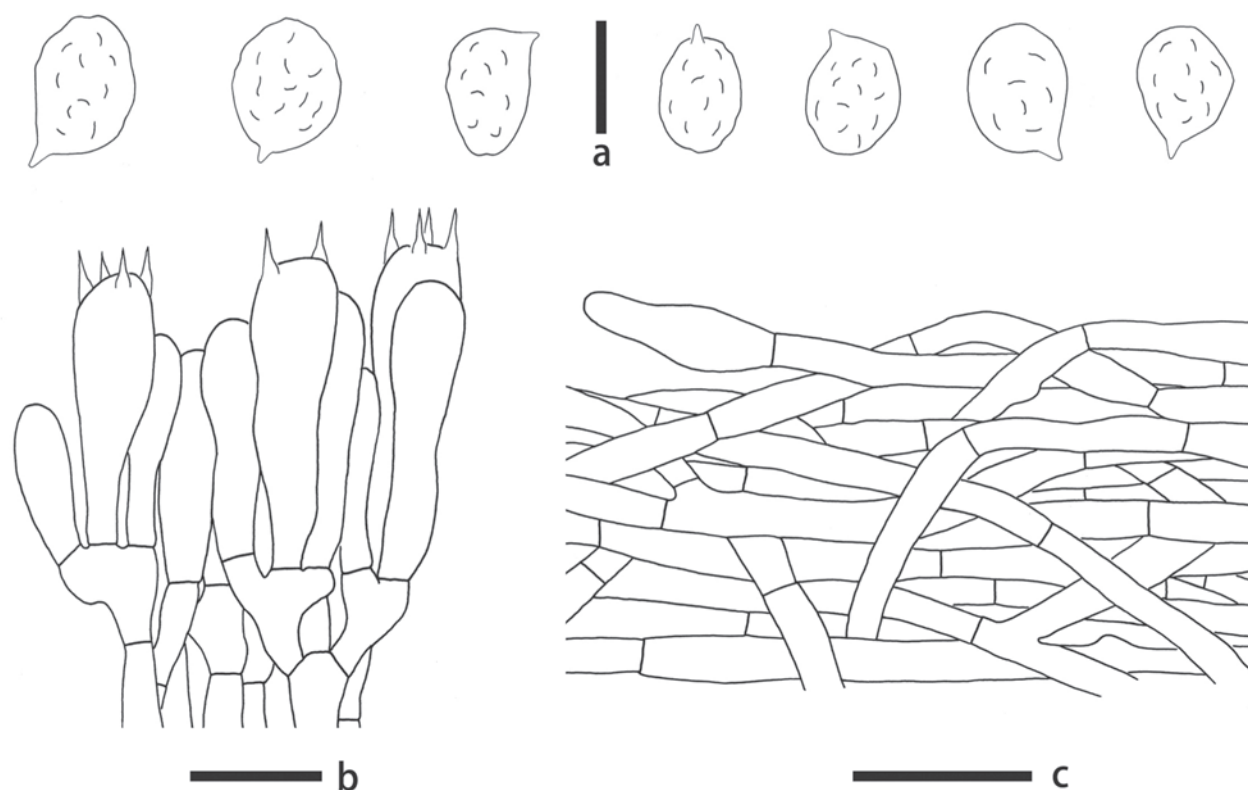


**Figure 7.** Microscopic features of *Rhodocybe zijinshanensis* (KUN-HKAS 145338, holotype) **a** hymenium and subhymenium **b** basidiospores. Scale bars: 5 µm (**a**); 10 µm (**b**); 20 µm (**c**).

**Etymology.** “*zijinshanensis*” indicates the source place, where it was located in Nanjing City, China.

**Diagnosis.** *Rhodocybe zijinshanensis* is similar to *R. subasyae*, but differs by its smaller yellow pileus, shorter and more slender stipes and the absence of cheilocystidia.

**Description.** Basidiomata omphalioid, small size. Pileus 10–15 mm wide, applanate to plano-concave; surface yellow (#eac7a2) over edge and brownish-yellow (#6c3620) over disc, distributing some radiate fibrillose, sometimes hygrophanous; margin slightly inflexed, even or undate; context about 1 mm thick. Lamellae adnate to subdecurrent, yellowish (#cdbead) to greyish-pink (#d1b4a2), dense or crowded, edges entire or undate, sometimes with transverse intervenose, concolorous with lamellae, lamellulae numerous. Stipe 7–19 × 1–2 mm, central to eccentric, cylindrical to tapering downwards, usually concolorous with pileus, densely fine scales dispersed around the top. Odour none.

Basidiospores (4.5) 5–6.5 × 3.5–5 µm,  $L_m \times W_m = 5.5 (\pm 0.54) \times 4.3 (\pm 0.31)$  µm,  $Q = 1.09–1.55$  ( $Q_{avg} = 1.28 \pm 0.11$ ) [41/2/2], hyaline, subglobose, subamygdaliform to broadly ellipsoid in profile view, ellipsoid in face view and minutely, but obviously angular in polar view (7–9 facets in total), undulate-pustulate in all views. Basidia 18.5–32 × 5.5–7.5 µm, clavate, hyaline, 2- or 4-spored; sterigmata up to 5 µm long. Lamellar trama regular, composed of 2.5–10.5 µm in diam., thin-walled, hyaline hyphae. Lamellae edges fertile. Pleurocystidia and cheilocystidia absent. Pileipellis a cutis composed of radially arranged, subregular hyphae, hyphae thin-walled, yellowish, smooth, cylindrical, 3.5–11.5 µm in diam., sometimes with oleiferous hyphae; pileal trama regular, composed of hyaline, thin-walled, cylindrical hyphae with a

diameter of 2–11 µm. Stipitipellis a cutis composed of compactly arranged, regular, thin-walled and hyaline hyphae with a diameter of 3.5–9.5 µm; Stipe trama regular, composed of thin-walled and hyaline hyphae with a diameter of 4–10.5 µm. Caulocystidia absent. Clamp connections absent.

**Ecology and distribution.** Solitary on rotten wood in broad-leaved forest, only found in Jiangsu Province, China, August to October.

**Additional specimens examined.** CHINA • Jiangsu Province, Nanjing City, Zijinshan, E 118.87, N 32.06, alt. 99 m, solitary on rotten wood, in mixed broad-leaf (i.e. *Quercus acutissima*, *Quercus aliena*, *Aphananthe aspera*, *Osmanthus fragrans*, *Liquidambar formosana*, *Photinia serratifolia* and *Ilex chinensis*) forest, 30 August 2024, collected by X. Chen, CX 665 (KUN-HKAS 145339).

**Notes.** *Rhodocybe zijinshanensis* belongs to *R.* sect. *Rufobrunnea* (Fig. 2). Species in this section are characterised by centrally stipitate basidiomata, pilei ranged from pinkish, reddish, brown, tan to fulvous (but never greyish or white), lamellae that are adnexed to adnate or decurrent, the absence of hymenial pseudocystidia and clamp connections (Baroni 1981). *Rhodocybe zijinshanensis* is similar to several other species, including *R. asyae* Sesli & Vizzini, *R. subasyae* T. Bau & Y.L. Sun, *R. pseudoalutacea* T.J. Baroni et al. and *R. alutacea* Singer. *Rhodocybe asyae*, first recorded in Turkey, can be differentiated from *R. zijinshanensis* by its relatively larger, smooth pileus (10–30 mm), longer and thicker stipe (25–30 × 2–5 mm) and flexuous cheilocystidia (20–30 × 4–6 µm) (Sesli and Vizzini 2017). *Rhodocybe subasyae*, a recently described species from Jilin, China, is also similar to *R. zijinshanensis*, but differs in having a smooth pileus, a longer and thicker stipe (22–37 × 5–7 mm), slightly larger basidiospores ( $Q_{avg} = 1.4$ ), and cheilocystidia measuring 22.4–28.2 × 3.9–6.8 µm (Sun and Bau 2023). For *R. pseudoalutacea*, it was reported from the Dominican Republic, featured by its slightly larger pileus (10–35 mm), slender yet thick stipe (15–50 × 2–6 mm) and pileipellis composed of finely encrusted cylindrical hyphae (Baroni et al. 2020). The last species which resembled *R. zijinshanensis* was *R. alutacea*, found in Florida, USA. It is characterised by the greater pileus size (25–35 mm), a longer stipe (23–35 × 2.5–5.5 mm), and septate, flexuous cheilocystidia (20–35 × 6.5–7 µm) (Singer 1946b; Baroni 1981).

## Discussion

In this study, we described two new species and documented a new record species in China: *C. parasiticus*, *R. zijinshanensis* and *C. baronii*. For the phylogenetic analysis, we utilised nearly all available sequences for the genera *Clitopilus* and *Rhodocybe*, uploaded by classified references or expert researchers (see Fig. 1). The phylogenetic tree indicates that *C. parasiticus* is closely related to *C. velutinus* T. J. Baroni & Angelini, which was discovered in the Dominican Republic. However, it can be distinguished by its larger pileus (10–25 mm), the existence of an eccentric stipe and larger basidiospores ( $L_m \times W_m = 8.0 \times 5.0$  µm) with more longitudinal ridges (10–14) (Baroni et al. 2020). Similarly, *C. baronii* is closer to *C. venososulcatus* Singer, which is occurring only in Florida, USA. Nonetheless, the latter typically exhibits a larger, venose and sulcate pileus (12–23 mm) and slightly larger basidiospores (8–8.5 × 4.5–5 µm) with 6–8 obscurely longitudinal ridges (Singer 1946a). Finally, *R. zijinshanensis* approaches

to *R. nuciolens* (Murrill) Singer and *R. gemina* (Paulet) Kuyper & Noordel., but the larger size of their basidiomata (particularly in the pileus and stipe) and the presence of cheilocystidia make them easy to distinguish from the former (Baroni 1981; Sesli and Vizzini 2017; Vizzini et al. 2018). The similar species of above species are compared in Table 3.

In the family Entolomataceae Kotl. & Pouzar, there are over 1500 described species worldwide (Co-David et al. 2009; Baroni and Matheny 2011; Karstedt et al. 2019). However, only a few species exhibit mycoparasitic capabilities, like *Entoloma abortivum* (Berk. & M.A. Curtis) Donk, *E. parasiticum* (Quél.) Kriess, *E. pseudoparasiticum* Noordel. and *Rhodophana stangliana* (Bresinsky & Pfaff) Vizzini (Noordeloos 1988; Læssøe and Rosendahl 1994; Czederpiltz et al. 2001). Thereinto, *Entoloma abortivum* is frequently reported to co-occur with *Armillaria* (Fr.) Staude, leading to the hypothesis that *Armillaria* attacks and parasitises the basidiomata of *Entoloma abortivum* (Watling 1974). On the contrary, Czederpiltz et al. (2001) demonstrated that *E. abortivum* can actually abort the growth of *Armillaria* in culture media. Furthermore, Koch and Herr (2021) explained this phenomenon using transcriptomics.

Notably, some species, such as *E. clypeatum* (L.) P. Kumm., *E. niphoides* Romagn. ex Noordel., *E. saepium* (Noulet & Dass.) Richon & Roze and *E. sericeoides* (J.E. Lange) Noordel., have been reported to associate with rosaceous woody plants. However, these species are more likely to be detrimental to roots rather than forming typical mycorrhizae (Agerer and Waller 1993; Gryndler et al. 2010; Shishikura et al. 2020). In the *Rhodocybe-Clitopilus* clade, *C. daamsii* has been observed growing on *Hydnoporia tabacina* (Sowerby) Spirin et al. (previously classified as *Hymenochaete tabacina* (Sowerby) Lév.), while *C. passeckerianu* and *C. fasciculatus* have been associated with the growing-beds of cultivated *Agaricus* L. (Noordeloos 1984; Noordeloos 1988; Noordeloos 1993), although Singer questioned the mycoparasitic behaviour of *C. passeckerianu* (Singer and Harris 1987).

To investigate the saprophytic and biotrophic abilities of *C. parasiticus*, we carefully examined different specimens to identify the discrepancies between various hosts and growth on soil. The results are presented in Table 4. We found that the basidiospores from specimens KUN-HKAS 145335 and 145337, which were collected from the leaves of *Oplismenus* sp. and *Dryopteris* sp., respectively, showed no significant differences. However, there was an obvious difference with specimen KUN-HKAS 145336, where the basidiospores of *C. parasiticus* growing on soil were larger than those from specimens growing on plant leaves. Larger basidiospores often indicate more robust growth of basidiomata (Kauserud et al. 2011; Halbwachs et al. 2017), suggesting that this species may be better suited to a soil habitat than to a biotrophic lifestyle.

Furthermore, the average temperature over a fortnight in 2024 was slightly higher than in 2023, while the average precipitation during the same period was slightly lower in 2024 compared to 2023. These subtle discrepancies could influence the nutritional mode and even the choice of parasitic host. Admittedly, our judgement that this species is biotrophic on the basis of only two collections from different plant leaves, is not entirely rigorous. More experiments, including physiological and genomic analyses, are necessary for a comprehensive assessment.



**Table 3.** The comparison of morphological characters amongst *C. parasiticus*, *C. baronii*, *R. zijinshanensis* and similar species.

Taxa	Badisiomata	Pileus	Basidiospores (ridges)	Hymenial cystidia	Habitat	Locality	References
<b><i>Clitopilus</i> sect. <i>Scyphoides</i></b>							
<i>C. baronii</i> (Holotype)	Orbicular to conchate or spatulate, sessile	5–40 mm, white to greyish	6.9–8.4 × 4.4–5.5 µm (8–10), Q = 1.68–1.71	Cheilocystidia lageniform	On a decaying trunk of <i>Quercus</i> sp.	Italy	Consiglio and Setti (2019)
<b><i>C. baronii</i></b>	<b>Conchate, sessile</b>	<b>3–15 mm, white to greyish</b>	<b>6.5–9.5 × 4–5 µm (8–10), Q = 1.4–1.98</b>	<b>None</b>	<b>On rotten wood</b>	<b>China</b>	<b>This study</b>
<i>C. daamsii</i> (Holotype)	Orbicular to conchate, sessile	2–8 mm, white	8–11.5 × 4.8–6.6 µm (6–9), Q = 1.4–2	None	On wood or other fungi	Netherlands	Noordeloos (1984)
<i>C. fasciculatus</i> (Holotype)	Fasciculata, sessile	Individual 24 × 20 mm, pale brown	4.7–6.3 × 3.0–3.5 µm (3–6), Q = 1.2–1.85	None	On beds of cultivated mushrooms	Netherlands	Noordeloos (1984)
<i>C. hobsonii</i> (Holotype)	Orbicular or slightly reniform, sessile	5–18 mm, white to pale greyish	6.5–9 × 4–5.5 µm (7–12), Q = 1.2–2	None	On plant debris or herbaceous stems	Britain	Orton (1960)
<b><i>C. parasiticus</i> (Holotype)</b>	<b>Conchate, sessile</b>	<b>2–8 mm, whitish to chalk white</b>	<b>5.5–8.5 × 3.5–5 µm (7–9), Q = 1.2–1.9</b>	<b>None</b>	<b>On soil, rotten wood and leaves of plants</b>	<b>China</b>	<b>This study</b>
<i>C. passeckerianus</i> (Holotype)	Reniform or resembling an ear, sessile	8–40 mm, white	7–9 × 4–5 µm (7–12), Q = 1.45–2.25	None	On mushroom-beds	Europe	Pilát (1935)
<i>C. pinsitus</i> (Holotype)	Spatulate, semi-cicular, sessile	15–40 mm, white to pale ochre	7–9 × 4.6–5.3 µm (7–8)	None	On trunk of <i>Quercus</i> sp.	Sweden	Josserand (1937)
<i>C. velutinus</i> (Holotype)	Clitocyboid	10–25 mm, pure white	7–9 × 5–6 µm (7–8), Q = 1.27–1.8	None	On soil	Dominican Republic	Baroni et al. (2020)
<i>C. venosulcatus</i> (Holotype)	Pleurotoid, sessile or sub sessile	12–23 mm, pallid white	8–8.5 × 4.5–5 µm (6–8)	None	On trunks or logs of <i>Ficus aurea</i>	USA	Singer (1946a)
<b><i>Rhodocybe</i> sect. <i>Rufobrunnea</i></b>							
<i>R. alutacea</i> (Holotype)	25–35 mm, yellowish, hygrophanous	23–35 × 2.5–5.5 mm, subequal	5.8–7.5 × 3.5–5 µm (7–9)	Cheilocystidia	On sandy soil and fallen leaves	USA	Singer (1946b)
<i>R. asyae</i> (Holotype)	10–30 mm, salmon pink	25–30 × 2–5 mm, tapering	5–7 × 4–5 µm, Q = 1.1–1.4	Cheilocystidia	On the grass	Turkey	Sesil and Vizzini (2017)
<i>R. gemina</i>	15–80 mm, reddish, incarnate	25–50 × 3–15 mm, subequal	5–6.5 × 4–5 µm	Cheilocystidia	On humus	Europe	Baroni (1981)
<i>R. nuciolens</i>	10–60 mm, pinkish cinnamon, hygrophanous	35–80 × 2–9 mm, equal	5.5–8 × 4–5 µm	Cheilocystidia	On humus, sandy soil or decaying wood	USA	Baroni (1981)
<i>R. pseudoalutacea</i> (Holotype)	10–35 mm, brown or brownish orange, hygrophanous	15–50 × 2–6 mm, equal or enlarged downwards	5.5–7 × 4–5 µm (7–10), Q = 1.2–1.6	None	On decaying humus or woody debris	Dominican Republic	Baroni et al. (2020)
<i>R. subasyae</i> (Holotype)	19–25 mm, beige red	22–37 × 5–7 mm, cylindrical	5.4–6.8 × 3.9–4.9 µm (6–8), Q = 1.2–1.6	Cheilocystidia	On sandy soil	China	Sun and Bau (2023)
<b><i>R. zijinshanensis</i> (Holotype)</b>	<b>10–15 mm, yellow, hygrophanous</b>	<b>7–19 × 1–2 mm, cylindrical to tapering</b>	<b>5–6.5 × 3.5–5 µm (7–9), Q = 1.09–1.55</b>	<b>None</b>	<b>On rotten wood</b>	<b>China</b>	<b>This study</b>

**Table 4.** The intraspecies comparison of *C. parasiticus* in morphological characters and microenvironment.

Taxa	Voucher specimen	Pileus	Basidiospores (ridges)	Crystals in pileipellis	Habitat	Temp. (°C)	Prec. (mm/d)
<i>C. parasiticus</i>	KUN-HKAS145335 (CX628)	2–8 mm	5.5–7.0 × 4–5.5 µm, $L_m \times W_m = 6.3 (\pm 0.47) \times 4.24 (\pm 0.35) \mu\text{m}$ , $Q = 1.20\text{--}1.84$ ( $Q_{\text{avg}} = 1.49 \pm 0.13$ ) (8–9) [63/3/1]	None	On leaves of <i>Oplismenus undulatifolius</i>	29.04	5.58
<i>C. parasiticus</i> (Holotype)	KUN-HKAS145336 (CX966)	3–7 mm	6.0–8.5 × 4–5 µm, $L_m \times W_m = 7.06 (\pm 0.6) \times 4.40 (\pm 0.30) \mu\text{m}$ , $Q = 1.40\text{--}1.81$ ( $Q_{\text{avg}} = 1.61 \pm 0.10$ ) (7–8) [62/3/1]	Present	On soil	31.25	4.43
<i>C. parasiticus</i>	KUN-HKAS145337 (CX967)	3–5.5 mm	5.5–7.5 × 3.5–5 µm, $L_m \times W_m = 6.33 (\pm 0.50) \times 4.09 (\pm 0.28) \mu\text{m}$ , $Q = 1.20\text{--}1.90$ ( $Q_{\text{avg}} = 1.55 \pm 0.13$ ) (7–9) [61/3/1]	Present	On leaves of <i>Dryopteris</i> sp.	31	4.42

Notes: Temp./Prec. means the average temperatures/precipitations one week before and one week after the date of collection.

## Acknowledgements

The authors are very grateful to Drs. Bang Feng, Xiang-Hua Wang (Kunming Institute of Botany, Chinese Academy of Sciences), Yu-Peng Ge (School of Horticulture, Ludong University) and Ms. Ya-Jun Hou for providing some constructive information and suggestions. The authors thank the herbaria KUN-HKAS for providing materials and pictures. The authors thank Mr. Ting Tang for supplying scanning electron microscope (SEM) images.

## Additional information

### Conflict of interest

The authors have declared that no competing interests exist.

### Ethical statement

No ethical statement was reported.

## Funding

This research was funded by the National Natural Science Foundation of China (No. 32060707) and the Funds of Sci-Tech Innovation System Construction for Tropical Crops of Yunnan Province (No. 655-4-3).

## Author contributions

Sipeng Jian conceived, designed and completed the experiments under the guidance of Chunxia Zhang. Xia Chen, Yiwei Fang and Tianwei Yang helped to collect samples, use and adjust the microscope, with some photographs. Xinjing Xu, Jing Liu and Feng Gao assisted with extracting DNA and PCR amplification. Sipeng Jian wrote the manuscript and Chunxia Zhang revised it.

## Author ORCIDs

Sipeng Jian  <https://orcid.org/0000-0002-2055-3169>

Xia Chen  <https://orcid.org/0009-0002-1239-1865>

## Data availability

In this study, DNA sequences have been deposited in GenBank. Specimens were placed at Herbarium of Kunming Institute of Botany, Chinese Academy of Sciences (KUN-HKAS).

## References

- Agerer R, Waller K (1993) Mycorrhizae of *Entoloma saepium*: Parasitism or symbiosis? Mycorrhiza 3: 145–154. <https://doi.org/10.1007/BF00203608>
- Aplin N, Cullington P, Douglas B, Janke E (2022) DNA barcoding reveals three *Rhodocybe* species new to Britain. Field Mycology : a Magazine for the Study and Identification of Wild Fungi 23: 41–47.
- Baroni TJ (1981) A revision of the genus *Rhodocybe* Maire (Agaricales). Beih Nova Hedwigia 67: 1–198.
- Baroni TJ, Matheny PB (2011) A re-evaluation of gasteroid and cyphelloid species of Entolomataceae from Eastern North America. Harvard Papers in Botany 16: 293–310. <https://doi.org/10.3100/0.25.016.0205>

- Baroni TJ, Hofstetter V, Largent DL, Vilgalys R (2011) *Entocybe* is proposed as a new genus in the Entolomataceae (Agaricomycetes, Basidiomycota) based on morphological and molecular evidence. *North American Fungi* 6: 1–19. <https://doi.org/10.2509/naf2011.006.012>
- Baroni TJ, Angelini C, Bergemann SE, Lodge DJ, Lacey L, Curtis TA, Cantrell SA (2020) *Rhodocybe-Clitopilus* clade (Entolomataceae, Basidiomycota) in the Dominican Republic: New taxa and first reports of *Clitocella*, *Clitopilus*, and *Rhodocybe* for Hispaniola. *Mycological Progress* 19: 1083–1099. <https://doi.org/10.1007/s11557-020-01619-y>
- Co-David D, Langeveld D, Noordeloos ME (2009) Molecular phylogeny and spore evolution of Entolomataceae. *Persoonia* 23: 147–176. <https://doi.org/10.3767/003158509X480944>
- Consiglio G, Setti L (2019) Nomenclatural novelties. *Index Fungorum* : Published Numbers 427: 1.
- Consiglio G, Contu M, Roy M, Selosse MA, Vizzini A (2007) *Rhodocybe praesidentialis* spec. nov. una nuova specie della Sezione *Rhodocybe*. *Rivista di Micologia* 50: 23–35.
- Cooper JA (2014) New species and combinations of some New Zealand agarics belonging to *Clitopilus*, *Lyophyllum*, *Gerhardtia*, *Clitocybe*, *Hydangium*, *Mycena*, *Rhodocollybia* and *Gerronema*. *Mycosphere* 5: 263–288. <https://doi.org/10.5943/mycosphere/5/2/2>
- Crous PW, Shivas RG, Wingfield MJ, Summerell BA, Rossman AY, Alves JL, Adams GC, Barreto RW, Bell A, Coutinho ML, Flory SL, Gates G, Grice KR, Hardy GE, Kleczewski NM, Lombard L, Longa CM, Louis-Seize G, Macedo F, Mahoney DP, Maresi G, Martin-Sanchez PM, Marvanova L, Minnis AM, Morgado LN, Noordeloos ME, Phillips AJ, Quaedvlieg W, Ryan PG, Saiz-Jimenez C, Seifert KA, Swart WJ, Tan YP, Tanney JB, Thu PQ, Videira SI, Walker DM, Groenewald JZ (2012) Fungal Planet description sheets: 128–153. *Persoonia* 29: 146–201. <https://doi.org/10.3767/003158512X661589>
- Crous PW, Wingfield MJ, Burgess TI, Hardy GESJ, Crane C, Barrett S, Cano-Lira JF, Leroux JJ, Thangavel R, Guarro J, Stchigel AM, Martín MP, Alfredo DS, Barber PA, Barreto RW, Baseia IG, Cano-Canals J, Cheewangkoon R, Ferreira RJ, Gené J, Lechat C, Moreno G, Roets F, Shivas RG, Sousa JO, Tan YP, Wiederhold NP, Abell SE, Accioly T, Albizu JL, Alves JL, Antoniolli ZI, Aplin N, Araújo J, Arzanlou M, Bezerra JDP, Bouchara JP, Carlavilla JR, Castillo A, Castroagudín VL, Ceresini PC, Claridge GF, Coelho G, Coimbra VRM, Costa LA, da cunha KC, da silva SS, Daniel R, de beer ZW, Dueñas M, Edwards J, Enwistle P, Fiuza PO, Fournier J, García D, Gibertoni TB, Giraud S, Guevara-Suarez M, Gusmão LFP, Haituk S, Heykoop M, Hirooka Y, Hofmann TA, Houbroken J, Hughes DP, Kautmanová I, Koppel O, Koukol O, Larsson E, Latha KPD, Lee DH, Lisboa DO, Lisboa WS, López-Villalba Á, Maciel JLN, Manimohan P, Manjón JL, Marincowitz S, Marney TS, Meijer M, Miller AN, Olariaga I, Paiva LM, Piepenbring M, Poveda-Molero JC, Raj KNA, Raja HA, Rougeron A, Salcedo I, Samadi R, Santos TAB, Scarlett K, Seifert KA, Shuttleworth LA, Silva GA, Silva M, Siqueira JPZ, Souza-Motta CM, Stephenson SL (2016) Fungal Planet description sheets: 469–557. *Persoonia - Molecular Phylogeny and Evolution of Fungi* 37: 218–403. <https://doi.org/10.3767/003158516X694499>
- Crous PW, Wingfield MJ, Burgess TI, Hardy GESJ, Barber PA, Alvarado P, Barnes CW, Buchanan PK, Heykoop M, Moreno G, Thangavel R, Van der spuy S, Barili A, Barrett S, Cacciola SO, Cano-Lira JF, Crane C, Decock C, Gibertoni TB, Guarro J, Guevara-Suarez M, Hubka V, Kolařík M, Lira CRS, Ordoñez ME, Padamsee M, Ryvarden L, Soares AM, Stchigel AM, Sutton DA, Vizzini A, Weir BS, Acharya K, Aloï F, Baseia IG, Blanchette RA, Bordallo JJ, Bratek Z, Butler T, Cano-Canals J, Carlavilla JR, Chander J, Cheewangkoon R, Cruz RHSF, Da silva M, Dutta AK, Ercole E, Escobio V, Esteve-Raventós

- F, Flores JA, Gené J, Góis JS, Haines L, Held BW, Horta jung M, Hosaka K, Jung T, Jurjević Ž, Kautman V, Kautmanova I, Kiyashko AA, Kozanek M, Kubátová A, Lafourcade M, La spada F, Latha KPD, Madrid H, Malysheva EF, Manimohan P, Manjón JL, Martín MP, Mata M, Merényi Z, Morte A, Nagy I, Normand AC, Paloi S, Pattison N, Pawłowska J, Pereira OL, Petterson ME, Picillo B, Raj KNA, Roberts A, Rodríguez A, Rodríguez-Campo FJ, Romański M, Ruszkiewicz-Michalska M, Scanu B, Schena L, Sempelbauer M, Sharma R, Shouche YS, Silva V, Staniaszek-Kik M, Stielow JB, Tapia C, Taylor PWJ, Toome-Heller M, Vabeikhekhei JMC, van Diepeningen AD, Van Hoa N, Van Tri M, Wiederhold NP, Wrzosek M, Zothanzama J, Groenewald JZ (2017) Fungal Planet description sheets: 558–624. *Persoonia - Molecular Phylogeny and Evolution of Fungi* 38: 240–384. <https://doi.org/10.3767/003158517X698941>
- Czederpiltz DLL, Volk TJ, Burdsall Jr HH (2001) Field observations and inoculation experiments to determine the nature of the carpophoroids associated with *Entoloma abortivum* and *Armillaria*. *Mycologia* 93: 841–851. <https://doi.org/10.1080/00275514.2001.12063219>
- Doyle JJ, Doyle JL (1987) A rapid DNA isolation procedure for small quantities of fresh leaf tissue. *Phytochemical Bulletin* 19: 11–15.
- Dutta AK, Gates GM, Rakshit S, Acharya K (2021) *Rhodocybe brunneoaurantiaca* (sect. *Rufrobrunnea*, Entolomataceae): A new species from India. *Nordic Journal of Botany* 39: 1–9. <https://doi.org/10.1111/njb.03061>
- Elkhateeb WA, Daba GM (2021) Fungi over fungi, endophytic fungi associated with mushroom fruiting bodies and lichens. *Pharmaceutics and Pharmacology Research* 4: 1–4. <https://doi.org/10.31579/2693-7247/028>
- Fatima N, Usman M, Khalid AN (2022) *Clitopilus chichawatniensis* sp. nov. (Entolomataceae, Agaricales) from Pakistan. *Phytotaxa* 567: 257–268. <https://doi.org/10.11646/phytotaxa.567.3.5>
- Gryndler M, Egertová Z, Soukupová L, Gryndlerová H, Borovička J, Hršelová H (2010) Molecular detection of *Entoloma* spp. associated with roots of rosaceous woody plants. *Mycological Progress* 9: 27–36. <https://doi.org/10.1007/s11557-009-0615-3>
- Halbwachs H, Heilmann-Clausen J, Bässler C (2017) Mean spore size and shape in ectomycorrhizal and saprotrophic assemblages show strong responses under resource constraints. *Fungal Ecology* 26: 59–64. <https://doi.org/10.1016/j.funeco.2016.12.001>
- Hall TA (1999) BioEdit: A user-friendly biological sequence alignment editor and analysis program for Windows 95/98/NT. *Nucleic Acids Symposium Series* 41: 95–98.
- He Z-M, Yang ZL (2022) The genera *Bonomyces*, *Harmajaea* and *Notholepista* from Northwestern China: Two new species and a new record. *Mycological Progress* 21: 26. <https://doi.org/10.1007/s11557-022-01786-0>
- He Z-M, Chen Z-H, Bau T, Wang G-S, Yang ZL (2023) Systematic arrangement within the family Clitocybaceae (Tricholomatineae, Agaricales): Phylogenetic and phylogenomic evidence, morphological data and muscarine-producing innovation. *Fungal Diversity* 123: 1–47. <https://doi.org/10.1007/s13225-023-00527-2>
- Hyde KD, Hongsanan S, Jeewon R, Bhat DJ, McKenzie EHC, Jones EBG, Phookamsak R, Ariyawansa HA, Boonmee S, Zhao Q, Abdel-Aziz FA, Abdel-Wahab MA, Banmai S, Chomnunti P, Cui B-K, Daranagama DA, Das K, Dayarathne MC, de Silva NI, Dissanayake AJ, Doilom M, Ekanayaka AH, Gibertoni TB, Góes-Neto A, Huang S-K, Jayasiri SC, Jayawardena RS, Konta S, Lee HB, Li W-J, Lin C-G, Liu J-K, Lu Y-Z, Luo Z-L, Manawasinghe IS, Manimohan P, Mapook A, Niskanen T, Norphanphoun C, Papizadeh M, Perera RH, Phukhamsakda C, Richter C, de A. Santiago ALCM, Drechsler-Santos



- ER, Senanayake IC, Tanaka K, Tennakoon TMD, Thambugala KM, Tian Q, Tibpromma S, Thongbai B, Vizzini A, Wanasinghe DN, Wijayawardene NN, Wu H-X, Yang J, Zeng X-Y, Zhang H, Zhang J-F, Bulgakov TS, Camporesi E, Bahkali AH, Amoozegar MA, Araujo-Neta LS, Ammirati JF, Baghela A, Bhatt RP, Bojantchev D, Buyck B, da Silva GA, de Lima CLF, de Oliveira RJV, de Souza CAF, Dai Y-C, Dima B, Duong TT, Ercole E, Mafalda-Freire F, Ghosh A, Hashimoto A, Kamolhan S, Kang J-C, Karunarathna SC, Kirk PM, Kytövuori I, Lantieri A, Liimatainen K, Liu Z-Y, Liu X-Z, Lücking R, Medardi G, Mortimer PE, Nguyen TTT, Promputtha I, Raj KNA, Reck MA, Lumyong S, Shahzadeh-Fazeli SA, Stadler M, Soudi MR, Su H-Y, Takahashi T, Tangthirasun N, Uniyal P, Wang Y, Wen T-C, Xu J-C, Zhang Z-K, Zhao Y-C, Zhou J-L, Zhu L (2016) Fungal diversity notes 367–490: Taxonomic and phylogenetic contributions to fungal taxa. *Fungal Diversity* 80: 1–270. <https://doi.org/10.1007/s13225-016-0373-x>
- Izhar A, Khan Z, Asif M, Bashir H, Rani AK, Niazi AR, Khalid AN (2023) *Clitopilus cretoalbus* sp. nov. (Entolomataceae, Agaricales), a new species from Pakistan. *European Journal of Taxonomy* 861: 168–184. <https://doi.org/10.5852/ejt.2023.861.2075>
- Jian SP, Bau T, Zhu XT, Deng WQ, Zhao ZW, Yang ZL (2020a) *Clitopilus*, *Clitocella* and *Clitopilopsis* in China. *Mycologia* 112: 371–399. <https://doi.org/10.1080/00275514.2019.1703089>
- Jian SP, Karadelev M, Wang PM, Deng WQ, Yang ZL (2020b) *Clitopilus abprunulus*, a new species from North Macedonia with notes on *C. ravus* and pleuromutilin producing taxa. *Mycological Progress* 19: 805–816. <https://doi.org/10.1007/s11557-020-01603-6>
- Jian SP, Wang XH, Deng WQ, Yang ZL (2023) *Clitopilus* in southern China: Two new species and comments on *C. subscyphoides*. *Mycological Progress* 22: 35. <https://doi.org/10.1007/s11557-023-01885-6>
- Josserand M (1937) Champignons de la région Lyonnaise. *Bulletin de la Société Mycologique de France* 53: 178–230.
- Karstedt F, Capelari M, Baroni TJ, Largent DL, Bergemann SE (2019) Phylogenetic and morphological analyses of species of the Entolomataceae (Agaricales, Basidiomycota) with cuboid basidiospores. *Phytotaxa* 391: 1–27. <https://doi.org/10.11646/phytotaxa.391.1.1>
- Katoh K, Kuma K, Toh H, Miyata T (2005) MAFFT version 5: Improvement in accuracy of multiple sequence alignment. *Nucleic Acids Research* 33: 511–518. <https://doi.org/10.1093/nar/gki198>
- Kausarud H, Heegaard E, Halvorsen R, Boddy L, Høiland K, Stenseth NC (2011) Mushroom's spore size and time of fruiting are strongly related: Is moisture important? *Biology Letters* 7: 273–276. <https://doi.org/10.1098/rsbl.2010.0820>
- Kemen E, Jones JDG (2012) Obligate biotroph parasitism: Can we link genomes to lifestyles? *Trends in Plant Science* 17: 448–457. <https://doi.org/10.1016/j.tplants.2012.04.005>
- Khan Z, Khalid AN (2024) Molecular phylogeny and morphology reveal a new species of genus *Rhodocybe* sensu stricto Maire (Entolomataceae; Agaricales) from Pakistan. *Cryptogamie. Mycologie* 45: 127–137. <https://doi.org/10.5252/cryptogamie-mycologie2024v45a10>
- Kim CS, Jo JW, Kwag Y-N, Sung G-H, Lee S-G, Kim S-Y, Shin C-H, Han S-K (2015) Mushroom flora of Ulleung-gun and a newly recorded bovista species in the Republic of Korea. *Mycobiology* 43: 239–257. <https://doi.org/10.5941/MYCO.2015.43.3.239>
- Kluting KL, Baroni TJ, Bergemann SE (2014) Toward a stable classification of genera within the Entolomataceae: A phylogenetic re-evaluation of the *Rhodocybe-Clitopilus* clade. *Mycologia* 106: 1127–1142. <https://doi.org/10.3852/13-270>

- Koch RA, Herr JR (2021) Transcriptomics reveals the putative mycoparasitic strategy of the mushroom *Entoloma abortivum* on species of the mushroom genus *Armillaria*. *mSystems* 6: 1–18. <https://doi.org/10.1128/msystems.00544-21>
- Kumla J, Suwannarach N, Sungpalee W, Sri-Ngernyuan K, Lumyong S (2019) *Clitopilus lampangensis* (Agaricales, Entolomataceae), a new species from northern Thailand. *MycKeys* 58: 69–82. <https://doi.org/10.3897/mycokeys.58.36307>
- Læssøe T, Rosendahl S (1994) *Rhodocybe stangliana*, a parasite on other agarics? *Mycological Research* 98: 88–90. [https://doi.org/10.1016/S0953-7562\(09\)80343-2](https://doi.org/10.1016/S0953-7562(09)80343-2)
- Liu J-W, Ge Z-W, Horak E, Vizzini A, Halling RE, Pan C-L, Yang ZL (2021) Squamanitaceae and three new species of *Squamanita* parasitic on *Amanita* basidiomes. *IMA Fungus* 12: 4. <https://doi.org/10.1186/s43008-021-00057-z>
- Luttrell ES (1974) Parasitism of fungi on vascular plants. *Mycologia* 66: 1–15. <https://doi.org/10.1080/00275514.1974.12019567>
- Matheny PB (2005) Improving phylogenetic inference of mushrooms with *RPB1* and *RPB2* nucleotide sequences (*Inocybe*; Agaricales). *Molecular Phylogenetics and Evolution* 35: 1–20. <https://doi.org/10.1016/j.ympev.2004.11.014>
- Matheny PB, Wang Z, Binder M, Curtis JM, Lim YW, Nilsson RH, Hughes KW, Hofstetter V, Ammirati JF, Schoch CL, Langer E, Langer G, McLaughlin DJ, Wilson AW, Froslev T, Ge ZW, Kerrigan RW, Slot JC, Yang ZL, Baroni TJ, Fischer M, Hosaka K, Matsuura K, Seidl MT, Vauras J, Hibbett DS (2007) Contributions of *rpb2* and *tef1* to the phylogeny of mushrooms and allies (Basidiomycota, Fungi). *Molecular Phylogenetics and Evolution* 43: 430–451. <https://doi.org/10.1016/j.ympev.2006.08.024>
- McTaggart AR, Shivas RG, Boekhout T, Oberwinkler F, Vánky K, Pennycook SR, Begerow D (2016) *Mycosarcoma* (Ustilaginaceae), a resurrected generic name for corn smut (*Ustilago maydis*) and its close relatives with hypertrophied, tubular sori. *IMA Fungus* 7: 309–315. <https://doi.org/10.5598/ima fungus.2016.07.02.10>
- Moncalvo J-M, Vilgalys R, Redhead SA, Johnson JE, James TY, Catherine Aime M, Hofstetter V, Verduin SJW, Larsson E, Baroni TJ, Greg Thorn R, Jacobsson S, Clémenceon H, Miller OK (2002) One hundred and seventeen clades of euagarics. *Molecular Phylogenetics and Evolution* 23: 357–400. [https://doi.org/10.1016/S1055-7903\(02\)00027-1](https://doi.org/10.1016/S1055-7903(02)00027-1)
- Moncalvo JM, Baroni TJ, Bhatt RP, Stephenson SL (2004) *Rhodocybe paurii*, a new species from the Indian Himalaya. *Mycologia* 96: 859–865. <https://doi.org/10.1080/15572536.2005.11832932>
- Moreno G, Contu M, Ortega A, Platas G, Pelaez F (2007) Molecular phylogenetic studies show *Omphalina giovanellae* represents a new section of *Clitopilus* (Agaricomycetes). *Mycological Research* 111: 1399–1405. <https://doi.org/10.1016/j.mycres.2007.09.009>
- Morgado LN, Noordeloos ME, Hausknecht A (2016) *Clitopilus reticulosporus*, a new species with unique spore ornamentation, its phylogenetic affinities and implications on the spore evolution theory. *Mycological Progress* 15: 26. <https://doi.org/10.1007/s11557-016-1165-0>
- Noordeloos ME (1984) Notulae ad floram agaricinam neerlandicam IV–V. *Clitopilus* and *Leucopaxillus*. *Persoonia* 12: 155–167.
- Noordeloos ME (1988) Entolomataceae. In: Bas C, Kuyper TW, Noordeloos ME, Vellinga EC (Eds) *Flora Agaricina Neerlandica*. Vol. 1. AA Balkema, Rotterdam, 182 pp.
- Noordeloos ME (1993) Studies in *Clitopilus* (Basidiomycetes, Agaricales) in Europe. *Persoonia* 15: 241–248.
- Nylander JAA (2004) MrModeltest v2. Program distributed by the author. Evolutionary Biology Centre, Uppsala University, Uppsala.

- Orton PD (1960) New check list of British Agarics and Boleti, part III (keys to *Crepidotus*, *Deconica*, *Flocculina*, *Hygrophorus*, *Naucoria*, *Pluteus* and *Volvaria*). Transactions of the British Mycological Society 43: 159–439. [https://doi.org/10.1016/S0007-1536\(60\)80065-4](https://doi.org/10.1016/S0007-1536(60)80065-4)
- Peng L, Shan X, Wang Y, Martin F, Vilgalys R, Yuan Z (2021) Hybrid genome assembly and gene repertoire of the root endophyte *Clitopilus hobsonii* QYL-10 (Entolomataceae, Agaricales, Basidiomycetes). Molecular Plant-Microbe Interactions 34: 711–714. <https://doi.org/10.1094/MPMI-11-20-0328-A>
- Pilát A (1935) Atlas des champignons de l'Europe II: *Pleurotus* Fries. Chez les éditeurs, Praha, 193 pp.
- Pölme S, Abarenkov K, Henrik Nilsson R, Lindahl BD, Clemmensen KE, Kauserud H, Nguyen N, Kjøller R, Bates ST, Baldrian P, Frøslev TG, Adojaan K, Vizzini A, Suija A, Pfister D, Baral H-O, Järv H, Madrid H, Nordén J, Liu J-K, Pawlowska J, Pöldmaa K, Pärtel K, Runnel K, Hansen K, Larsson K-H, Hyde KD, Sandoval-Denis M, Smith ME, Toome-Heller M, Wijayawardene NN, Menolli N, Reynolds NK, Drenkhan R, Maharachchikumbura SSN, Gibertoni TB, Læssøe T, Davis W, Tokarev Y, Corrales A, Soares AM, Agan A, Machado AR, Argüelles-Moyao A, Detheridge A, de Meiras-Otoni A, Verbeken A, Dutta AK, Cui B-K, Pradeep CK, Marín C, Stanton D, Gohar D, Wanasinghe DN, Otsing E, Aslani F, Griffith GW, Lumbsch TH, Grossart H-P, Masigol H, Timling I, Hiiesalu I, Oja J, Kupagme JY, Geml J, Alvarez-Manjarrez J, Ilves K, Loit K, Adamson K, Nara K, Küngas K, Rojas-Jimenez K, Bitenieks K, Irinyi L, Nagy LG, Soonvald L, Zhou L-W, Wagner L, Aime MC, Öpik M, Mujica MI, Metsoja M, Ryberg M, Vasar M, Murata M, Nelsen MP, Cleary M, Samarakoon MC, Doilom M, Bahram M, Hagh-Doust N, Dulya O, Johnston P, Kohout P, Chen Q, Tian Q, Nandi R, Amiri R, Perera RH, dos Santos Chikowski R, Mendes-Alvarenga RL, Garibay-Orijel R, Gielen R, Phookamsak R, Jayawardena RS, Rahimlou S, Karunarathna SC, Tibpromma S, Brown SP, Sepp S-K, Mundra S, Luo Z-H, Bose T, Vahter T, Netherway T, Yang T, May T, Varga T, Li W, Coimbra VRM, de Oliveira VRT, de Lima VX, Mikryukov VS, Lu Y, Matsuda Y, Miyamoto Y, Kõljalg U, Tedersoo L (2021) FungalTraits: A user-friendly traits database of fungi and fungus-like stramenopiles. Fungal Diversity 105: 1–16. <https://doi.org/10.1007/s13225-020-00466-2>
- Raj KNA, Manimohan P (2018) A new species and a new record of *Clitopilus* and a description of *C. orientalis* from India based on morphology and molecular phylogeny. Phytotaxa 343: 47–59. <https://doi.org/10.11646/phytotaxa.343.1.4>
- Rogerson CT, Samuels GJ (2018) Polyporiculous species of *Hypomyces*. Mycologia 85: 213–272. <https://doi.org/10.1080/00275514.1992.12026272>
- Ronquist F, Huelsenbeck JP (2003) MrBayes 3: Bayesian phylogenetic inference under mixed models. Bioinformatics (Oxford, England) 19: 1572–1574. <https://doi.org/10.1093/bioinformatics/btg180>
- Sanchez-Garcia M, Matheny PB (2017) Is the switch to an ectomycorrhizal state an evolutionary key innovation in mushroom-forming fungi? A case study in the Tricholomatineae (Agaricales). Evolution 71: 51–65. <https://doi.org/10.1111/evo.13099>
- Sesli (2021) *Rhodocybe cistetorum* (Basidiomycota, Entolomataceae), a new species from the Colchic ecoregion of Turkey. Nordic Journal of Botany 39: 1–9. <https://doi.org/10.1111/njb.03078>
- Sesli, Vizzini A (2017) Two new *Rhodocybe* species (sect. *Rufobrunnea*, Entolomataceae) from the East Black Sea coast of Turkey. Turkish Journal of Botany 41: 200–210. <https://doi.org/10.3906/bot-1607-1>
- Shi J, Wang X, Wang E (2023) Mycorrhizal symbiosis in plant growth and stress adaptation: From genes to ecosystems. Annual Review of Plant Biology 74: 569–607. <https://doi.org/10.1146/annurev-arplant-061722-090342>

- Shishikura M, Takemura Y, Sotome K, Maekawa N, Nakagiri A, Endo N (2020) Four mycelial strains of *Entoloma clypeatum* species complex form ectomycorrhiza-like roots with *Pyrus betulifolia* seedlings in vitro, and one develops fruiting bodies 2 months after inoculation. *Mycorrhiza* 31: 31–42. <https://doi.org/10.1007/s00572-020-00994-4>
- Silva-Filho AGS, Baroni TJ, Komura DL, Moncalvo JM, Baseia IG, Wartchow F (2020) *Rhodocybe fusipes* (Entolomataceae), a new species from Amazonian ‘terra-firme’ forest of Brazil. *Sydowia* 72: 163–170. <https://doi.org/10.12905/0380.sydowia72-2020-0163>
- Singer R (1946a) The Boletineae of Florida with notes on extralimital species. IV. The lamellate families (Gomphidiaceae, Paxillaceae, and Jugasporaceae). *Farlowia* 2: 527–567. <https://doi.org/10.5962/p.316017>
- Singer R (1946b) Two new species in the Agaricales. *Mycologia* 38: 687–690. <https://doi.org/10.1080/00275514.1946.12024092>
- Singer R (1986) The Agaricales in Modern Taxonomy. 4<sup>th</sup> edn. Koeltz Scientific Books, Koenigstein, 981 pp.
- Singer R, Harris B (1987) Mushrooms and Truffles: Botany, Cultivation, and Utilization. 2<sup>nd</sup> edn. Koeltz Scientific Books, Welling, Germany, 272 pp.
- Sleiman S, Bellanger JM, Richard F, Stephan J (2021) First molecular-based contribution to the checklist of Lebanon macrofungi. *Mycotaxon* 136: 1–12. <https://doi.org/10.5248/136.687>
- Smith SA, Dunn CW (2008) Phyutility: A phyloinformatics tool for trees, alignments and molecular data. *Bioinformatics* (Oxford, England) 24: 715–716. <https://doi.org/10.1093/bioinformatics/btm619>
- Stamatakis A (2006) RAxML-VI-HPC: Maximum likelihood-based phylogenetic analyses with thousands of taxa and mixed models. *Bioinformatics* (Oxford, England) 22: 2688–2690. <https://doi.org/10.1093/bioinformatics/btl446>
- Sulzbacher MA, Grebenc T, Giachini AJ, Baseia IG (2017) Sclerotium-forming fungi from soils of the Atlantic rainforest of Northeastern Brazil. *Plant Ecology and Evolution* 150: 358–362. <https://doi.org/10.5091/plecevo.2017.1148>
- Sun YL, Bau T (2023) *Rhodocybe subasyae*, a new species of *Rhodocybe* sect. *Rufobrunnea* (Entolomataceae, Agaricales) from northeast China. *Mycoscience* 64: 96–100. <https://doi.org/10.47371/mycosci.2023.03.001>
- Tudzynski P, Scheffer JAN (2004) *Claviceps purpurea*: Molecular aspects of a unique pathogenic lifestyle. *Molecular Plant Pathology* 5: 377–388. <https://doi.org/10.1111/j.1364-3703.2004.00237.x>
- Varga T, Krizsán K, Földi C, Dima B, Sánchez-García M, Sánchez-Ramírez S, Szöllősi GJ, Szarkándi JG, Papp V, Albert L, Andreopoulos W, Angelini C, Antonín V, Barry KW, Bougher NL, Buchanan P, Buyck B, Bense V, Catcheside P, Chovatia M, Cooper J, Dámon W, Desjardin D, Finy P, Geml J, Haridas S, Hughes K, Justo A, Karasiński D, Kautmanova I, Kiss B, Kocsubé S, Kotiranta H, LaButti KM, Lechner BE, Liimatainen K, Lipzen A, Lukács Z, Mihaltcheva S, Morgado LN, Niskanen T, Noordeloos ME, Ohm RA, Ortiz-Santana B, Ovrebo C, Rácz N, Riley R, Savchenko A, Shiryayev A, Soop K, Spirin V, Szebenyi C, Tomšovský M, Tulloss RE, Uehling J, Grigoriev IV, Vágvölgyi C, Papp T, Martin FM, Miettinen O, Hibbett DS, Nagy LG (2019) Megaphylogeny resolves global patterns of mushroom evolution. *Nature Ecology & Evolution* 3: 668–678. <https://doi.org/10.1038/s41559-019-0834-1>
- Vizzini A, Musumeci E, Ercole E, Contu M (2011) *Clitopilus chrischonensis* sp. nov. (Agaricales, Entolomataceae), a striking new fungal species from Switzerland. *Nova Hedwigia* 92: 425–434. <https://doi.org/10.1127/0029-5035/2011/0092-0425>



- Vizzini A, Picillo B, Ercole E, Vila J, Contu M (2016) *Rhodocybe formosa* (Agaricales, Entolomataceae): New collections, molecular data and synonymy, and *Rhodocybe griseonigrella* comb. nov. *Phytotaxa* 255: 34–46. <https://doi.org/10.11646/phytotaxa.255.1.3>
- Vizzini A, Ferrari RJ, Ercole E, Fellin A (2018) A new species of *Rhodocybe* sect. *Rufobrunnea* (Entolomataceae, Agaricales) from Italy. *MycKeys* 36: 21–33. <https://doi.org/10.3897/mycokeys.36.27094>
- Vizzini A, Alvarado P, Consiglio G, Angelini C (2023) *Lulesia* Singer (1970), an older name for *Clitocella* Kluting, T.J. Baroni & Bergemann (2014, Entolomataceae). *Rivista Micologica Romana, Bollettino dell'Associazione Micologica Ecologica Romana* 39: 3–23. <https://doi.org/10.57624/AMER.2023.18>
- Vu D, Groenewald M, de Vries M, Gehrmann T, Stielow B, Eberhardt U, Al-Hatmi A, Groenewald JZ, Cardinali G, Houbraken J, Boekhout T, Crous PW, Robert V, Verkley GJM (2019) Large-scale generation and analysis of filamentous fungal DNA barcodes boosts coverage for kingdom fungi and reveals thresholds for fungal species and higher taxon delimitation. *Studies in Mycology* 92: 135–154. <https://doi.org/10.1016/j.simyco.2018.05.001>
- Wang D, Deng WQ, He XL, Peng WH, Gan BC (2017) *Clitopilus fusiformis* (Entolomataceae; Agaricales), a new species from southwest China. *Phytotaxa* 321: 201–207. <https://doi.org/10.11646/phytotaxa.321.2.5>
- Watling R (1974) Dimorphism in *Entoloma abortivum*. *Bulletin Mensuel de la Societe Linneenne de Lyon* 43: 449–470.
- White TJ, Bruns T, Lee S, Taylor J (1990) Amplification and direct sequencing of fungal ribosomal RNA genes for phylogenetics. In: Innis MA, Gelfand DH, Sninsky JJ, White TJ (Eds) *PCR protocols: a guide to methods and applications*. Academic Press, San Diego, California, 315–322. <https://doi.org/10.1016/B978-0-12-372180-8.50042-1>
- Xavier MD, Silva-Filho AGS, Wartchow F, Baseia IG (2022) Fine-scale diversity in *Rhodocybe mellea* (Entolomataceae, Basidiomycota), with a description of a new variety and notes on sclerotia formation in *Rhodocybe*. *Phytotaxa* 538: 87–99. <https://doi.org/10.11646/phytotaxa.538.2.1>
- Xiao Y-Q, Xu Y-D, Chen Z-H, He Z-M (2024) *Lulesia umbrinomarginata* (Entolomataceae, Agaricales), a newly discovered species from Southern China. *Phytotaxa* 650: 60–72. <https://doi.org/10.11646/phytotaxa.650.1.5>
- Zhang P, Ge Y, Bau T (2022) Two new species of *Crepidotus* (Crepidotaceae) from China. *Phytotaxa* 552: 22–34. <https://doi.org/10.11646/phytotaxa.552.1.2>

# Two new species of *Penicillium* (Eurotiales, Aspergillaceae) from China based on morphological and molecular analyses

Rui-Na Liang<sup>1,2</sup>, Xiang-Hao Lin<sup>1</sup>, Miao-Miao An<sup>1</sup>, Guo-Zhu Zhao<sup>1,2</sup>

<sup>1</sup> College of Biological Sciences and Technology, Beijing Forestry University, Beijing 100083, China

<sup>2</sup> National Engineering Research Center of Tree Breeding and Ecological Restoration, Beijing Forestry University, Beijing 100083, China

Corresponding author: Guo-Zhu Zhao (zhaogz@bjfu.edu.cn)

## Abstract

*Penicillium* is a large and significant genus of fungi, exhibiting widespread distribution across diverse substrates. Ongoing taxonomic and nomenclatural revisions have led to an annual increase in the number of newly described species. This study described two new *Penicillium* species, i.e., *P. lentum* and *P. tibetense*, discovered in China. They have been identified and characterized through morphological examination and both single gene and multigene phylogenetic analyses. Based on these analyses, *P. lentum* was classified within the section *Brevicompacta*, while *P. tibetense* was placed in the section *Lanata-Divaricata*. Both species exhibited the morphological features typical of their respective sections. *Penicillium lentum* is characterized by restricted growth with dense colonies on agar media and predominantly generates terverticillate conidiophores. *Penicillium tibetense* demonstrates rapid growth on media and has vigorous growth on CYA at 30 °C, producing biverticillate conidiophores. Comprehensive descriptions and detailed illustrations of these new species were presented. A morphological comparison between the new species and their closely related taxa was provided.

**Key words:** Aspergillaceae, DNA barcodes, section *Brevicompacta*, section *Lanata-Divaricata*, taxonomy



Academic editor: Ning Jiang

Received: 11 February 2025

Accepted: 27 March 2025

Published: 25 April 2025

**Citation:** Liang R-N, Lin X-H, An M-M, Zhao G-Z (2025) Two new species of *Penicillium* (Eurotiales, Aspergillaceae) from China based on morphological and molecular analyses. MycoKeys 116: 255–274. <https://doi.org/10.3897/mycokeys.116.149376>

Copyright: © Rui-Na Liang et al.

This is an open access article distributed under terms of the Creative Commons Attribution License (Attribution 4.0 International – CC BY 4.0).

## Introduction

*Penicillium* is widely distributed across various substrates, primarily in soil, as well as in the atmosphere, food, plant tissues, and other environments. Several species possess considerable value for human applications in food production, biocontrol, and biotechnology. For instance, *P. sclerotiorum* exhibits antagonistic activity against certain plant pathogens, demonstrating potential as a biocontrol agent (Jahan et al. 2024). The food industry utilizes *P. nalgioense* as starter cultures for dry-fermented sausages (Ludemann et al. 2010). The capability of certain species to synthesize pigments has prompted the evaluation of these species for the production of highly stable and safe natural pigments (Morales-Oyervides et al. 2020). Nevertheless, mycotoxins generated by specific species present a significant risk to human and animal health (Nielsen et al. 2017). Notably, patulin exhibits multiple toxicities, including genotoxicity and immunotoxicity, and is predominantly produced by *P. expansum* and *P. griseofulvum* (Bandoh et al. 2009; Puel et al. 2010; Tannous et al. 2014).

Link (1809) introduced the generic name *Penicillium*, which is classified in the family Aspergillaceae. Traditional taxonomy of *Penicillium* primarily relied on morphological characters, including colony diameter, texture, conidial color, and conidiophore branching patterns. However, the variability in morphology has presented substantial challenges in accurately identifying novel species, frequently resulting in the erroneous classification of new isolates under known species (Visagie et al. 2016). Conversely, contemporary taxonomy adopts a polyphasic strategy that incorporates morphological, extrolite, genetic, and multigene phylogenetic data (Visagie et al. 2014). Houbraken et al. (2020) delivered the most comprehensive update on the genus *Penicillium* based on a phylogenetic approach combined with phenotypic, physiologic, and extrolite data. This study recognized 483 species and introduced a novel series classification, which is deemed highly predictive of potential functional traits (Houbraken et al. 2020). Subsequently, Visagie et al. (2024b) applied GCPSR (Genealogical Concordance Phylogenetic Species Recognition) and phylogenetic analyses to reassess the list of *Penicillium* species published up to 31 December 2022, resulting in an updated count of 535 species. An additional 100 species of this genus were described from 1 January 2023 to 31 December 2024 (Ansari et al. 2023; Crous et al. 2023; da Silva et al. 2023; Khuna et al. 2023; Li et al. 2023; Liu et al. 2023; Tan 2023; Tan and Shivas 2023, 2024; Tan et al. 2023, 2024a, 2024b; Wang et al. 2023; Zhang et al. 2023; Araújo et al. 2024; Crous et al. 2024; Liang et al. 2024; Lima et al. 2024; Nóbrega et al. 2024; Song et al. 2024; Visagie et al. 2024a, 2024c; Zhang et al. 2024). The increase in species numbers in recent years indicates the possibility of numerous undiscovered *Penicillium* species, and their biodiversity, ecological functions, and potential for resource development warrant further investigation.

During a comprehensive survey of *Penicillium* biodiversity in China, we found two isolates that could not be classified within existing species. In this paper, we compare these isolates with related species using multi-locus phylogenetic analyses and morphological character assessments. As a result, the isolates are described as species new to science. This study is expected to offer new perspectives on the diversity, function, ecology, and distribution of *Penicillium* members.

## Materials and methods

### Isolates

Soil samples were collected from the rhizosphere of plants in the Kangyu Tunnel, Tibet, China, while indoor dust samples were sourced from Beijing Forestry University, Beijing, China. To isolate the fungus, the samples were suspended in sterile water at a ratio of 1:10, vortexed to ensure homogeneity, and then diluted to  $10^{-4}$  concentrations. Each of 100  $\mu\text{L}$  from  $10^{-2}$ ,  $10^{-3}$ , and  $10^{-4}$  dilutions was spread on potato dextrose agar (PDA) and Martin medium with 50 ppm penicillin and 50 ppm streptomycin. The cultures were incubated at 25 °C for 5–7 days. Individual colonies were then picked from the plates and transferred to fresh PDA plates until pure cultures were obtained. Type specimens, preserved as dry cultures, were deposited in the Fungarium (HMAS), Institute of Microbiology, Chinese Academy of Sciences, while ex-type strains, maintained as living cultures, were stored at the China General Microbiological Culture Collection Centre (CGMCC).

## Morphological studies

Morphological observations of colonies were conducted under strictly standardized conditions, encompassing media preparation, inoculation technique, incubation parameters, and description methods (Visagie et al. 2014). Colony characters and diameters were recorded from cultures grown on Czapek yeast autolysate agar (CYA), malt extract agar (MEA), yeast extract sucrose agar (YES), dichloran 18% glycerol agar (DG18), and creatine sucrose agar (CREA) at 25 °C for 7 days. Additional CYA plates were incubated at 30 and 37 °C. Color names and codes adhered to the book “Color Standards and Color Nomenclature” (Ridgway 1912). Ehrlich reaction was employed to assess the production of indole metabolites; a violet ring observed within ten min was deemed a positive result, while other color changes were interpreted as negative (Lund 1995; Houbraeken et al. 2016).

For light microscopic observations, slides were prepared from cultures grown on MEA, and phenol glycerin solution was used as mounting fluid, with cotton blue staining if necessary. In addition, a field emission scanning electron microscope (Hitachi SU8010, Japan) was employed to examine microstructural characteristics. Agar blocks (3–4 mm × 3–4 mm) were fixed in 2.5% v/v glutaraldehyde at 4 °C for 8–12 hr, then washed three times for 10 min each with 0.1M phosphate buffer. Dehydration was performed with a gradient of ethanol (30, 50, 70, 95, and 100% v/v) for 10–20 min per step, followed by replacement with tert-butanol and ultimate vacuum freeze-dried and gold-sprayed for observation (Wei et al. 2024).

## DNA extraction, sequencing, and phylogenetic analyses

Colonies were cultivated on MEA plates for 5–7 days, and DNA extraction was conducted using the E.Z.N.A.® Fungal DNA Mini Kit (Omega Bio-Tek, Inc., United States). The internal transcribed spacer (ITS), beta-tubulin (*BenA*), calmodulin (*CaM*), and RNA polymerase II second largest subunit (*RPB2*) genes were amplified using primer pairs ITS1/ITS4 (White et al. 1990), Bt2a/Bt2b (Glass and Donaldson 1995), CMD5/CMD6 (Hong et al. 2006), and RPB2-5F/RPB2-7CR (Liu et al. 1999), respectively. Polymerase chain reaction (PCR) amplification followed Visagie et al. (2014). Sequencing reactions were performed by Sangon Biotech (Shanghai) Company Limited, China. DNAMAN software (Lynnon Biosoft) was used for the assembly and trimming of the Sanger chromatograms. Sequences were submitted to GenBank ([www.ncbi.nlm.nih.gov](http://www.ncbi.nlm.nih.gov)).

Sequence similarity searches were conducted using the mega BLAST program of basic local alignment search tool (BLAST) within the NCBI core nucleotide database (core\_nt). Comprehensive sequence datasets were compiled containing newly generated sequences alongside reference sequences sourced from GenBank (Table 1). Sequence alignments were performed using the ClustalW algorithm and subsequently manually edited using MEGA 11 (Tamura et al. 2021). The resulting multiple sequence alignments have been deposited in TreeBASE (submission number: 31847) ([www.treebase.org](http://www.treebase.org)). Phylogenetic trees were constructed based on the ITS, *BenA*, *CaM*, and *RPB2* genes as well as the concatenated sequences of the latter three genes. Phylogenetic analyses were conducted using both maximum likelihood (ML) and Bayesian Inference (BI). ML phylogenies were performed using IQtree v. 1.6.12 (Nguyen et al. 2015), including 1000 standard non-parametric boot-



**Table 1.** Strains of *Penicillium* used for phylogenetic analyses.

Species	Strain	Substrate and origin	GenBank accession numbers			
			ITS	<i>BenA</i>	<i>CaM</i>	<i>RPB2</i>
<i>P. abidjanum</i>	CBS 246.67 <sup>T</sup>	Soil, Ivory Coast	GU981582	GU981650	MN969234	JN121469
<i>P. alagoense</i>	URM 8086 <sup>T</sup>	Leaves of <i>Miconia</i> sp., Brazil	MK804503	MK802333	MK802336	MK802338
<i>P. amphipolaria</i>	CBS 140997 <sup>T</sup>	Soil, Antarctica	KT887872	KT887833	KT887794	MN969177
<i>P. annulatum</i>	CBS 135126 <sup>T</sup>	Air sample, South Africa	JX091426	JX091514	JX141545	KF296410
<i>P. araracuaraense</i>	CBS 113149 <sup>T</sup>	Leaf litter, Colombia	GU981597	GU981642	MN969237	KF296414
<i>P. astrolabium</i>	CBS 122427 <sup>T</sup>	Grapes, Portugal	DQ645804	DQ645793	DQ645808	JN406634
<i>P. ausonianum</i>	CBS 148237 <sup>T</sup>	Sediment of freshwater stream, Spain	LR655808	LR655809	LR655810	LR655811
<i>P. austrosinense</i>	CGMCC 3.18797 <sup>T</sup>	Acidic soil, China	KY495007	KY495116	MN969328	KY495061
<i>P. bialowiezense</i>	CBS 227.28 <sup>T</sup>	Soil under conifers, Poland	EU587315	AY674439	AY484828	JN406604
<i>P. bissettii</i>	CBS 140972 <sup>T</sup>	Soil from spruce forest, Canada	KT887845	KT887806	KT887767	MN969178
<i>P. brasilianum</i>	CBS 253.55 <sup>T</sup>	Herbarium exsiccata, Brazil	GU981577	GU981629	MN969239	KF296420
<i>P. brevicompactum</i>	NRRL 28139	Stroma of a wood decay fungus, USA	AY484917	DQ645795	AY484825	–
	CV1492	Unknown, South Africa	JX091398	JX091533	JX141574	–
	CBS 257.29 <sup>T</sup>	Unknown, Belgium	AY484912	AY674437	AY484813	JN406594
<i>P. buchwaldii</i>	CBS 116980	Wheat, United Kingdom	JX313163	JX313181	JX313147	–
	CBS 116935	Wheat, United Kingdom	JX313156	JX313174	JX313140	–
	CBS 116929	Wheat flour, Denmark	JX313152	JX313170	JX313136	–
	CBS 117181 <sup>T</sup>	<i>Hordeum vulgare</i> , Denmark	JX313164	MN969374	JX313148	JN406637
<i>P. camponoti</i>	CBS 140982 <sup>T</sup>	Carpenter ants, Canada	KT887855	KT887816	KT887777	MN969179
<i>P. cataractarum</i>	CBS 140974 <sup>T</sup>	Fallen nuts of <i>Carya cordiformis</i> , Canada	KT887847	KT887808	KT887769	MN969180
<i>P. coffeatum</i>	CGMCC 3.25152 <sup>T</sup>	Soil, China	OQ870815	OR051121	OR051298	OR051466
<i>P. daleae</i>	CBS 211.28 <sup>T</sup>	Soil under conifer, Poland	GU981583	GU981649	MN969251	KF296427
<i>P. echinulonalgiovense</i>	CBS 328.59 <sup>T</sup>	Unknown, Japan	GU981587	GU981631	KX961269	KX961301
<i>P. excelsum</i>	DTO 357-D7 <sup>T</sup>	Brazil nut shell, Brazil	KR815341	KP691061	KR815342	MN969166
	ITAL 7804	Flowers, Brazil	KT749963	KT749959	KT749962	–
<i>P. expansum</i>	CBS 325.48 <sup>T</sup>	<i>Malus sylvestris</i> , USA	AY373912	AY674400	DQ911134	JF417427
<i>P. fengjieense</i>	CGMCC 3.25157 <sup>T</sup>	Soil, China	OQ870765	OR051156	OR051333	OR051489
<i>P. fennelliae</i>	CBS 711.68 <sup>T</sup>	Soil, Congo	JX313169	MN969382	JX313151	JN406536
<i>P. flaviroseum</i>	CGMCC 3.18805 <sup>T</sup>	Acidic soil, China	KY495032	KY495141	MN969329	KY495083
<i>P. fructuariae-cellae</i>	CBS 145110 <sup>T</sup>	Dried fruit of <i>Vitis vinifera</i> , Italy	MK039434	KU554679	MK045337	–
<i>P. globosum</i>	CBS 144639 <sup>T</sup>	Acidic soil, China	KY495014	KY495123	MN969330	KY495067
<i>P. griseoflavum</i>	CGMCC 3.18799 <sup>T</sup>	Acidic soil, China	KY495011	KY495120	MN969331	KY495064
<i>P. griseopurpureum</i>	CBS 406.65 <sup>T</sup>	Soil under <i>Pinus</i> sp., United Kingdom	KF296408	KF296467	MN969261	KF296431
<i>P. guaibinense</i>	CCDCA 11512 <sup>T</sup>	Soil, Brazil	MH674389	MH674391	MH674393	–
<i>P. guangxiense</i>	CBS 144526 <sup>T</sup>	Soil, China	KY494986	KY495095	MN969332	KY495045
<i>P. hainanense</i>	CGMCC 3.18798 <sup>T</sup>	Acidic soil, China	KY495009	KY495118	MN969333	KY495062
<i>P. infrabuccalum</i>	CBS 140983 <sup>T</sup>	<i>Camponotus pennsylvanicus</i> , Canada	KT887856	KT887817	KT887778	MN969181
<i>P. jianfenglingense</i>	CGMCC 3.18802 <sup>T</sup>	Acidic soil, China	KY495016	KY495125	MN969334	KY495069
<i>P. jinyunshanicum</i>	CGMCC 3.25162 <sup>T</sup>	Soil, China	OQ870766	OR051157	OR051334	OR051490
<i>P. kongii</i>	AS3.15329 <sup>T</sup>	leaf sample of <i>Cotoneaster</i> sp., China	KC427191	KC427171	KC427151	–
<i>P. laevigatum</i>	CGMCC 3.18801 <sup>T</sup>	Acidic soil, China	KY495015	KY495124	MN969335	KY495068
<b><i>P. lentum</i></b>	<b>CGMCC 3.28596<sup>T</sup></b> <b>= B24</b>	<b>Indoor dust, Beijing, China</b>	<b>PQ643282</b>	<b>PQ519854</b>	<b>PQ519855</b>	<b>PQ519856</b>
<i>P. mariae-crucis</i>	CBS 271.83 <sup>T</sup>	<i>Secale cereale</i> , Spain	GU981593	GU981630	MN969275	KF296439
<i>P. marykayhuntingiae</i>	BRIP 74934a <sup>T</sup>	Soil, Australia	OR271913	OR269446	–	OR269440
<i>P. neocrassum</i>	CBS 122428 <sup>T</sup>	Grapes, Madeira	DQ645805	DQ645794	DQ645809	JN406633
<i>P. newtonturnerae</i>	BRIP 74909a <sup>T</sup>	Soil, Australia	OP903478	OP921964	OP921962	OP921963
<i>P. ochrochloron</i>	CBS 357.48 <sup>T</sup>	Copper sulphate solution, USA	GU981604	GU981672	MN969280	KF296445
	DTO 189-A6	Unknown, Japan	KC346347	KC346324	KC346341	KC346318

Species	Strain	Substrate and origin	GenBank accession numbers			
			ITS	BenA	CaM	RPB2
<i>P. olsonii</i>	CBS 232.60 <sup>T</sup>	<i>Musa</i> , France	EU587341	AY674445	DQ658165	JN121464
<i>P. onobense</i>	CBS 174.81 <sup>T</sup>	Soil, andosol, Spain	GU981575	GU981627	MN969281	KF296447
<i>P. panissanguineum</i>	CBS 140989 <sup>T</sup>	Soil near termite mound, Tanzania	KT887862	KT887823	KT887784	MN969182
<i>P. paraherquei</i>	CBS 338.59 <sup>T</sup>	Soil, Japan	AF178511	KF296465	MN969285	KF296449
<i>P. pauciramulum</i>	CGMCC 3.25164 <sup>T</sup>	Soil, associated with nest of Formicidae, China	OQ870726	OR051111	OR051288	OR051457
<i>P. pedernalense</i>	CBS 140770 <sup>T</sup>	<i>Litopenaeus vannamei</i> , Ecuador	KU255398	KU255396	MN969322	MN969184
<i>P. penarojense</i>	CBS 113178 <sup>T</sup>	Leaf litter, Colombia	GU981570	GU981646	MN969287	KF296450
<i>P. piscarium</i>	CBS 362.48 <sup>T</sup>	Cod-liver oil emulsion, Germany	GU981600	GU981668	MN969288	KF296451
<i>P. pulvillorum</i>	CBS 280.39 <sup>T</sup>	Acidic soil, United Kingdom	AF178517	GU981670	MN969289	KF296452
	CBS 275.83	Rye grain, Spain	GU981601	GU981671	KC346336	KF296423
<i>P. rolfsii</i>	CBS 368.48 <sup>T</sup>	Fruit of <i>Ananas sativus</i> , USA	JN617705	GU981667	MN969294	KF296455
<i>P. roodeplaatense</i>	DTO 444-C8	Soil, South Africa	OR819195	OR820176	OR820180	OR820186
<i>P. rotoruae</i>	CBS 145838 <sup>T</sup>	<i>Pinus radiata</i> timber stake in ground contact, New Zealand	MN315103	MN315104	MN315102	MT240842
<i>P. rubriannulatum</i>	CGMCC 3.18804 <sup>T</sup>	Acidic soil, China	KY495029	KY495138	MN969336	KY495080
<i>P. salamii</i>	CBS 135391 <sup>T</sup>	Salami, Italy	HG514431	HG514437	HG514432	MN969160
<i>P. simplicissimum</i>	CBS 372.48 <sup>T</sup>	<i>Secale cereale</i> , Spain	GU981588	GU981632	MN969297	JN121507
<i>P. singorense</i>	CBS 138214 <sup>T</sup>	House dust, Thailand	KJ775674	KJ775167	KJ775403	MN969138
<i>P. skrjabinii</i>	CBS 439.75 <sup>T</sup>	Soil, Russia	GU981576	GU981626	MN969299	EU427252
<i>P. soliforme</i>	CGMCC 3.18806 <sup>T</sup>	Acidic soil, China	KY495038	KY495147	MN969337	KY495047
	NN072390	Acidic soil, China	KY495019	KY495128	KY494959	KY495072
	NN072399	Acidic soil, China	KY495022	KY495131	KY494962	KY495074
<i>P. spathulatum</i>	CBS 117192 <sup>T</sup>	Mouldy chestnut ( <i>Castanea</i> sp.), France	JX313165	MN969400	JX313149	JN406636
<i>P. spinuliferum</i>	CBS 144483 <sup>T</sup>	Acidic soil, associated with <i>Litchi chinensis</i> , China	KY495040	KY495149	MN969338	KY495090
<i>P. stangiae</i>	URM 8347 <sup>T</sup>	Soil, Brazil	MW648590	MW646388	MW646390	MW646392
<i>P. stolkiaie</i>	CBS 315.67 <sup>T</sup>	Soil, South Africa	AF033444	JN617717	AF481135	JN121488
<i>P. subfuscum</i>	CBS 147455 <sup>T</sup>	Soil, South Africa	MT949907	MT957412	MT957454	MT957480
<i>P. subrubescens</i>	CBS 132785 <sup>T</sup>	Soil of <i>Helianthus tuberosus</i> field, Finland	KC346350	KC346327	KC346330	KC346306
<i>P. subrutilans</i>	CGMCC 3.25174 <sup>T</sup>	Soil, China	OQ870816	OR051137	OR051314	OR051479
<i>P. svalbardense</i>	CBS 122416 <sup>T</sup>	Glacial ice, Svalbard	GU981603	DQ486644	KC346338	KF296457
<i>P. taii</i>	CGMCC 3.25176 <sup>T</sup>	Soil, China	OQ870778	OR051170	OR051347	OR051496
<i>P. tanzanicum</i>	CBS 140968 <sup>T</sup>	Soil near termite mound, Tanzania	KT887841	KT887802	KT887763	MN969183
<i>P. terrarumae</i>	CBS 131811 <sup>T</sup>	Soil contaminated by heavy metals, China	MN431397	KX650295	MN969323	MN969185
	CS23-08	Unknown, China	OQ870751	OR051141	OR051318	OR051481
<i>P. tularense</i>	CBS 430.69 <sup>T</sup>	Soil under <i>Pinus ponderosa</i> and <i>Quercus kelloggii</i> , USA	AF033487	KC427175	JX313135	JN121516
	CBS 431.69	Soil under <i>Pinus ponderosa</i> and <i>Quercus kelloggii</i> , USA	JX313167	AY674433	JX313134	–
<i>P. vanderhammenii</i>	CBS 126216 <sup>T</sup>	Leaf litter, Colombia	GU981574	GU981647	MN969308	KF296458
<i>P. vasconiae</i>	CBS 339.79 <sup>T</sup>	Soil, Spain	GU981599	GU981653	MN969309	MN969144
<i>P. vickeryae</i>	BRIP 72552a <sup>T</sup>	Soil, Australia	OP903479	OP921966	–	OP921965
<i>P. viridissimum</i>	CGMCC 3.18796 <sup>T</sup>	Acidic soil, China	KY495004	KY495113	MN969339	KY495059
<i>P. wotroi</i>	CBS 118171 <sup>T</sup>	Leaf litter, Colombia	GU981591	GU981637	MN969313	KF296460
<b><i>P. tibetense</i></b>	<b>CGMCC 3.28597<sup>T</sup> = XZ5-3</b>	<b>Rhizosphere soil, Tibet, China</b>	<b>PQ643284</b>	<b>PQ519857</b>	<b>PQ519858</b>	<b>PQ519859</b>
<i>P. yuyongnianii</i>	CGMCC 3.25187 <sup>T</sup>	Soil, China	OQ870820	OR051175	OR051352	OR051499
<i>P. zonatum</i>	CBS 992.72 <sup>T</sup>	Soil, USA	GU981581	GU981651	MN969315	KF296461

strap replicates with the best partition scheme and substitution model selected using ModelFinder (Kalyaanamoorthy et al. 2017). BI phylogenies were run in MrBayes v. 3.2.7 (Ronquist et al. 2012). Best fit models were selected according to the Akaike information criterion (AIC) using MrModeltest v. 2.4 (Nylander 2004). Posterior probabilities (PP) were estimated using Markov Chain Monte Carlo (MCMC) sampling, set to run for 1,000,000 generations with the average standard deviation of split frequencies less than 0.01 as the stopping criterion. In cases where this threshold was not achieved, the run was continued until the condition was met. Additionally, the initial 25% of the generated trees were discarded as burn-in.

## Results

### Morphology

Two novel species, *Penicillium lentum* and *P. tibetense*, were introduced within the sections *Brevicompacta* and *Lanata-Divaricata*, respectively, based on comprehensive phylogenetic analyses. General morphological characteristics and ecological information for the species included in these sections are provided in Table 2. Both newly described species exhibited morphological traits consistent with their respective sections. Specifically, *P. lentum* displayed limited growth with dense colonies on agar media and primarily produced terverticillate conidiophores. In contrast, *P. tibetense* demonstrated rapid growth on agar media, particularly exhibiting robust development on CYA at 30 °C, and predominantly formed biverticillate conidiophores. The morphological features of the new species and their closely related species are summarized in Table 3.

**Table 2.** Morphological and ecological data pertaining to the sections of the new species in this study.

Section	Morphology	Ecology	References
<i>Brevicompacta</i>	Colonies restricted (occasionally moderately fast), texture velutinous; conidiophores terverticillate or multiramulate branched with wide stipes, smooth-walled.	Mainly soil and foods, also on plant leaves and rotting wood.	(Houbraken and Samson 2011; Frisvad et al. 2013; Wang and Wang 2013; Houbraken et al. 2020)
<i>Lanata-Divaricata</i>	Colonies grow rapidly, occasionally moderately fast; conidiophores monoverticillate, biverticillate or divaricate, occasionally terverticillate.	Commonly found in soil, also on rotting leaf litter and vegetable.	(Houbraken and Samson 2011; Houbraken et al. 2020)

**Table 3.** Morphological features of new species and their closely related taxa.

Species	Growth rates (mm)			Conidiophores branching	Cleistothecia /sclerotia	Conidia			Acid production on CREA
	CYA	CYA 30 °C	CYA 37 °C			Size	Shape	Roughening	
<i>P. lentum</i>	7–10	No growth	No growth	Terverticillate, sometimes biverticillate	Absent	2–3 × 1.5–2.5 µm	Broadly ellipsoidal	Smooth	Absent
<i>P. tularense</i> <sup>a</sup>	n.a.	n.a.	n.a.	Asymmetric and divaricate	Cleistothecia	2.2–2.6 µm	Globose to subglobose	Smooth	n.a.
<i>P. tibetense</i>	42–50	42–52	21–27	Biverticillate	Absent	1.5–3 µm	Globose to subglobose	Finely rough	Absent
<i>P. excelsum</i> <sup>b</sup>	35–50	n.a.	8–22	Biverticillate, sometimes terverticillate	Absent	4–5 × 2–3.2 µm	Ellipsoidal	Smooth	Absent

<sup>a</sup>Description based on Paden (1971), <sup>b</sup>Description based on Taniwaki et al. (2016).

## Phylogenetic analyses

A BLAST search revealed that strain CGMCC 3.28596 is most closely related to *Penicillium tularense* (Identities: ITS: 97.52%, *BenA*: 81.13%, *CaM*: 84.91%, *RPB2*: 91.00%) within section *Brevicompecta*, and strain CGMCC 3.28597 exhibits the highest similarity to *P. excelsum* (Identities: ITS: 98.64%, *BenA*: 94.37%, *CaM*: 89.66%, *RPB2*: 94.84%) within section *Lanata-Divaricata*.

## Section *Brevicompecta*

The analyses of the concatenated dataset (*BenA*, *CaM*, and *RPB2*) comprised 20 predominantly ex-type strains, each with a total sequence length of 1876 bp (*BenA*: 469 bp, *CaM*: 512 bp, *RPB2*: 895 bp). Phylogenetic analyses divided section *Brevicompecta* into four distinct clades, with the new species *Penicillium lentum* forming a robustly supported clade alongside *P. tularense* (100% bs, 1.00 pp) (Fig. 1). In the phylogenetic analyses of individual genes, the new species, together with *P. tularense*, consistently formed a well-supported clade, mostly with high support values (>97% bs, 1.00 pp), except for ITS (Fig. 2).

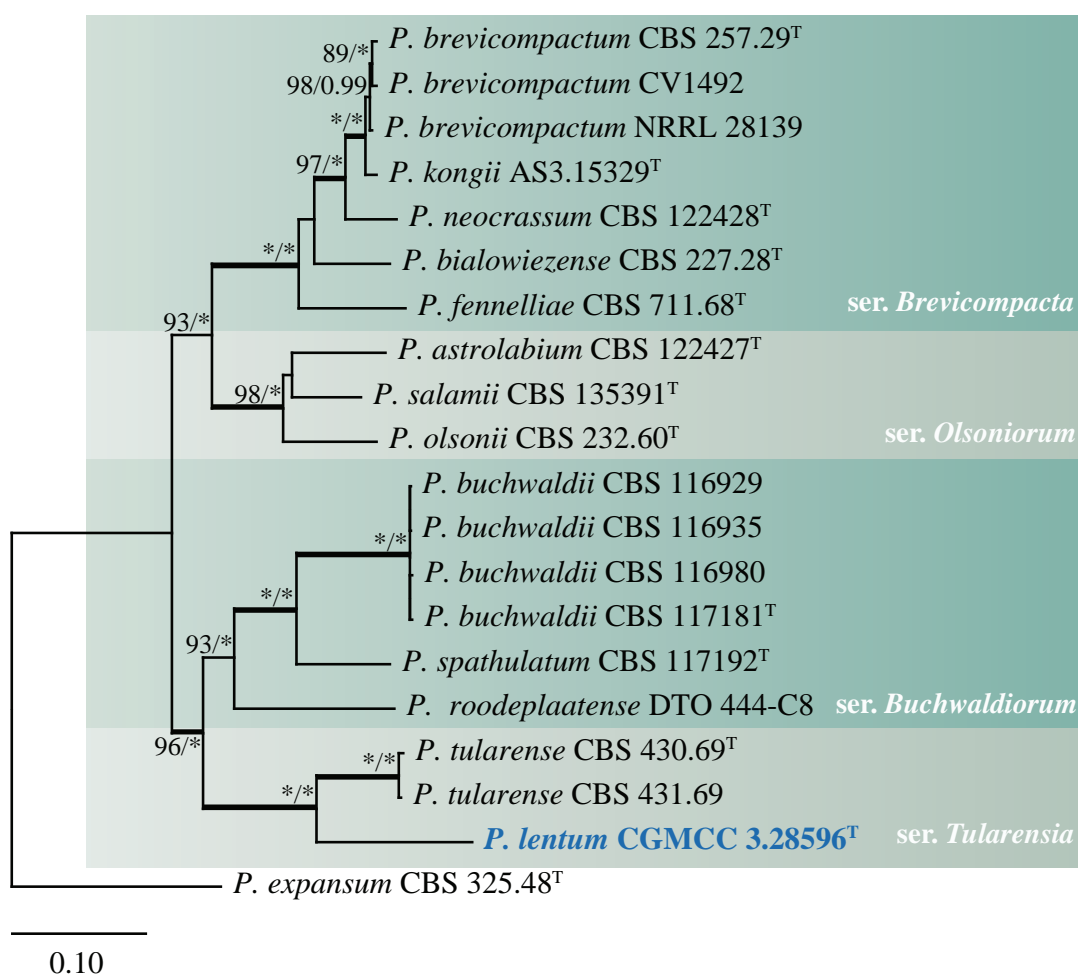


**Figure 1.** ML tree based on the concatenated data set (*BenA*, *CaM*, and *RPB2*) of section *Brevicompecta*. *Penicillium expansum* CBS 325.48<sup>T</sup> was designated as the outgroup. Nodes display bootstrap values (bs) exceeding 70% or posterior probabilities (pp) greater than 0.95. Branches with bs of 95% or higher and pp of 1.00 are depicted in bold. The strain described as the new species *P. lentum* is indicated with blue text. \* Indicates bs = 100% or pp = 1.00, <sup>T</sup> = ex-type strain.



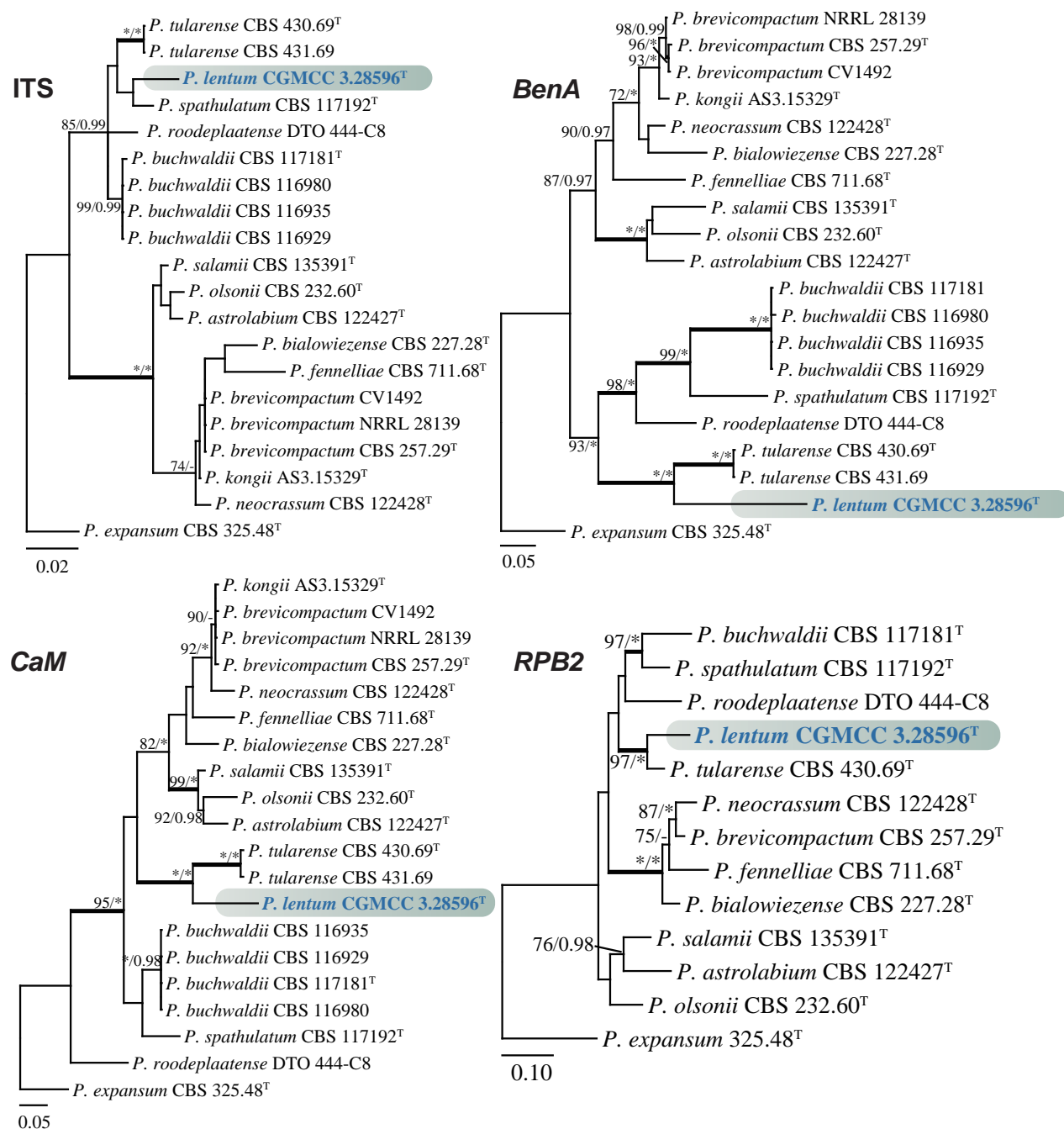


**Figure 2.** ML trees for section *Brevicompecta* based on ITS, *BenA*, *CaM*, and *RPB2*. *Penicillium expansum* CBS 325.48<sup>T</sup> was designated as the outgroup. Nodes display bootstrap values (bs) exceeding 70% or posterior probabilities (pp) greater than 0.95. Branches with bs of 95% or higher and pp of 1.00 are depicted in bold. The strain described as the new species *P. lentum* is indicated with blue text. \* Indicates bs = 100% or pp = 1.00, <sup>T</sup> = ex-type strain.

### Section *Lanata-Divaricata*

In this section, we selected the series *Simplicissima*, *Dalearum*, and *Rolfsiorum*, comprising 71 predominantly ex-type strains, for phylogenetic analyses based on the concatenated dataset totaling 1876 bp (*BenA*: 504 bp, *CaM*: 617 bp, *RPB2*: 755 bp). The resulting phylogenies revealed that *Penicillium tibetense* is closely related to *P. excelsum* (64% bs, 0.97 pp; not depicted in Fig. 3). However, the significant evolutionary divergence observed supports the recognition of

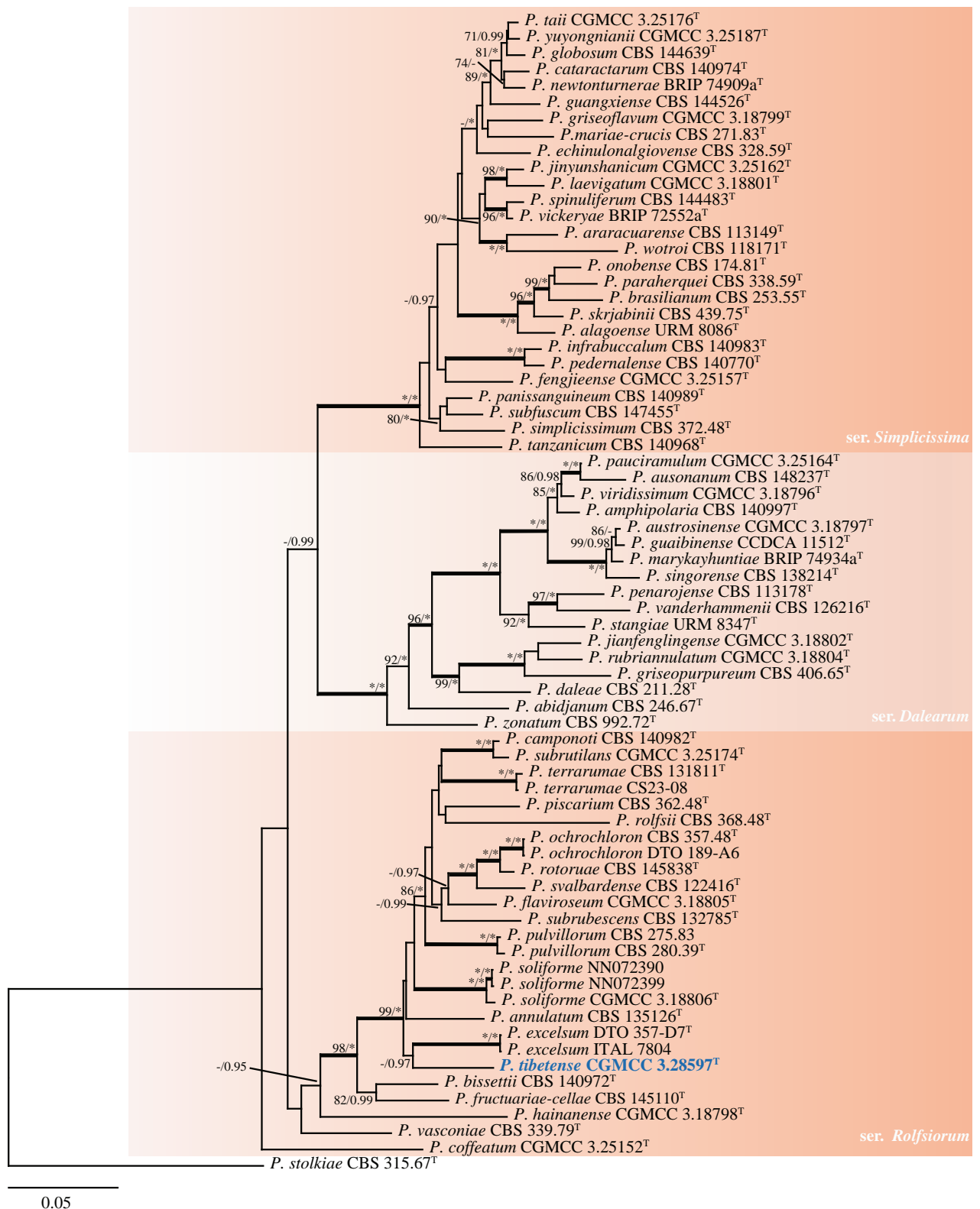


**Figure 3.** ML tree based on the concatenated data set (*BenA*, *CaM*, and *RPB2*) of section *Lanata-Divaricata* (series *Simplicissima*, *Dalearum*, and *Rolfsiorum*). *Penicillium stolckiae* CBS 315.67<sup>T</sup> was designated as the outgroup. Nodes display bootstrap values (bs) exceeding 70% or posterior probabilities (pp) greater than 0.95. Branches with bs of 95% or higher and pp of 1.00 are depicted in bold. The strain described as the new species *P. tibetense* is indicated with blue text. \* Indicates bs = 100% or pp = 1.00, <sup>T</sup> = ex-type strain.

*P. tibetense* as a distinct species (Fig. 3). Phylogenetic analyses of individual genes within series *Rolfisiorum* demonstrated generally weak clustering support, with variations observed among the ITS, *BenA*, *CaM*, and *RPB2* datasets. Furthermore, *P. ochrochloron* and *P. rotoruae* share identical ITS sequences, making them indistinguishable through ITS phylogeny alone (Fig. 4).

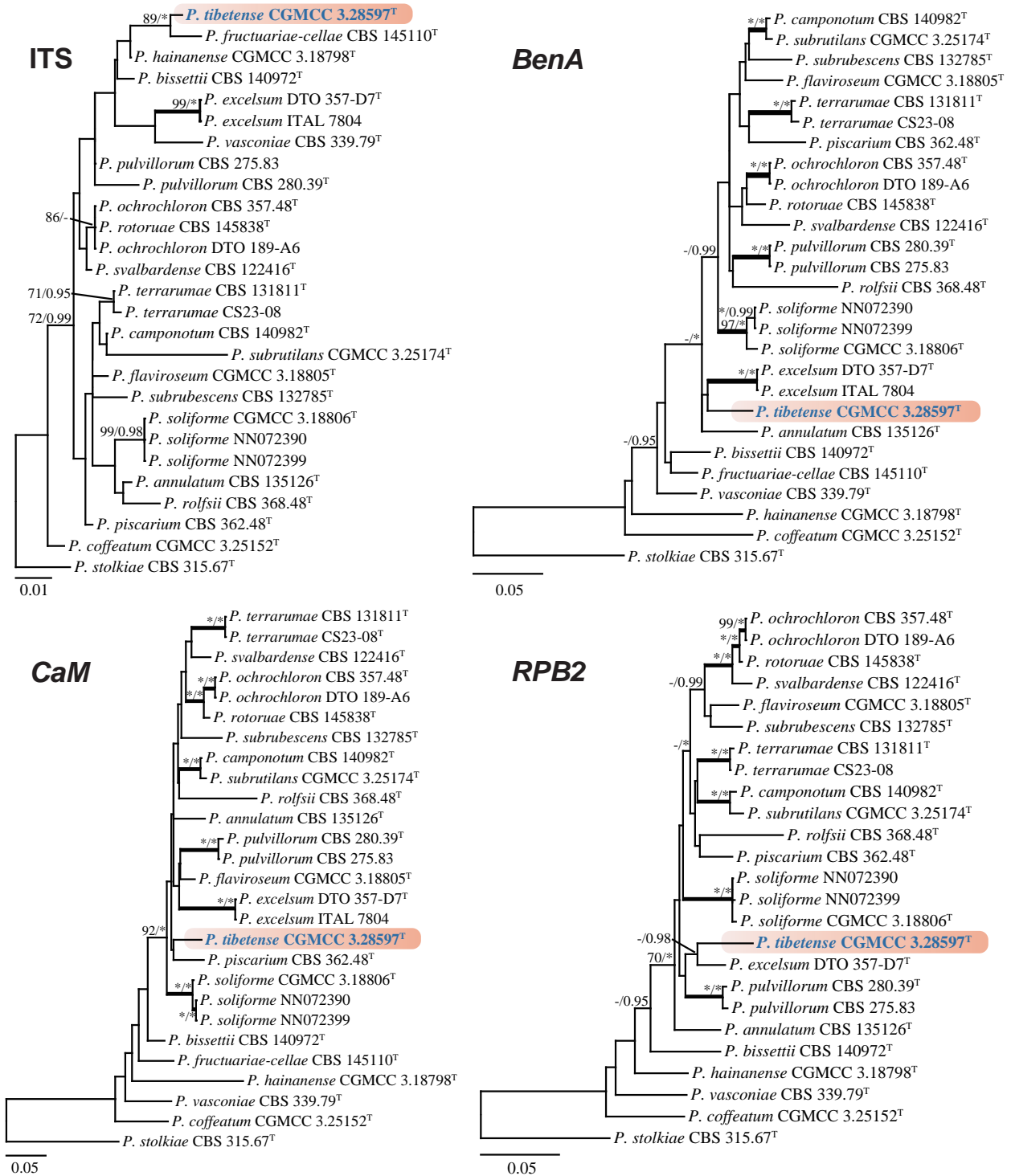


**Figure 4.** ML trees for section *Lanata-Divarcata* series *Rolfisiorum* based on ITS, *BenA*, *CaM*, and *RPB2*. *Penicillium stolkia* CBS 315.67<sup>T</sup> was designated as the outgroup. Nodes display bootstrap values (bs) exceeding 70% or posterior probabilities (pp) greater than 0.95. Branches with bs of 95% or higher and pp of 1.00 are depicted in bold. The strain described as the new species *P. tibetense* is indicated with blue text. \* Indicates bs = 100% or pp = 1.00, <sup>T</sup> = ex-type strain.

## Taxonomy

### *Penicillium lentum* R.N. Liang & G.Z. Zhao, sp. nov.

MycoBank No: 857346

Fig. 5

**Infrageneric classification.** Subgenus *Penicillium*, section *Brevicompecta*, series *Tularensia*.

**Etymology.** The specific epithet "*lentum*" is derived from *lentus* (Latin), reflecting the slow growth rate characteristic of this species.

**Type.** CHINA • Beijing, Haidian District, Beijing Forestry University, 40°0'20"N, 116°20'51"E, from indoor dust, 1 February 2024, collected by G.Z. Zhao, B24 (holotype HMAS 353385, dried culture; culture ex-type CGMCC 3.28596).

**Colony diameter after 7 d (mm).** CYA 7–10; CYA 30 °C, 37 °C no growth; MEA 6–9; YES 9–13; DG18 7–11; CREA 3.5–5.

**Colony characteristics (7 d).** CYA at 25 °C: Colonies deep, raised at center, margins low, narrow, irregular; mycelium white; texture velutinous, floccose areas present; sporulation moderate to good, conidia antique green (R. Pl. VI); exudate clear; reverse capucine buff (R. Pl. III); soluble pigment absent. MEA at 25 °C: Colonies deep, raised at center, margins low, narrow, entire; mycelium white; texture velutinous, floccose areas present; sporulation moderate to good, conidia celandine green (R. Pl. XLVII) to deep turtle green (R. Pl. XXXII); exudate clear; reverse light orange-yellow (R. Pl. III); soluble pigment absent. YES at 25 °C: Colonies deep, radially and concentrically sulcate, raised at center, margins low, narrow, entire; mycelium white; texture velutinous and fasciculate; sporulation good to strong, conidia glaucous-green (R. Pl. XXXIII); exudate absent; reverse cinnamon (R. Pl. XXIX); soluble pigment absent. DG18 at 25 °C: Colonies low, plane, margins low, wide, entire; mycelium white; texture velutinous and fasciculate; sporulation good, conidia bluish gray-green (R. Pl. XLII); exudate absent; reverse antimony yellow (R. Pl. XV); soluble pigment absent. CREA at 25 °C: Weak growth, no acid production. Ehrlich reaction negative.

**Micromorphology.** *Conidiophores* biverticillate to terverticillate; *stipes* smooth-walled, 70–236.5 × 2.5–4.5 µm; *rami* two when present, 6.5–18 × 2–4 µm; *metulae* divergent, 2–4 per branch/ramus, 4.0–13.0 × 2.5–4.5 µm; *phialides* ampulliform, 3–8 per metula, 4.5–8.0 × 2–3 µm; *conidia* broadly ellipsoidal, smooth-walled, 2–3 × 1.5–2.5 µm.

**Notes.** *Penicillium lentum* belongs to section *Brevicompecta* and is most closely related to *P. tularensis* (Fig. 1). *Penicillium tularensis* produces light brown to pale tan cleistothecia, which are not found in the new species (Paden 1971). Additionally, *P. lentum* has broadly ellipsoidal conidia, while *P. tularensis* produces globose to subglobose conidia (Table 3).

### *Penicillium tibetense* R.N. Liang & G.Z. Zhao, sp. nov.

MycoBank No: 857347

Fig. 6

**Infrageneric classification.** Subgenus *Aspergilloides*, section *Lanata-Divaricata*, series *Rolfisiorum*.



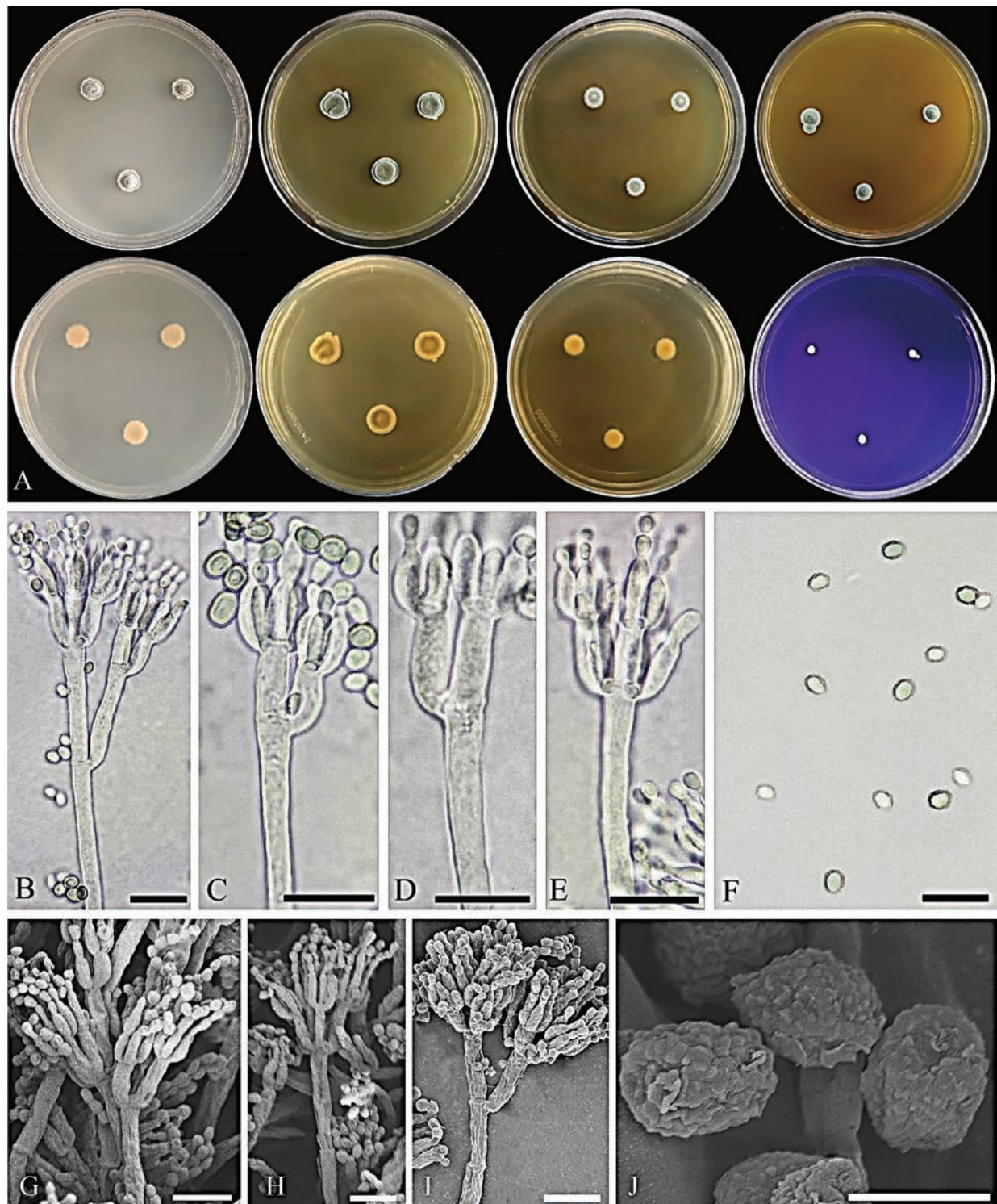


**Figure 5.** *Penicillium lentum* CGMCC 3.28596. **A** Colonies on medium at 25 °C for 7d (left to right, top row: CYA, YES, DG18, MEA obverse; second row: CYA reverse, YES reverse, DG18 reverse, CREA obverse) **B–E** conidiophores **F** conidia **G–I** SEM micrograph of conidiophores **J** SEM micrograph of conidia. Scale bars: 10 µm (**B–I**); 2 µm (**J**).

**Etymology.** The specific epithet “*tibetense*” denotes the geographical origin of the species, indicating its discovery in Tibet.

**Type.** CHINA • Tibet, Changdu City, Basu County, Kangyu Tunnel, 30°33'53"N, 96°15'25"E, from rhizosphere soil of grasses, 19 July 2023, collected by X.W. Peng, XZ5-3 (holotype HMAS 353386, dried culture; culture ex-type CGMCC 3.28597).



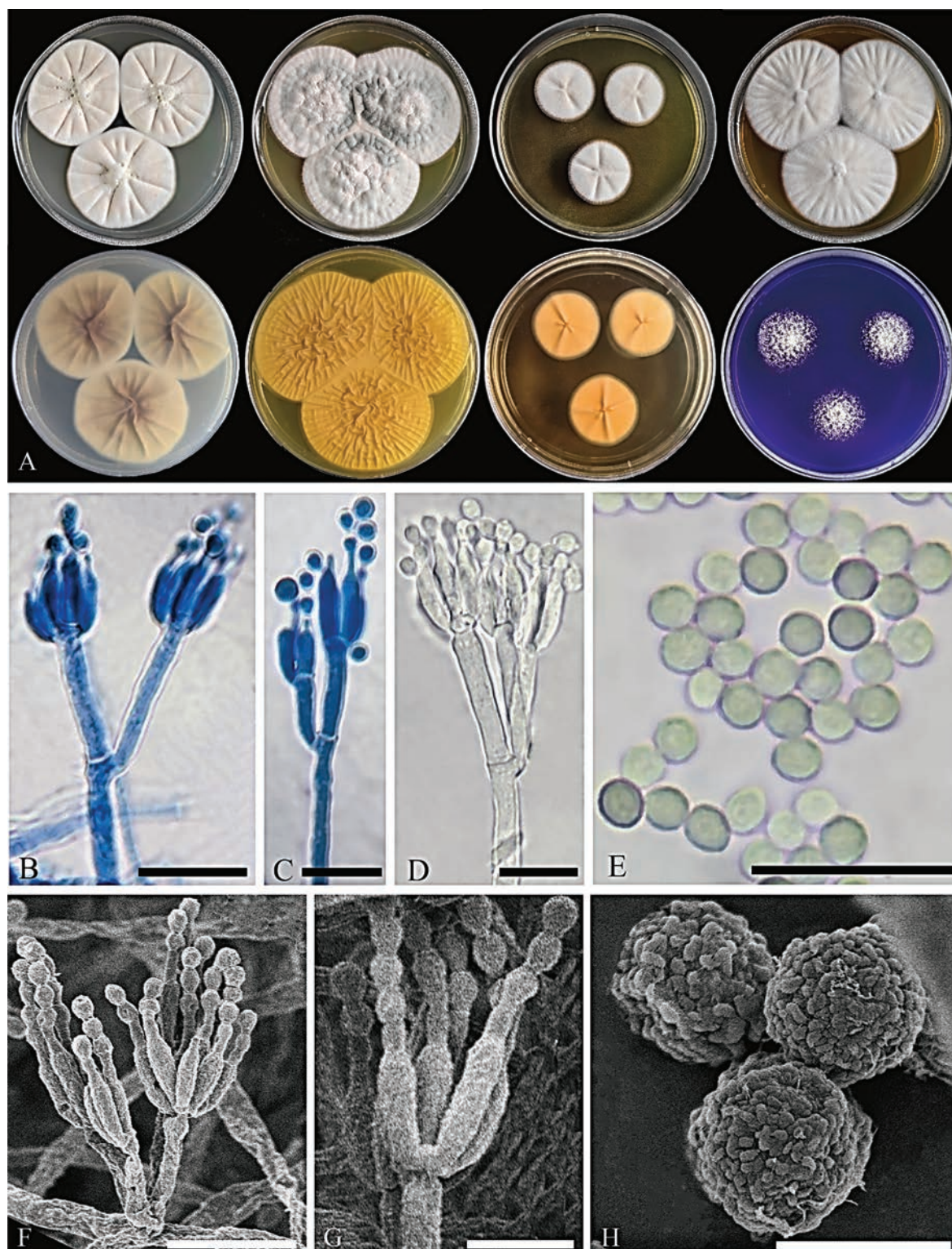


**Figure 6.** *Penicillium tibetense* CGMCC 3.28597. **A** Colonies on medium at 25 °C for 7d (left to right, top row: CYA, YES, DG18, MEA obverse; second row: CYA reverse, YES reverse, DG18 reverse, CREA obverse) **B–D** conidiophores **E** conidia **F, G** SEM micrograph of conidiophores **H** SEM micrograph of conidia. Scale bars: 10 µm (**B–G**); 2 µm (**H**).

**Colony diameter after 7 d (mm).** CYA 42–50; CYA 30 °C 42–52; CYA 37 °C 21–27; MEA 48–52; YES 46–52; DG18 20–26; CREA 24–26.

**Colony characteristics (7 d).** CYA at 25 °C: Colonies low to moderately deep, radially sulcate, margins low, narrow, entire; mycelium white; texture floccose;

sporulation moderate, conidia livid pink (R. Pl. XXVII); exudate clear; reverse light purple-drab (R. Pl. XLV) to avellaneous (R. Pl. XL); soluble pigment absent. CYA at 30 °C: Colonies low to moderately deep, radially sulcate, margins low, narrow, entire; mycelium white; texture floccose; sporulation moderate, conidia livid pink (R. Pl. XXVII); exudate clear; reverse brownish vinaceous (R. Pl. XXXIX); soluble pigment absent. CYA at 37 °C: Colonies moderately deep, radially sulcate, margins low, narrow, entire; mycelium white; texture floccose; sporulation sparse, conidia livid pink (R. Pl. XXVII); exudate clear; reverse light buff (R. Pl. XV); soluble pigment absent. MEA at 25 °C: Colonies low to moderately deep, radially sulcate, margins low, narrow, entire; mycelium white; texture floccose; sporulation sparse to moderate, conidia pale brownish vinaceous (R. Pl. XXXIX); exudate clear; reverse antimony yellow (R. Pl. XV); soluble pigment absent. YES at 25 °C: Colonies moderately deep, randomly sulcate, margins low, wide, entire; mycelium white; texture floccose; sporulation moderate, conidia antique green (R. Pl. VI); exudate clear; reverse antimony yellow (R. Pl. XV); soluble pigment absent. DG18 at 25 °C: Colonies low, radially sulcate, margins low, wide, entire; mycelium white; texture floccose; sporulation sparse, conidia ecru-drab (R. Pl. XLVI); exudate absent; reverse orange-pink (R. Pl. II); soluble pigment absent. CREA at 25 °C: Strong growth, no acid production. Ehrlich reaction negative.

**Micromorphology.** *Conidiophores* biverticillate; *stipes* finely rough-walled, 27–364.5 × 2–3 µm; *metulae* appressed to divergent, 2–4 per stipe, 8–15 × 1.5–3 µm; *phialides* ampulliform to cylindrical, 2–6 per metula, 5–10.5 × 1.5–3 µm; *conidia* globose to subglobose, finely rough-walled, 1.5–3 µm diam.

**Notes.** *Penicillium tibetense* is classified in section *Lanata-Divaricata* and exhibits a close phylogenetic relationship to *P. excelsum* (Fig. 3). This novel species generates globose to subglobose, finely rough-walled conidia that distinguish it from *P. excelsum* (Table 3). Additionally, *P. tibetense* demonstrates more robust growth on CYA at 37 °C compared to *P. excelsum* (21–27 mm vs. 8–22 mm) (Taniwaki et al. 2016).

## Discussion

*Penicillium*, a ubiquitous and diverse fungal genus, plays pivotal roles in natural ecosystems while maintaining substantial economic importance and significant relevance to human affairs. The recent rapid increase in newly described species within this genus suggests that numerous taxa remain undiscovered. Given the extensive biotechnological applications of *Penicillium* species, accurate taxonomic identification is paramount, necessitating comprehensive species delineation through polyphasic approaches. In the present study, we introduced two novel species: one belonging to section *Brevicompecta* and the other to section *Lanata-Divaricata*.

Section *Brevicompecta* currently comprises 15 species distributed across four series (Visagie et al. 2024a, 2024b) and is represented in our findings by the newly described *P. lentum* sp. nov. This species, classified within series *Tularensia*, is characterized by predominantly terverticillate conidiophores and demonstrates a close relationship with other members of section *Brevicompecta* (Table 2). Section *Lanata-Divaricata* is characterized by its remarkable species diversity and rapid colony growth, primarily comprising soil-inhabiting

species, with over 90 taxa currently recognized across five series (Houbraken et al. 2020; Visagie et al. 2024b). The newly identified *Penicillium tibetense* assigned to series *Rolfsiorum* exhibits characteristic rapidly expanding colonies and produces biverticillate conidiophores, consistent with the morphological features typical of this series. Members of section *Lanata-Divaricata* are ecologically significant as decomposers of organic matter (Lichtner et al. 2022), with notable biotechnological potential exemplified by *P. subrubescens*, which has demonstrated efficient inulinase production (Mansouri et al. 2013).

Phylogenetic analyses of section *Brevicompacta* demonstrated that our strain *P. lentum* formed a well-supported clade with its closest relative, *P. tularense* (Fig. 1), a relationship corroborated by shared morphological characteristics such as conidiophore branching patterns and growth rates. However, our strain could be clearly distinguished from *P. tularense* based on distinct phenotypic features, including the presence or absence of cleistothecia and differences in conidial morphology (Table 3). The phylogenetic relationships within section *Lanata-Divaricata* remain unresolved, primarily due to the poor support values in certain clades (Houbraken et al. 2020), exemplified by a clade comprising *P. camponoti*, *P. piscarium*, *P. rolfsii*, *P. subrutilans*, and *P. terrarumae* (Fig. 3), which highlights the persistent challenges in resolving certain taxonomic groups even with multigene phylogenetic approaches.

To address these limitations, we recommend expanding the taxonomic sampling to include strains from diverse geographical origins and ecological niches. This strategy would not only generate additional reference sequences but also facilitate the discovery of novel species and the detection of infraspecific variation (Visagie and Houbraken 2020). Furthermore, sequencing additional gene regions represents a promising approach to enhance phylogenetic resolution (Visagie et al. 2021). The rapid development of high-throughput sequencing technologies has resulted in an accelerated increase in genomic data availability (Kapli et al. 2020), positioning phylogenomics as an essential tool in modern fungal taxonomy and systematics. By leveraging genome-scale data, phylogenomics is poised to overcome the limitations of single gene or multigene analyses, providing robust statistical support for clade resolution and enabling the reconstruction of a highly resolved fungal tree of life (Burki et al. 2020; Zhou and May 2023). These advancements underscore the transformative potential of phylogenomics in addressing long-standing taxonomic challenges and refining our understanding of fungal evolutionary relationships.

## Acknowledgements

We express our sincere gratitude to Professor Xia-Wei Peng for her invaluable assistance in the collection of soil samples from Tibet.

## Additional information

### Conflict of interest

The authors have declared that no competing interests exist.

### Ethical statement

No ethical statement was reported.



## Funding

This work was funded by the National Natural Science Foundation of China (No. 31570019, 31093440) and the Survey Project of Alien Invasive Species and Grassland Pest in Mentougou District (2022HXFWSWXY038).

## Author contributions

Rui-Na Liang: Formal analysis, investigation, data curation, writing – original draft preparation, visualization; Xiang-Hao Lin and Miao-Miao An: Investigation, visualization; Guo-Zhu Zhao: Conceptualization, methodology, validation, resources, writing – review and editing, supervision, funding acquisition. All authors have read and agreed to the published version of the manuscript.

## Data availability

All of the data that support the findings of this study are available in the main text. All sequences generated in this study have been submitted to GenBank.

## References

- Ansari L, Asgari B, Zare R, Zamanizadeh HR (2023) *Penicillium rhizophylum*, a novel species in the section *Exilicaulis* isolated from the rhizosphere of sugarcane in South-west Iran. *International Journal of Systematic and Evolutionary Microbiology* 73: 006028. <https://doi.org/10.1099/ijsem.0.006028>
- Araújo KS, Alves JL, Pereira OL, de Queiroz MV (2024) Five new species of endophytic *Penicillium* from rubber trees in the Brazilian Amazon. *Brazilian Journal of Microbiology* 55: 3051–3074. <https://doi.org/10.1007/s42770-024-01478-9>
- Bandoh S, Takeuchi M, Ohsawa K, Higashihara K, Kawamoto Y, Goto T (2009) Patulin distribution in decayed apple and its reduction. *International Biodeterioration & Biodegradation* 63: 379–382. <https://doi.org/10.1016/j.ibiod.2008.10.010>
- Burki F, Roger AJ, Brown MW, Simpson AGB (2020) The New Tree of Eukaryotes. *Trends in Ecology & Evolution* 35: 43–55. <https://doi.org/10.1016/j.tree.2019.08.008>
- Crous PW, Osieck ER, Shivas RG, Tan Y, Bishop-Hurley SL, Esteve-Raventós F, Larsson E, Luangsa-ard JJ, Pancorbo F, Balashov S, Baseia IG, Boekhout T, Chandranayaka S, Cowan DA, Cruz R, Czachura P, De la Peña-Lastra S, Dovana F, Drury B, Fell J, Flakus A, Fotedar R, Jurjevic Z, Kolecka A, Mack J, Maggs-Kölling G, Mahadevakumar S, Mateos A, Mongkol-samrit S, Noisripoom W, Plaza M, Overy DP, Pigtek M, Sandoval-Denis M, Vauras J, Wingfield MJ, Abell SE, Ahmadpour A, Akulov A, Alavi F, Alavi Z, Altés A, Alvarado P, Anand G, Ashtekar N, Assyov B, Banc-Prandi G, Barbosa KD, Barreto GG, Bellanger JM, Bezerra JL, Bhat DJ, Bilanski P, Bose T, Bozok F, Chaves J, Costa-Rezende DH, Danteswari C, Darmostuk V, Delgado G, Denman S, Eichmeier A, Etayo J, Eyssartier G, Faulwetter S, Ganga KGG, Ghosta Y, Goh J, Góis JS, Gramaje D, Granit L, Groenewald M, Gulden G, Gusmao LFP, Hammerbacher A, Heidarian Z, Hywel-Jones N, Jankowiak R, Kaliyaperumal M, Kaygusuz O, Kezo K, Khonsanit A, Kumar S, Kuo CH, Læssre T, Latha KPD, Loizides M, Luo S, Macía-Vicente JG, Manimohan P, Marbach PAS, Marinho P, Marney TS, Marques G, Martín MP, Miller AN, Mondello F, Moreno G, Mufeeda KT, Mun HY, Nau T, Nkomo T, Okrasinska A, Oliveira J, Oliveira RL, Ortiz DA, Pawlowska J, Pérez-De-Gregorio MA, Podile AR, Portugal A, Privitera N, Rajeshkumar KC, Rauf I, Rian B, Rigueiro-Rodriguez A, Rivas-Torres GF, Rodriguez-Flakus P, Romero-Gordillo M, Saar I, Saba M, Santos CD, Sarma P, Siquier JL, Sleiman S, Spetik M, Sridhar KR, Stryjak-Bogacka M, Szczepanska K, Taskin H, Tennakoon DS, Thanakitpipattana D, Trovao J, Tuerkecul J, van Iperen AL,

- van 't P, Vasquez G, Visagie CM, Wingfield BD, Wong PTW, Yang WX, Yarar M, Yarden O, Yilmaz N, Zhang N, Zhu YN, Groenewald JZ (2023) Fungal Planet description sheets: 1478–1549. *Persoonia* 50: 158–310. <https://doi.org/10.3767/persoonia.2023.50.05>
- Crous PW, Wingfield MJ, Jurjević Ž, Balashov S, Osiek ER, Marin-Felix Y, Luangsa-Ard JJ, Mejía LC, Cappelli A, Parra LA, Lucchini G, Chen J, Moreno G, Faraoni M, Zhao RL, Weholt Ø, Borovička J, Jansen GM, Shivas RG, Tan YP, Akulov A, Alfenas AC, Alfenas RF, Altés A, Avchar R, Barreto RW, Catcheside DEA, Chi TY, Esteve-Raventós F, Fryar SC, Hanh LTM, Larsbrink J, Oberlies NH, Olsson L, Pancorbo F, Raja HA, Thanh VN, Thuy NT, Ajithkumar K, Akram W, Alvarado P, Angeletti B, Arumugam E, Atashi Khalilabad A, Bandini D, Baroni TJ, Barreto GG, Boertmann D, Bose T, Castañeda-Ruiz RF, Couceiro A, Cykowska-Marzencka B, Dai YC, Darmostuk V, Da Silva SBG, Dearnaley JDW, De Azevedo Santiago ALCM, Declercq B, De Freitas LWS, De La Peña-Lastra S, Delgado G, De Lima CLF, Dhotre D, Dirks AC, Eisevand P, Erhard A, Ferro LO, García D, García-Martín A, Garrido-Benavent I, Gené J, Ghobad-Nejhad M, Gore G, Gunaseelan S, Gusmão LFP, Hammerbacher A, Hernández-Perez AT, Hernández-Restrepo M, Hofmann TA, Hubka V, Jiya N, Kaliyaperumal M, Keerthana KS, Ketabchi M, Kezo K, Knoppersen R, Kolarczyková D, Kumar TKA, Læssøe T, Langer E, Larsson E, Lodge DJ, Lynch MJ, Maciá-Vicente JG, Mahadevakumar S, Mateos A, Mehrabi-Koushki M, Miglio BV, Noor A, Oliveira JA, Pereira OL, Piatek M, Pinto A, Ramírez GH, Raphael B, Rawat G, Renuka M, Reschke K, Ruiz Mateo A, Saar I, Saba M, Safi A, Sánchez RM, Sandoval-Denis M, Savitha AS, Sharma A, Shelke D, Sonawame D, Souza MGAP, Stryjak-Bogacka M, Thines M, Thomas A, Torres-Garcia D, Traba JM, Vauras J, Vermaas M, Villarreal M, Vu D, Whiteside EJ, Zafari D, Starink-Willemse M, Groenewald JZ (2024) Fungal Planet description sheets: 1697–1780. *Fungal Systematics and Evolution* 14: 325–577. <https://doi.org/10.3114/fuse.2024.14.19>
- da Silva IJS, Sousa TF, de Queiroz CA, dos Santos Castro G, Caniato FF, de Medeiros LS, Angolini CFF, Hanada RE, Koolen HHF, da Silva GF (2023) *Penicillium amapaense* sp. nov., section *Exilicaulis*, and new records of *Penicillium labradorum* in Brazil isolated from Amazon River sediments with potential applications in agriculture and biotechnology. *Mycological Progress* 22: 23. <https://doi.org/10.1007/s11557-023-01868-7>
- Frisvad JC, Houbraken J, Popma S, Samson RA (2013) Two new *Penicillium* species *Penicillium buchwaldii* and *Penicillium spathulatum*, producing the anticancer compound asperphenamate. *FEMS Microbiology Letters* 339: 77–92. <https://doi.org/10.1111/1574-6968.12054>
- Glass NL, Donaldson GC (1995) Development of primer sets designed for use with the PCR to amplify conserved genes from filamentous ascomycetes. *Applied and Environmental Microbiology* 61: 1323–1330. <https://doi.org/10.1128/aem.61.4.1323-1330.1995>
- Hong SB, Cho HS, Shin HD, Frisvad JC, Samson RA (2006) Novel *Neosartorya* species isolated from soil in Korea. *International Journal of Systematic and Evolutionary Microbiology* 56: 477–486. <https://doi.org/10.1099/ijs.0.63980-0>
- Houbraken J, Samson RA (2011) Phylogeny of *Penicillium* and the segregation of Trichocomaceae into three families. *Studies in Mycology* 70: 1–51. <https://doi.org/10.3114/sim.2011.70.01>
- Houbraken J, Wang L, Lee HB, Frisvad JC (2016) New sections in *Penicillium* containing novel species producing patulin, pyripyropens or other bioactive compounds. *Persoonia* 36: 299–314. <https://doi.org/10.3767/003158516X692040>
- Houbraken J, Kocsube S, Visagie CM, Yilmaz N, Wang XC, Meijer M, Kraak B, Hubka V, Bensch K, Samson RA, Frisvad JC (2020) Classification of *Aspergillus*, *Penicillium*, *Talaromyces* and related genera (Eurotiales): An overview of families, genera,

- subgenera, sections, series and species. *Studies in Mycology* 95: 5–169. <https://doi.org/10.1016/j.simyco.2020.05.002>
- Jahan I, Wang YH, Li P, Hussain S, Song JY, Yan J (2024) Comprehensive analysis of *Penicillium sclerotiorum*: Biology, secondary metabolites, and bioactive compound potential—a review. *Journal of Agricultural and Food Chemistry* 72: 9555–9566. <https://doi.org/10.1021/acs.jafc.3c09866>
- Kalyaanamoorthy S, Minh BQ, Wong TKF, von Haeseler A, Jermiin LS (2017) ModelFinder: Fast model selection for accurate phylogenetic estimates. *Nature Methods* 14: 587–589. <https://doi.org/10.1038/nmeth.4285>
- Kapli P, Yang ZH, Telford MJ (2020) Phylogenetic tree building in the genomic age. *Nature Reviews. Genetics* 21: 428–444. <https://doi.org/10.1038/s41576-020-0233-0>
- Khuna S, Kumla J, Thitla T, Hongsanan S, Lumyong S, Suwannarach N (2023) *Penicillium thailandense* (Aspergillaceae, Eurotiales), a new species isolated from soil in northern Thailand. *Phytotaxa* 612: 33–45. <https://doi.org/10.11646/phytotaxa.612.1.2>
- Li M, Raza M, Song S, Hou LW, Zhang ZF, Gao M, Huang JE, Liu F, Cai L (2023) Application of culturomics in fungal isolation from mangrove sediments. *Microbiome* 11: 272. <https://doi.org/10.1186/s40168-023-01708-6>
- Liang RN, Yang QQ, Li Y, Yin GH, Zhao GZ (2024) Morphological and phylogenetic analyses reveal two new *Penicillium* species isolated from the ancient Great Wall loess in Beijing, China. *Frontiers in Microbiology* 15: 1329299. <https://doi.org/10.3389/fmicb.2024.1329299>
- Lichtner FJ, Jurick WM, Bradshaw M, Broeckling C, Bauchan G, Broders K (2022) *Penicillium raperi*, a species isolated from Colorado cropping soils, is a potential biological control agent that produces multiple metabolites and is antagonistic against postharvest phytopathogens. *Mycological Progress* 21: 62. <https://doi.org/10.1007/s11557-022-01812-1>
- Lima J, Barbosa R, Bento D, Barbier E, Bernard E, Bezerra J, Souza-Motta C (2024) *Aspergillus*, *Penicillium*, and *Talaromyces* (Eurotiales) in Brazilian caves, with the description of four new species. *Fungal Systematics and Evolution* 14: 89–107. <https://doi.org/10.3114/fuse.2024.14.06>
- Link HF (1809) *Observationes in ordines plantarum naturales*. Dissertatio I. *Magazin der Gesellschaft Naturforschenden Freunde Berlin* 3: 3–42.
- Liu YJ, Whelen S, Hall BD (1999) Phylogenetic relationships among ascomycetes: Evidence from an RNA polymerase II subunit. *Molecular Biology and Evolution* 16: 1799–1808. <https://doi.org/10.1093/oxfordjournals.molbev.a026092>
- Liu C, Wang XC, Yu ZH, Zhuang WY, Zeng ZQ (2023) Seven new species of Eurotiales (Ascomycota) isolated from tibial flat sediments in China. *Journal of Fungi (Basel, Switzerland)* 9: 960. <https://doi.org/10.3390/jof9100960>
- Ludemann V, Greco M, Rodríguez MP, Basílico JC, Pardo AG (2010) Conidial production by *Penicillium nalgiovense* for use as starter cultures in dry fermented sausages by solid state fermentation. *Lebensmittel-Wissenschaft + Technologie* 43: 315–318. <https://doi.org/10.1016/j.lwt.2009.07.011>
- Lund F (1995) Differentiating *Penicillium* species by detection of indole metabolites using a filter paper method. *Letters in Applied Microbiology* 20: 228–231. <https://doi.org/10.1111/j.1472-765X.1995.tb00434.x>
- Morales-Oyervides L, Ruiz-Sánchez JP, Oliveira JC, Sousa-Gallagher MJ, Méndez-Zavala A, Giuffrida D, Dufossé L, Montañez J (2020) Biotechnological approaches for the production of natural colorants by *Talaromyces*/*Penicillium*: A review. *Biotechnology Advances* 43: 107601. <https://doi.org/10.1016/j.biotechadv.2020.107601>

- Mansouri S, Houbroken J, Samson RA, Frisvad JC, Christensen M, Tuthill DE, Koutaniemi S, Hatakka A, Lankinen P (2013) *Penicillium subrubescens*, a new species efficiently producing inulinase. *Antonie van Leeuwenhoek* 103: 1343–1357. <https://doi.org/10.1007/s10482-013-9915-3>
- Nguyen LT, Schmidt HA, von Haeseler A, Minh BQ (2015) IQ-TREE: A fast and effective stochastic algorithm for estimating maximum-likelihood phylogenies. *Molecular Biology and Evolution* 32: 268–274. <https://doi.org/10.1093/molbev/msu300>
- Nielsen JC, Grijseels S, Prigent S, Ji BY, Dainat J, Nielsen KF, Frisvad JC, Workman M, Nielsen J (2017) Global analysis of biosynthetic gene clusters reveals vast potential of secondary metabolite production in *Penicillium* species. *Nature Microbiology* 2: 17044. <https://doi.org/10.1038/nmicrobiol.2017.44>
- Nóbrega JP, do Nascimento Barbosa R, Lima JMdS, de Medeiros Bento D, de Souza-Motta CM, Melo RFR (2024) Six new *Penicillium* species in the section *Lanata-Divaricata* from a cave in Amazon rainforest, Brazil. *Mycological Progress* 23: 71. <https://doi.org/10.1007/s11557-024-02007-6>
- Nylander J (2004) MrModeltest v2. Program distributed by the author. *Bioinformatics* (Oxford, England) 24: 581–583. <https://doi.org/10.1093/bioinformatics/btm388>
- Paden JW (1971) Three new species of *Eupenicillium* from soil. *Mycopathologia et Mycologia Applicata* 43: 259–268. <https://doi.org/10.1007/BF02051745>
- Puel O, Galtier P, Oswald IP (2010) Biosynthesis and toxicological effects of patulin. *Toxins* 2: 613–631. <https://doi.org/10.3390/toxins2040613>
- Ridgway R (1912) *Color Standards and Color Nomenclature*. Washington, D.C., 43 pp. [+ 53 pls.] <https://doi.org/10.5962/bhl.title.62375>
- Ronquist F, Teslenko M, van der Mark P, Ayres DL, Darling A, Höhna S, Larget B, Liu L, Suchard MA, Huelsenbeck JP (2012) MrBayes 3.2: efficient Bayesian phylogenetic inference and model choice across a large model space. *Systematic Biology* 61: 539–542. <https://doi.org/10.1093/sysbio/sys029>
- Song H, Ding YJ, Zhuang WY, Ding GZ, Wang XC (2024) Three new species of *Penicillium* from East and Northeast China. *Journal of Fungi* (Basel, Switzerland) 10: 342. <https://doi.org/10.3390/jof10050342>
- Tamura K, Stecher G, Kumar S (2021) MEGA11: Molecular evolutionary genetics analysis version 11. *Molecular Biology and Evolution* 38: 3022–3027. <https://doi.org/10.1093/molbev/msab120>
- Tan YP (2023) Nomenclatural novelties. *Index of Australian Fungi* 26: 1–6. <https://zenodo.org/records/10211858>
- Tan YP, Shivas RG (2023) Nomenclatural novelties. *Index of Australian Fungi* 9: 1–19. <https://zenodo.org/record/8151939>
- Tan YP, Shivas RG (2024) Nomenclatural novelties. *Index of Australian Fungi* 46: 1–17. <https://zenodo.org/records/13905938>
- Tan YP, Sbaraini N, Chooi YH, Piggott AM, Foster C, Lacey E (2023) Nomenclatural novelties. *Index of Australian Fungi* 24: 1–13. <https://zenodo.org/records/10146062>
- Tan YP, Minns SA, Valter S, Lacey E (2024a) Nomenclatural novelties. *Index of Australian Fungi* 47: 1–14. <https://zenodo.org/records/14177441>
- Tan YP, Gilchrist GLM, Sbaraini N, Vuong D, Coulits CA, Lacey E (2024b) Nomenclatural novelties. *Index of Australian Fungi* 32: 1–15. <https://zenodo.org/records/10816340>
- Taniwaki MH, Pitt JI, Iamanaka BT, Massi FP, Fungaro MHP, Frisvad JC (2016) *Penicillium excelsum* sp. nov from the Brazil nut tree ecosystem in the Amazon basin. *PLoS One* 10: e0143189. <https://doi.org/10.1371/journal.pone.0143189>



- Tannous J, El Khoury R, Snini SP, Lippi Y, El Khoury A, Atoui A, Lteif R, Oswald IP, Puel O (2014) Sequencing, physical organization and kinetic expression of the patulin biosynthetic gene cluster from *Penicillium expansum*. *International Journal of Food Microbiology* 189: 51–60. <https://doi.org/10.1016/j.ijfoodmicro.2014.07.028>
- Visagie CM, Houbraken J (2020) Updating the taxonomy of *Aspergillus* in South Africa. *Studies in Mycology* 95: 253–292. <https://doi.org/10.1016/j.simyco.2020.02.003>
- Visagie CM, Houbraken J, Frisvad JC, Hong SB, Klaassen CH, Perrone G, Seifert KA, Varga J, Yaguchi T, Samson RA (2014) Identification and nomenclature of the genus *Penicillium*. *Studies in Mycology* 78: 343–371. <https://doi.org/10.1016/j.simyco.2014.09.001>
- Visagie CM, Renaud JB, Burgess KM, Malloch DW, Clark D, Ketch L, Urb M, Louis-Seize G, Assabgui R, Sumarah MW, Seifert KA (2016) Fifteen new species of *Penicillium*. *Persoonia* 36: 247–280. <https://doi.org/10.3767/003158516X691627>
- Visagie CM, Frisvad JC, Houbraken J, Visagie A, Samson RA, Jacobs K (2021) A re-evaluation of *Penicillium* section *Canescentia*, including the description of five new species. *Persoonia* 46: 163–187. <https://doi.org/10.3767/persoonia.2021.46.06>
- Visagie CM, Houbraken J, Yilmaz N (2024a) The re-identification of *Penicillium* and *Talaromyces* (Eurotiales) catalogued in South African culture collections. *Persoonia* 53: 29–61. <https://doi.org/10.3767/persoonia.2024.53.02>
- Visagie CM, Yilmaz N, Kocsubé S, Frisvad JC, Hubka V, Samson RA, Houbraken J (2024b) A review of recently introduced *Aspergillus*, *Penicillium*, *Talaromyces* and other Eurotiales species. *Studies in Mycology* 107: 1–66. <https://doi.org/10.3114/sim.2024.107.01>
- Visagie CM, Yilmaz N, Allison JD, Barreto RW, Boekhout T, Boers J, Delgado MA, Dewing C, Fitza KNE, Furtado ECA, Gaya E, Hill R, Hobden A, Hu DM, Hülsewig T, Khonsanit A, Luangsa-ard JJ, Mthembu A, Pereira CM, Price JL, Pringle A, Qikani N, Sandoval-Denis M, Schumacher RK, Seifert KA, Slippers B, Tennakoon DS, Thanakitpipattana D, van Vuuren NI, Groenewald JZ, Crous PW (2024c) New and Interesting Fungi. 7. *Fungal Systematics and Evolution* 13: 441–494. <https://doi.org/10.3114/fuse.2024.13.12>
- Wang B, Wang L (2013) *Penicillium kongii*, a new terverticillate species isolated from plant leaves in China. *Mycologia* 105: 1547–1554. <https://doi.org/10.3852/13-022>
- Wang XC, Zhang ZK, Zhuang WY (2023) Species diversity of *Penicillium* in Southwest China with discovery of forty-three new species. *Journal of Fungi (Basel, Switzerland)* 9: 1150. <https://doi.org/10.3390/jof9121150>
- Wei QY, Yuan Y, Zhang JH, Wang J (2024) Fungicidal efficiency of DBD cold plasma against *Aspergillus niger* on dried jujube. *Food Microbiology* 121: 104523. <https://doi.org/10.1016/j.fm.2024.104523>
- White TJ, Bruns T, Lee S, Taylor J (1990) Amplification and direct sequencing of fungal ribosomal RNA genes for phylogenetics. Academic Press, Inc., New York, 315–322 pp. <https://doi.org/10.1016/B978-0-12-372180-8.50042-1>
- Zhang ZY, Li X, Chen WH, Liang JD, Han YF (2023) Culturable fungi from urban soils in China II, with the description of 18 novel species in Ascomycota (Dothideomycetes, Eurotiomycetes, Leotiomyces and Sordariomycetes). *Mycosphaera* 98: 167–220. <https://doi.org/10.3897/mycokeys.98.102816>
- Zhang ZY, Pan H, Tao G, Li X, Han YF, Feng Y, Tong SQ, Ding CY (2024) Culturable mycobiota from Guizhou Wildlife Park in China. *Mycosphere: Journal of Fungal Biology* 15: 654–763. <https://doi.org/10.5943/mycosphere/15/1/5>
- Zhou LW, May TW (2023) Fungal taxonomy: Current status and research agendas for the interdisciplinary and globalisation era. *Mycology* 14: 52–59. <https://doi.org/10.1080/21501203.2022.2103194>

# Two new species of *Penicillium* and a new genus in Xylariomycetidae from the forest dump-sites in Chiang Mai, Thailand

Tanapol Thitla<sup>1\*</sup>, Jutamart Monkai<sup>2,3\*</sup>, Weiqian Meng<sup>1</sup>, Surapong Khuna<sup>1</sup>, Ning Xie<sup>1</sup>, Sinang Hongsanan<sup>1,3</sup>, Saisamorn Lumyong<sup>3,4,5</sup>

<sup>1</sup> Shenzhen Key Laboratory of Microbial Genetic Engineering, College of Life Science and Oceanography, Shenzhen University, Shenzhen 518060, China

<sup>2</sup> Office of Research Administration, Chiang Mai University, Chiang Mai 50200, Thailand

<sup>3</sup> Department of Biology, Faculty of Science, Chiang Mai University, Chiang Mai 50200, Thailand

<sup>4</sup> Center of Excellence in Microbial Diversity and Sustainable Utilization, Chiang Mai University, Chiang Mai 50200, Thailand

<sup>5</sup> Academy of Science, The Royal Society of Thailand, Bangkok 10300, Thailand

Corresponding authors: Saisamorn Lumyong (schoi009@gmail.com); Sinang Hongsanan (sinang333@gmail.com)



This article is part of:

**Exploring the Hidden Fungal Diversity: Biodiversity, Taxonomy, and Phylogeny of Saprobic Fungi**

Edited by Samantha C. Karunarathna, Danushka Sandaruwan Tennakoon, Ajay Kumar Gautam

Academic editor:

Samantha C. Karunarathna

Received: 18 February 2025

Accepted: 5 April 2025

Published: 29 April 2025

**Citation:** Thitla T, Monkai J, Meng W, Khuna S, Xie N, Hongsanan S, Lumyong S (2025) Two new species of *Penicillium* and a new genus in Xylariomycetidae from the forest dump-sites in Chiang Mai, Thailand. MycoKeys 116: 275–301. <https://doi.org/10.3897/mycokeys.116.150635>

Copyright: © Tanapol Thitla et al.

This is an open access article distributed under terms of the Creative Commons Attribution License (Attribution 4.0 International – CC BY 4.0).

## Abstract

Waste accumulation in forest regions can have a severe impact on the soil mycobiome. However, research on soil fungi inhabiting forest disposal sites remains limited. Therefore, this study focused on the taxonomy and phylogeny of ascomycetes isolated from soil in forest dump-sites in Chiang Mai, Thailand. The fungal strains were identified using morphological characterisations and multigene phylogenetic reconstruction. A new genus, *Pseudoleptodontidium*, typified by *Ps. Chiangmaiense* sp. nov. (Amphisphaeriales genera incertae sedis, Xylariomycetidae), along with two new species, *Penicillium Chiangmaiense* (series *Janthinella*, section *Lanata-Divaricata*) and *P. terrae* (series *Erubescens*, section *Exilicaulis*) (Aspergillaceae, Eurotiales), are described in detail and compared with closely-related species. Our discovery offers valuable insights into the soil ascomycetes associated with forest disturbances.

**Key words:** Eurotiomycetes, new taxa, *Pseudoleptodontidium*, soil fungi, Sordariomycetes, taxonomy

## Introduction

The disposal of waste materials through open burning, landfilling and dumping in land areas or water resources contributes to environmental issues, such as air pollution (PM<sub>2.5</sub>), as well as water and soil pollution, which can endanger the health and livelihood of humans, animals, plants and other organisms (Lin et al. 2020; Wanthongchai et al. 2021). Soil serves as a natural habitat for a wide range of fauna and flora, including fungi. Fungi are a major component of soil ecosystems, playing crucial roles in the cycling of nutrients and the decomposition of organic materials (Frąc et al. 2018; Coleine et al. 2022). The most abundant soil fungi belong to the Ascomycota, which includes the classes Arthoniomycetes, Dothideomycetes, Eurotiomycetes, Leotiomyces and Sordariomycetes (Tedersoo et al. 2021; Gomes de Farias et al. 2023). Amongst

\* These authors have contributed equally to this work.

these, *Fusarium*, *Penicillium* and *Phoma* are the most frequently isolated genera (Tedersoo et al. 2021; Yasanthika et al. 2023). However, contamination with pollutants may adversely affect their diversity, population and ecological functions (Frąc et al. 2018; Schlöter et al. 2018; Coleine et al. 2022). The ability to synthesise a wide range of enzymes for breaking down various substrates enables soil fungi to adapt and thrive in diverse environments and harsh conditions (Singh et al. 2021; Coleine et al. 2022; Sun et al. 2024).

Extensive studies have focused on isolating and characterising soil fungi from contaminated areas, landfills and urban dump-sites (Sangale et al. 2019; Verma and Gupta 2019; Ren et al. 2021; Khan et al. 2022; Gong et al. 2023; Sathiyabama et al. 2024; Sun et al. 2024). These studies have revealed diverse soil fungal communities and identified numerous new fungal taxa and strains from these polluted habitats. Moreover, they have demonstrated a significant potential for biodegradation and bioremediation. For example, Yasanthika et al. (2021) studied soil ascomycetes in China and reported a new species, *Juxtiphoma yunnanensis*, as well as two new records, *Lecanicillium dimorphum* and *Scopulariopsis brevicaulis*, from urban-industrialised soils. Ren et al. (2021) isolated 29 fungal strains from soils contaminated with explosive materials in China. Amongst them, the isolate of *Fusarium solani* demonstrated the ability to decompose alkyne-terminated polybutadiene with urethane segments (PUPB) (Ren et al. 2021). Similarly, Sangale et al. (2019) obtained 109 fungal isolates from the dumping sites of mangrove rhizosphere soil and revealed that the strains of *Aspergillus terreus* and *A. sydowii* were the most effective in breaking down polythene. Additionally, the strain of *Penicillium citrinum*, isolated from municipal landfill soils in Bhopal, India, has demonstrated efficacy in degrading low-density polyethylene (LDPE) without prior pretreatment (Khan et al. 2022).

Dump-sites, especially those located within forested areas, represent an underexplored yet ecologically significant niche. Forest dump-sites provide a distinctive habitat, characterised by decreased soil nutrients, fluctuating temperature and moisture levels and potential exposure to pollutants (Kooch et al. 2023; Sun et al. 2024). It is essential for exploring novel soil fungi from this habitat in order to determine fungal diversity and investigate their biodegradation strategies. Therefore, the present study aims to isolate and identify soil ascomycetes from disposal sites located in forests of northern Thailand. The topsoil samples from forest dump-sites in Chiang Mai Province were collected and isolated for fungi, leading to the discovery of five novel Ascomycota strains. Based on molecular analyses and morphological characteristics, two new species of *Penicillium* and a new genus in Xylariomycetidae were introduced and described.

## Materials and methods

### Fungal isolation

Soil samples (0–10 cm depth) were collected from three forest dump-sites in June 2024 in Chiang Mai Province, Thailand: (1) Papae, Mae Taeng District, (2) Suthep, Muang Chiang Mai District and (3) Mae Sa, Mae Rim District (Fig. 1). The collection details were noted (Rathnayaka et al. 2024) and the soil samples were placed in plastic bags and taken to the Sustainable Development of Biological Resources Laboratory (SDBR), at the Department of Biology, Faculty of Science, Chiang Mai





**Figure 1.** Forest dump-sites used for soil fungal isolation in this study **A** Papae, Mae Tang District, Chiang Mai Province **B** Suthep, Muang Chiang Mai District, Chiang Mai Province **C** Mae Sa, Mae Rim District, Chiang Mai Province.

University, Thailand. Upon arrival, soil fungi were isolated immediately using the serial dilution plating method with three serial dilutions in sterile water (Yasanthika et al. 2022). After dilution, 100 µl of the soil suspension was dropped and spread on potato dextrose agar (PDA; CONDALAB, Spain) supplemented with 100 µg/ml of streptomycin. The isolation plates were incubated at 25 °C in the dark for 5 days. The appearing fungal colonies were transferred to fresh PDA using the hyphal tip method (Korhonen and Hintikka 1980). The pure cultures were deposited and permanently preserved in a metabolically inactive state at the Culture Collection of Microbial Shenzhen University (MBSZU), Shenzhen University, China.

### Morphological characterisation

The morphological characteristics of the obtained fungi were observed in both macro-morphology and micro-morphology, with different details depending on each fungus.

To investigate the morphology of *Penicillium* (comprising MBSZU 24-007 to MBSZU 24-010), the colony characteristics, growth rate, pigment production, sporulation or related features were investigated on Blakeslee's Malt extract agar (MEAbI), creatine sucrose agar (CREA), Czapek yeast autolysate agar with 5% NaCl (CYAS), Czapek's agar (CZ), Dichloran 18% glycerol agar (DG18), malt extract agar (MEA), oatmeal agar (OA), PDA and yeast extract sucrose agar (YES) at 25 °C in darkness for 7 days. The experiment was also performed on Czapek yeast autolysate agar (CYA) at 25, 30 and 37 °C in darkness for 7 days to characterise the macro-morphology (Visagie et al. 2014; Khuna et al. 2023). Micro-morphologically, the characteristics of conidiophores, stipes, conidiogenous cells, conidia or other structures were observed under a light microscope (Nikon DS-Ri2; Nikon, Japan), using fungal colonies grown on MEA at 25 °C in darkness for 7 days. Size data were evaluated by at least 50 measurements per structure.

The colony characteristics, growth rate and pigment production of *Pseudo-leptodontidium* (MBSZU 25-005) were studied on PDA and MEA at 25 °C in darkness for 14 days. Micro-morphology was observed under a light microscope using a fungal colony grown on PDA at 25 °C in darkness for 14–21 days. The size of each morphological structure was measured at least 50 times per structure.



## DNA extraction, amplification and sequencing

Fungal genomic DNA from each strain was extracted from the fungal mycelium, which had grown on PDA at 25 °C for a week, using an E.Z.N.A® Tissue DNA Kit (Omega, USA). The polymerase chain reaction (PCR) technique was used to amplify each region. Each target locus was amplified using the specific primers (Table 1). PCR amplifications were performed in 20 µl reaction mixtures, consisting of 1 µl of genomic DNA, 1 µl of each primer, 10 µl of 2× Phanta Max Master Mix (Dye Plus) (Vazyme, China) and 7 µl of deionised water. The PCR amplification was performed using a T100 Thermal Cycler (BIO-RAD, USA), with an initial denaturation step at 95 °C for 5 min, followed by 35 cycles of denaturation, annealing and elongation steps. The denaturation and elongation steps were performed at 95 °C for 30 s and 72 °C for 60 s, respectively. The annealing step was performed at different conditions depending on each target locus (Table 1). A final elongation step was performed at 72 °C for 10 minutes. The success or failure of the PCR product was determined through 1% agarose gel electrophoresis, followed by purification of the product using the E.Z.N.A® Gel Extraction Kit (Omega, USA). The quality and quantity of the purified PCR products were assessed using 1% agarose gel electrophoresis and a Nanodrop 2000 Spectrophotometer (Thermo Scientific, USA). Subsequently, the products were sequenced by BGI-Shenzhen Company (Shenzhen, Guangdong, China).

The bidirectional sequence data were assembled using the software Sequencher 5.4.6 (Nishimura 2000). The consensus sequence data were searched for sequence similarity via the Basic Local Alignment Search Tool (BLAST) in the National Center for Biotechnology Information (NCBI) website.

**Table 1.** The specific primer and annealing condition of each locus used in this study.

Loci*	Primer	Annealing condition		References
		Temperatures (°C)	Annealing period (s)	
ITS	ITS4/ITS5	52	30	White et al. (1990)
LSU	LR0R/LR5	52	30	Vilgalys and Hester (1990); Rehner and Samuels (1994)
CAM	CF1/CF4	51	60	Peterson et al. (2005)
	Cmd5/Cmd6	58	30	Hong et al. (2006)
RPB2	fRPB2-5F/ fRPB2-7cR	56	60	Liu et al. (1999)
TUB	Bt2a/Bt2b	52	30	Glass and Donaldson (1995)
	T1/Bt2b	55	45	Glass and Donaldson (1995); O'Donnell and Cigelnik (1997)

\* ITS – Internal Transcribed Spacer region of the rRNA; LSU – 28S large subunit of the nuclear rRNA; TUB – beta-tubulin gene; CAM – calmodulin gene; RPB2 – RNA polymerase II second largest subunit genes.

## Phylogenetic analysis

The multi-loci phylogenetic dataset was obtained, based on previous studies of *Penicillium* section *Exilicaulis* (Ansari et al. 2023; Liu et al. 2023; Wang et al. 2023b; Visagie et al. 2024a, 2024b), *Penicillium* section *Lanata-Divaricata* (Lenz et al. 2022; Liu et al. 2023; Wang et al. 2023b; Araújo et al. 2024; Visagie et al. 2024b) and Xylariomycetidae (Samarakoon et al. 2022; Crous et al. 2023; Li et al. 2024; Samarakoon 2024) (Suppl. material 1: tables S1–S3).

The sequence data for each locus were individually aligned using MUSCLE through the software MEGA 6 (Edgar 2004) and manually adjusted in BioEdit v.7.2.5 (Hall 2004). The concatenation of the ITS, *TUB*, *CAM* and *RPB2* loci was performed for the phylogenetic analysis of *Penicillium*; in contrast, the combined ITS, LSU, *RPB2* and *TUB* loci were used for the analysis of Xylariomycetidae. Maximum Likelihood (ML) and Bayesian Inference (BI) analyses were applied to generate a phylogenetic tree. The ML analysis was conducted with 25 categories and 1,000 bootstrap (BS) replications under the GTRCAT model using RAxML-HPC2 on XSEDE (v.8.2.12) in the CIPRES web portal (Felsenstein 1985; Stamatakis 2006; Miller et al. 2009). The best-fit models of nucleotide substitution for individual locus were determined by using MrModelTest v.2.3 based on the Akaike Information Criterion (AIC) (Nylander 2004). The GTR+I+G substitution model was the best fit for all loci. The BI analysis was performed using MrBayes v.3.2.6 (Ronquist and Huelsenbeck 2003). Bayesian Posterior Probability (PP) was examined by Markov Chain Monte Carlo (MCMC) sampling. Six simultaneous Markov chains were run with random initial trees, wherein every 100<sup>th</sup> generation was sampled. The first 20% of generated trees, representing the burn-in phase of the analysis, were discarded, while the remaining trees were used to calculate PP in the majority-rule consensus tree. The tree topologies were visualised in FigTree v.1.4.0 with BS support and PP values equal to or higher than 75% and 0.95, respectively, in branches (Rambaut 2019). The final alignment and phylogram were submitted to TreeBASE (<http://purl.org/phylo/treebase/phyloids/study/TB2:S32075>, accessed 19 March 2025).

## Results

### Phylogenetic analysis

Phylogenetic analysis of 72 taxa from *Penicillium*, section *Exilicaulis* (including *P. terrae* MBSZU 24-007 and MBSZU 24-008) was performed using a combined ITS, *TUB*, *CAM* and *RPB2* sequence dataset. *Penicillium janthinellum* CBS 340.48 and *P. limosum* CBS 339.97 were selected as the outgroup. The combined dataset comprised 2,630 characters (ITS, 1–564 bp; *TUB*, 565–1,102 bp; *CAM*, 1,103–1,701 bp; *RPB2*, 1,702–2,630 bp), including gaps. RAxML analysis of the integrated dataset yielded the best-scoring tree with a final ML optimisation likelihood value of -26380.0905. The matrix contained 1,279 distinct alignment patterns, with 13.06% of the characters being undetermined or gaps. The estimated base frequencies were recorded as follows: A = 0.2238, C = 0.2765, G = 0.2706 and T = 0.2291, while the substitution rates were as follows: AC = 1.0947, AG = 3.5202, AT = 1.1705, CG = 0.7818, CT = 5.4306 and GT = 1.0000. The gamma distribution shape parameter alpha value was equal to 0.2342, while the tree length was equal to 2.4771. The final average standard deviation of the split frequencies at the end of the total MCMC generations was computed as 0.003644 via BI analysis.

Phylogenetic analysis of 111 taxa from *Penicillium* section *Lanata-Divaricata* (including *P. Chiangmaiense* MBSZU 24-009 and MBSZU 24-010) was performed using a combined ITS, *TUB*, *CAM* and *RPB2* sequence dataset.

*Penicillium alogum* CBS 140996 and *P. stolkiaie* CBS 315.67 were selected as outgroups. The combined dataset comprised 2,549 characters (ITS, 1–563 bp; *TUB*, 564–1,114 bp; *CAM*, 1,115–1,794 bp; *RPB2*, 1,795–2,549 bp), including gaps. RAxML analysis of the integrated dataset yielded the best scoring tree with a final ML optimisation likelihood value of -35195.9174. The matrix contained 1,381 distinct alignment patterns with 12.17% undetermined characters or gaps. The estimated base frequencies were recorded as follows: A = 0.2214, C = 0.2908, G = 0.2615 and T = 0.2263, while the substitution rates were as follows: AC = 1.1361, AG = 3.5568, AT = 1.5061, CG = 0.7521, CT = 5.3860 and GT = 1.0000. The gamma distribution shape parameter alpha value was equal to 0.2744, while the tree length was equal to 3.5928. The final average standard deviation of the split frequencies at the end of the total MCMC generations was computed as 0.005628 via BI analysis.

Phylogenetic analysis of species in subclass Xylariomycetidae was performed using a combined ITS, LSU, *RPB2* and *TUB* sequence dataset of MBSZU 25-005 (proposed as *Pseudoleptodontidium Chiangmaiensis*), together with 118 taxa of the subclass. *Achaetomium macrosporum* CBS 532.94, *Chaetomium elatum* CBS 374.66 and *Sordaria fimicola* CBS 723.96 were selected as outgroups. The combined dataset comprised 3,560 characters (ITS, 1–693 bp; LSU, 694–1,592 bp; *RPB2*, 1,593–2,656 bp; *TUB*, 2,657–3,560 bp), including gaps. RAxML analysis of the integrated dataset yielded the best scoring tree with a final ML optimisation likelihood value of -83630.121273. The matrix contained 2,615 distinct alignment patterns with 39.42% undetermined characters or gaps. The estimated base frequencies were recorded as follows: A = 0.256414, C = 0.231937, G = 0.280501 and T = 0.231149, while the substitution rates were as follows: AC = 0.888171, AG = 2.661198, AT = 1.161270, CG = 0.868099, CT = 3.494813 and GT = 1.000000. The gamma distribution shape parameter alpha value was equal to 0.351763, while the tree length was equal to 15.592567. The final average standard deviation of the split frequencies at the end of the total MCMC generations was computed as 0.009989 via BI analysis.

Topologically, the ML and BI phylogenetic trees of all fungal species had similar results; therefore, only the ML phylogram was demonstrated in this study. The phylogram of *Penicillium* section *Exilicaulis* showed that two new strains (MBSZU 24-007 and MBSZU 24-008) separated from other recognised species with 100% BS and 1.00 PP supports (Fig. 2). These fungal strains formed a sister clade with *P. laeve* DTO270G8 (BS 99% and PP 1.00) and belonged to the series *Erubescencia*.

While the phylogram of *Penicillium* section *Lanata-Divaricata* exhibited that MBSZU 24-009 and MBSZU 24-010 formed a distinct clade, clearly separated from other taxa with significant support (BS 100% and PP 1.00; Fig. 3). These strains also formed a sister clade with *P. brefeldianum* CBS 235.81 (BS 100% and PP 1.00) within the Series *Janthinella* clade.

The phylogram of Xylariomycetidae showed that MBSZU 25-005 clustered amongst families and taxa in Amphisphaeriales. This strain also formed a sister clade to *Neoleptodontidium aciculare* CBS 123.86 and *N. aquaticum* CBS 149455 (BS 96% and PP 1.00; Fig. 4).

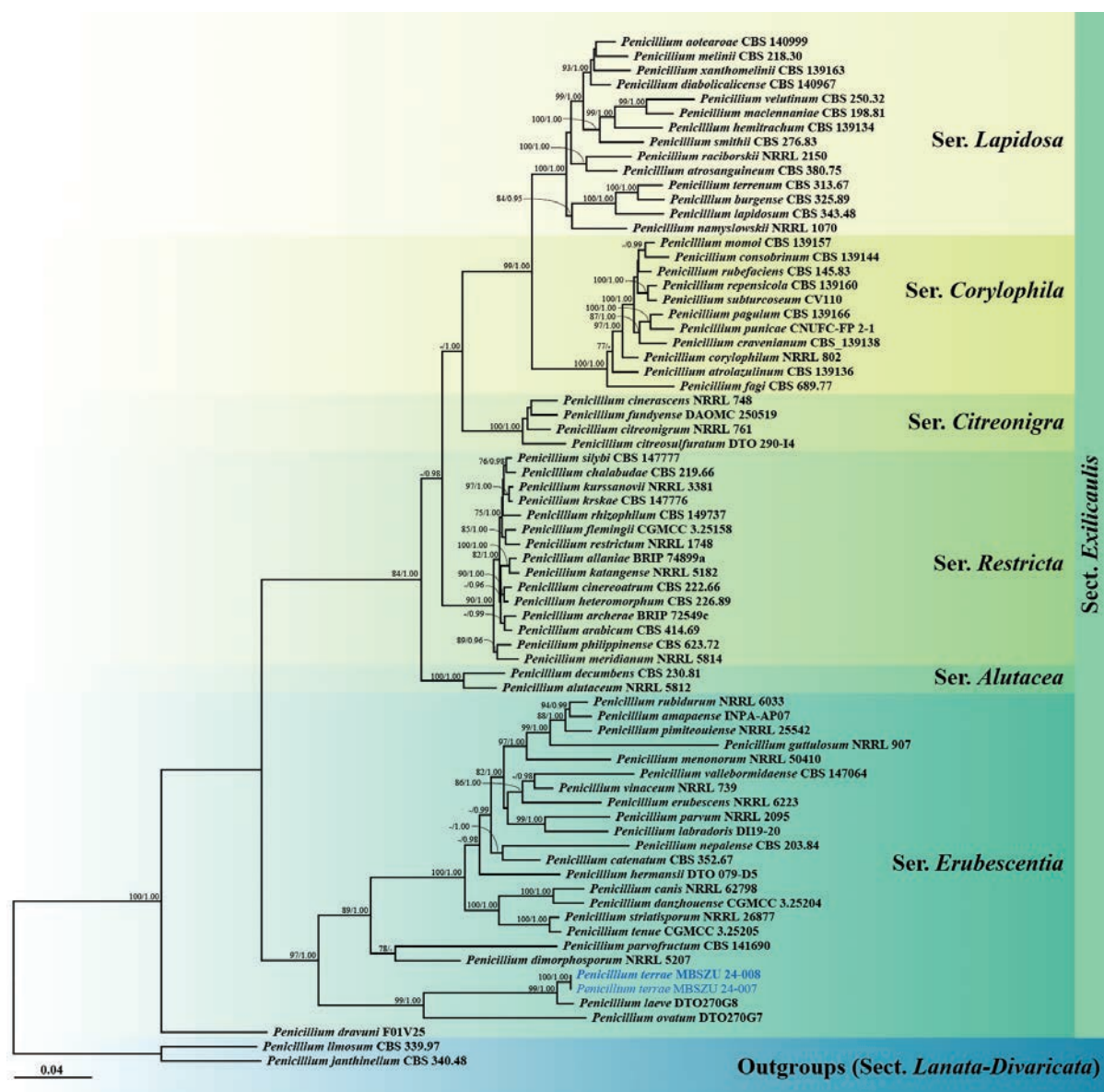


**Figure 2.** Phylogram generated from Maximum Likelihood analysis of 72 specimens belonging to the genus *Penicillium* section *Exilicaulis*, using the combined ITS, *TUB*, *CAM* and *RPB2* genes. *Penicillium janthinellum* CBS 340.48 and *P. limosum* CBS 339.97 were used as the outgroup. The numbers above branches show bootstrap percentages (left) and Bayesian Posterior Probabilities (right). Bootstrap values  $\geq 75\%$  and Bayesian Posterior Probabilities  $\geq 0.95$  are shown. The scale bar reflects the estimated number of nucleotide substitutions per site. The fungal strains in this study are blue. Type species are bold.

## Taxonomy

### *Penicillium terrae* Thitla, Monkai, Lumyong & Hongsan, sp. nov.

MycoBank No: 857423

**Etymology.** The specific epithet *terrae* refers to the soil substrate, from which this species was isolated.

**Holotype.** THAILAND • Chiang Mai Province, Mae Taeng District, Papae, on soil in the forest dump-sites, 20 June 2024, T. Thitla & J. Monkai; VR040 (SZU25-005, holotype); ex-type living culture, MBSZU 24-008, dried culture permanently preserved in a metabolically inactive state, SZU25-005.



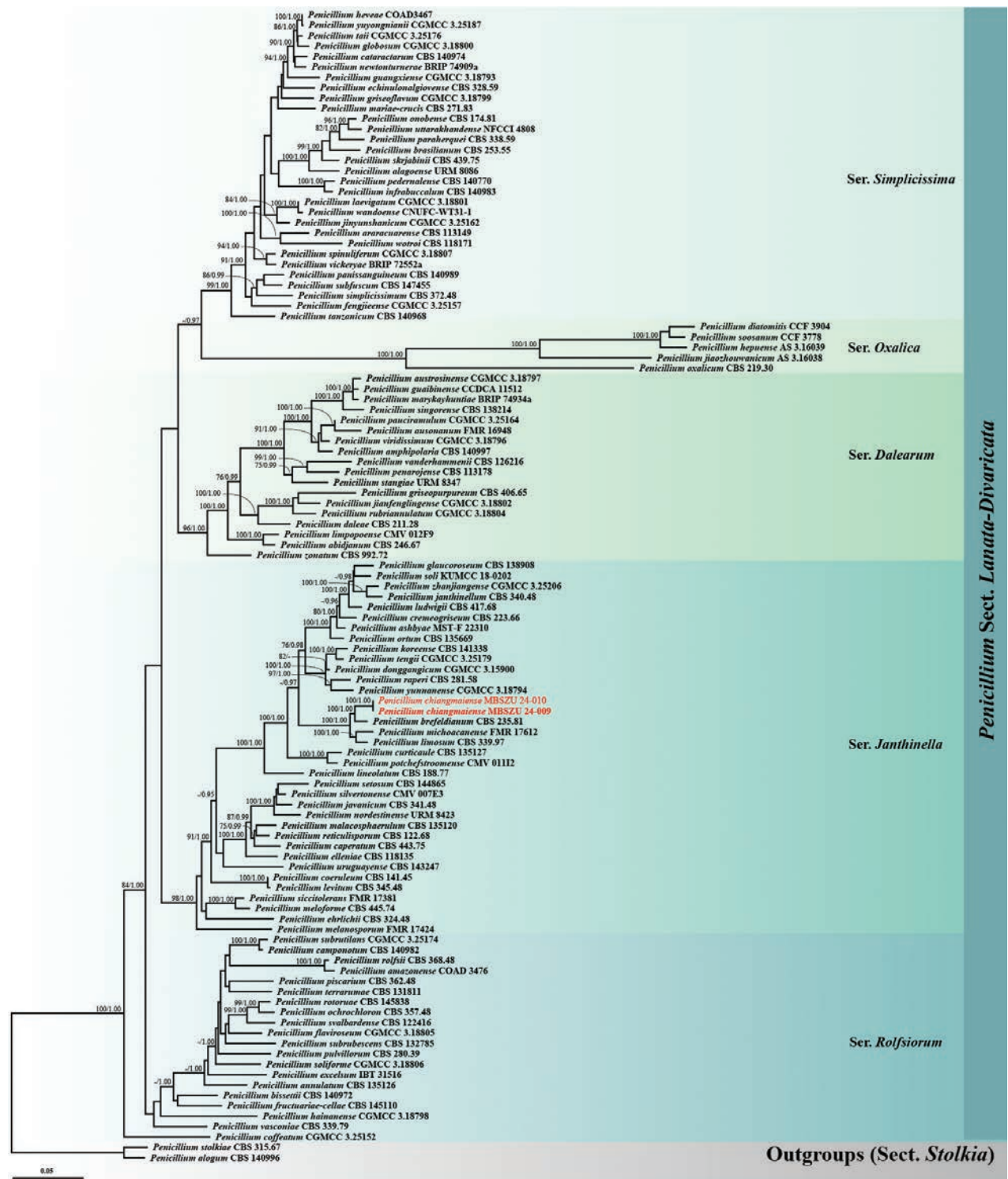


**Figure 3.** Phylogram generated from Maximum Likelihood analysis of 111 specimens belonging to the genus *Penicillium* section *Lanata-Divaricata* using the combined ITS, *TUB*, *CAM* and *RPB2* genes. *Penicillium alogum* CBS 140996 and *P. stolckiae* CBS 315.67 were used as the outgroup. The numbers above branches show bootstrap percentages (left) and Bayesian Posterior Probabilities (right). Bootstrap values  $\geq 75\%$  and Bayesian Posterior Probabilities  $\geq 0.95$  are shown. The scale bar reflects the estimated number of nucleotide substitutions per site. The fungal strains in this study are red. Type species are bold.

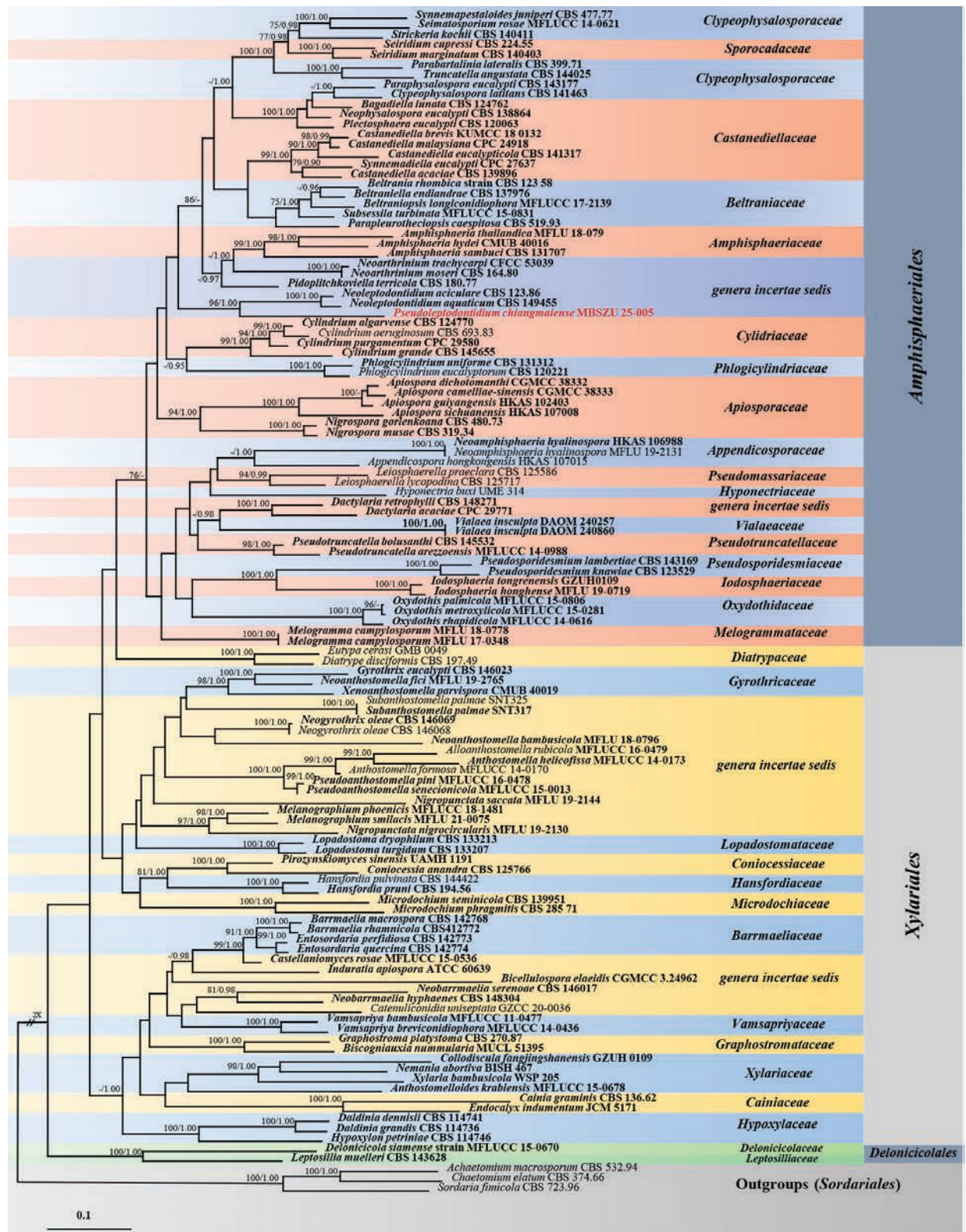


**Figure 4.** Phylogram generated from Maximum Likelihood analysis of 119 specimens belonging to the subclass Xylariomycetidae of the combined ITS, LSU, *RPB2* and *TUB* genes. *Achaetomium macrosporum* CBS 532.94, *Chaetomium elatum* CBS 374.66 and *Sordaria fimicola* CBS 723.96 were used as the outgroup. The numbers above branches show bootstrap percentages (left) and Bayesian Posterior Probabilities (right). Bootstrap values  $\geq 75\%$  and Bayesian Posterior Probabilities  $\geq 0.95$  are shown. The scale bar reflects the estimated number of nucleotide substitutions per site. The fungal strains in this study are red. Type species are bold.



**Colony diam.** (in mm) 7 days, 25 °C: CREA 8–11, CYA 13–18, CYAS 7–9, CZ 11–15, DG18 12–16, MEA 15–19, MEAb1 16–19, OA 13–19, PDA 12–15 and YES 9–13. 7 days, 30 °C: CYA 10–15. 7 days, 37 °C: CYA no growth.

**Culture characteristics.** Colonies at 25 °C for 7 days on CREA thin colonies; acid production absent (Fig. 5A). Colonies on CYA circular, convex, wrinkled texture, entire margin; white mycelia; soluble pigment absent; reverse yellowish-brown (Fig. 5B). Colonies on CYAS barely growing, circular, raised, wrinkled texture, undulate margin; white mycelia; soluble pigment absent; reverse white (Fig. 5C). On CZ thin colonies, circular, flat, entire margin; white mycelia; soluble pigment absent; reverse white (Fig. 5D). On DG18 circular, flat, wrinkled at the centre, margin smooth and entire; grey mycelia at the centre, white mycelia at the margin; soluble pigment absent; reverse greenish-grey to light yellow (Fig. 5E). Colonies on MEA circular, flat, smooth texture, entire margin; light grey mycelia; soluble pigment absent; reverse light yellow to white (Fig. 5F). On MEAb1 circular, flat, wrinkled at the centre, margin smooth and entire; light grey at the centre, white at the margin; soluble pigment absent; reverse yellowish-brown (Fig. 5G). On OA circular, flat, smooth textured, entire margin; light brown mycelia at the centre, white mycelia at the margin; soluble pigment absent; reverse white (Fig. 5H). Colonies on PDA circular, flat, wrinkled texture, entire margin; white mycelia; soluble pigment absent; reverse white to light yellow (Fig. 5I). Colonies on YES circular, convex, wrinkled texture, entire margin; white mycelia; soluble pigment absent; reverse light brown (Fig. 5J). Sporulation abundantly produces on all media.

**Micromorphology.** Conidiophores mononematous, growing out at right angles from hyphae, unbranched, smooth, hyaline,  $3\text{--}14 \times 1\text{--}3 \mu\text{m}$  (Fig. 5K–P). Phialides solitary, terminal, ampulliform, smooth, hyaline,  $5\text{--}12 \times 1\text{--}4 \mu\text{m}$  (Fig. 5K–P). Conidia globose to subglobose,  $2\text{--}4 \mu\text{m}$  diam., smooth, hyaline (Fig. 5K–N, Q). Sclerotia not observed. Sexual morph absent.

**Additional strain examined.** THAILAND • Chiang Mai Province, Mae Taeng District, Papae, on soil in the forest dump-sites, 20 June 2024, T. Thitla & J. Monkai; CMUVR039; living culture, MBSZU 24-007, dried culture permanently preserved in a metabolically inactive state, CMUVR039.

**Habitat and distribution.** Soil; only known from Chiang Mai Province, Thailand.

**Notes.** *Penicillium* section *Exilicaulis* was first established by Pitt (1980), with *P. restrictum* as the type species. This section was initially proposed to accommodate *Penicillium* species characterised by monoverticillate conidiophores and non-vesiculated stipes. Subsequently, phylogenetic studies expanded the section to include species with bi-verticillate conidiophores and those with conidiophores bearing solitary phialides (Houbraken and Samson 2011; Visagie et al. 2016a, b; da Silva et al. 2023). Species of the sect. *Exilicaulis* have been isolated from diverse environments, including soil, marine ecosystems, air, plants and insects (Ansari et al. 2023). Currently, this section comprises over 60 species across six series: *Alutacea*, *Citreonigra*, *Corylophila*, *Erubescens*, *Lapidosa* and *Restricta* (Ansari et al. 2023; Visagie et al. 2024a).

*Penicillium terrae* is classified within section *Exilicaulis*, series *Erubescens*. Phylogenetically, this species is closely related to *P. laeve* and *P. ovatum* (Fig. 2). However, *P. laeve* and *P. ovatum* were unable to grow on CREA and CYAS media, while *P. terrae* can grow on these media. Regarding growth rates, *P. laeve* exhibited slower growth than *P. terrae*, including CYA (8–9 mm), DG18

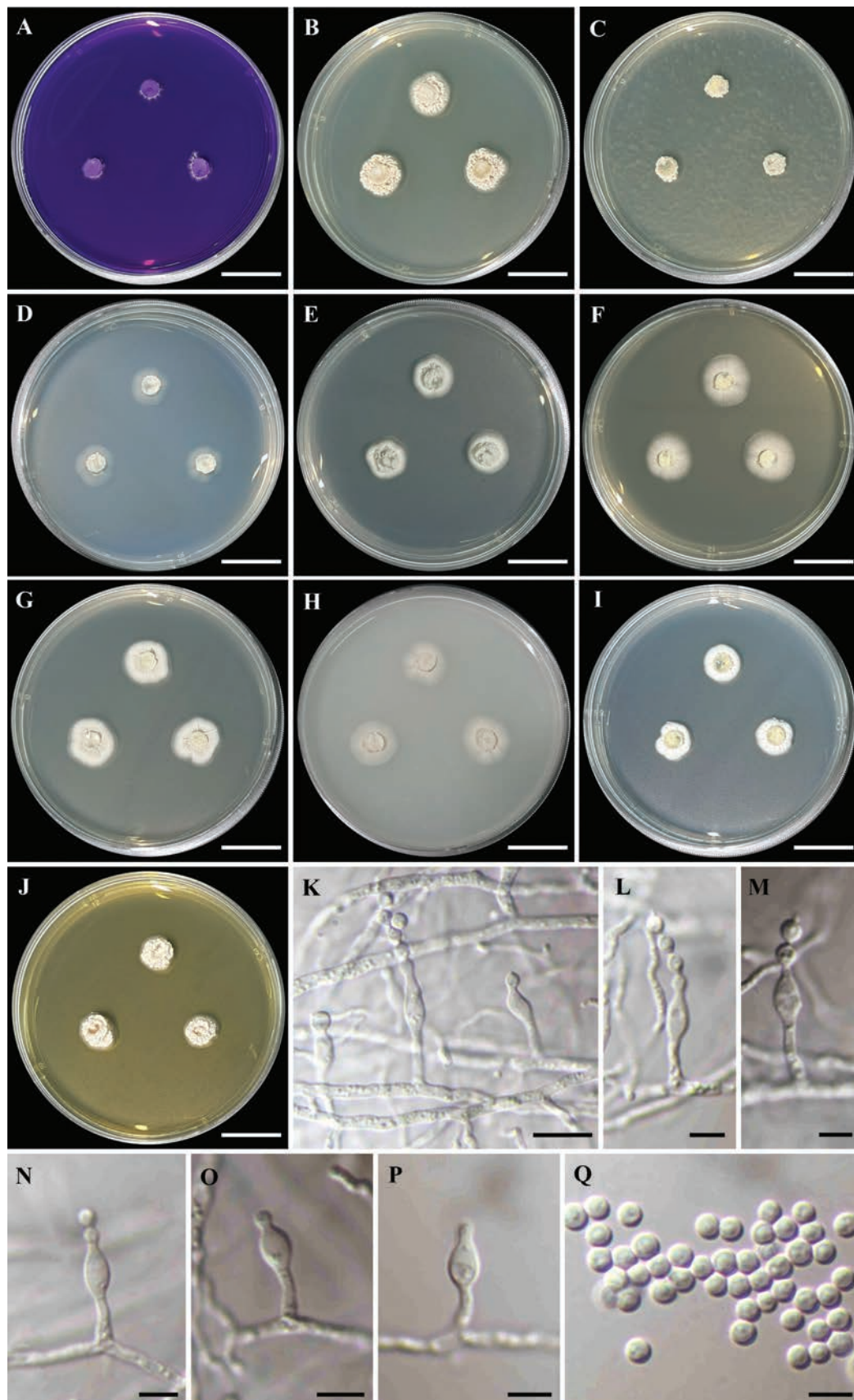


**Figure 5.** *Penicillium terrae* (MBSZU 24-008, ex-type living culture) **A–J** colonies at 25 °C for 7 days on CREA, CYA, CYAS, CZ, DG18, MEA, MEAbI, OA, PDA and YES, respectively **K–P** conidiophores, phialides and conidia **Q** conidia. Scale bar: 2 cm (**A–J**); 10 µm (**K**); 5 µm (**L–Q**).



(5–7 mm), OA (7–8 mm) and YES (8–9 mm) at 25 °C, as well as CYA at 30 °C (4–5 mm) (Visagie et al. 2016a). Similarly, *P. ovatum* also demonstrated slower growth compared to *P. terrae* on CYA (10–11 mm), DG18 (9–11 mm), MEA (7–8 mm) and OA (10–11 mm) at 25 °C (Visagie et al. 2016a). Micromorphologically, the phialides of *P. laeve* (4–6 µm × 2–3 µm) and *P. ovatum* (4.5–7 µm × 2–3 µm) were shorter than *P. terrae* (Visagie et al. 2016a). In terms of conidia, *P. terrae* produced globose to subglobose conidia with 2–4 µm, while *P. laeve* produced globose conidia measuring 2.5–3 µm diam. and *P. ovatum* produced ellipsoidal conidia with 2–3 × 1.5–2 µm (Visagie et al. 2016a). Furthermore, a pairwise nucleotide comparison between *P. terrae* and *P. laeve* showed differences of 0.86% (5/581 bp, including gaps) in ITS, 2.87% (13/453 bp, including gaps) in *TUB*, 2.62% (13/497 bp, including gaps) in *CAM* and 1.39% (13/938 bp, including gaps) in *RPB2*. Similarly, the comparison between *P. terrae* and *P. ovatum* revealed nucleotide differences of 2.64% (15/569 bp, including gaps) in ITS, 14.41% (65/451 bp, including gaps) in *TUB*, 17.74% (91/513 bp, including gaps) in *CAM* and 12.37% (116/938 bp, including gaps) in *RPB2*.

***Penicillium Chiangmaiense* Thitla, Monkai, Lumyong & Hongsanan, sp. nov.**

MycoBank No: 857424

**Etymology.** The specific epithet “*Chiangmaiense*” refers to the type locality “Chiang Mai Province, Thailand”.

**Holotype.** THAILAND • Chiang Mai Province, Mae Rim District, Mae Sa, on soil in the forest dump-sites, 27 June 2024, T. Thitla & J. Monkai; VR005 (SZU25-006, holotype); ex-type living culture, MBSZU 24-009, dried culture permanently preserved in a metabolically inactive state, SZU25-006.

**Colony diam.** (in mm) 7 days, 25 °C: CREA 40–44, CYA 50–52, CYAS 35–38, CZ 48–49, DG18 34–39, MEA 47–51, MEAb1 51–53, OA 53–54, PDA 49–50 and YES 32–38. 7 days, 30 °C: CYA 59–61. 7 days, 37 °C: CYA 55–56.

**Culture characteristics.** Colonies at 25 °C for 7 days on CREA thin colonies; acid production absent (Fig. 6A). Colonies on CYA and CYAS wrinkled texture, velvety, circular, flat, entire margin; white mycelia; soluble pigment absent; reverse light brown (Fig. 6B, C). On CZ, thin colonies, circular, flat, filamentous margin; white mycelia; soluble pigment absent; reverse white (Fig. 6D). On DG18, wrinkled texture, velvety, circular, flat, entire margin; white mycelia; soluble pigment absent; reverse white to pale yellow (Fig. 6E). Colonies on MEA and MEAb1 smooth texture, circular, flat, entire margin; pale yellow at the centre, white at the margin; soluble pigment absent; reverse pale brown to white (Fig. 6F, G). On OA, smooth textured, velvety, circular, flat, entire margin; white mycelia; soluble pigment absent; reverse light yellow to white (Fig. 6H). Colonies on PDA circular, flat, smooth texture, entire margin; white mycelia; soluble pigment absent; reverse white to light yellow (Fig. 6I). Colonies on YES circular, flat, wrinkled texture, velvety, entire margin; white mycelia; soluble pigment absent; reverse brownish-yellow (Fig. 6J). Sporulation abundantly produces on DG18, MEA and MEAb1 media. Sclerotia produces MEA, MEAb1 and OA (Fig. 6P).

**Micromorphology.** Conidiophores monoverticillate, sometimes divaricate. Stipes hyaline, smooth-walled, 80–270 × 2–3 µm (Fig. 6K–N). Phialides



**Figure 6.** *Penicillium chiangmaiense* (MBSZU 24-009, ex-type living culture) **A–J** colonies at 25 °C for 7 days on CREA, CYA, CYAS, CZ, DG18, MEA, MEAbI, OA, PDA and YES, respectively **K–N** conidiophores, phialides and conidia **O** conidia **P** sclerotia produced on culture media. Scale bar: 2 cm (**A–J**); 10 µm (**K–O**); 100 µm (**P**).

terminal, ampulliform, hyaline, smooth-walled 6–17 × 2–3.5 µm (Fig. 6K–N). Conidia globose to subglobose, 2–4 µm diam., smooth, hyaline (Fig. 6K–O). Sclerotia pale brown to brown, globose to irregular, 180–260 µm diam. (Fig. 6P). Sexual morph absent.

**Additional strain examined.** Thailand • Chiang Mai Province, Mae Rim District, Mae Sa, on soil in the forest dump-sites, 27 June 2024, T. Thitla & J. Monkai; CMUVR005-2; living culture, MBSZU 24-010, dried culture permanently preserved in a metabolically inactive state, CMUVR005-2.

**Habitat and distribution.** Soil; only known from Chiang Mai Province, Thailand.

**Notes.** *Penicillium* section *Lanata-Divaricata* was established by Thom (1930) to include species with biverticillate conidiophores, which usually contain a main conidiophore axis and metulae that diverge (referred to as divaricate conidiophores), as well as broadly spreading colonies (Houbraken and Samson 2011; Pangging et al. 2021). Species within this section have been isolated from various sources, including soil, air, fluvial sediments and plants (Nóbrega et al. 2024). Currently, the section is divided into five series: *Dalearum*, *Janthinella*, *Oxalica*, *Rolfsiorum* and *Simplicissima* (Ansari et al. 2023; Visagie et al. 2024a).

*Penicillium chiangmaiense* is classified within section *Lanata-Divaricata*, series *Janthinella*. In the phylogenetic tree (Fig. 3), the new species is closely related to *P. brefeldianum*, *P. limosum* and *P. michoacanense*. However, *P. brefeldianum* produces sexual structures on cornmeal agar and *P. limosum* produces on CZ, MEA and OA, while *P. chiangmaiense* does not exhibit any sexual features (Dodge 1933; Ueda 1995). Furthermore, the growth rate of *P. limosum* on MEA (42 mm in 14 days) was slower than that of *P. chiangmaiense* (47–51 mm in 7 days) (Ueda 1995). In the case of *P. michoacanense*, the stipes ( $15\text{--}60 \times 1\text{--}1.5 \mu\text{m}$ ) and phialides ( $4\text{--}5 \times 1.5 \mu\text{m}$ ) were shorter than those of *P. chiangmaiense* (stipes  $80\text{--}270 \times 2\text{--}3 \mu\text{m}$ ; phialides  $6\text{--}17 \times 2\text{--}3.5 \mu\text{m}$ ) (Rodríguez-Andrade et al. 2021). Moreover, *P. michoacanense* produced weak acid on CREA, while *P. chiangmaiense* does not produce it (Rodríguez-Andrade et al. 2021). Additionally, the pairwise nucleotide comparison of *P. chiangmaiense* with related species revealed significant differences. The comparison of *P. chiangmaiense* to *P. brefeldianum* showed 0.90% (5/556 bp) difference in ITS, 4.73% (21/444 bp) in *TUB*, 4.28% (24/561 bp) in *CAM* and 1.46% (11/755 bp) in *RPB2*, including gaps. Differences in *P. chiangmaiense* and *P. limosum* were 1.09% (6/548 bp) in ITS, 5.00% (22/440 bp) in *TUB*, 6.28% (35/557 bp) in *CAM* and 0.93% (7/755 bp) in *RPB2*, including gaps. In comparison between *P. chiangmaiense* and *P. michoacanense*, the differences were 0.73% (4/548 bp) in ITS, 2.84% (11/388 bp) in *TUB*, 8.35% (34/407 bp) in *CAM* and 1.61% (12/745 bp) in *RPB2*, including gaps.

***Pseudoleptodontidium* Thitla, Monkai, Lumyong & Hongsanan, gen. nov.**  
MycoBank No: 857466

**Etymology.** The name refers to its morphological similarity to *Leptodontidium*.

**Classification.** Sordariomycetes, Xylariomycetidae, Amphisphaerales, *incertae sedis*.

Asexual morph: Mycelium composed of hyaline to black, thin- to thick-walled, smooth, branched, septate. Conidiophores arising from hyphae, solitary, erect, cylindrical, pale brown to dark brown, thick-walled, occasionally roughened on lower part, septate. Conidiogenous cells terminal and intercalary on conidiophores, occasionally lateral on hyphae, obclavate, sympodially proliferate, denticulate, hyaline to pale brown, smooth, septate. Conidia hyaline, smooth, aseptate, subglobose to ellipsoidal, slightly curved. Chlamydospores solitary, terminal on hyphae, medium brown to dark brown, smooth, thick-walled, aseptate, subglobose. Sexual morph: absent.

**Type species.** *Pseudoleptodontidium chiangmaiense* Thitla, Monkai, Lumyong & Hongsanan, sp. nov.



**Notes.** Hernández-Restrepo et al. (2017) established *Leptodontidium* in Leptodontidiaceae (Helotiales, Leotiomycetes), characterised by erect conidiophores and conidiogenous cells with a long rachis bearing denticles, as well as the presence of a *Beauveria*-like synasexual morph. *Neoleptodontidium* was introduced by Crous et al. (2023) due to its morphological resemblance to *Leptodontidium*, but it differs in having minute, terminal and lateral exophiala-like phialides. Based on LSU phylogeny, the type species of *Neoleptodontidium* (*N. aquaticum*) clustered with *Leptodontidium aciculare* (Crous et al. 2023). Hence, Crous et al. (2023) transferred *L. aciculare* to *Neoleptodontidium* as *N. aciculare* by the morphological and phylogenetic congruence.

*Pseudoleptodontidium* is morphologically similar to *Neoleptodontidium*, sharing septate, subcylindrical conidiophores, terminal and lateral phialidic conidiogenous cells and aseptate subcylindrical conidia (Crous et al. 2023). However, *Pseudoleptodontidium* can be distinguished from *Neoleptodontidium* by its obclavate, sympodially proliferating, denticulate conidiogenous cells and subglobose to ellipsoidal conidia. The phylogeny, based on a combined ITS, LSU, *RPB2* and *TUB* dataset, revealed that *Pseudoleptodontidium* forms an independent lineage, sister to *Neoleptodontidium* with significant support (BS 96% ML and PP 1.00; Fig. 4). Although Crous et al. (2023) placed *Neoleptodontidium* in Xylariales genera *incertae sedis*, our phylogeny indicates that *Pseudoleptodontidium* and *Neoleptodontidium* are closely related to the Amphisphaeriaceae, Cylidriaceae, Phlogicylindriaceae and Amphisphaeriales genera *incertae sedis* (*Neoarthrinium*, *Pidoplitchkoviella*) (Fig. 4). Therefore, due to their distinct morphology and phylogeny, *Pseudoleptodontidium* is introduced as a genus *incertae sedis* in Amphisphaeriales, with *Ps. chiangmaiense* designated as the type species.

***Pseudoleptodontidium chiangmaiense* Thitla, Monkai, Lumyong & Hongsanan, sp. nov.**

MycoBank No: 857467

**Etymology.** The specific epithet *chiangmaiense* refers to the type locality, Chiang Mai Province, Thailand.

**Holotype.** Thailand•Chiang Mai Province, Mueang Chiang Mai District, Su Thep, on soil in the forest dump-sites, 21 June 2024, T. Thitla & J. Monkai; VR044 (SZU25-007, holotype); ex-type living culture, MBSZU 25-005, dried culture permanently preserved in a metabolically inactive state, SZU25-007.

**Colony diam.** (in mm) 14 days, 25 °C: PDA 36–40 and MEA 31–38.

**Culture characteristics.** Colonies at 25 °C for 14 days on PDA velvety, circular, flat, entire margin; dark green at the centre, greenish-yellow at the middle, white at the margin; soluble pigment absent; reverse dark green to pale yellow, white at the margin (Fig. 7A). Colonies on MEA velvety, circular, flat, entire margin; dark green to black at the centre, yellowish-green to white at the margin; soluble pigment absent; reverse dark green at the centre, pale yellow to white at the margin (Fig. 7B).

**Micromorphology.** Mycelium composed of hyaline to black, thin- to thick-walled, smooth, branched, septate, 2–4.5 µm diam. hyphae (Fig. 7C–L). Conidiophores arising from hyphae, solitary, erect, cylindrical, pale brown to dark



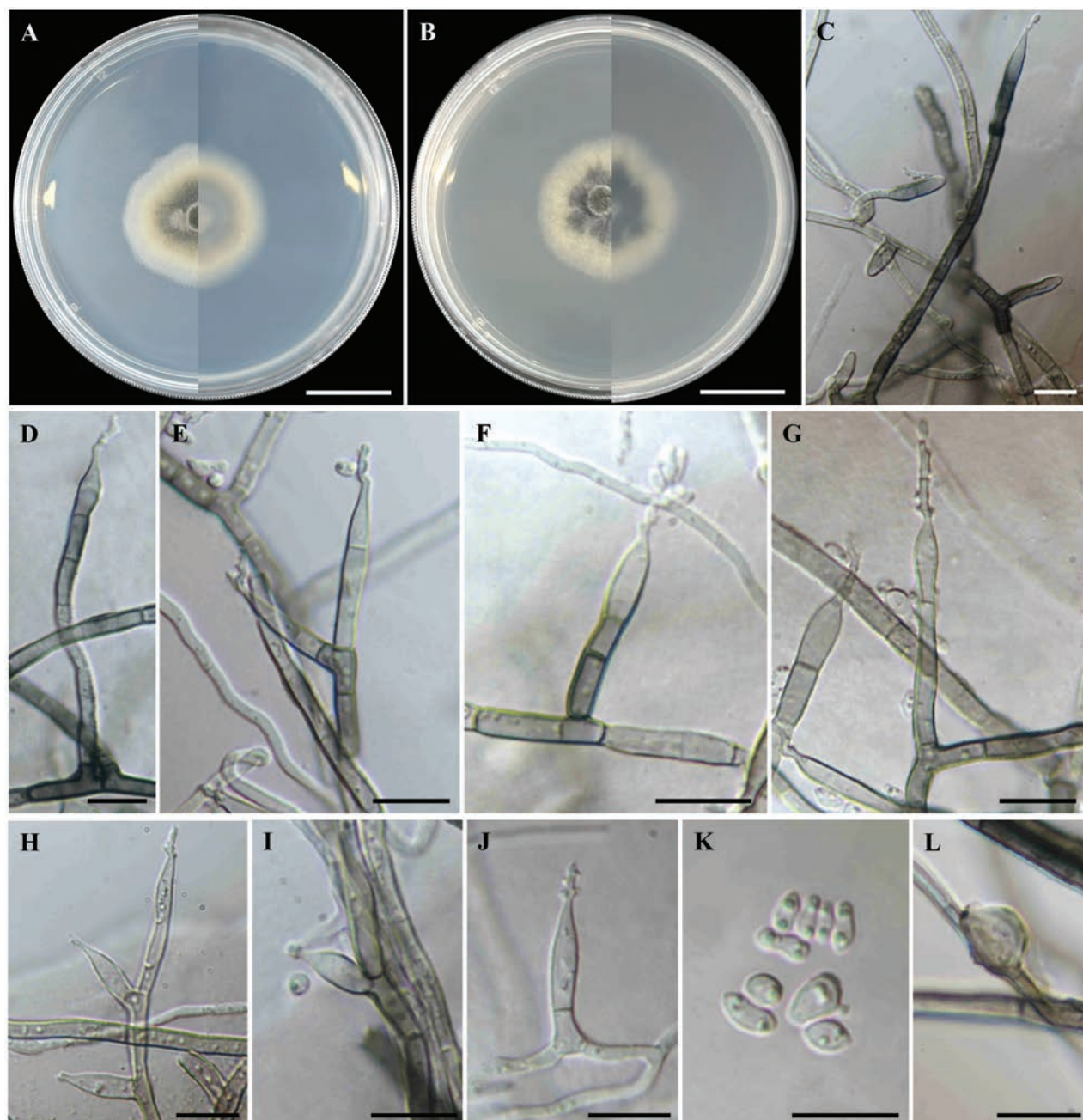


**Figure 7.** *Pseudoleptodontidium chiangmaiense* (MBSZU 25-005, ex-type living culture) **A, B** colonies from surface and reverse view at 25 °C for 14 days on PDA and MEA, respectively **C–J** conidiophores, conidiogenous cells and conidia **K** conidia **L** chlamydospore. Scale bar: 2 cm (**A, B**); 10 µm (**C–L**).

brown, thick-walled, occasionally roughened on lower part, septate,  $7\text{--}70 \times 2.5\text{--}5 \mu\text{m}$  (Fig. 7C–G). Conidiogenous cells terminal and intercalary on conidiophores, occasionally lateral on hyphae, obclavate, sympodially proliferate, denticulate, hyaline to pale brown, smooth, 0–1 septate,  $7.5\text{--}26 \times 3\text{--}5 \mu\text{m}$  (Fig. 7C–J). Conidia hyaline, smooth, aseptate, subglobose to ellipsoidal, slightly curved,  $3\text{--}7.5 \times 1.5\text{--}4 \mu\text{m}$  (Fig. 7K). Chlamydospores solitary, terminal on hyphae, medium brown to dark brown, smooth, thick-walled, aseptate, subglobose,  $6\text{--}8 \times 4.5\text{--}6 \mu\text{m}$  (Fig. 7L). Sexual morph absent.

**Habitat and distribution.** Soil; only known from Chiang Mai Province, Thailand.

**Notes.** *Pseudoleptodontidium chiangmaiense* has a close relationship with *Neoleptodontidium aciculare* and *N. aquaticum* (Fig. 4). However, their morphological characteristics are distinct: *Ps. chiangmaiense* has broader conidiogenous cells ( $7.5\text{--}26 \times 3\text{--}5 \mu\text{m}$ ) than *N. aciculare* ( $15\text{--}30 \times 2\text{--}3 \mu\text{m}$ ) and *N. aquaticum* ( $10\text{--}30 \times 2\text{--}2.5 \mu\text{m}$ ) and larger conidia ( $3\text{--}7.5 \times 1.5\text{--}4 \mu\text{m}$ ) than *N. aciculare* ( $3\text{--}4 \times 1\text{--}2 \mu\text{m}$ ) and *N. aquaticum* ( $3\text{--}4 \times 1.5 \mu\text{m}$ ) (Rao and De Hoog 1986; Hernández-Restrepo et al. 2017). The pairwise nucleotide comparison between *Ps. chiangmaiense* and *N. aciculare* revealed differences of 16.38% (95/580 bp, including gaps) in the ITS region and 4.92% (40/813 bp, including gaps) in the LSU region. Additionally, the comparison between *Ps. chiangmaiense* and *N. aquaticum* revealed differences of 16.23% (87/536 bp, including gaps) in the ITS region and 4.80% (39/813 bp, including gaps) in the LSU region.

## Discussion

This study identifies a new genus in Xylariomycetidae, namely *Pseudoleptodontidium*, accommodating *Ps. chiangmaiense* sp. nov., along with two new species of *Penicillium*: *P. terrae* in section *Exilicaulis* and *P. chiangmaiense* in section *Lanata-Divaricata*. These species were isolated from soil collected in forest dump-sites in Chiang Mai Province, Thailand. They were characterised through morphological observations and multigene phylogenetic analyses (Figs 2–6).

*Penicillium* is a highly impactful genus, with species ranging from mycotoxin-producing plant pathogens and opportunistic animal and human pathogens to valuable sources of enzymes, antibiotics and bioactive compounds (Oshikata et al. 2013; Perrone and Susca 2017; Costa et al. 2019; Toghuego and Boyom 2020; Wolski 2023; Suwannarach et al. 2024). The genus was proposed by Link (1809) and currently comprises two subgenera, 34 sections, 102 series and 535 accepted species (Visagie et al. 2024a). *Penicillium* was traditionally identified, based on macro-morphology (such as colony characteristics and pigment production) and micro-morphology (including conidiophores, branches, metula, phialides and conidia) (Khuna et al. 2023). However, relying solely on morphological characteristics has proven insufficient for accurate identification. Consequently, an integrated approach combining morphology, molecular data and extrolite analysis is currently used to identify species within the genus *Penicillium* (Visagie et al. 2014; Labuda et al. 2021; Nguyen and Pham 2022; Visagie et al. 2024a, 2024b). In section *Exilicaulis*, key genetic data for species identification include the internal transcribed spacer region (ITS), beta-tubulin (*TUB*), calmodulin (*CAM*) and RNA polymerase II subunit (*RPB2*) genes (Visagie et al. 2016c). Initially, *P. laeve* and *P. ovatum* were introduced under the genus *Torulomyces* as *T. laevis* and *T. ovatus*, respectively (Ando et al. 1998). Subsequently, phylogenetic analyses using RNA polymerase II largest subunit (*RPB1*), *RPB2*, the protein required for processing of 20S pre-rRNA in the cytoplasm (*Tsr1*) and the subunit of the cytosolic chaperonin Cct ring complex (*Cct8*) led to transfer to *Penicillium* section *Torulomyces* (Houbraken and Samson 2011). Visagie et al. (2016a) reclassified these species into section *Exilicaulis* using ITS, *TUB*, *CAM* and *RPB2* sequence data. Currently, *P. laeve* and *P. ovatum* belong to the series *Erubescens*, characterised by species with monoverticillate conidiophores, short stipes and the ability to grow at 37 °C (Houbraken et al.

2020). However, both *P. laeve* and *P. ovatum*, along with *P. terrae*, produce conidiophores with solitary phialides and were unable to grow at 37 °C. Additionally, the phylogenetic clade of these species formed a basal clade with other species in this series with strong support (BS 97% and PP 1.00) (Fig. 2). In our opinion, this distinct clade may represent a potential new series within section *Exilicaulis* and should be further studied in the future.

Prior to this study, *P. laeve* was the only species in section *Exilicaulis* reported from Thailand (Ando et al. 1998). The discovery of *P. terrae* from soil in Thailand marks the second species from this section identified in the country. Furthermore, this new species represents the 69<sup>th</sup> global species in section *Exilicaulis*, as shown in Suppl. material 1: table S1, excluding *P. janthinellum* and *P. limosum*. In addition, this study proposed a new species, *P. Chiangmaiense* in section *Lanata-Divaricata*, which is the second species recorded in Thailand from this section, following the first species (*P. singorensis*) described by Visagie et al. (2014b). Additionally, this new species represents the 108<sup>th</sup> global species in section *Lanata-Divaricata*, as outlined in Suppl. material 1: table S2, excluding *P. alogum* and *P. stolckiae*.

Ecologically, *Penicillium* species have been isolated from different environments (Ansari et al. 2023; Nóbrega et al. 2024). For instance, *P. Chiangmaiense* and its closely-related species, including *P. brefeldianum*, *P. limosum* and *P. michoacanense*, have been found in the human digestive tract, marine sediments and soil (Dodge 1933; Ueda 1995; Rodríguez-Andrade et al. 2021). Similarly, *P. terrae* and its relatives, including *P. laeve* and *P. ovatum*, have primarily been reported from soil, with *P. laeve* specifically found in forest soils in Thailand (Ando et al. 1998). These findings highlight the ecological plasticity of *Penicillium* species, which can potentially thrive in disturbed ecosystems. Future studies examining their functional traits and metabolic profiles could further enhance better understanding of their ecological significance.

Xylariomycetidae is a large subclass within Sordariomycetes comprising numerous taxa that are polyphyletic and paraphyletic (Wendt et al. 2017; Daranagama et al. 2018; Konta et al. 2020; Samarakoon et al. 2022). The taxonomic classification of Xylariomycetidae has undergone considerable change (Maharachchikumbura et al. 2016; Samarakoon et al. 2016, 2022). Earlier, Amphisphaeriales was considered a synonym of Xylariales (Maharachchikumbura et al. 2016). However, based on morphology, molecular data, divergence estimates and ancestral state reconstruction, Samarakoon et al. (2016, 2022) subsequently reclassified Amphisphaeriales, Delonicolales and Xylariales in Xylariomycetidae. Molecular phylogeny, based on concatenated ITS, LSU, *RPB2*, *TUB* and *TEF-1α* sequence data, demonstrated the placement of Amphisphaeriales in a sister clade to Xylariales (Samarakoon et al. 2022), which is consistent with our study (Fig. 4). However, we did not incorporate *TEF-1α* into the phylogenetic tree, as the number of taxa with available sequence data was low. The classification of taxa within Xylariomycetidae remains ambiguous, as more than 50 *incertae sedis* genera await taxonomic resolution (Samarakoon et al. 2022). Likewise, our study was unable to assign the novel genus *Pseudoleptodontidium* to any family within the Xylariomycetidae (Fig. 4). The new lineage of *Pseudoleptodontidium* and *Neoleptodontidium* also lacks significant statistical support for placement within other taxa and families in Amphisphaeriales, though it is likely linked to Amphisphaeriaceae, Cylindriaceae and Phlogicylindriaceae (Fig. 4). Further taxonomic and phylogenetic studies, including the collection of new

specimens and the examination of additional isolates, are necessary to confirm the familial placement of *Pseudoleptodontidium* and *Neoleptodontidium*.

Members of Xylariomycetidae have a worldwide distribution and occupy various ecological niches, including saprobes, endophytes and pathogens (U'Ren et al. 2016; Daranagama et al. 2018; Sugita et al. 2022; Samarakoon 2024). Recently, several new taxa have been reported as saprobes on dead plant materials from Thailand (Monkai et al. 2022; Afshari et al. 2023; Samarakoon et al. 2023; Karimi et al. 2023, 2024; Samarakoon 2024; Thakshila et al. 2024). In this study, *Pseudoleptodontidium* was isolated from soil associated with a forest dump-site in Thailand, whereas *Neoleptodontidium* species have been found in hydroponic water and decomposing wood in the USA and India (Rao and De Hoog 1986; Hernández-Restrepo et al. 2017). This demonstrates that these taxa have a broad distribution range, highlighting their adaptability in diverse environments.

These findings significantly contribute to our understanding of fungal diversity and ecology, particularly within the Ascomycota and highlight the richness and diversity of soil fungal communities in Thailand. *Penicillium* and some Xylariomycetidae taxa, such as *Amphisphaeria*, *Annulohyphoxylon* and *Hypoxylon* are recognised for possessing a wide variety of secondary metabolites, which have prospective agricultural and therapeutic uses (Toghueo and Boyom 2020; Becker and Stadler 2021; Wang et al. 2023a; Wolski 2023). The discovery of novel fungi in forest dump areas presents an opportunity to explore and characterise these fungi for various applications. Therefore, further research is necessary to evaluate the capabilities of new fungal strains for extracellular enzyme production and the degradation of synthetic materials.

## Acknowledgements

This research work is partially funded by Chiang Mai University. Shaun Pennycook is thanked for the nomenclatural advice. Sinang Hongsanant would like to thank the National Natural Science Foundation of China (32400012), 2023 Shenzhen Pengcheng Distinguished Positions and scientific research funds for high-tech talents /high-level talents and Shenzhen University 2035 Program for Excellent Research, Grant No. 2024C006. Ning Xie would like to thank the Natural Science Foundation of Guangdong Province (2024B1515020034) and National Key R&D Program of China (2021YFA0910800).

## Additional information

### Conflict of interest

The authors have declared that no competing interests exist.

### Ethical statement

No ethical statement was reported.

### Funding

This work was funded by the Natural Science Foundation of Guangdong Province (2024B1515020034), the International Research Fellowship (Visiting Researcher Program), Chiang Mai University (Grant No. 014/2567), and the National Key R&D Program of China (2021YFA0910800).



## Author contributions

Conceptualisation: Tanapol Thitla, Jutamart Monkai, Sinang Hongsanan, Saisamorn Lumyong. Collection and morphological examinations: Tanapol Thitla, Jutamart Monkai, Weiqian Meng, Surapong Khuna. Molecular sequencing and phylogenetic analyses: Tanapol Thitla, Jutamart Monkai, Weiqian Meng, Surapong Khuna. Original draft preparation: Tanapol Thitla, Jutamart Monkai, Surapong Khuna. Review and editing, supervision: Tanapol Thitla, Jutamart Monkai, Weiqian Meng, Surapong Khuna, Ning Xie, Sinang Hongsanan, Saisamorn Lumyong. All authors have read and agreed to the published version of the manuscript.

## Author ORCIDs

Tanapol Thitla  <https://orcid.org/0000-0003-3092-0679>

Jutamart Monkai  <https://orcid.org/0000-0001-6043-0625>

Weiqian Meng  <https://orcid.org/0009-0006-3840-0992>

Surapong Khuna  <https://orcid.org/0000-0003-1999-4001>

Ning Xie  <https://orcid.org/0000-0002-5866-8535>

Sinang Hongsanan  <https://orcid.org/0000-0003-0550-3152>

Saisamorn Lumyong  <https://orcid.org/0000-0002-6485-414X>

## Data availability

The datasets generated during and/or analysed during the current study are available in the MycoBank repository (included in the manuscript) and GenBank (included in Suppl. material 1: tables S1–S3). Additionally, the datasets generated during and/or analysed during the current study are available from the corresponding author on reasonable request.

## References

- Afshari N, Karimi O, De Farias ARG, Suwannarach N, Bhunjun CS, Zeng X-Y, Lumyong S (2023) Additions to Diatrypaceae (Xylariales): Novel taxa and new host associations. *Journal of Fungi* (Basel, Switzerland) 9: 1151. <https://doi.org/10.3390/jof9121151>
- Ando K, Nawawi A, Manoch L, Pitt JI (1998) Three new species and a new combination in the genus *Torulomyces* from soil. *Mycoscience* 39(3): 313–318. <https://doi.org/10.1007/BF02464014>
- Ansari L, Asgari B, Zare R, Zamanizadeh HR (2023) *Penicillium rhizophilum*, a novel species in the section *Exilicaulis* isolated from the rhizosphere of sugarcane in Southwest Iran. *International Journal of Systematic and Evolutionary Microbiology* 73(9). <https://doi.org/10.1099/ijsem.0.006028>
- Araújo KS, Alves JL, Pereira OL, de Queiroz MV (2024) Five new species of endophytic *Penicillium* from rubber trees in the Brazilian Amazon. *Brazilian Journal of Microbiology* 55: 3051–3074. <https://doi.org/10.1007/s42770-024-01478-9>
- Becker K, Stadler M (2021) Recent progress in biodiversity research on the Xylariales and their secondary metabolism. *The Journal of Antibiotics* 74: 1–23. <https://doi.org/10.1038/s41429-020-00376-0>
- Coleine C, Stajich JE, Selbmann L (2022) Fungi are key players in extreme ecosystems. *Trends in Ecology & Evolution* 37: 517–528. <https://doi.org/10.1016/j.tree.2022.02.002>
- Costa JH, Bazioli JM, De Moraes Pontes JG, Fill TP (2019) *Penicillium digitatum* infection mechanisms in citrus: What do we know so far? *Fungal Biology* 123: 584–593. <https://doi.org/10.1016/j.funbio.2019.05.004>

- Crous PW, Akulov A, Balashov S, Boers J, Braun U, Castillo J, Delgado MA, Denman S, Erhard A, Gusella G, Jurjević Ž, Kruse J, Malloch DW, Osieck ER, Polizzi G, Schumacher RK, Sloatweg E, Starink-Willemse M, Van Iperen AL, Verkley GJM, Groenewald JZ (2023) New and Interesting Fungi. 6. Fungal Systematics and Evolution 11: 109–156. <https://doi.org/10.3114/fuse.2023.11.09>
- da Silva IJS, Sousa TF, de Queiroz CA, Castro GDS, Caniato FF, de Medeiros LS, Angolini CFF, Hanada RE, Koolen HHF, da Silva GF (2023) *Penicillium amapaense* sp. nov., section *Exilicaulis*, and new records of *Penicillium labradorum* in Brazil isolated from Amazon River sediments with potential applications in agriculture and biotechnology. Mycological Progress 22(4): 23. <https://doi.org/10.1007/s11557-023-01868-7>
- Daranagama DA, Hyde KD, Sir EB, Thambugala KM, Tian Q, Samarakoon MC, McKenzie EHC, Jayasiri SC, Tibpromma S, Bhat JD, Liu X, Stadler M (2018) Towards a natural classification and backbone tree for Graphostromataceae, Hypoxylaceae, Lopadostomataceae and Xylariaceae. Fungal Diversity 88: 1–165. <https://doi.org/10.1007/s13225-017-0388-y>
- Dodge BO (1933) The perithecium and ascus of *Penicillium*. Mycologia 25: 90–104. <https://doi.org/10.1080/00275514.1933.12020653>
- Edgar RC (2004) MUSCLE: A multiple sequence alignment method with reduced time and space complexity. BMC Bioinformatics 5: e113. <https://doi.org/10.1186/1471-2105-5-113>
- Felsenstein J (1985) Confidence limits on phylogenies: An approach using the bootstrap. Evolution; International Journal of Organic Evolution 39: 783–791. <https://doi.org/10.2307/2408678>
- Frąc M, Hannula SE, Bełka M, Jędrzycka M (2018) Fungal biodiversity and their role in soil health. Frontiers in Microbiology 9: 707. <https://doi.org/10.3389/fmicb.2018.00707>
- Glass NL, Donaldson GC (1995) Development of primer sets designed for use with the PCR to amplify conserved genes from filamentous ascomycetes. Applied and Environmental Microbiology 61: 1323–1330. <https://doi.org/10.1128/aem.61.4.1323-1330.1995>
- Gomes de Farias AR, Yasanthika WAE, Monkai J (2023) Insights into the profile of soil fungal diversity in Thailand. Asian Journal of Mycology, 305–317. <https://doi.org/10.5943/ajom/6/2/11>
- Gong Z, Jin L, Yu X, Wang B, Hu S, Ruan H, Sung Y-J, Lee H-G, Jin F (2023) Biodegradation of low density polyethylene by the fungus *Cladosporium* sp. recovered from a landfill Site. Journal of Fungi (Basel, Switzerland) 9: 605. <https://doi.org/10.3390/jof9060605>
- Hall T (2004) Bioedit Version 6.0.7. <http://www.mbio.ncsu.edu/bioedit/bioedit> [Accessed November 2024]
- Hernández-Restrepo M, Gené J, Castañeda-Ruiz RF, Mena-Portales J, Crous PW, Guarro J (2017) Phylogeny of saprobic microfungi from Southern Europe. Studies in Mycology 86: 53–97. <https://doi.org/10.1016/j.simyco.2017.05.002>
- Hong SB, Cho HS, Shin HD, Frisvad JC, Samson RA (2006) Novel *Neosartorya* species isolated from soil in Korea. International Journal of Systematic and Evolutionary Microbiology 56: 477–486. <https://doi.org/10.1099/ijs.0.63980-0>
- Houbraken J, Samson RA (2011) Phylogeny of *Penicillium* and the segregation of Trichocomaceae into three families. Studies in Mycology 70(1): 1–51. <https://doi.org/10.3114/sim.2011.70.01>
- Houbraken J, Kocsubé S, Visagie CM, Yilmaz N, Wang XC, Meijer M, Kraak B, Hubka V, Bensch K, Samson RA, Frisvad JC (2020) Classification of *Aspergillus*, *Penicilli-*

- um, *Talaromyces* and related genera (Eurotiales): An overview of families, genera, subgenera, sections, series and species. *Studies in Mycology* 95: 5–169. <https://doi.org/10.1016/j.simyco.2020.05.002>
- Karimi O, Chethana KWT, Farias ARG, Li Q (2023) Two new records of Xylariales species from Northern Thailand. *Phytotaxa* 598: 187–205. <https://doi.org/10.11646/phytotaxa.598.3.1>
- Karimi O, Afshari N, Asghari R, Li Q, Chethana KWT, Hyde KD, Alotibi FO (2024) Novel discoveries of Xylariomycetidae (Ascomycota) taxa from peat swamp forests and other terrestrial habitats in Thailand. *MycKeys* 107: 219–247. <https://doi.org/10.3897/mycokeys.107.127749>
- Khan S, Ali SA, Ali AS (2022) Biodegradation of low density polyethylene (LDPE) by mesophilic fungus '*Penicillium citrinum*' isolated from soils of plastic waste dump yard, Bhopal, India. *Environmental Technology* 44: 2300–2314. <https://doi.org/10.1080/09593330.2022.2027025>
- Khuna S, Kumla J, Thitla T, Hongsanant S, Lumyong S, Suwannarach N (2023) *Penicillium thailandense* (Aspergillaceae, Eurotiales), a new species isolated from soil in northern Thailand. *Phytotaxa* 612(1): 033–045. <https://doi.org/10.11646/phytotaxa.612.1.2>
- Konta S, Hyde KD, Phookamsak R, Xu JC, Maharachchikumbura SSN, Daranagama DA, McKenzie EH, Boonmee S, Tibpromma S, Eungwanichayapant PD, Samarakoon MC (2020) Polyphyletic genera in Xylariaceae (Xylariales): *Neoxylaria* gen. nov. and *Stilbohypoxylon*. *Mycosphere* 11: 2629–2651. <https://doi.org/10.5943/mycosphere/11/1/17>
- Kooch Y, Nouraei A, Haghverdi K, Kolb S, Francaviglia R (2023) Landfill leachate has multiple negative impacts on soil health indicators in Hyrcanian forest, northern Iran. *The Science of the Total Environment* 896: 166341. <https://doi.org/10.1016/j.scitotenv.2023.166341>
- Korhonen K, Hintikka V (1980) Simple isolation and inoculation methods for fungal cultures. *Karstenia* 20: 19–22. <https://doi.org/10.29203/ka.1980.192>
- Labuda R, Bacher M, Rosenau T, Gasparotto E, Gratzl H, Doppler M, Sulyok M, Kubátová A, Berger H, Cank K, Raja HA, Oberlies NH, Schüller C, Strauss J (2021) Polyphasic approach utilized for the identification of two new toxigenic members of *Penicillium* section *Exilicaulis*, *P. krskae* and *P. silybi* spp. nov. *Journal of Fungi* (Basel, Switzerland) 7(7): 557. <https://doi.org/10.3390/jof7070557>
- Lenz AR, Balbinot E, de Abreu FP, de Oliveira NS, Fontana RC, de Avila E, Silva S, Park MS, Lim YW, Houbraken J, Camassola M, Dillon AJP (2022) Taxonomy, comparative genomics and evolutionary insights of *Penicillium ucsense*: A novel species in series *Oxalica*. *Antonie van Leeuwenhoek* 115: 1009–1029. <https://doi.org/10.1007/s10482-022-01746-4>
- Li WL, Liang RR, Yang J, Liu JK (2024) Morpho-molecular characterization reveals a new genus, three novel species and two new host records in Xylariomycetidae. *Journal of Fungi* (Basel, Switzerland) 10: 189. <https://doi.org/10.3390/jof10030189>
- Lin D, Yang G, Dou P, Qian S, Zhao L, Yang Y, Fanin N (2020) Microplastics negatively affect soil fauna but stimulate microbial activity: Insights from a field-based microplastic addition experiment. *Proceedings. Biological Sciences* 287: 20201268. <https://doi.org/10.1098/rspb.2020.1268>
- Link JHF (1809) *Observationes in ordines plantarum naturales. Dissertatio I.* *Magazin Der Gesellschaft Naturforschenden Freunde Berlin* 3: 3–42. [in Latin]
- Liu YJ, Whelen S, Hall BD (1999) Phylogenetic relationships among ascomycetes: Evidence from an RNA polymerase II subunit. *Molecular Biology and Evolution* 16: 1799–1808. <https://doi.org/10.1093/oxfordjournals.molbev.a026092>

- Liu C, Wang XC, Yu ZH, Zhuang WY, Zeng ZQ (2023) Seven new species of Eurotiales (Ascomycota) isolated from tidal flat sediments in China. *Journal of Fungi* (Basel, Switzerland) 9: 960. <https://doi.org/10.3390/jof9100960>
- Maharachchikumbura SSN, Hyde KD, Jones EBG, McKenzie EHC, Bhat JD, Dayarathne MC, Huang S-K, Norphanphoun C, Senanayake IC, Perera RH, Shang Q-J, Xiao Y, D'souza MJ, Hongsanan S, Jayawardena RS, Daranagama DA, Konta S, Goonasekara ID, Zhuang W-Y, Jeewon R, Phillips AJL, Abdel-Wahab MA, Al-Sadi AM, Bahkali AH, Boonmee S, Boonyuen N, Cheewangkoon R, Dissanayake AJ, Kang J, Li Q-R, Liu JK, Liu XZ, Liu Z-Y, Luangsa-Ard JJ, Pang K-L, Phookamsak R, Promputtha I, Suetrong S, Stadler M, Wen T, Wijayawardene NN (2016) Families of Sordariomycetes. *Fungal Diversity* 79: 1–317. <https://doi.org/10.1007/s13225-016-0369-6>
- Miller MA, Holder MT, Vos R, Midford PE, Liebowitz T, Chan L, Hoover P, Warnow T (2009) The CIPRES Portals. CIPRES. [http://www.phylo.org/sub\\_sections/portal](http://www.phylo.org/sub_sections/portal) [Accessed November 2024]
- Monkai J, Phookamsak R, Tennakoon DS, Bhat DJ, Xu S, Li Q, Xu J, Mortimer PE, Kumla J, Lumyong S (2022) Insight into the taxonomic resolution of *Apiospora*: Introducing novel species and records from bamboo in China and Thailand. *Diversity* 14: 918. <https://doi.org/10.3390/d14110918>
- Nguyen VD, Pham TT (2022) *Penicillium vietnamense* sp. nov., the first novel marine fungi species described from vietnam with a unique conidiophore structure and molecular phylogeny of *Penicillium* section *Charlesia*. *Mycobiology* 50(3): 155–165. <https://doi.org/10.1080/12298093.2022.2068750>
- Nishimura D (2000) Sequencher 3.1.1. Biotech Software & Internet Report 1: 24–30. <https://doi.org/10.1089/152791600319231>
- Nóbrega JP, do Nascimento Barbosa R, Lima JMds, Bento DdM, de Souza-Motta CM, Melo RFR (2024) Six new *Penicillium* species in the section *Lanata-Divaricata* from a cave in Amazon rainforest, Brazil. *Mycological Progress* 23: 71. <https://doi.org/10.1007/s11557-024-02007-6>
- Nylander JAA (2004) MrModeltest 2.0. Program distributed by the author. Evolutionary Biology Centre, Uppsala University, Uppsala.
- O'Donnell K, Cigelnik E (1997) Two divergent intragenomic rDNA ITS2 types within a monophyletic lineage of the fungus *Fusarium* are nonorthologous. *Molecular Phylogenetics and Evolution* 7: 103–116. <https://doi.org/10.1006/mpev.1996.0376>
- Oshikata C, Tsurikisawa N, Saito A, Watanabe M, Kamata Y, Tanaka M, Tsuburai T, Mitomi H, Takatori K, Yasueda H, Akiyama K (2013) Fatal pneumonia caused by *Penicillium digitatum*: A case report. *BMC Pulmonary Medicine* 13: 16. <https://doi.org/10.1186/1471-2466-13-16>
- Pangging M, Nguyen TTT, Lee HB (2021) Seven new records of *Penicillium* species belonging to section *Lanata-Divaricata* in Korea. *Mycobiology* 49: 363–375. <https://doi.org/10.1080/12298093.2021.1952814>
- Perrone G, Susca A (2017) *Penicillium* species and their associated mycotoxins. *Methods in Molecular Biology* (Clifton, N.J.): 107–119. [https://doi.org/10.1007/978-1-4939-6707-0\\_5](https://doi.org/10.1007/978-1-4939-6707-0_5)
- Peterson SW, Vega FE, Posada F, Nagai C (2005) *Penicillium coffeae*, a new endophytic species isolated from a coffee plant and its phylogenetic relationship to *P. fellutanum*, *P. thiersii* and *P. brocae* based on parsimony analysis of multilocus DNA sequences. *Mycologia* 97(3): 659–666. <https://doi.org/10.1080/15572536.2006.11832796>
- Pitt JI (1980) [1979] The Genus *Penicillium* and its Teleomorphic States *Eupenicillium* and *Talaromyces*. Academic Press, London.



- Rambaut A (2019) FigTree tree figure drawing tool version 131; Institute of Evolutionary 623 Biology (Edinburgh, Scotland: University of Edinburgh). <http://treebioedacuk/software/figtree/> [Accessed November 2024]
- Rao V, De Hoog GS (1986) New of critical hyphomycetes from India. *Studies in Mycology* 28: 1–84.
- Rathnayaka AR, Tennakoon DS, Jones GE, Wanasinghe DN, Bhat DJ, Priyashantha AH, Stephenson SL, Tibpromma S, Karunarathna SC (2024) Significance of precise documentation of hosts and geospatial data of fungal collections, with an emphasis on plant-associated fungi. *New Zealand Journal of Botany* 63: 462–489. <https://doi.org/10.1080/0028825X.2024.2381734>
- Rehner SA, Samuels GJ (1994) Taxonomy and phylogeny of gliocladium analyzed from nuclear large subunit ribosomal DNA sequences. *Mycological Research* 98: 625–634. [https://doi.org/10.1016/S0953-7562\(09\)80409-7](https://doi.org/10.1016/S0953-7562(09)80409-7)
- Ren GC, Pang AM, Gao Y, Wu SX, Ge ZQ, Zhang TF, Wanasinghe DN, Khan S, Mortimer PE, Xu JC, Gui H (2021) Polyurethane-degrading fungi from soils contaminated with rocket propellant and their ability to decompose alkyne terminated polybutadiene with urethane. *Studies in Fungi* 6: 224–239. <https://doi.org/10.5943/sif/6/1/15>
- Rodríguez-Andrade E, Stchigel AM, Cano-Lira JF (2021) New xerophilic species of *Penicillium* from soil. *Journal of Fungi (Basel, Switzerland)* 7: 126. <https://doi.org/10.3390/jof7020126>
- Ronquist F, Huelsenbeck JP (2003) MrBayes 3: Bayesian phylogenetic inference under mixed models. *Bioinformatics (Oxford, England)* 19: 1572–1574. <https://doi.org/10.1093/bioinformatics/btg180>
- Samarakoon MC (2024) Additions to the Xylariomycetidae (Sordariomycetes) Fungal Flora from Northern Thailand: *Amphisphaeria chiangmaiensis* sp. nov. and *A. hydei* sp. nov. *New Zealand Journal of Botany* 62: 253–269. <https://doi.org/10.1080/0028825X.2023.2284420>
- Samarakoon MC, Hyde KD, Promputtha I, Hongsanan S, Ariyawansa HA, Maharachchikumbura SSN, Daranagama DA, Stadler M, Mapook A (2016) Evolution of Xylariomycetidae (Ascomycota: Sordariomycetes). *Mycosphere* 7: 1746–1761. <https://doi.org/10.5943/mycosphere/7/11/9>
- Samarakoon MC, Hyde KD, Maharachchikumbura SSN, Stadler M, Jones EBG, Promputtha I, Suwannarach N, Camporesi E, Bulgakov TS, Liu J-K (2022) Taxonomy, phylogeny, molecular dating and ancestral state reconstruction of Xylariomycetidae (Sordariomycetes). *Fungal Diversity* 112: 1–88. <https://doi.org/10.1007/s13225-021-00495-5>
- Samarakoon MC, Lumyong S, Manawasinghe IS, Suwannarach N, Cheewangkoon R (2023) Addition of five novel fungal flora to the Xylariomycetidae (Sordariomycetes, Ascomycota) in northern Thailand. *Journal of Fungi (Basel, Switzerland)* 9: 1065. <https://doi.org/10.3390/jof9111065>
- Sangale MK, Shahnawaz M, Ade AB (2019) Potential of fungi isolated from the dumping sites mangrove rhizosphere soil to degrade polythene. *Scientific Reports* 9: 5390. <https://doi.org/10.1038/s41598-019-41448-y>
- Sathiyabama M, Boomija RV, Sathiyamoorthy T, Mathivanan N, Balaji R (2024) Myco-degradation of low-density polyethylene by *Cladosporium sphaerospermum*, isolated from platisphere. *Scientific Reports* 14: 8351. <https://doi.org/10.1038/s41598-024-59032-4>
- Schlöter M, Nannipieri P, Sørensen SJ, Van Elsas JD (2018) Microbial indicators for soil quality. *Biology and Fertility of Soils* 54: 1–10. <https://doi.org/10.1007/s00374-017-1248-3>

- Singh M, Singh D, Rai PK, Suyal DC, Saurabh S, Soni R, Giri K, Yadav AN (2021) Fungi in remediation of hazardous wastes: current status and future outlook. *Fungal Biology*, 195–224. [https://doi.org/10.1007/978-3-030-68260-6\\_8](https://doi.org/10.1007/978-3-030-68260-6_8)
- Stamatakis A (2006) RAxML-VI-HPC: Maximum likelihood-based phylogenetic analyses with thousands of taxa and mixed models. *Bioinformatics (Oxford, England)* 22: 2688–2690. <https://doi.org/10.1093/bioinformatics/btl446>
- Sugita R, Hirayama K, Shirouzu T, Tanaka K (2022) *Spirodecosporaceae* fam. nov. (Xylariales, Sordariomycetes) and two new species of *Spirodecospora*. *Fungal Systematics and Evolution* 10: 217–229. <https://doi.org/10.3114/fuse.2022.10.09>
- Sun Y, Xie S, Zang J, Wu M, Tao J, Li S, Du X, Wang J (2024) Terrestrial plastisphere as unique niches for fungal communities. *Communications Earth & Environment* 5: 483. <https://doi.org/10.1038/s43247-024-01645-8>
- Suwannarach N, Khuna S, Chaiwong K, Senwanna C, Nuangmek W, Kumla J (2024) Identification and fungicide sensitivity of the blue mold pathogen in postharvest-stored elephant garlic Bulbs in Thailand. *Studies in Fungi* 0: 1–9. <https://doi.org/10.48130/sif-0024-0015>
- Tedersoo L, Mikryukov V, Anslan S, Bahram M, Khalid AN, Corrales A, Agan A, Vasco-Palacios A-M, Saitta A, Antonelli A, Rinaldi AC, Verbeken A, Sulistyo BP, Tamgnoue B, Furneaux B, Ritter CD, Nyamukondiwa C, Sharp C, Marín C, Dai DQ, Gohar D, Sharmah D, Biersma EM, Cameron EK, De Crop E, Otsing E, Davydov EA, Albornoz FE, Brearley FQ, Buegger F, Gates G, Zahn G, Bonito G, Hiiesalu I, Hiiesalu I, Zettur I, Barrio IC, Pärn J, Heilmann-Clausen J, Ankuda J, Kupagme JY, Sarapuu J, Maciá-Vicente JG, Fovo JD, Geml J, Alatalo JM, Alvarez-Manjarrez J, Monkai J, Põldmaa K, Runnel K, Adamson K, Bråthen KA, Pritsch K, Tchan KI, Armolaitis K, Hyde KD, Newsham KK, Panksep K, Adebola LA, Lamit LJ, Saba M, Da Silva Cáceres ME, Tuomi M, Gryzenhout M, Bauters M, Bálint M, Wijayawardene N, Hagh-Doust N, Yorou NS, Kurina O, Mortimer PE, Meidl P, Nilsson RH, Puusepp R, Casique-Valdés R, Drenkhan R, Garibay-Orijel R, Godoy R, Alfarraj S, Rahimlou S, Pölme S, Dudov SV, Mundra S, Ahmed T, Netherway T, Henkel TW, Roslin T, Fedosov VE, Onipchenko VG, Yasanthika W, Lim YW, Piepenbring M, Klavina D, Kõljalg U, Abarenkov K (2021) The Global Soil Mycobiome consortium dataset for boosting fungal diversity research. *Fungal Diversity* 111: 573–588. <https://doi.org/10.1007/s13225-021-00493-7>
- Thakshila SAD, Bhunjun CS, Samarakoon MC, Rathnayaka AR, Gajanayake AJ (2024) Morpho-molecular analyses reveal a novel species, *Xenoanthostomella thailandica* (Gyrothricaceae, Xylariales), from northern Thailand. *New Zealand Journal of Botany* 62: 336–366. <https://doi.org/10.1080/0028825X.2024.2304776>
- Thom C (1930) *The Penicillia*. The Williams & Wilkins Company, Baltimore.
- Toghueo RMK, Boyom FF (2020) Endophytic *Penicillium* species and their agricultural, biotechnological, and pharmaceutical applications. *3 Biotech* 10. <https://doi.org/10.1007/s13205-020-2081-1>
- U'Ren JM, Miadlikowska J, Zimmerman NB, Lutzoni F, Stajich JE, Arnold AE (2016) Contributions of North American endophytes to the phylogeny, ecology, and taxonomy of Xylariaceae (Sordariomycetes, Ascomycota). *Molecular Phylogenetics and Evolution* 98: 210–232. <https://doi.org/10.1016/j.ympev.2016.02.010>
- Ueda SA (1995) New species of *Eupenicillium* from marine sediment. *Mycoscience* 36: 451–454. <https://doi.org/10.1007/BF02268631>
- Verma N, Gupta S (2019) Assessment of LDPE degrading potential *Aspergillus* species isolated from municipal landfill sites of Agra. *SN Applied Sciences* 1: 701. <https://doi.org/10.1007/s42452-019-0746-3>

- Vilgalys R, Hester M (1990) Rapid genetic identification and mapping of enzymatically amplified ribosomal DNA from several *Cryptococcus* species. *Journal of Bacteriology* 172: 4238–4246. <https://doi.org/10.1128/jb.172.8.4238-4246.1990>
- Visagie CM, Houbraken J, Frisvad JC, Hong SB, Klaassen CHW, Perrone G, Seifert KA, Varga J, Yaguchi T, Samson RA (2014) Identification and nomenclature of the genus *Penicillium*. *Studies in Mycology* 78: 343–371. <https://doi.org/10.1016/j.simyco.2014.09.001>
- Visagie CM, Hirooka Y, Tanney JB, Whitfield E, Mwange K, Meijer M, Amend AS, Seifert KA, Samson RA (2014b) *Aspergillus*, *Penicillium* and *Talaromyces* isolated from house dust samples collected around the world. *Studies in Mycology* 78: 63–139. <https://doi.org/10.1016/j.simyco.2014.07.002>
- Visagie CM, Houbraken J, Dijksterhuis J, Seifert KA, Jacobs K, Samson RA (2016a) A taxonomic review of *Penicillium* species producing conidiophores with solitary phialides, classified in section *Torulomyces*. *Persoonia* 36: 134–155. <https://doi.org/10.3767/003158516X690952>
- Visagie CM, Renaud JB, Burgess KM, Malloch DW, Clark D, Ketch L, Urb M, Louis-Seize G, Assabgui R, Sumarah MW, Seifert KA (2016b) Fifteen new species of *Penicillium*. *Persoonia* 36: 247–280. <https://doi.org/10.3767/003158516X691627>
- Visagie CM, Seifert KA, Houbraken J, Samson RA, Jacobs K (2016c) A phylogenetic revision of *Penicillium* sect. *Exilicaulis*, including nine new species from fynbos in South Africa. *IMA Fungus* 7: 75–117. <https://doi.org/10.5598/ima fungus.2016.07.01.06>
- Visagie CM, Yilmaz N, Kocsubé S, Frisvad JC, Hubka V, Samson RA, Houbraken J (2024a) A review of recently introduced *Aspergillus*, *Penicillium*, *Talaromyces* and other Eurotiales species. *Studies in Mycology* 107: 1–66. <https://doi.org/10.3114/sim.2024.107.01>
- Visagie CM, Houbraken J, Yilmaz N (2024b) The re-identification of *Penicillium* and *Talaromyces* (Eurotiales) catalogued in South African culture collections. *Persoonia* 53: 29–61. <https://doi.org/10.3767/persoonia.2024.53.02>
- Wang X, Wanasinghe DN, Zhang J, Ma J, Zhou P, Zhang L, Lu Y, Zhang Z (2023a) Insights from the endophytic Fungi in *Amphisphaeria* (Sordariomycetes): *A. orixae* sp. nov. from *Orixa japonica* and Its Secondary Metabolites. *Microorganisms* 11: 1268. <https://doi.org/10.3390/microorganisms11051268>
- Wang XC, Zhang ZK, Zhuang WY (2023b) Species diversity of *Penicillium* in Southwest China with discovery of forty-three new species. *Journal of Fungi (Basel, Switzerland)* 9: 1150. <https://doi.org/10.3390/jof9121150>
- Wanthongchai K, Tanpipat V, Noochaiya P, Sirimongkonlertkun N, Macatangay R, Thamavongsa L, Oo TN, Bran SH, Solanki R (2021) Integrated highland wildfire, smoke, and haze management in the Upper Indochina region. *APN Science Bulletin* 11: 133–143. <https://doi.org/10.30852/sb.2021.1704>
- Wendt L, Sir EB, Kuhnert E, Heitkamp S, Lambert C, Hladki AI, Romero AI, Luangsa-Ard JJ, Srikitikulchai P, Peršoh D, Stadler M (2017) Resurrection and emendation of the Hypoxylaceae, recognised from a multigene phylogeny of the Xylariales. *Mycological Progress* 17: 115–154. <https://doi.org/10.1007/s11557-017-1311-3>
- White TJ, Bruns T, Lee S, Taylor JW (1990) Amplification and direct sequencing of fungal ribosomal RNA genes for phylogenetics. In: Innes MA, Gelfand DH, Sninsky JJ and White TJ (Eds) *PCR Protocols: A Guide to Methods and Applications*. Academic Press, San Diego, 315–322. <https://doi.org/10.1016/B978-0-12-372180-8.50042-1>

- Wolski EA (2023) The versatility of *Penicillium* species to degrade organic pollutants and its use for wastewater treatment. *Studies in Fungi* 8: 1–10. <https://doi.org/10.48130/SIF-2023-0002>
- Yasanthika E, Wanasinghe DN, Ren G-C, Karunarathna SC, Tennakoon DS, Monkai J, Gui H, Mortimer PE, Lumyong S, Hyde KD (2021) Taxonomic and phylogenetic insights into novel Ascomycota from contaminated soils in Yunnan, China. *Phytotaxa* 513: 203–225. <https://doi.org/10.11646/phytotaxa.513.3.2>
- Yasanthika W, Wanasinghe D, Mortimer P, Monkai J, Farias A (2022) The importance of culture-based techniques in the genomic era for assessing the taxonomy and diversity of soil fungi. *Mycosphere : Journal of Fungal Biology* 13: 724–751. <https://doi.org/10.5943/mycosphere/13/1/8>
- Yasanthika WAE, De Farias ARG, Wanasinghe DN, Chethana KWT, Zare R, Cai L, Maharachchikumbura SSN, Tennakoon DS, Perera RH, Luangharn T, Chomnunti P (2023) a web-based platform for soil-inhabiting Ascomycota species. *Studies in Fungi* 8: 16. <https://doi.org/10.48130/SIF-2023-0016>

## Supplementary material 1

### Additional information

Authors: Tanapol Thitla, Jutamart Monkai, Weiqian Meng, Surapong Khuna, Ning Xie, Sinang Hongsanant, Saisamorn Lumyong

Data type: docx

Explanation note: **table S1**. GenBank accession numbers of *Penicillium* section *Exilicaulis* used in multi-locus phylogenetic analysis. **table S2**. GenBank accession numbers of *Penicillium* section *Lanata-Divariata* used in multi-locus phylogenetic analysis. **table S3**. GenBank accession numbers of taxa in Xylariomycetidae used in multi-genes phylogenetic analysis.



Copyright notice: This dataset is made available under the Open Database License (<http://opendatacommons.org/licenses/odbl/1.0/>). The Open Database License (ODbL) is a license agreement intended to allow users to freely share, modify, and use this Dataset while maintaining this same freedom for others, provided that the original source and author(s) are credited.

Link: <https://doi.org/10.3897/mycokeys.116.150635.suppl1>





# Four new species of *Entoloma* subgenus *Cyanula* (Entolomataceae, Agaricales) from subtropical regions of China

Lin-Gen Chen<sup>1</sup>, Hong Chen<sup>1</sup>, Ling Ding<sup>1</sup>, Yu-Qin Xu<sup>1</sup>, Hui Zeng<sup>2</sup>, Sheng-Nan Wang<sup>1,3</sup>, Jun-Qing Yan<sup>1</sup>

<sup>1</sup> Jiangxi Provincial Key Laboratory of Excavation and Utilization of Agricultural Microorganisms, Jiangxi Agricultural University, Nanchang 330045, China

<sup>2</sup> Institute of Edible mushroom, Fujian Academy of Agricultural Sciences, Fuzhou 350011, China

<sup>3</sup> Jiangxi Provincial Key Laboratory of Subtropical Forest Resource Cultivation, College of Forestry, Jiangxi Agricultural University, Nanchang 330045, China

Corresponding author: Jun-Qing Yan (yanjunqing1990@jxau.edu.cn)

## Abstract

In this study, four species of *Entoloma* subgenus *Cyanula* (*E. orientosinense*, *E. subgriseosquamulosum*, *E. subpraegracile*, and *E. wuyishanense*) from subtropical regions of China, are described as new to science based on morphological and phylogenetic analyses. Morphologically, *E. orientosinense* is characterized by the white basidiomata, relatively large basidiospores, and carneogriseum-type lamellae edge; *E. subgriseosquamulosum* is recognized by the fuscous pileus, crowded and adnate lamellae, and medium-sized basidiospores; *E. subpraegracile* is identified by the yellow pileus and intervenose lamellae with sterile or heterogeneous edge; *E. wuyishanense* is distinct by the blue basidiomata and fertile lamellae edge with slightly bluish pigmentation near the stipe. *Entoloma orientosinense* belongs to sect. *Caesiocincta*, subsect. *Queletia*, and *E. wuyishanense* belongs to sect. *Poliopodes*. The remaining two species each form independent branches and do not belong to any known sections. Detailed descriptions, color photos, and a key to related species are presented.

**Key words:** Basidiomycetes, new taxa, phylogeny, taxonomy



This article is part of:

**Diversity, taxonomy, and systematics of macrofungi from tropical Asia**

Edited by Olivier Raspé, Rui-Lin Zhao, Jennifer Luangsa-ard

Academic editor: Olivier Raspé

Received: 30 December 2024

Accepted: 8 April 2025

Published: 29 April 2025

**Citation:** Chen L-G, Chen H, Ding L, Xu Y-Q, Zeng H, Wang S-N, Yan J-Q (2025) Four new species of *Entoloma* subgenus *Cyanula* (Entolomataceae, Agaricales) from subtropical regions of China. MycoKeys 116: 303–325. <https://doi.org/10.3897/mycokeys.116.145568>

Copyright: © Lin-Gen Chen et al.

This is an open access article distributed under terms of the Creative Commons Attribution License (Attribution 4.0 International – CC BY 4.0).

## Introduction

*Entoloma* (Fr.) P. Kumm. is one of the most diverse genera within Agaricales, well-characterized by pink to brownish spore prints and angular basidiospores viewed in all views (Co-David et al. 2009). It shows extremely wide geographical distribution, occurring from the frigid zone to the tropics, and from alpine to basins, with most members being saprobic on shady and humid soil, mosses, or rotten wood in forests (Horak 1980; Noordeloos 1981; Largent 1994; Reschke et al. 2022b). So far, approximately 2000 *Entoloma* species have been reported in the world. In China, however, there are relatively few reports about the species of this genus, with approximately 200. Among them, some of the newly discovered species published earlier were not classified into specific subgenera (Bi et al. 1986; Zhang et al. 1994; He et al. 2011).

In the past, based on morphological taxonomy, *Cyanuli* was introduced by Romagnesi (1974) as a section within *Rhodophyllus* Quél (= *Entoloma*). The combination *Entoloma* section *Cyanula* (Romagn.) Noordeloos belonged to *Entoloma* subgenus

*Leptonia* of wide sense. However, the subg. *Leptonia*, traditionally divided into three sections, viz. *Leptonia*, *Cyanula*, and *Griseorubida* (Noordeloos 2004), turned out to be polyphyletic. Sect. *Leptonia* of belonged to the */Nolanea-Claudopus* clade, and *Cyanula* and *Griseorubida* to the */Inocephalus-Cyanula* clade (Co-David et al. 2009). Morphologically, species of sect. *Leptonia* exhibited clamp connections, whereas species of *Cyanula* lacked clamp connections. Based on these, sect. *Cyanula* was elevated to subgenus rank (Noordeloos and Gates 2012; Noordeloos et al. 2022a).

The species of *Entoloma* subg. *Cyanula* are mainly characterized by their collybioid habit, vividly colorful (often blue, violaceous to brown) and squamulose pileus, absence of clamp connections, and presence of brilliant granules and intracellular pigments in hyphae. So far, at least 500–600 species of *E. subg. Cyanula* have been discovered worldwide.

According to previous studies, there are 13 species belonging to *Entoloma* subg. *Cyanula* in China, 7 of which were newly described (He et al. 2011, 2012; He et al. 2017). In the past few years, during our surveys on the diversity of macrofungi in the subtropical regions of China, we have found that the species diversity under *E. subg. Cyanula* is extremely rich. In this study, four species of this subgenus are newly described based on morphological comparisons and phylogenetic analyses.

## Materials and methods

### Morphological studies

The collection sites of the specimens in this study were all located in the subtropical region of East China, and these specimens were deposited in the Herbarium of Fungi, Jiangxi Agricultural University (HFJAU). Fresh specimens were photographed in the field and macroscopically recorded. The color notations followed the Methuen Handbook of Colour (Kornerup and Wanscher 1978). Microscopic structures were studied under an Olympus BX53 microscope (Olympus corporation, Tokyo, Japan) by making squash preparations of sections of dried specimens. The sections were hydrated with 5% KOH solution or H<sub>2</sub>O, and 1% Congo red was used as the staining agent when observing colorless tissues. Melzer's reagent was selected for determining whether the spores were amyloid or not (Horak 2005). At least 20 basidiospores, basidia, and cystidia were measured for each collection. The range of spore size is expressed as the form (a) b–c (d), in which "a" and "d" represent the minimum and maximum values, and 90% of the spores falling within the range "b–c". The meanings of the other spore characteristics were as follows: "Q" stood for the ratio of length and width; "av" symbolized average value; "n" meant the number of measurements; and "Qm" indicated average "Q"  $\pm$  standard deviation (Bas 1969). The morphological descriptions were based on the work of Noordeloos et al. (2022a).

### DNA extraction, PCR amplification, and sequencing

Genomic DNA was extracted from dried specimens with the NuClean Plant Genomic DNA kit (CWBIQ, China) (Wang et al. 2022). The nrDNA ITS and LSU regions were amplified respectively using the primer pairs of ITS1F/ITS4, LR0R/LR5 (White et al. 1990).

PCR amplification was conducted with a 25 µL reaction system as follows: 1 µL DNA, 1 µL each for forward and reverse primers, 9.5 µL ddH<sub>2</sub>O, and 12.5 µL 2 × Taq Master Mix (Dye Plus, Vazyme Biotechnology Co. Ltd., Nanjing City, China). PCR was carried out using a touchdown amplification procedure following Chen et al. (2024). The PCR products were sequenced by Qing Ke Biotechnology Co. Ltd. (Wuhan City, China).

### Alignment and phylogenetic analyses

In total, 173 sequences (126 ITS sequences and 47 LSU sequences) of 126 samples were used for phylogenetic analyses based on Bayesian inference (BI) and Maximum likelihood (ML). The selection of sequences for the phylogenetic analyses was based on the results of ITS BLAST and of Noordeloos et al. (2022a) (Table 1). Some species of *Entoloma* subg. *Nolanea* were designated as outgroups. The ITS sequences and the LSU sequences were separately aligned on the MAFFT online server using the automatic selection of algorithm (Katoh et al. 2019). First, phylogenetic trees were constructed separately for ITS and LSU and their congruence was checked. BI and ML phylogenetic analyses of the concatenated sequences were run using MRBAYES v.3.2.7a (Ronquist et al. 2012) and IQTREE v.2.1.2 (Nguyen et al. 2015), respectively. For the ML analysis, models of sequence evolution were assessed in IQ-Tree prior to the analysis and allowing the partitions of sequences to have different seeds (-spp) and the results were the following: TPM2 + F + I + G4 for ITS and HKY + F + I + G4 for LSU. Ultrafast bootstrap support values were calculated from 1000 replicates. For the BI analysis, the best-fit models were determined by PARTITIONFINDER (Zhang et al. 2020) based on Bayesian information criterion (BIC) and the results were the following: GTR + F + I + G4 for ITS and HKY + F + I + G4 for LSU. The Monte Carlo Markov chains were run for 40 million generations. The first 25% of trees were discarded as burn-in. The nodes with Bayesian posterior probabilities (BI-PP) ≥ 0.95 and ML bootstrap proportions (ML-BP) ≥ 95% were considered as statistically supported. A nexus file containing sequence alignment and the original trees of ML and BI analyses are provided in Suppl. material 1.

**Table 1.** Details of sequences used in the phylogenetic analyses. Newly generated sequences were in bold.

Species	Location	Voucher Number	GenBank No. (ITS)	GenBank No. (LSU)	Sequence origin
<i>Entoloma albidosimulans</i>	Australia	MEN 2004-065, isotype	—	MK277956	Varga et al. (2019)
<i>E. albinellum</i>	USA	TENN:070403	KY777375	—	Unpublished in GenBank
<i>E. argus</i>	Vietnam	LE F-312694, holotype	OM987263	OM996175	Morozova et al. (2022)
<i>E. argus</i>	Vietnam	LE F-315916	OM987264	—	Morozova et al. (2022)
<i>E. arion</i>	Vietnam	LE F-312691, holotype	OM987259	OM996176	Morozova et al. (2022)
<i>E. arion</i>	Vietnam	LE F-312692	OM987260	—	Morozova et al. (2022)
<i>E. arion</i>	Vietnam	LE F-315917	OM987261	—	Morozova et al. (2022)
<i>E. asprellum</i>	Estonia	TUF106064	UDB011486	—	UNITE
<i>E. atropapillatum</i>	Brazil	FK0898, holotype	KF679354	KF738940	Karstedt et al. (2020)
<i>E. azureosquamulosum</i>	China	HKAS53408	JQ410334	JQ410326	He et al. (2012)
<i>E. azureosquamulosum</i>	China	GDGM29254	JQ410335	—	He et al. (2012)
<i>E. azureosquamulosum</i>	China	GDGM27355, holotype	NR_137086	NG_059214	He et al. (2012)
<i>E. caespitosum</i>	China	GDGM27564	JQ281477	JQ320130	He et al. (2012)
<i>E. caespitosum</i>	China	GDGM24025	JQ281490	JQ410327	He et al. (2012)
<i>E. caespitosum</i>	China	GDGM24026	JQ281491	JQ320133	He et al. (2012)



Species	Location	Voucher Number	GenBank No. (ITS)	GenBank No. (LSU)	Sequence origin
<i>E. calceus</i>	Norway	O-F-259457, holotype	NR_182489	—	Noordeloos et al. (2022b)
<i>E. calceus</i>	France	LIP0402265	ON008492	—	Noordeloos et al. (2022b)
<i>E. calceus</i>	Norway	JL12-19	ON008493	—	Noordeloos et al. (2022b)
<i>E. callipygmaeum</i>	Russia	LE312488	MZ145205	—	Dima et al. (2021)
<i>E. callipygmaeum</i>	Russia	LE312487	MZ145206	—	Dima et al. (2021)
<i>E. callipygmaeum</i>	Russia	LE253784, holotype	MZ145207	—	Dima et al. (2021)
<i>E. carneogriseum</i>	Norway	O-F-256479	UDB07673714	—	UNITE
<i>E. cetratum</i>	Sweden	LE311888, neotype	OL338280	—	Reschke et al. (2022a)
<i>E. chalybeum</i>	Russia	LE254353	KC898445	KC898500	Morozova et al. (2014)
<i>E. chalybeum</i>	Denmark	TUF105760	UDB034191	—	UNITE
<i>E. consanguineum</i>	New Zealand	PDD80751	MW775252	—	Unpublished in GenBank
<i>E. consanguineum</i>	New Zealand	PDD80751	MW775268	—	Unpublished in GenBank
<i>E. coracis</i>	Norway	O-F-256850, holotype	MW934571	MW934251	Crous et al. (2021b)
<i>E. coracis</i>	Norway	O-F-67255	MW934572	—	Crous et al. (2021b)
<i>E. coracis</i>	Norway	O-F-251952	MW934573	—	Crous et al. (2021b)
<i>E. corvinum</i>	France	FA4261	OR419868	—	Armada et al. (2023)
<i>E. cyanostipitum</i>	China	GDGM31318, holotype	KY711237	KY972694	He et al. (2017)
<i>E. cyanostipitum</i>	China	SAAS2239	KY711238	KY972695	He et al. (2017)
<i>E. cyanostipitum</i>	China	GDGM31294	KY972700	KY972693	He et al. (2017)
<i>E. dislocatum</i>	Spain	L0607565, holotype	ON008483	—	Noordeloos et al. (2022b)
<i>E. dislocatum</i>	Spain	SFC-080612-01	ON008484	—	Noordeloos et al. (2022b)
<i>E. dislocatum</i>	Italy	TUF105920, paratype	UDB0799300	—	UNITE
<i>E. exile</i>	Germany	Lueck8	KP965773	KP965791	Karich et al. (2015)
<i>E. exile</i>	—	KM187354	MF977976	—	Unpublished in GenBank
<i>E. griseocyaneum</i>	Russia	LE254351	KC898444	KC898498	Morozova et al. (2014)
<i>E. griseocyaneum</i>	Germany	KaiR997	MZ611684	—	Reschke et al. (2022b)
<i>E. icarus</i>	Vietnam	LE F-312696, holotype	OM987257	OM996174	Morozova et al. (2022)
<i>E. icarus</i>	Vietnam	LE F-312697	OM987258	—	Morozova et al. (2022)
<i>E. incanum</i>	Sweden	LE312503, neotype	OK161247	OK161275	Crous et al. (2021b)
<i>E. incanum</i>	Russia	LE311794	OK161249	OK161276	Crous et al. (2021b)
<i>E. incanum</i>	Russia	LE315858	OK161250	—	Crous et al. (2021b)
<i>E. isborscanum</i>	Russia	LE312486	MW934564	—	Crous et al. (2021a)
<i>E. isborscanum</i>	Russia	LE302088, holotype	MW934566	MW934253	Crous et al. (2021a)
<i>E. linkii</i>	Norway	O-F-256353	UDB07673651	—	UNITE
<i>E. mastoideum</i>	China	GDGM28820	JQ281476	JQ410328	He et al. (2012)
<i>E. mastoideum</i>	China	GDGM26597	JQ291564	JQ320126	He et al. (2012)
<i>E. meridionale</i>	Greece	ACAM2014-0127	OL679698	—	Lebeuf et al. (2021)
<i>E. meridionale</i>	Greece	ACAM2018-0152	OL679699	—	Lebeuf et al. (2021)
<i>E. meridionale</i>	Greece	ACAM2018-0153, holotype	OL679700	—	Lebeuf et al. (2021)
<i>E. minutigranulosum</i>	Russia	LE312484	MZ145210	—	Dima et al. (2021)
<i>E. minutigranulosum</i>	Russia	LE312483	MZ145212	—	Dima et al. (2021)
<i>E. minutigranulosum</i>	Russia	LE302096, holotype	MZ145214	—	Dima et al. (2021)
<i>E. mougeotii</i>	Estonia	TUF106917	UDB015645	—	UNITE
<i>E. mougeotii</i>	Estonia	TUF101633	UDB016265	—	UNITE
<i>E. mougeotii</i>	Estonia	TUF106505	UDB019720	—	UNITE
<i>E. mutabilipes</i>	Finland	TUR610/12	LN850550	—	Kokkonen (2015)
<i>E. mutabilipes</i>	Estonia	TUR8788	LN850551	—	Kokkonen (2015)
<i>E. notabile</i>	Cyprus	L-0607514, holotype	OL343537	—	Vila et al. (2021)
<i>E. olivaceomarginatum</i>	USA	PUL00036174	ON561593	—	Unpublished in GenBank
<b><i>E. orientosinense</i></b>	<b>China</b>	<b>HFJAU1414, holotype</b>	<b>PQ584686</b>	—	<b>This work</b>
<b><i>E. orientosinense</i></b>	<b>China</b>	<b>HFJAU1907</b>	<b>PQ584690</b>	<b>PQ584707</b>	<b>This work</b>
<b><i>E. orientosinense</i></b>	<b>China</b>	<b>HFJAU2616</b>	<b>PQ584687</b>	—	<b>This work</b>
<b><i>E. orientosinense</i></b>	<b>China</b>	<b>HFJAU2920</b>	<b>PQ584688</b>	<b>PQ584708</b>	<b>This work</b>
<b><i>E. orientosinense</i></b>	<b>China</b>	<b>HFJAU4048</b>	<b>PQ584689</b>	<b>PQ584709</b>	<b>This work</b>
<i>E. pallidostriatum</i>	Spain	L-0607566, holotype	NR_177630	—	Vila et al. (2021)

Species	Location	Voucher Number	GenBank No. (ITS)	GenBank No. (LSU)	Sequence origin
<i>E. perasprellum</i>	France	GC01100310, holotype	MZ145177	—	Dima et al. (2021)
<i>E. perasprellum</i>	Sweden	GB-0204547 / JBJ 19-107	MZ145179	—	Dima et al. (2021)
<i>E. perasprellum</i>	Sweden	GB-0204548 / JBJ 19-122	MZ145180	—	Dima et al. (2021)
<i>E. perchalybeum</i>	Sweden	GB-0209474, holotype	NR_182490	—	Noordeloos et al. (2022b)
<i>E. perchalybeum</i>	Finland	TUR190180	ON008495	—	Noordeloos et al. (2022b)
<i>E. poliopus</i>	Estonia	TUF120264	UDB024655	—	UNITE
<i>E. praegracile</i>	China	GDGM29251	JQ281482	JQ320129	He et al. (2013)
<i>E. praegracile</i>	China	GDGM29256	JQ320107	—	He et al. (2013)
<i>E. pseudocoelestinum</i>	Germany	Lueck10	KP965774	KP965792	Karich et al. (2015)
<i>E. pseudocoelestinum</i>	—	KM132400	MF977966	—	Unpublished in GenBank
<i>E. pseudosubcorvinum</i>	Thailand	SDBR-CMUNK0985, holotype	MZ215769	MZ203540	Bhunjun et al. (2022)
<i>E. pseudosubcorvinum</i>	Thailand	SDBR-CMUNK1367	MZ215770	MZ203541	Bhunjun et al. (2022)
<i>E. pulchripes</i>	Russia	LE312485	MZ145187	—	Dima et al. (2021)
<i>E. pulchripes</i>	Russia	LE311808, holotype	MZ145188	—	Dima et al. (2021)
<i>E. pulchripes</i>	Russia	LE311809	MZ145189	—	Dima et al. (2021)
<i>E. queletii</i>	Turkey	OKA-TR1002	MT741747	—	Unpublished in GenBank
<i>E. queletii</i>	Estonia	TUF141044	UDB07674927	—	UNITE
<i>E. riparium</i>	Italy	L-0607563, holotype	NR_177632	—	Vila et al. (2021)
<i>E. riparium</i>	Estonia	TUF120259	UDB024650	—	UNITE
<i>E. septentrionale</i>	Norway	O-F-254295, holotype	NR_174647	—	Noordeloos et al. (2021)
<i>E. sericeum</i>	Germany	KaiR237	OL338118	OL338542	Reschke et al. (2022a)
<i>E. sericeum</i>	—	VHAs03 2	DQ367430	DQ367423	Unpublished in GenBank
<i>E. serrulatum</i>	Norway	O-F-158208/DMS-730296	MZ869016	—	Reschke et al. (2022b)
<i>E. serrulatum</i>	Russia	LE254361	KC898447	KC898501	Morozova et al. (2014)
<i>E. serrulatum</i>	Iran	EnSe-1	KT833862	—	Unpublished in GenBank
<i>E. sicoense</i>	Portugal	PO F2244, holotype	OR026624	—	Fachada et al. (2023)
<i>E. sicoense</i>	Portugal	PO F2245	OR026625	—	Fachada et al. (2023)
<i>E. subcaesiocinctum</i>	China	SAAS103	KY711235	KY972698	He et al. (2017)
<i>E. subcaesiocinctum</i>	China	SAAS133, holotype	KY711236	KY972697	He et al. (2017)
<i>E. subcorvinum</i>	USA	MGW1494	KY744168	—	Unpublished in GenBank
<i>E. subcorvinum</i>	USA	SAT1518905	KY744169	—	Unpublished in GenBank
<b><i>E. subgriseosquamulosum</i></b>	<b>China</b>	<b>HFJAU3967</b>	<b>PQ584696</b>	<b>—</b>	<b>This work</b>
<b><i>E. subgriseosquamulosum</i></b>	<b>China</b>	<b>HFJAU3969, holotype</b>	<b>PQ584697</b>	<b>PQ584721</b>	<b>This work</b>
<b><i>E. subpraegracile</i></b>	<b>China</b>	<b>HFJAU1822, holotype</b>	<b>PQ584698</b>	<b>PQ584710</b>	<b>This work</b>
<b><i>E. subpraegracile</i></b>	<b>China</b>	<b>HFJAU3094</b>	<b>PQ584706</b>	<b>PQ584711</b>	<b>This work</b>
<b><i>E. subpraegracile</i></b>	<b>China</b>	<b>HFJAU3164</b>	<b>PQ584700</b>	<b>PQ584712</b>	<b>This work</b>
<b><i>E. subpraegracile</i></b>	<b>China</b>	<b>HFJAU3168</b>	<b>PQ584705</b>	<b>—</b>	<b>This work</b>
<b><i>E. subpraegracile</i></b>	<b>China</b>	<b>HFJAU5110</b>	<b>PQ584701</b>	<b>—</b>	<b>This work</b>
<b><i>E. subpraegracile</i></b>	<b>China</b>	<b>HFJAU5115</b>	<b>PQ584699</b>	<b>PQ584713</b>	<b>This work</b>
<b><i>E. subpraegracile</i></b>	<b>China</b>	<b>HFJAU5140</b>	<b>PQ584702</b>	<b>PQ584714</b>	<b>This work</b>
<b><i>E. subpraegracile</i></b>	<b>China</b>	<b>HFJAU5175</b>	<b>PQ584703</b>	<b>PQ584715</b>	<b>This work</b>
<b><i>E. subpraegracile</i></b>	<b>China</b>	<b>HFJAU5177</b>	<b>PQ584704</b>	<b>PQ584716</b>	<b>This work</b>
<i>E. subserrulatum</i>	USA	TENN:068464	KY744143	—	Unpublished in GenBank
<i>E. subserrulatum</i>	USA	TENN:070407	KY744177	—	Unpublished in GenBank
<i>E. subtenuicystidium</i>	China	GDGM 28459, holotype	JQ320109	JQ320116	He et al. (2013)
<i>E. subtenuicystidium</i>	China	GDGM 29246	JQ320114	JQ320132	He et al. (2013)
<i>E. turci</i>	Austria	WU25055	UDB0802163	—	UNITE
<i>E. viridomarginatum</i>	The Netherlands	JAC15761	MW775255	—	Unpublished in GenBank
<i>E. viridomarginatum</i>	The Netherlands	JAC12344	MW775264	—	Unpublished in GenBank
<b><i>E. wuyishanense</i></b>	<b>China</b>	<b>HFJAU3571, holotype</b>	<b>PQ584691</b>	<b>—</b>	<b>This work</b>
<b><i>E. wuyishanense</i></b>	<b>China</b>	<b>HFJAU3871</b>	<b>PQ584692</b>	<b>PQ584717</b>	<b>This work</b>
<b><i>E. wuyishanense</i></b>	<b>China</b>	<b>HFJAU3874</b>	<b>PQ584694</b>	<b>PQ584718</b>	<b>This work</b>
<b><i>E. wuyishanense</i></b>	<b>China</b>	<b>HFJAU3878</b>	<b>PQ584693</b>	<b>PQ584719</b>	<b>This work</b>
<b><i>E. wuyishanense</i></b>	<b>China</b>	<b>HFJAU3881</b>	<b>PQ584695</b>	<b>PQ584720</b>	<b>This work</b>

## Results

### Phylogenetic analysis

A total of 2136 characters were used in subsequent analyses (ITS, 841 bp; LSU, 1,295 bp), of which 1382 were constant, 670 were parsimony-informative, and 84 were singleton. For Bayesian analysis, the average standard deviation of split frequencies was less than 0.01 after 20 million generations.

The results of the phylogenetic analysis were shown in Fig. 1. The results were consistent with previous studies (Noordeloos et al. 2022a; Brandrud et al. 2023). The four new species were clustered in the subg. *Cyanula* clade and formed separate and well-supported branches, respectively. Among them, *Entoloma orientosinense* formed a separate and well-supported lineage (BI-PP = 1, ML-BP = 99%), and groups together with *E. albinellum* (Peck) Hesler and *E. queletii* (Boud.) Noordel. nested in the sect. *Caesiocincta*, subsect. *Queletia* (BI-PP = 1, ML-BP = 100%). *Entoloma subgriseosquamulosum* independently

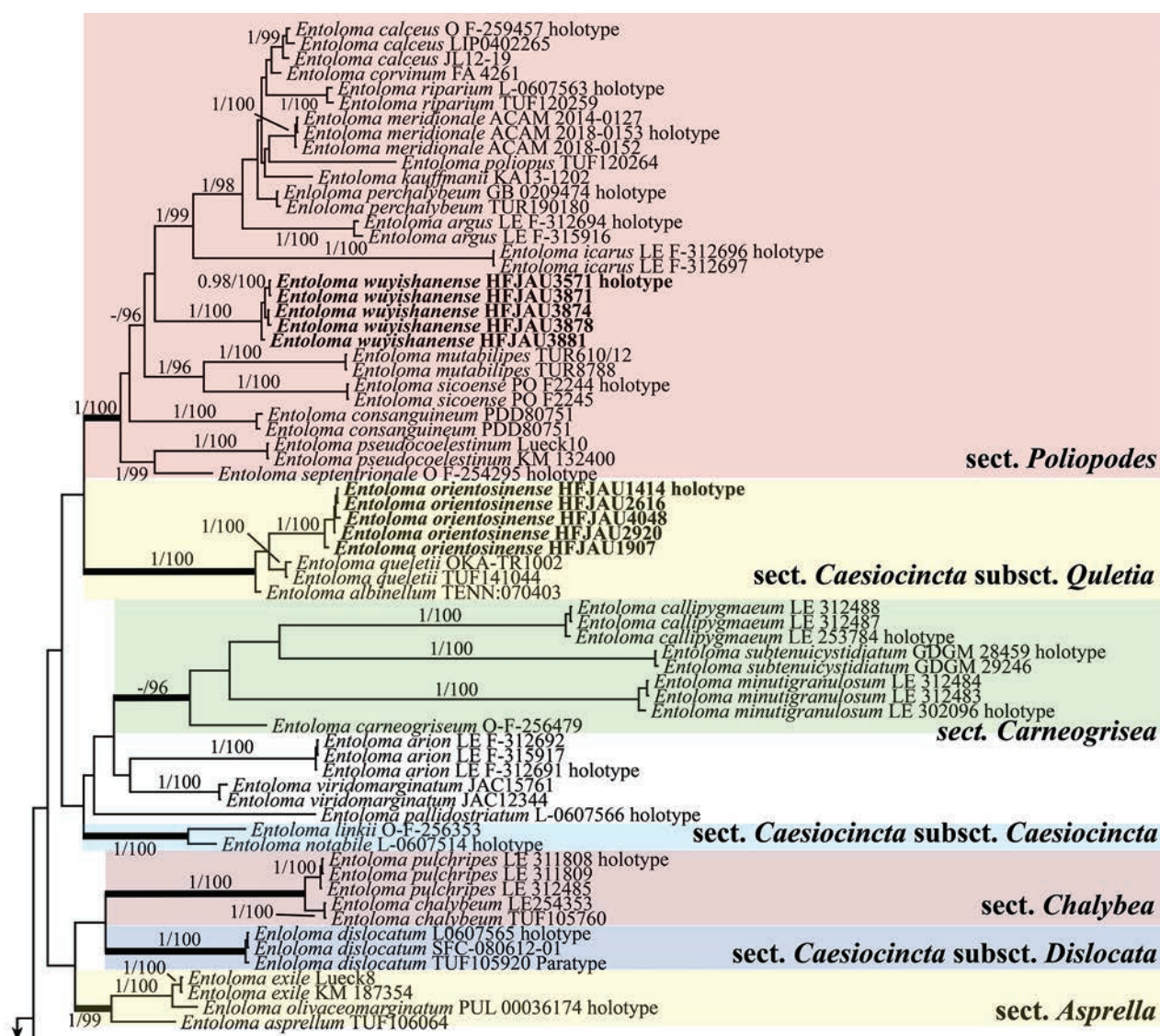


**Figure 1.** Phylogram of *Entoloma* subg. *Cyanula* spp. generated by Bayesian inference (BI) analysis based on ITS and LSU, rooted with *E. subgenus Nolanea* spp. Bayesian inference (BI-PP)  $\geq 0.95$  and ML bootstrap proportions (ML-BP)  $\geq 95\%$  are indicated as PP/BP. The new taxa are marked in bold.



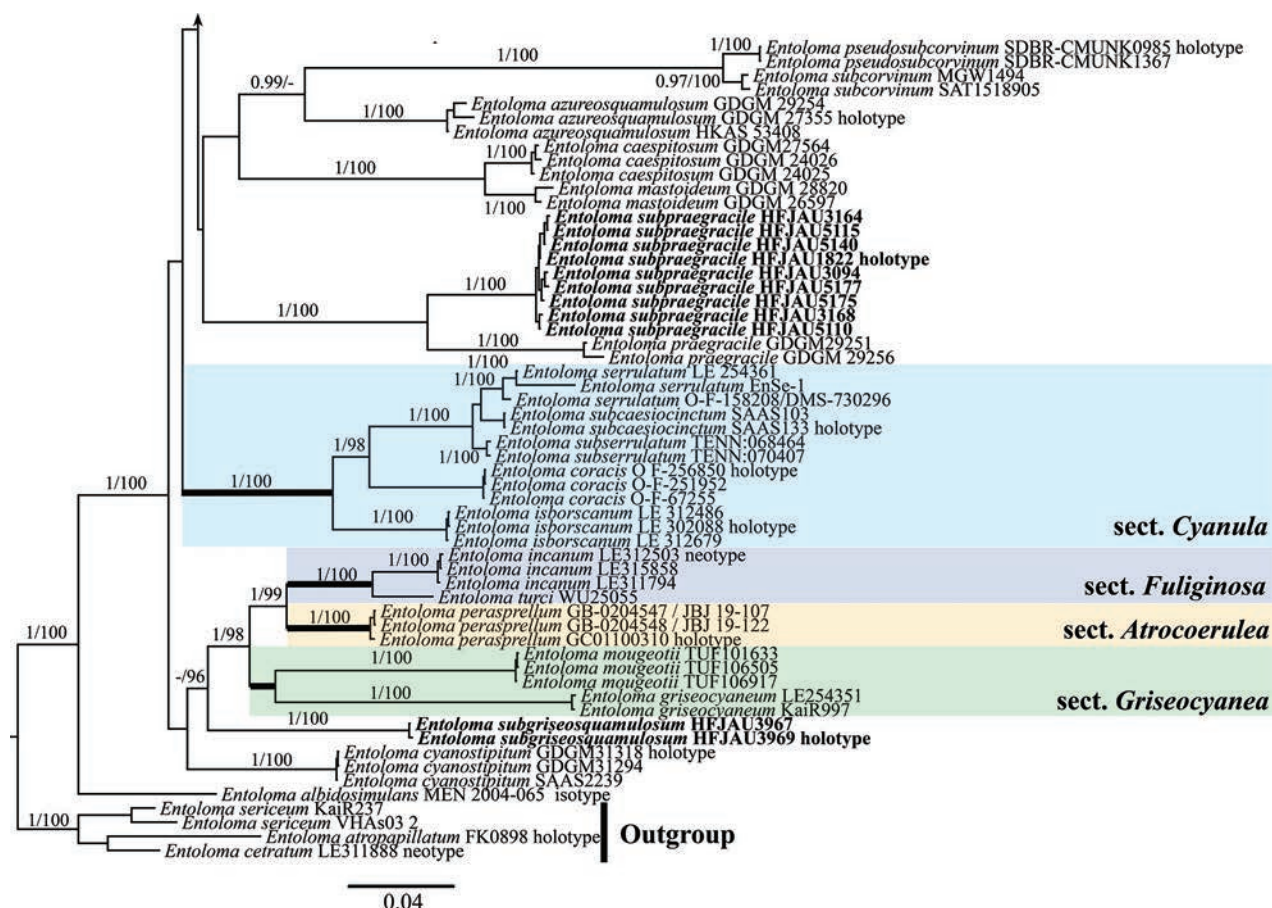


Figure 1. Continued.

formed a well-supported branch (BI-PP = 1, ML-BP = 100%). *Entoloma subpraegracile* formed a sister lineage with *E. praegracile* Xiao L. He & T.H. Li (BI-PP = 1, ML-BP = 100%), well clustered in a small clade (BI-PP = 1, ML-BP = 100%). *Entoloma wuyishanense* formed a well-supported lineage within the sect. *Poliopodes* (BI-PP = 1, ML-BP = 100%).

## Taxonomy

***Entoloma orientosinense* J.Q. Yan, L.G. Chen & S.N. Wang, sp. nov.**

MycoBank No: 858361

Fig. 2

**Etymology.** Refers to its type specimen originating from the eastern regions of China.

**Holotype.** CHINA • Anhui Province, Chizhou City, Shitan County, Guniujiang Nature Reserve, 30.0303°N, 117.5290°E, alt. 783 m, 9 October 2019, collected by Yu-Peng Ge, HFJAU1414.

**Diagnosis.** *Entoloma orientosinense* is mainly characterized by the white, collybioid basidiomata, fibrillous and not striate pileus, narrow, adnate to decurrent lamellae, glabrous stipe, 5–6 angled basidiospores, sterile lamellae edge of carneogriseum-type, cylindrical to subclavate cheilocystidia, absence of cell pigments and clamp connections in hyphae. It differs from *E. albinellum* by its non-striate pileus, adnate to decurrent lamellae, and smaller basidiospores.



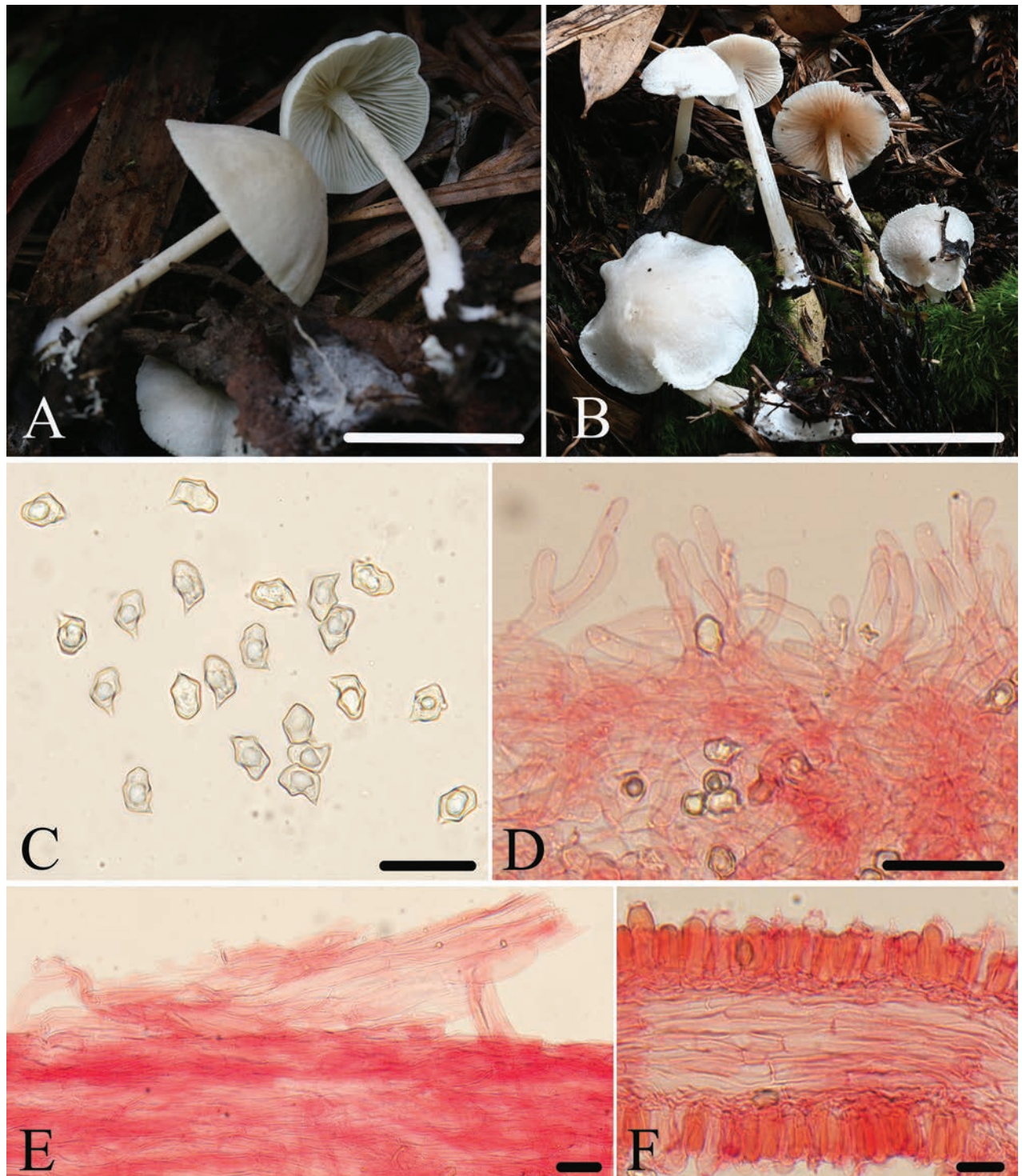


**Figure 2.** *E. orientosinense* **A, B** basidiomata **A** HFJAU1414, holotype **B** HFJAU2616 **C** basidiospores **D** cheilocystidia **E** pileipellis **F** lamellar trama. All microscopic structures were observed in 5% KOH, and used 1% Congo red as the stain except **C**. Scale bars: 10 mm (**A, B**); 20 µm (**C**); 30 µm (**D–F**).

**Macromorphology.** Basidiomata rather small, collybioid. Pileus 8–20 mm wide, convex then flattened with depressed center, with entire margin, slightly hygrophanous, fibrillous when young, then repent or raised scaly, not translucently striate, white (3A1–2). Lamellae moderately distant, 1.5–2.0 mm wide, with three types of lamellulae, adnate to decurrent, subventricose, initially white, then pink (11B4–6),

with serrulate and concolorous edge. Stipe 20–25 × 2.0–3.0 mm, central, terete, tapered upwards, hollow, concolorous or paler with the pileus, minutely tomentose in the upper part elsewhere smooth and glabrous, base with white tomentum. Context thin, concolorous to the surface. Odor indistinct, taste not tested.

**Micromorphology.** Basidiospores (8.5)9.3–11.0(12.5) × (6.0)6.5–8.0(9.0) µm, (av = 10.1 × 7.3 µm), Q = 1.2–1.6(1.7) (Qm = 1.4 ± 0.07, n = 200), heterodiametrical, 5–6 angles in profile view, thick-walled, inamyloid. Basidia 40–52 × 11–13 µm, clavate, 4-spored, sterigmata 5.0–10 µm long, clampless. Pleurocystidia absent. Lamellae edge sterile of carneogriseum-type. Cheilocystidia regularly dispersed in the lamellae edge, 17–47 × 4.0–7.0 µm, narrowly cylindrical to subclavate, septate, with slightly inflated apex. Lamellar trama regular, made up of cylindrical hyphae 7.0–13 µm wide. Pileipellis a cutis made up of cylindrical hyphae 8.0–11 µm broad, with transitions to a trichoderm towards the margin with clavate terminal elements 10–18 µm wide, not pigmented. Stipitipellis a cutis composed of densely arranged, cylindrical hyphae, up to 11 µm wide, slightly constricted at the septa, with acute or tapered end. Clamp connections absent.

**Habitat.** Solitary or scattered on soil in mixed coniferous-broad-leaved forest, or on rotten wood, soil, and moss in broadleaved forest.

**Distribution.** So far known from eastern China.

**Additional specimens examined.** CHINA • Fujian Province, Wuyishan City, 27.7139°N, 117.6533°E, alt. 1113 m, 27 June 2022, collected by Jun-Qing Yan and Bing-Ring Ke, HFJAU4048 • Zhejiang Province, Lishui City, Suichang County, Huangtakou Village, 28.2679°N, 118.9435°E, alt. 346 m, 12 July 2020, collected by Jun-Qing Yan and Yan-Liu Chen, HFJAU1907 • Qingtian County, Shigu Lake, 28.2063°N, 120.0415°E, alt. 1130 m, 31 July 2021, collected by Jun-Qing Yan, Bing-Ring Ke, and Zhi-Heng Zeng, HFJAU2616 • Nanyang Village, 27.9603°N, 120.0020°E, alt. 522 m, 6 August 2021, collected by Yu-Peng Ge and Lan-Yu Sun, HFJAU2920.

**Notes.** Morphologically, *Entoloma orientosinense* has much in common with *E. albidosimulans* G.M. Gates & Noordel. and *E. albinellum* with regard to the white and collybioid basidiomata. However, *E. albidosimulans* is distinct by its broader (up to 6 mm), adnate-emarginate lamellae, and belonging to *E. subg. Alboleptonia* species (Gates and Noordeloos 2007). *Entoloma albinellum* differs from new species by its striate pileus, adnexed lamellae, and larger basidiospores (11–12.5 × 7.5–8.5 µm) (Hesler 1967).

In the molecular data, *E. orientosinense* fits well within subg. *Cyanula*, sect. *Caesiocincta*, subsect. *Queletia* including *E. albinellum* and *E. queletii*. *E. queletii* is distinguished from new species by the vinaceous-pink pileus and larger basidiospores (10–13 × 6.5–9.0 µm) (Bas et al. 1988a).

***Entoloma subgriseosquamulosum* J.Q. Yan, L.G. Chen & S.N. Wang, sp. nov.**

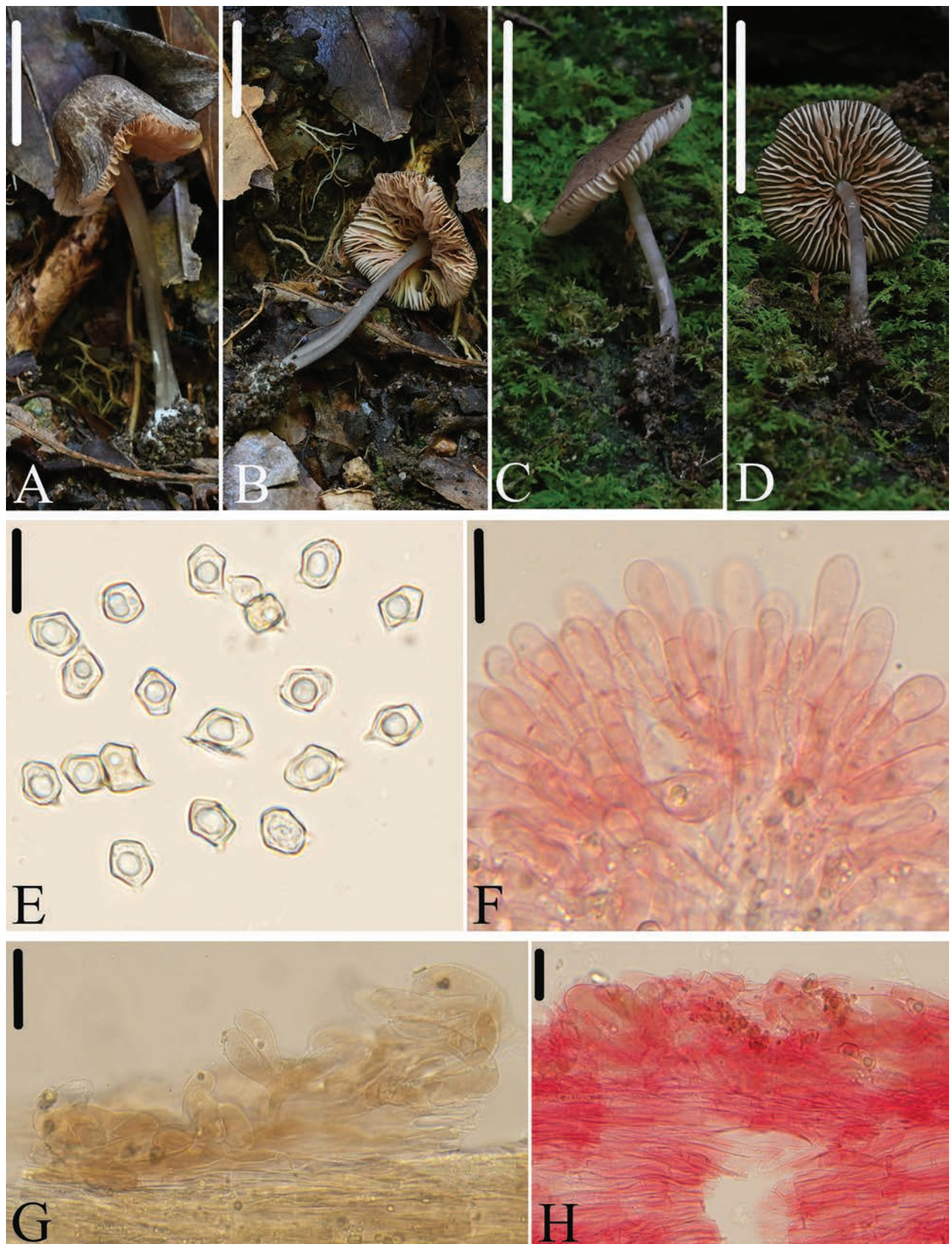
MycoBank No: 858362

Fig. 3

**Etymology.** Refers to its morphology similar to “*Entoloma griseosquamulosum*”.

**Holotype.** CHINA • Fujian Province, Wuyishan City, Yangzhuang Town, Xiyuan Village, 27.7632°N, 117.8139°E, alt. 533 m, 26 June 2022, collected by Jun-Qing Yan, Cheng-Feng Nie, and Lin-Gen Chen, HFJAU3969.





**Figure 3.** *E. subgriseosquamulosum* **A–D** basidiomata **A, B** HFJAU3969, holotype **C, D** HFJAU3967 **E** basidiospores **F** cheilocystidia **G** basidia **G, H** pileipellis. **G** was observed in H<sub>2</sub>O, remaining microstructures all were observed in 5% KOH, and used 1% Congo red as the stain except **E**. Scale bars: 10 mm (**A–D**); 20 µm (**E**); 30 µm (**F–H**).

**Diagnosis.** *Entoloma subgriseosquamulosum* is mainly characterized by the rather small, collybioid basidiomata, fuscous pileus, crowded and adnate lamellae, glabrous stipe, medium-sized basidiospores with 5–6 angles, mostly 5 angles, and absence of clamp connections. It differs from *E. griseosquamulosum* G.M. Gates & Noordel. by its gray stipe, smaller basidiospores, and absence of brilliant granules in hyphae.

**Macromorphology.** Basidiomata rather small, collybioid. Pileus 11–20 mm wide, campanulate to convex with slight depressed center, with entire margin, not hygrophanous, gray hairy scaly with denser center, translucently striate almost up to 1/2 of the radius, fuscous (4D2–4F2) to dark gray (1F1–4F1), darker at center. Lamellae relatively crowded, 2.0–4.0 mm wide, with two types of lamellulae, adnate to emarginate, ventricose, initially white, then brownish-rose, with entire and concolorous edge. Stipe 20–42 × 1.5–3.0 mm, central, terete, equal, hollow, gray (1C1–1E1), darker downwards, sparsely white fibrillose in the upper part elsewhere smooth and glabrous, base with white mycelium. Context thin, white. Odor indistinct, taste not tested.

**Micromorphology.** Basidiospores (8.1)8.4–10.5(11) × (6.0)6.5–8.0(8.5) µm, (av = 9.3 × 7.4 µm), Q = 1.1–1.4(1.5) (Qm = 1.3 ± 0.07, n = 100), subisodiametrical or heterodiametrical, 5–6 angles, mostly 5 angles in profile view, thick-walled, inamyloid. Basidia 27–36 × 10–13 µm, clavate, 4-spored, sterigmata 6.0–9.0 µm long, clampless. Pleurocystidia absent. Lamellae edge sterile of polipus-type. Cheilocystidia 27–64 × 9.0–14 µm, clavate. Lamellar trama regular, made up of cylindrical hyphae 7.0–12 µm wide. Pileipellis a trichoderm made up of cylindrical hyphae 6.0–12 µm broad, with clavate terminal elements and yellow-brown intracellular pigment. Stipitipellis a cutis composed of densely arranged, cylindrical hyphae, 7.0–17 µm wide, slightly constricted at the septa, with acute or attenuated end. Clamp connections absent.

**Habitat.** Solitary on soil or moss in broad-leaved forest.

**Distribution.** So far known from Fujian Province in China.

**Additional specimens examined.** CHINA • Fujian Province, Wuyishan City, Yangzhuang Town, Xiyuan Village, 27.7652°N, 117.8164°E, alt. 512 m, 26 June 2022, collected by Jun-Qing Yan, Cheng-Feng Nie, and Lin-Gen Chen, HFJAU3967.

**Notes.** Morphologically, several similar species within *Entoloma* subg. *Cyanula* that share brown to brown-gray pileus can be distinguished from the new species as follows: *E. anatinum* (Lasch) Donk is characterized by its larger basidiospores (9.0–13.5 × 7.5–9.0 µm) with 6–9 angles, and fertile lamellae edge (Donk 1949); *E. glaucobasis* Huijsman ex Noordel. has larger basidiospores (10–13.5 × 7.0–8.0 µm) (Noordeloos 1985); *E. griseosquamulosum* differs from the new species by the gray-violet stipe, larger basidiospores (9.0–12 × 7.0–9.0 µm), and presence of abundant brilliant granules in all hyphae (Noordeloos and Gates 2009); *E. phaeomarginatum* E. Horak is recognized by the fibrillose pileus, brown lamellae edge, and larger basidiospores (10–13 × 7.0–8.0 µm) (Horak 1973); *E. saponicum* G.M. Gates & Noordel. is distinct by the blackish brown lamellae edge and presence of abundant brilliant granules in all hyphae (Noordeloos and Gates 2009).

Phylogenetically, *E. cyanostipitum* Xiao L. He & W.H. Peng is closest to the new species. However, *E. cyanostipitum* is distinct by the deep blue pileus margin, lamellae edge and stipe, and the ITS region, with an 84% similarity (He et al. 2017).



***Entoloma subpraegracile* J.Q. Yan, L.G. Chen & S.N. Wang, sp. nov.**

MycoBank No: 856754

Fig. 4

**Etymology.** Refers to its macroscopic morphology similar to “*Entoloma praegracile*”

**Holotype.** CHINA • Zhejiang Province, Lishui City, Qingyuan County, Bandai-houshang Village, 27.6748°N, 119.0780°E, alt. 1084 m, 7 July 2020, collected by Jun-Qing Yan and Yan-Liu Chen, HFJAU1822.

**Diagnosis.** *Entoloma subpraegracile* is mainly characterized by the yellow, glabrous, and striate pileus, white, adnexed to adnate lamellae with tiny lateral veins, 5–7 angled and medium-sized basidiospores, sterile or heterogeneous lamellae edge of serrulatum-type, cylindrical or clavate cheilocystidia, and absence of clamp connections. It differs from *E. praegracile* by the larger basidiomata, and sterile or heterogeneous lamellae edge.

**Macromorphology.** Basidiomata rather small. Pileus 10–20 mm wide, conical when young, then convex to flattened with depressed, rarely cuspidate center, with entire margin, not hygrophanous, smooth and glabrous, translucently striate almost up to the center, ochre (7B4–6), grayish yellow (1A4–5) to tawny (2C4–6), darker at center. Lamellae relatively dense, 1.5–2.0 mm wide, with tiny lateral veins and two or three types of lamellulae, adnate to adnexed, subventricose, white, with entire and concolorous edge. Stipe 25–35 × 2.0–2.5 mm, central, terete. equal, hollow, concolorous or paler with the pileus, smooth and glabrous, sometimes grooved, white tomentose at the base. Context thin, concolorous to the surface. Odor indistinct, taste not tested.

**Micromorphology.** Basidiospores (7.0)8.5–10.5(12) × (6.0)6.5–7.5(8.5) μm, (av = 9.6 × 7.0 μm), Q = 1.2–1.6(1.7) (Qm = 1.4 ± 0.08, n = 200), heterodiametrical, 5–7(8) angles in profile view, appearing nodulose, thick-walled, inamyloid. Basidia 27–37 × 9–12 μm, clavate, slightly constricted at middle, mainly 2-spored, sterigmata 6.0–12 μm long, clampless. Pleurocystidia absent. Lamellae edge sterile or heterogeneous of poliporus-type. Cheilocystidia dense clusters on lamellae edge, 21–53 × 7.0–14 μm, cylindrical or clavate. Lamellar trama regular, made up of cylindrical hyphae 4.0–8.0 μm wide. Pileipellis a cutis made up of cylindrical hyphae 5.0–12 μm broad, with transitions to a trichoderm towards the center with clavate terminal elements 10–16 μm wide, with tawny intracellular pigment. Stipitipellis a cutis composed of densely arranged, cylindrical hyphae, 7.0–15 μm wide, slightly constricted at the septa, with rounded end. Clamp connections absent.

**Habitat.** Solitary or scattered on soil in mixed coniferous-broad-leaved forest.

**Distribution.** So far known from eastern China.

**Additional specimens examined.** CHINA • Fujian Province, Wuyishan City, 27.8594°N, 117.9096°E, alt. 372 m, 12 August 2021, collected by Jun-Qing Yan and Ze-Wei Liu, HFJAU3094 • 27.8563°N, 117.8661°E, alt. 668 m, 13 August 2021, collected by Qin Na, Yu-Peng Ge, and Lan-Yu Sun, HFJAU3164, HFJAU3168 • 27.7221°N, 117.7072°E, alt. 654 m, 16 August 2023, collected by Nian-Kai Zeng, Cheng-Feng Nie, Hua-Zhi Qin, Hui Deng, Tian Jiang, and Run-Xiang Zhao, HFJAU5110, HFJAU5115, HFJAU5140, HFJAU5175, HFJAU5177.

**Notes.** In the phylogenetic tree, *E. subpraegracile* groups together with *E. praegracile*. *Entoloma praegracile* differs from the new species by the smaller pileus (less than 10 mm), fertile lamellae edge, and the ITS sequence with 86% similarity (He et al. 2011).

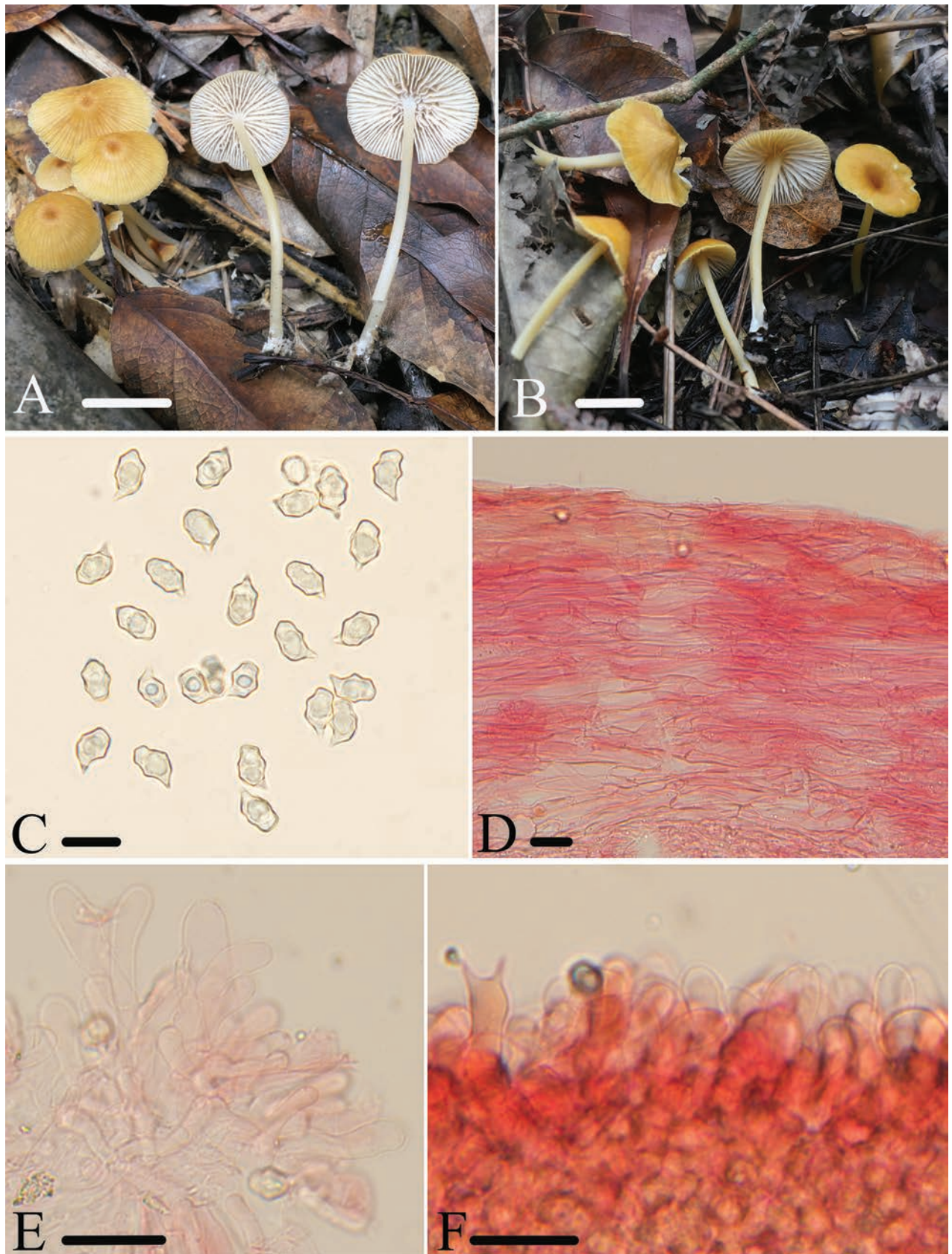


**Figure 4.** *E. subpraegracile* **A, B** basidiomata **A** HFJAU1822, holotype **B** HFJAU5115 **C** basidiospores **D** pileipellis **E** cheilocystidia **F** heterogeneous lamellae edge. All microscopic structures were observed in 5% KOH, and used 1% Congo red as the stain except **C**. Scale bars: 10 mm (**A, B**); 20  $\mu$ m (**C**); 30  $\mu$ m (**D–F**).

Some similar species with a yellow pileus within subg. *Cyanula* can be distinguished from the new species as follows: *E. chloropolium* (Fr.) M.M. Moser is recognized by the fertile to heterogeneous lamellae edge, and septate cheilocystidia (Noordeloos 2004); *E. formosum* (Fr.) Noordel. is characterized by its squamulose pileus, larger basidiospores ( $9.0\text{--}12.5 \times 6.0\text{--}8.0\ \mu\text{m}$ ), and fertile or heterogeneous lamellae edge (Bas et al. 1988b). *E. luteoochraceum* Ribes & Vila is distinct by the squamous pileus, 4-spored basidia, and fertile lamellae edge (Ribes and Vila 2013); *E. pseudoturci* Noordel. has tomentose to squamous and not striate pileus, porphyrogriseum-type lamellae edge, and brilliant granules in tissue cells (Noordeloos 1984).

***Entoloma wuyishanense* J.Q. Yan, L.G. Chen & S.N. Wang, sp. nov.**

MycoBank No: 858363

Fig. 5

**Etymology.** Refers to the collection locality of the holotype specimen – Wuyishan National Natural Park.

**Holotype.** CHINA • Fujian Province, Nanping City, Wuyishan National Natural Park,  $27.5418^{\circ}\text{N}$ ,  $117.4743^{\circ}\text{E}$ , alt. 422 m, 7 June 2022, collected by Jun-Qing Yan and Lin-Gen Chen, HFJAU3571.

**Diagnosis.** *Entoloma wuyishanense* is mainly characterized by the rather small and blue basidiomata, squamous and striate pileus, white and adnexed lamellae with fertile edge with slightly bluish pigmentation near the stipe, relatively large basidiospores with 5–6 angles, pileipellis with fuscous intracellular pigment. It differs from *E. azureosquamulosum* Xiao L. He & T.H. Li by the striate pileus, adnexed lamellae, larger basidiospores, and fertile lamellae edge.

**Macromorphology.** Basidiomata rather small. Pileus 2.0–11 mm wide, conical when young, then convex to flattened with depressed center, with entire, straight or wavy margin, not hygrophanous, squamous with denser center, translucently striate almost up to the center, deep blue (20E4–7) to light gray-blue (20B2–3), darker at center. Lamellae moderately distant, 1.0–3.0 mm wide, with two types of lamellulae, adnexed, ventricose, white, with entire and bluish edge near the stipe. Stipe 9.0–26  $\times$  1.0–2.0 mm, central, terete, equal, hollow, concolorous with pileus, paler downwards, white fibrillose, glabrescent with age, base with white mycelium. Context thin, gray-blue. Odor indistinct, taste not tested.

**Micromorphology.** Basidiospores  $(9.5)10\text{--}13.5(15) \times (6.5)7.5\text{--}9.5(10)\ \mu\text{m}$ , ( $\text{av} = 11.7 \times 8.5\ \mu\text{m}$ ),  $Q = 1.2\text{--}1.7(2.0)$  ( $Q_m = 1.4 \pm 0.11$ ,  $n = 200$ ), heterodiametrical, 5–6 angles in profile view, sometimes appearing nodulose, thick-walled, inamyloid. Basidia 25–33  $\times$  10–13  $\mu\text{m}$ , clavate, slightly constricted at middle, 4- or 2-spored, sterigmata 6.0–10  $\mu\text{m}$  long, clampless. Lamellae edge fertile. Cystidia absent. Lamellar trama regular, made up of cylindrical hyphae 5.0–11  $\mu\text{m}$  wide. Pileipellis a trichoderm made up of clavate to pyriform terminal cells, 41–65  $\times$  22–36  $\mu\text{m}$ . Pigment fuscous, intracellular, diffuse in pileipellis. Stipitipellis a cutis composed of densely arranged, cylindrical hyphae, 5.0–12  $\mu\text{m}$  wide, with rounded end. Clamp connections absent.

**Habitat.** Solitary or scattered on moss in mixed coniferous-broad-leaved forest.

**Distribution.** So far known from eastern China.



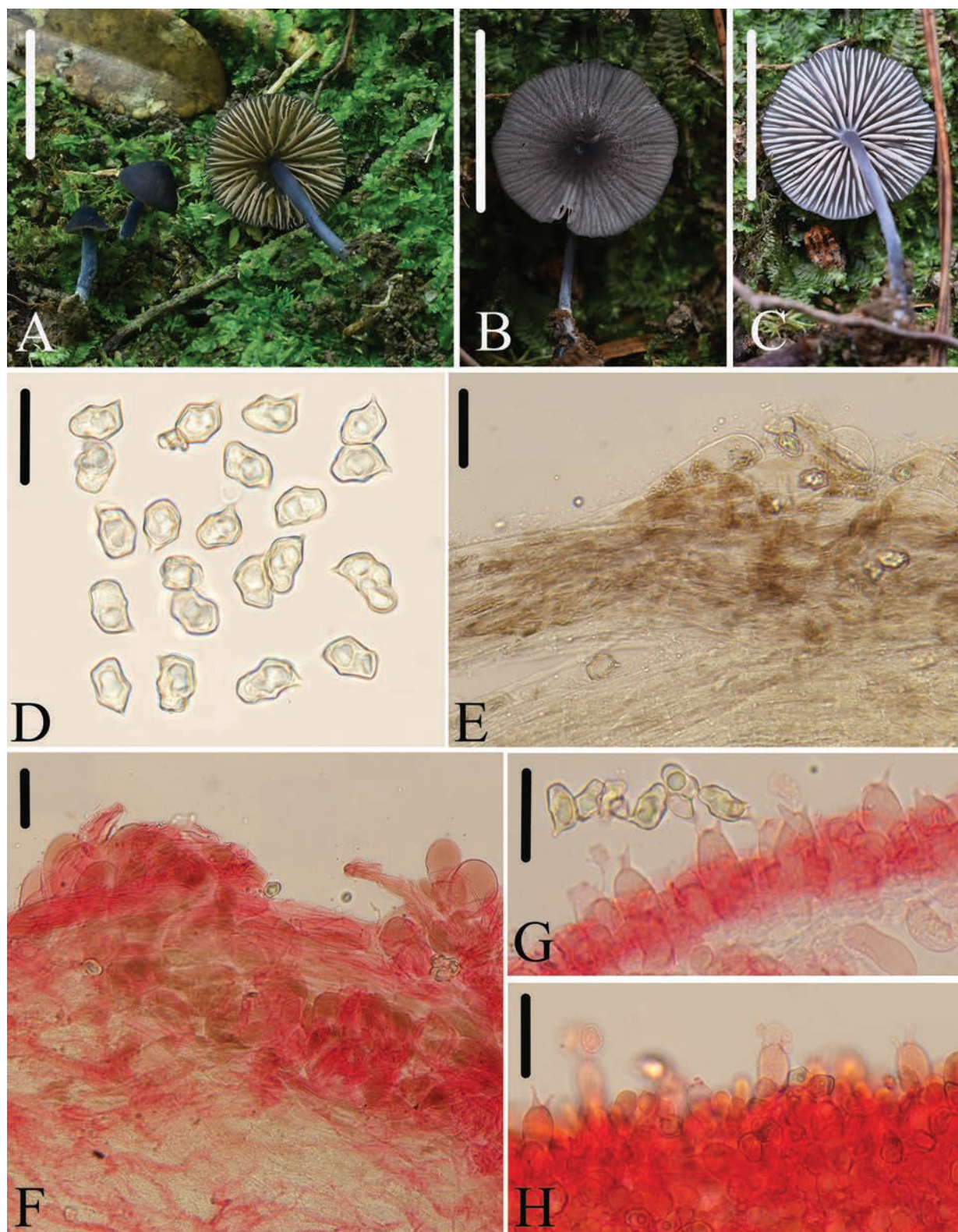


Figure 5. *E. wuyishanense* A–C basidiomata HFJAU3571, holotype B, C HFJAU3871 D basidiospores E, F pileipellis G basidia H fertile lamellar edge. E was observed in H<sub>2</sub>O D, F–H were observed in 5% KOH, and used 1% Congo red as the stain except D. Scale bars: 10 mm (A–C); 20 µm (D); 30 µm (E–H).

**Additional specimens examined.** CHINA • Zhejiang Province, Lishui City, Songyang County, Zicao Village, 28.4874°N, 119.5783°E, alt. 722 m, 2 July 2022, collected by Jun-Qing Yan, Cheng-Feng Nie, and Meng-Hui Han, HFJAU3871,



HFJAU3874, HFJAU3878 • Lishui City, Yunhe County, Chongtou Town, Xiayang Village, 28.0499°N, 119.4732°E, alt. 592 m, 4 July 2022, collected by Jun-Qing Yan and Cheng-Feng Nie, HFJAU3881.

**Notes.** Morphologically, *E. azureosquamulosum* is the most similar species with the distinction that *E. azureosquamulosum* exhibits not striate pileus, adnate lamellae, smaller basidiospores ( $8\text{--}10.5 \times 6.5\text{--}8.0\ \mu\text{m}$ ), and sterile lamellae edge (He et al. 2012).

In the phylogenetic tree, *E. wuyishanense* belongs to *Cyanula* sect. *Poliopodes*, within which several species have blue pileus, including *E. argus* O.V. Morozova, E.S. Popov, A.V. Alexandrova & Noordel., *E. calceus* Noordel., Bendiksen, Brandrud, P.-A. Moreau & Vila, *E. corvinum* (Kühner) Noordel., *E. icarus* O.V. Morozova, E.S. Popov & Noordel., and *E. perchalybeum* Noordel., J.B. Jordal & Dima. However, the lamellae edge of the latter in all species is sterile. In addition, *E. argus* is characterized by the adnate lamellae and smaller basidiospores ( $\leq 10\ \mu\text{m}$ ) (Morozova et al. 2022); *E. calceus* shows 6–9 angled basidiospores (Noordeloos et al. 2022b); *E. corvinum* is recognized by its not striate pileus, adnate lamellae, and smaller basidiospores ( $8.0\text{--}11 \times 6.5\text{--}7.5\ \mu\text{m}$ ) (Noordeloos 1982); *E. icarus* can be easily differentiated by the lateral stipe and adnate lamellae (Morozova et al. 2022); *E. perchalybeum* is distinct by the adnate lamellae and 6–7 rather bluntly angled basidiospores (Noordeloos et al. 2022b).

## Discussion

*Entoloma* subg. *Cyanula* currently is divided into 11 sections (Noordeloos et al. 2022a; Dima et al. 2023), and which formed well-supported clades and confirmed taxonomic positions within subgenus in this study. It is worth mentioning that two of the four newly discovered species in this study, along with the majority of previously reported new taxa of subg. *Cyanula* from China, do not belong to any known sections. To address this issue, continued phylogenetic studies of subg. *Cyanula* based on both morphological characters and molecular markers for more representative specimens of this subgenus from China are necessary. This will result in a more natural classification in the future.

Notably, based on the results of this phylogenetic analysis, we have realized that the sect. *Caesiocincta* is divided into three clades. However, since none of the originating branches of these scattered clades is supported, the cause of this result cannot be determined. Additional specimen data are needed for further analysis.

The present study expands our understanding of entolomoid species by providing descriptions and phylogenetic analyses for four new species. The findings enrich our knowledge of the distribution of *E.* subg. *Cyanula* species in China and the overall diversity of *Entoloma*.

## Key to *Entoloma* subg. *Cyanula* species reported in China

- 1 Pileus white to pink .....2
- Pileus other colored .....3
- 2 Pileus white, not striate, with depressed center; lamellae adnate to decurrent; basidiospores 5–6 angled; pigment not.....***E. orientosinense***
- Pileus pink, striate, with umbonate center; lamellae subfree to adnexed; basidiospores 6–8 angled; pigment yellow encrusting .....***E. mastoideum***

3	Pileus yellow-brown to grayish-brown.....	4
–	Pileus blue to violaceous .....	13
4	Pileus glabrous to fibrillose .....	5
–	Pileus squamulose to velvety .....	8
5	Basidiospores $Lav \geq 11 \mu m$ ; pileus striate, with depressed center; lamellae adnate; lamellae edge sterile or heterogeneous .....	<b><i>E. subtenuicystidium</i></b>
–	Basidiospores $Lav < 11 \mu m$ .....	6
6	Pileus $\geq 20 mm$ , with margin exceeding lamellae; lamellae adnate-emarginate to adnexed .....	<b><i>E. caespitosum</i></b>
–	Pileus $< 20 mm$ .....	7
7	Lamellae edge sterile or heterogeneous; pileus not hygrophanous .....	<b><i>E. subpraegracile</i></b>
–	Lamellae edge fertile; pileus hygrophanous .....	<b><i>E. praegracile</i></b>
8	Lamellae edge fertile; pileus striate; lamellae adnate or emarginate; basidiospores $8.0-14 \times 5.5-10 \mu m$ .....	<b><i>E. insidiosum</i></b>
–	Lamellae edge sterile .....	9
9	Basidiospores $Lav \geq 10 \mu m$ ; pileus striate; lamellae adnexed; pigment yellow-brown intracellular .....	<b><i>E. longistriatum</i></b>
–	Basidiospores $Lav < 10 \mu m$ .....	10
10	Cheilocystidia cylindrical to clavate .....	11
–	Cheilocystidia fusiform, lageniform, vesiculose to spheropedunculate .....	12
11	Pileus striate; lamellae adnate to emarginate; lamellae edge entire and concolorous with lamellae.....	<b><i>E. subgriseosquamulosum</i></b>
–	Pileus not striate; lamellae adnexed to short decurrent; lamellae edge serrulate and blue-black.....	<b><i>E. subcaesiocinctum</i></b>
12	Cheilocystidia fusiform to lageniform; pileus not striate; lamellae adnexed to free; lamellae edge concolorous with lamellae...	<b><i>E. pseudosubcorvinum</i></b>
–	Cheilocystidia vesiculose or spheropedunculate; pileus not striate; lamellae adnate-emarginate; lamellae edge brown .....	<b><i>E. pulchripes</i></b>
13	Lamellae edge fertile; pileus squamous, striate; lamellae adnexed; lamellae edge blue; basidiospores $10-13.5 \times 7.5-9.5 \mu m$ .....	<b><i>E. wuyishanense</i></b>
–	Lamellae edge sterile .....	14
14	Pileus not striate .....	15
–	Pileus striate.....	16
15	Lamellae adnate-emarginate; cheilocystidia fusoid .....	<b><i>E. azureosquamulosum</i></b>
–	Lamellae short decurrent; cheilocystidia cylindrical to subclavate .....	<b><i>E. cyanostipitum</i></b>
16	Cheilocystidia subglobose or sphaeropedunculate; lamellae edge concolorous with lamellae .....	<b><i>E. ekaterinae</i></b>
–	Cheilocystidia broadly clavate or lageniform; lamellae edge blackish purple .....	<b><i>E. callipygmaeum</i></b>

## Acknowledgments

The authors are very grateful for assistance of Yu-Peng Ge and Meng-Hui Han in the field specimen collection and the anonymous reviewers of the manuscript.

## Additional information

### Conflict of interest

The authors have declared that no competing interests exist.

### Ethical statement

No ethical statement was reported.

### Funding

This work was financed by the National Natural Science Foundation of China (32460326, 31960008), Jiangxi Provincial Natural Science Foundation (20224BAB205003), Fujian Provincial Natural Science Foundation (2023J01379), and the Project of FAAS (XTCX-GC2021007).

### Author contributions

Conceptualization, Jun-Qing Yan; methodology, Jun-Qing Yan and Sheng-Nan Wang; software, Lin-Gen Chen, Hong Chen, Ling Ding and Yu-Qin Xu; formal analysis, Hui Zeng, Jun-Qing Yan, and Sheng-Nan Wang; investigation, Lin-Gen Chen, Hong Chen, Ling Ding, and Jun-Qing Yan; resources, Hui Zeng and Jun-Qing Yan; writing – original draft, Lin-Gen Chen; writing – review and editing, Jun-Qing Yan; visualization, Jun-Qing Yan and Sheng-Nan Wang; supervision, Jun-Qing Yan; project administration, Jun-Qing Yan; funding acquisition, Jun-Qing Yan. All authors have read and agreed to the published version of the manuscript.


### Author ORCIDs

Lin-Gen Chen  <https://orcid.org/0009-0000-2506-181X>

Hong Chen  <https://orcid.org/0009-0004-0107-3962>

Ling Ding  <https://orcid.org/0009-0000-5293-046X>

Hui Zeng  <https://orcid.org/0000-0003-2025-844X>

Sheng-Nan Wang  <https://orcid.org/0000-0003-0648-271X>

Jun-Qing Yan  <https://orcid.org/0000-0003-1128-5171>

### Data availability

All of the data that support the findings of this study are available in the main text or Supplementary Information.

## References

- Armada F, Bellanger J-M, Moreau P-A (2023) Champignons de la zone alpine. Contribution à l'étude des champignons supérieurs alpins. Fédération mycologique et botanique Dauphiné-Savoie, 376.
- Bas C (1969) Morphology and subdivision of *Amanita* and a monograph of its section *Lepidella*. Persoonia-Molecular Phylogeny and Evolution of Fungi 5: 285–573.
- Bas C, Wkuyper TH, Noordeloos ME, Vellinga EC, Boekhout T, Arnolds E (1988a) Flora Agaricina Neerlandica: Critical monographs on families of agarics and boleti occurring in the Netherlands. Balkema, Netherlands, 191.
- Bas C, Wkuyper TH, Noordeloos ME, Vellinga EC, Boekhout T, Arnolds E (1988b) Flora agaricina Neerlandica: critical monographs on families of agarics and boleti occurring in the Netherlands Vol.1 Entolomataceae. Balkema, Rotterdam, 191.

- Bhunjun CS, Niskanen T, Suwannarach N, Wannathes N, Chen YJ, Mckenzie E, Maharachchikumbura S, Buyck B, Zhao CL, Fan YG, Zhang JY, Dissanayake AJ, Sandamali D, Jayawardena RS, Kumla J, Padamsee M, Chen YY, Liimatainen K, Ammirati JF, Phukhamsakda C, Liu J-KJ, Phonrob W, Randrianjohany E, Hongsan S, Cheewangkoon R, Bundhun D, Khuna S, Yu WJ, Deng LS, Lu YZ, Hyde KD, Lumyong S (2022) The numbers of fungi: Are the most speciose genera truly diverse? *Fungal Diversity* 114: 387–462. <https://doi.org/10.1007/s13225-022-00501-4>
- Bi ZS, Zheng GY, Li TH (1986) Taxonomic studies on the genus *Entoloma* from Guangdong. *Acta Mycologica Sinica* 5: 161–169. <https://doi.org/10.13346/j.mycosystema.1986.03.005>
- Brandrud TE, Bendiksen E, Jordal JB, Weholt Ø, Iorås J, Dima B, Noordeloos ME (2023) *Entoloma* species of subgenus *Cyanula* (Tricholomatinae, Basidiomycota) in Norway, with emphasis on habitat preferences and distribution. *Agarica: Mykologisk Tidsskrift* 43: 85–137. <https://doi.org/10.5617/agarica.10985>
- Chen LG, Ding L, Hong C, Zeng H, Zeng ZH, Wang SN, Yan JQ (2024) Seven New Species of *Entoloma* Subgenus *Cubospora* (Entolomataceae, Agaricales) from Subtropical Regions of China. *Journal of Fungi* (Basel, Switzerland) 10: 594. <https://doi.org/10.3390/jof10080594>
- Co-David D, Langeveld D, Noordeloos ME (2009) Molecular phylogeny and spore evolution of Entolomataceae. *Persoonia-Molecular Phylogeny and Evolution of Fungi* 23: 147–176. <https://doi.org/10.3767/003158509X480944>
- Crous PW, Cowan DA, Maggs-Kölling G, Yilmaz N, Thangavel R, Wingfield MJ, Noordeloos ME, Dima B, Brandrud TE, Jansen GM, Morozova OV, Vila J, Shivas R, Tan YP, Bishop-Hurley SL, Lacey E, Marney TS, Larsson E, Floch GL, Lombard L, Nodet P, Hubka V, Alvarado P, Berraf-Tebbal A, Reyes JD, Delgado G, Eichmeier A, Jordal JB, Kachalkin A, Kubátová A, Macia-Vicente JG, Malysheva E, Papp V, Rajeshkumar KC, Sharma A, Spetik M, Strašitáková D, Tomashevskaya MA, Abad JA, Abad ZG, Alexandrova AV, Anand G, Arenas F, Ashtekar ND, Balashov S, Bañares Á, Baroncelli R, Bera I, Biketova AY, Blomquist CL, Boekhout T, Boertmann D, Bulyonkova T, Burgess TI, Carnegie A, Díaz JFC, Corriol G, Cunningham J, Cruz M, Damm U, Davoodian N, Santiago A, Dearnaley JDW, Freitas LWSd, Dhileepan K, Dimitrov RA, Piazza SD, Fatima S, Fuljer F, Galera H, Ghosh A, Giraldo A, Glushakova AM, Gorczak M, Gouliamova D, Gramaje D, Groenewald M, Gunsch CK, Gutiérrez A, Holdom D, Houbraken J, Ismailov A, Istel Ł, Iturriaga T, Jeppson M, Jurjević Ž, Kalinina L, Kapitonov VI, Kautmanová I, Khalid AN, Kiran M, Kiss L, Kovács Á, Kurose D, Kušan I, Lad S, Læssøe T, Lee HB, Luangsa-Ard JJ, Lynch M, Popov E, Matočec N, Reschke K (2021a) Fungal Planet description sheets: 1182–1283. *Persoonia-Molecular Phylogeny and Evolution of Fungi* 46: 313–528. <https://doi.org/10.3767/persoonia.2021.46.11>
- Crous PW, Osieck ER, Jurjević Ž, Boers J, Iperen AV, Starink M, Dima B, Balashov S, Bulgakov T, Johnston PR, Morozova OV, Pinruan U, Sommai S, Alvarado P, Decock C, Lebel T, McMullan-Fisher SJM, Moreno G, Shivas R, Zhao L, Abdollahzadeh J, Abrinbana M, Ageev D, Akhmetova C, Alexandrova A, Altés A, Amaral AGG, Angelini C, Antonín V, Arenas F, Asseman P, Badali F, Baghela A, Bañares Á, Barreto RW, Baseia I, Bellanger J-M, Berraf-Tebbal A, Biketova AY, Bukharova N, Burgess TI, Cabero J, Camara MPS, Cano J, Ceryngier P, Chavez R, Cowan DA, Lima AFd, Oliveira R, denman S, Quynh DN, Dovana F, Duarte IG, Eichmeier A, Erhard A, Esteve-Raventós F, Fellin A, Ferisin G, Ferreira RJ, Ferrer A, Finy P, Gaya E, Geering ADW, Gil-Durán C, Glässnerova K, Glushakova AM, Gramaje D, Guard F, Serrudo AG, Haelewaters D, Halling RE, Hill R, Hirooka Y, Hubka V, Iliushin VA, Ivanova DD, Ivanushkina NE, Jangsantear P, Justo A, Kachalkin A, Kato S, Khamsuntorn P, Kirtsideli I,



- Knapp DG, Galina K, Koukol O, Kovács GM, Kruse J, Kumar TKA, Kušan I, Læssøe T, Larsson E, Lebeuf R, Levican G, Loizides M, Marinho P, Luangsa-Ard JJ, Lukina EG, Magaña V, Maggs-Kölling G, Malysheva E, Malysheva V, Martín B, Martín MP, Matočec N, McTaggart A, Mehrabi-Koushki M, Mesic A, Miller AN, Mironova P, Moreau P-A, Morte A, Müller K, Nagy LG, Nanu S, Navarro-Ródenas A, Nel W, Nguyen TH, Nóbrega T, Noordeloos ME, Olariaga I, Overton B, Ozerskaya SM, Palani P, Pancorbo F, Papp V, Pawłowska J, Thu PQ, Phosri C, Popov E, Portugal A, Pošta A, Reschke K, Reul M, Ricci GM, Rodríguez A, Romanowski J, Ruchikachorn N, Saar I, Safi A, Sakolrak B, Salzmann F, Sandoval-Denis M, Sangwichein E, Sanhueza L, Sato T, Sastoque AP, Senn-Irllet BJ, Shibata A, Siepe K, Somrithipol S, Špetík M, Pichai S, Stchigel AM, Štůsková K, Suwannasai N, Tan YP, Thangavel R, Tiago I, Tiwari S, Tkalcic Z, Tomashevskaya MA, Tonegawa C, Tran H, Tran NT, Trovão J, Trubitsyn V, Wyk JJV, Vieira WADS, Vila J, Visagie CM, Vizzini A, Volobuev S, Vu DT, Wangsawat N, Yaguchi T, Ercole E, Ferreira BW, Souza APd, Vieira BS, Groenewald JZ (2021b) Fungal Planet description sheets: 1284–1382. *Persoonia-Molecular Phylogeny and Evolution of Fungi* 47: 1284–1382. <https://doi.org/10.3767/persoonia.2021.47.06>
- Dima B, Brandrud TE, Corriol G, Jansen GM, Jordal JB, Khalid AN, Larsson E, Lorås J, Morozova OV, Naseer A, Noordeloos ME, Rossi W, Santamaria S, Sarwar S, Sesli E, Usman M, Afshan NUS, Ahmad I, Banerjee A, Banerjee K, Bendiksen E, Colombo DRdS, Kesel AD, Dovana F, Ferisin G, Hussain S, Islam S, Jesus ALd, Kaygusuz O, Krisai-Greilhuber I, Mahammad S, Mishra DK, Nath PS, Paixão SCdOd, Panja B, Papp V, Zottarelli C, Radnoti A, Rana D, Saha R, Türkecul İ, Haelewaters D (2021) Fungal systematics and evolution: FUSE 7. *Sydowia* 73: 271–340. <https://doi.org/10.12905/0380.sydowia73-2021-0271>
- Dima B, Noordeloos ME, Morozova OV, Jansen GM, Reschke K, Brandrud TE, Vila J (2023) Nomenclatural novelties. Index Fungorum no 546: Donk MA (1949) New and revised nomina generica conservanda proposed for Basidiomycetes (Fungi). *Bulletin of the Botanical Gardens Buitenzorg* 18: 83–168.
- Donk MA (1949) New and revised nomina generica conservanda proposed for Basidiomycetes (Fungi). *Bulletin of the Botanical Gardens Buitenzorg* 18: 83–168.
- Fachada V, Pedreiro H, Raimundo S, Noordeloos ME, Dima B, Marques G (2023) *Entoloma sicoense*, a new species in the subgenus *Cyanula* (Entolomataceae). *Phytotaxa* 606: 133–146. <https://doi.org/10.11646/phytotaxa.606.2.4>
- Gates GM, Noordeloos ME (2007) Preliminary studies in the genus *Entoloma* in Tasmania – II. *Persoonia-Molecular Phylogeny and Evolution of Fungi* 19: 157–226.
- He XL, Li TH, Jiang ZD, Shen YH (2011) *Entoloma mastoideum* and *E. praegracile* – Two new species from China. *Mycotaxon* 116: 413–419. <https://doi.org/10.5248/116.413>
- He XL, Li TH, Jiang ZD, Shen YH (2012) Four new species of *Entoloma* s.l. (Agaricales) from southern China. *Mycological Progress* 11: 915–925. <https://doi.org/10.1007/s11557-012-0807-0>
- He XL, Li TH, Xi PG, Jiang ZD, Shen YH (2013) Phylogeny of *Entoloma* s.l. subgenus *Pouzarella* with descriptions of five new species from China. *Fungal Diversity* 58: 227–243. <https://doi.org/10.1007/s13225-012-0212-7>
- He XL, Wang D, Peng WH, Gan BC (2017) Two new *Entoloma* s.l. species with serrulatum-type lamellar edge from Changbai Mountains. *Northeast China*. 16: 761–768. <https://doi.org/10.1007/s11557-017-1313-1>
- Hesler LR (1967) *Entoloma* in Southeastern North America. *Beihefte zur Nova Hedwigia*, Germany, 196.
- Horak E (1973) Fungi agaricini Novazelandiae I–V: I. *Entoloma* (Fr.) and related genera. *Beihefte zur Nova Hedwigia*, Germany, 86.

- Horak E (1980) *Entoloma* (Agaricales) in Indomalaya and Australasia. Beihefte zur Nova Hedwigia, Germany, 352.
- Horak E (2005) Röhrlinge und Blätterpilze in Europa: Bestimmungsschlüssel für Polyporales (pp), Boletales, Agaricales, Russulales. Elsevier, Spektrum, Akad. Verl., Munich, Germany, 557.
- Karich A, Kellner H, Schmidt M, Ullrich R (2015) Ein bemerkenswertes Mykotop im Zittauer Gebirge mit *Microglossum rufescens* als Erstnachweis für Deutschland. *Boletus* 36: 151–163.
- Karstedt F, Bergemann SE, Capelari M (2020) Five *Nolanea* spp. nov. from Brazil. *Mycotaxon* 135: 589–612. <https://doi.org/10.5248/135.589>
- Katoh K, Rozewicki J, Yamada KD (2019) MAFFT online service: multiple sequence alignment, interactive sequence choice and visualization. *Briefings in Bioinformatics* 20: 1160–1166. <https://doi.org/10.1093/bib/bbx108>
- Kokkonen K (2015) A survey of boreal *Entoloma* with emphasis on the subgenus *Rhodopolia*. *Mycological Progress* 14: 116. <https://doi.org/10.1007/s11557-015-1135-y>
- Kornerup A, Wanscher JH (1978) *The Methuen Handbook of Colour*. Eyre Methuen Ltd, UK, 252.
- Largent DL (1994) *Entolomatoid fungi of the western United States and Alaska*. Mad River Press, Eureka, California, USA, 495.
- Lebeuf R, Alexandrova A, Mendoza AC, Guivin MAC, Silva GAd, Ricaldi AMdIS, Dima B, Fryssouli V, Gkilas M, Guerrero-Abad JC, Lamoureux Y, Landry J, Mesic A, Morozova OV, Noordeloos ME, Oehl F, Paul A, Pham THG, Polemis E, Santos VM, Svetasheva T, Tkalec Z, Vallejos-Tapullima A, Vila J, Zervakis GI, Baral H-O, Bulynkova T, Kalinina L, Krisai-Greilhuber I, Malysheva E, Myhrer J, Pärtel K, Pennanen M, Stallman J, Haelewaters D (2021) *Fungal Systematics and Evolution: FUSE* 8. *Sydowia* 74: 193–249. <https://doi.org/10.12905/0380.sydowia74-2021-0193>
- Morozova OV, Noordeloos ME, Vila J (2014) *Entoloma* subgenus *Leptonia* in boreal-temperate Eurasia: Towards a phylogenetic species concept. *Persoonia-Molecular Phylogeny and Evolution of Fungi* 32: 141–169. <https://doi.org/10.3767/003158514X681774>
- Morozova OV, Popov E, Alexandrova A, Pham THG, Noordeloos ME (2022) Four new species of *Entoloma* (Entolomataceae, Agaricomycetes) subgenera *Cyanula* and *Claudopus* from Vietnam and their phylogenetic position. *Phytotaxa* 549: 1–21. <https://doi.org/10.11646/phytotaxa.549.1.1>
- Nguyen LT, Schmidt HA, Haeseler Av, Minh BQ (2015) IQ-TREE: A fast and effective stochastic algorithm for estimating maximum-likelihood phylogenies. *Molecular Biology and Evolution* 32: 268–274. <https://doi.org/10.1093/molbev/msu300>
- Noordeloos ME (1981) Introduction to the taxonomy of the genus *Entoloma* sensu lato (Agaricales). *Persoonia-Molecular Phylogeny and Evolution of Fungi* 11: 121–151.
- Noordeloos ME (1982) Notes on *Entoloma*. New and rare species of *Entoloma* from Scandinavia. New names and combinations. *Nordic Journal of Botany* 2: 155–162. <https://doi.org/10.1111/j.1756-1051.1982.tb01176.x>
- Noordeloos ME (1984) Studies in *Entoloma* – 10–13. *Persoonia-Molecular Phylogeny and Evolution of Fungi* 12: 195–223.
- Noordeloos ME (1985) Notulae ad floram Agaricinam Neerlandicam X–XI. *Entoloma*. *Persoonia-Molecular Phylogeny and Evolution of Fungi* 12: 457–462.
- Noordeloos ME (2004) *Entoloma* s.l. *Fungi Europaei* 5. Edizioni Candusso, Alassio, Italy, 618.
- Noordeloos ME, Gates G (2009) Preliminary studies in the genus *Entoloma* in Tasmania-II. *Cryptogamie. Mycologie* 30: 107–140.

- Noordeloos ME, Gates GM (2012) The Entolomataceae of Tasmania. Springer, Dordrecht, The Netherlands, 400. <https://doi.org/10.1007/978-94-007-4679-4>
- Noordeloos ME, Lorås J, Eidissen SE, Brandrud TE, Bendiksen E, Morozova OV, Jordal JB, Weholt Ø, Jansen GM, Larsson E, Dima B (2021) Three new *Entoloma* species of the *Cyanula* clade from (sub)alpine habitats in Northern Norway and Sweden. *Sydowia* 73: 185–196. <https://doi.org/10.12905/0380.sydowia73-2020-0185>
- Noordeloos ME, Dima B, Morozova OV, Reschke K, Jansen GM, Brandrud TE, Jordal JB, Bendiksen E, Vila J (2022a) *Entoloma Sensu Lato*. Subgenera *Cyanula*, *Leptonia*, *Nolanea*, *Trichopilus*, and the *Rhombisporum* Clade. Candusso Edtrice di Lidia Carla Candusso Via Saronnino 41/47 I-21040–Origgio VA, Italy, 968.
- Noordeloos ME, Vila J, Jordal JB, Kehlet T, Brandrud TE, Bendiksen E, Moreau P-A, Dondl M, Lorås J, Larsson E, Dima B (2022b) Contributions to the revision of the genus *Entoloma* (Basidiomycota, Agaricales) in Europe: Six new species from subgenus *Cyanula* and typification of *E. incarnatofuscescens*. *Fungal Systematics and Evolution* 9: 87–97. <https://doi.org/10.3114/fuse.2022.09.06>
- Reschke K, Morozova OV, Dima B, Cooper JA, Corriol G, Biketova AY, Piepenbring M, Noordeloos ME (2022a) Phylogeny, taxonomy, and character evolution in *Entoloma* subgenus *Nolanea*. *Persoonia-Molecular Phylogeny and Evolution of Fungi* 49: 136–170. <https://doi.org/10.3767/persoonia.2022.49.04>
- Reschke K, Noordeloos ME, Manz C, Hofmann TA, Rodríguez-Cedeño J, Dima B, Piepenbring M (2022b) Fungal diversity in the tropics: *Entoloma* spp. in Panama. *Mycological Progress* 21: 93–145. <https://doi.org/10.1007/s11557-021-01752-2>
- Ribes MÁ, Vila J (2013) *Entoloma luteoochraceum* y *E. luteoviolaceum*, dos nuevas especies de las Islas Canarias. *Fungi Non Delineati : Raro Vel Haud Perspecte et Explore Descripti aut Definite Picti* 146: 86–92.
- Romagnesi H (1974) Essai d'une classification des rhodophylles. *Bulletin Mensuel de la Societe Linneenne de Lyon* 43: 325–332. <https://doi.org/10.3406/linly.1974.10142>
- Ronquist F, Teslenko M, Mark PVD, Ayres DL, Darling A, Höhna S, Larget B, Liu L, Suchard MA, Huelsenbeck J (2012) MrBayes 3.2: efficient Bayesian phylogenetic inference and model choice across a large model space. *Systematic Biology* 61: 539–542. <https://doi.org/10.1093/sysbio/sys029>
- Varga T, Krizsán K, Földi C, Dima B, Sánchez-García M, Sánchez-Ramírez S, Szöllősi GJ, Szarkándi JG, Papp V, Albert L, Andreopoulos W, Angelini C, Antonín V, Barry KW, Bougher NL, Buchanan P, Buyck B, Bense V, Catcheside P, Chovatia M, Cooper J, Dämon W, Desjardin D, Finy P, Geml J, Haridas S, Hughes K, Justo A, Karasiński D, Kautmanova I, Kiss B, Kocsubé S, Kotiranta H, LaButti KM, Lechner BE, Liimatainen K, Lipzen A, Lukács Z, Mihaltcheva S, Morgado LN, Niskanen T, Noordeloos ME, Ohm RA, Ortiz-Santana B, Ovrebo C, Rácz N, Riley R, Savchenko A, Shiryayev A, Soop K, Spirin V, Szebenyi C, Tomšovský M, Tulloss RE, Uehling J, Grigoriev IV, Vágvölgyi C, Papp T, Martin FM, Miettinen O, Hibbett DS, Nagy LG (2019) Megaphylogeny resolves global patterns of mushroom evolution. *Nature Ecology & Evolution* 3: 668–678. <https://doi.org/10.1038/s41559-019-0834-1>
- Vila J, Noordeloos ME, Reschke K, Moreau P-A, Battistin E, Ribes MÁ, Marulli U, Corriol G, Polemis E, Loizides M, Dima B (2021) New species of the genus *Entoloma* (Basidiomycota, Agaricales) from Southern Europe. *Asian Journal of Mycology* 29: 123–153.
- Wang SN, Fan YG, Yan JQ (2022) *lugisporipsathyra reticulopilea* gen. et sp. nov. (Agaricales, Psathyrellaceae) from tropical China produces unique ridge-ornamented spores with an obvious suprahilar plage. *MycoKeys* 90: 147–162. <https://doi.org/10.3897/mycokeys.90.85690>

- White TJ, Bruns TD, Lee SB, Taylor JW, Innis MA, Gelfand DH, Sninsky J (1990) Amplification and direct sequencing of fungal ribosomal RNA genes for phylogenetics. Academic Press, Inc, San Diego, USA, 315–322. <https://doi.org/10.1016/B978-0-12-372180-8.50042-1>
- Zhang D, Gao F, Jakovlić I, Zou H, Zhang J, Li W, Wang GT (2020) PhyloSuite: An integrated and scalable desktop platform for streamlined molecular sequence data management and evolutionary phylogenetics studies. *Molecular Ecology Resources* 20: 348–355. <https://doi.10.1111/1755-0998.13096>
- Zhang WM, Li TH, Bi ZS, Zheng GY (1994) Taxonomic studies on the genus *Entoloma* from Hainan Province of China (I). *Acta Mycologica Sinica* 13: 188–196. <https://doi.org/10.13346/j.mycosystema.1994.03.006>

## Supplementary material 1

### Supplementary data

Authors: Lin-Gen Chen, Hong Chen, Ling Ding, Yu-Qin Xu, Hui Zeng, Sheng-Nan Wang, Jun-Qing Yan

Data type: nex

Explanation note: A nexus file contains alignment sequence and original tree of ML and Bayes.

Copyright notice: This dataset is made available under the Open Database License (<http://opendatacommons.org/licenses/odbl/1.0/>). The Open Database License (ODbL) is a license agreement intended to allow users to freely share, modify, and use this Dataset while maintaining this same freedom for others, provided that the original source and author(s) are credited.

Link: <https://doi.org/10.3897/mycokeys.116.145568.suppl1>





# *Biconidium sinense* gen. et sp. nov. (Hypocreales, Bionectriaceae) and *Didymocyrtis shanxiensis* sp. nov. (Phaeosphaeriaceae, *Didymocyrtis*) isolated from urban soil in China

Hai-Yan Wang<sup>1</sup>, Chunbo Dong<sup>1</sup>, Yan-Wei Zhang<sup>2</sup>, Wan-Hao Chen<sup>3</sup>, Yan-Feng Han<sup>1</sup>

<sup>1</sup> Institute of Fungus Resources, Department of Ecology, College of Life Science, Guizhou University, Guiyang 550025, Guizhou, China

<sup>2</sup> Key Laboratory of Development and Utilization of Biological Resources in Colleges and Universities of Guizhou Province/Key Laboratory of Ecology and Management on Forest Fire in Higher Education Institutions of Guizhou Province, Guizhou Education University, Guiyang 550018, Guizhou, China

<sup>3</sup> Center for Mycomedicine Research, Basic Medical School, Guizhou University of Traditional Chinese Medicine, Guiyang 550025, Guizhou, China

Corresponding authors: Yan-Wei Zhang (zyw\_email@163.com); Yan-Feng Han (swallow1128@126.com)

## Abstract

During a fungal diversity survey in various urban habitats across China, 5 fungal isolates were discovered from soil samples. Detailed morphological observations and multi-gene phylogenetic analyses confirmed the identification of two novel taxa: *Biconidium sinense* **gen. et sp. nov.** and *Didymocyrtis shanxiensis* **sp. nov.** These species were formally described, illustrated, and discussed, highlighting their distinct characteristics and taxonomic placement. The study expands our understanding of fungal diversity in urban environments, emphasizing the importance of combining morphological and molecular approaches for accurate species delineation and discovery.

**Key words:** Fungal taxonomy, mycodiversity, new taxa, phylogeny



Academic editor: Ajay Kumar Gautam

Received: 14 January 2025

Accepted: 20 March 2025

Published: 29 April 2025

**Citation:** Wang H-Y, Dong C, Zhang Y-W, Chen W-H, Han Y-F (2025)

*Biconidium sinense* gen. et sp. nov.

(Hypocreales, Bionectriaceae) and

*Didymocyrtis shanxiensis* sp. nov.

(Phaeosphaeriaceae, *Didymocyrtis*) isolated from urban soil in China.

MycoKeys 116: 327–344. <https://doi.org/10.3897/mycokeys.116.146683>

**Copyright:** © Hai-Yan Wang et al.

This is an open access article distributed under

terms of the Creative Commons Attribution

License (Attribution 4.0 International – CC BY 4.0).

## Introduction

Soil fungi play an important role in mediating the processes of geochemical cycling, ecosystem material cycling and energy flow. For instance, they influence soil fertility, mineral breakdown, and organic matter cycling, as well as plant health and nutrition (Guo et al. 2017; Lu 2018). Moreover, some soil fungi can produce a lot of metabolites that are essential for human life and production (Zhang et al. 2023; Wang et al. 2024). For example, among the fungal species in the soil, the strains of the genera *Aspergillus*, *Penicillium*, *Paecilomyces* and *Trichoderma* produce flavins, ankaflavin, quinones, and anthraquinone (Akilandeswari and Pradeep 2016). *Penicillium griseofulvum* can produce a range of secondary metabolites including chanoclavine I, elymoclavine, fulvic acid, and griseofulvin, all of which can be used for antimicrobial activity (Yogabaanu et al. 2017). *Acrophialophora levis* QHDZ1–2 isolated from a zoo soil can produce some compounds, such as amino acid, amines, fatty acid, and vitamins (Wang 2024). Due to a multitude of factors, it is suspected that species are disappearing before they are discovered in many habitats (Wang et al. 2018; Löbl et al. 2023; Wang et al. 2024). This implies that we still need to make

more efforts to delve deeper into soil fungi resources, contribute to the study of our Earth's fungal diversity, and provide fungal resources for social industrial production. Currently, numerous studies have investigated fungal diversity in various soil habitats across China, including caves, forests, farmland, deserts and grasslands (Guo et al. 2017; Ma et al. 2021; Ma 2023; Guo 2024; Song et al. 2024). However, the composition and diversity of soil fungi in various urban various environments appear to have been neglected.

Urbanization has been the most impactful human activity in altering landscape patterns over the past century and is widely regarded as a significant threat to global biodiversity (Grimm et al. 2008; Nugent and Allison 2022). Developing countries are experiencing the swiftest rates of urbanization, with projections indicating that approximately 68% of the global population will reside in urban areas by 2050 (Desa 2019). The process of urbanization will reshape the land landscape, impacting elements such as surface vegetation, hydrology and soil, which in turn affects biodiversity and can lead to species homogenization or even extinction of species (Buczowski and Richmond 2012; Yan et al. 2022). Urbanization has had a profound impact on soil fungi. It fragments the original habitats, resulting in a decline in fungal diversity and the potential disappearance of some native fungal species (Zhao et al. 2012; Hou et al. 2014; Rai et al. 2018). Consequently, in the context of urbanization, the composition and distribution of soil fungi across various urban habitats should be paid more attention. In recent years, the composition and diversity of green soil fungi in different urban habitats were explored (Zhang et al. 2021, 2023, 2024; Li et al. 2022a, 2022b; Ren et al. 2022; Wang et al. 2023, 2024). Fortunately, many new species and genera have been discovered and documented in these urban settings.

Bionectriaceae Samuels & Rossman was proposed by Rossman et al. (1999) based on the sexual morph-typified genus *Bionectria* Speg. (Spegazzini 1919). It is including 26 genera. Its diagnostic characteristics are the presence of white, pale tan orange or brown, uniloculate, perithecial, rarely cleistothecial ascomata and generally not changing color in KOH.

Barr (1979) proposed the family Phaeosphaeriaceae using *Phaeosphaeria* with *Ph. oryzae* as the type species. The new genus *Diederichomyces* was described by Trakunyingcharoen et al. (2014) to include most of the lichenicolous *Phoma* species that were assigned to the Phaeosphaeriaceae by Lawrey et al. (2012). Vainio (1921) established *Didymocyrtis* Vain., based on the type species *Didymocyrtis consimilis* Vain. With the development of phylogeny, the lichenicolous species of genus *Didymocyrtis* had been assigned to *Diederichia* D. Hawksw., *Diederichomyces* Crous & Trakun., *Leptosphaeria* Pass. and *Phoma* Sacc. (Trakunyingcharoen et al. 2014). Recently, the genus *Didymocyrtis* was resurrected for these species, and the new combinations, *Didymocyrtis bryonthae* (Arnold) Hafellner, *Didymocyrtis cladoniicola* (Diederich, Kocourk. & Etayo) Ertz & Diederich, *Didymocyrtis foliaceiphila* (Diederich, Kocourk. & Etayo) Ertz & Diederich, *Didymocyrtis infestans* (Speg.) Hafellner, *Didymocyrtis kaernefeltii* (S.Y. Kondr.) Hafellner, *Didymocyrtis melanelixiae* (Brackel) Diederich, R.C. Harris & Etayo, *Didymocyrtis pseudeverniae* (Etayo & Diederich) Ertz & Diederich, *Didymocyrtis ramalinae* (Roberge ex Desm.) Ertz, Diederich & Hafellner, *Didymocyrtis slaptoniensis* (D. Hawksw.) Hafellner & Ertz, and *Didymocyrtis xanthomendozae* (Diederich & Freebury) Diederich & Freebury were created (Ertz et al. 2015). Presently, the genus *Didymocyrtis* includes twenty-nine species in the Index Fungorum.

During a continuous survey of fungal diversity exploration from different urban green soils in China, five strains from green soils of sewage treatment plant were isolated and purified. Based on the multi-gene phylogeny and morphological characteristics, these isolated strains were identified as two new taxa, *Biconidium sinense* gen. et sp. nov. and *Didymocyrtis shanxiensis* sp. nov., which are described and illustrated.

## Materials and methods

### Sample collection and fungal isolation

Soil samples, from 3–10 cm below the soil surface, were collected from green soil of sewage treatment plant in some cities in China. Samples were placed in sterile Ziploc plastic bags, and brought back to the laboratory. Then, the 2 g of each soil samples for fungal isolation, were placed into a sterile conical flask containing 20 mL sterile water in a 50 mL sterile conical flask, and thoroughly shaken using a Vortex vibration meter. Subsequently, the soil suspension was diluted to a concentration of  $10^{-3}$ . Then, 1 mL of the diluted sample was transferred to a sterile Petri dish with Sabouraud's dextrose agar (SDA; peptone 10 g/L, dextrose 40 g/L, agar 20 g/L, 3.3 mL of 1% Bengal red aqueous solution) medium containing 50 mg/L penicillin and 50 mg/L streptomycin. The plates were incubated at 25 °C for 1 week, then every single colony was selected from the plates and transferred to new potato dextrose agar (PDA, potato 200 g/L, dextrose 20 g/L, agar 20 g/L) plates.

### Morphological study

Strains of potentially new species were transferred to plates of malt extract agar (MEA), oatmeal agar (OA) and potato dextrose agar (PDA), and were incubated at 25 °C for examining their colony morphology and microscopic morphology. After 7 days, the colony colors according to national standard color card and diameters on the surface and reverse of inoculated Petri dishes were observed and recorded. Meanwhile, fungal hyphae and conidiogenous structures were examined, and images were captured by making direct wet mounts with 25% lactic acid on PDA, with an optical microscope (DM4 B, Leica). Strains of two novel species were deposited in the Institute of Fungus Resources, Guizhou University (GZUIFR = GZAC). Taxonomic descriptions and nomenclature of one new genus and two new species were uploaded in MycoBank (<https://www.mycobank.org/>).

### DNA extraction, PCR amplification and sequencing

Using the BioTeke Fungus Genomic DNA Extraction kit (DP2032, BioTeke), total genomic DNA was extracted following the manufacturer's instruction. The extracted DNA was stored at –20 °C. Primer combinations: ITS1/ITS4 (White et al. 1990), LR0R/LR5 (Wang et al. 2022) and T1/TUB4Rd (O'Donnell and Cigelnik 1997; Woudenberg et al. 2009) were used for amplification of the internal transcribed spacers (ITS), the 28S nrRNA locus (LSU) and beta-tubulin gene (*tub2*), respectively. The PCR amplification conditions: ITS, 94 °C: 5 min, (94 °C: 30 s, 51 °C: 50 s, 72 °C: 45 s) × 35 cycles, 72 °C: 10 min (White et al. 1990); LSU, 94 °C:



5 min, (94 °C: 30 s, 51 °C: 1 min, 72 °C: 2 min) × 35 cycles, 72 °C: 10 min (Zhang et al. 2023); *tub2*, 94 °C: 5 min, (94 °C: 30 s, 52 °C: 30 s, 72 °C: 30 s) × 35 cycles, 72 °C: 10 min (Woudenberg et al. 2009). In this study, the PCR products were sent to Quintarabio (Wuhan, China) for purification and sequencing. Strains sequences of two new species were submitted to GenBank (<https://www.ncbi.nlm.nih.gov/>) (Table 1 and Table 2).

## Phylogenetic analysis

The relevant strains sequences were downloaded from GenBank in this paper (Table1 and Table2). *Flammoclaadiella decora* (Wallr.) Lechat & J. Fourn. and *Flammoclaadiella aceris* Crous, L. Lombard & R.K. Schumach. were used as the outgroup in phylogenetic tree 1 (Fig. 1). *Parathyridaria philadelphi* Crous & R.K. Schumach. was used as the outgroup in phylogenetic tree 2 (Fig. 3). The multiple datasets of ITS, LSU and *tub2* were aligned and trimmed in MEGA v.6.06 (Tamura et al. 2013). Using the “Concatenate Sequence” function, the concatenation of loci was conducted in PhyloSuite v.1.16 (Zhang et al. 2020). Then, the phylogenetic construction of each loci dataset was processed by both Maximum Likelihood (ML) and the Bayesian Inference (BI) methods. In ModelFinder, the Akaike Information Criterion correction (AICc) was used for the best-fit substitution model (Kalyaanamoorthy et al. 2017). With 1000 bootstrap tests using the ultrafast algorithm (Minh et al. 2013), the ML analysis was conducted in IQ-TREE v.1.6.11 (Nguyen et al. 2015). The BI analysis was performed in MrBayes v.3.2 (Ronquist et al. 2012) and Markov chain Monte Carlo (MCMC) simulations were used for 2×10<sup>6</sup> generations. Using FigTree version 1.4.3, the phylogenetic trees were visualized and edited in Microsoft PowerPoint.

## Results

### Phylogenetic analysis

In this study, using ITS sequences, our five isolates were identified and assigned to potential genera and species based on a BLASTn in NCBI. Five strains belonging to Bionectriaceae or *Didymocyrtis* were screened and tested for further identification through morphological characterization and phylogenetic analyses. Using ML and BI analyses, the two phylogenetic trees were consistent and supported strongly in branches. The ML analysis for the combined dataset provided the best scoring tree. The concatenated sequences of Fig. 1 and Fig. 3 included 90 and 16 taxa, respectively. The dataset in Fig. 1 was composed of ITS (1–382 bp) and LSU (383–782 bp) sequence data. The dataset in Fig. 3 was composed of ITS (1–402 bp) and *tub2* (403–731 bp) sequence data.

The phylogeny shows that each genus clusters into a monophyletic clade, and three strains of the genus *Biconidium* clustered in a well-separated clade, with a high support value (ML/BI 100/1) (Fig. 1). Two strains of the genus *Didymocyrtis* also clustered together, with a high support value (ML/BI 98/1) (Fig. 3). Therefore, a new genus, *Biconidium* H.Y. Wang & Y.F. Han, is introduced, and *Biconidium sinense* H.Y. Wang & Y.F. Han and *Didymocyrtis shanxiensis* H.Y. Wang & Y.F. Han as new species are proposed according to the phylogenetic analysis.

**Table 1.** Strains of Bionectriaceae and corresponding GenBank numbers included in phylogenetic analyses.

Species	Strains	ITS	LSU	Reference
<i>Gliomastix murorum</i>	CBS 154.25T	OQ429613	HQ232063	Hou et al. (2023)
<i>Gliomastix murorum</i>	CBS 253.79	OQ429614	OQ055521	Hou et al. (2023)
<i>Gliomastix roseogrisea</i>	CBS 134.56T	OQ429639	OQ055545	Hou et al. (2023)
<i>Gliomastix tumulicola</i>	CBS 127532T	OQ429641	OQ055547	Hou et al. (2023)
<i>Paracylindrocarpon aloicola</i>	CBS 141300T	KX228277	KX228328	Hou et al. (2023)
<i>Paracylindrocarpon aloicola</i>	CBS 135907	OQ429762	OQ055661	Hou et al. (2023)
<i>Paracylindrocarpon aurantiacum</i>	CBS 135909T	OQ429763	OQ055662	Hou et al. (2023)
<i>Paracylindrocarpon multiseptatum</i>	CBS 337.77T	OQ429768	OQ055666	Hou et al. (2023)
<i>Fusariella curvata</i>	MFLUCC 15-0844T	KX025152	KX025154	Hou et al. (2023)
<i>Fusariella atrovirens</i>	CBS 311.73	OQ429594	OR052105	Hou et al. (2023)
<i>Fusariella arenula</i>	CBS 330.77	OQ429592	OQ055503	Hou et al. (2023)
<i>Fusariella arenula</i>	CBS 329.77	OQ429593	OQ055504	Hou et al. (2023)
<i>Selinia pulchra</i>	A.R. 2812	HM484859	GQ505992	Hou et al. (2023)
<i>Roumegueriella rufula</i>	CBS 346.85	OQ429827	OQ430088	Hou et al. (2023)
<i>Verrucostoma martinicense</i>	CBS 138731T	OQ429934	OR052121	Hou et al. (2023)
<i>Verrucostoma freycinetiae</i>	MAFF 240100T	HM484866	GQ506013	Hou et al. (2023)
<i>Synnemellisia aurantia</i>	COAD 2070 T	KX866395	KX866396	Hou et al. (2023)
<i>Musananaesporium tectonae</i>	CBS 725.87T	OQ429714	OQ055615	Hou et al. (2023)
<i>Gossypinidium sporodochiale</i>	CBS 101694T	OQ429643	OQ055549	Hou et al. (2023)
<i>Caespitomonium squamicola</i>	CBS 701.73	OQ429515	OQ055426	Hou et al. (2023)
<i>Caespitomonium squamicola</i>	CBS 392.73	OQ429514	OQ055425	Hou et al. (2023)
<i>Monohydropisphaera fusigera</i>	CBS 124147T	OQ429713	OQ055614	Hou et al. (2023)
<i>Hydropisphaera fungicola</i>	CBS 122304T	OQ429666	OR052107	Hou et al. (2023)
<i>Hydropisphaera suffulta</i>	CBS 122.87	OQ429672	OQ055577	Hou et al. (2023)
<i>Paragliomastix rosea</i>	CBS 277.80AT	OQ429775	OQ055673	Hou et al. (2023)
<i>Paragliomastix chiangraiensis</i>	MFLUCC 14-0397T	MN648324	MN648329	Hou et al. (2023)
<i>Septofusidium berolinense</i>	CBS 731.70	OQ429859	OQ430110	Hou et al. (2023)
<i>Pseudoacremonium sacchari</i>	CBS 137990T	KJ869144	KJ869201	Hou et al. (2023)
<i>Lasionectria olida</i>	CBS 799.69T	OQ429693	OQ055598	Hou et al. (2023)
<i>Lasionectria olida</i>	CBS 798.69	OQ429692	OQ055597	Hou et al. (2023)
<i>Lasionectria castaneicola</i>	CBS 122792T	OQ429680	OQ055585	Hou et al. (2023)
<i>Lasionectria atrorubra</i>	CBS 123502T	OQ429674	OQ055579	Hou et al. (2023)
<i>Verruciconidia persicina</i>	CBS 310.59T	OQ429921	OQ430172	Hou et al. (2023)
<i>Verruciconidia persicina</i>	CBS 113716	OQ429922	OQ430173	Hou et al. (2023)
<i>Verruciconidia erythrolyi</i>	CBS 728.87T	OQ429910	OQ430161	Hou et al. (2023)
<i>Verruciconidia infusata</i>	CBS 100888T	OQ429911	OQ430162	Hou et al. (2023)
<i>Verruciconidia quercina</i>	CBS 469.67T	OQ429925	OQ430176	Hou et al. (2023)
<i>Verruciconidia quercina</i>	CBS 355.77	OQ429927	OQ430178	Hou et al. (2023)
<i>Lasionectriopsis dentifera</i>	CBS 650.75	OQ429700	OQ055602	Hou et al. (2023)
<i>Lasionectriopsis dentifera</i>	CBS 574.76T	KY607540	KY607555	Hou et al. (2023)
<i>Ochronectria thailandica</i>	MFLUCC 15-0140T	KU564071	KU564069	Hou et al. (2023)
<i>Lasionectriopsis germanica</i>	CBS 143538T	OQ429701	MK276528	Hou et al. (2023)
<i>Ochronectria calami</i>	CBS 134535	OQ429755	OQ055654	Hou et al. (2023)
<i>Lasionectriella arenuloides</i>	CBS 576.76T	OQ429696	OQ055601	Hou et al. (2023)
<i>Lasionectriella marigotensis</i>	CBS 131606T	OQ429698	KR105613	Hou et al. (2023)
<i>Lasionectriella rubioi</i>	CBS 140157T	OQ429699	KU593581	Hou et al. (2023)
<i>Ramosiphorum polyporicola</i>	CBS 123779T	OQ429823	OQ430084	Hou et al. (2023)
<i>Ramosiphorum polyporicola</i>	CBS 109.87	OQ429822	OQ430083	Hou et al. (2023)
<i>Ramosiphorum thailandicum</i>	CBS 101914T	OQ429825	OQ430086	Hou et al. (2023)

Species	Strains	ITS	LSU	Reference
<i>Protocreopsis rutila</i>	CBS 396.66T	OQ429814	OQ430077	Hou et al. (2023)
<i>Protocreopsis rutila</i>	CBS 229.70	OQ429813	OQ430076	Hou et al. (2023)
<i>Protocreopsis finnmarkica</i>	CBS 147428T	OQ429803	OQ055699	Hou et al. (2023)
<i>Protocreopsis phormiicola</i>	CBS 567.76T	OQ429806	OQ430069	Hou et al. (2023)
<i>Protocreopsis freycinetiae</i>	CBS 573.76T	OQ429804	OR052113	Hou et al. (2023)
<i>Nectriopsis lindauiana</i>	CBS 897.70T	OQ429729	OQ055629	Hou et al. (2023)
<i>Nectriopsis fuliginicola</i>	CBS 400.82T	KU382175	OQ055628	Hou et al. (2023)
<i>Nectriopsis violacea</i>	CBS 914.70T	OQ429733	OQ055632	Hou et al. (2023)
<i>Nectriopsis violacea</i>	CBS 849.70	OR050510	MH871773	Hou et al. (2023)
<i>Nectriopsis sporangiicola</i>	CBS 166.74T	AF210661	AF210662	Hou et al. (2023)
<i>Clonostachys spinulosispora</i>	CBS 133762T	MH634702	KY006568	Hou et al. (2023)
<i>Clonostachys phyllophila</i>	CBS 921.97T	AF210664	OQ055445	Hou et al. (2023)
<i>Stephanonectria keithii</i>	CBS 943.72	OQ429872	OQ430121	Hou et al. (2023)
<i>Stephanonectria keithii</i>	CBS 100007	OQ429871	OQ430120	Hou et al. (2023)
<i>Mycocitrus odoratus</i>	CBS 100104T	OQ429717	OQ055618	Hou et al. (2023)
<i>Mycocitrus odoratus</i>	CBS 120610	OQ429715	OQ055616	Hou et al. (2023)
<i>Mycocitrus zonatus</i>	CBS 400.70	OQ429719	OQ055620	Hou et al. (2023)
<i>Mycocitrus phyllostachydis</i>	CBS 330.69	OQ429718	OQ055619	Hou et al. (2023)
<i>Emericellopsis fuci</i>	CBS 116467	OQ429564	OQ055477	Hou et al. (2023)
<i>Emericellopsis fuci</i>	CBS 485.92	OQ429565	OQ055478	Hou et al. (2023)
<i>Emericellopsis maritima</i>	CBS 491.71T	OQ429566	OQ055480	Hou et al. (2023)
<i>Emericellopsis pallida</i>	CBS 490.71T	OQ429574	OQ055487	Hou et al. (2023)
<i>Emericellopsis brunneiguttula</i>	CBS 111360T	OQ429545	OQ055457	Hou et al. (2023)
<i>Stanjemonium grisellum</i>	CBS 655.79T	OQ429868	OQ430117	Hou et al. (2023)
<i>Stanjemonium ochroroseum</i>	CBS 656.79T	OQ429869	OQ430118	Hou et al. (2023)
<i>Proliferophialis apiculata</i>	CBS 303.64T	OQ429796	OQ055692	Hou et al. (2023)
<i>Proliferophialis apiculata</i>	CBS 365.64	OQ429797	OQ055693	Hou et al. (2023)
<i>Acremonium subulatum</i>	CBS 588.73AT	OQ429491	OQ055402	Hou et al. (2023)
<i>Acremonium subulatum</i>	CBS 115996	OQ429490	OQ055401	Hou et al. (2023)
<i>Acremonium aerium</i>	CBS 189.70T	OQ429441	OQ055352	Hou et al. (2023)
<i>Acremonium longiphialidicum</i>	CBS 451.70T	OQ429475	OQ055386	Hou et al. (2023)
<i>Acremonium purpurascens</i>	CBS 149.62T	OQ429485	OQ055396	Hou et al. (2023)
<i>Acremonium ellipsoideum</i>	CBS 147433T	OQ429468	OQ055379	Hou et al. (2023)
<i>Acremonium ellipsoideum</i>	CBS 147434	OQ429467	OQ055378	Hou et al. (2023)
<i>Acremonium brunneisporum</i>	CBS 413.76T	OQ429444	OQ055355	Hou et al. (2023)
<i>Acremonium brunneisporum</i>	CBS 142823	OQ429445	OQ055356	Hou et al. (2023)
<i>Acremonium multiramum</i>	CBS 147436T	OQ429476	OQ055387	Hou et al. (2023)
<i>Waltergamsia pilosa</i>	CBS 124.70T	OQ429949	OQ430199	Hou et al. (2023)
<i>Waltergamsia pilosa</i>	CBS 511.82	OQ429948	OQ430198	Hou et al. (2023)
<i>Waltergamsia alkalina</i>	CBS 741.94T	OQ429935	OQ430185	Hou et al. (2023)
<i>Waltergamsia dimorphospora</i>	CBS 139050T	LN810515	LN810506	Hou et al. (2023)
<i>Geosmithia microcorthyli</i>	CCF 3861T	NR_137566	NG_067560	Hou et al. (2023)
<i>Geosmithia pallidum</i>	CBS 260.33T	OQ429599	OQ055509	Hou et al. (2023)
<i>Bulbithecium spinosum</i>	CBS 136.33T	OQ429512	OQ055423	Hou et al. (2023)
<i>Bulbithecium spinosum</i>	CBS 915.85	OQ429510	OQ055421	Hou et al. (2023)
<i>Bulbithecium arxii</i>	CBS 737.84T	OQ429505	OQ055416	Hou et al. (2023)
<i>Bulbithecium ellipsoideum</i>	CBS 993.69T	OQ429507	OQ055418	Hou et al. (2023)
<i>Ovicillium oosporum</i>	CBS 110151T	OQ429758	OQ055657	Hou et al. (2023)
<i>Ovicillium asperulatum</i>	CBS 130362T	OQ429756	OQ055655	Hou et al. (2023)
<i>Ovicillium asperulatum</i>	CBS 426.95	KU382192	KU382233	Hou et al. (2023)

Species	Strains	ITS	LSU	Reference
<i>Proxiovicillium blochii</i>	CBS 427.93T	OQ429816	OQ430079	Hou et al. (2023)
<i>Proxiovicillium blochii</i>	CBS 324.33	OQ429815	OQ430078	Hou et al. (2023)
<i>Proxiovicillium lepidopterorum</i>	CBS 101239T	OQ429817	OQ430080	Hou et al. (2023)
<i>Hapsidospora flava</i>	CBS 596.70T	OQ429649	OQ055555	Hou et al. (2023)
<i>Hapsidospora flava</i>	CBS 316.72	OQ429648	OQ055554	Hou et al. (2023)
<i>Hapsidospora variabilis</i>	CBS 100549T	OQ429663	OQ055569	Hou et al. (2023)
<i>Hapsidospora stercoraria</i>	CBS 516.70T	OQ429662	OQ055568	Hou et al. (2023)
<i>Alloacremonium humicola</i>	CBS 613.82T	OQ429496	OQ055407	Hou et al. (2023)
<i>Alloacremonium ferrugineum</i>	CBS 102877T	OQ429495	OQ055406	Hou et al. (2023)
<i>Stilbocrea walteri</i>	CBS 144627T	OR050519	OQ430124	Hou et al. (2023)
<i>Stilbocrea macrostoma</i>	CBS 114375	OQ429873	OQ430122	Hou et al. (2023)
<i>Flammocladia decora</i>	CBS 142776	MF611693	MF614949	Hou et al. (2023)
<i>Flammocladia aceris</i>	CBS 138906T	OQ429591	KR611901	Hou et al. (2023)
<b><i>Biconidium sinense</i></b>	<b>GZUIFR 24.013T</b>	<b>PQ595985</b>	<b>PQ595988</b>	<b>This study</b>
<b><i>Biconidium sinense</i></b>	<b>GZUIFR 24.014</b>	<b>PQ595986</b>	<b>PQ595989</b>	<b>This study</b>
<b><i>Biconidium sinense</i></b>	<b>GZUIFR 24.015</b>	<b>PQ595987</b>	<b>PQ595990</b>	<b>This study</b>

Note: T = Ex-type; New isolates in this study are in bold; The line “–” represents the absence of GenBank record. ITS: the internal transcribed spacer region and intervening 5.8S nrRNA; LSU: 28S large subunit.

**Table 2.** Strains of *Didymocyrtis* and corresponding GenBank numbers included in phylogenetic analyses.

Species	Strains	ITS	tub2	Reference
<i>Didymocyrtis banksiae</i>	CSN1049	MT813909	–	Monteiro et al. (2022)
<i>Didymocyrtis banksiae</i>	CSN1065	MT813919	–	Monteiro et al. (2022)
<i>Didymocyrtis brachylaenae</i>	CPC 32651	MH327821	MH327896	Monteiro et al. (2022)
<i>Didymocyrtis cladoniicola</i>	CBS 131731	KP170644	KP170694	Monteiro et al. (2022)
<i>Didymocyrtis cladoniicola</i>	CBS 131732	KP170645	KP170695	Monteiro et al. (2022)
<i>Didymocyrtis consimilis</i>	CBS 129140	MH865190	–	Monteiro et al. (2022)
<i>Didymocyrtis consimilis</i>	CBS 129338	MH865230	–	Monteiro et al. (2022)
<i>Didymocyrtis epiphyscia</i>	Freebury 1411	KT383824.1	–	Monteiro et al. (2022)
<i>Didymocyrtis foliaceiphila</i>	CBS 131729	KP170649	KP170699	Monteiro et al. (2022)
<i>Didymocyrtis foliaceiphila</i>	CBS 131730	KP170650	KP170700	Monteiro et al. (2022)
<i>Didymocyrtis melanelixiae</i>	Harris 57476 (NY)	KT383831	–	Monteiro et al. (2022)
<i>Didymocyrtis melanelixiae</i>	Harris 57475 (NY)	KT383828	–	Monteiro et al. (2022)
<i>Didymocyrtis pini</i>	CAA 1002 T	MW732246	MW759031	Monteiro et al. (2022)
<i>Didymocyrtis pini</i>	CAA 1003	MW732247	MW759030	Monteiro et al. (2022)
<i>Didymocyrtis pseudeverniae</i>	Diederich 17327b	KT383833	–	Monteiro et al. (2022)
<i>Didymocyrtis pseudeverniae</i>	Diederich 17327a	KT383832	–	Monteiro et al. (2022)
<i>Didymocyrtis ramalinae</i>	Paul 10i13	KT383839	–	Monteiro et al. (2022)
<i>Didymocyrtis ramalinae</i>	Paul 27i13	KT383836	–	Monteiro et al. (2022)
<i>Didymocyrtis septata</i>	KNU-JJ-1827	LC552949	–	Monteiro et al. (2022)
<i>Didymocyrtis slaptonensis</i>	MoraA (BR)	KT383841	–	Monteiro et al. (2022)
<i>Didymocyrtis trassii</i>	AB298	MG519614	–	Monteiro et al. (2022)
<i>Didymocyrtis trassii</i>	AB297	MG519613	–	Monteiro et al. (2022)
<i>Didymocyrtis xanthomendozae</i>	CBS 129666	KP170651	KP170701	Monteiro et al. (2022)
<i>Parathyridaria philadelphi</i>	CBS 143432	MH107905	–	Monteiro et al. (2022)
<b><i>Didymocyrtis shanxiensis</i></b>	<b>GZUIFR 24.004T</b>	<b>PQ065635</b>	<b>PQ119783</b>	<b>This study</b>
<b><i>Didymocyrtis shanxiensis</i></b>	<b>GZUIFR 24.005</b>	<b>PQ065636</b>	<b>PQ119784</b>	<b>This study</b>

Note: T = Ex-type; New isolates in this study are in bold; The line “–” represents the absence of GenBank record. ITS: the internal transcribed spacer region and intervening 5.8S nrRNA; tub2:  $\beta$ -tubulin.



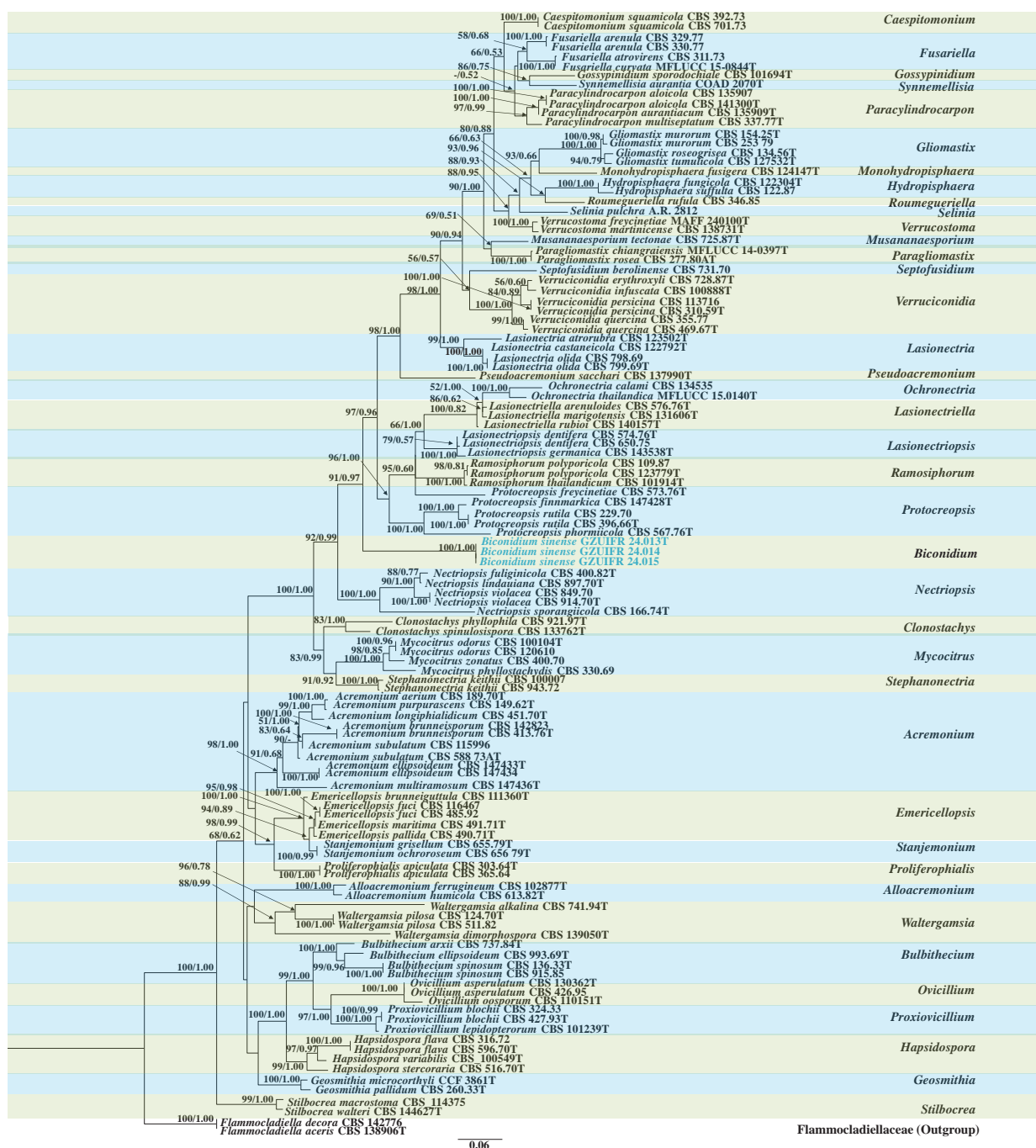


**Figure 1.** Phylogenetic tree of Bionectriaceae constructed from the dataset of ITS and LSU. Notes: Statistical support values (ML/BI) were shown at nodes. ML bootstrap values  $\geq 50\%$  and posterior probabilities  $\geq 0.50$  are shown above the internal branches. '–' indicates the absence of statistical support ( $< 50\%$  for bootstrap proportions from ML analysis;  $< 0.50$  for posterior probabilities from Bayesian analysis). Three new strains are shown in blue font.

**Sordariomycetes O.E. Erikss. & Winka**

**Hypocreales Lindau**

**Bionectriaceae Samuels & Rossman**

***Biconidium* H.Y. Wang & Y.F. Han, gen. nov.**

MycoBank No: MB857281

**Etymology.** Referring to the bicellular conidia.

**Description.** *Mycelium* hyaline, septate, smooth, thin-walled. *Conidiophores* hyaline, septate, smooth-walled, solitary, straight, (sub-)erect, arising directly from hyphae, unbranched or branched, bearing 1–5 levels with 1–6 phialides per node. *Conidiogenous cells* enteroblastic, monophialidic, lateral or terminal, awl-shaped, hyaline, smooth, with globose to cylindric thickening at conidiogenous loci. *Conidia* bicellular, podiform, unsymmetrically at both ends, hyaline, thick-walled, smooth, arranged in slimy heads. Chlamydospores and sexual morph absent.

**Type species.** *Biconidium sinense* H.Y. Wang & Y.F. Han

**Notes.** Three isolates from green soil of sewage treatment plant clearly form an independent clade on the ITS and LSU tree (Fig. 1), and are phylogenetically segregated from other genera, representing the new species with conidiogenous cells with globose to cylindric thickening at conidiogenous loci and podiform conidia arranged in slimy heads. Therefore, we introduce *Biconidium* as a new genus to accommodate this species.

***Biconidium sinense* H.Y. Wang & Y.F. Han, sp. nov.**

MycoBank No: MB857282

Fig. 2

**Etymology.** Referring to China where the species was isolated.

**Type.** CHINA • Zhejiang Province, Hangzhou City, sewage treatment plant (30°10'53"N, 120°10'2"E), soil, August 2021, Yulian Ren, ex-type culture GZUIFR 24.013, dried holotype GZAC 24.013. ITS sequences, GenBank PQ595985; LSU sequences, GenBank PQ595988.

**Description.** Culture characteristics (7 days of incubation at 25 °C): Colony on PDA, 20–30 mm diam., fleshy, plicated, beige (RAL1001) at the center, villiform, traffic white (RAL 9016) at the edge, reverse, light ivory (RAL1015) at the center, cream (RAL9001) at the edge, nearly round, margin partial; Colony on MEA, 25–30 mm diam., flocculence, traffic white (RAL 9016), reverse, broom yellow (RAL1032), margin entire, round. Colony on OA, 30–35 mm diam., thin, short villous, signal white (RAL9003), reverse, cream (RAL9001), margin entire, round.

On PDA, *Mycelium* hyaline, septate, smooth, thin-walled 1.2–2.7 µm wide. *Conidiophores* hyaline, septate, smooth, solitary, straight, (sub-)erect, arising directly from hyphae, branched or unbranched, bearing 1–5 levels with 1–6 phialides, 1–3 septate at base or middle, 20–52 µm long, 1.5–2.7 µm wide at base. *Phialides* lateral or terminal, from the conidiophores or directly from the mycelia, awl-shaped, hyaline, smooth-walled, 9.5–35 µm long, 1–2.3 µm wide at base, with globose to cylindric thickening at conidiogenous loci. polyphialides not observed. *Conidia* podiform, 1-septate, 2.5–6.0 × 1.0–3.0 µm (mean ± SD = 3.5 ± 1.0 × 2.0 ± 0.5 µm, n = 30), center-empty, unsymmetrically at both ends, apex angular, base subobtuse, hyaline, thick-, smooth-walled, arranged in slimy heads. Chlamydospores and sexual morph not observed.

**Additional specimens examined.** CHINA • Zhejiang Province, Hangzhou City, sewage treatment plant (30°10'53"N, 120°10'2"E), soil, August 2021, living cultures GZUIFR 24.014 (ITS sequences, GenBank PQ595986; LSU sequences, GenBank PQ595989), GZUIFR 24.015 (ITS sequences, GenBank PQ595987; LSU sequences, GenBank PQ595990).

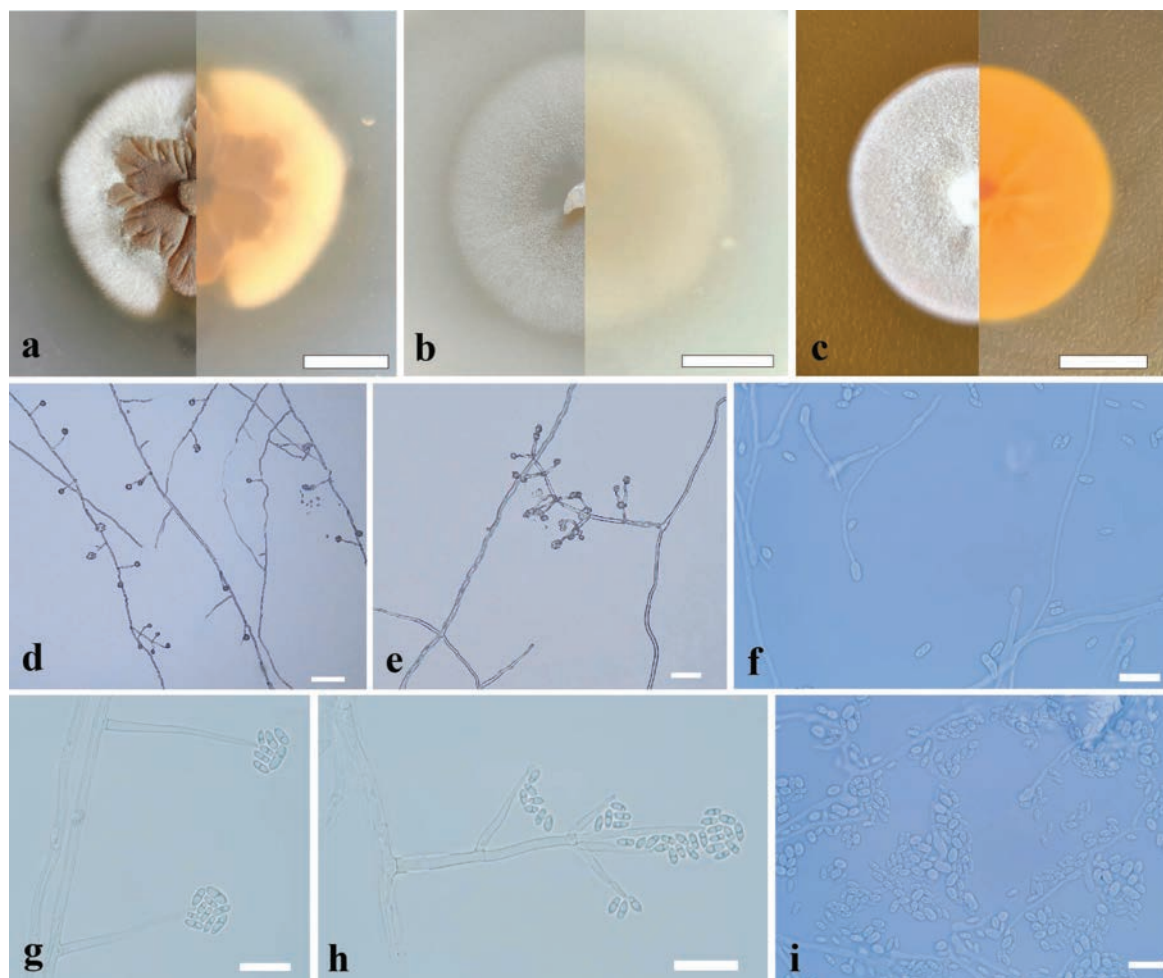


**Figure 2.** Morphological characteristics of *Biconidium sinense* sp. nov. **a–c** front and reverse of colony on PDA, OA and MEA after 7 days at 25 °C **d, e** conidiophores and conidial heads **f–h** conidiophores and conidia **i** conidia. Scale bars: 10 mm (**a–c**); 50 µm (**d**); 20 µm (**e**); 10 µm (**f–i**).

**Notes.** Phylogenetically, our three strains (GZUIFR 24.013, GZUIFR 24.014 and GZUIFR 24.015) can apparently separate with other species in Bionectriaceae, and clustered in a single clade with a high support value (BI pp = posterior probability 1, ML BS 100) (Fig. 1). *Biconidium sinense* is distinguished from other species of Bionectriaceae by conidiogenous cells with globose to cylindric thickening at conidiogenous loci, and podiform conidia arranged in slimy heads in the morphological characteristics.

**Dothideomycetes** O.E. Erikss. & Winka

**Pleosporales** Luttr. ex M.E. Barr

**Phaeosphaeriaceae** M.E. Barr

***Didymocyrtis* Vain.**

***Didymocyrtis shanxiensis* H.Y. Wang & Y.F. Han, sp. nov.**

MycoBank No: MB857280

Fig. 4

**Etymology.** shanxiensis, referring to Shanxi province where the type locality was isolated.

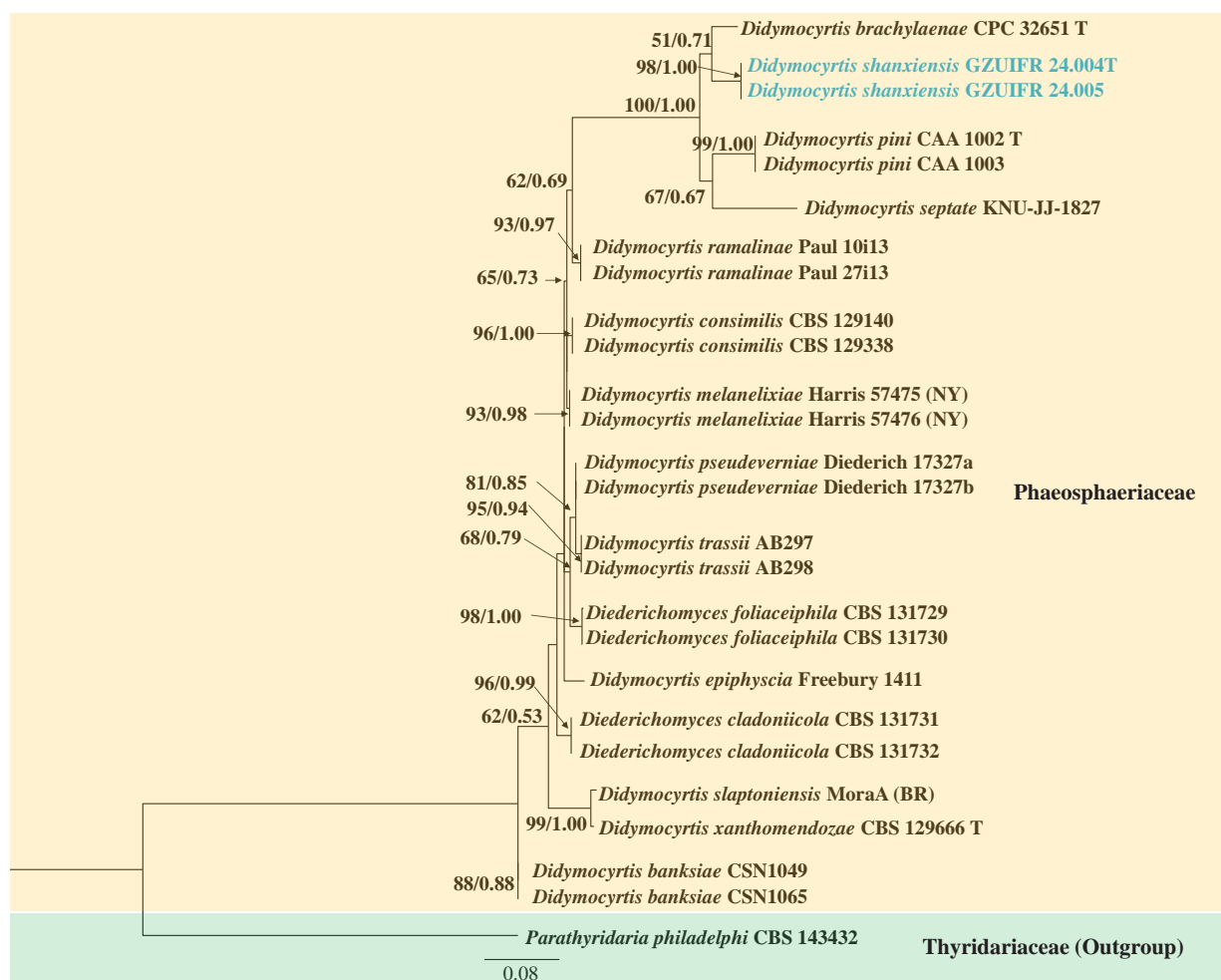


**Figure 3.** Phylogenetic tree of the genus *Didymocyrtis* constructed from the dataset of ITS and *tub2*. Notes: Statistical support values (ML/BI) were shown at nodes. ML bootstrap values  $\geq 50\%$  and posterior probabilities  $\geq 0.50$  are shown above the internal branches. Two new strains are shown in blue font.

**Type.** CHINA • Shanxi Province, Datong City, sewage treatment plant (40°2'42"N, 113°20'48"E), soil, August 2021, Yulian Ren, ex-type culture GZUIFR 24.004, dried holotype GZAC 24.004. ITS sequences, GenBank PQ065635; *tub2* sequences, GenBank PQ119783.

**Description.** Culture characteristics (7 days of incubation at 25 °C): Colony on PDA, 30–35 mm diam., thin, villiform, cream (RAL9001), reverse cream (RAL9001), regular in the margin; Colony on MEA, 20–25 mm diam., thick, villiform, light Ivory (RAL1015), reverse dahlia yellow (RAL1033), regular in the margin; Colony on OA, 30–35 mm diam., texture velvety, olive yellow (RAL1020), reverse stone gray (RAL7030), regular in the margin. Black spots produced after incubating 15 days on PDA.

On PDA medium after 30 days of incubation at 25 °C, **Hyphae** septate, hyaline, smooth, thick-walled, 1.0–2.5  $\mu\text{m}$  wide. **Conidiomata** submersed, brown to black, globose, 150–250  $\mu\text{m}$  diam. **Conidiophores** reduced to conidiogenous cells. **Conidiogenous cells** globose to subglobose, also ampulliform, aseptate, hyaline, smooth, thick-walled, 4.5–10.0  $\times$  2.0–6.0  $\mu\text{m}$  (mean  $\pm$  SD = 7.0  $\pm$  1.9  $\times$  3.5  $\pm$  1.0  $\mu\text{m}$ , n = 15). **Conidia** abundant, cymbiform mostly, brown, smooth, apex subobtuse, base truncate, 1-septate, 5.0–11.0  $\times$  1.5–3.0  $\mu\text{m}$  (mean  $\pm$  SD = 7.5  $\pm$  1.6  $\times$  2.0  $\pm$  0.4  $\mu\text{m}$ , n = 30).



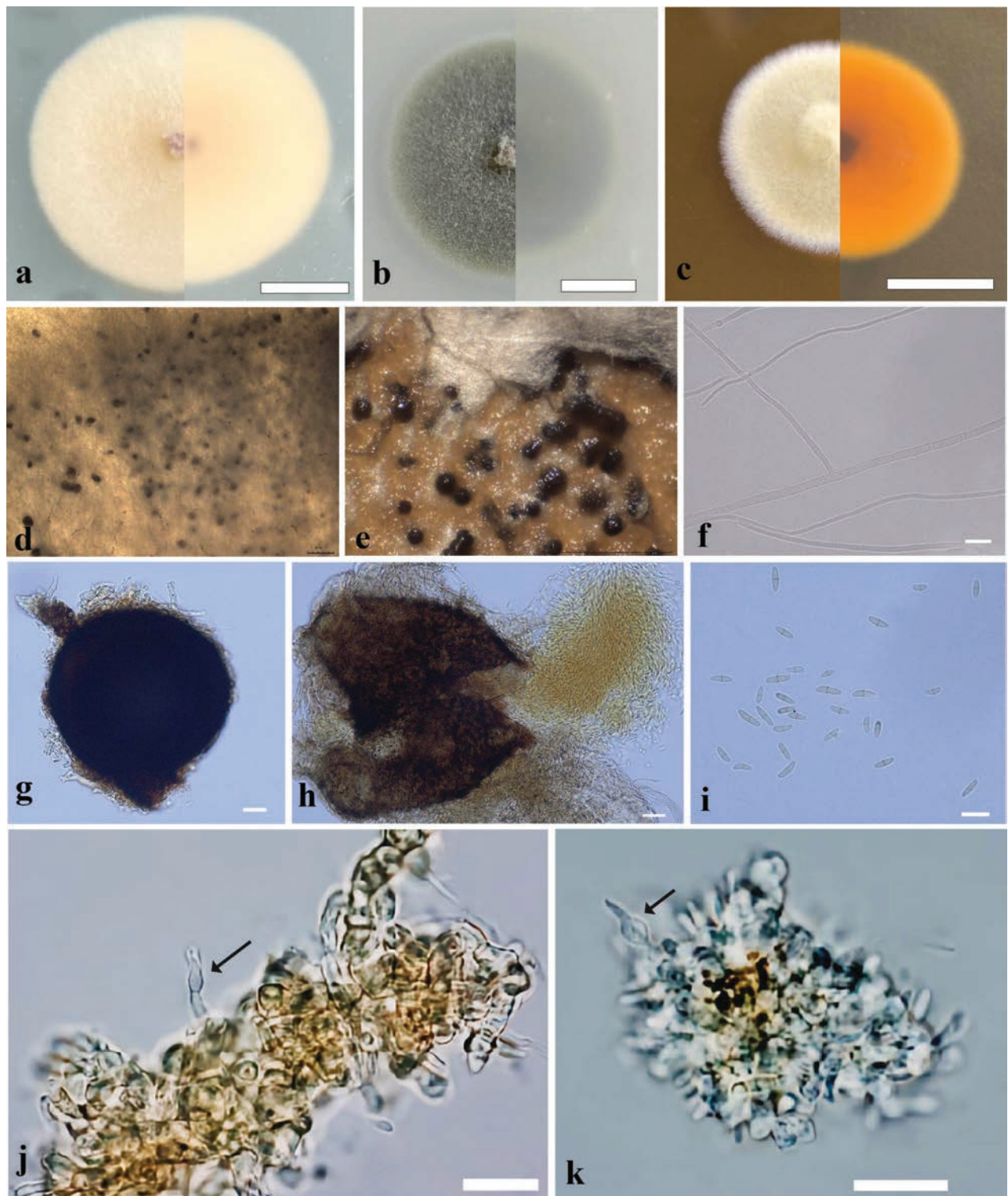


**Figure 4.** Morphological characteristics of *Didymocyrtis shanxiensis* sp. nov. **a–c** front and reverse of colony on PDA, OA and MEA after 7 days at 25 °C **d, e** conidiomata on culture **f** hyphae **g, h** conidiomata and ruptured conidiomata with conidia mass **i** conidia **j, k** conidiogenous cells. Scale bars: 10 mm (**a–c**); 20 µm (**g, h**); 10 µm (**i**); 20 µm (**j, k**).

**Additional specimens examined.** CHINA • Shanxi Province, Datong City, sewage treatment plant (40°2'42"N, 113°20'48"E), soil, August 2021, living cultures GZUIFR 24.005. ITS sequences, GenBank PQ065636; *tub2* sequences, GenBank PQ119784.

**Notes.** Twenty-nine species of the genus *Didymocyrtis* are recorded in the Index Fungorum. However, the DNA sequence data of fifteen species have no

records in NCBI database. Phylogenetically, our two strains (GZUIFR 24.004 and GZUIFR 24.005) clustered in a single clade with a high support value (ML/BI 98/1) (Fig. 3). In the phylogenetic tree, although our new species *D. shanxiensis* and *Didymocyrtis brachylaenae* Crous are closely related species, they were obviously different in morphological characteristics. *Didymocyrtis shanxiensis*, having conidiophores reduced to conidiogenous cells, globose to subglobose and ampulliform conidiogenous cells, and cymbiform conidia, can be distinguished from *D. brachylaenae* with subcylindrical and branched conidiophores, lining the inner cavity and ampulliform to doliiform conidiogenous cells, and fusoidellipsoid to subcylindrical conidia (Crous et al. 2018).

## Discussion

Hou et al. (2023) reevaluated acremonium-like fungi in Hypocreales, and found most species of *Acremonium* s. lat. grouped in genera of Bionectriaceae. Therefore, the phylogenetic tree of Bionectriaceae is provided based on multi-locus (ITS, LSU, *rpb2*, *tef-1a*) DNA sequencing analyses to accommodate 183 species and 39 genera including 10 new genera. In this study, employing ITS and LSU sequences can well distinguish the species of Bionectriaceae. From the phylogenetic tree (Fig. 1), three strains of our new species *Biconidium sinense* cluster in a well-separated clade with a high support value (ML/BI 100/1). Meanwhile, *B. sinense* having conidiogenous cells with globose to cylindrical thickening at conidiogenous loci, and podiform conidia arranged in slimy heads differs from all other species of Bionectriaceae. Therefore, *Biconidium* is introduced to accommodate a new species *B. sinense* combined with phylogenetic and morphological analyses. Bionectriaceae are including both sexual morphs and asexual taxa (Hou et al. 2023). Species of the Bionectriaceae are mostly found in terrestrial or freshwater environments, with fewer commonly found in marine habitats, and they are common coprophilous, corticolous, fungicolous, lichenicolous or herbicolous (Zhao et al. 2023). In this study, our three strains of *B. sinense* were isolated from green soils of sewage treatment plant.

In this study, although *D. shanxiensis*, *D. brachylaenae*, *D. pini* and *D. septata* clustered as the sister subclades, they were obviously different in morphological characteristics. Morphologically, the main characteristics of *D. shanxiensis* are having globose conidiomata, conidiophores reduced to conidiogenous cells, globose to subglobose and ampulliform conidiogenous cells, and the smaller size of cymbiform conidia (mean size =  $7.5 \times 2.0 \mu\text{m}$ ). While, *D. brachylaenae* can be distinguished from *D. shanxiensis* by having subcylindrical and branched conidiophores, and fusoidellipsoid to subcylindrical conidia (Crous et al. 2018); *Didymocyrtis pini* can be distinguished from *D. shanxiensis* by having fusiform conidia (mean size =  $8.5 \times 2.4 \mu\text{m}$ ) (Monteiro et al. 2022); *Didymocyrtis septata* differed from *D. shanxiensis* by having irregular conidiomata, and fusiform, clavate to subcylindrical conidia (mean size =  $8.2 \times 2.3 \mu\text{m}$ ) (Das et al. 2021). At the same time, *D. shanxiensis* has a clear morphological difference from fifteen species without DNA sequence data (Joshi et al. 2024), so it is proposed as a new species in the genus *Didymocyrtis*. Up to now, the most species of *Didymocyrtis* are lichenicolous fungi living parasitic life-style (Ertz et al. 2015; Sujja et al. 2021). Some *Didymocyrtis* spp. are pathogenic fungi and saprophytic fungi. For example, *D. brachylaenae* and *D. pini* as pathogeny

live on plant leaves (Crous et al. 2018; Monteiro et al. 2022), and *D. septata* is saprophytic in containing plant soil (Das et al. 2021). Our two strains of new species were also isolated from green land soil in this study and possible to be saprophytic. Presently, this genus includes twenty-nine species in the Index Fungorum (<http://www.indexfungorum.org/Names/Names.asp>, retrieval on 10 January 2025). Here, together with *D. shanxiensis*, the genus *Didymocyrtis* has a total of thirty species.

Though two new species were reported in this study, we believed that more new taxa will be found and reported from the various soil habitats, which are deserving to be explored in the future.

## Acknowledgements

We appreciate Tianpeng Wei for the photomicrograph.

## Additional information

### Conflict of interest

The authors have declared that no competing interests exist.

### Ethical statement

No ethical statement was reported.

## Funding

The work was supported by the National Natural Science Foundation of China (no. 32160007, 32260003) and “Hundred” Talent Projects of Guizhou Province (Qian Ke He [2020] 6005).

## Author contributions

Hai-Yan Wang: Writing – review & editing, Formal analysis, Project administration. Chunbo Dong, Yan-Wei Zhang and Wan-Hao Chen: Data acquisition, Data analysis, Investigation, Data curation. Yan-Wei Zhang and Yan-Feng Han: Supervision, Project administration, Funding acquisition.

## Author ORCIDs

Hai-Yan Wang  <https://orcid.org/0000-0001-9190-0490>

Chunbo Dong  <https://orcid.org/0000-0001-7074-5700>

Yan-Wei Zhang  <https://orcid.org/0000-0003-1251-5821>

Wan-Hao Chen  <https://orcid.org/0000-0001-7240-6841>

Yan-Feng Han  <https://orcid.org/0000-0002-8646-3975>

## Data availability

All of the data that support the findings of this study are available in the main text.

## References

Akilandeswari P, Pradeep B (2016) Exploration of industrially important pigments from soil fungi. *Applied Microbiology and Biotechnology* 100(4): 1631–1643. <https://doi.org/10.1007/s00253-015-7231-8>

- Barr ME (1979) A classification of Loculoascomycetes. *Mycologia* 71: 935–957. <https://doi.org/10.1080/00275514.1979.12021099>
- Buczowski G, Richmond DS (2012) The effect of urbanization on ant abundance and diversity: A temporal examination of factors affecting biodiversity. *PLOS ONE* 7(8): e41729. <https://doi.org/10.1371/journal.pone.0041729>
- Crous PW, Wingfield MJ, Burgess TI, Hardy GSJ, Gené J, Guarro J, Baseia IG, García D, Gusmão LFP, Souza-Motta CM, Thangavel R, Adamčík S, Barili A, Barnes CW, Bezerra JDP, Bordallo JJ, Cano-Lira JF, de Oliveira RJV, Ercole E, Hubka V, Iturrieta-González I, Kubátová A, Martín MP, Moreau PA, Morte A, Ordoñez ME, Rodríguez A, Stchigel AM, Vizzini A, Abdollahzadeh J, Abreu VP, Adamčíková K, Albuquerque GMR, Alexandrova AV, Álvarez Duarte E, Armstrong-Cho C, Banniza S, Barbosa RN, Bellanger JM, Bezerra JL, Cabral TS, Caboň M, Caicedo E, Cantillo T, Carnegie AJ, Carmo LT, Castañeda-Ruiz RF, Clement CR, Čmoková A, Conceição LB, Cruz RSHF, Damm U, da Silva BDB, da Silva GA, da Silva RMF, de A Santiago ALCM, de Oliveira LF, de Souza CAF, Dénier F, Dima B, Dong G, Edwards J, Félix CR, Fournier J, Gibertoni TB, Hosaka K, Iturriaga T, Jadan M, Jany JL, Jurjević Ž, Kolařík M, Kušan I, Landell MF, Leite Cordeiro TR, Lima DX, Loizides M, Luo S, Machado AR, Madrid H, Magalhães OMC, Marinho P, Matočec N, Mešić A, Miller AN, Morozova OV, Neves RP, Nonaka K, Nováková A, Oberlies NH, Oliveira-Filho JRC, Oliveira TGL, Papp V, Pereira OL, Perrone G, Peterson SW, Pham THG, Raja HA, Raudabaugh DB, Řehulka J, Rodríguez-Andrade E, Saba M, Schauflerová A, Shivas RG, Simonini G, Siqueira JPZ, Sousa JO, Stajsic V, Svetasheva T, Tan YP, Tkalčec Z, Ullah S, Valente P, Valenzuela-Lopez N, Abrinbana M, Viana Marques DA, Wong PTW, Xavier de Lima V, Groenewald JZ (2018) Fungal planet description sheets: 716–784. *Persoonia. Molecular Phylogeny and Evolution of Fungi* 40: 240–393. <https://doi.org/10.3767/persoonia.2018.40.10>
- Das K, Lee SY, Jung HY (2021) Morphology and phylogeny of two novel species within the Class Dothideomycetes collected from Soil in Korea. *Mycobiology* 49: 15–23. <https://doi.org/10.1080/12298093.2020.1838114>
- Desa UN (2019) World population prospects 2019: Highlights. New York (US). United Nations Department for Economic and Social Affairs 11(1): 125.
- Ertz D, Diederich P, Lawrey JD, Berger F, Freebury CE, Coppins B, Gardiennet A, Hafellner J (2015) Phylogenetic insights resolve Dacampiaceae (Pleosporales) as polyphyletic: *Didymocyrtis* (Pleosporales, Phaeosphaeriaceae) with *Phoma*-like anamorphs resurrected and segregated from *Polycoccum* (Trypetheliales, Polycoccaceae fam. nov.). *Fungal Diversity* 74: 53–89. <https://doi.org/10.1007/s13225-015-0345-6>
- Grimm NB, Faeth SH, Golubiewski NE, Redman CL, Wu J, Bai X, Briggs JM (2008) Global change and the ecology of cities. *Science* 319: 756–760. <https://doi.org/10.1126/science.1150195>
- Guo H (2024) Effects of different stubble and nitrogen application rates on yield traits and soil microorganisms of winter wheat. Master Thesis, Henan Agricultural University, Zhengzhou, Chain.
- Guo CJ, Zhang LR, Shen RQ, Xu BL (2017) Diversity of rhizosphere soil fungi in sand-fixation plants in Tengger Desert of Ningxia Autonomous Region. *Junwu Xuebao* 36(5): 552–562. <https://doi.org/10.13346/j.mycosystema.160083>
- Hou Y, Zhou HP, Zhang C (2014) Effects of urbanization on community structure of soil microorganism. *Shengtai Huanjing Xuebao* 23(7): 1108–1112. <https://doi.org/10.16258/j.cnki.1674-5906.2014.07.002>
- Hou LW, Giraldo A, Groenewald JZ, Rämä T, Summerbell RC, Zang P, Cai L, Crous PW (2023) Redisposition of *acremonium*-like fungi in Hypocreales. *Studies in Mycology* 105: 23–203. <https://doi.org/10.3114/sim.2023.105.02>



- Joshi Y, Bisht S, Bansal P (2024) *Didymocyrtis pertusariae*: A new species from Central Himalaya, India and a worldwide key to all recognized *Didymocyrtis* (Phaeosphaeriaceae; Pleosporales) species. *Journal of Asia-Pacific Biodiversity* 17(3): 550–561. <https://doi.org/10.1016/j.japb.2024.04.005>
- Kalyaanamoorthy S, Minh BQ, Wong TKF, von Haeseler A, Jermiin LS (2017) ModelFinder: Fast model selection for accurate phylogenetic estimates. *Nature Methods* 14(6): 587–589. <https://doi.org/10.1038/nmeth.4285>
- Lawrey JD, Diederich P, Nelsen MP, Freebury C, Van den Broeck D, Sikaroodi M, Ertz D (2012) Phylogenetic placement of lichenicolous *Phoma* species in the Phaeosphaeriaceae (Pleosporales, Dothideomycetes). *Fungal Diversity* 55: 195–213. <https://doi.org/10.1007/s13225-012-0166-9>
- Li X, Zhang ZY, Chen WH, Liang JD, Huang JZ, Han YF, Liang ZQ (2022a) A new species of *Arthrographis* (Eremomycetaceae, Dothideomycetes), from the soil in Guizhou, China. *Phytotaxa* 538(3): 175–181. <https://doi.org/10.11646/phytotaxa.538.3.1>
- Li X, Zhang ZY, Ren YL, Chen WH, Liang JD, Pan JM, Huang JZ, Liang ZQ, Han YF (2022b) Morphological characteristics and phylogenetic evidence reveal two new species of *Acremonium* (Hypocreales, Sordariomycetes). *MycKeys* 91: 85–96. <https://doi.org/10.3897/mycokeys.91.86257>
- Löbl I, Klausnitzer B, Hartmann M, Krell FT (2023) The silent extinction of species and taxonomists—An appeal to science policymakers and legislators. *Diversity* 15(10): 1053. <https://doi.org/10.3390/d15101053>
- Lu M (2018) Effects of wetlands degradation on structure and biodiversity of soil microbial community in Napahai plateau wetlands. PhD Thesis, Beijing Forestry University, Beijing, China.
- Ma CX (2023) The Influence of Moso Bamboo Forest and Chinese Fir Forest on Soil Microorganisms of Typical Subtropical. *Shandong Nongye Daxue Xuebao* 54(3): 391–396. <https://doi.org/10.3969/j.issn.1000-2324.2023.03.009> [Natural Science Edition]
- Ma YS, Lu ZY, Yang HL, Zhang ZB, Yan RM, Jiang YM, Zhu D (2021) Comparison of soil microbial community structure in different seasons in Longgong Cave, Jiangxi Province. *Journal of Jiangxi Normal University* 45(2): 162–171. <https://doi.org/10.16357/j.cnki.issn1000-5862.2021.02.09> [Natural Science]
- Minh BQ, Nguyen MAT, von Haeseler A (2013) Ultrafast approximation for phylogenetic bootstrap. *Molecular Biology and Evolution* 30(5): 1188–1195. <https://doi.org/10.1093/molbev/mst024>
- Monteiro P, Gonçalves MF, Pinto G, Silva B, Martín-García J, Díez JJ, Alves A (2022) Three novel species of fungi associated with pine species showing needle blight-like disease symptoms. *European Journal of Plant Pathology* 162: 183–202. <https://doi.org/10.1007/s10658-021-02395-5>
- Nguyen LT, Schmidt HA, von Haeseler A, Minh BQ (2015) IQ-TREE: A fast and effective stochastic algorithm for estimating maximum-likelihood phylogenies. *Molecular Biology and Evolution* 32(1): 268–274. <https://doi.org/10.1093/molbev/msu300>
- Nugent A, Allison SD (2022) A framework for soil microbial ecology in urban ecosystems. *Ecosphere* 13(3): e3968. <https://doi.org/10.1002/ecs2.3968>
- O'Donnell K, Cigelnik E (1997) Two divergent intragenomic rDNA ITS2 types within a monophyletic lineage of the fungus *Fusarium* are nonorthologous. *Molecular Phylogenetics and Evolution* 7(1): 103–116. <https://doi.org/10.1006/mpev.1996.0376>
- Rai PK, Rai A, Singh S (2018) Change in soil microbial biomass along a rural-urban gradient in Varanasi (U.P., India). *Geology, Ecology, and Landscapes* 2: 15–21. <https://doi.org/10.1080/24749508.2018.1438743>

- Ren YL, Zhang ZY, Chen WH, Liang JD, Han YF, Liang ZQ (2022) Morphological and phylogenetic characteristics of *Phaeomycocentrospora xinjiangensis* (Pleosporales, Dothideomycetes), a new species from China. *Phytotaxa* 558(1): 125–132. <https://doi.org/10.11646/phytotaxa.558.1.9>
- Ronquist F, Teslenko M, van der Mark P, Ayres DL, Darling A, Höhna S, Larget B, Liu L, Suchard MA, Huelsenbeck JP (2012) MrBayes 3.2: Efficient bayesian phylogenetic inference and model choice across a large model space. *Systematic Biology* 61(3): 539–542. <https://doi.org/10.1093/sysbio/sys029>
- Rossmann AY, Samuels GJ, Rogerson CT, Lowen R (1999) Genera of Bionectriaceae, Hypocreaceae and Nectriaceae (Hypocreales, Ascomycetes). *Studies in Mycology* 42: 1–248.
- Song JQ, Yin YL, Zhang W, Liu Y, Sui QQ, Huo JY, Zheng WX, Li SX (2024) Characteristics of spatial differentiation of soil microbial communities in degraded grassland on the “black soil beaches” of Qinghai Plateau. *Shengtai Huanjing Xuebao* 33(11): 1696–1707. <https://doi.org/10.16258/j.cnki.1674-5906.2024.11.004>
- Spegazzini C (1919) Fungi Costaricensis Nonnulli. *Fungi Costaricensis Nonnulli*. *Boletín de la Academia Nacional de Ciencias en Córdoba* 23: 563.
- Suija A, Delhoume A, Poumarat S, Diederich P (2021) *Didymocyrtis microxanthoriae* (Phaeosphaeriaceae, Dothideomycetes), a new lichenicolous fungus from France. *Bulletin de la Société des naturalistes luxembourgeois* 123: 129–136.
- Tamura K, Stecher G, Peterson D, Filipowski A, Kumar S (2013) MEGA6: Molecular evolutionary genetics analysis version 6.0. *Molecular Biology and Evolution* 30(12): 2725–2729. <https://doi.org/10.1093/molbev/mst197>
- Trakunyingcharoen T, Lombard L, Groenewald JZ, Cheewangkoon R, Toanun C, Alfenas AC, Crous PW (2014) Mycoparasitic species of *Sphaerellopsis*, and allied lichenicolous and other genera. *IMA Fungus* 5(2): 391–414. <https://doi.org/10.5598/ima fungus.2014.05.02.05>
- Vainio EA (1921) *Lichenographia Fennica* I. *Acta Societatis pro Fauna et Flora Fennica*. 49(2): 1–274.
- Wang HY (2024) Study on the diversity and keratinophilic functional strains of heat-tolerant fungi in zoo soils. Master Thesis, Guizhou University, Guiyang, China.
- Wang MX, Liu KY, Xing YJ (2018) Association analysis of soil microorganism and plant species diversity under climate change. *Zhongguo Nongxue Tongbao* 34(20): 111–117.
- Wang XW, Han PJ, Bai FY, Luo A, Bensch K, Meijer M, Kraak B, Han DY, Sun BD, Crous PW, Houbraken J (2022) Taxonomy, phylogeny and identification of Chaetomiaceae with emphasis on thermophilic species. *Studies in Mycology* 101(1): 121–243. <https://doi.org/10.3114/sim.2022.101.03>
- Wang HY, Zhang ZY, Ren YL, Shao QY, Li X, Chen WH, Liang JD, Liang ZQ, Han YF (2023) *Multiverruca sinensis* gen. nov., sp. nov., a thermotolerant fungus isolated from soil in China. *International Journal of Systematic and Evolutionary Microbiology* 73(2): 005734. <https://doi.org/10.1099/ijsem.0.005734>
- Wang HY, Li X, Dong CB, Zhang YW, Chen WH, Liang JD, Han YF (2024) Two new species of Sordariomycetes (Chaetomiaceae and Nectriaceae) from China. *MycKeys* 102: 301–315. <https://doi.org/10.3897/mycokeys.102.114480>
- White TJ, Bruns T, Lee S, Taylor J (1990) Amplification and direct sequencing of fungal ribosomal RNA genes for phylogenetics. *PCR protocols: a guide to methods and applications* 18(1): 315–322. <https://doi.org/10.1016/B978-0-12-372180-8.50042-1>
- Woudenberg JHC, Aveskamp MM, de Gruyter J, Spiers AG, Crous PW (2009) Multiple *Didymella* teleomorphs are linked to the *Phoma clematidina* morphotype. *Persoonia* 22(1): 56–62. <https://doi.org/10.3767/003158509X427808>

- Yan B, Lu Q, Xia S, Li JS (2022) An overview of advances in soil microbial diversity of urban environment. *Shengwu Duoyangxing* 30: 22186. <https://doi.org/10.17520/biods.2022186>
- Yogabaanu U, Weber JFF, Convey P, Rizman-Idid M, Alias SA (2017) Antimicrobial properties and the influence of temperature on secondary metabolite production in cold environment soil fungi. *Polar Science* 14: 60–67. <https://doi.org/10.1016/j.polar.2017.09.005>
- Zhang D, Gao FL, Jakovlić I, Zou H, Zheng J, Li WX, Wang GT (2020) PhyloSuite: An integrated and scalable desktop platform for streamlined molecular sequence data management and evolutionary phylogenetics studies. *Molecular Ecology Resources* 20(1): 348–355. <https://doi.org/10.1111/1755-0998.13096>
- Zhang ZY, Shao QY, Li X, Chen WH, Liang JD, Han YF, Huang JZ, Liang ZQ (2021) Culturable fungi from urban soils in China I: Description of 10 new taxa. *Microbiology Spectrum* 9: e00867–e21. <https://doi.org/10.1128/Spectrum.00867-21>
- Zhang ZY, Li X, Chen WH, Liang JD, Han YF (2023) Culturable fungi from urban soils in China II, with the description of 18 novel species in Ascomycota (Dothideomycetes, Eurotiomycetes, Leotiomycetes and Sordariomycetes). *MycKeys* 98: 167–220. <https://doi.org/10.3897/mycokeys.98.102816>
- Zhang ZY, Pan H, Tao G, Li X, Han YF, Feng Y, Tong SQ, Ding CY (2024) Culturable mycobiota from Guizhou wildlife park in China. *Mycosphere: Journal of Fungal Biology* 15(1): 654–763. <https://doi.org/10.5943/mycosphere/15/1/5>
- Zhao D, Li F, Wang RS, Yang QR, Ni HS (2012) Effect of soil sealing on the microbial biomass, N transformation and related enzyme activities at various depths of soils in urban area of Beijing, China. *Journal of Soils and Sediments* 12: 519–530. <https://doi.org/10.1007/s11368-012-0472-6>
- Zhao L, Groenewald JZ, Hernández-Restrepo M, Schroers HJ, Crous PW (2023) Revising *Clonostachys* and allied genera in Bionectriaceae. *Studies in Mycology* 105: 205–266. <https://doi.org/10.3114/sim.2023.105.03>